PETROLOGY AND GEOCHEMISTRY OF SHETLAND GRANITES

Thesis submitted in accordance with the requirements
of the University of Liverpool
for the degree of Doctor in Philosophy

By Ali Saif Gamil

April, 1991

ABSTRACT.

A GEOCHEMICAL AND PETROLOGICAL STUDY OF SHETLAND GRANITOIDS AND THEIR RELATIONSHIP TO THE SCOTTISH GRANITOIDS.

This study is concerned with the distribution, age, chemistry and geotectonic setting of the 21 granites in Shetland. The granites range in size from a few metres to 8 Km across and in age from Pre-Moine to early Carboniferous. The granites occupy a unique position in being placed approximately half way between Scotland and Norway Caledonides and about 320 Km east of southeast coast of Greenland, if Greenland is restored to its pre-continental Drift position as predicted by the best fit of Greenland and Europe. The Shetland granites have been subdivided into 5 groups according to their location to the east or west of Walls Boundary Fault (a continuation of Great Glen Fault), mineralogical content and their occurrence in situ as granitic pebbles, as follows;

Granites to the east of WBF include (1) hornblende-bearing granites (2) hornblende-free granites and (3) Granitic pebbles a) the Rova Head conglomerate & b) the Funzie conglomerate.

Granites to the west of WBF include (4) Ronas Hill granite and its satellites and (5) Sandsting & Bixter granites which are grouped together because of their proximity and because the Bixter granite seems to be the acidic end product of the Sandsting granitoid.

A detailed petrological and geochemical study has been made of each group. Samples from each occurrence have been examined for mineralogical content and analysed by a variety of methods for major and trace elements (XRF, INAA, RNAA). This information has been used to derive the mechanisms which may have been responsible for the observed differentiation trends.

To the east of the Walls Boundary Fault (WBF) are hornblende-bearing granites, hornblende-free granites and Funzie and Rova Head granitic pebbles. The hornblende-bearing granites are truncated by the WBF and characterized by high Sr and Ba values. The Spiggie granite within this hornblende-bearing group also contains considerable amounts of primary epidote. The hornblende-free granites are a miscellaneous group of granitic rocks ranging between two-mica granites and garnet bearing granites, albite keratophyre and trondhjemite dykes. To the west of WBF are Ronas Hill granophyre and its satellites (with drusy cavities containing crystals of stilpnomelane, quartz and epidote), Sandsting complex and Bixter granites. Major element modelling suggests that a plagioclase, biotite and

hornblende fractionation process is appropriate for hornblende-bearing granites and Sandsting granite. Graphical and trace element modelling do not conflict with this too, but rare earth element modelling requires extraction of a quartz-feldspar phase.

The classification of Shetland granitoids on the basis of ages and petrology has not been previously attempted. According to the Read classification, the Caledonian hornblende-free granites could be classified as Pretectonic and Syntectonic intrusions equivalent to his older granites. In contrast to the hornblende-bearing granites to the east of WBF (Graven, Brae complexes and the Spiggie granite), the Graven and Brae appear to belong to the Appinite Suite while the Spiggie granite seems to be a forceful Newer Granite. According to Read the forceful Newer Granites were emplaced just after the Appinite Suite but in Shetland the Graven and Spiggie granites appear to be the same age (400 Ma). The Ronas Hill granite and its satellites, Sandsting and Bixter granites to the west of WBF are Upper Devonian granites and equivalent to the permitted last intrusions of Read, but do not appear to be of the cauldeeron or ring complex type typical of those in Scotland. In terms of ages the hornblende-bearing granites have given K-Ar ages of about 400-430 Ma. The Ronas Hill granite and its satellites, Sandsting complex and Bixter granite give K-Ar ages about 360 Ma.
Consideration of typology indicates that the hornblende-bearing granites, Ronas Hill & its satellites, the Sandsting complex and Bixter granite are I-Caledonian type whereas some of the hornblende-free granites are close to S-type. On the De La Roche classification system the Shetland granites are high-K calc-alkaline (except trondhjemite dykes and keratophyre in the hornblende-free granites group) and mostly plotted in the shoshonitic trend.
The geochemical comparison of the the post Devonian Ronas Hill granite and its satellites on the one hand and the closely associated late Devonian Shetland volcanics on the other, reveals that there is no link between them.
A comparison of the Shetland and Scottish granitoids in terms of major, trace and rare earth elements reveals very close similarities between these two Caledonian regions. Both show the same high K-calc-alkaline (Peccerillo & Taylor, 1976), the high alumina and alkali (Kuno, 1966) character, also show a general alkali-calcic character (Peacock, 1930) and they also have very good correlation in terms of some trace element variation diagrams such as Sr and Ba.

ACKNOWLEDGEMENT.

Table of Contents.

Chapter One

General Introduction

1.1 Aims of Research

A review of research on Shetland granitoids indicates that little is known about the chemistry, ages and types of Shetland graintoids. The fundamental aim of the research embodied in this thesis is to investigate the geochemical and petrological characteristics of the Shetland granitoids. In particular it was considered important to examine each of the eighteen separate plutons of Shetland granitoid, as initial indications were that there are significant differences between them. Also two areas of granitic pebbles in the Funzie and Rova Head conglomerates were included in order to determine their provenance.

One of the main lines of investigation is to establish whether there is any geochemical and/or genetic link between the Shetland and Scotland granitoids and to relate the origin of the individual granitoid to the development of the Caledonian orogen in the Shetland area.

1.2 Location of Shetland

Shetland lies about 240 Km north-northeast of the Scottish mainland, about 200 mls west of Bergen in Norway, approximately half way between Scotland and Norway, and about 320 Km east of southeast coast of Greenland, if Greenland is restored to its pre-continental Drift position as predicted by the best fit of Greenland and Europe (Carey 208; Bullard et al. 1965, Fig. 7). Thus Shetland is geographically in a position of some importance for correlating the various parts of the disrupted Caledonian orogenic belt. It forms a large exposure of Caledonian rocks lying between the three parts of the Caledonian orogenic belt which are separated by post-Caledonian sediments and sea. Shetland is an erosional monadnock-like remnant of Caledonian rocks rising above the continental shelf to the north of Scotland and is a part of the stable Shetland platform, the northward

submarine continuation of Scotland. The platform is limited to the east by the north-south trending Viking graben and to the west by the north-northeast trending west Shetland basin, a half graben, fault-bounded to the east (Ziegler 1981). Both these structures and the platform itself came into being in Triassic times when a propagating rift started to form in the north sea but failed to develop further.

1.3 Summary Of The Geology Of Shetland

The geology of Shetland is complex and can not be considered as a single unit. In Fig. 1.1 the Islands have been divided into a number of different geological areas and Shetland as a whole is divided into two geologically different parts by the Walls Boundary Fault (WBF), an extension or branch of the Great Glen Fault (Figure 1.2). To the west of the Walls Boundary Fault are metamorphic rocks which are probably of diverse ages. They have a rather restricted outcrop area and are overlain by Old Red Sandstones and contemporaneous volcanics. The western plutonic complexes (e.i. to the west of WBF) give K-Ar ages near to 350 Ma (Miller and Flinn, 1966). The field relationships show that metamorphics and Old Red Sandstone rocks are cut by the Sandsting granite. In the case of Ronas Hill granite and Muckle Roe granophyre, connected by the Mangaster Voe diorite, a net-veined complex, and the Eastern granite which forms the eastern boundary of the net-veined complex, none of these latter complexes cut the Old Red Sandstone, but they are cut by a diverse series of dykes, some of which cut the Walls Sandstones to the south.

To the east of the Walls Boundary Fault most of the area is undelain by metamorphic rocks. In the southeast, these are unconformably covered by Old Red Sandstone. The metamorphic rocks can be divided into four stratigraphic units. In the Mainland, to the east of the Walls Boundary Fault, nearly all the metamorphic rocks belong to a continuous stratigraphic succession which will be called the East Mainland succession (Flinn,1966). These rocks have been intruded after their
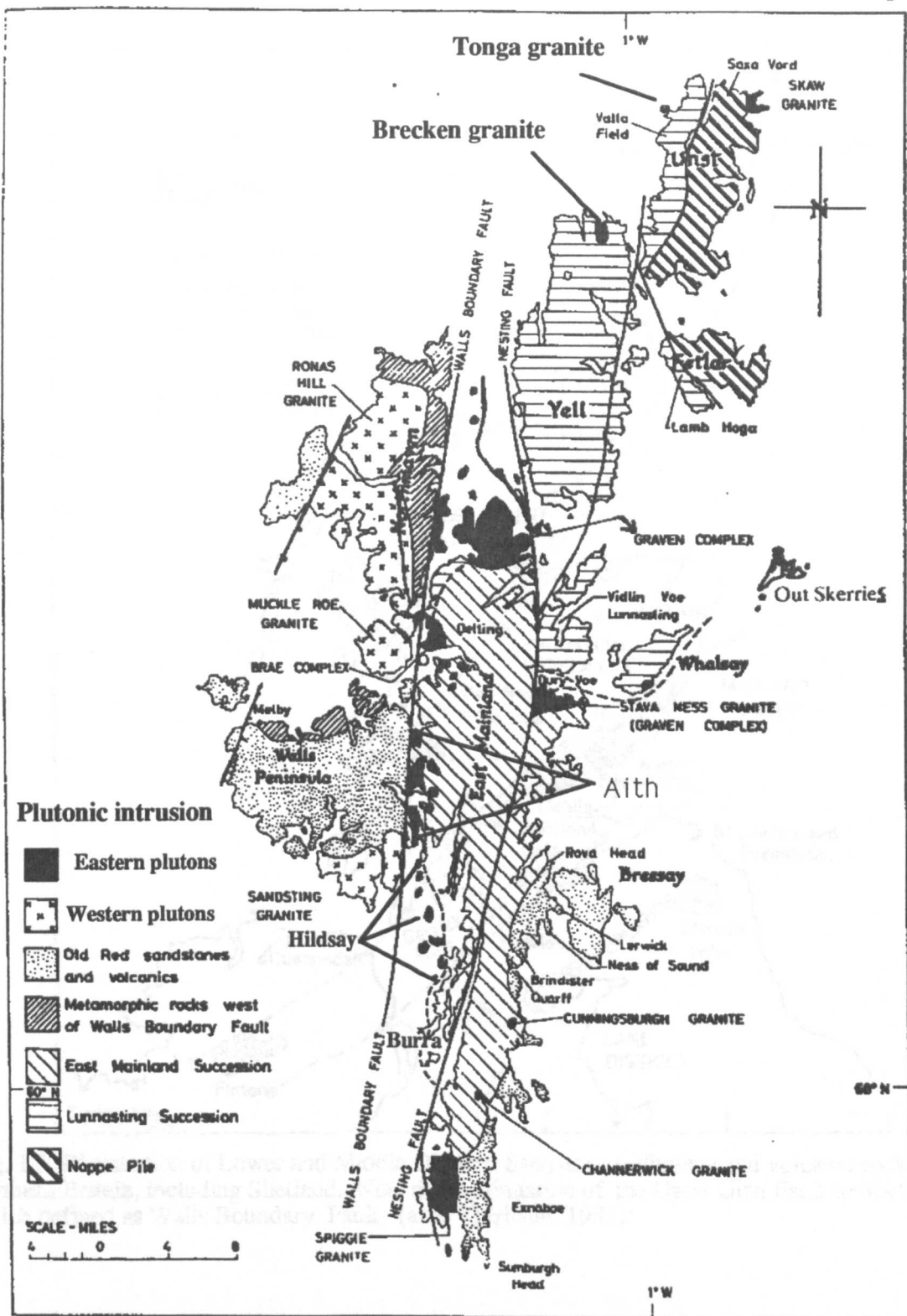
Figure 1.1 Locality map and geology of Shetland (after Flinn, 1966).
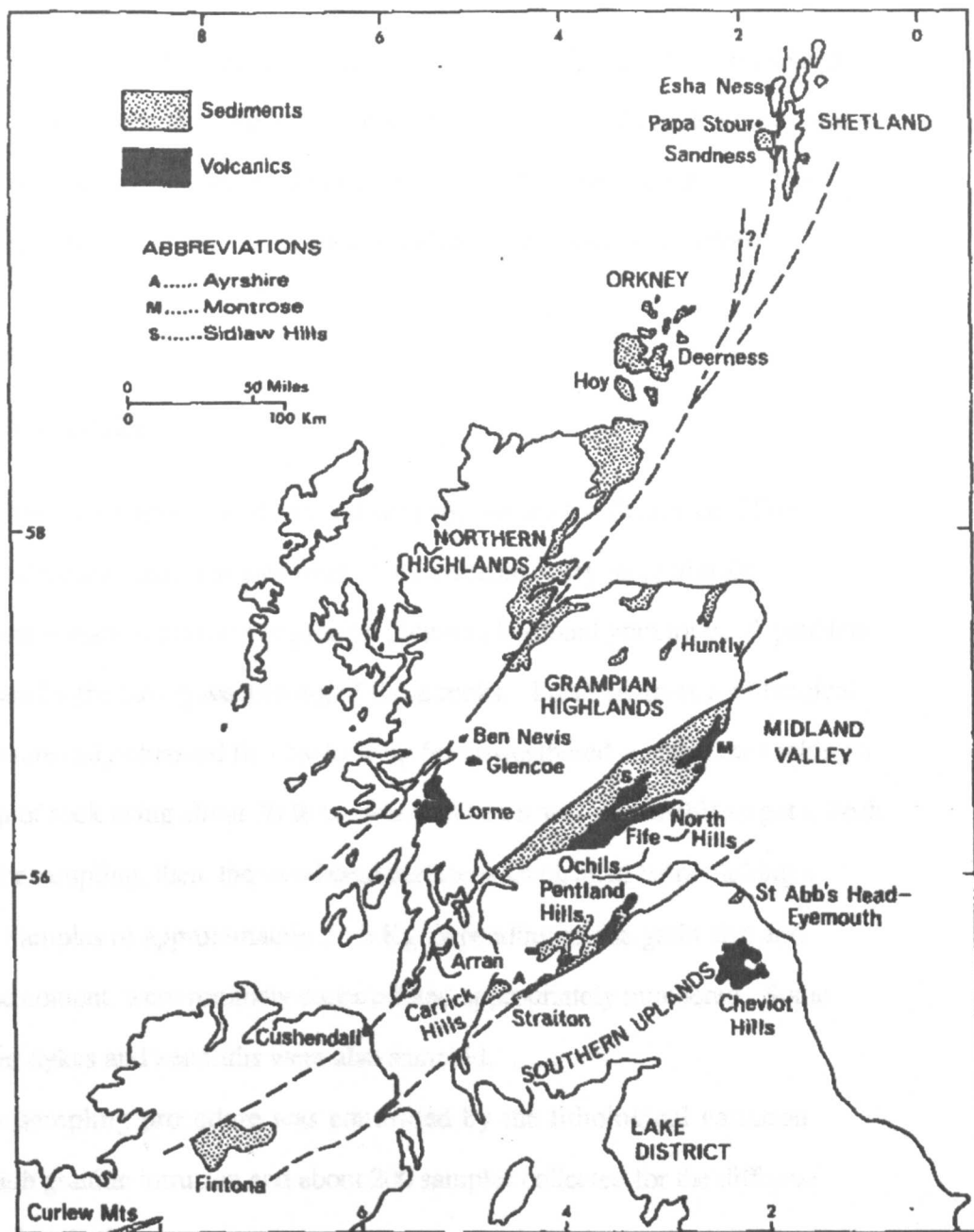
Fig. 1.2 Distribution of Lower and Middle Old Red Sandstone sediments and volcanic rocks in northern Britain, including Shetland. Note the continuation of the Great Glen Fault to Shetland, which defined as Walls Boundary Fault. (after Thirlwall, 1981).

metamorphism by the Graven and Brae Complexes, the Spiggie, Cunningsburgh and Channerwick granites, and a suite of lamprophyres. The Spiggie granite and the lamprophyres are unconformably covered by the Old Red Sandstone. The eastern complexes give K-Ar ages about 400 Ma (Miller and Flinn, 1966)

1.4 Rock Sampling

The field work was carried out and well supervised by Professor Flinn. Representative and fresh samples were collected from every recognisable petrological variation from every granitic pluton in Shetland granitoids. A problem was caused by the strong weathering of these rocks. Fresh samples for chemical analysis were only obtained first by looking for unweathered surface, then taking a big lump of rock using about 20 lb hammer. When it was impossible to get a fresh surface for sampling, then the weathered surface wast cleaned before taking a sample. Samples of approximately 2 - 3 Kg depending on the grain size and xenolithic content, were routinely collected and appropriately numbered. Some associated dykes and xenoliths were also sampled.

The sampling procedure was controlled by the lithological variation within each granitic intrusion and about 200 samples collected for the different aspects of analysis.

In all cases care was taken to sample as far away as possible from contacts to avoid contamination and also to avoid areas which were strongly veined and/or xenolithic. This clearly was one of the main purposes of field study, the other one is to make a detailed map of the Skaw granite.

1.5   Method of Investigation

The field mapping has been carried out by using a topographic map scale 1 : 10,000 as a base map. The samples collected in the field were studied in detail by means of polarizing microscope, X-ray flourescence, wet chemical analysis, electron microprobe and Neutron activation analysis. Details of these techniques are described in the appendix 1.

1.6 Presentation of Data .

In total, over 130 samples from the Shetland granitoids,their xenoliths and associated dioritic and gabbroic rocks have been analysed for major element oxides and selected trace elements, neutron activation analyses, REE analyses and microprobe analyses during the course of the study. A complete list of analyses is given in Appendix 2, along with modal analyses and a brief petrographic describtion of each rock. The sample localities are superimposed on a topographic base map of the area of study, and then reduced to several maps at various stages throughout the thesis.

Chapter Two.

2.1 Field Studies Of the Skaw Granite

The Skaw granite lies in the north-eastern corner of the Isle of Unst. It is a partially

tectonized, very coarsely porphyritic granite (Read 1934). It is bounded to the west

by a major shear zone and to the north, south and east by the North sea. It is

composed of a pink foliated augen-granite, the augen being red potash-feldspars

which reach a length of a 8cm or more and are set in a granulitic base of quartz and

mica (Flinn in Mykura 1976). The present author confirms Read's report (1934,

p.677) that the foliation of the granite, the orientation of the feldspar phenocrysts

and the attitude of the stratification of the xenoliths are all coincident and have an

overall north-east to easterly strike.

The Skaw granite has given a wide range of ages. A K-Ar age of biotite of

355 ± 12 Ma (Miller and Flinn, 1966), and Ar-Ar ages of 430 ± 10 Ma and $431 \pm$

11 Ma (xenoliths) , 433 ± 11 Ma (K-feldspar), and 380 ± 10 Ma (biotite) (Taylor,

1984).

Flinn (Personal Comunication) reports that the Skaw Granite was not thrust into

place as claimed by READ (1934), but was intruded in a semiconsolidated state,

so that the granite developed a strong L-tectonic fabric as it was intruded and at the

same time metamorphosed the contacted country rocks, sillimanite being devloped

in them, adjacent to the granite.

2.1.1 The Lithological Subdivision.

The Skaw granite is a member of Shetland Granitoids to the east of

Walls Boundary Fault (WBF), and also part of the Caledonian granite series. It is a

biotite granite and it can be divided in the field according to the Colour Index which

is the total percentage of mafic constituents in a rock. In this case there is only one

mafic constituent, biotite, and instead of using the three terms leucocratic,

mesocratic and melanocratic, the Skaw granite is subdivided as follows:-

1) Light granite 2) Darkish granite 3) Dark granite

These lithologies have gradational contacts and are easily recognized in the field (Figure 2.1). This petrological variation of the Skaw granite can be identified microscopically as the Dark granite contains the highest contents of biotite, up to 18% of the modal analysis, while the Light granite contains the lowest biotite value about 11% of the modal analysis. In between there is a Darkish granite which occurs as very small discrete patches within the Dark granite, especially in the north part of Skaw. Macroscopically the Dark and Light granites are composed of pink foliated augen-granite (plate 2.1B-E). The augen are red potash-feldspars which reach 12cm in length in some places and 6cm width and include mica inclusions (mainly biotite) (plate 2.1B and 2.1D), they are set in a granulitic matrix of quartz, microcline and mica. The augen texture and foliation appear more clearly in the dark granite than in the light granite (plate 2.1B). In addition to the augen texture and foliation, the Skaw granite is characterized by exfoliation weathering which always occur in the arid tropical regions (Plate 2.1A).

2.1.2 Subdivision Of the Skaw Granite into two Zones according to the shape and size of K-feldspar phenocrysts.

The K-feldspar phenocrysts shows a wide variation in size and shape. Twelve sites were chosen for measuring the length and width of the K-feldspar phenocrysts. This has led to a division the Skaw granite into two zones named *Zone A* and *Zone B* (Figure 2).

Zone A includes the dark granite and darkish granite which appears as patches within the dark one. This zone is characterized by the largest size of red K-feldspars phencrysts (12cm length by 7cm width).

Zone B is smaller than *Zone A* and lie to the west of A. This zone is clear of dark and darkish granite, the largest phenocryst length recorded in this zone is 5cm
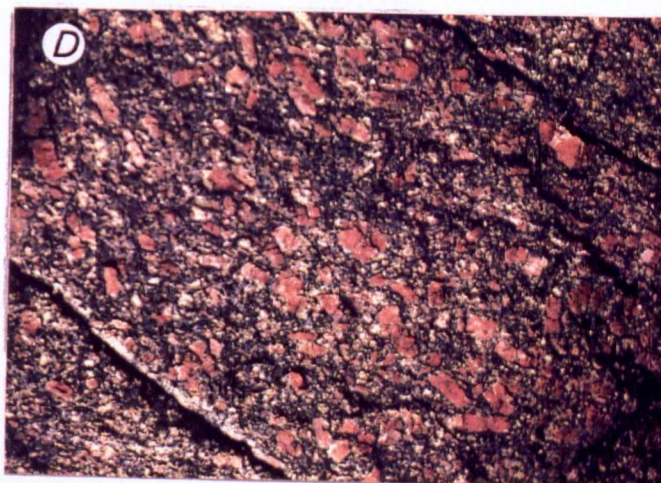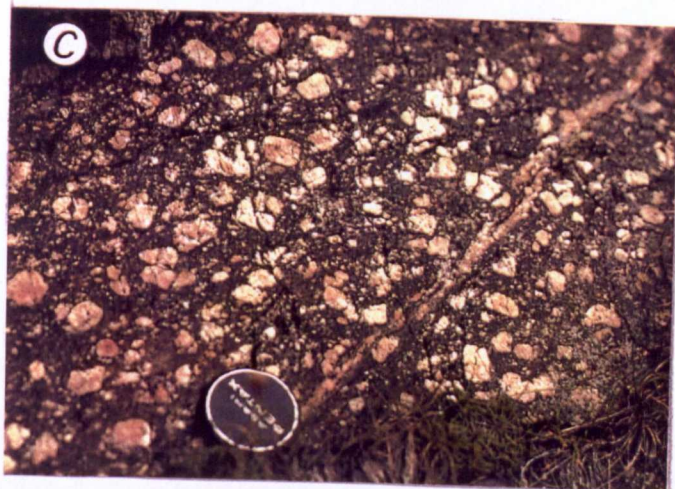
Plate 2.1. Macroscopic structures in the Skaw granite (light and dark Skaw granite) and Brecken granite. **A.** Exfoliation weathering in the light Skaw granite. **B.** Shear zone in the dark Skaw granite which fragmented the large feldspar crystals. **C** (light Skaw granite), **D** (dark Skaw granite) and **E** (light Skaw granite). **F.** Shows the gneisose texture in the Brecken granite.
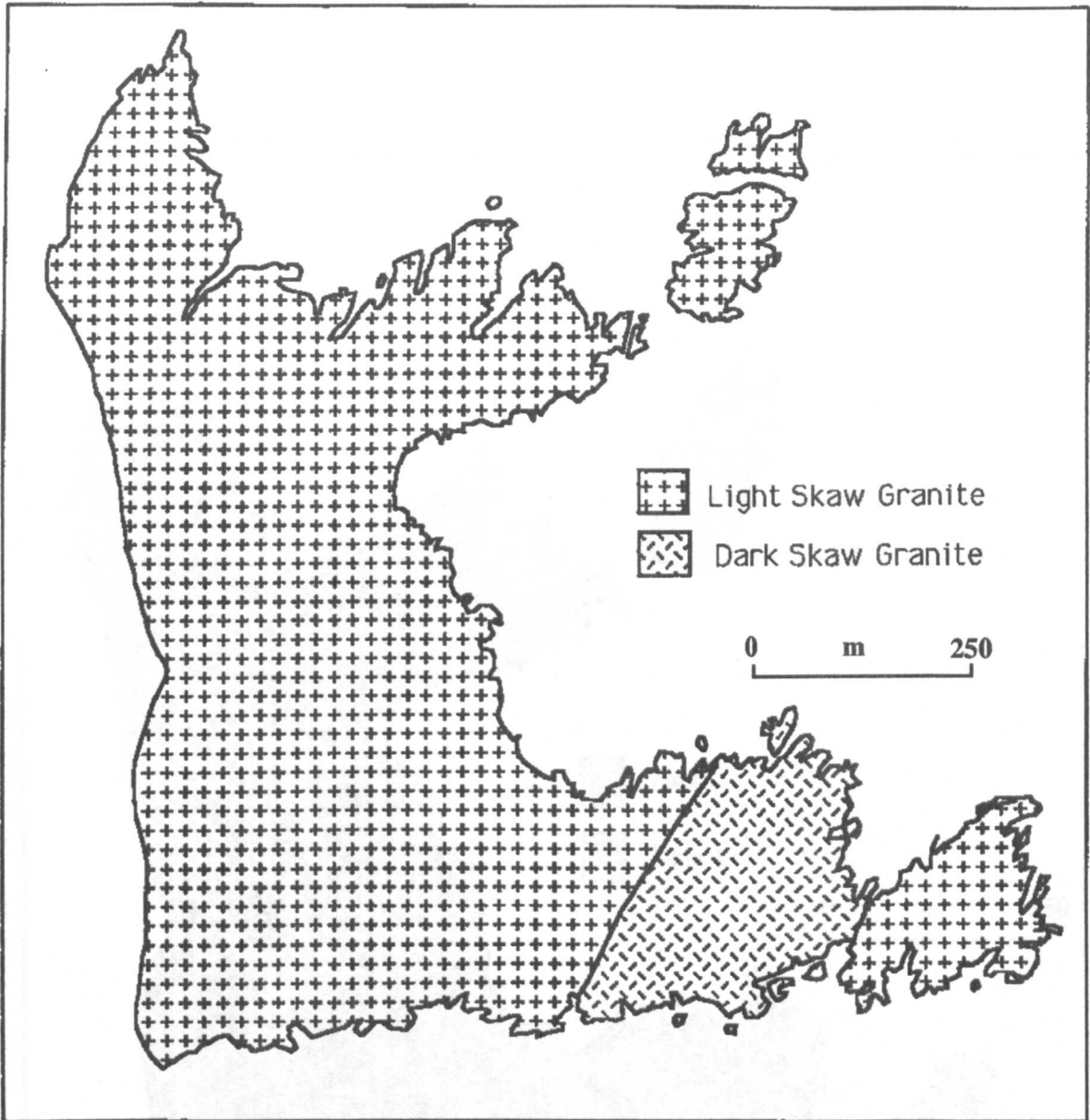
Figure.2.1 A geological map for Skaw granite, showing the
Dark and Light Skaw granites.
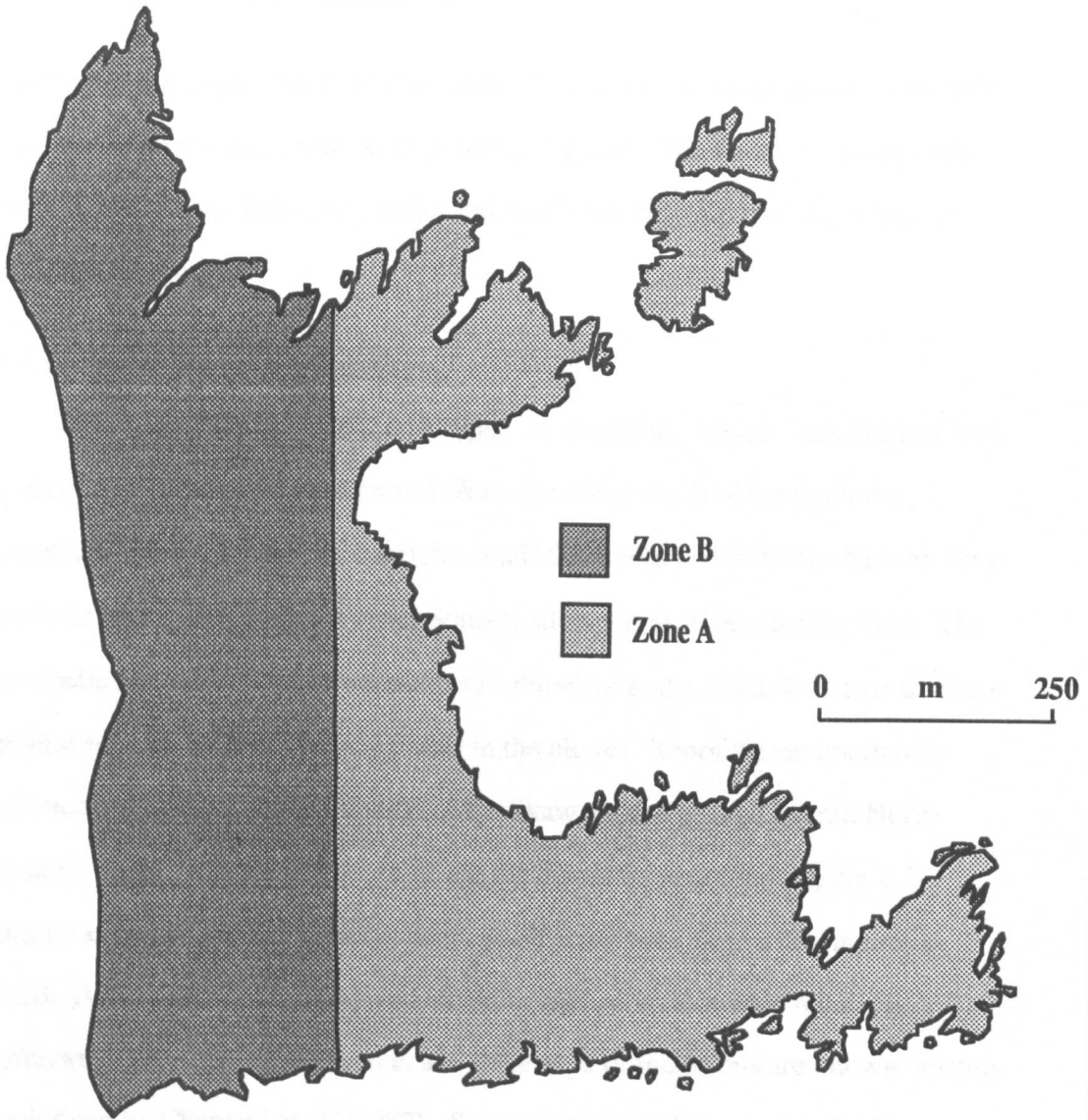
Figure 2.2 A map showing The subdivision Skaw into Zones A and B.

by 4cm width. The foliations of the granite in *Zone B* mostly strike between 035 to 045 and dip from 25 to 35 NW while the foliations in *Zone an strike* range from 030 to 080 and dip between 10 to 40 NW. The lineation associated with the foliation, plunges between 15 to 30 NE (Figure 2.3).

2.2 Structure of Skaw Granite.

Faulting in the Skaw granite is prominent. It is very easy to recognize in the field, but there is no evidence what kind of faults they are. The faults in Skaw granite have an overall North-Easterly strike and North-westerly dip in Zone A and in Zone B (Figure 2.3).

2.2.1 Skaw Granite Xenoliths.

There are two very different types of xenoliths, which are diorites and quartzites. The south eastern part of Skaw granite is much richer in diorite xenoliths and to some extent quartzite xenoliths. These xenoliths can be seen very easily in two sites, one in the Inner Sound and the other in the Herring Geo. The semipelitic and quartz schist xenoliths are abundant to the North-East side of Skaw granite and can be seen in many places in the pluton. Xenoliths are commonly oriented subparallell to the foliation of the Skaw granite with an overall North-Easterly strike. Diorite and quartzite are the dominant xenoliths (Figure 2.3). Diorite xenoliths are fine grained, occur in different sizes from a few metres at Heilla Pool to a few cm nearby and could be inclusions that were relatively refractory fragments of the source, and these type of inclusions are known restites as defined by Chappell et al. (1987). Some diorite xenoliths contain feldspar porphyroblasts which are similar to the large feldspar phenocrysts in the host Skaw granite.

2.2.2 Minor Intrusions.

A swarm of sub-parallel North-East trending acid and basic dykes cuts the Skaw granite (Figure 2.3). The acid dykes are composed of aplite and quartz,
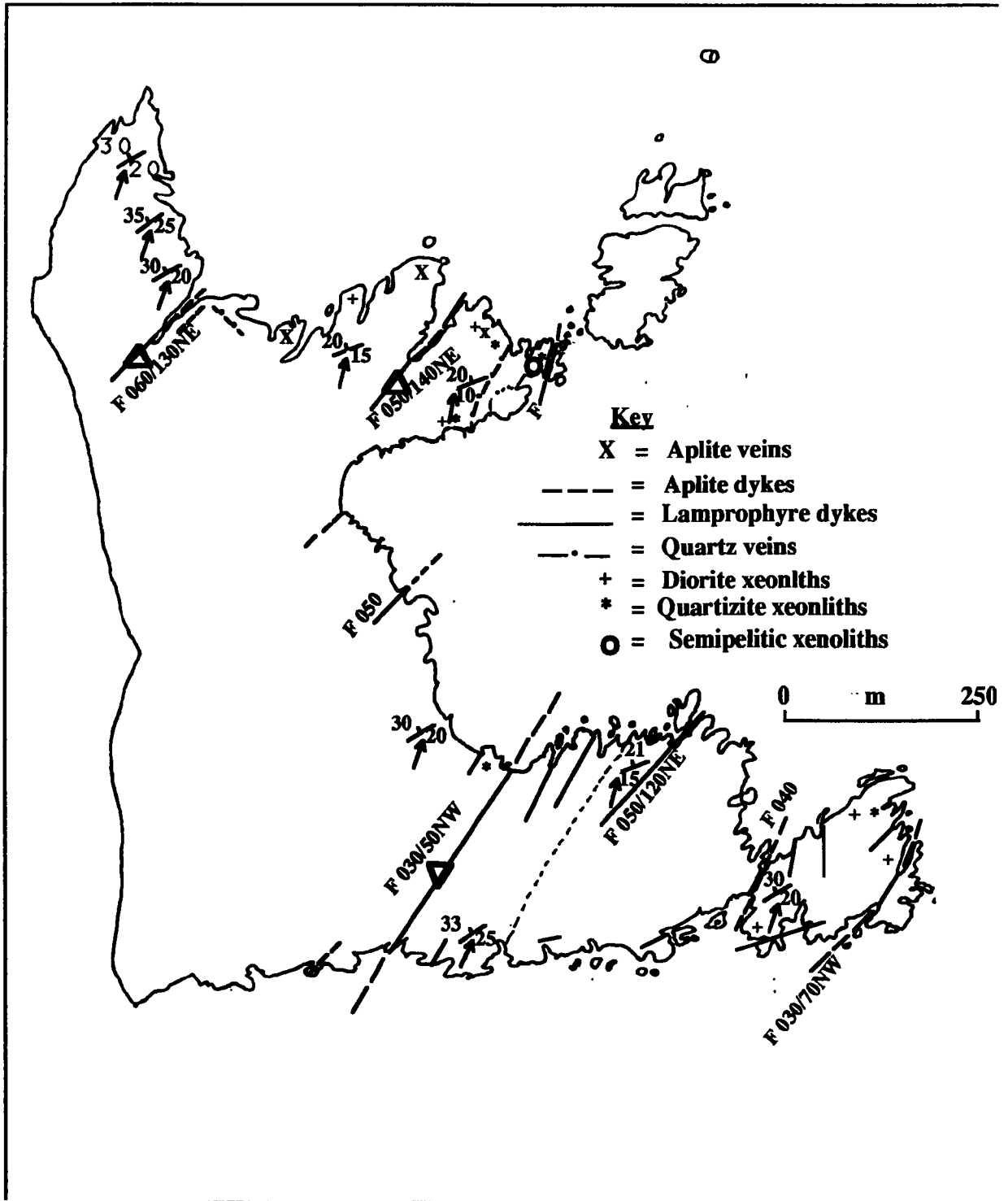
Figure 2.3 Skaw granite structural map and xenolith locations.

they are mostly veins, while the basic ones are lamprophyres. The lamprophyre

dykes are concentrated in the south-eastern part of the Skaw granite, whereas aplite

and quartz veins are restricted to the North-Eastern part of the Skaw granite. The

lamprophyre dykes, aplite and quartz veins have NE to ENE strike and some of

them in the North of Skaw granite have North-west strike.

2.3 Geochemical Evidence for Skaw Subdivision.

2.3.1 Major and Trace Elements.

The Harker major elements plots (Figs. 4.2a-b) show a good negative variation

for TiO_2, total iron as Fe_2O_3, MgO, CaO and P_2O_5 with the increasing silica

contents, from a slightly basic dark granite toward a slightly acidic light granite.

The trace element variation diagrams (Figs. 4.2c-e) also show a very good negative

correlation for Ba, Ce, La, Nd, Sc, Sr, V, Y, Zn and Zr with the increasing SiO_2

contents, and positive correlations for Pb, Rb, Th, Co and Cr with SiO_2 contents.

2.3.2 Rare Earth Elements.

The Dark and Light Skaw granite REE patterns are shown in Figure 4.10b in

evolutionary sequence from Dark to Light Skaw granites. The Dark granite has the

highest total REE compared with the Light granite which has total rare earth

depletion. Both of them have negative Eu anomalies and flat heavy REE patterns.

The conclusion from major and trace element variations diagrams that the

Light Skaw granite evolved from the Dark Skaw granite, and REE depletion from

Dark to Light Skaw granites and REE modelling of Light from Dark granite are

strong evidence to support the petrological subdivision of Skaw into Dark and

Light granites, which is already based on the field observation and petrographical

studies.

Chapter Three.

3.1 General Petrology Of the Shetland granitoids.

The Shetland granitoids are composed of intermediate to acid ~ "I" and "S" type (sensu Chappell and White, 1974) granitoid intrusions. The Hornblende-bearing granites, tend to be more basic in composition than the Hornblende-free granites. This is reflected in the mineralogy of the plutons, with hornblende, biotite and plagioclase forming the bulk of the more basic rocks of the Hornblende-bearing type, and K-feldspar, plagioclase and quartz forming the bulk of the Hornblende-free granites. Ronas Hill and Muckle Roe are miarolitic granophyric granites to the west of WBF within the late Caledonian calc-alkaline Northmaven plutonic complex, Mykura, (1979). Muscovite is found as an alteration product in the Hornblende-bearing granites, but it occurs in most of the Hornblende-free granites as a primary phase together with garnet. The accessory minerals in the granites are those found in acid/intermediate "I" and "S" type plutons (White et al., 1977a), namely sphene, epidote, apatite, allanite, garnet and zircon. Opaque minerals in Shetland granites are magnetite and ilmenite.

3.2 Petrology of the Hornblende-Bearing Granites to the East of Walls Boundary Fault (WBF) .

3.2.1 The Graven Complex

This intrusive complex occupies an area which extends from the Walls Boundary Fault (WBF) in North- Maven eastward via Sullom Voe, North Delting, and the adjoining islands in Yell Sound to the Nesting fault. It reappears further south in North Nesting, where it is exposed along the south shore of Dury Voe, having been displaced dextrally 14 to 16 Km by the Nesting fault (Figs. 3.2 & 3.7).

Name of Shetland granites arranged   as numbered in Figure 4.1a :

a) Alphabetically		b) Numerically
1) Aith granite	(12a)	1) Skaw granite
Bixter granite	(19a)	2) Tonga granite
Brae Complex	(7)	3) Funzie conglomerate
Brecken granite	(4a)	4) Brecken granite
Brecken Graveland granite	(4b)	5) Out Skerries granite
Channerwick granite	(10)	6) Graven complex
Colla Firth permeation belt granite	(9)	7) Brae complex
Cunningsburgh granite	(11)	8) Rova Head conglomerate
Eastern granite	(15)	9) Colla Firth granite
Foula granite	(20)	10) Channerwick granite
Graven complex	(6)	11) Cunningsburgh granite
Hildsay granite	(12b)	12) Spiggie granite
Keratophyre	(13)	13) Keratophyre
Muckle Ossas granite	(21)	14) Ronas Hill granite
Muckle Roe granophyre	(17)	15) Eastern granite
Net Veined granite	(16)	16) Net Veined granite
Out Skeries	(5)	17) Muckle Roe granophyre
Ronas Hill granite	(14)	18) Vementry granite
Rova Head Conglomerate	(8)	19a) Bixter granite
Sandsting Complex	(19)	19) Sandsting complex
Skaw granite (1)Skaw granite	(1)	20) Foula granite
Spiggie granite	(12c)	21) Muckle Ossas granite
Tonga granite	(2)	

Trondhjemite dykes associated with ultrabasic rocks   (3a)

Trondhjemite dykes associated with Green Stone rocks   (3b)

Trondhjemite and granitic pebbles associated with Funzie Conglomeratae   (3c)

Granites to the East of WBF.
Hornblende-bearing granites

430-400 Ma

Hornblende-free granites

433 Ma?

530 Ma

?

Garnet-bearing granites

Colla Firth granites

Tonga and Brecken granites

No K-feldspar granites

Trondhjemite dykes

Granitic pebbles in Funzie Conglomerate

Granites to the west of WBF.

360 Ma
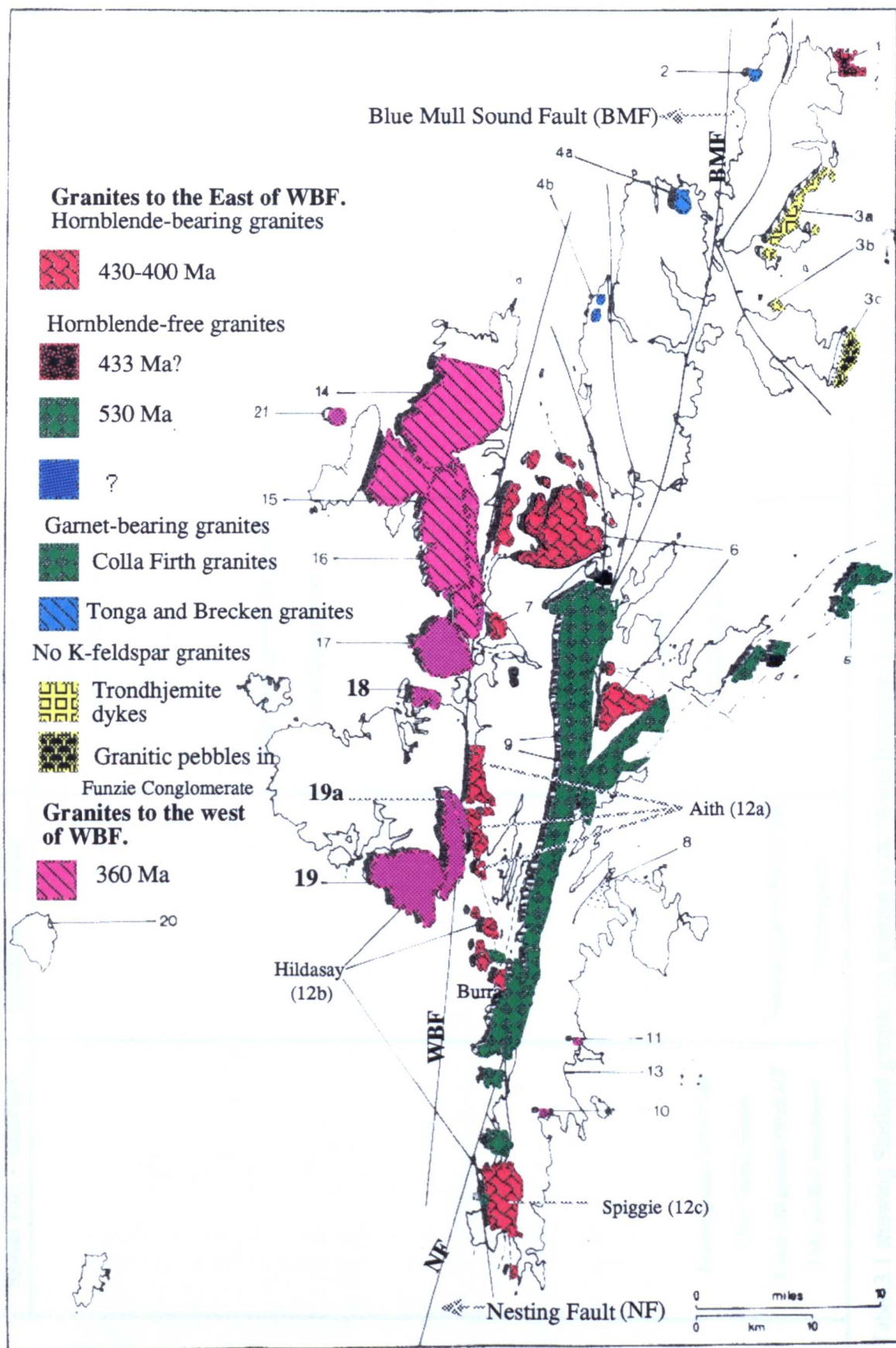
Figure 3.1. Showing the locations and different types of Shetland granitoids in relation to the ages and to the Walls Boundary Fault (WBF).

AGES	Granites to the west of the WBF		Granites to the East of the WBF		
	Ronas Hill + satellites	Sandsting + Bixter	Hbl-free	Hbl-bearing	Pebbles
600			? Brecken granite ? Tonga granite ? Albite-keratophyre		
575					
550					
525			Colla Firth granite 530±25 Ma*		
500			? Out Skerries granite		
475					? Funzie granitic pebbles (older than 475 Ma)
450					? Rova Head granite pebbles (older than 450 Ma)
425			Skaw granite 430±10 Ma (Ksp)⁺ 355±12 Ma (Bt)⁺	Brae granite 430±?? Ma⁺	
400	Eastern granite 385±?? Ma⁺ ? Net-Veined granite		Channerwick granite 399±8 Ma⁺	Graven granitoid 400±?? Ma⁺ Spiggie-Aith-Hildasay granites 399±8 Ma⁺	
375			? Cunningsburgh granite		
350	Ronas Hill granite 359±8 Ma⁺ ? Muckle Roe granophyre	Sandsting granite 360±11 Ma⁺ ? Bixter granite			

Table 3.1 showing Shetland granites in relation to the Walls Boundary Fault (WBF), and their relative ages. (Hbl = hornblende, Ksp = K-feldspar, Bt = biotite, * = Rb-Sr method, + = K-Ar method)
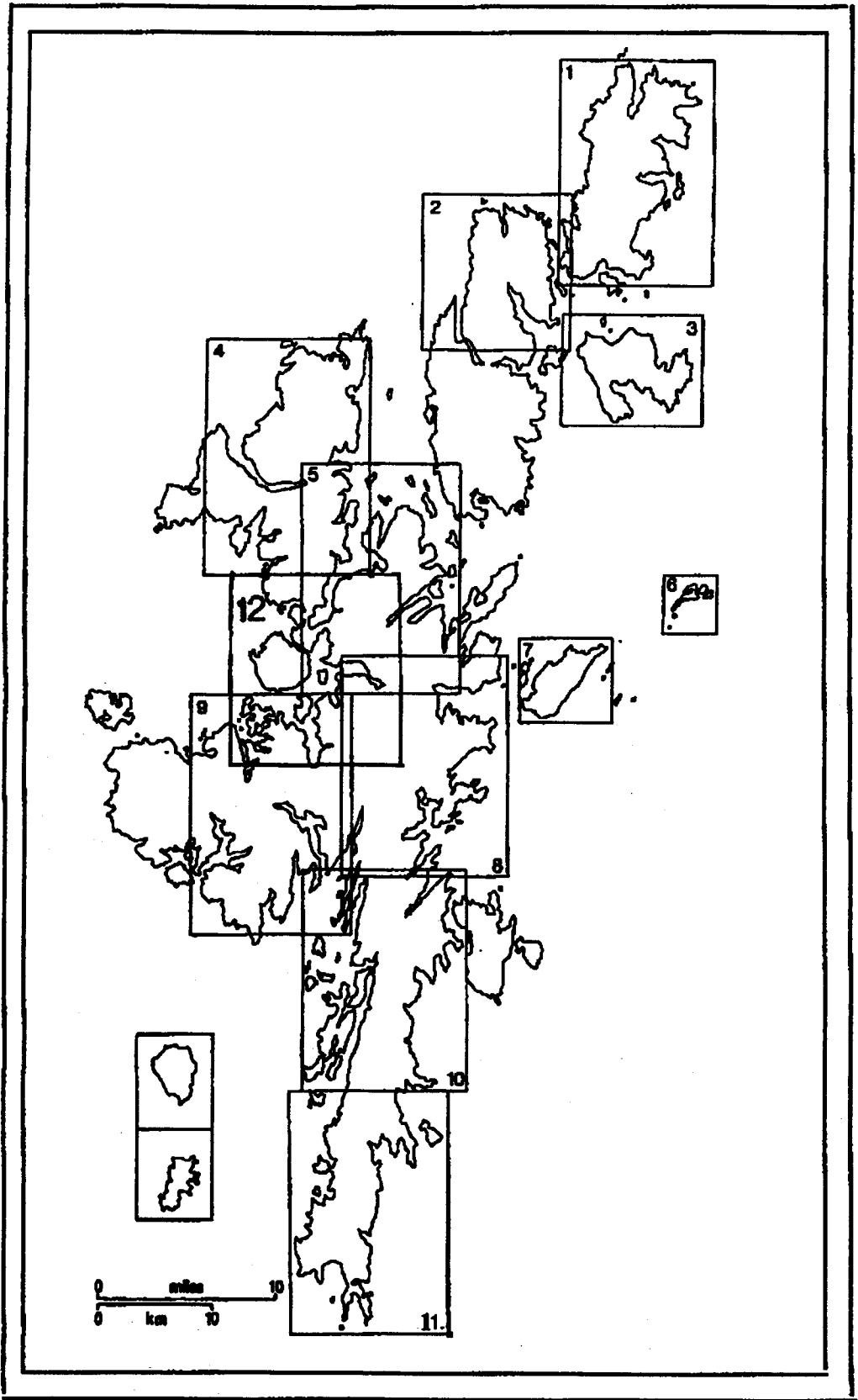
Figure 3.1. An outline map of Shetland. Boxes refer to the enlarged figures in text.
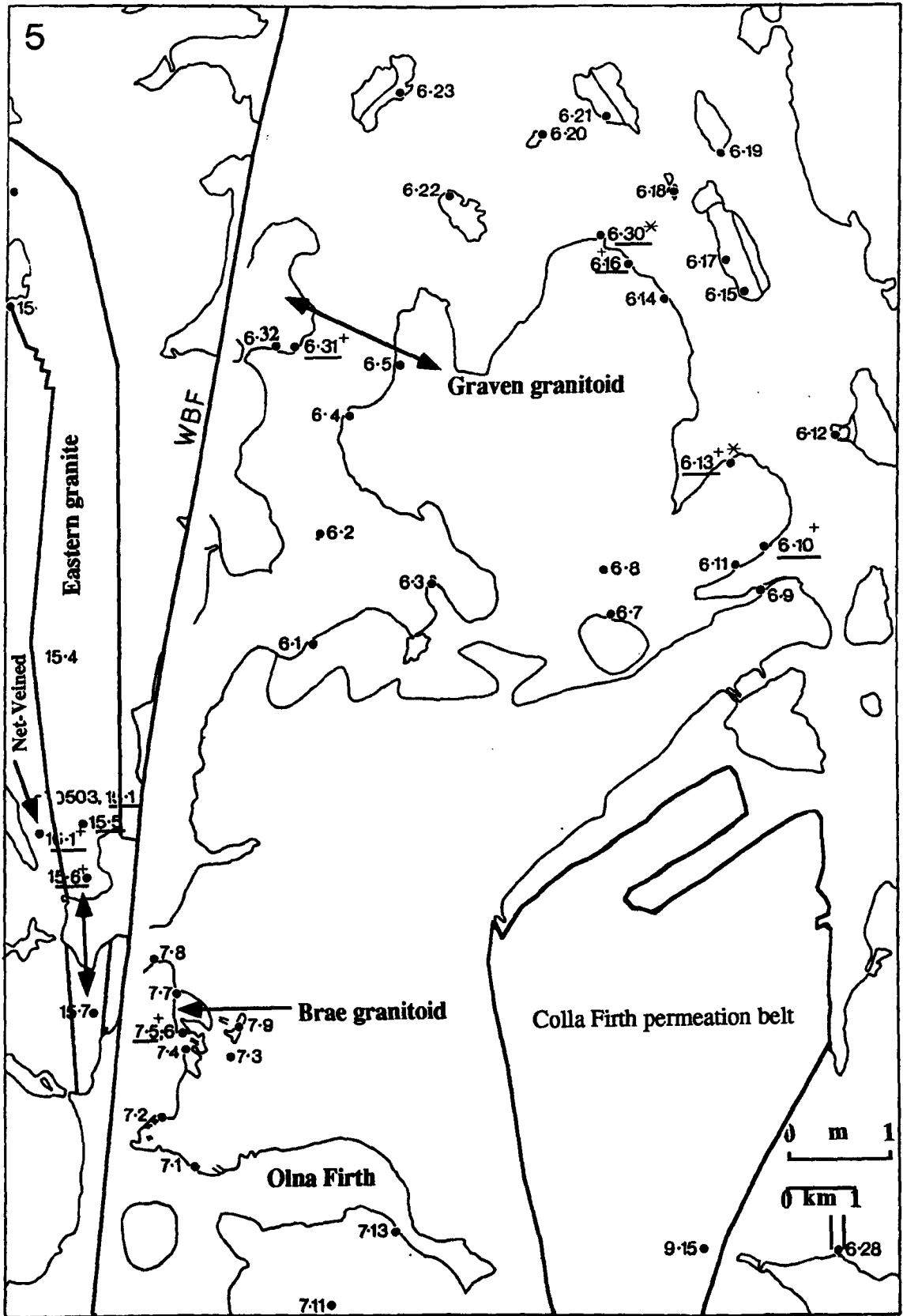
Figure 3.2. Map 5 showing locations of granites and samples of the Graven complex, Brae complex, Eastern and Net-Veined granites. (—) analysed samples by XRF, (+) INAA and (*) REE analyses.

3.2.2 Geological setting

Flinn in a series of papers (Flinn 1953; Flinn & Miller 1966; Mykura 1976; Flinn 1985), has stated that the Graven complex is emplaced along the contact between the Yell Sound division (the Moine) and the Whiteness division (the Dalradian), and cuts both. The Graven complex was emplaced as granodiorite forming a net-work of medium-to fine-grained hybrid plutonic rocks, which Flinn has collectively termed the "inclusion granite". This consists of a continously variable mixture of diorite, monzonite, granodiorite and granite, and is characterized by an abundance of small round cognate xenoliths of almost pure hornblende rock. The most granitic portion of the complex forms the Stava Ness Granite. It is also full of oriented angular xenoliths and larger enclaves of country rocks. The effects of thermal metamorphism by the intrusive rocks of the complex are most marked in the xenoliths, which contain abundant sillimanite in the psammitic rocks and diopside in the calcareous ones. The net vein granodiorite cuts the lamprophyre and porphyrite dykes.

Flinn and Miller (1966) collected rocks from the Graven complex (28445- a biotite facies of the early pegmatites and 28432 the later Stava Ness granite) for dating purposes, the age obtained for biotite from the pegmatite being 397 ± 5 Ma and for the Stava Ness Granite is 405 ± 14 Ma. The biotite was thermally metamorphosed by granodiorite.

Flinn (1985) described the Graven complex as a hornblende granodiorite with appinitic affinities. The granodiorite is characterized by the presence of innumerable tiny size xenoliths of hornblendite and in places passes into complex associations of hornblendite and hornblende diorite. The pegmatites previously reported as a first stage in the emplacement of the complex are widely distributed through the Yell Sound Division and are probably completely unrelated to the Graven complex

3.2.3 **Petrology of the Graven granitoid.**

The mineralogical composition of the Graven granodiorite (mineral contents are listed in appendix 2) include zoned plagioclase (An_{26}), zoned K-feldspar megacrysts, amphibole and biotite. Plagioclase is volumetrically the most important phase in Graven granitoid, whether acid, intermediate or basic. Crystals are euhedral to subhedral, occur singly and as large composite grains. Regular zoning of both normal and oscillatory types are seen in most crystals (plate 3.1B). Twinning on the albite law is very common with that on the pericline law being less so. Synneusis twins, indicative of magmatic crystal growth (Vance,1969) can be seen in plate (3.1D). Zoned crystals with anorthite-rich cores show to some extent a degree of alteration. Plagioclase is generally free of inclusions, but occasionally contains small euhedra of apatite and zircon. Some thin-sections showing late myrmekitic intergowths are ubquitous where plagioclase crystals adjoin microcline. K-feldspar is composed of microcline and microperthite and varies in size from small crystals to megacrysts. It is interstitial to the other minerals (see plate 3.1A) or encloses them completely. The most frequent inclusions are small zoned plagioclase, some of which are oriented parallel to the crystal suface of the host microperthite (plate 3.1C), biotite, zircon and apatite. Myrmekite is ubiquitous at plagioclase-K-feldspar boundaries, sometimes the process is so advanced that the smaller microcline grains are completely eaten away. Quartz is generally interstitial to all other minerals, especially to the plagioclase and also often to the K-feldspar. Boundaries between them tend to be irregular and mostly interlocking lobate. Hornblende forms euhedral to subhedral crystals (plate 3.1C) which are strongly pleochroic from dark bluish-green to pale yellowish green and commonly twinned. Small euhedral inclusions of apatite are common, individual hornblende crystals do occur, but most are found in multi-granular aggregates along with biotite, sphene and magnetite. Alteration of hornblende to green chlorite and to biotite is generally very common . Biotite occurs as euhedral to anhedral plates clotted together in
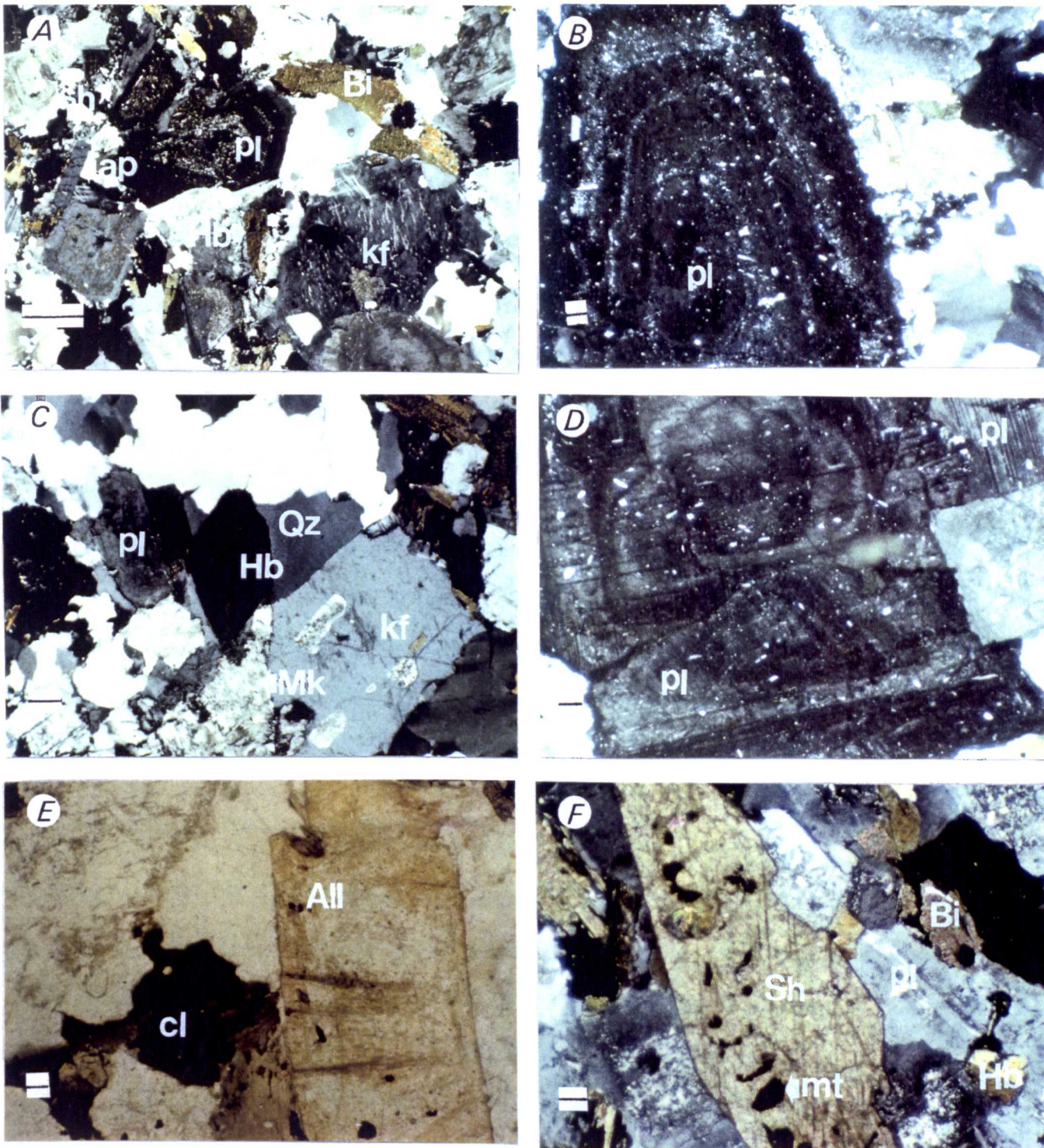
Plate 3.1 **A.** General texture and mineralogy of Graven granodiorite, showing euhedral zoned plagioclase (Pl), K-feldspar (kf) as microcline and perthite, biotite (Bi), hornblende (Hb) and the accessory minerals sphene (sh) and apatite (ap) (scale bar, 0.5 mm). **B.** Euhedral plagioclase showing excellent oscillatory zoning (scale bar, 0.5 mm). **C.** Twinning euhedral hornblende crystal and myrmekitic (Mk) texture (pointed arrow) (scale bar, 0.5 mm). **D.** Synneusis twinning in plagioclase (scale bar, 0.5 mm). **E.** Showing chlorite (cl) and allanite crystal (All) (scale bar, 0.5 mm). **F.** Sphene crystale encloses tiny magnetite minerals (scale bar, 1 mm).

groups along with the other minerals. Biotite commonly encloses numerous small crystals of apatite, zircon and iron ore. Some thin-sections show that the biotite is much more prone to secondary alteration than hornblende and breaks down, especially along cleavage plane to an association of epidote, sphene and iron ore. Accessories are allanite, sphene and occasionally magnetite. Allanite is very common in the Graven granodiorite (plate 3.1E) which is a variety of epidote usually containing several weight % of light rare earth elements and thorium content. Since allanite contains high concentration of thorium and uranium its structure is prone to radiation damage, alteration to a metamict state occurs frequently and is accompanied by the formation of radiating cracks in the rock around the crystals due to expansion on alteration and hydration. It occurs as brown or yellow coloured euhedral allanite prisms which often display a very pronounced zoning. Inclusions of magnetite and zircon in allanite are present (plate 3.1E). Sphene is the most abundant accessory mineral of the Graven granitoid occurring as euhedral crystals with a faint pleochroism from brown to very pale brown (plate 3.1F). Small euhedral plagioclase and magnetite are seen included in sphene.

3.2.4 **Brae Intrusive Complex.**

The Brae complex lies a few miles immediately south of the Graven complex, and occupies approximately 5.4 Km^2 of the south-western peninsula of Delting, which is bounded to the west by Busta Voe and to the south by Olna Firth. The main outcrop is centred around Brae Village, with satellite bodies south of Olna Firth (Fig. 3.2). The main intrusion is truncated on its western margin by the WBF (Walls Boundary Fault).

3.2.5 **Geological Setting.**

Flinn (1954) reported that contact of the Brae complex with the country rocks can be seen only on the the coast by Mangaster Burn and its age

cannot be determined. The rocks of the complex range from serpentines to acid pegmatite, the two dominant types being granite and very variable dark-coloured hornblende-biotite-feldspar rock. A mass of metamorphic rocks can be seen within the complex on the coast to the South of Wethersta.

Flinn (1966) demonstrated the contact relationship of the Brae complex as a cross-cutting mass of very variable composition, which metamorphoses the schist and permeation gneisses it cuts. The highest grade of thermally metmorphosed rock produced is a coarsely crystalline cordierite-sillimanite-garnet hornfels. A specimen of diorite (28435) was collected for age determination by K-Ar method and yields a biotite age 385 ± 6 Ma. (Miller and Flinn, 1966)

Flinn in Mykura (1976) described the Brae complex as a series of complexes with a family similarity. All have amphibole as their most characteristic mineral. Their emplacement may well represent an early phase in the igneous activity which culminated in the formation of the Graven complex. The Brae complex is unlike the Graven complex, in that, it is a compact, composite stock-like intrusion, which is largely composed of a two-pyroxene diorite with andesine, potash-feldspar and biotite. Scattered throughout the complex are masses of ultramafic rocks; the largest of which lies in S. W. corner. These vary from peridotite and pyroxenite, to dunite. In two places along the south coast, there are small xenolithic enclaves of altered mteasedimentary and ultrabasic rocks and they are associated with two-pyroxene gabbro, characterized by the presence of reddish-brown hornblende and are richer in iron than similar rocks in the rest of the complex, Gill (1965) considers them to be an early phase of emplacement.

Flinn (1985) has stated that the Brae complex is cut by Lamprophyre dykes which are cut by the Graven grandiorite, and that the Brae complex is a series of plugs formed by the multiple intrusion of rocks, varying from a two pyroxene mica diorite to ultramafic rocks on the one hand and granite rocks on the other. Flinn also mentioned that the lithologies of the complex are remarkably similar to those of Garabal Hill complex of Scotland.

Moffat (1978) described the Brae complex as a calc-alkaline suite, comprising a plutonic ultramafic-gabbro-diorite-granodiorite-granite association, with a wide compositional range (ca. 40 - 70 wt % SiO_2). Emplacement of younger granitic and dioritic magmas in the same igneous locus giving increased scope for variability and lithological diversity. Moffat described all lithologies represented in the Brae complex, two of which are: A) Granitic leucocratic rocks (biotite-hornblende tonalite, two-mica tonalite, biotite granodiorite, biotite granite). B) Granitic pegmatites, aplites and minette lamprophyres.

Age-constraints, Moffat concluded that the Brae plutonic complex is a late to post tectonic Caledonian pluton intruded at about 430 Ma (early Silurian using the time scale of Harland et al 1982). The critical observations in support of this conclusion, which have been taken into consideration are cross-cuting relations; xenoliths. (a) Radiometric dating of the adjacent migmatite belt given by Rb / Sr muscovite age of 526 Ma (Flinn & Pringle 1976), which is a reliable maximum possible age for the intrusion of the Brae complex. (b) K-Ar radiometric date for two rocks from the plutonic complex, consisting of a hypersthene diorite from Burra Voe and a biotite two pyroxene diorite from E. of Mill Burn, with biotite ages of 390 Ma (Flinn, pers. comm. in Gill, 1965) and 433 ± Ma (Gill, 1965) respectively; the younger of these ages may have been affected by partial Ar loss and resetting. (c) A hornblende separated from the hornblende gabbro from a satellite intrusion south of Olna Firth at the Loch of Gon Firth, gives a ^{40}Ar / ^{39}Ar plateau age of 427 ± 8 Ma (fig.7.2). Moffat concluded that the relation between the different rock types of the plutonic complex are very difficult to determine, given the relatively poor inland exposure and the multi-intrusion history, involving possible hybridization and assimilation, xenolith-host relationships and contacts scarce minor intrusive. Nevertheless, age relations between the granitic rock suite and the other plutonic units which comprise the Brae complex consistently indicate that the granitic rocks are younger.

Granular textures are present and overprint the penetrative gneissose

schistosity of the country rock and extend up to 100 m from the pluton-country rock contact. They are accompanied by the development of sillimanite, generally within 100 m of the contact.

The petrography and mineralogy. The granitic leucocratic rocks of Brae complex as studied by Moffat are late intrusive bodies and comprise < 10 % of the plutonic complex. They are biotite granodiorite, tonalite, minor amounts of biotite-hornblende tonalite, rare two mica tonalite and biotite granite; thus the most common rock types are grandiorite and tonalite. They are generally medium-grained (mean grain size = 1-5 mm), equigranular or porphyritic, subhedral-to anhedral-granular and characterized by abundant quartz, plagioclase (oligoclase), and a low mafic mineral contents ± microcline or orthoclase ± apatite ± zircon and Fe-Ti oxide. Aplites (quartz-microcline-oligoclase) and granitic pegmatites are common throughout the plutonic complex.

Moffat (1978) summarized and concluded as follows: A) The ordering and emplacement of successive basic or ultrabasic to acidic magmas in the Brae plutonic complex is consistent with possible storage and differentiation of primitive magma(s) in a lower-level reservoir. Transfer of successively more differentiated magmas into the exposed level of the plutonic complex, occurring with time. B) The limited Fe-enrichment along with lithological and mineralogical variations within the Brae plutonic complex are typical of calc-alkaline suites from destructive plate margins (cf. Best & Mercy, 1967; Lopez-Escobar et al, 1979). C) The Brae complex is late to post-tectonic and was intruded into metamorphic rocks of the East Mainland succession in a continental crust (sialic) setting at about 430 Ma (early Sillurian; time scale of Harland et al 1982).

Flinn (personal communication) says the difference between the two sets of radiometric ages, i.e between 390 and 430 Ma is broadly the result of a late regional K-metasomatism of the area giving rise in the Brae complex to newly formed biotites. It from these biotites, seen in thin section to be of late origin, that the young ages were obtained.

3.2.6 Petrology of Brae Granite.

The mineral constituents of the Brae plutonic granitoid rocks are plagioclase, K-feldspar, hornblende and biotite. Some of the hornblende, especially in the tonalite, appears to be altered to biotite and green chlorite (minerals are listed in appendix 2). Plagioclase forms euhedral to subhedral crystals, faint regular zoning of both normal and oscillatory types is seen in most crystals. Some thin sections show that the plagioclase is strongly altered to sericite (plate 3.7A). K-feldspar is microcline-microperthite and occurs as euhedral to anhedral crystals and is interstitial to the other minerals. Quartz is generally interstitial to all the other minerals, especially plagioclase. Boundaries between quartz crystals tend to be irregular and interlocking lobate. Hornblende forms euhedral prismatic crystals, some of the hornblendes have been recrystallized and changed to biotite and green chlorite.The tonalite rocks are characterized by zoned plagioclases + quartz ± microcline ± hornblende + biotite, and secondary biotite and chlorite. Accessory minerals are very scarce and are trace of apatite, rutile and allanite (plate 3.7A). The hornblende appears to have been the earliest essential mineral to commence crystallization because euhedral crystals of this mineral are found. Some have been recrystallized and changed to biotite. Aggregate mafic minerals biotite, chlorite, epidote allanite, and magnetite may be a decomposition of older pyroxene or hornblende. Biotite occurs as anhedral small plates usually clotted together in groups along with the other mafic minerals. Zoning of secondary amphibole is common. The granodiorite consists of zoned plagioclase + porphryritic microcline (occasionally poikilitic) + quartz + hornblende + biotite. The secondary minerals are chlorite and occasionally muscovite. The accessory minerals are sphene, apatite, zircon and occasionally allanite.

3.2.7 **Spiggie Granite.**

Outcrops in the southern tip of east Mainland on the east side of the Nesting fault between Spiggie and Quendale. Its most southerly outcrop is on Lady's Holm to the west of Scatsness (Fig. 3.3).

3.2.8 **Geological Setting**

Miller and Flinn (1966) have obtained a K-Ar age determination of muscovite from the Spiggie Granite aureole of 398 ± 5 Ma. The lithological units comprising the Spiggie complex are mainly granodiorite and porphyritic adamellite, but monzonite, pyroxenite and serpentinites are also present (Mykura 1976). The order of the emplacement of intrusion is as follows: (1) ultrabasic rocks; (2) monzonite and related rocks; (3) granodiorite an of porphryritic adamellite. Serpentinitic ultrabasic rocks occur along the margin at Scousburgh (345 535), as a band of serpentinite up to 350 m wide (Mykura1976). The monzonite in the Spiggie area crops out alongside the serpentinite at Scousburgh and around Bakka Setter where it is extensively decomposed. Strips of hornblende-rich rock occur at the edge of the complex at Noss (358 166), Quedale (372 132), The porphyrtic and non porphyritic facies occur in the same area. The thermal effect of the Spiggie Granite has been studied by Flinn (1967), who showed that marginal feldspathisation occurs at its contact. The zone of alteration is limited to a few metres and the changes in the rocks are not very noticeable, except where the granite cuts the Dunrosseness phyllites at Spiggie & Garthss Ness. There the thermal effects are spectacular and of considerable interest.

Flinn (1985), has stated that the Spiggie complex is all post-metamorphic and post-tectonic (except for faulting). The calc-alkaline trend of the Spiggie complex is described by Moffat (1987) and it ranges in composition from serpentinized dunite to granite(s.s). The more felsic rocks granodiorite,
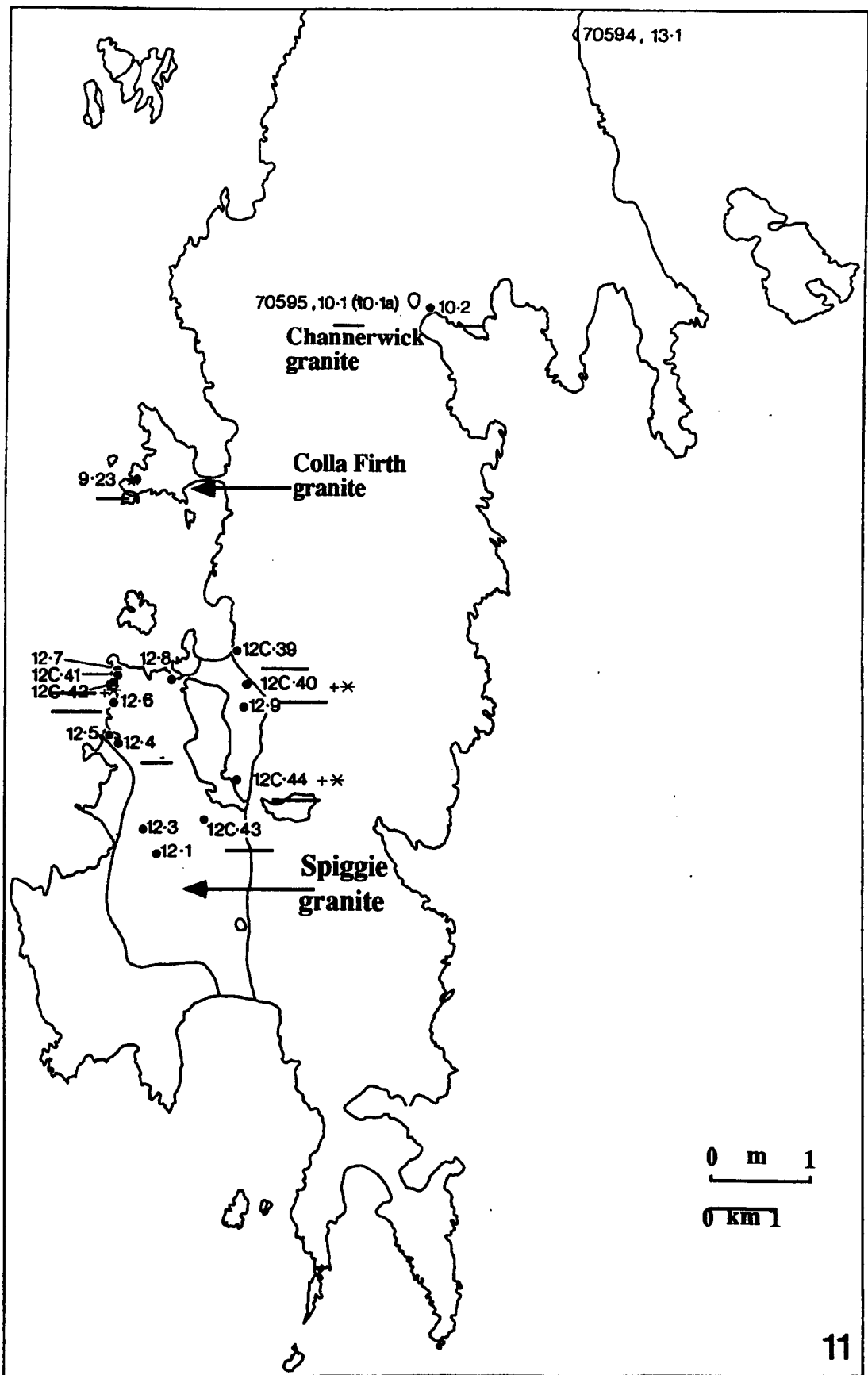
Figure 3.3. Map 11 showing locations of granites and samples in
Spiggie granite, Channerwick granite and the rest of Colla Firth granite.
(——) analysed samples by XRF, (+) INAA and (*) REE analyses.

hornblende-syenite and porphyritic granite comprise > 75 % of the outcrops. Xenolithic marginal facies are also found, and particularly the hornblende-biotite diorite, monzonite and granite.

3.2.9 Petrology of the Spiggie Granite.

Monzonite, porphyritic granodiorite and monzogranite occurs as coarse grained rocks containing K-feldspar megacrysts (See the list of Spiggie granite mineral constituents, appendix 2), large plagioclase and small amounts of hornblende, biotite and chlorite (plate 3.2D & 3.2E). Plagioclase (An_{36}) occurs as subhedral crystals, most of which are intensively altered. Small plagioclase crystals are commonly enclosed by K-feldspar. K-feldspar is microcline to microcline perthite and occurs as large subhedral poikilitic twinned crystals. Quartz occurs as large patches and aggregates of small grains interstitial to other minerals. Biotite occurs mostly as clusters of flakes and is totally altered to chlorite. Small chlorite flakes are poikilitically enclosed by K-feldspar. Hornblende occurs as small euhedral crystals partially altered to epidote and lack any pyroxene core. Among the accessory minerals, sphene commonly forms well-formed wedge-shaped crystals, apatite mostly occurs as inclusion in biotite which is now altered to chlorite and iron ore.

3.2.10 Aith granite.

The Aith Granite outcrops between the south-west shore of Aith Voe in the north & the sea to the south, and is truncated by the WBF to the west (Fig. 3.11).

3.2.11 Geological Setting.

Flinn in Mykura (1976) has found that the Aith granite has the same lithological components as the Hildsay and Spiggie granites, viz. granodiorite and porphyritic adamellite and which are respectively inner and marginal facies of a single major intrusion. The sequence of intrusion is as in the Hildsay and Spiggie areas. A band or a sizable outcrop of serpentinite occurs east of Houlland

(345535), 1.5 Km north of Bixter. Monzonitic and related rocks are cut by granitic and pegmatitic veins as exposed in a roadside quarry 1 Km east of Bixter (342521). At this locality pyroxene-bearing rock occurs with granulitized and recrystallized feldspars and pronounced linear fabric. Both the porphyritic and nonporphyritic facies of the granite also occur in the Sand Sound-Aith area. A weakly developed foliation is also present and is due to the presence of flattened quartz grain aggregates.

Flinn (1985) maintains that the Aith Granite and Hildsay & Spiggie Granites are all post-metmorphic and post-tectonic (except for faulting). Moffat (1987) pointed out that a calc-alkaline trend also exists in the Aith Granite which ranges in composition from ultramafic to granitic.

3.2.12 Petrology of Aith Granite.

Monzonite and granodiorite in the Aith area contains the same mineral constituents as the Spiggie granite (mineral are listed in appendix 2), the Aith Granite contains microcline (occasionally porphyritic), plagioclase (An_{36}) (occasionally zoned), amphibole, biotite, epidote. Pyroxene is found in the Aith monzonite. Pyroxene occurs as euhedral to subhedral prismatic crystals with green hornblende growth at the edges and along cleavage planes (plate 3.9A & 3.9B), which in turn is altered to biotite and epidote. Epidote forms euhedral/subhedral crystals, solitary epidote crystals do occur, but most are found in multi-granular aggregate along with biotite and well shaped allanite. The secondary minerals are chlorite and epidote. Accessory minerals are allanite, sphene, apatite, zircon and magnetite (occur in association with multi-granular aggregates).

3.2.13 Hildasay Granite.

The Hildsay Granite is exposed in a group of islands west of Scalloway between Hamna Voe on Burra Isle in the south and Sandsound in the north (Figure 3.8).

3.2.14 Geological Setting

Granodiorite and porphyritic adamellite form respectively the inner and

marginal facies of a single major intrusion, their relationship is best seen at Hamna Voe and on the islands to the N-W of West Burra. On the island of Papa (365375), the rock adjoining the eastern margin of the mass is packed with cube shaped microcline phenocrysts with about 1 cm in size. Further west the phenocrysts become progressively less abundant, but individually larger and in the central parts of the island, they are well scattered and up to 4 cm long. At the west end of the island and on Oxna (350 370) and Cheynies (347 386) the rock is a non porphyritic granodiorite (Mykura 1976). There is a weakly-developed foliation as in the Spiggie Granite. Under the microscope the rock shows the effects of incipient granulitization and recrystallization and contains abundant secondary epidote and pronounced linear fabric. Most of the Hildasay Granite is cut by veins of pegmatite up to 1m thick (Flinn in Mykura 1976). The sequence of intrusions is the same as in Spiggie area. Biotite-pyroxenite occurs as a raft in monzonite south of Hamna Voe (366 355) and form the inner Skerry (363 340) off the coast of W-Burra.

Flinn (1985) has shown that the granite is post-metamorphic and post-tectonic (except for faulting) as in the Aith and Spiggie Granites. A calc-alkaline trend has been reported by Moffat (1987) for all the different rock types of Spiggie and its two offshoots Aith and Hildsay granites. Xenolithic marginal facies are also found as the same in the Spiggie Granite.

3.2.15 Petrology of Hildasay Granite.

The mineralogical components of the Hildsay (minerals and modes are listed in appendix 2) Granite are the same as in the Spiggie and Aith areas, i.e. plagioclase, K-feldspar megacrysts, hornblende, biotite and epidote (plate 3.2A-C). Plagioclase crystals are subhedral, occurring both singly and as large composite grains, twinning on the albite law is common with that on the pericline law being less so. They display varying degrees of alteration to fine sericite, but where the rock has been exposed to prolonged surface weathering or deuteric alteration near fractures, then alteration to sericite is sometimes almost complete. Sericitisation is most noticeable in strongly zoned crystals, with the more anorthite-rich core
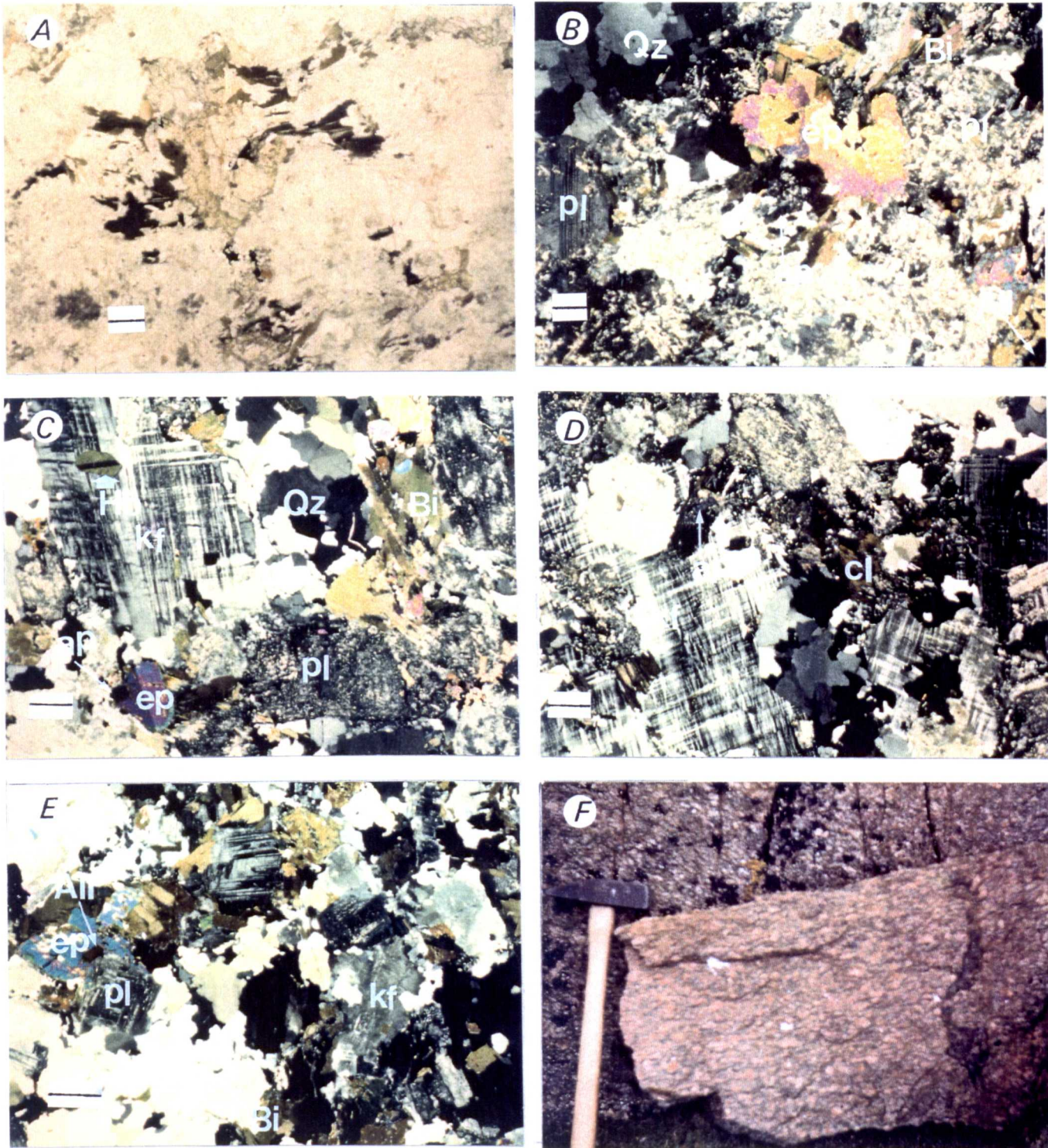
Plate 3.2. **A.** Hildsay granodiorite under plain polarized light (scale bar, 0.5 mm). **B.** Hildsay granodiorite under X nicols showing the high alteration of plagioclase (pl), euhedral primary epidote crystals (ep), biotite (Bi), quartz (Qz) and accessory minerals apatite (ap) and allanite (All) (scale bar, 0.5 mm). **C.** Hildsay monzonite showing twined hornblende (Hb) enclosed in K-feldspar (kf) (scale bar, 0.5 mm). **D and E.** Are from Spiggie granite, note the subhedral poikilitic microcline (kf, D) in coarse grained granite and break down of biotite into chlorite (cl, D), note the biotite in E does not break down into biotite (scale bar, 0.5 mm). **F.** Gneisose Tonga granite.

showing the greatest degree of replacement. K-feldspar is a microcline, subhedral to anhedral crystals show simple cross-hatch twinning. The most frequent inclusions are small altered plagioclase, small euhedral hornblende crystals, biotite flakes. Hornblende occurs as small euhedral twinned crystals which are strongly pleochroic from dark bluish-green to pale yellowish-green. Epidote forms euhedral to anhedral crystals and, commonly, twinned epidote crystals; pale pinkish and greenish rims are ubiquitous. Biotite is the commonest mafic mineral, being on average about two times as abundant as hornblende. It occurs as anhedral plates which are usually clotted together in groups, along with the other mafic minerals. A strong pleochroism is displayed, varying from deep olive-green or brown-black to pale yellow. The biotite is much more prone to secondary alteration than hornblende , breaking down, especially along the cleavage planes to an assemblage epidote ± chlorite ± sphene ± ore. Quartz is generally interstitial to all the other minerals, especially to plagioclase and also often to the microcline, the crystals are usually relatively strained, boundaries between them tend to be irregular. Accessory minerals are allanite (usually in association with epidote), zircon, apatite and occur as small crystals in the interiors of biotite, sphene and magnetite.

3.3 Petrology of the Hornblende-free Granites to the East of WBF.

3.3.1 Skaw Granite

The Skaw Granite oocupies the north-eastern corner of Unst. It is an interesting and spectacular tectonic unit. It and its relation to the adjacent schists can be studied in the cliffs making Lamba Ness, and around Houlls and Skaw (Figure 3.4).

3.3.2 Geological Setting.

For the Skaw Granite some restricted work has been done by the following workers: READ (1934a) described the main rock of the Skaw Granite as an augen -granite, which carries abundant xenoliths of semipeltic and siliceous schist. It is known locally as the "granite with pebbles", on account of the large
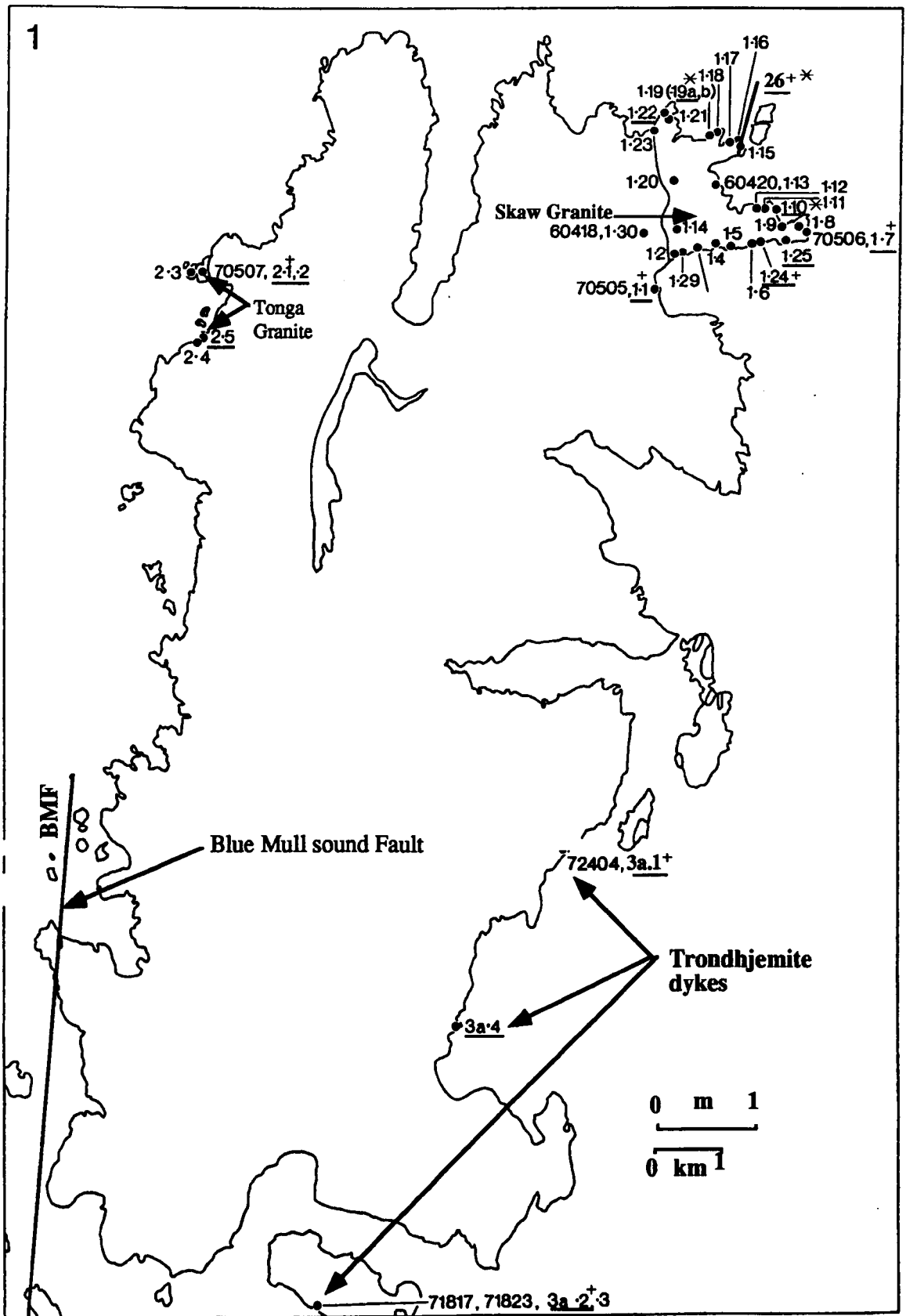
Figure 3.4. Map1 showing locations of granites and samples in the Skaw granite, Tonga granite, and Trondhjemite dykes. Note that the underlined samples are analysed for major and trace elements by XRF, single asterisks allocated for REE analysed samples and crosses for INAA analyses .

feldspar crystals, that reach a length of 3 inches or more. The degree of rock

foliation, varies from slightly deformed porphyritic granite to plane foliated

ribboned pink and gray rock. The feldspar phenocrysts are orthoclase with

microcline patches, microperthite, and acid plagioclase, with usually rounded or

embayed margins. Most of them are seen to be broken and displaced. The

fractures are healed by quartz.They are set in a granulitic base of quartz and biotite,

which flows around the larger feldspar phenocrysts. Over most of its outcrop the

augen-granite contains large and small xenolithic masses of sedimentary origin.

The augen-granite foliation, the feldspar phenocrysts and the attitude of

stratification in the xenoliths are all coincident, and have over all a NE-SW strike.

Some of the xenoliths contain feldspar porphyroblasts, which are similar to the

large feldspars in the granite.

Miller and Flinn (1966) demonstrated that the Skaw Granite is a gneissose augen-

granite,which appears to be an integral part of the nappe pile. It is cut by

lamprophyres. A biotite from this granite has given a K-Ar age of 355 ± 12 Ma

(table 7.1). Both the appearance and relation to the surounding rocks are unlike

those of the Ronas Hill and Sandsting Granites which give similar ages. They

mention that the Skaw Granite is extremely rotten and in places has been dug as a

source of grit for road. This alteration may explain the very young age obtained.

G. K. Taylor (1984) had studied 3 samples from the Skaw Granite for

the purpose of Ar-Ar step heating age determination. The first one designated

R1544, a hornfelsed honblendic xenolith. This sample failed to yield a concordant

plateau, instead it yielded a complex disjointed series of apparent ages. The

anomalous ages of the first four steps are probably a result of their small size (all <

2 % of total Ar released) steps 6-8 and 9-12 are each concordant and yield ages of

430 ± 10 and 431 ± 11Ma respectively. The highest temperature steps yield

increasing apparent ages, and possibly are a relict of the originally metamorphosed

rocks . The second sample is feldspar phenocryst. This was cut from a fresh

sample of the granite. It yields an almost ideal concordant age plateau which is
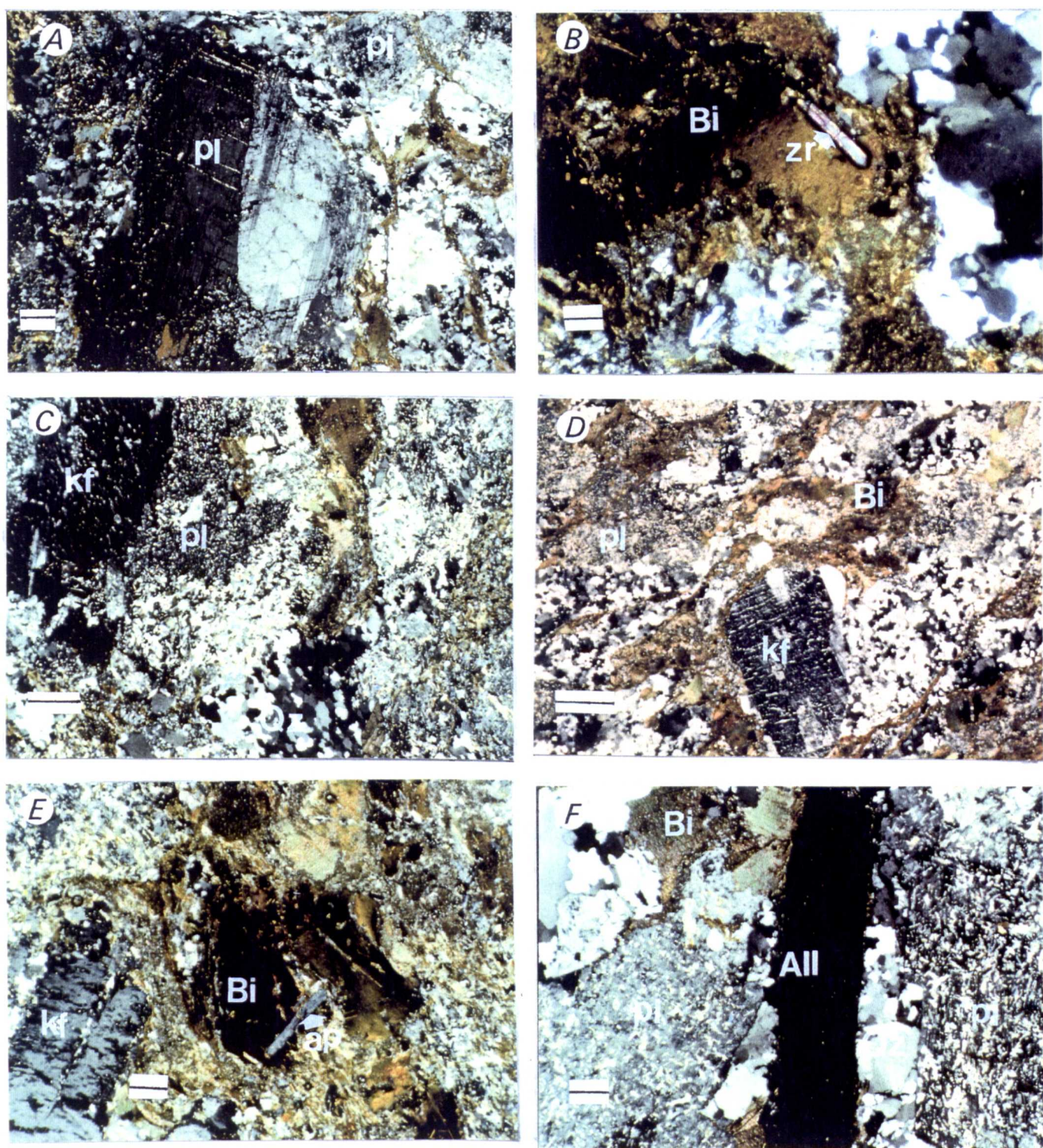
Plate 3.3. **A.** Euhedral plagioclase (pl) phenocryst in Skaw darkish granite, note that the quartz and biotite flow round the longer feldspar pheocrysts (scale bar, 0.5 mm). **B.** Euhedral zircon (zr) crystal enclosed in biotite (Bi) in dark Skaw granite (scale bar, 0.5 mm). **C.** Note the recrystallized quartzs (Qz) have been stretched in a micro shear zone; perthitic K-feldspar (kf) (scale bar, 0.5 mm). **D.** The augen granite foliation of Skaw (scale bar, 0.5 mm). **E.** K-feldspar (kf); biotite (Bi) and apatite (ap) are broken and displaced and later healed by quartz, (scale bar, 0.5 mm). **F.** Euhedral crystal of allanite (All) and highly altered plagioclase (pl) (scale bar, 0.5 mm).

433 ± 11 Ma. The third sample is composed of the biotite -feldspar-quartz matrix . This sample was cut from the same specimen as was used for sample R1556. This sample gives a good plateau and an age of 380 ± 10Ma.

3.3.3 Petrology of Skaw granite.

The mineral constituents of the Skaw granite are plagioclase, microcline-perthite, quartz and biotite. Plagioclase occurs as euhedral to subhedral crystals, varying in size from minute crystals up to megacrysts (plate 3.3A), small crystals are strongly altered to sericite. Twinning on the albite law and Carlsbad is very common. K-feldspar is orthoclase with micocline patches, microperthite, varying in size from minute size crystals up to 12cm in length. Most of them are seen to be broken and displaced (plate 3.3E), the fractures are healed by quartz. K-feldspars and plagioclase are set in a granulitic base of quartz and biotite, which flows around the longer feldspar phenocrysts (plate 3.3A & D). Quartz is interstitial to the other minerals, boundaries between them tend to be interlocking and lobate. Biotite is considered an important mafic phase as it reached to 18 % of the modal mineralogy of the Skaw granite. It occurs as subhedral to anhedral plates, solitary plates do occur, but mostly clotted together in groups. Apatite and zircon occur as euhedral crystals and included in the interiors of the biotite (plate 3.3B & E). Accessory minerals are euhedral crystals of apatite, allanite (most abundant accessory mineral), zircon and ilmenite (plate 3.3F).

3.3.4 Tonga Granite

This Granite lies on the west coast of Unst in the Valla Field Block (Figure 3.4) and it is shown on the British Geological Survey map of Shetland (B.G.S.) as foliated granite and granodiorite (plate 3.2F). It outcrops in the Tonga peninsular and in the cliffs to the south.

3.3.5 Geological Setting

Read (1934) reported this as granite sills which are well

developed on Tonga. They vary from a few cms in thickness to 150 metres or more and intrude a series of micaceous and hornblende schists and gneisses . They consist of red augen granite, and are traversed by sheets and veins of coarse pegmatite. Both granite and pegmatite are well foliated. Pegmatites are also abundant in the schist and gneisses which contain these granite sheets.

3.3.6 Petrology of Tonga Granite.

The Tonga syenogranites are characterized by allotriomorphic texture (plate 3.5C) and occur as coarse grained porphyritic rocks containing large K-feldspar, plagioclase and appreciable amounts of large garnet (plate 3.5A-B), part of which has broken down into biotite and quartz, biotite, muscovite and chlorite (after biotite). Plagioclase forms eubhedral crystals; single crystals occur more than the composite ones. K-feldspar is microcline and occurs as large twinned subhedral to anhedral crystals. Quartz occurs as anhedral patches and as aggregates of small grains which are interstitial to other minerals. Biotite occurs as anhedral plates, strong pleochroism is displayed, varying from dark brown to pale yellow. Tonga biotite is free of inclusions and occurs singly or clotted together in groups. Muscovite forms colourless anhedral plates which exist along with biotite. Accessory minerals are apatite and ilmenite.

3.3.7 Brecken Granite

3.3.8 Geological Setting

Flinn (1988) described the Brecken granite as an orthogneiss (plate 2.1F), in North Yell which occurs as a large lense and several smaller sheets (Graveland gneiss), in the Graveland lens (fig. 3.5), in Moine metasediments. All are tectonized granitoids and are associated with otherwise unusually large scale and complex folds of very irregular type in the adjacent rocks. No signs of an aureole were detected adjacent to them. However, several kilometres west of the Brechen gneiss, a small band of pelitic schist, in the west
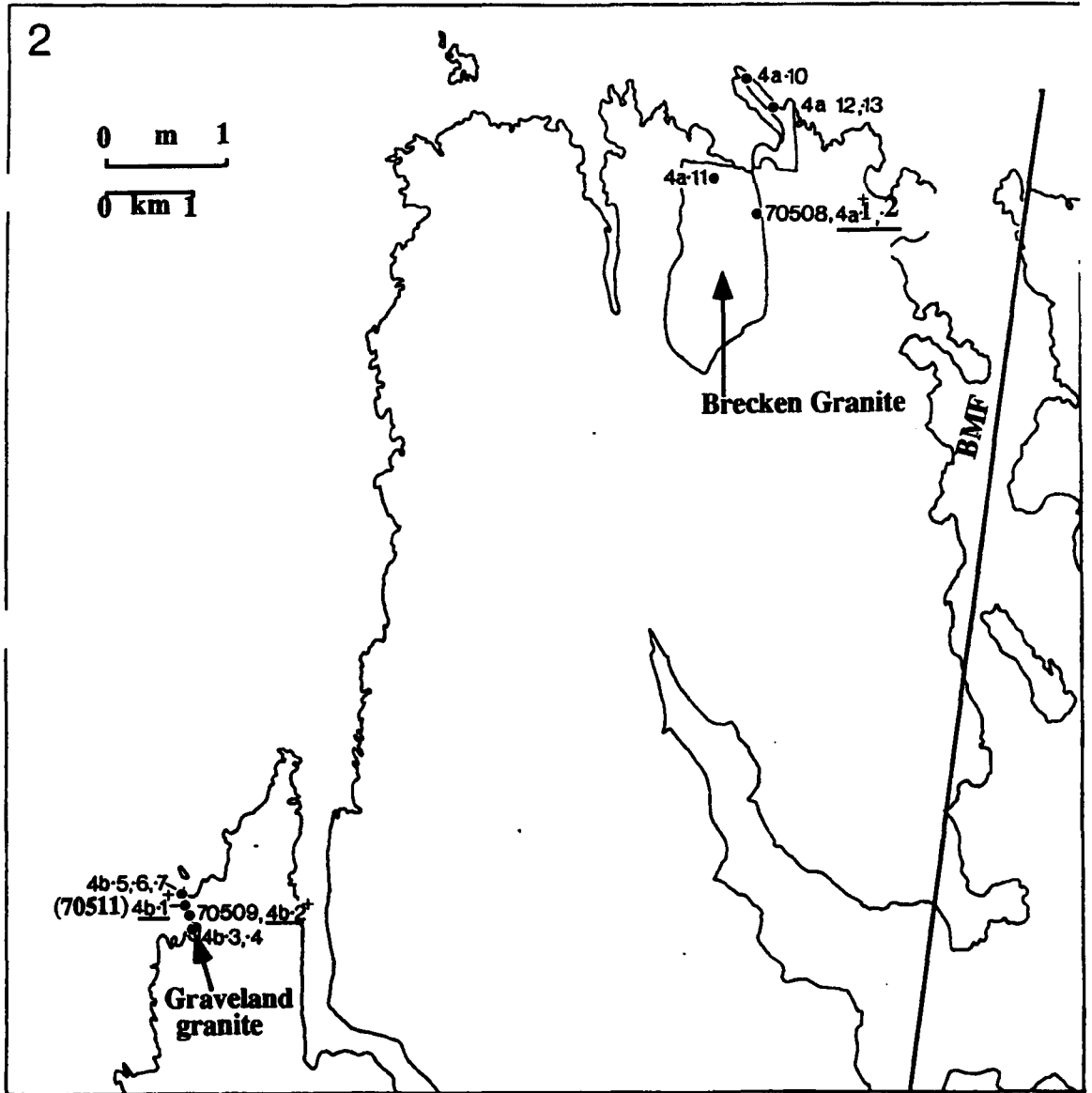
Figure 3.5. Map showing locations of granites and samples of the Brecken and Graveland granites. Underlined samples analysed by XRF and (+) by INAA.
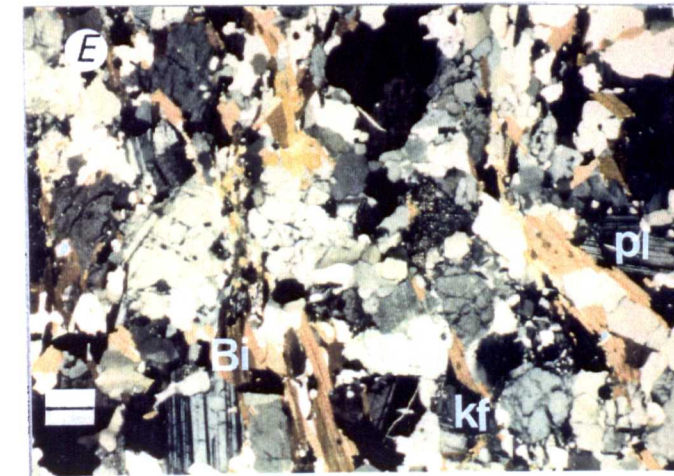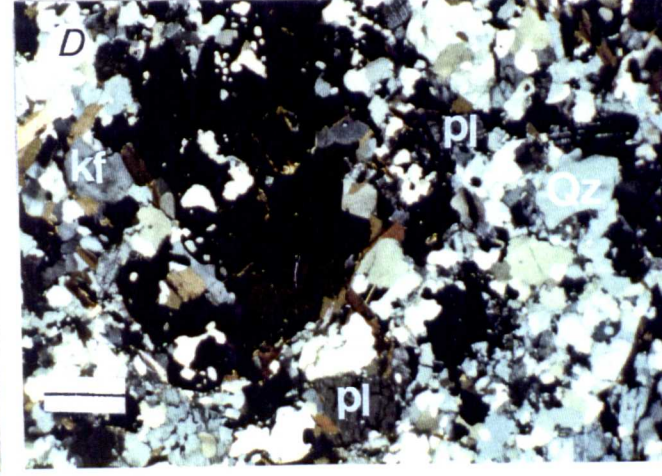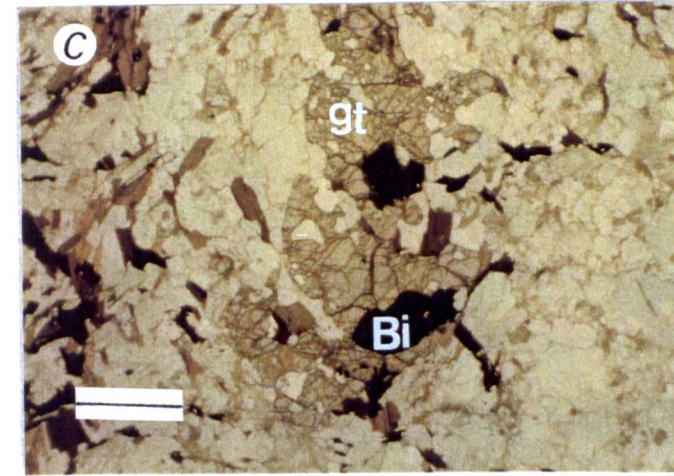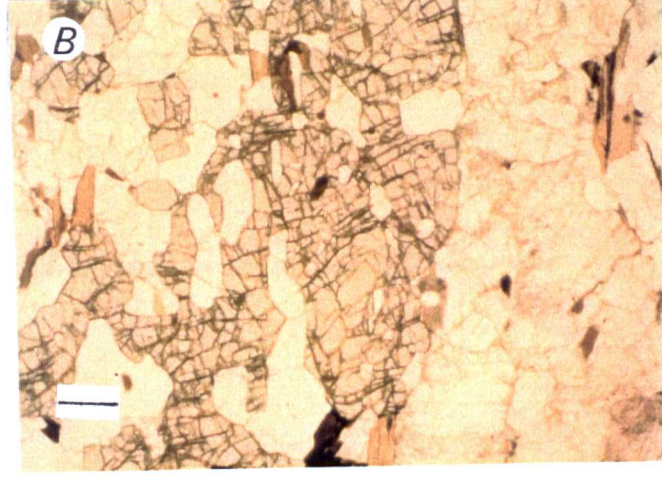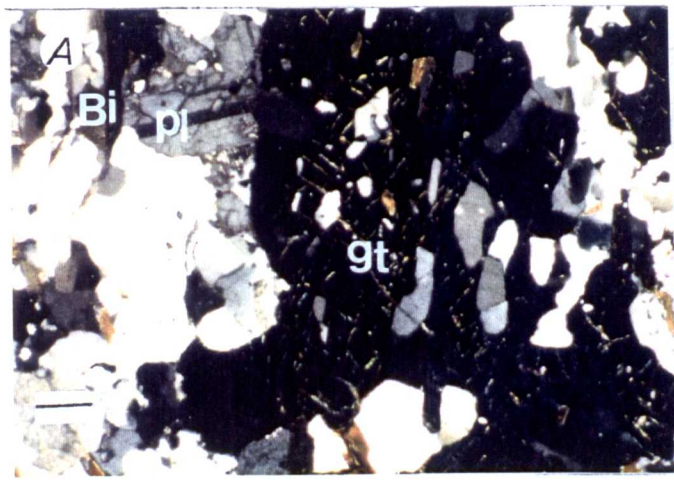
Plate 3.4. **A.** Garnet megacryst (gt) in Brecken granite, part of it altered into biotite and quartz; twinned plagioclase (pl) and biotite (Bi) (scale bar, 0.5 mm). **B.** The same section under PPL (scale bar, 0.5 mm). **C and D.** under X nicols and Plain PL showing the break down of garnet into reddish biotite (Bi) and quartz (Qz) (scale bar, 0.5 mm). **E and F.** Showing allotriomorphic texture and plagioclase twinning on the albite law is very common, note that Brecken plagioclase (pl) have a strange dusty appearance and are cracked (scale bar, 0.5 mm).

cliffs of Yell, contains many kyanite pseudomorphs of chiastolite which are easily visible in the field. The chiastolite must have formed as the result of thermal metamorphism of the Moine sediments prior to the regional metamorphism, possibly due to an intrusion of granite of the type forming the protolith of the Brecken and Graveland gneisses, which now lies beneath the sea immediately west of the cliffs. No other rocks are known to occur which could have produced this effect.

3.3.9 Petrology of Brecken Granite.

There are two exposures of Brecken granite, one situated in the west of Yell on the Graveland coast, which are geographically separated from each other. One will be called **Graveland granite b.** (Fig 3.5). The other granite will be called **Brecken granite a.** (Fig 3.5), occurring in the north of Yell (mineral constituents of both groups are listed in the appendix 2).

The Brechen Granite a. is characterized by an allotriomorphic texture (plate 3.4E) and is mainly composed of plagioclase (occasionally zoned), microcline phenocrysts, quartz, biotite, garnet and muscovite and very rare chlorite. Plagioclases occur singly and are seldom seen as composite grains. Twinning on the albite law is common, most Brecken granite plagioclases have a strange dusty appearance and are cracked (plate 3.4E & F), whereas the K-feldspar is clear. K-feldspar is microcline and has highly irregular outlines, filling interstitial areas between other minerals. Most of them show microcline cross-hatched twinning with that on the carlsbad twins law being less common. Quartz is interstitial to all the other minerals, the grain size of quartz is greatly reduced and has serrated or scalloped margins resulting from grain boundary migration indicating tectonic events to which Brecken granite has been exposed after its emplacement. Biotite occurs as anhedral plates which are usually clotted together, strong pleochroism is displayed from brown-black to pale yellow. Biotite commonly encloses apatite and zircon. Muscovite is colourless anhedral plates and occurs along with biotite, sometimes the plates are strongly aligned resulting in a good foliation in the rock.
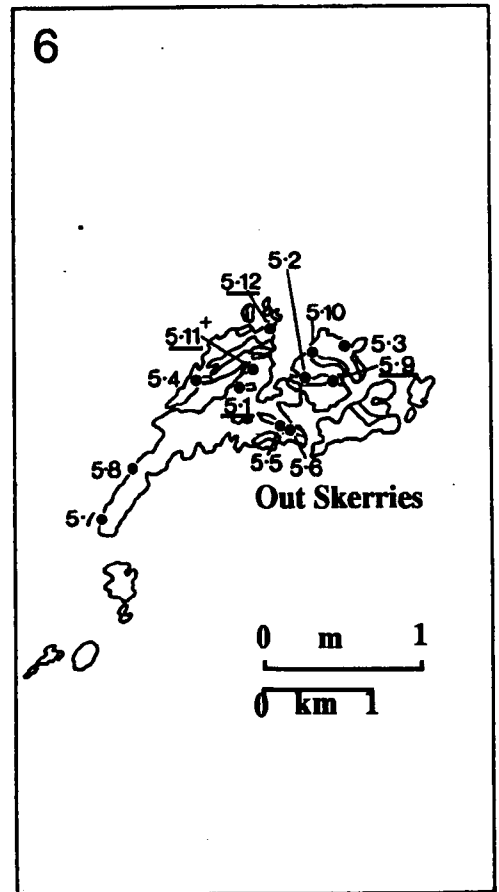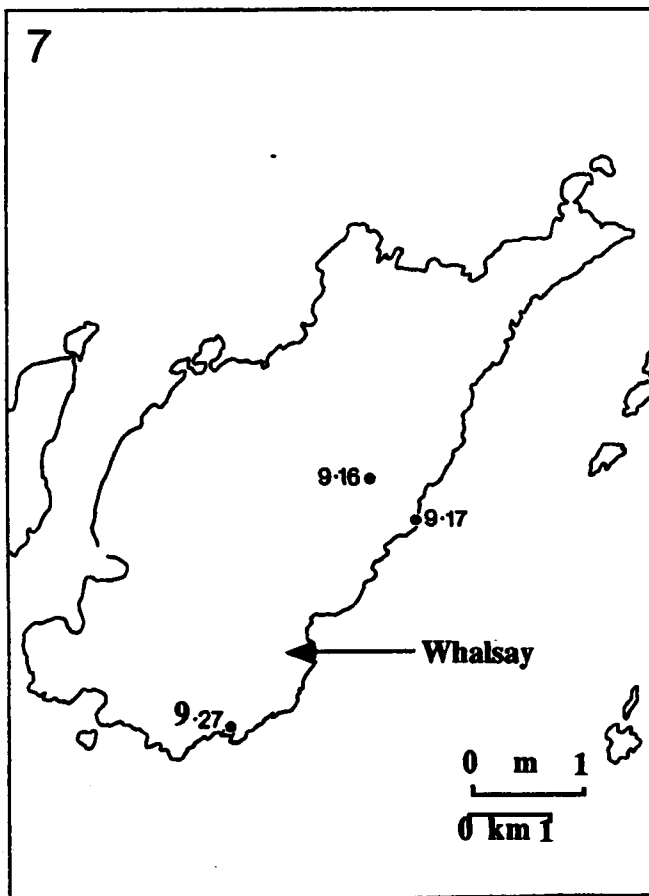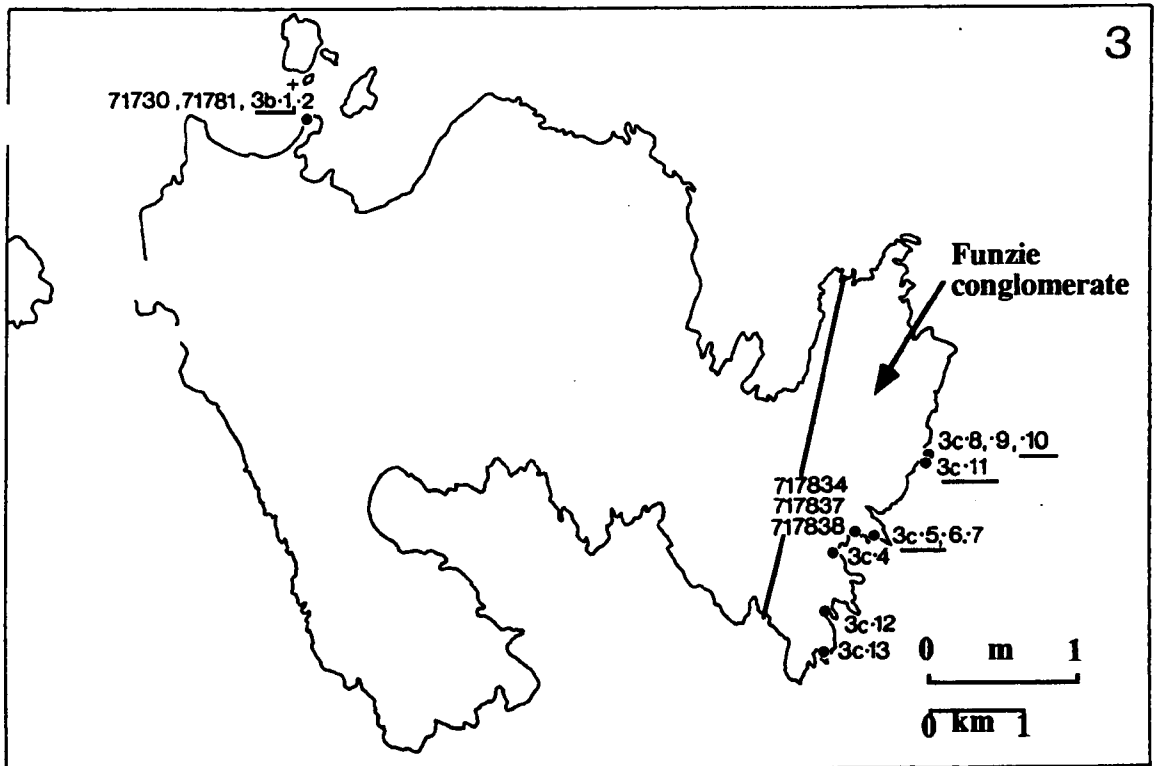
Figure 3.6. Map 3, 6 & 7 showing locations of granites and samples of Funzie conglomerate, Out Skeries granite and Whalsay granite. Underlined samples analysed by XRF and (+) by INAA.

Garnet megacrysts occur in appreciable amounts, part of them altered into biotite and quartz (plate 3.4A & D). Accessory minerals are few and include amounts of metamict allanite, sphene, apatite (most abundant accessory mineral) and zircon. **The Graveland granite b.** consists of plagioclase, K-feldspar, quartz, biotite and muscovite. The Graveland granite b. differ from Brecken granite a. in containing no garnet. K-feldspar is microcline and large plagioclase phenocrysts occur. It seems to be more calcic on the basis that calcic plagioclases show characteristic broad lamellae albite twinning. The cracked dusty appearance of plagioclase of the **Brecken granite a.** does not appear here. Secondary chlorite is more common in b. than a. Accessory minerals are allanite, apatite and zircon.

3.3.10 The Out Skerries Granite

The Out Skerries granite occurs in the Out Skerries Isles to the North east of Whalasay Isle and south of Fetlar Isle. They are a small group of Islands (Figure 3.6).

3.3.11 Geological Setting.

Flinn in Mykura (1976) reported that the rocks of the Out Skeries have been invaded by pegmatite and granite veins and ribs, some of which are several hundred meters long. The edge of a somewhat larger granite intrusion occurs in the extreme north of the group of Islands. Flinn (personal comunication) has made a detailed map of Out Skerries which shows a clear-cut relationship of the invaded granite veins and ribs to the different country rocks.

3.3.12 Petrology of Out Skerries Granite.

The constituent minerals of Out Skerries granite (mineral constituents are listed in appendix 2) are plagioclase, K-feldspar megacrysts, quartz, biotite and muscovite. Plagioclase occurs as euhedral to subhedral crystals, the zoning is normal and common; crystals which show zoning have altered cores (plate 3.5E & F). Twinning on the albite law is very common. K-feldspar forms anhedral
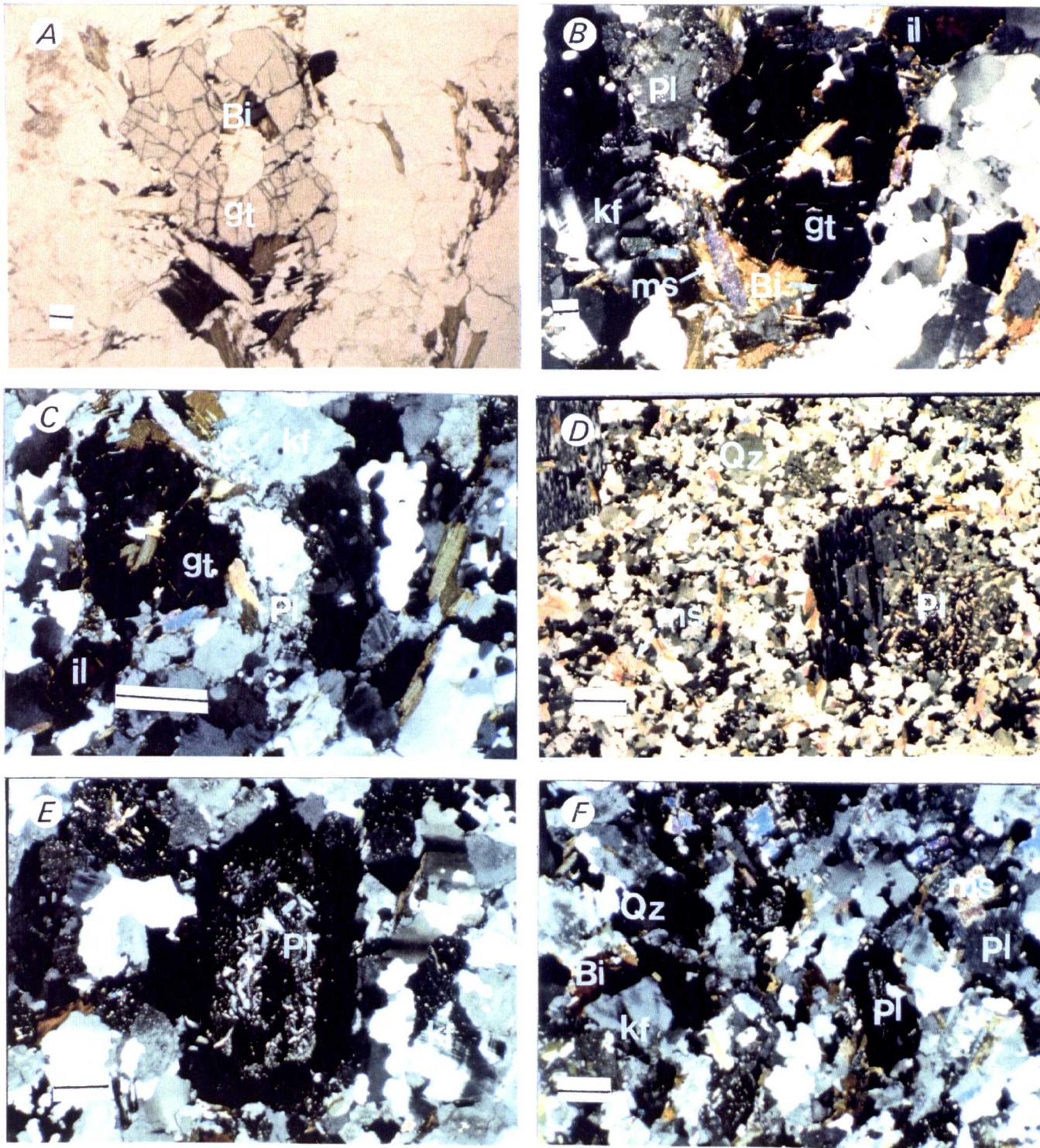
Plate 3.5. **A.** Garnet crystal (gt) in Tonga granite breaking down into biotite (Bi) and quartz (scale bar, 0.5 mm). **B.** The same section under X nicols showing mineralogical composition; plagioclase (Pl), K-feldspar (kf), biotite (Bi), muscovite (ms), garnet (gt) and quartz (Qz) and accessory mineral ilmenite (il) (scale bar, 0.5 mm). **C.** Showing alltriomorphic texture in Tonga granite (scale bar, 0.5 mm). **D.** plagioclase phenocryst, mostly albite (Pl) in a fine grained quartz(Qz), plagioclase and muscovite (ms) groundmass in Cunningsburgh granite,which show complex twin pattern something like that chess-board albite (scale bar, 0.5 mm). **E and F.** Shows euhedral plagioclase (Pl) normal zoning with altered cores in the Out Skeries granite, microcline K-feldspar (kf), quartz (Qz), biotite (Bi) and muscovite (ms) (scale bar, 0.5 mm).
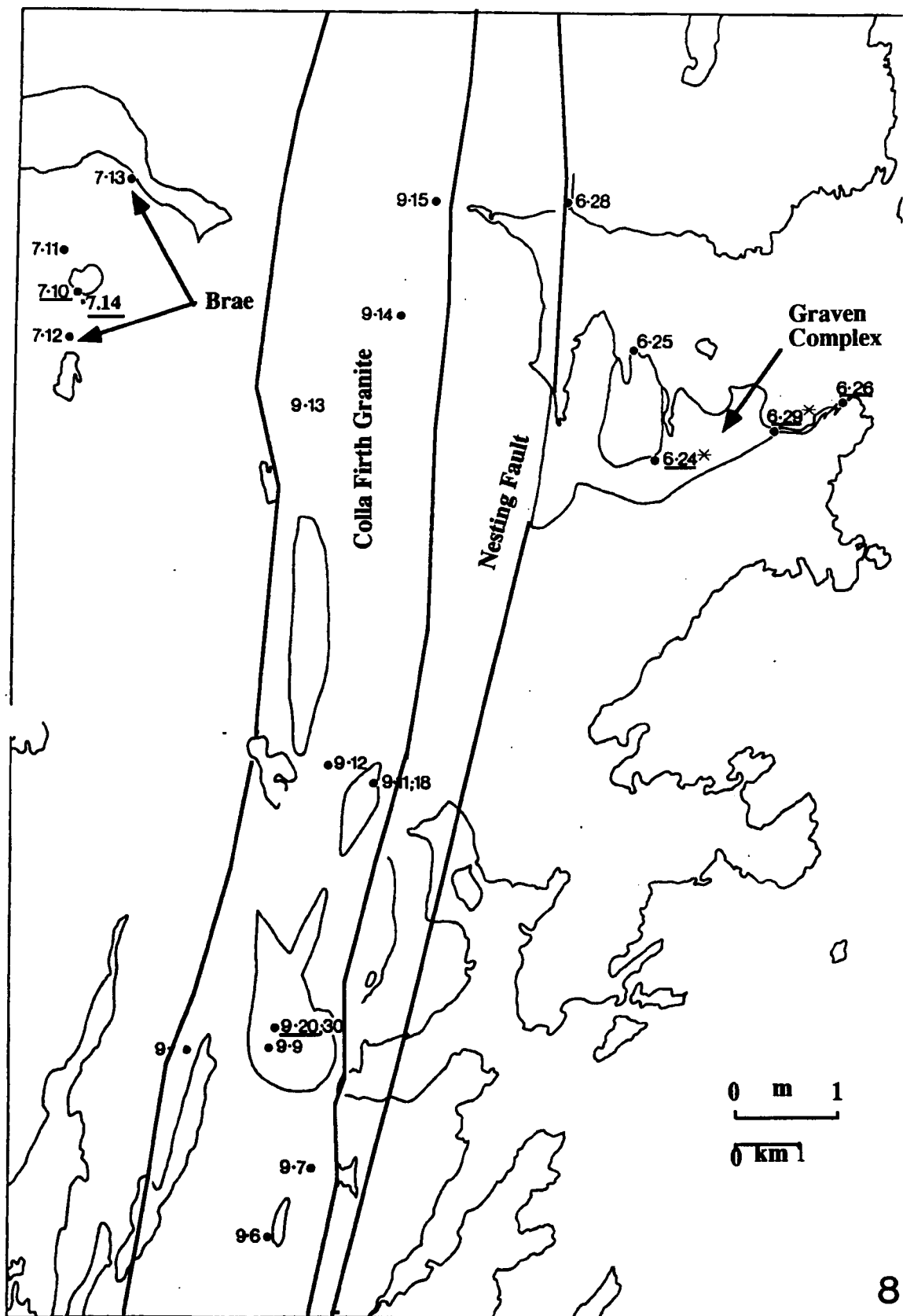
Figure 3.7. Map 8 showing locations of granites and samples from the rest of Graven and Brae granitoid and from Colla Firth granite. (—) analysed samples by XRF and (*) REE analyses.

Figure 3.8. Map 10 showing locations of granites and samples of Hildasay granite,
Colla Firth granite, Rova Head conglomerate, Cunningsburgh granite
and albite-keratophyre. (——) analysed samples by XRF, (+) INAA and (*)
REE analyses.

microcline crystals, interstitial to the other minerals and contain small euhedral plagioclase crystals as inclusions and occasionally small euhedral zircons. Quartz is anhedral and interstitial to all other minerals, boundaries between large crystals tend to be irregular and interlocking lobate. Biotite occurs as anhedral plates which are usually clotted together in groups along with muscovite, sometimes the plates are strongly aligned resulting in a good foliation in the rock as it in the Colla Firth granite. A strong pleochroism is displayed, varying from brown black to pale yellow. Biotite commonly encloses numerous small crystals of apatite, zircon and ilmenite.

3.3.13 Granitic Associated With Colla Firth Permeation Belt.

The Colla Firth Permeation belt lies in the south-east of the Delting area, running parallel to general strike of the rocks (Figs. 3.7 & 3.8). The belt is up to 2.5 Km wide and can be traced from Swining Voe in Delting southwards to south of Burra, a distance of 43 Km. Its extension on the east side of the Nesting fault passes through Nesting and extends from Cat Firth to Stava Ness.

3.3.14 Geological Setting.

An early paper by Flinn (1954) recognized a migmatic gneiss, termed the Colla Firth permeation belt as a localized phase of recrystallization following the regional metamorphism. Around and within this belt, the country rocks have suffered a thermal metamorphism, which may be regarded as a contact effect of the permeation process, and which produced sillimanite, andalusite and shimmer aggregate (composed almost entirely of sericite) in the pelitic rocks, and clinopyroxene & microcline in the calcareous rocks. The permeated rock of the Colla Firth belt are not confined to an area of high grade regional metamorphism. The field relations suggest that the regional metamorphism and the permeation were independent processes at the present level of exposure. The problem of their relations, and the length of the time interval separating them have been discussed by Flinn and

interpreted as follows: Permeation took place after the regional metamorphism and under conditions sufficiently different from those prevailing during the regional metamorphism for the more reactive rock types in the belt of permeation to develop new minerals. This conclusion was based on the observation that thermal metamorphism associated with the permeation was superimposed on the tectonic fabric of the regional metamorphic rocks, and was stronger in the areas in which garnet had developed in the regional metamorphic rocks, than in areas where it had not developed. Thus the permeation must be later than the tectonizing metamorphism.

Along its eastern boundary and extending up to half Km beyond the last signs of permeation is a zone of intrusive granite and pegmatite rocks. Deformed veins of granitic, pegmatite and quartz-tourmaline rock are very abundant within and just outside the migmatite belt, most of the granite veins are concordant sheets and lenses with sharp margins against the gneiss, but cross-cutting veins are also common. The largest granite mass has a maximum thickness of 500 m and extends for 6.5 Km along the strike. Many of the concordant sheets are boudinaged and most have marked schistosity which is parallel to, and continous with, the regional foliation. The cross-cutting veins have been folded by buckling.

Flinn and Pringle (1976), have made an age determination for the aplo-granite intrusive veins associated with Colla Firth permeation belt. A Rb-Sr age of 530 Ma was obtained.

3.3.15 Petrology of Colla Firth Granite Veins.

The Colla Firth granite is characterized by allotriomorphic texture and the constituent minerals (listed in appendix 2) are plagioclase, K-feldspar megacrysts, biotite, garnet and muscovite. Plagioclase occurs as anhedral crystals, twinning on the albite law is very common while that on the pericline law is less so. Plagioclase is free of inclusions, but occasionally small euhedral apatite crystals occur;
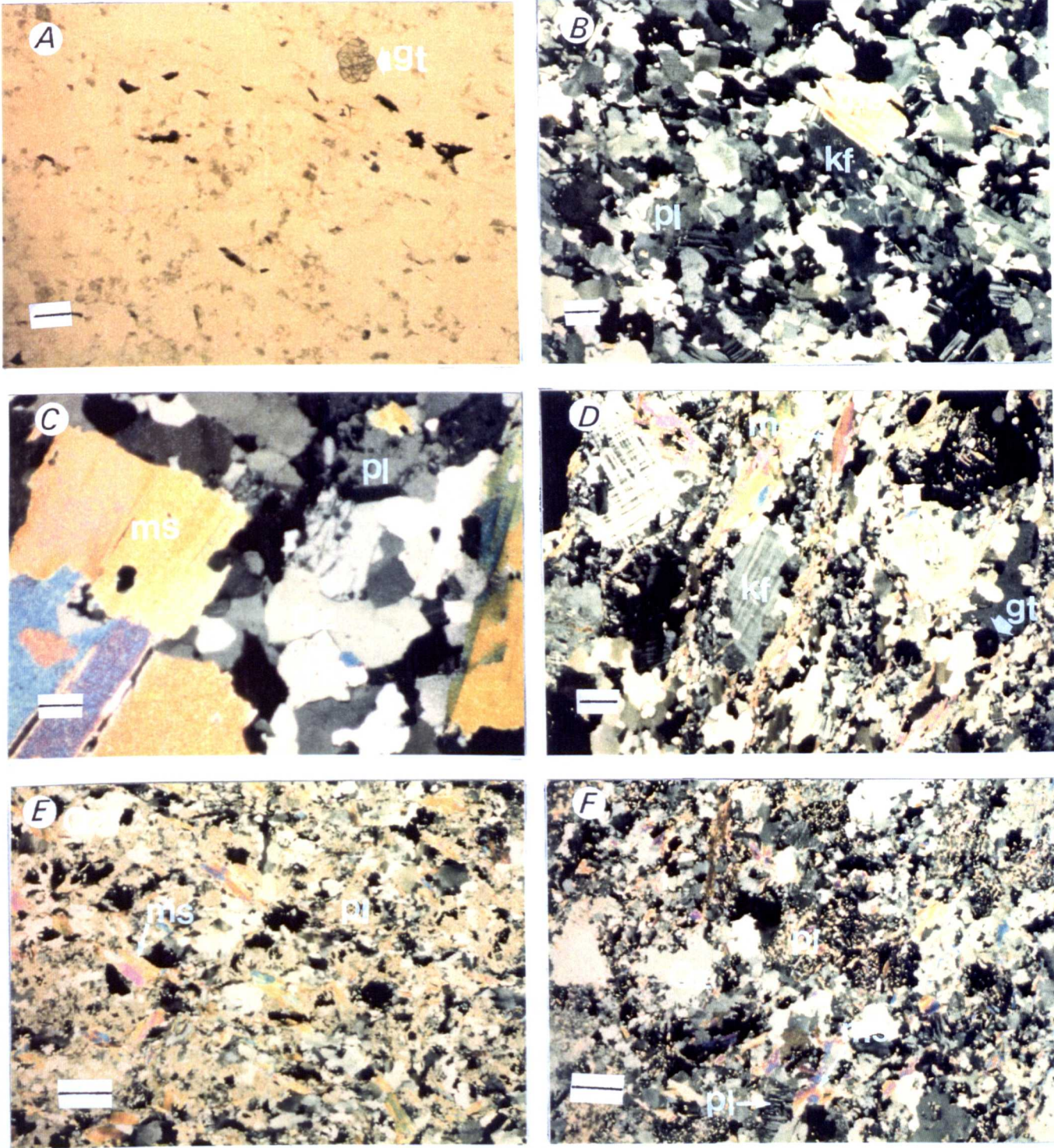
Plate 3.6. **A.** Thin section under PPL showing garnet crystal (gt) in Colla Firth granite (scale bar, 0.5 mm). **B.** The same thin section under X nicols showing the allotriomorphic texture, plagioclase (pl), K-feldspar (kf) and muscovite (ms) (scale bar, 0.5 mm). **C and D.** Showing strongly aligned abundant moscovites (ms), microcline K-feldspar (kf) near extinction showing faint microcline cross twinning, turbid plagioclase (pl) in C, quartz (Qz) and garnet (gt) (scale, bar, 0.5 mm). **E and F.** Showing allotriomorphic texture in Channerwick granite and the constituent minerals are plagioclase (pl) mostly albite, muscovite (ms) and quartz (Qz). Note that the plagioclase is mostly altered.

zoning very rare. K-feldspar is microcline with cross-hatching twinning (plate 3.6D). It is seen to have highly irregular outlines, filling interstitial areas between the other minerals. Quartz is generally interstitial to all other minerals. It seems from the serrated or scalloped margins and greatly reduced grain size of quartz that grain boundary migration has taken place. Biotite is less abundant than muscovite (plate 3.6C) and both are strongly aligned resulting in a good foliation in the rock. Garnet occurs as many small grains (plate 3.6A & B), in contrast with the few large garnet in the Tonga and Brecken granites. Chlorite exists in a small quantity as alteration of biotite. Accessory minerals are apatite and ilmenite.

3.3.16 Channerwick Granite.

The Channerwick granite consist of a number of inter-connected sill-like bodies up to 25 m thick (Flinn in Mykura,1976), which are exposed close to the main road at Channerwick, 18 Km S.S.W. of Lerwick (Figure 3.3).

3.3.17 Geological Setting.

Flinn (1967), has shown that the Channerwick granite has a very small outcrop with a form reminiscent of a cedar tree laccolith. In hand specimen it appears to be rather altered. It is composed of albite, muscovite, and quartz. The Channerwick granite intrude the Clift Hill series (fig. 10.1). The eastern part of the aureole of the granite is made visible in the field by the presence of white and dark spots in the Dunrossness phyllite to the east of the granite. The dark spots are shimmer aggregates. Thin sections show both types of spots crystallized after the tectonizing metamorphism. No relics of the minerals which originally formed the spots were found. Knox (1936), considered the shimmer aggregates to be after andalusite, the hornfelsed rocks contain no biotite, but much pale chlorite, which looks as if it is retrogressive after biotite. The chloritoid in the Dunrossness phyllites near to the aureole in the Channerwick area is of recrystallized type. The Dunrossness phyllites are much more sensitive to the thermal metamorphism than the Clift Hills phyllites, so it is possible that the recrystallization of this chloritoid is

one of the thermal effects of the Channerwick granite.

The Channerwick granite has a tiny exposure but a remarkable thermal effect or contact aureole with a diameter of about 900 m. Miller and Flinn (1966) used the K-Ar age method for muscovite from the Channerwick granite and obtained an age of 399 ± 8 Ma .

3.3.18 Petrology of Channerwick Granite.

The Channerwick granite has an allotriomorphic texture (plate 3.6E) and the constituent minerals (mineral are listed in appendix 2) are albite, muscovite and quartz. Albite occurs in two types, one show normal polysynthetic twinning, though rather broad for albite. The other has a much more complex twin pattern (plate 3.6F), something like that of chess-board albite (Flinn,1967). The muscovite occur in two types, one normal and the other cloudy in thin-section but yellow in hand specimen. The muscovite appears to be late and the first mentioned type of albite contains much coarse sericite. The finer grained specemens show gradation towards the associated quartz-porphyry sheets, though the latter contain some microcline (Flinn 1967). The microphotograph available here of Channerwick granite (plate 3.6E & F), shows that the albite is intensively altered to sericite. No accessory minerals were recorded in the available samples.

3.3.19 Cunningsburgh Granite.

The Cunningsburgh Granite occurs to the south of Lerwick and NE of Channerwick (Figure 3.8).

3.3.20 Geological Setting.

The Cunnigsburgh Granite is accessible only in one tiny exposure (fig.11.1). In thin section it is very similar to the Channerwick granite (Flinn 1967). In spite of its tiny exposure it had a considerable effect on the country rocks which are thermally metamorphosed pelitic Dunrossness phyllites. Most of the Cunningsburgh aureole is composed of mimetically recrystallized muscovite - green

chlorite schists with cross-cutting porphyroblasts of staurolite. In exposures very close to the granite, biotite occurs instead of the green chlorite and there are a few shimmer aggregates which may represent the beginning of the andalusite zone (Flinn 1976). The Cunningsburgh granite is even smaller than the Channerwick granite, but as it intrudes the Dunrossness phyllites, which are very sensitive to thermal metamorphism, its aureole is extensive and consists of an inner zone in containing porphyroblasts of staurolite, a middle zone in which chloritoid has partially replaced staurolite and an outer zone of completely recrystallized chloritoid (Mykura 1976).

Flinn (1966), pointed out that a series of quartz-porphyry sheets occur in the area between Cunningsburgh and Channerwick grarnites and that they are probably associated with Channerwick and Cunningsburgh granites.

3.3.21 Petrology Of Cunningsburgh Granite.

The Cunningsburgh granite has an allotriomorphic texture and the constituent minerals (listed in appendix 2) are the same as in Channerwick granite consisting of albite, muscovite and quartz. Albite varying in size from small altered crystals, up to phenocrysts which show a complex twin pattern something like chess-board albite. The muscovite occurs in both normal and cloudy forms in thin-section (plate 3.5D), but yellow in hand specemens. Accessory minerals are the same as in Channerwick granite.

3.3.22 Albite-Keratophyre.

The albite-keratophyre occurs as a small exposure on the coast of southeast Shetland in the Cunnigsburgh area. It occurs as a small mass and as tiny veins in metavolcanic rocks associated with komatiitic serpintenites (Figure 3.8).

3.3.23 Geological Setting.

Flinn and Moffat (1985) described a series of komatiitic serpentinites providing evidence of composition and the presence of the spinifex texture, in the

Cunnigsburgh area. The ultramafic unit is associated with large masses of metamorphosed basic volcanic rock and contains rounded masses of hornblende metagabbro up to 10 m diameter. This ultramafic unit interdigitates to the east with an underlying layer of basic metavolcanic rocks whose protoliths are difficult to determine in the field. Occasional well weathered exposures show that these rocks include tuffs, agglomerates, lavas and pillow lavas. Minor amounts of metasediments occur especially at the junction with the ultramafic layer to the west. A very minor component of this layer is albite-keratophyre forming thin veins and more equant larger bodies.

3.3.24 Petrology of the Albite Keratophyre.

The albite-keratophyre is composed appoximately of 99 % albite and 1 % of quartz. The accessory mineral is pyrite.

3.4 Petrology of Shetland Granites to the West of the WBF and North of Bixter Voe.

3.4.1 Ronas Hill Granite.

The Ronas Hill Granite is the major component of the granitic Northmaven plutonic complex. Although faulted against the Old Red Sandstone lavas and tuffs of Eshaness and truncated to south and west by the sea, it occupies a land area of about 60 Km^2 (Phemister 1979). Its outcrop is divided into two parts by the long fiord of Ronas Voe (Figure 3.9). The southern part on the Hillswick-Eshaness peninsula, forms a plateau of 100 to 120 m in elevation, in contrast, on the north side of Ronas Voe the northern part rises steeply to a general elevation of 210 to 250 m above which the broad summits of Ronas Hill; Roga Field and Collafirth Hill decline successively eastwards from 450 to 366 to 226m.

3.4.2 Geological Setting.

Many authors in the latter part of the 19 th century have described and discussed the
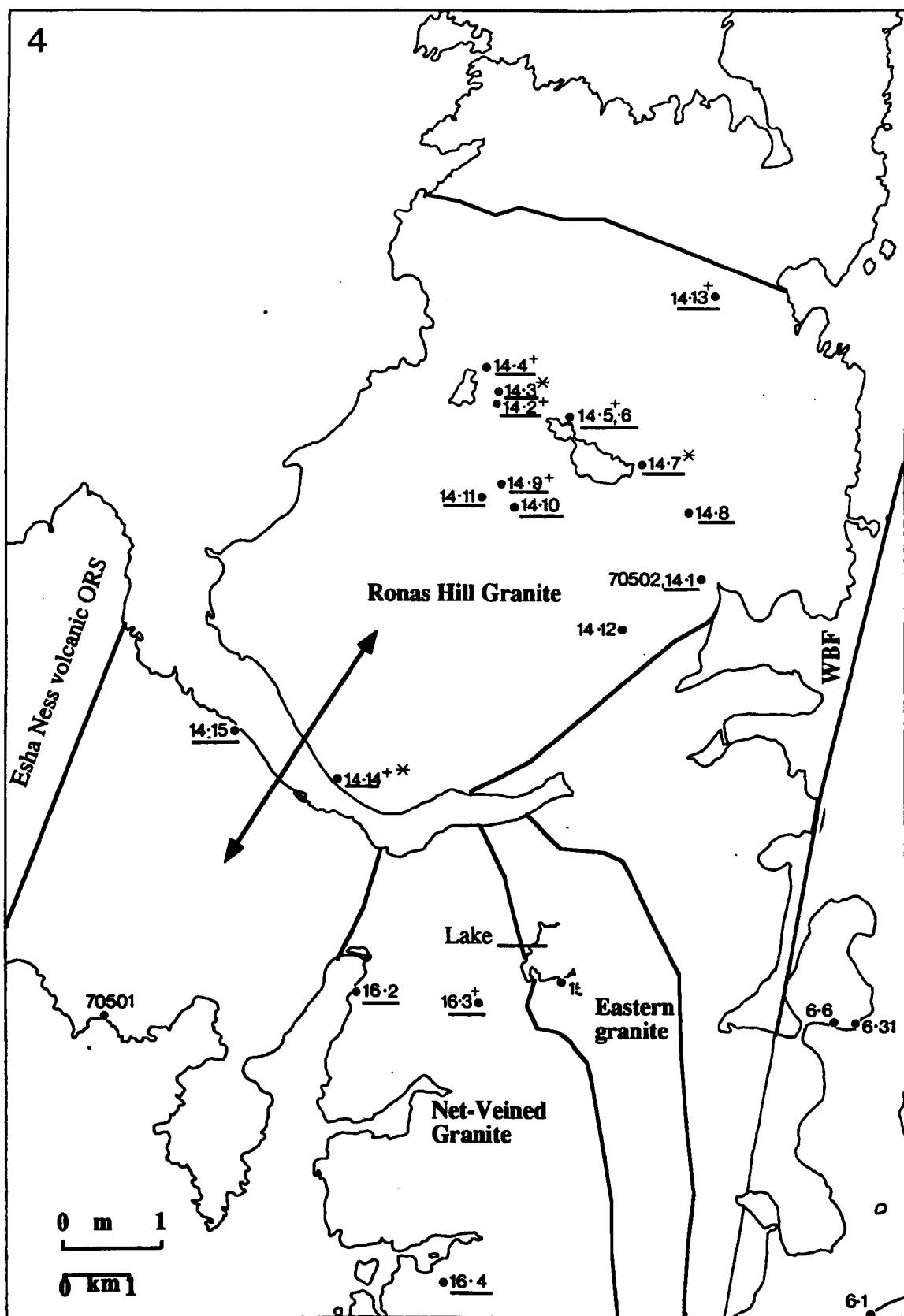
Figure 3.9. Map 4 showing locations of Granites and samples from Ronas Hill, Eastern and Net-Veined granites. Underlined samples analysed by XRF, samples with asterisk analysed for REE and samples with cross analysed by INAA.

intrusive complex of Northmaven area. For example Heddle (1879) insisted with reference to the neptunist / plutonist controversy, on the intrusive nature of the granites of western Shetland, and called attention to the importance, from the point of view of rock metamorphism, of the breccia with granitic matrix that crops out at the eastern margin of the granite at the Brig of Collafirth.

Peach and Horne (1879) in their study of the glaciation of Shetland, described the Ronas Hill Granite mass as a sheet intruded between the metamorphic basement and Old Red sandstone strata.

Peach and Horne (1884), based their account of the Old Red volcanic rocks of Shetland on the microscopical descriptions of acid and basic members and of dykes of the complex and chemical analysis of the granite and a basic dyke from localities on Ronas Voe.

Finlay (1930) made a comperhensive study of the Old Red Sandstone of Shetland. He includes a fuller petrographic description of the gabbro, diorite and granite components of the complex. He supported the view of Peach and Horne that the Ronas Hill granite is an intrusive sheet. He extended this hypothesis to include the basic and intermediate components as a gravitational differentiated lower member, and separated the dyke swarms into three series, comprising in order of decreasing age, lamprophyre, quartz-porphyries and very acid riebeckite-bearing granophyric dykes. The vertical disposition of the contacts of country rock with the Ronas Hill Granite, the occurrence of xenoliths of an amygdaloidal igneous rock at the margin of the granite in Collafirth, and the existence of a dyke-like intrusion in which a breccia of thermally altered country rock is cemented by granite in the Skelberry-Collafirth area has been noted by Wilson (1933).

Pringle (1970) carried out a recent study of the geological structure of the North Roe area and gives a condensed summary of the field relations and petrography of the components of the complex. In particular he identified the black micaceous mineral of the granite as stilpnomelane and distinguished biotite granite as a constituent part of the granitic mass. Pringle has found that the Ronas Hill
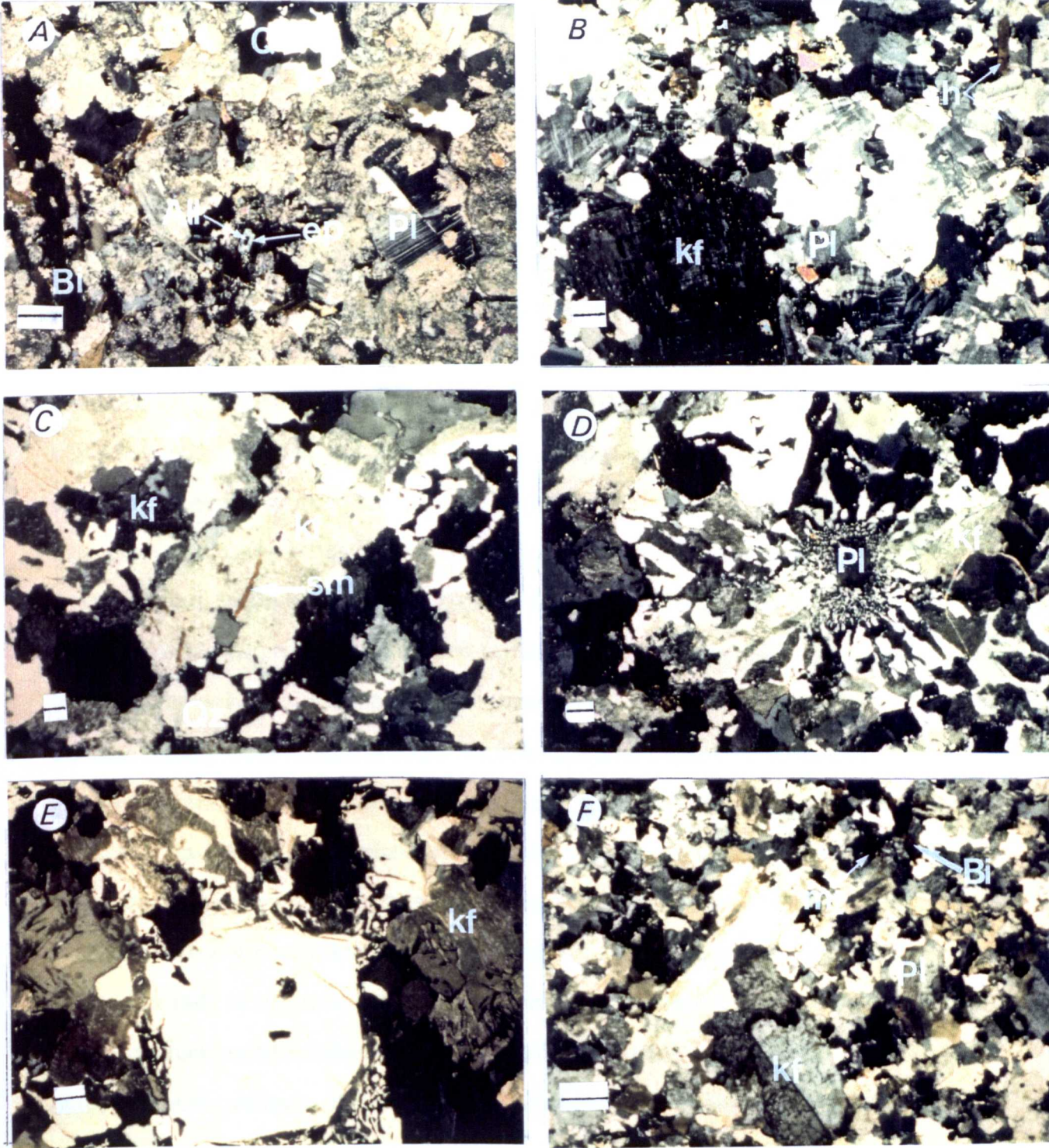
Plate 3.7. **A.** Highly altered plagioclase (Pl) in Brae tonalite, quartz (Qz), biotite (Bi), and biotite breaking down into epidote (ep) and euhedral allanite (All) enclosed by epidote (scale bar, 0.5 mm). **B.** Subhedral poikilitic K-feldspar (kf) in Spiggie monzonite, plagioclase, quartz (Qz) and accessory mineral sphene (sh) (scale bar, 0.5 mm). **C.** Showing the Ronas Hill perthite-granite and granophyre constituent minerals, K-feldspar as perthite (kf), quartz (Qz) and stilpnomelane (sm). (scale bar, 0.5 mm). **D and E.** Showing granophyric intergrowth between quartz and K-feldspar round a nucleus crystal (plagioclase in D and quartz in E) (scale bar, 0.5 mm). **F.** Constituent minerals in two feldspar biotite granite, plagioclase (Pl), K-feldspar (kf), biotite (Bi) and magnetite (mt) (scale, bar, 0.5 mm).

intrusion in the North Voe area is formed of approximately 40 Km^2 of drusy red granophyre, 1.5 Km^2 of biotite granophyre and 5 Km^2 of diorite and gabbroic xenoliths (fig. 14.2).The relationship of the Ronas Hill granite to the felsite dykes has been observed by Phillips (1926) and the special petrographical features of the dykes has been given.

Phemister et al (1950) have shown that the aegirine-riebeckite-bearing felsite dykes contain a higher percentage of iron than the granite, and the similarity in composition and petrology suggest that they are part of the same igneous episode. The higher iron content of the riebeckite-bearing felsites which are younger than the granite may be related to the occurrence of stilpnomelane associated with alteration of the feldspar in the granite and are presented as a concentration of iron in the later stages of the igneous episode. The junction of the Ronas Hill Granite with adjoining gneiss has been shown by Phemister to be sharp and steep everywhere and he believes that the intrusion of the granite was preceded by the formation of an arcuate zone fracture and brecciation, along part of which an early ring dyke was intruded. The main body of the magma then punched out a clean plug from the loosened country rocks within this zone. The K-Ar age determination of the biotite-granite member of the granitic mass has been recorded as 358 ± 8 Ma by Miller & Flinn (1966). The emplacement of granite has been suggested by **Phemister** to have been in three stages; two sheets or laccoliths followed by a stock, but the corresponding units can be delimited only appoximately for the sheets and conjecturally for the stock on the available evidence. The thermal alteration of the country rock can be studied only along the northern and north-eastern margins of the granite, the existence of the thermal aureole along the other sides is known.

3.4.3 Petrology of Ronas Hill Granite.

The present author supports the view of three lithological units comprising the Ronas Hill Granite (mineral constituents are listed in appendix 2) and defined by Phemister (1979). They are termed as follows **a) Perthite-granite and**

granophyre, forming the main granite massif and composed of chiefly a pink or red granitic rock with drusy and large cavities containing crystals of stilpnomelane, quartz and epidote. **b) Two feldspar-biotite granite** (plate 3.7F), a pink medium to fine-grained granite which crops out over an area about 2.5 km^2 between the Hevadale diorite and the northern of the Roerwater diorites. A few euhedral hornblende crystals are seen in thin-section. The same granite occurs in many localities within the main granite (Ronas Hill granite). **c) Altered granite** which is an unusual kind of alteration of granite to muscovite-chlorite rock, the altered rock resembles Cornish Peach but contain neither boron nor tin. A further subdivision into two groups has been made to the perthite granite and granophyre based on the pattern of the quartz-feldspar intergrowths. In one group the pattern is defined by the enclosure of small pieces of feldspar in quartz without regular arrangement. Since feldspar of this kind is dominantly perthite or antiperthite, this group is referred to as the perthite-granite (plate 3.7C), characterized by xenomorphic quartz and perthitic feldspar with a varying proportion of plagioclase prisms occurring as cores or shells to perthite. In the other group, the intergrowth is a micropegmatite with a regular pattern produced by enclosures of radial concentric or subparallel strips of feldspar in quartz, the two components of intergrowth being approximately equal in amount. The group has been termed granite granophyre (plate 3.7D & E). The group can be subdivided into granophyric granite and granophyre, in which the patterned intergrowth is respectively subordinate and dominant. **The perthite-granite and granophyre and two-feldspar biotite granite** of Ronas Hill contains alkali feldspar (brick-red with miarolitic cavities), plagioclase, quartz, hornblende and biotite. Secondary minerals are epidote, stilpnomelane, chlorite. Accessory minerals are very rare with ± allanite ± sphene ± zircon ± rutile ± iron ore.

3.4.4 <u>Eastern Granite.</u>

The Eastern Granite extends 14.5 Km from south of Mavis Grind northwards to Ronas Voe (Figures 3.9 & 3.2), over this length, the width varies from 1.6 Km near Eela water to 150 m between Busta Voe and Ellwick, thus having a dyke-like outcrop. It has been described by Finlay (1930) as a dyke. The form of the intrusion, however, is uncertain.

3.4.5 Geological Setting.

The eastern margin is near-vertical and appears to be controlled by the existence of an early dislocation parallel to the WBF zone. On its western margin the contact relations are entirely different (Mykura 1976). The contact with Mangaster net vein complex takes the form of a plexus of large and small sheets, dykes, and veins of granite in the diorite. The relationship indicates that the Eastern Granite was intruded by basic magma while still in a magmatic state and later it veined the consolidated basic rock before itself crystallizing (plate 3.10C & E) (M. P. Atherton, personal communication).

Mykura and Phemister (1976) have stated that the Eastern Granite throughout its extent from Busta Voe to the northern margin maintains the aspect of a pink to red leucogranite, some specimens of the rock are slightly cavernous; the small vacules may be druses, but in many cases seem to be due to loose interstitial aggregate. The Eastern Granite has been described by Phemister (1979) as a drusy and coarse grained red leucocratic granite. Quartz in large xenomorphic grains encloses irregular small pieces of perthitic feldspar. Prisms of zircon are abundant in magnetite-rich aggregates.

3.4.6 Petrology of the Eastern Granite.

The mineral constituents of the Eastern Granite are (listed in appendix 2) K-feldspar, plagioclase, quartz and biotite. K-feldspar is perthite, the pattern of the quartz-feldspar intergrowth is very similar to the quartz-feldspar intergrowth in the

Ronas Hill granite. The pattern is formed by the enclosure of small pieces of feldspar in quartz without regular arrangement. Since the feldspar of this kind is dominantly perthite, the group is referred to the perthite granite (plate 3.9C), characterized by xenomorphic quartz and perthite feldspar. Plagioclase prisms occur as cores or shells to perthite. In the other group, the intergrowth is a micropegmatite with a regular pattern produced by the enclosure of radial, concentric or subparallel strips of feldspar in quartz, the two components of intergrowth being approximately equal in amount. The group can be subdivided into granophyric granite and granophyre, in which the patterned intergrowth is respectively subordinate and dominant (plate 3.9E). Biotite is present in very small amount and displays a pleochroism ranging from dark brown to pale yellow. Secondary minerals are muscovite, chlorite and epidote. Accessory minerals are zircon and magnetite.

3.4.7 The Muckle Ossas Granite.

The Ossas Granite is exposed on two small rocky islets in the Atlantic Ocean about 2.4 Km west of Ockran Head. The larger, the Muckle Ossas, is 450 m long. The smaller, the Little Ossas, is 225 m long.

3.4.8 Geological Setting.

On the one-inch-to-one mile geological survey map of Northern Shetland this exposure is shown to be composed of a granite-diorite complex and granodiorite hybrid rocks. Eight specimens from the two islets have been studied by Phemister (1979). Macroscopically the rocks are composed of a matrix of anhedral cleaved red feldspar among which are set inconspicuous grains of quartz, numerous whitish prisms of plagioclase and microgranular groups of dark minerals. None of the specimens show foliation. Microscopically the rock of both islets is a biotite-pyroxene-granodiorite composed of plagioclase, quartz, micropegmatite, pyroxene and biotite with accessory abundant magnetite and apatite and scarce zircon. Large and small prisms of plagioclase are mantled, in some cases very thinly by turbid K-
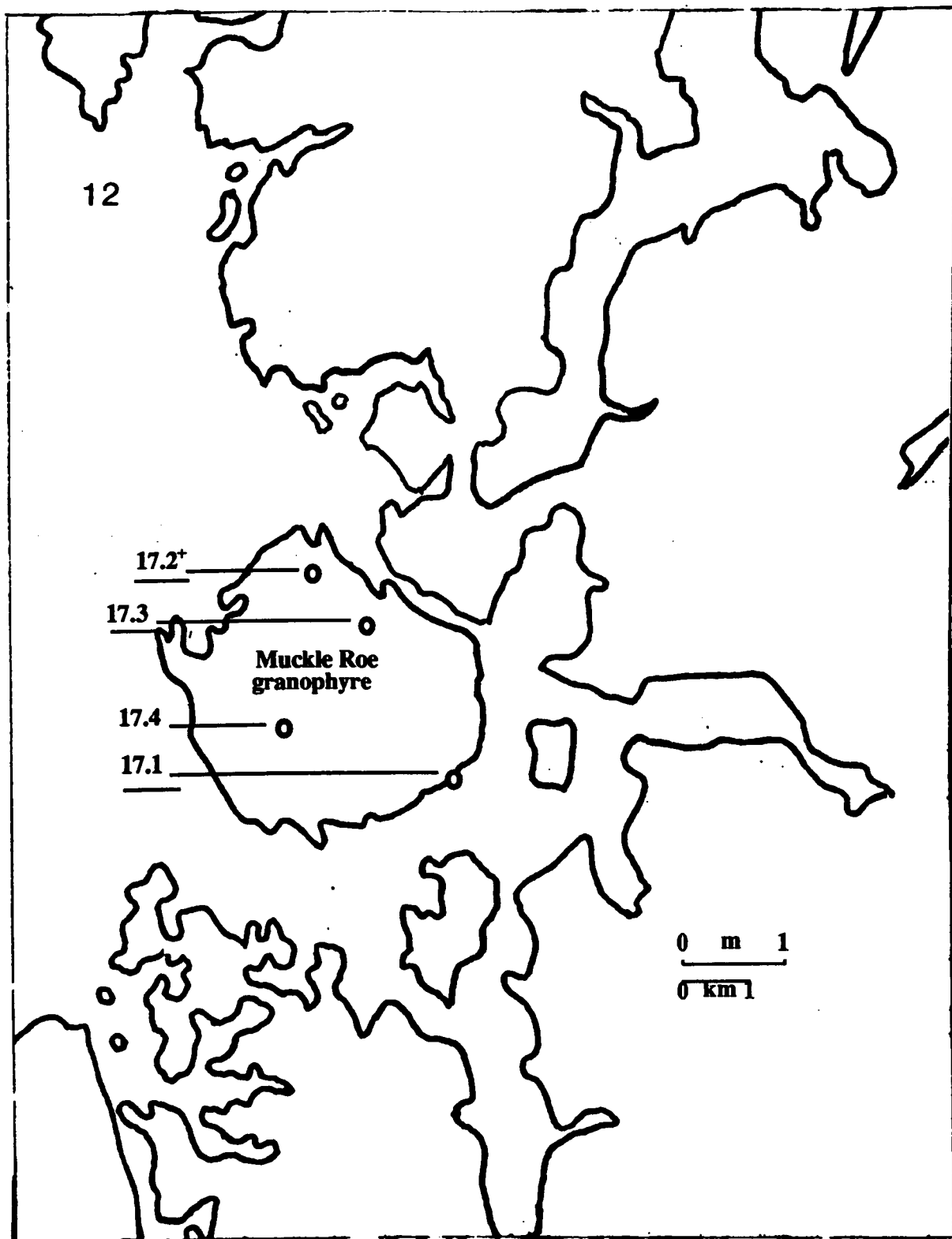
Figure 3.10. Map 12 showing location of Muckle Roe granophyre and samples.
(—) analysed by XRF and (+) INAA analyses.
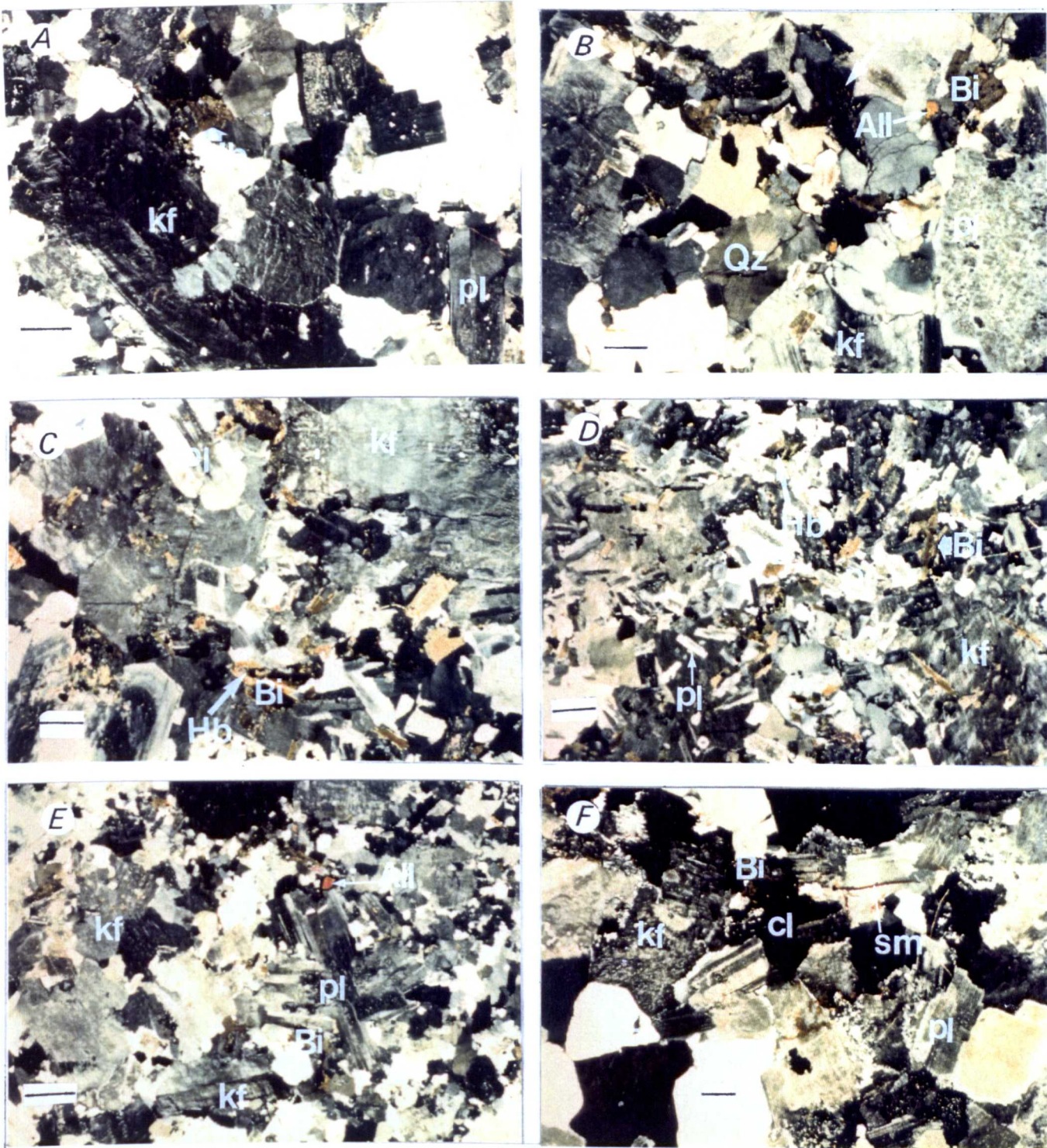
Plate 3.8. **A.** Poikilitic perthite K-feldspar (kf) in Bixter granite, euhedral plagioclase (pl), quartz (Qz) and hornblende (Hb) (scale bar, 0.5 mm). **B and C.** Showing mineral constituents in the Sandsting granodiorite and granite, plagioclase (pl), perthitic K-feldspar (kf), quartz (Qz), biotite (Bi), hornblende (Hb) and accessory mineral allanite (All) (scale bar, 0.5 mm). **D.** Poikilitic perthite K-feldspar (kf) in porphyritic microadamelite, small euhedral plagioclase (pl), biotite (Bi) and hornblende (Hb) (scale bar, 0.5 mm). **E.** phenocryst of plagioclase (pl) in the Sandsting coarse grained granite, perthitic K-feldspar (kf), biotite (Bi) and allanite (All) (scale bar, 0.5 mm). **F.** Constituent minerals of Vementry granite, plagioclase (pl), perthitic K-feldspar (kf), quartz (Qz), chlorite (cl) and stiplomelane (sm) (scale bar, 0.5 mm).
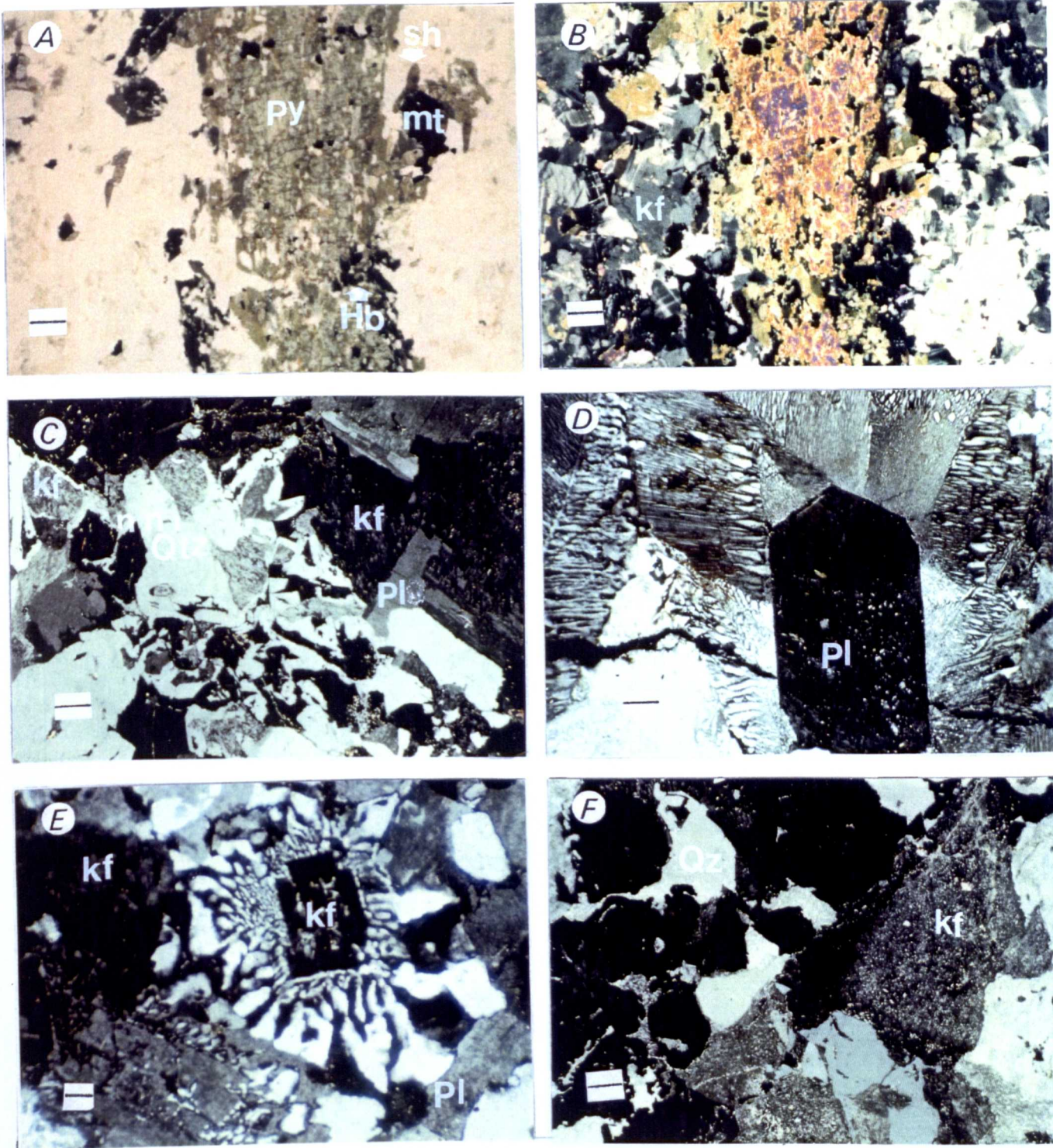
Plate 3.9. **A.** Aith-Spiggie monzonite under PPL showing prismatic pyroxene (Py), hornblende (Hb), sphene (sh) and magnetite (mt) (scale, bar, 0.5 mm). **B.** The same thin section under X nicols (scale bar, 0.5 mm). **C and E.** from Eastern granite showing the mineral constituents, plagioclase (Pl), K-feldspar (kf) and quartz (Qz) and the granophyric intergrowth between quartz and K-feldspar in E (scale bar, 0.5 mm). **D and F.** from Muckle Roe granophyre showing the typical granophyric intergrowth of quartz and K-feldspar in D and perthitic K-feldspar (kf) and quartz (Qz) in F (scale bar 0.5 mm).
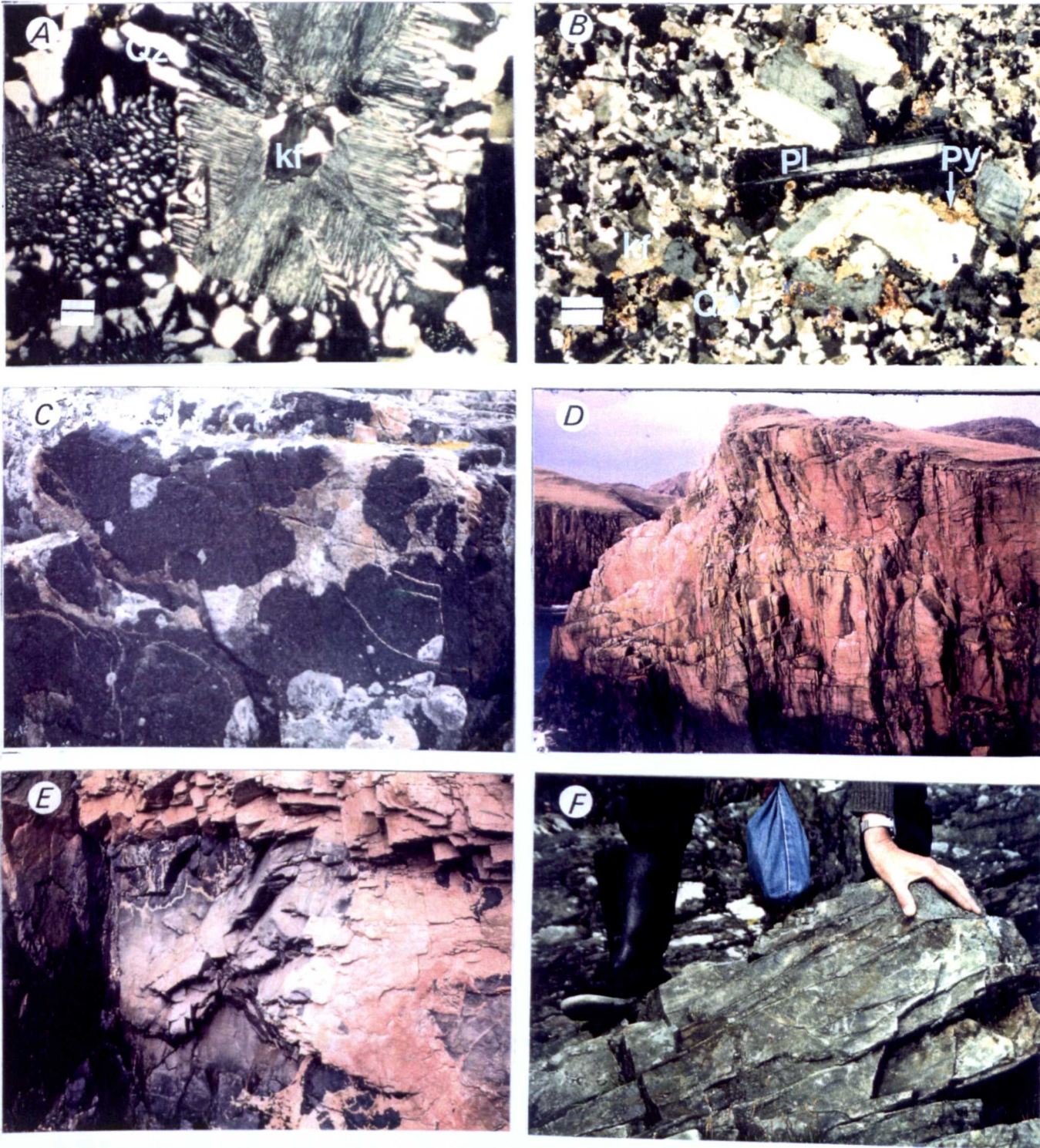
Plate 3. 10. **A.** Granophyric intergrowth between quartz (Qz) and K-feldspar (kf) in Net Veined granite (scale bar, 0.5 mm). **B.** The patchy plagioclase (Pl) in Muckle Ossas; K-feldspar (kf), quartz and pyroxene (scale bar, 0.5 mm). **C.** Showing the basic magma intruding the Eastern granite magma and later veining the consolidated basic rock. **D.** Shows the impressive coastal cliffs of Muckle Roe granophyre. **E.** Relationship between basic and acidic magmas in the Net Veined granite. **F.** Showing the Cunningsburgh albite Keratophyre tiny exposure.

feldspar which passes into micrographic intergrowth with the interstitial quartz. The
plagioclase is baordly zoned with core composition about An35-An40. Monoclinic
pyroxene occurs in two forms as stout colourless prisms, which interfer with all
felsic constituents and interlock with magnetite and apatite crystals, and as
aggregates of small grains which with black ore granules are cemented together by a
reddish amphibole. Apart from its unusual colour the mineral is a monoclinic
pyroxene similar to others from appinites and granodiorite hybrid rocks of the
Scottish lower Old Red Sandstone which, however, have the usual green to yellow
pleochroism; the high content of $Na_2 O$ is notable. Though the specimens from the
Ossas show evidence of hybrid composition in a patchy distribution of plagioclase
and pyroxene relative to micropegmatite, the product, as exemplified by the
available specimens, appears to be fairly homogeneous. In this respect it differs
from the randomly variable and local products of hybridisation in the main diorite, it
differs also from them in its pyroxene and granophyric character.

The granodiorite of Muckle Ossas is an intrusion and its emplacement was not
directly related to the emplacement of the North Roe granite. The absence of
foliation and stress effects, the geographical situation and the petrographical
character of the rock, nevertheless, justify its inclusion within the Old Red
Sandstone igneous province of western Shetland.

3.4.9 Petrology of Muckle Ossas granite.

The mineral constituents of Muckle Ossas rocks are (listed in appendix 2)
plagioclase, K-feldspar, pyroxene, hornblende and biotite. Plagioclase varying in
size from small to large prisms, in many cases thinly mantled with turbid K-
feldspar (plate 3.10B), which in some thin-sections passes into micrographic
intergrowth with interstitial quartz. The patchy plagioclase distribution which is
evidence of hybrid composition is very common (plate 3.10B). K-feldspar in the
form of microcline is found in one thin-section out of seven thin-sections available.
It is interstitial to all other minerals and present in very small amounts. Pyroxene

and hornblende co-exists together and some of euhedral hornbelende present in the core of pyroxene. Accessory minerals are apatite and magnetite.

3.4.10 Muckle Roe Granite.

The Muckle Roe granophyre forms the greater part of the Muckle Roe island. The granophyre forms a mass which, though its western and southern boundries are cut off by the sea, seems to have a roughly circular outline (Figure 3.10): 5 Km diameter.

3.4.11 Geological Setting.

Mykura (1976) pointed out that the Muckle Roe granophyre is closely jointed and gives rise to rugged topography with extensive inland scree slopes and impressive coastal cliffs. It is pink in colour with quartz blebs and feldspar cleavage planes are sometimes seen. Drusy cavities are common and some of these are lined with well-shaped quartz crystals. Drusy cavities containing more or less well terminated crystals of quartz are common and a black ferromagnesian mineral is a minor constituent present as shapeless clots, as reported by Mykura & Phemister (1976).

The cross-cutting relation to the gneiss and to the Mangaster net veined complex suggests that the mass is of stock form and of late date in the plutonic history of the district. Its intrusion is earlier than dykes of felsite, porphyrite, and basalt or dolerite by which it is cut. The shape of the low gravity anomaly over the granophyre, though incomplete, is consistent with its occurrence as a stock-form body of roughly circular-section and low density. It includes no member of the aegirine riebeckite minor intrusive group which is a feature of the complex north of Ronas Voe, but on the other hand includes two small outcrops of ultrabasic rock which is unrepresented to the north, but is similar to material in the Sandsting complex.

3.4.12 Petrology of Muckle Roe Granophyre

The present author confirmed the view that drusy cavities are abundant in Muckle

Roe granophyre and some of these are lined with well-shaped quartz crystals.

Drusy cavities containing more or less well terminated crystals of quartz are

common and black ferromagnesian mineral is a minor constituent present as

shapeless clots. K-feldspar is microperthite and the quartz-feldspar intergowth very

much like that in the perthite granite (plate 3.9D & F), and granite-granophyre of

Ronas Hill granite. The xenomorphic quartz and a varying porportion of

plagioclase prisms which occurs as cores or shells to perthite are a characteristic

feature of these rocks.

3.4.13 Vementry Granite.

The Vementry Granite crops out in the north-eastern part of the island of Vementry,

where it occupies an area of 0.85 Km^2 (Figure 3.11). Its outcrop may, however,

continue northward under Swarbacks Minn, possibly linking with the granophyre

of Muckle Roe.

3.4.14 Geological Setting.

Mykura (1976) pointed out that the Vementry Granite, which forms the Hill of

Muckle Ward consists of two lithological types, an outer coarse-grained pink

leucocratic quartz-rich granite with very low proportion of dark minerals and an

inner porphyritic granite composed of quartz and feldspar phenocrysts in a medium

to fine-grained rather darker matrix. Its boundary with the surrounding coarse

grained granite is not everywhere clearly defined and in one area there is a

transitional zone up to 90 m wide. The inner porphyritic granite is of particular

interest, in that it forms the focus of a large number of acid dykes which appear to

radiate from its centre. The junction with adjoining metamorphic rock is straight and

sharp and where seen it is inclined at 40° to 50° away from the granite. The

Vementry Granite and the adjoining metamorphic rocks are traversed by a number
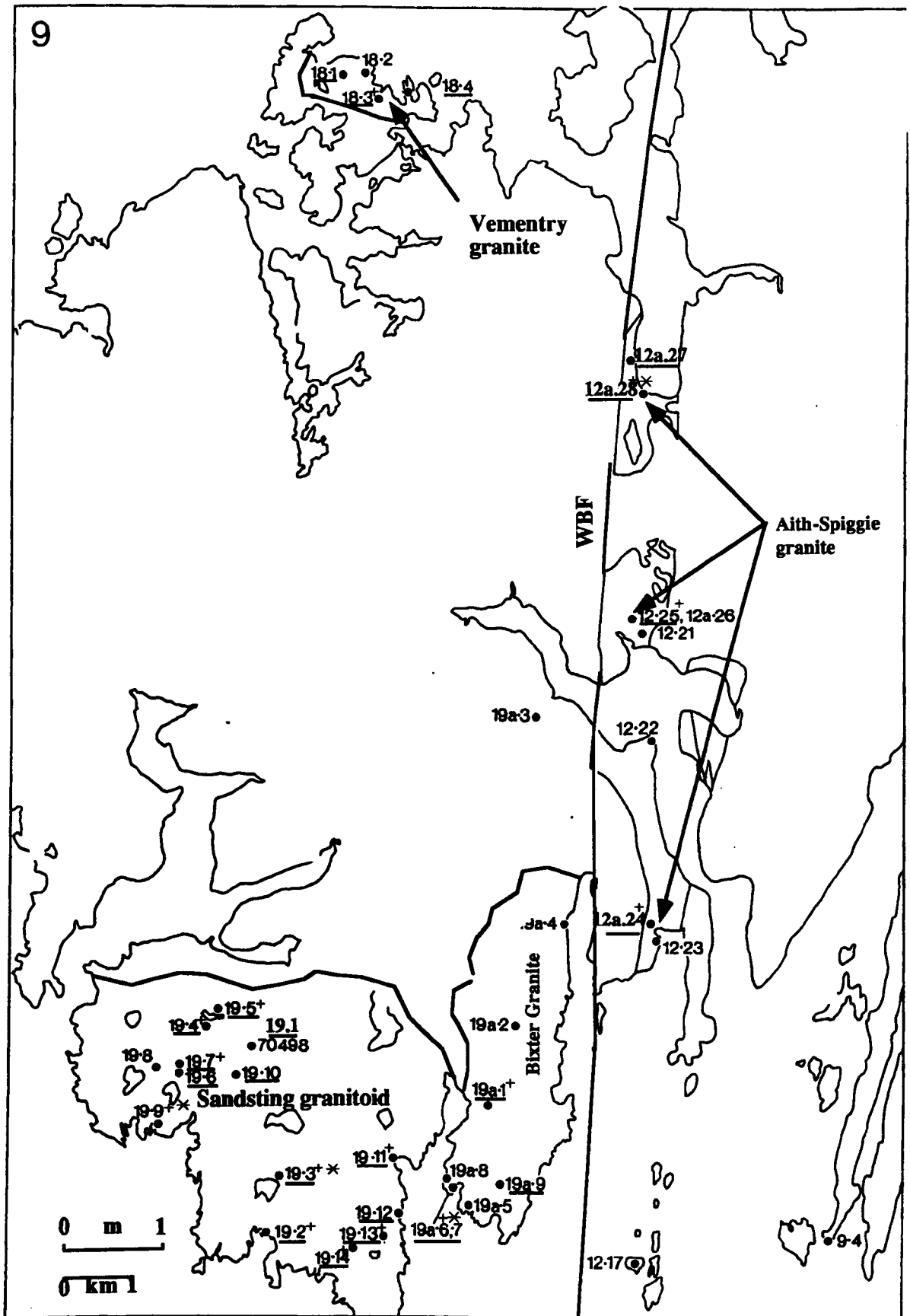
Figure 3.11. Map 9 showing locations of granites and samples of the Aith granite, Vementry granite, Bixter and Sandsting granites. (—) analysed samples by XRF, (+) INAA and (*) REE analyses.

of crush belts and the granite has strong joints, which give rise to strong linear depressions inland and deep geos along the coast (Mykura & Phemister 1976). In thin section it is composed of 70 % feldspar and 30 % quartz, and rutile is accessroy mineral of euhedral form. Finlay (1930 p.687) has recorded flourite in the granite, but this has not been confirmed. The inner porphyritic granite has a slightly higher proportion of dark minerals (biotite) than the outer granite. Phenocrysts form about 40 % of the total volume of the rock. The Vementry Granite differs from the typical biotite Sandsting-Granite in its relative lack of ferromagnesian minerals, the absence of apatite and sphene and the complete lack of liquid inclusions in quartz. There is, however, a very wide range in composition and texture within the Sandsting Granite, and the Vementry Granite corresponds most closely to the coarse quartz-rich variaties from the easternpart of the Sandsting complex (The Bixter Granite).

3.4.15 Petrology of Vementry Granite.

The mineral constituents of the Vementry Granite (minerals are listed in appendix 2) are K-feldspar, plagioclase, quartz and biotite (plate 3.8F). K-feldspar is subhedral to anhedral microperthite. Plagioclase forms subhedral crystals and also occurs as cores or shells to perthites. Quartz-feldspar intergrowth resembles the Ronas Hill perthite granite intergrowth, but on a small scale. Mafic minerals include biotite, magnetite and stilpnomelane. Secondary minerals are chlorite, epidote and very scarce muscovite. Accessory minerals are of the outer granite are zircon, and magnetite and for the inner granite are allanite, sphene, apatite, zircon and magnetite.

3.5   Petrology of Shetland Granites to the West of WBF and South of Bixter Voe.

3.5.1 Bixter Granite

The Bixter Granite lies to the east of the Sandsting complex, but is very poorly exposed (Figure 3.11). It appears to form now a series of near vertical sill-like intrusions with north-north westerly trend, which thin and finger out in a northerly direction.

3.5.2 Geological Setting.

Mykura & Phemister (1976) pointed out that the Bixter Granite and graphic microgranite sills are in some aspects similar to sheets of granite and felsite which cut the Walls Formation on the shores of Seli Voe, Gruting Voe and Vaila Sound. The granite outcrop near Gard House toward Bixter Voe contains coarse-grained granite with microperthite and antiperthite as described above. This granite grades into graphic granite which becomes progressively finer-grained and has more extensive zones of graphic intergrowth as it is traced northward. The coarse-grained granite of the sill differs from the main mass in that it contains a higher proportion of quartz (up to 40 %) with serrate margins and rudimentary graphic intergrowth. Oligoclase is fairly abundant, forming clusters of euhedral crystals. Hornblende is absent and interstitial biotite is present. Dykes and veins of felsite are many, highly irregular, branching and locally shattered by the later movements associated with the WBF.

3.5.3 Petrology of the Bixter Granite.

The mineral constituents of the Bixter granite shows that the rock is composed of plagioclase, K-feldspar megacrysts and biotite (proportion very low compared with Sandsting granite). Plagioclase occurs as euhedral to subhedral crystals, singly and as composite aggregates, normal zoning is very common and the zoned

crystals cores are showing alteration (plate 3.8A). K-feldspar is microcline.
Microperthite occurs as zoned suhedral crystals, they are not generally interstitial to
the other minerals . The most frequent small plagioclase inclusions are small
plagioclases oriented parallel to the face of the host microperthite (plate 3.8A).
Quartz is interstitial to all other minerals, and commonly forms large anhedral
crystals. Biotite occurs as subhedral to anhedral plates with weak pleochroism
from dark brown to pale yellow, and it seems that some crystals of hornblende are
pesudomorphed by biotite. Secondary minerals are chlorite, epidote and
muscovite. Accessory minerals are allanite, apatite, sphene (more abundant
accessory mineral), zircon and magnetite.

3.5.4 Sandsting Plutonic Complex.

The Sandsting Plutonic Complex occurs in the south-eastern part of the Walls
Peninsula and intrudes Middle Devonian (ORS) Walls Sandstone Formation
(Figure 3.11).

3.5.5 Geological Setting.

The Sandsting complex comprises predominantly granitic and dioritic
rock types with minor gabbroic and metagabbroic / ultramafic lithological units
(Mykura & Phemister 1976). Age relations between the granitic rock suite and the
other plutonic units which comprise the Sandsting Plutonic Complex have been
shown by Mykura & Phemister (1976) consistently to indicate that the granitic
rocks are younger. However, mafic dykes intrude all the major plutonic units and
represent a widespread later stage magmatic event. The sequence of events in the
Sandsting Plutonic Complex can be ordered according to apparent relative age
(Mykura & Phemister 1976) into: (a) diorite, including melamicrodiorite, biotite and
hornblende-diorite, tonalite, monzonite, gabbro (which form at least two small
dyke-like masses within diorite) and melaolivine gabbronorite / plagioclase-bearing
lherzolite; (b) granodiorite; (c) coarse grained biotite granite grading locally into
graphic granite; (d) porphyritic granite and microgranite; (e) porphyritic

microgranite and mafic dykes which cut both the plutonic complex and adjoining

sediments; (f) hydrothermal brecciation and scapolitization (cf. Mykura & Young

1969). The emplacement of the granitic rock suite of Sandsting has been described

by Mykura (1976) as a sheet-like mass of granite emplaced in several pulses of

magmatic activity. Scapolite occurs in the area around Wester Wick and in the

Skelda Ness peninsula as a vein-filling mineral and a replacement product in

mylonite belts which do not appear to be connected with the Walls Boundary Fault

(WBF). The Sandsting Granitic suite has been described by Mykura & Phemister

(1976) as consisting of four granitic members: 1) a coarse grained granodiorite

sheet overlying the Culswick diorite with inclusions of baked sediment between

them (seen on the west shore of Keolki field). 2) A porphyritic microadamelite

sheet-like intercalation in the Culswick diorite with distinctive field characteristics in

hand specimen due to the presence of pink or white feldspar phenocrysts. Its main

outcrop extends from Green Head on the White Ness Peninsula eastward via west

Culswick to the Head of the Culswick valley where it is displaced southward by the

Culswick fault. 3) A locally porphyritic microgranite forming a high proportion of

the veins and major cross-cutting intrusions within the diorite. 4) A coarse grained

quartz-rich biotite granite forming over half of the outcrop of the Sandsting

Complex, with grain size fairly consistent throughout the great part of the outcrop.

The amount of mafic minerals present decreases slightly to the east . The

proportion of quartz increases to the east and the proportion of plagioclase

decreases.

NNW of Garderhouse the granite forms a series of near vertical sheets in the

steeply inclined sediments of the Walls Formation. A large number of individual

sills occur in different places and show granophyric textures towards Bixter Voe.

(Fig. 20.1). As to age relationships, the contacts between granodiorite and

microadamellite and between microadamellite and coarse grained granite are

unclear.

Miller & Flinn (1966) used K-Ar radiometric dating of biotite from the Sandsting

granite and obtained an age of 334 ± 13 Ma. Biotites from a granite N-E of Culswick gives an age of 360 Ma (Mykura & Phemister 1976). Hornblende from a diorite at Hestinsetter Hill give a K-Ar age of 369 Ma. The significant disparity (about 30 Ma) between the two age groupings possibly reflect a prolonged intrusion history or the different closure temperatures of biotite and hornblende.

3.5.6 Petrology of Sandsting Granite.

The mineral constituents of the Sandsting granite (listed in appendix 2) are zoned plagioclase, poikilitic microcline-microperthite varying in size from small crystals to megacrysts, hornblende and biotite. Plagioclase is volumetrically the most important phase in the Sandsting granite. Plagioclase occurs both as clusters of large euhedral to subhedral crystals and as small and large discrete euhedral crystals. In strongly zoned crystals, with the more anorthite-rich cores showing the greatest degree of alteration. Plagioclase is generally free of inclusions, but occasionally contains small euhedral inclusions of hornblende and apatite and anhedral crystals of biotite. K-feldspar is microcline-microperthite and forms subhedral to anhedral crystals. Microperthite contains euhedral inclusions of all the other minerals. The most frequent inclusions are small zoned plagioclases, some of which are oriented parallel to the crystal faces of the host microperthite (plate 3.8B & C). This kind of plagioclase orientation in K-feldspar is called intergrowth texture. Quartz is interstitial to all the other minerals, especially the plagioclase and also often to the K-feldspar. Hornblende forms euhedral crystals (plate 3.8C & D) which are pleochroic from dark bluish green to pale yellowish green and commonly twinned. Small euhedral inclusions of apatite are common. Hornblende crystals occur either singly or in multi-granular aggregates along with biotite and iron ore. Biotite occurs as subhedral to anhedral plates either singly or clotted together in groups along with the other minerals. Biotite commonly encloses small crystals of zircon and apatite. The secondary minerals are chlorite and epidote. Accessory minerals are allanite, sphene, zircon, rutile and magnetite.

3.6 Petrology of Granitic Pebbles in Conglomerates to the East of the WBF.

3.6.1 Ophiolite-Na-Granite

There is a typical ophiolite sequence in Unst and Fetlar. This igneous mass is well known from the work of H.H.Read (1934), and Flinn (1958), to form a number of tectonic blocks (Figure 3.4). It has been shown that these blocks are parts of a typical ophiolite complex , composed of rocks ranging from harzbergite to sheeted dyke complex .

Na-Granite. This occurs in two forms. One as intrusive sheets in the sheeted dyke complex of the ophiolite, and the other as pebbles in metaconglomeratic sediments derived by erosion from the ophiolite complex as it was obducted.

3.6.3 Geological Setting.

A) Na-Granite as minor intrusions:

Flinn (1958) described minor intrusions of quartz-albite-porphyry indistinguishable from that occurring as pebbles in some of the conglomerates (Figure 3.3). These minor intrusions take the shape of lenticles less than one metre thick and the others form an irregular masses some tens of metres across, intruding the greenstone slice in the thrust at Staves Geo (Fetlar) and at North Tonga in the Muness phyllite about one metre thick. Prichard (1982) has analysed a sample from a Na-granite vein in the sheeted dyke complex of the Muness phyllite block (K symbol in the appendix 2). ·

B) Na-Granite as pebbles. These type of pebbles occur within conglomeratic sediments in a) the Funzie conglomerate and in b) the Muness-phyllite Group conglomerates (Figure 3.6). a) Funzie conglomerate occurs on the east coast side of Fetlar and is a very large body of deformed metaconglomerate of pre- Middle Old Red sandstone age, which contains elongated and flattened pebbles, that are mostly of quartzite, occasionally of granite and rarely of marble {Flinn 1958}. More than

half of the Funzie conglomeratic pebbles are a fairly pure quartzite, nearly all the

remainder are of gneissose, biotite-albite-granite. The pebbles of granophyre and

quartz-albite-porphyry are indistinguishable from those occurring in the sheeted

dyke in the ophiolite complex. Pebbles of rocks which cannot be matched

eleswhere in the area, are also present (Flinn 1958). The Funzie conglomerate

was formed after the phyllite conglomerate, the former differ from the latter, in that

it contains many more pebbles types than the conglomeratic band in the phyllite.

The Funzie conglomerate is a typical polymictic conglomerate (Pittijohn, 1949), and

may be interpreted as an erosion product of a newly formed relief.

Phyllite Group conglomerate. The conglomeratic bands in the Phyllite Group,

contain pebbles of Na-granophyre and quartz-albite porphyry. The Na-granophyre

pebbles are a rare but distinctive albite-granophyre occasionally

carrying plates of pale amphibole. These granophyre pebbles are indistinguishable

from those in the greenstone conglomerate. The porphyry pebbles are deformed ,

while the granophyre ones are not (Flinn 1958).

In 1970 Flinn analysed samples of three types of conglomerate pebbles (see

appendix 2) the sample 13 and 14 come from greenstone pebbles, they show

dioritic or quartz-diorite composition . A second type of conglomerate contains

quartz-albite-porphyry pebbles, the analysed pebble is unusual, in that the feldspar

phenocrysts are intergrown with epidote (No. 15, appendix 2). A third type of

conglomerate contains pebbles of albite-granophyre, which occasionally contain

plates of amphibole (No. 16, table 1). Flinn inferred that the diorite pebbles,

quartz-albite-porphyry pebbles and albite granophyre pebbles are related to each

other and to the rocks of the ophiolite, by their association with each other and with

the other pebbles derived from the rocks of the ophiolite, as well as by the fact that

some resemble intrusives cutting the ophiolite nappes and by the compositional

characteristics of the four pebbles.

3.6.4   Petrology.

The mineral constituents of the Na-granite (minerals contents are listed in

appendix 2) are essentially plagioclase (mostly albite), quartz and mafic aggregate. Plagioclase is intensely altered and small amounts being less so (plate 3.11F). Quartz phenocrysts are very common in the quartz-albite porphyry (plate 3.11F). Reduction in the grain size of quartz is very common due to disintegration of quartz phenocrysts by deformation. The mafic aggregate is composed of hornblende, magnetite and a little biotite (mostly occur as anhedral flakes). Very rare secondary muscovite and epidote occur. Accessory minerals are rutile and occur occasionally.

3.6.5 Rova Head Granitic pebbles.

There are several occurrences of conglomerate in the Old Red Sandstones of south-east Shetland. The largest is at Rova Head and on the nearby coast of Bressay (Figure 3.8).

3.6.6 Geological Setting..

In the paper by Flinn (1966), he recognized the Rova Head conglomerate as a local facies of the Lerwick sandstones. It should not be considered a stratigraphic marker horizon. Wherever the metamorphic rocks and the Rova Head conglomerate are seen close together, the latter becomes a breccia matrix and the boundary is probably an unconformity, although later movement may have taken place along it.

Mykura (1976) described the Rova Head conglomerate, a coarse conglomerate with rounded pebbles of granite and quartzite which locally reach 1m in diameter. To the east or south east the conglomerate interdigitates with the Lerwick sandstone, though to the north of Lerwick the junction between the Rova head conglomerate and the metamorphic basement is sheared and along it the basal breccia consists of fine breccia. This suggests the conglomerate passes down without any intervening sediment into basal breccia, which may be thin and discontinuous. Palaeocurrent data suggest that these coarse sediments came principally from the north-west direction. Allen (1980) observed that the Rova Head conglomerate is dominated by
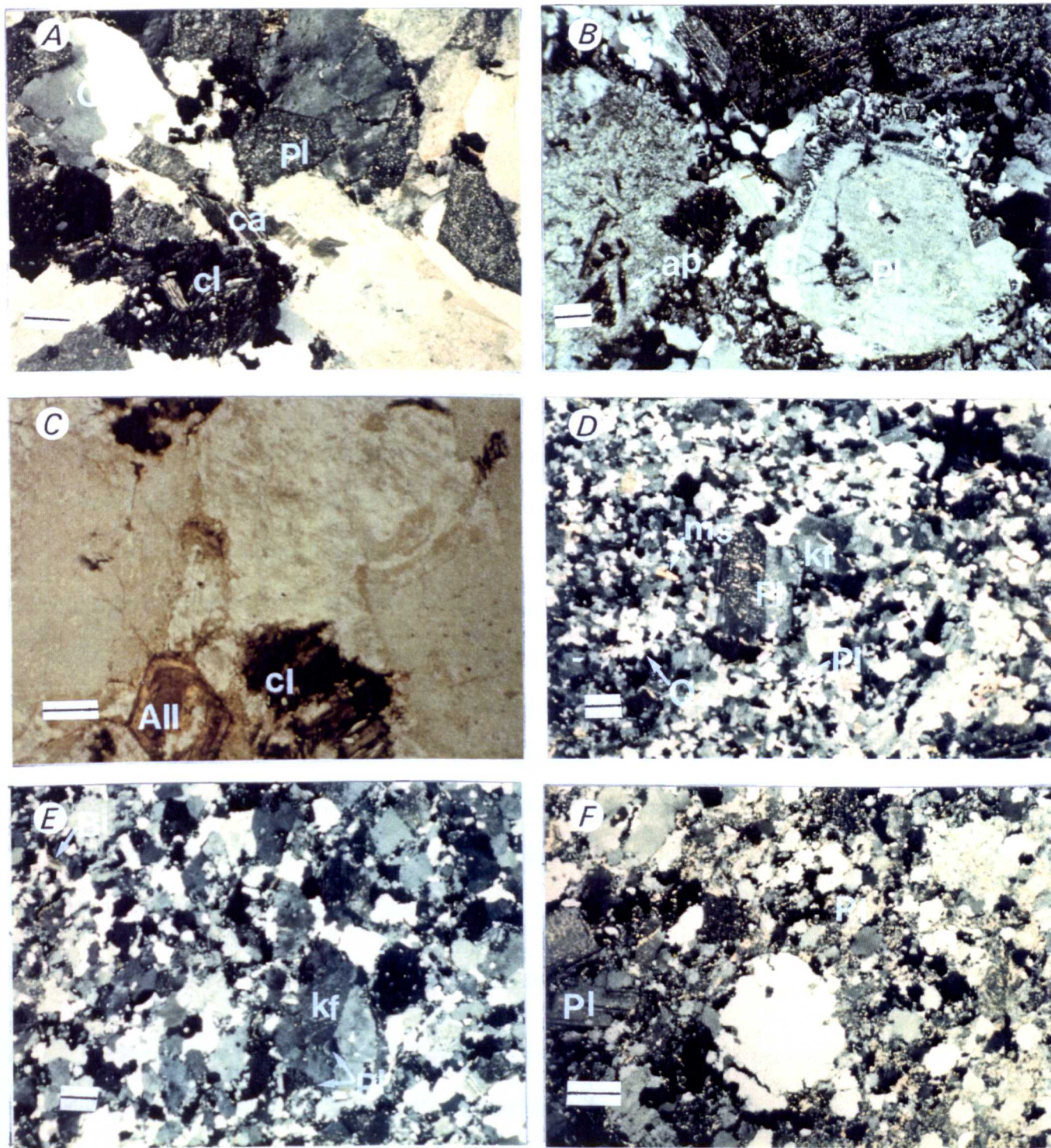
Plate 3.11. **A.** Basic granodioritic pebble of Rova Head, showing the mafic minerals have been altered to chlorite (cl), small fracture healed by calcite (ca), plagioclase (Pl) and quartz (Qz) (scale bar, 0.5 mm). **B.** Showing micrographic texture in the basic micrographic granite and accessory mineral apatite (ap) (scale bar, 0.5 mm). **C.** Euhedral allanite (All) and chlorite (cl) in the basic granodiorite pebble (scale bar, 0.5 mm). **D and E.** Leucocratic porphyritic granite of Rova Head showing plagioclase (Pl) and K-feldspar (kf) phenocrysts set in a fine grained quartz and feldspar groundmass (scale bar, 0.5 mm). **F.** Funzie trondhjemite pebble showing the rounded quartz (Qz) and plagioclase phenocrysts (Pl) set in a fine grained quartz and plagioclase groundmass (scale bar, 0.5 mm).

thick conglomerate and outcrops over an area approximately 7 Km long, and has up to 5 m thick beds and is 0.5-1.3 Km wide. The western limit is defined by a major northeast-trending fault, which juxtaposes conglomerates against older metmorphic rocks. An offshoot from this fault marks the base of the Old Red Sandstone deposits in the north of the area west of Rova Head. The conglomerate is often inverse to normal graded framework-supported gravels and composed of clasts of well rounded to moderate sphericity of quartzite and granite, with small proportions of psammite, felsite, schist and foliated granodiorite. The granitic pebbles within the Rova Head Conglomerate indicate a large granitic source-terrain. The high percentage of quartzite may be due to recycling of older conglomerates. Finally, Allen have recognized three types of conglomerate in the Rova Head area which are termed type A or inverse to normal conglomerate, type B or inverse and ungraded, and type C or normal conglomerate. Allen and J.E.A.Marshal (1981) have distinguished six major depositional environments, where the Old Red Sandstone sediments of south east Shetland were deposited, one of these environments, termed alluvial fun environment, is where the Rova Head conglomerate had been built and deposited. The quartzite clasts may originate from the lower Dalradian Scatsa Division (Flinn 1967, Mykura 1976), but the granite clasts probably came from further field. Large post-Devonian displacements along the WBF and associated faults obscure the provenance of these granitic clasts.

3.6.7 Petrology of Rova Head Granitic Pebbles.

The Rova Head Conglomerate (RHC) includes four types of granitic pebbles:-basic granodiorite, leucocratic porphyritic granodiorite, basic micrographic granite and leucocratic granite. The mineral constituents of RHC are (listed in appendix 2) plagioclase, K-feldspar, quartz and altered mafic aggregates confined to basic granodiorite and to basic micrographic granite (plate 3.11A & B). Plagioclase displays differences in composition and size between the different kinds of the RHC granites, twinning on the albite law is very common. Large plagioclase

phenocrysts (most likely albite) and xenomorphs of quartz are found in the leucocratic granodiorite, highly altered in the basic granodiorite to sericite. Plagioclase in the basic micrographic granite resembles the Ossas micrographic granite in that the plagioclase is thinly mantled with turbid K-feldspar which passes into micrographic intergrowth with interstitial quartz. K-feldspar is microcline megacrysts in both basic and leucocratic granodiorite and encloses small euhedral plagioclase crystals. In leucocratic granite with allotriomorphic texture (plate 3.11E), K-feldspar is orthoclase with a very few crystals displaying carlsbad twinning, and plagioclase is very small grains in the groundmass, small compared with K-feldspar. Quartz grain size seems to have been reduced by later deformation. Quartz is interstitial in all rocks to all other minerals. Mafic aggregates in basic granodiorite are large clots of altered chlorite after biotite and aegirine-riebeckite (a relict of aegirine-riebeckite is present) in the basic micrographic granite. A few plates of chlorite associated with iron ore are present in the leucocratic granodiorite. Accessory minerals are well shaped allanite (plate 3.11C) (only in basic granodiorite), apatite and iron ore.

Chapter Four.

4.1 Mineral Chemistry of Shetland Granitoids.

Many of the late Caledonian granitoid plutons of Shetland are composite bodies with coarse-grained amphibole and biotite. From field relations, Graven Complex, Brae Complex, Spiggie Complex and Sandsting Complex appear to be formed by multiple intrusion and differentiation comes to mind as an explanation for the relationship between the individual facies. Constituent minerals such as amphibole, biotite, pyroxene, plagioclase, K-feldspar, magnetite, ilmenite and others from representative rocks of the Shetland granites were analyzed by electron microprobe, using a Link Systems Model 290-2KX energy-dispersive spectrometer, attached to a Cambridge Instruments Geoscan.

4.2 Mineralogy of Shetland granites to the east and west of Walls Boundary Fault (WBF).

4.2.1 Amphibole.

Amphibole represents a significant proportion of the mafic minerals in the hornblende-bearing plutons and is absent only in some of the most evolved rocks. Representative analyses of amphibole from the hornblende-bearing granites from different Shetland granitoids including the Graven Complex granitoid, Brae Complex granitoid and Spiggie-Aith-Hildsay granites are listed in the appendix (2); analyses have been recalculated to a base of 23 oxygens. According to the nomenclature of Leake (1978), the amphiboles of the Graven and Sandsting granitoids vary from actinolitic-hornblende to magnesio-hornblende, and those of the Aith and Hildsay granites vary from magnesio to ferro-hornblendes (Figure 5.1). The Xmg values (atomic Mg/(Mg+Fe) ratio) range from 0.41 to 0.79 and in the Graven, Sandsting and Bixter granites are higher than in the Spiggie, Aith and Hildsay granites (Figure 5.1). Tetrahedral Al varies from 0.606 to 1.69 and
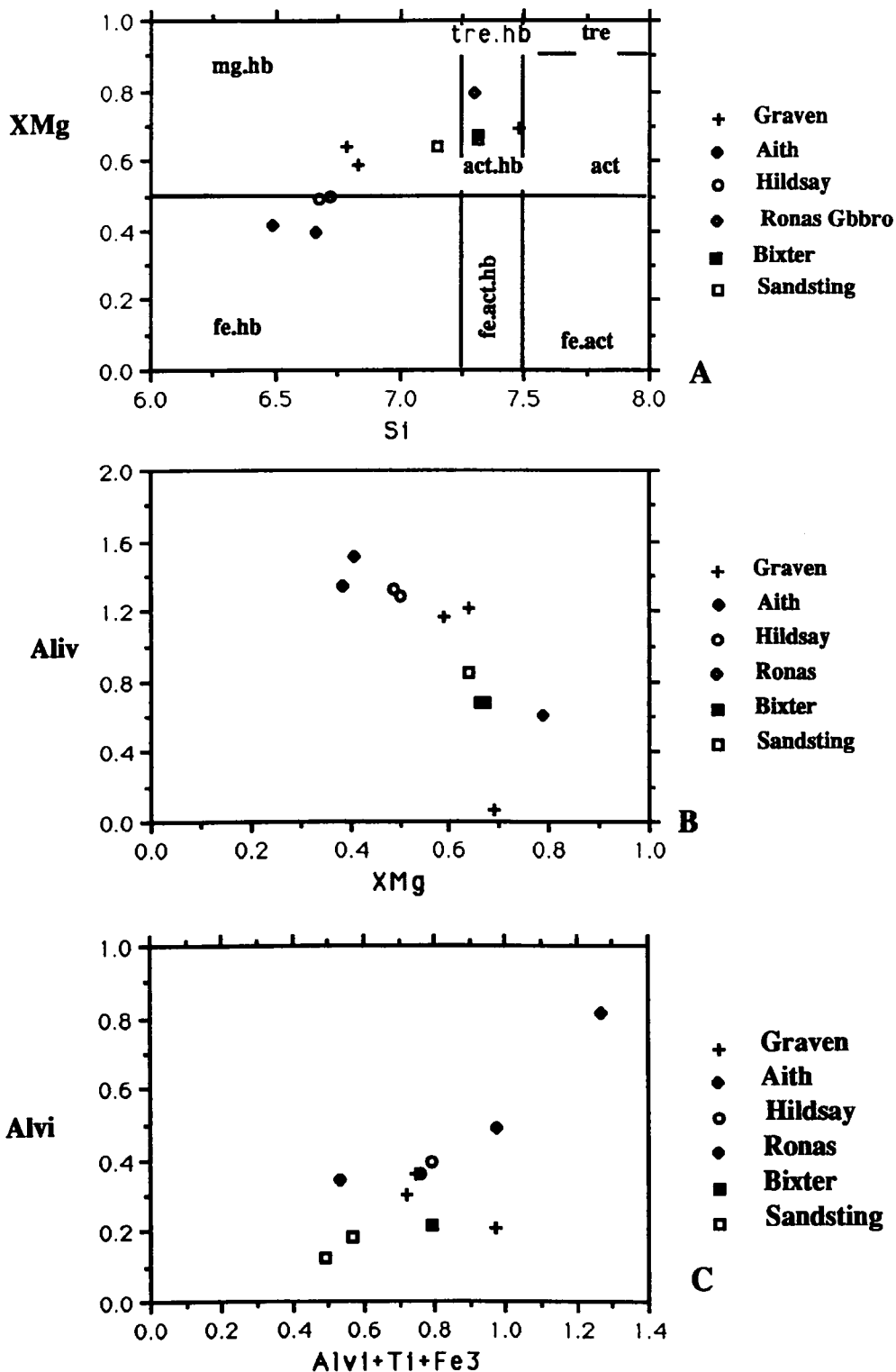
Figure 5.1 variation of hornblende compositions in Shetland granitoid rocks in terms A) XMg v Si atoms in the unit cell formula after the nomenclature of Leake, 1978. (Cation based on 23 oxygens). B and C) Variation in tetrahedral aluminium v XMg (Mg/(Mg+Fe) and octahedral $Al_{vi}+Ti+Fe3$. Note that the different facies of Shetland granitoids contain differenrt types of hornblende ranging from act. hornblende through magnesio-hornblende to ferro-hornblende.

octahedral Al from 0.13 to 0.81, Ti from 0.41 to 0.53. Fe^{+3} {calculated using the computer program recalc (Holland and Powell, 1989)} ranges from 0.16 to 0.41 . The Si content (number of Si atoms to 23 oxygens) varies between 6.49 and 7.48. The Aliv values are generally higher on the whole than the Alvi values (0.06-1.69 to 0.16-0.41 respectively), they show a large spread in the hornblende composition for the different facies of Shetland granitoid rocks (Figure 5.1).

4.2.2 **Biotite.**

Biotite is present in most of the rocks of Shetland granitoids and shows an increase with decreasing acidity. Analysed biotites are plotted on Figure 5.2, from which it can be seen that the biotites from all the hornblende-bearing granites fall in the phlogopite field, and those from hornblende-free granites fall in the annite field; the Mg/(Mg+Fe) values are restricted to 0.67-0.73 and 0.42-0.55 respectively. This indicates that the Mg values do not vary markedly with increasing acidity from the Graven granite through the Hildsay-Spiggie granite (to the east of WBF) to the Bixter and Sandsting granitoids (to the west of WBF) (Figure 5.1). Skaw biotites of the hornblende-free granites plot in the annite field (Figure 5.2) which indicates a MgO decrease and FeO increase relative to the hornblende-bearing granites. Biotites have Mg contents of 1.24-3.053 and Fe^{+2}+Mn values of 0.91-1.51 and plot as individual groups on an Mg-Fe^{+2}+Mn-Alv$_i$+Fe^{+3}+Ti ternary diagram (5.4A). Thus the biotites of the hornblende-bearing granites fall in the Mg-biotite field, while the Skaw (hornblende-free granite) fall in the Fe-biotite field of Foster (1960). Tetrahedral Al varies from 2.21 to 2.41 in the hornblende-bearing granites and from 2.36 to 2.52 in the hornblende-free granite over the stated Fe/(Fe+Mg) 0.28- 0.29- to 0.52-0.58 respectively (Figure 5.3). Total Al ranges from 2.52 to 2.88 in the hornblende-bearing granites and from 2.97 to 3.22 in the hornblende-free granites and Ti from 0.17-0.61 to 0.21-0.28 respectively. No zoning or core to rim trends are evident from the analyses.
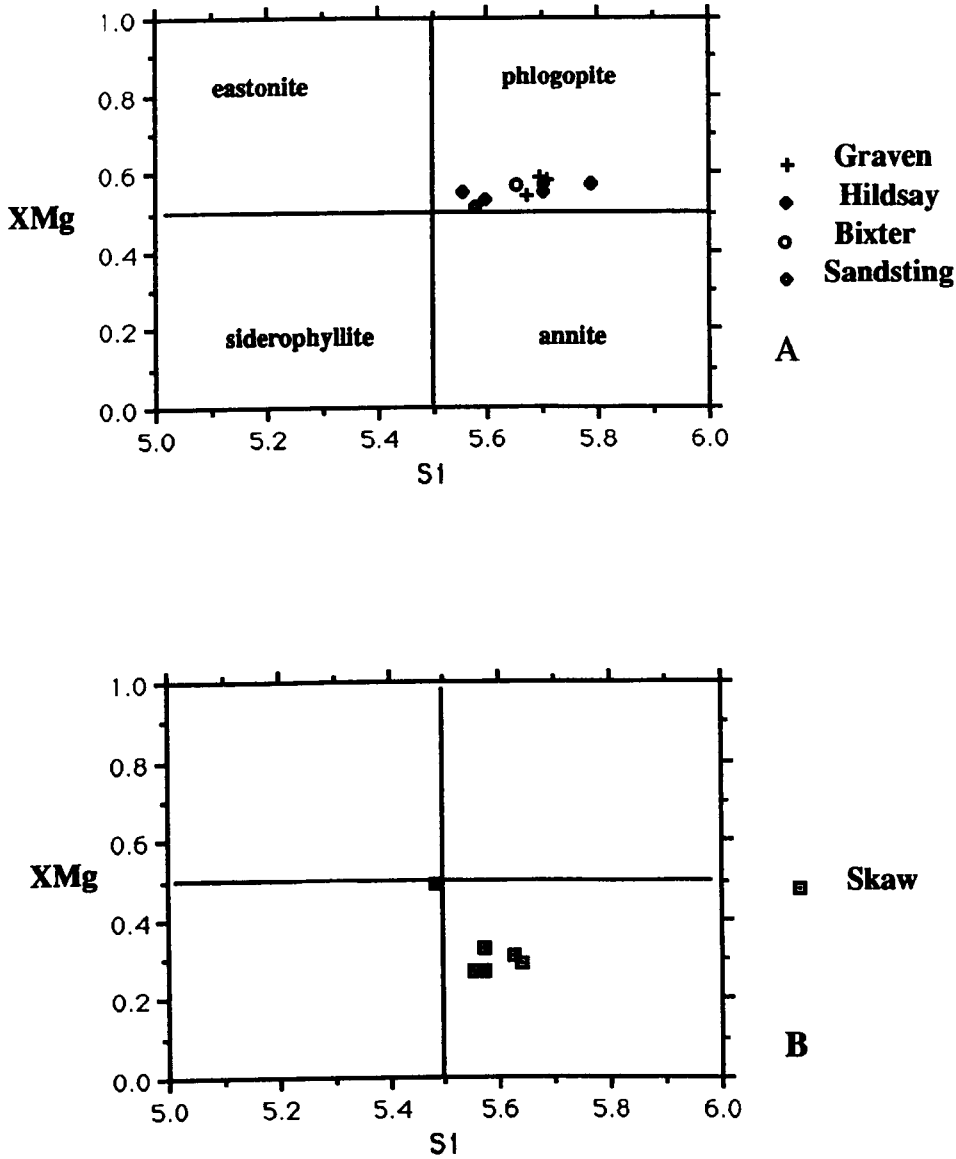
Figure 5.2 Variation of biotite compositions in Shetland granitoid rocks in terms of XMg Mg/(Mg+FE) v Si atoms in the standard biotite unit cell (calculated on the basis of 22 oxygens). Note that the hornblende-bearing granite plus Bixter and Sandsting fall within t he phlogopite field while hornblende-free granite-Skaw fall within the annite field and one sample of Skaw lies on the boundary between eastonite and siderophyllite.
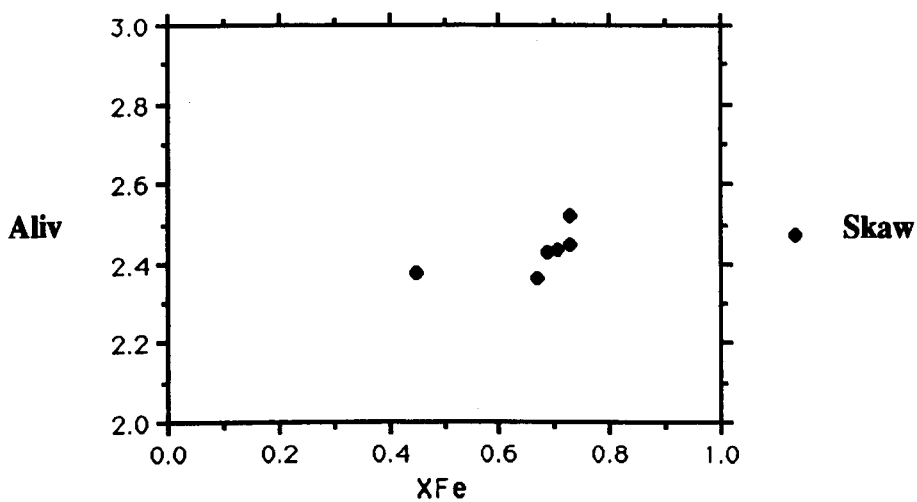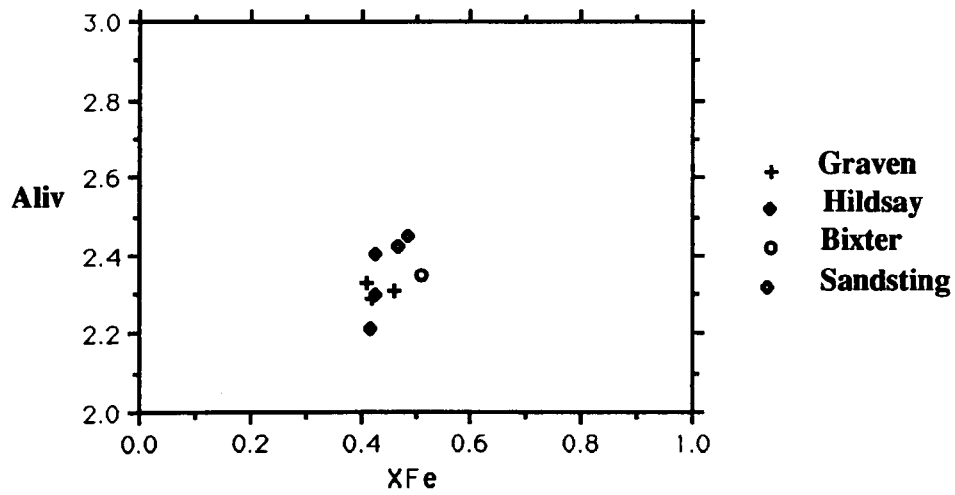
Figure 5.3 Variation of biotite composition in tetrahedral aluminium versus XFe (Fe2O3/Fe2O3+FeO) for the Shetland granitoid rocks. Note t here is no large spread of the tetrahedral Al for the biotite composition of Shetland granitoid rocks.

4.2.3 Pyroxene

The nomenclature used to describe the chemistry of the pyroxenes is illustrated in
Figure 5.4B The presence of clinopyroxene is a definitive characteristic of the basic
monzonitic rocks of the Aith-Hildsay-Spiggie granite. They occur as prismatic
crystals, some are subhedral and enclosed partly within hornblende crystals,
probably indicating that it reacted with magma at the beginning of hornblende
crystallization. Frequently sphene euhedra are associated with clinopyroxene.
Pyroxene is salite in Aith-Hildsay-Spiggie granite and augite in Ronas Hill gabbro
(Figure 5.4B).

4.2.4 Plagioclase

Plagioclase compositions from the main facies of the hornblende-bearing granites to
the east and west of Walls Boundary Fault (WBF) determined by microprobe
analyses are plotted on a triangular Or-Ab-An diagram (Figure 5.5A). Microprobe
analysis of Graven granite plagioclase indicate its sodic nature as the An-contents
range between 26 to 15 (An_{26-15}). The Spiggie granite plagioclase composition is
restricted to a fairly narrow range (An_{36-31}), which is more An-rich than Graven
granite plagioclase (Figure 5.5A). The plagioclase from hornblende-bearing and
hornblende- free granites including one sample from the eastern granite (to the west
of WBF) have a similar compositional ($An_{23.97}Ab_{75.93}Or_{0.10}$) except for the
Ronas Hill Gabbro which has An-content of An83-75 (Figure 5.5C).

4.2.5 K-feldspar

Microprobe analysis of K-feldspar shows a composition for the Graven granite of
$Or_{92.8}$-$Ab_{7.2}$-$An_{0.0}$ and the compositional range for the Spiggie granite is
$Or_{89.7-94}Ab_{6-10}An_{0.0-0.03}$. These compositions are plotted on a triangular Or-
Ab-An (Figure 5.5) diagram. K-feldspar is compositionally restricted to a
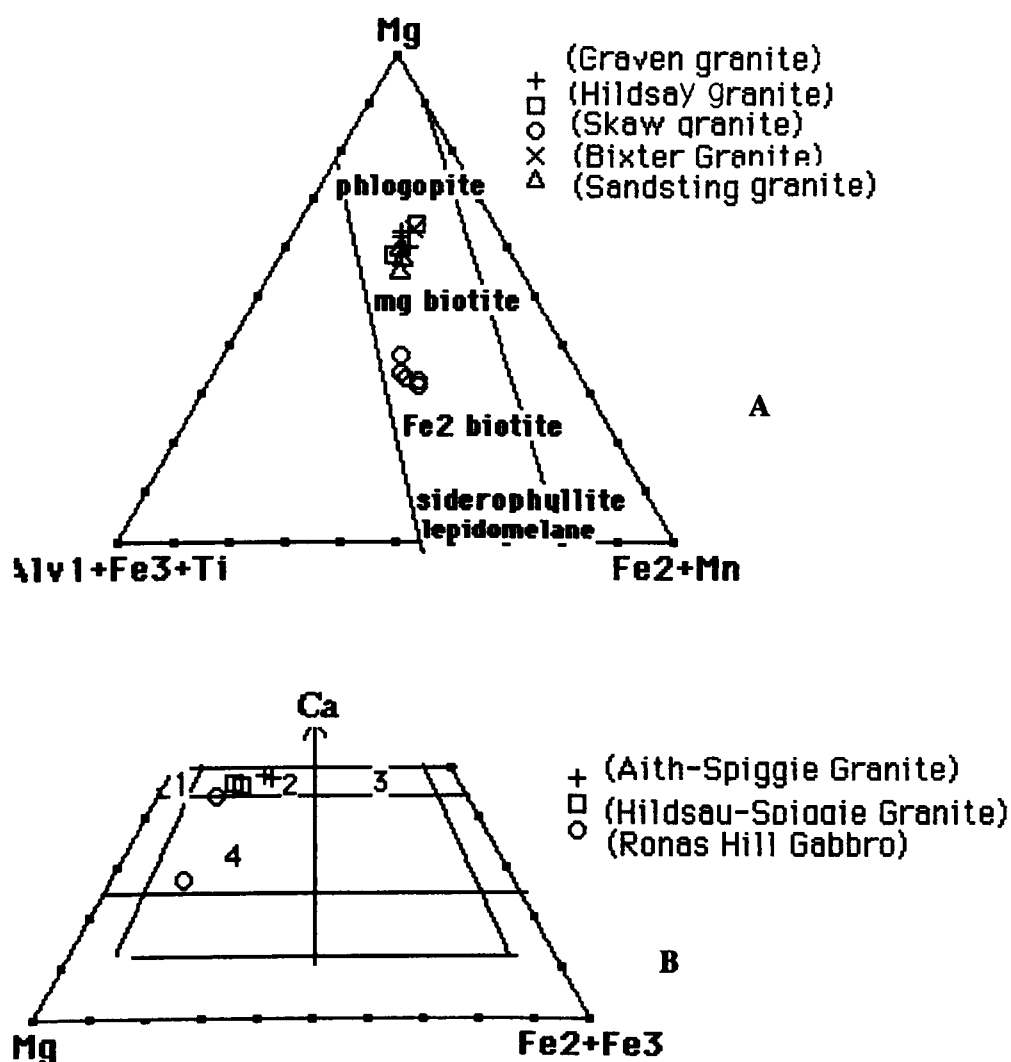
KEY:

field 1 - diopside

field 2 - salite

field 3 - ferrosalite

field 4 - augite

· Figure 5.4 B) for Aith-Hildsay-Spiggie granite and Ronas Hill gabbro

clinopyroxene represented upon the pyroxene quadrilateral. pyroxene nomenclature after Poldervaart and Hess (1951). A) Biotite classification (after Foster, 1960).
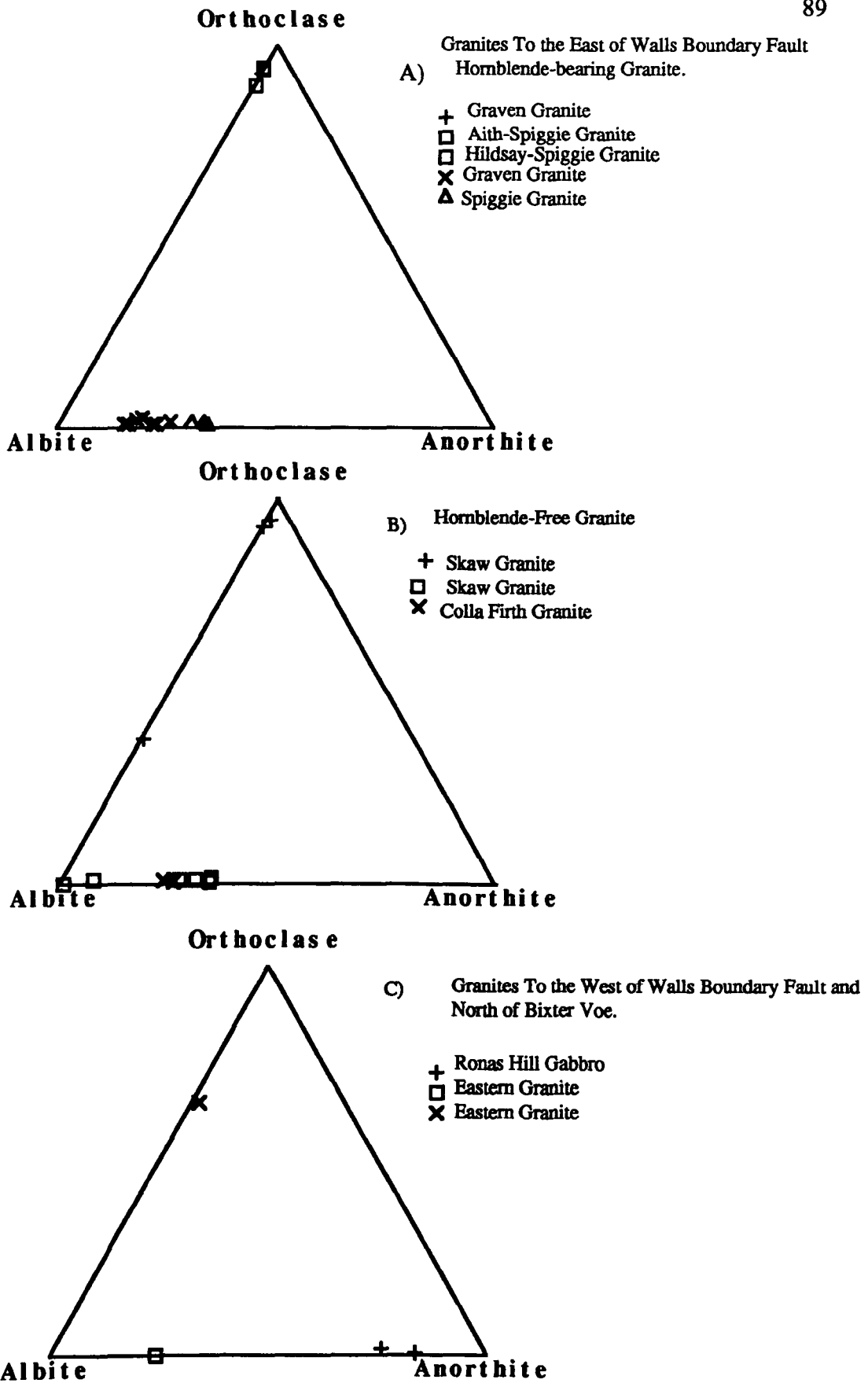
Figure 5.5A-C Ternary Or-Ab-An plots showing the variation in feldspar compositions from the various Shetland granitoid facies.

maximum Ab content of about 7% in the hornblende-bearing granites, while it reachs to 62% in a perthitic intergrowth and 99% in a lamella of albite in the hornblende-free granites (Figure 5.5B). The perthitic intergrowth in the Eastern granite contain $Or_{65.09}Ab_{33.27}An_{1.64}$ (Figure 5.5C).

4.2.6 Epidote

Epidote occurs as skeletal intergrowths with biotite and amphibole, as epitaxial rims on allanite and as a breakdown saussuritization product in plagioclase cores. In the Spiggie -Aith-Hildsay granite epidote forms euhedral crystals (plate 3.2) and interstitial grains trapped between phenocrysts and matrix phases, which suggests that it is primary. Epidotes in the Skaw granite are secondary minerals and microprobe analysis show that it is more aluminous than the primary epidote of Spiggie-Hildasay granite so that it is expected to be a saussurite epidote (see appendix 2).

4.3 Accessory Minerals

4.3.1 Ore Phases

The oxide minerals of the Shetland granitoids are mostly magnetite in the hornblende -bearing granites and mostly ilmenite in the hornblende-free granites. They occur within or in contact with hornblende and biotite. Microprobe analyses of magnetite show them to be nearly end-member compositions. Microprobe analyses of ilmenite show high Ti contents and very limited contents of Mg and Mn as the formula of ilmenite is a titanate of ferrous iron ($Fe^{+2}Ti^{+4}O_3$) and this can be expressed as (Fe, Mg, Mn)TiO3.

4.3.2 Sphene

Microprobe analyses of sphene shows that they are all have high Ca and Ti

contents and are more or less constant over eight analyses from the different facies

of Shetland granitoids.

4.3.3 Apatite

Apatite is very abundant in the hornblende-bearing granites, varying in shape from

stumpy to acicular. In general, the smaller crystals are needle-shaped and included

in the interiors of the mafic minerals whereas the larger crystals have a smaller

length/breadth ratio and are found along grain boundaries at the edge of the mafic

minerals or in the adjacent felsic minerals. Microprobe analyses of apatite shows

that it is pure Ca and P.

4.3.4 Allanite

Allanite is an abundant mineral in both the Skaw granite about 1.5% of the modal

analysis (hornblende-free granite) and about 2% modal analysis in the hornblende-

bearing granites, is the only member of the epidote group in which Fe^{+2} is an

essential component. Radioactive components are usually present in allanite and

most of the Skaw granite allanite, part of these in the Graven Complex granitoid

and the Spiggie granite and its two offshoots Hildsay and Aith granites are

commonly in the metamict state due to the partial destruction of its crystalline

structure by alpha particle bombardment from the disintegration of the radioactive

components in the mineral. Epitaxial subhedral epidote overgrowths commonly

fringe part or sometimes all of the allanite crystals. The boundary between yellow

allanite and the almost colourless epidote is always sharp, indicating a distinct break

in the conditions of crystal growth. Mineral composition of allanite is given in

appendix 2.

CHAPTER FIVE

Chemical Aspects

5.1 Introduction

No comprehensive geochemical study has been done on the Shetland granitoids and very little data has been published. The Shetland granitoids have been subdivided into five main groups according to their location to the east or west of the Walls Boundary Fault (WBF) which is a continuation of the Great Glen Fault and according to their mineralogical content (Figure 4.1) as the follows :

Granites to the east of WBF have been subdivded on the basis of their mineralogical content into (1) hornblende-bearing granites, (2) hornblende-free granites and (3) The granitic pebbles which were subdivided according to ther location into a) the Funzie and b) the Rova Head conglomerates.

Granites to the west of WBF include (4) Ronas Hill granite and its satellites and (5) Sandsting and Bixter granites. The Ronas Hill and its satellites are perthite and granophyre granites characterized by drusy and large cavities containing crystals of stilpnomelane, quartz and epidote. The Sandsting granitoid and the Bixter granite were grouped together because of their proximity and because on Harker diagrams the Bixter granite represent the acidic end of the Sandsting granitoid which varies from porphyritic microadamellite through granodiorite containing minor amounts of hornblende to granite. The aim of this chapter is to constrain the mechanism which may have been responsible for the observed trends. There will be a detailed discussion of each group in the following sections.

5.2 Major Element chemistry of Hornblende-bearing Granites.

The hornblende-bearing granites to the east of Wall Boundary Fault include the Graven complex, Brae complex and Spiggie granite with its two displaced offshoots the Hildasay and Aith granites. The Spiggie granite is truncated by the Walls Boundary Fault and is exposed discontinously northward *via* a group of islands including Burra Isle (Figure 4.1). Although the field relations of Graven and Brae Complexes do not show any link between them, on major and trace element variation diagrams they always plot together and form continuous fields or trends.

Samples of the hornblende-bearing Granites were collected from the Graven complex, the Brae complex and the Spiggie Granite and its two offshoots the Hildasay and the Aith and have been analysed for major and trace elements (see appendix 1 for methods) in order to establish the general trends in the chemistry of hornblende-bearing granites. The variation of major element oxides with increasing SiO_2 is shown on the Harker diagrams, in Figures 4.2a & 4.2b.

Generally the major element variations in the hornblende-bearing granites are consistent with a differentiation model. Such trends are commonly attributed to a differentiating silicate magma (Gribble, 1969). On the TiO_2 plot there are two distinct trends, one representing Graven and Brae and the other for the Spiggie pluton and its two offshoot granites (Aith and Hildsay). On the CaO diagram the Spiggie granite is distinct from its two offshoots in that it has lower CaO values. The H_2O and CO_2 show a crude negative correlation with increasing silica contents. A summary of the patterns in relation to crystallizing phases seen in the rocks is given below:

TiO_2:- decreases with increasing SiO2 caused by crystallisation of rutile and ilmenite.

$Al2O_3$:- shows slight decreases with increasing SiO_2 caused by crystallisation

of plagioclase and biotite.

Total Iron as Fe2O3 :- decreases with increasing SiO2 due to crystallisation of hornblende and biotite and the ore phases haematite, ilmenite and magnetite.

MnO:- no clear trend with increasing in SiO2 occurs.

MgO:- decreases with increasing SiO2 due to crystallisation of hornblende and biotite.

CaO:- decreases with increasing SiO2 due to plagioclase and hornblende crystallisation.

Na2O:- the diagram shows no apparent change in the value of Na2O, with Graven and Brae range values around 4%.

K2O:- shows increase with increasing SiO2 due to removal only in biotite and later K-feldspar crystallisation.

P2O5:- decreases with increasing SiO2 due to crystallisation of apatite.

5.3 Trace Element Chemistry Of Hornblende-Bearing Granites.

The trace element data for the hornblende-bearing granites is given in appendix 2   and the methods of analyses in appendix 1. Values of trace elements determined are plotted against SiO2 in Figures 4.2a & 4.2b. Trends with variable scatter, and of decreasing elemental concentrations with increasing silica contents can be seen for the elements Ba, Ce, La, Nd, Ni, Sc, Sr, V, Y, Zn and Zr. The most remarkable variations are in Nd, Sr and Zn contents. There are no particular trends or correlations between the elements Co, Cr, Pb, Rb and Th and silica contents, although some samples of Graven and Brae Complexes are relatively high in Cr and Ni compared with Spiggie and its two offshoots Aith and Hildasay, Figure (4.2c & d).

The Th contents are markedly high in four samples, three of them from Spiggie and the fourth highest one from Hildasay. The sympathetic relation between Th and K contents in plutonic rocks has been recognized by Heir and Rogers (1963), Clark
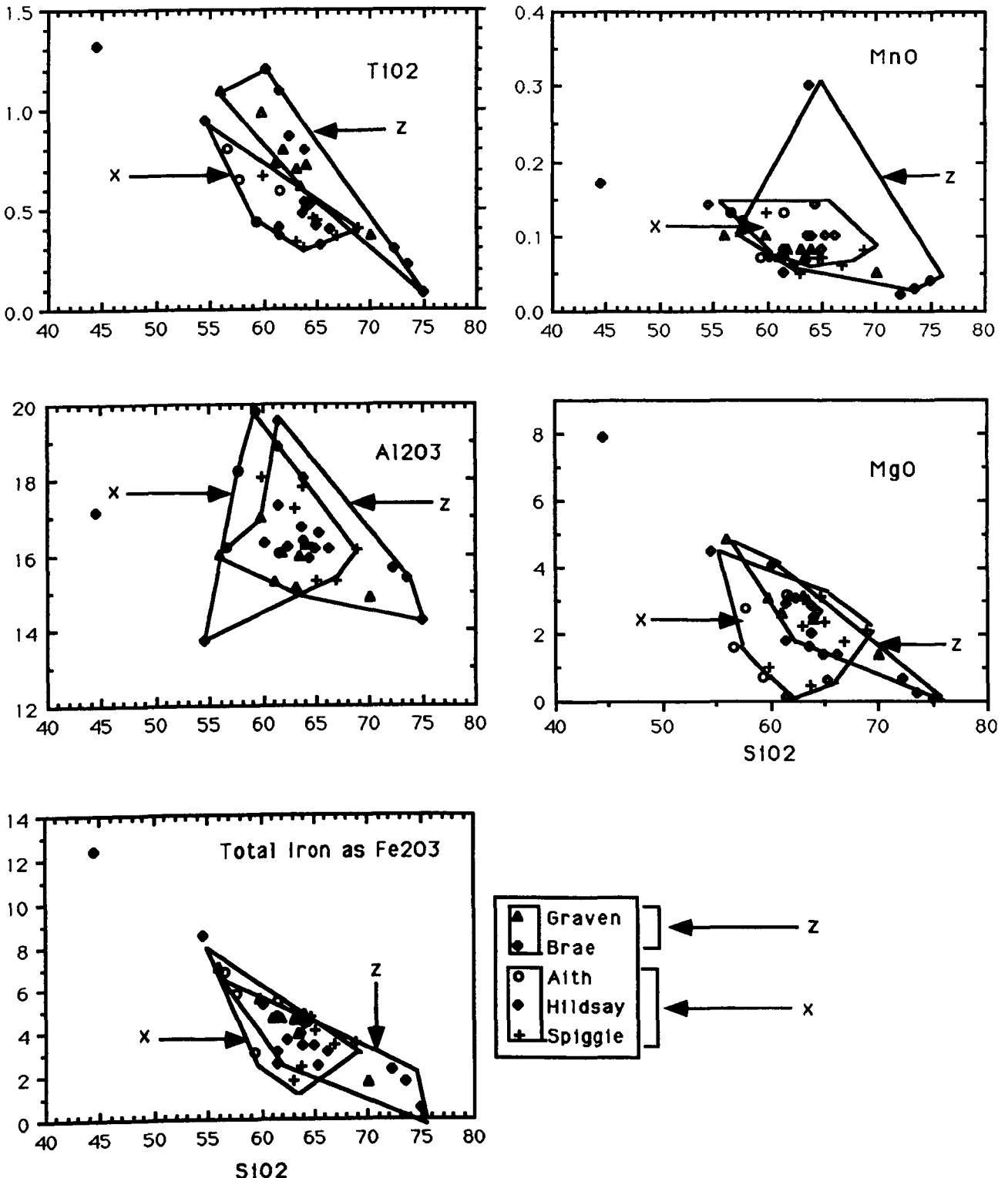
FIGURE 5.2a Plots of 5 major element oxides (TiO2, Al2O3, Fe2O3, MnO, MgO) vs. SiO2 for Hornblende-bearing Granites; to the east of Walls Boundary Fault, values are in wt%.
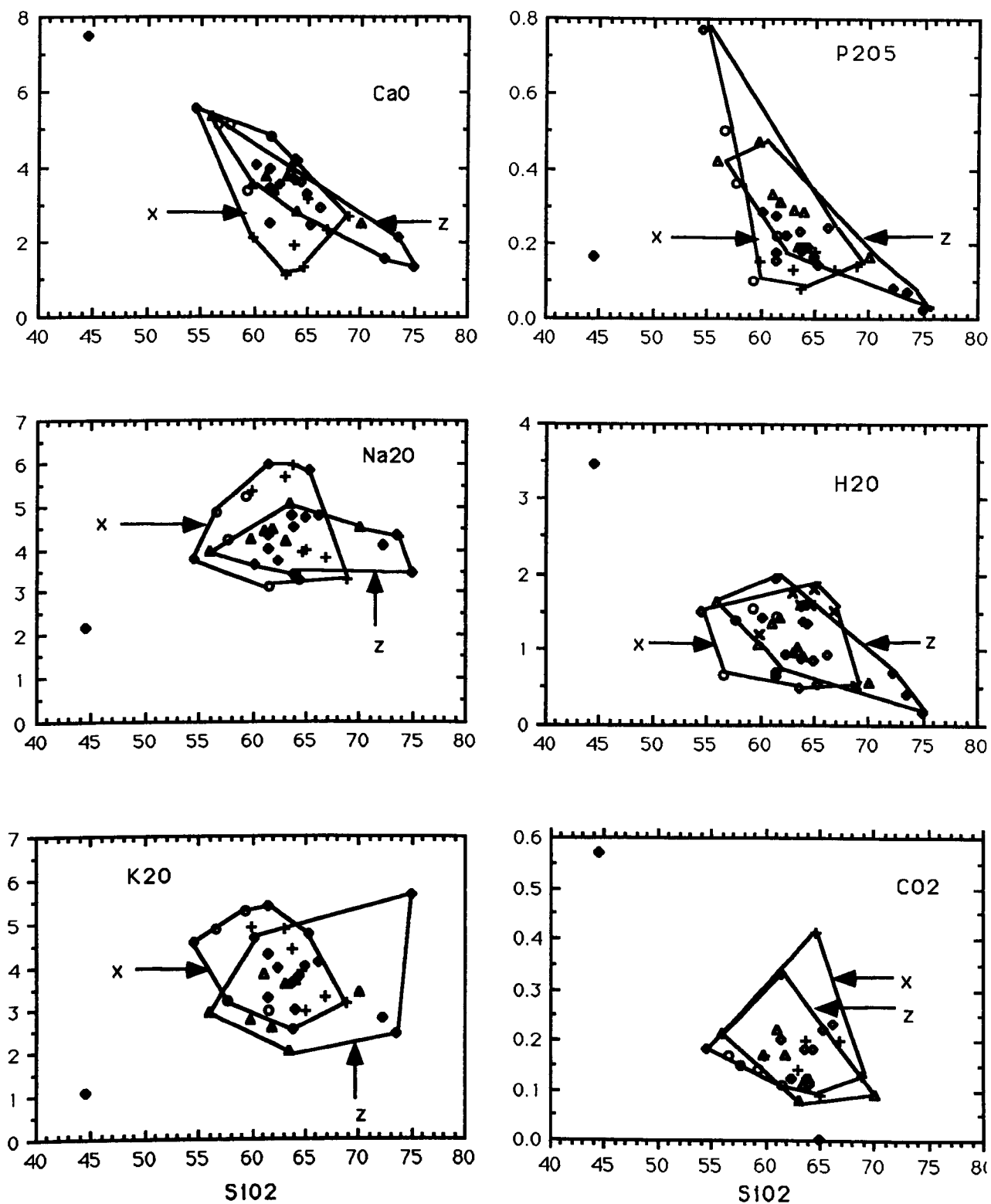
FIGURE 5.2b plots of 6 major element oxides (CaO, Na2O, K2O, P2O5, H2O, CO2) vs. SiO2 for Hornblende-bearing Granites. See Fig. 4.1a for key.
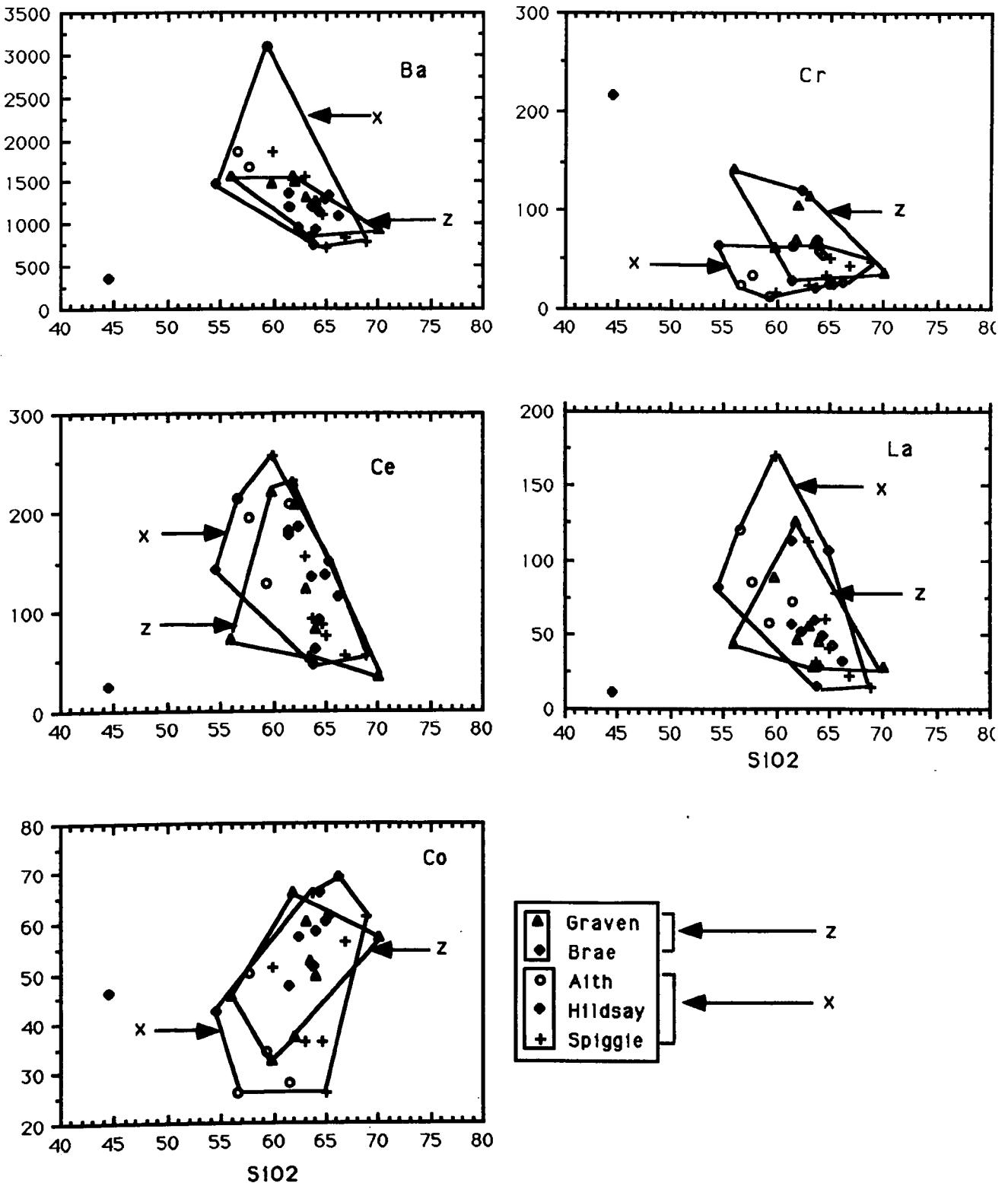
FIGURE 5.2c plots of 5 trace elements (Ba, Ce, Co, Cr, La) in ppm vs. wt% SiO2 for Hornblende-bearing Granites.
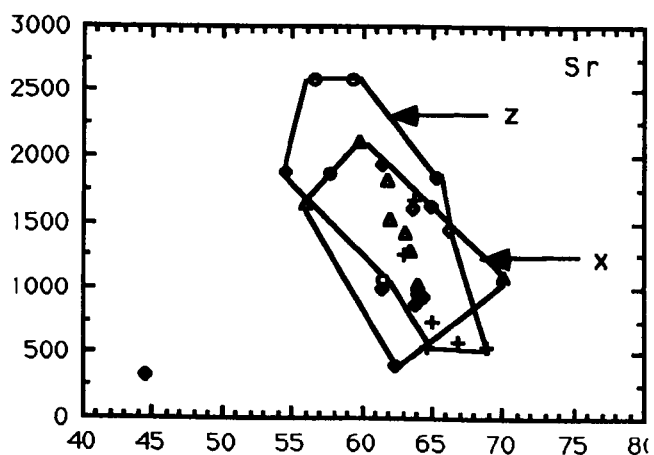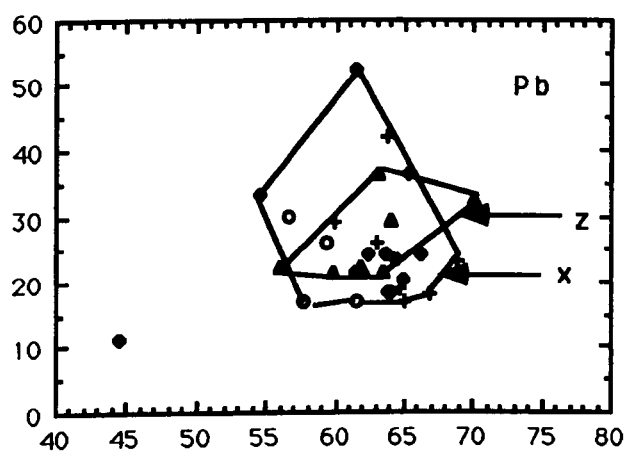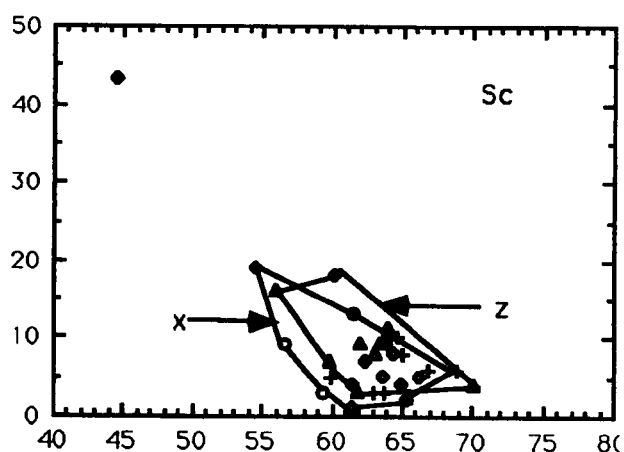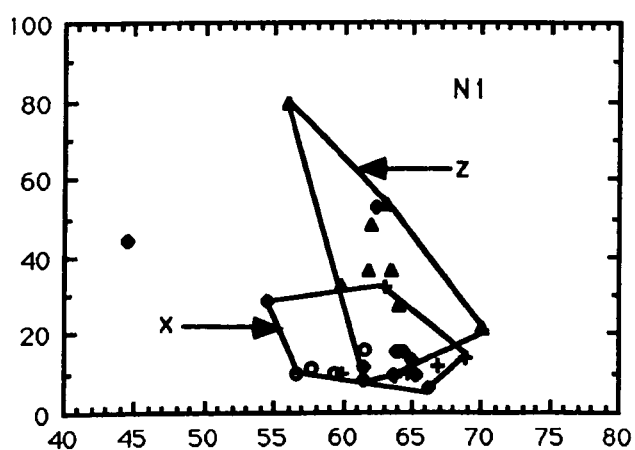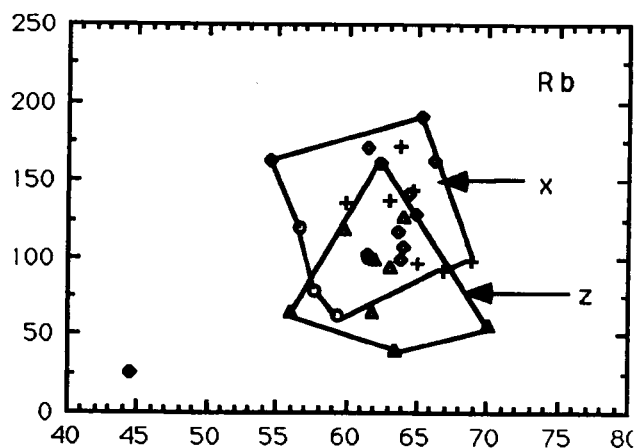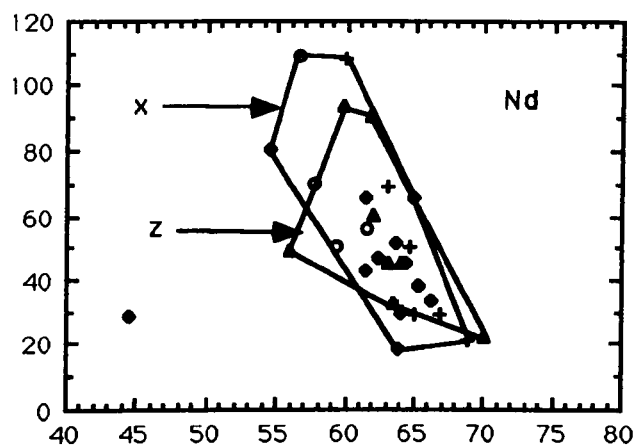
FIGURE 5.2d plots of 6 trace elements (Nd, Ni, Pb, Rb, Sc, Sr) in ppm vs. wt% SiO2 for Hornblenbende-bearing Granites. See Fig. 4.1c for key.
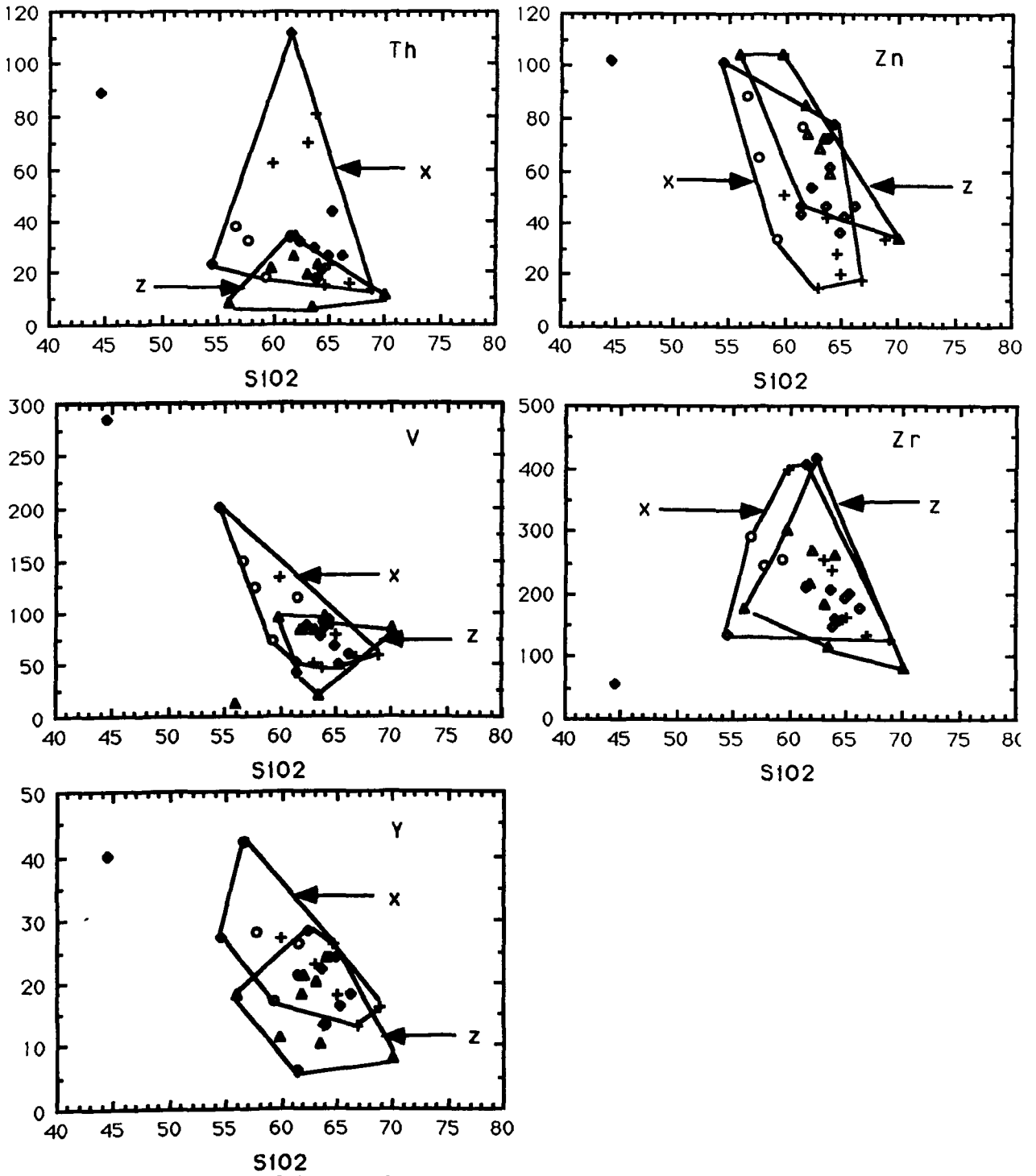
Figure 5.2e plots of 5 trace elements (Th, V, Y, Zn, Zr) in ppm versus wt% SiO2 for hornblende-bearing granites. See Fig. 4.2c for key.

et al., (1966), Adam et al., (1967) . Sawka and Chappell (1985) have
demonstrated that the thorium and potassium increase in plutonic rocks can be
related directly to increase in allanite (+ thorite?) and K-feldspar abundances with
acidity. K_2O is also high in the monzonitic rocks of the Spiggie granite and its two
offshoots and together with the high Th abundances may perhaps be due to
increase of allanites and K-feldspar in these rocks.

On the V content plot versus SiO2, it is clear that the Spiggie granite and its
offshoots show higher V content coupled with a fair negative correlation with silica
content compared with Graven and Brae granites data which form a field rather
than a trend. Both Sc and V are strongly concentrated in the ferromagnesian
minerals presumably substituting for Fe^{3+} (Curtis, 1964) the highest concentration
occurring in hornblende, and to a lesser extent in augite (Ewart and Taylor, 1969).
In the case of the Spiggie granite and its two offshoots the decrease in
clinopyroxene (see modal data appendix 2) and hornblende from quartz diorite
through granodiorite to monzonite may account for the decrease of V. The
extraction of these elements by clinopyroxene and hornblende during fractionation
emphasis their compatible character.

5.3.1 Rubidium-Strontium Ratio

The Rubidium is concentrated in the residual liquid during crystallisation essentially
following K^+ which enters potash feldspar. Strontium on the other hand is
removed from the liquid phase and is concentrated primarily in early formed calcic-
plagioclase. As a consequences, the Rb/Sr ratio tends to increase with
differentiation particularly towards the end of the spectrum where the slope of the
curve increases dramatically (Faure and Powell, 1972).

In the hornblende-bearing granites the Rb/Sr ratio (Figure 4.8a-A) ranges between
0.02-0.4 and does not vary with increasing differentiation Index. This lack of a
variation is attributed to the Sr enrichment of hornblende-bearing granites, which
appear to define a unique curve for the Shetland hornblende-bearing granites.

5.4 Major Element Chemistry of Hornblende-free Granites.

These are a miscellaneous group of rocks to the east of Walls Boundary Fault, which encompass different granitoids of totally different age. They can be arranged in order of decreasing age from older to younger as follows; Breckin (not dated), Tonga ?, Colla Firth (530 Ma) and Skerries (420 Ma), Skaw (357-407 Ma) and Channerwick (399 Ma). Keratophyre and trondhjemite dykes are not dated yet. Brecken, Tonga and Skaw granites occur on the Isle of Unst which is the furthermost of the northern Isles of Shetland, Out Skerries granite which is a continuation of Colla Firth occurs on Out Skerries Island while the Colla Firth occurs on the Mainland of Shetland. Despite different ages and separate localities they show similarities in some aspects of major and trace element chemistry.

The Harker variation diagrams (Figures 4.3a and 4.3b) of rocks from Skaw, Tonga & Brecken, Colla Firth and Out Skerries show three clear trends and it is obvious that the Skaw rocks exibit most abundant constituents of major element oxides on account of their low silica contents and lie mostly on a good negative trend. Thus TiO_2, total iron, MgO, CaO, and P_2O_5 show variations which are consistent with a differentiation model. The good negative trends shown by the Skaw granite which is part of the Unst nappe structure may be attributed in part to its wide range of SiO_2 content (64-70%) compared with Tonga and Breckin (73-75.5%), Colla Firth and Skerries (70-73%) Channerwick (73-75% except one sample 69%) and to the order of crystallisation of the carrier phases of these elements such as rutile, ilmenite, magnetite, biotite, plagioclase and apatite. Chemically the compositionally restricted rocks show little variation in the major and trace element Harker diagrams. However, negative trends for TiO_2, Total Iron, MgO and CaO (only for Colla Firth & Skerries granites) with increasing silica contents can be seen. Al_2O_3 plots show constant variation for Skaw and Colla Firth and Skerries granites at between 14-16%; Channerwick and Tonga & Breckin granites show a weak negative trend with increasing silica contents. Na_2O contents show constant
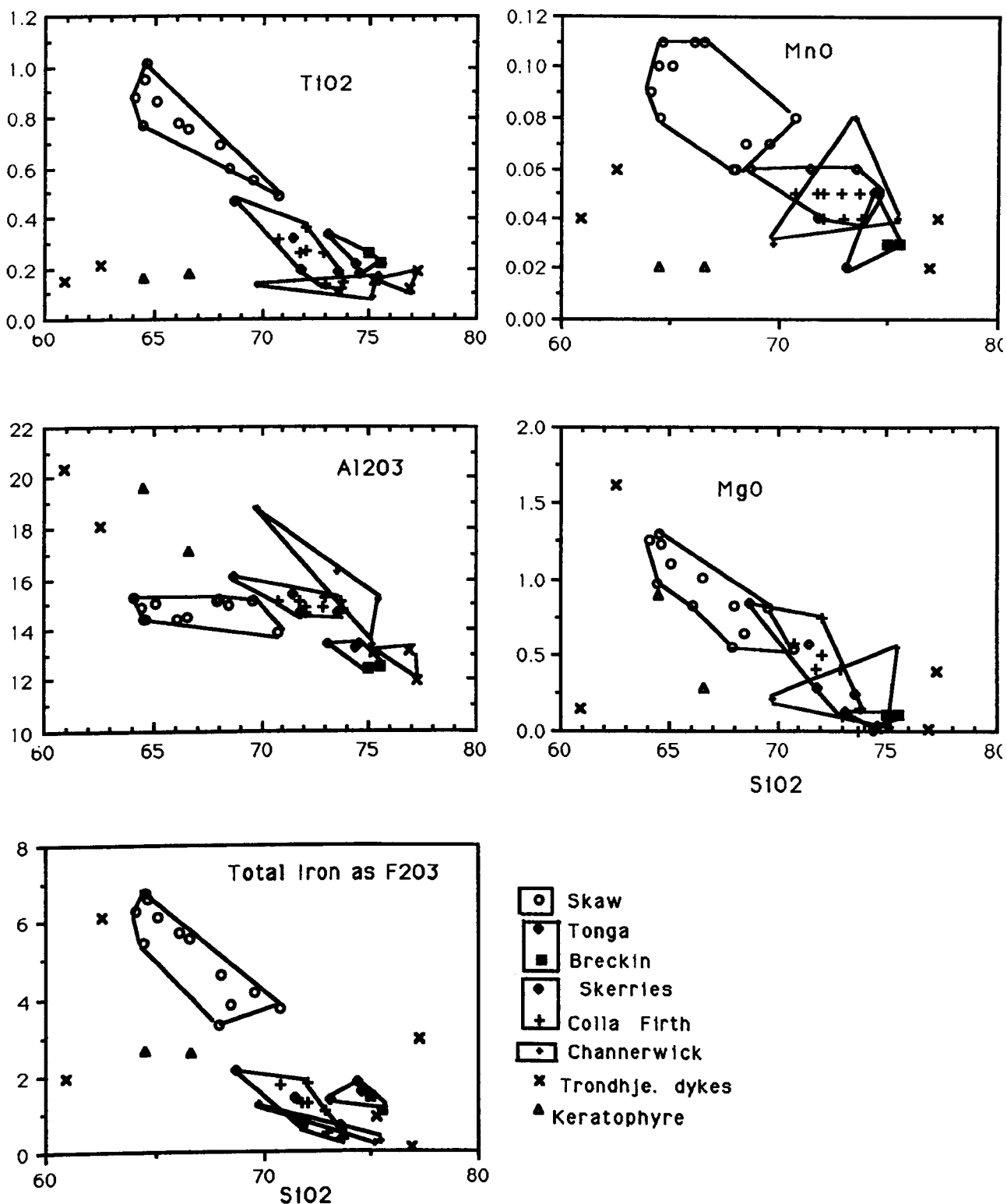
FIGURE 5.3a plots of 5 major element oxides (TiO2, Al2O3, Fe2O3, MnO. MgO) vs. SiO2 for Hornblende-free Granites, values are in wt%.
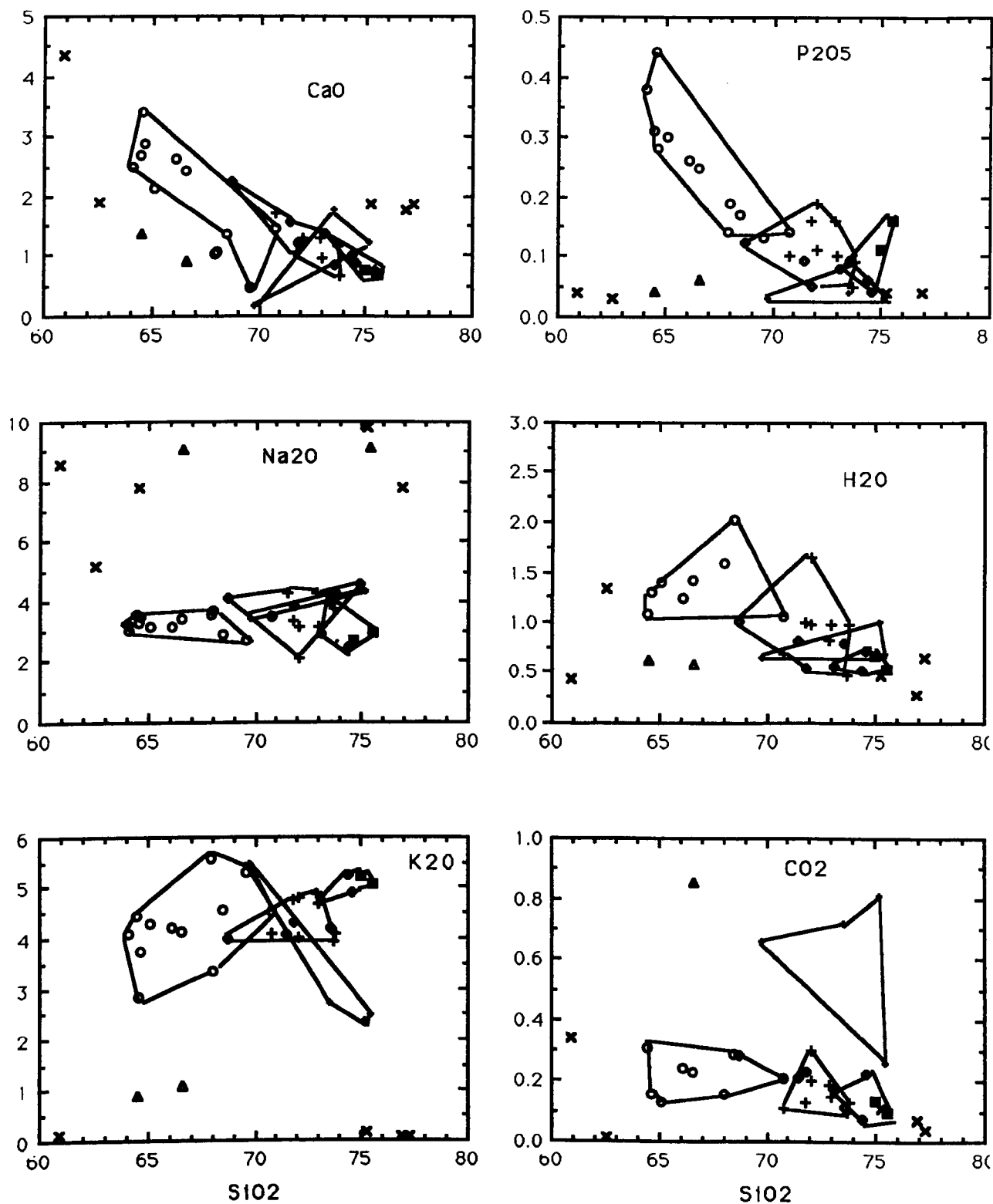
FIGURE 5.3b plots of 6 major element oxides (CaO, Na2O, K2O, P2O5, H2O, CO2) vs. SiO2 for Hornblende-free Granites, values are in wt%. See Fig. 4.3a for key.
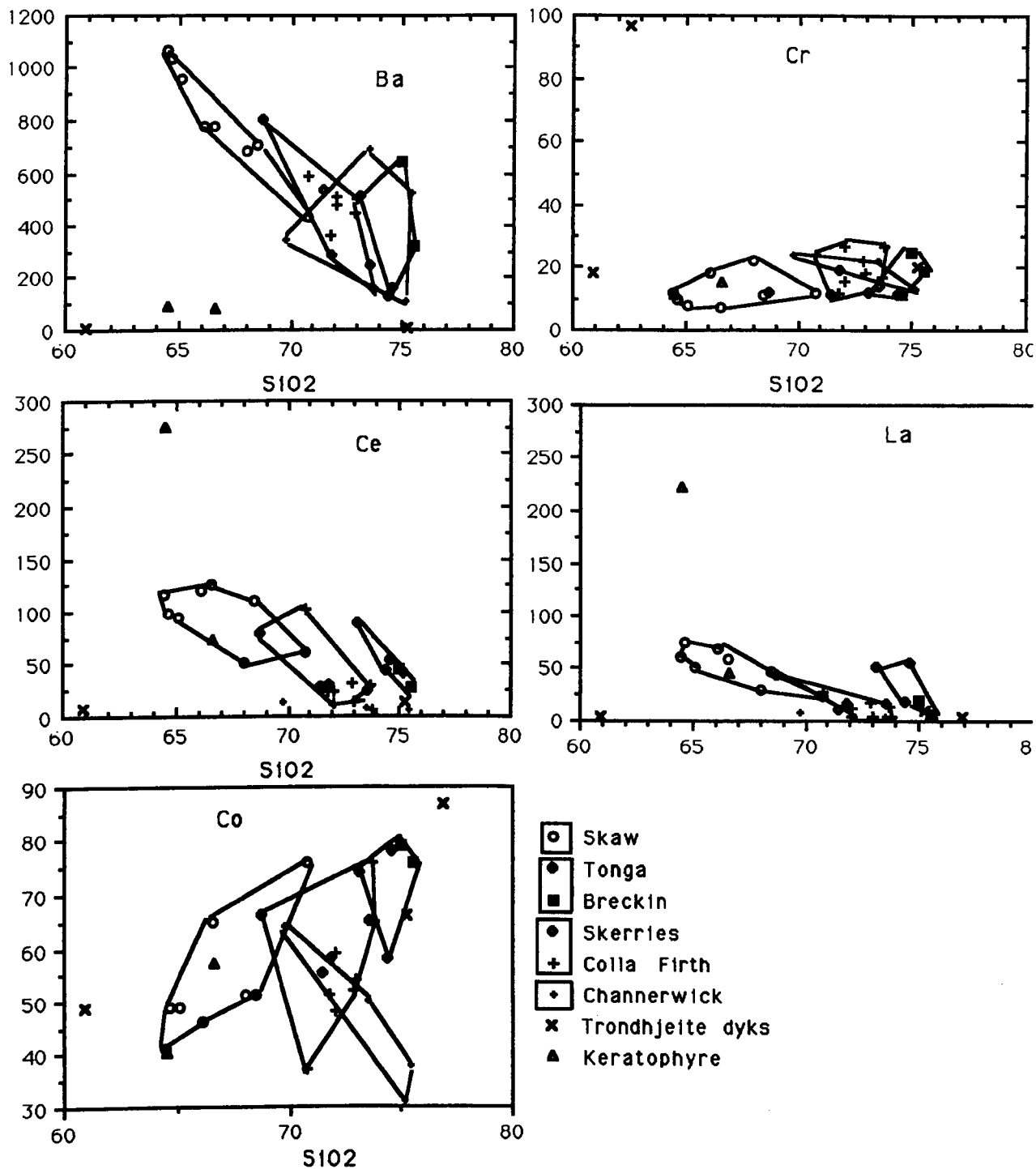
Figure 5.3c plots of 5 trace elements (Ba, Ce, Co, Cr, La) in ppm versus wt% SiO2 for hornblende-free granites.
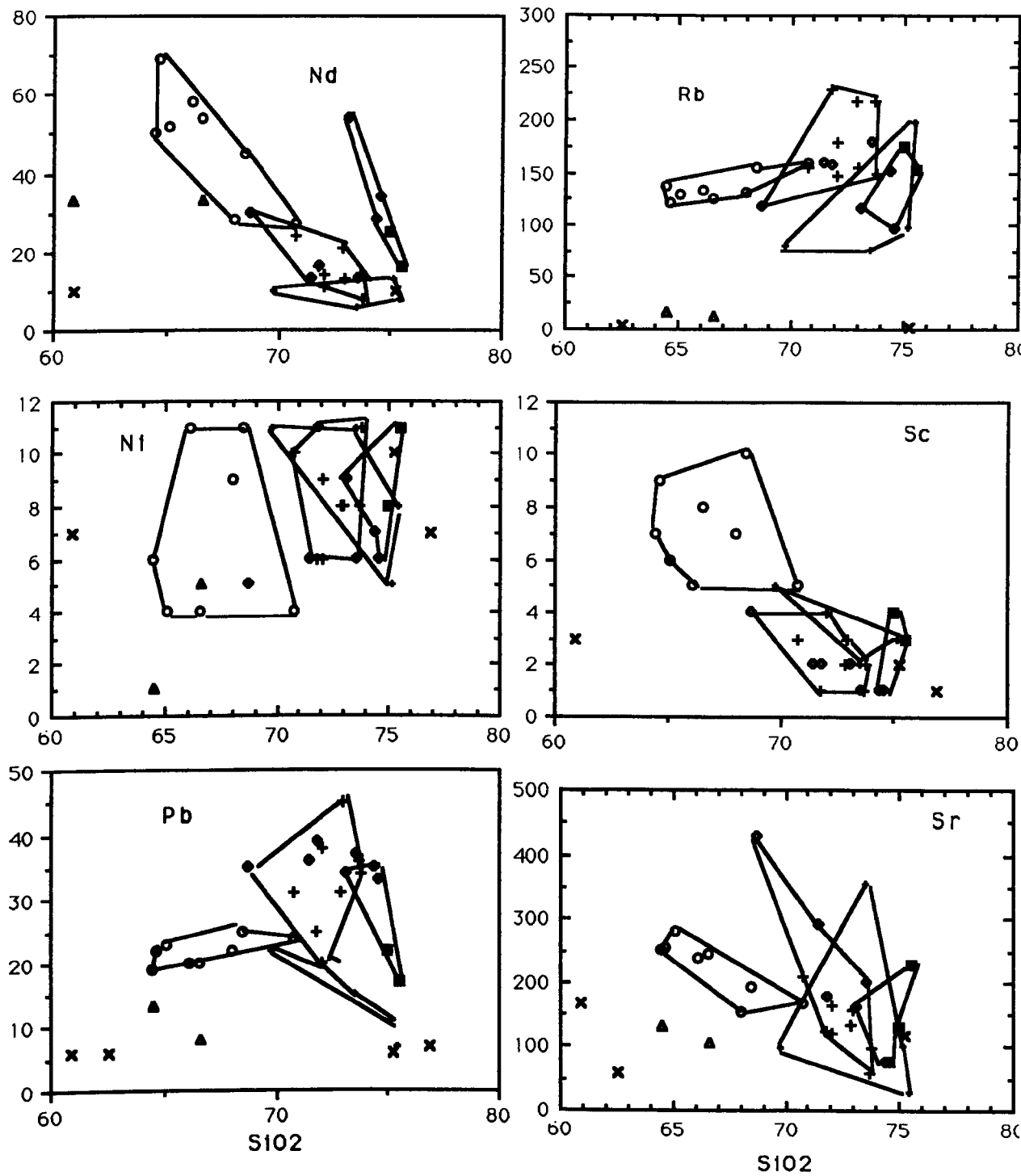
Figure 5.3d plots of 6 trace elements (Nd, Ni, Pb, Rb, Sc, Sr) in ppm versus wt% SiO2 for hornblende-free granites. See Fig. 4.3c for key.
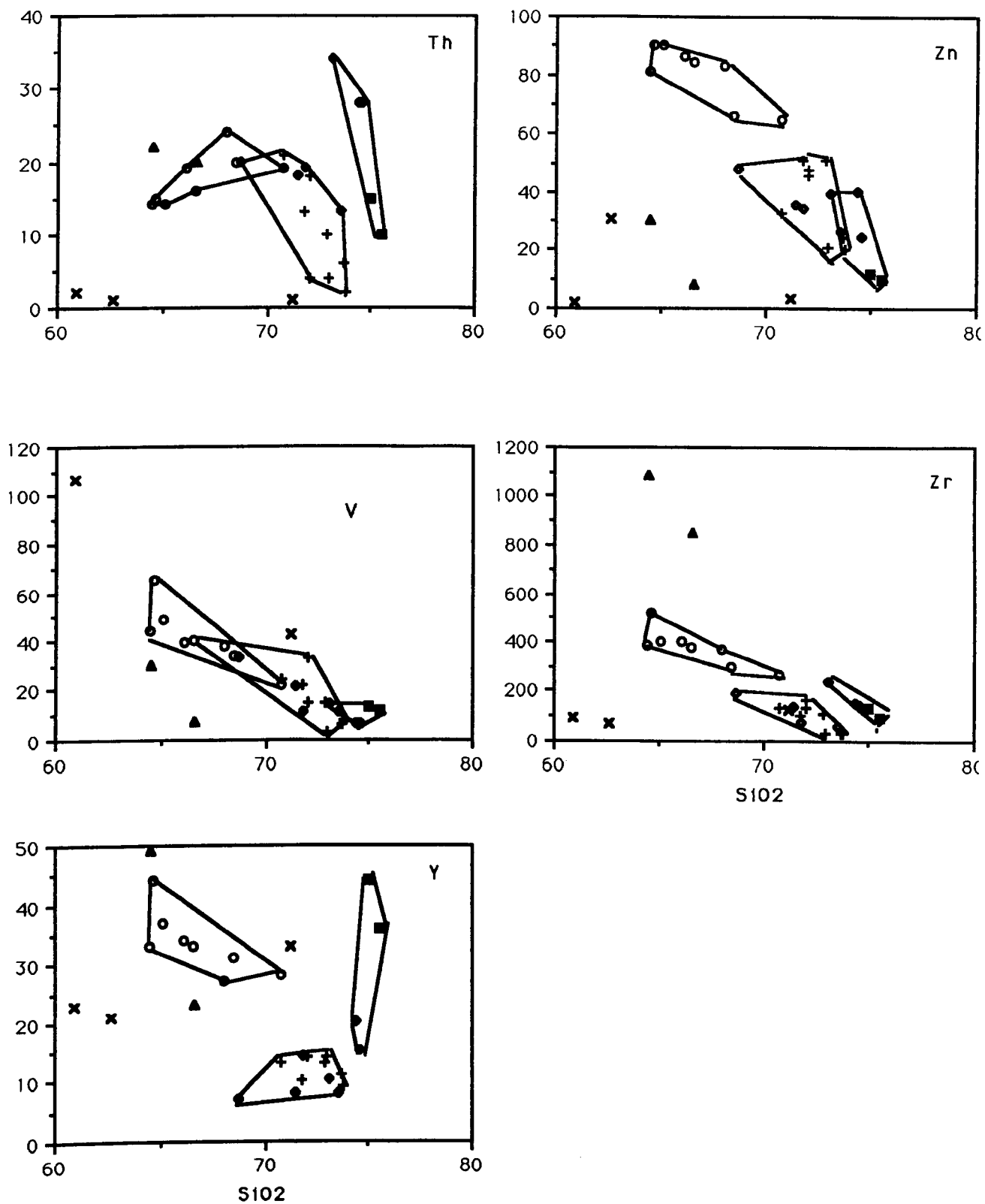
FIGURE 5.3e plots of 5 trace elements (Th, V, Y, Zn, Zr) in ppm vs.wt%
SiO2 for hornblende-free granites. See Fig. 4.3c for key.

variation for most members of the hornblende-free Granites. No particular correlations are found in the plots of K2O, MnO, H2O and CO2 with increasing silica contents; instead they form fields.

Superficially it seems that from Harker variation diagrams (MgO, CaO, P2O5 , TiO2 and Fe2O3, Figure 4.3a and 4.3b), the older granitoids rocks of Breckin and Tonga could be derived by fractionation of the younger Skaw-Colla Firth and Skerries granites which obviously is not true based on their relative age.

5.5 Trace Element Chemistry of Hornblende-free Granites.

The hornblende-free granites trace element data is given in appendix 2. The values of trace elements determined are plotted versus SiO2 in Figures 4.3c, 4.3d and 4.3e. There are three clear trends for Skaw, Tonga & Brecken, Colla Firth & Out Skerries granites of decreasing elemental concentrations with increasing silica content for Ba, Ce, La, Nd, Sr and V. The Co-content shows no correlation with silica contents except for the Skaw granite which show positive correlation. Since the ionic radius and electronegativity of cobalt are similar to those of ferrous iron, it would therefore be camouflaged in the Skaw biotite minerals which will give positive cobalt trend in the Skaw granite. Cr-contents show constant trend with increasing silica contents, Ni, Pb, Rb, Th, show no particular trend with increasing silica.

5.5.1 Rubidium-strontium Ratio versus DI.

In the hornblende-free granites the variation of Rb/Sr (Figure 4.8a) shows a common trend at high DI of increasing Rb/Sr ratio. Each member of this group has its own trend which can be drawn. At least three coherent curves can be seen for the following granites; Skaw (Rb/Sr = 0.46-0.94), Colla Firth (Rb/Sr = 0.74-3.7), Out Skerries (Rb/Sr = 0.27-0.89), and Tonga (Rb/Sr = 0.72-2.04). All show increasing Rb/Sr with increasing DI, except Breckin (Rb/Sr = 0.67-1.34)

which exibits a limited variation and no correlation with DI. Channerwick appears to have wide variation and no correlation (Rb/Sr = 0.21-7.11) with increasing DI. The keratophyre and trondhjemite rocks are charactrized by very low Rb/Sr ratio and this is due to their possession of very low K contents. The Rb/Sr ratio for this group defines its own unique curve with DI.

5.6 Major Element Chemistry of Ronas Hill Granite and its Granitic Satellites

The Ronas Hill Granite and its satellites lie to the west of the Walls Boundary Fault and North of Bixter Voe. The samples of Ronas Hill Granite and its satellites were collected and analysed for major elements (data set in appendix 2) which were plotted on the variation diagrams (Figures 4.4a and 4.4b) to establish the general trend in the geochemistry of the suite. The Ronas Hill Rafts which are fine and coarse-grained gabbro and diorites, have a silica content ranging between 50 and 58 wt % and plot in areas distinct from the Ronas Hill granite and its satellites on the Harker diagrams. The granitic portion of Ronas Hill and its satellites are compositionally very restricted (73-77% SiO_2) and show considerable overlap on both major and trace element variation Harker diagrams .

The Harker variation diagrams (Figure 4.4a & 4.4b) show very weak decreasing trends for TiO_2, Al_2O_3, Total iron and CaO with increasing silica contents. Na_2O and K_2O contents are approximately constant at between 4 and 5%. MgO slightly decrease wirh SiO_2 increase and MnO content are constant at between 0.03 and 0.39%. The H_2O content shows a weak decrease with increasing silica content and the CO_2 content varies randomly. Gabbros and diorites rafts always plot separately and there are no intermediate rock compositions, suggesting mixing between the basic and acidic rocks was restricted or did not occur.
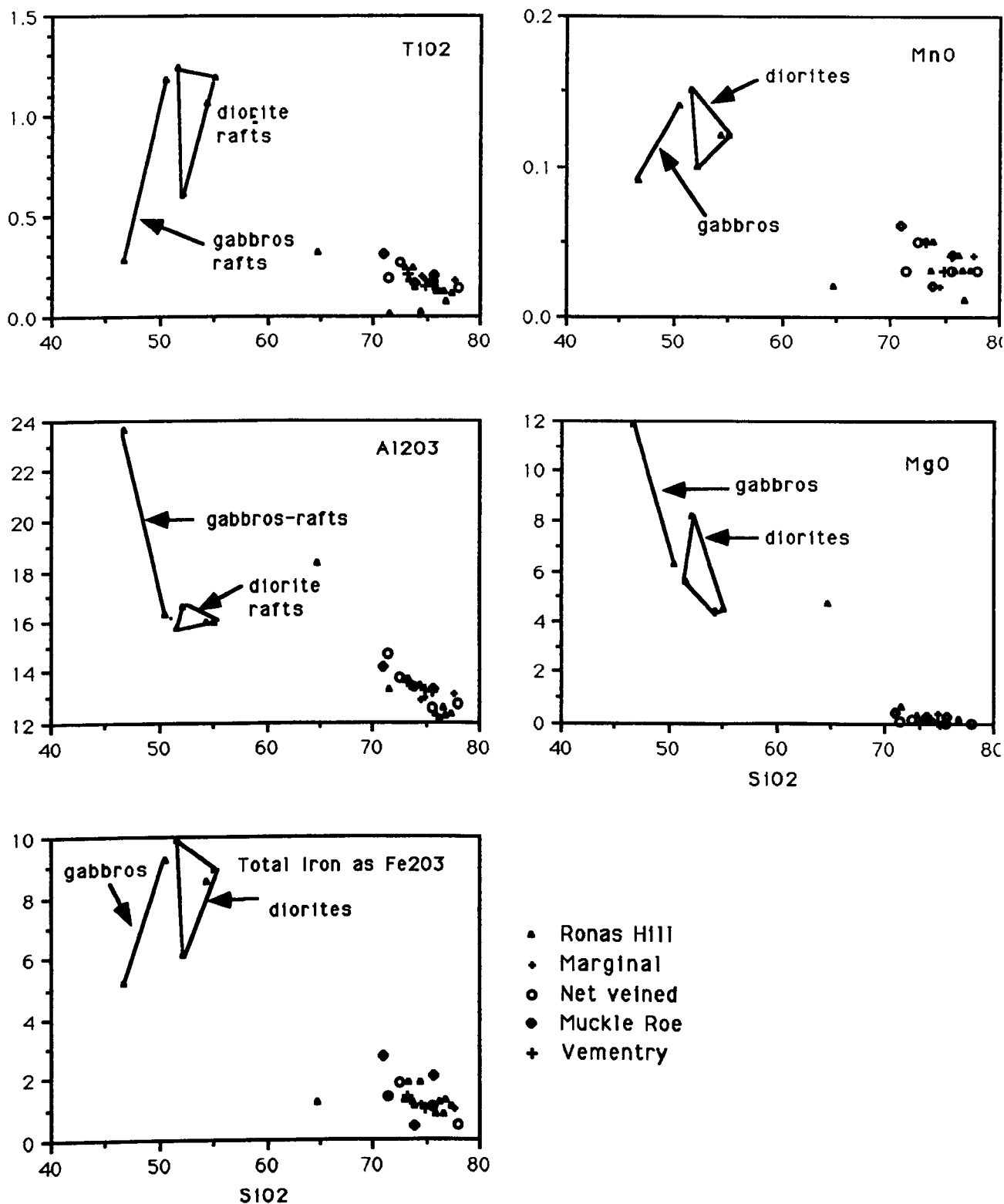
FIGURE 5.4a plots of 5 major element oxides (TiO2, Al2O3, Fe2O3, MnO, MgO) vs. SiO2 for Granites to the North of Bixter Voe and west of WBF, all values are in wt%.
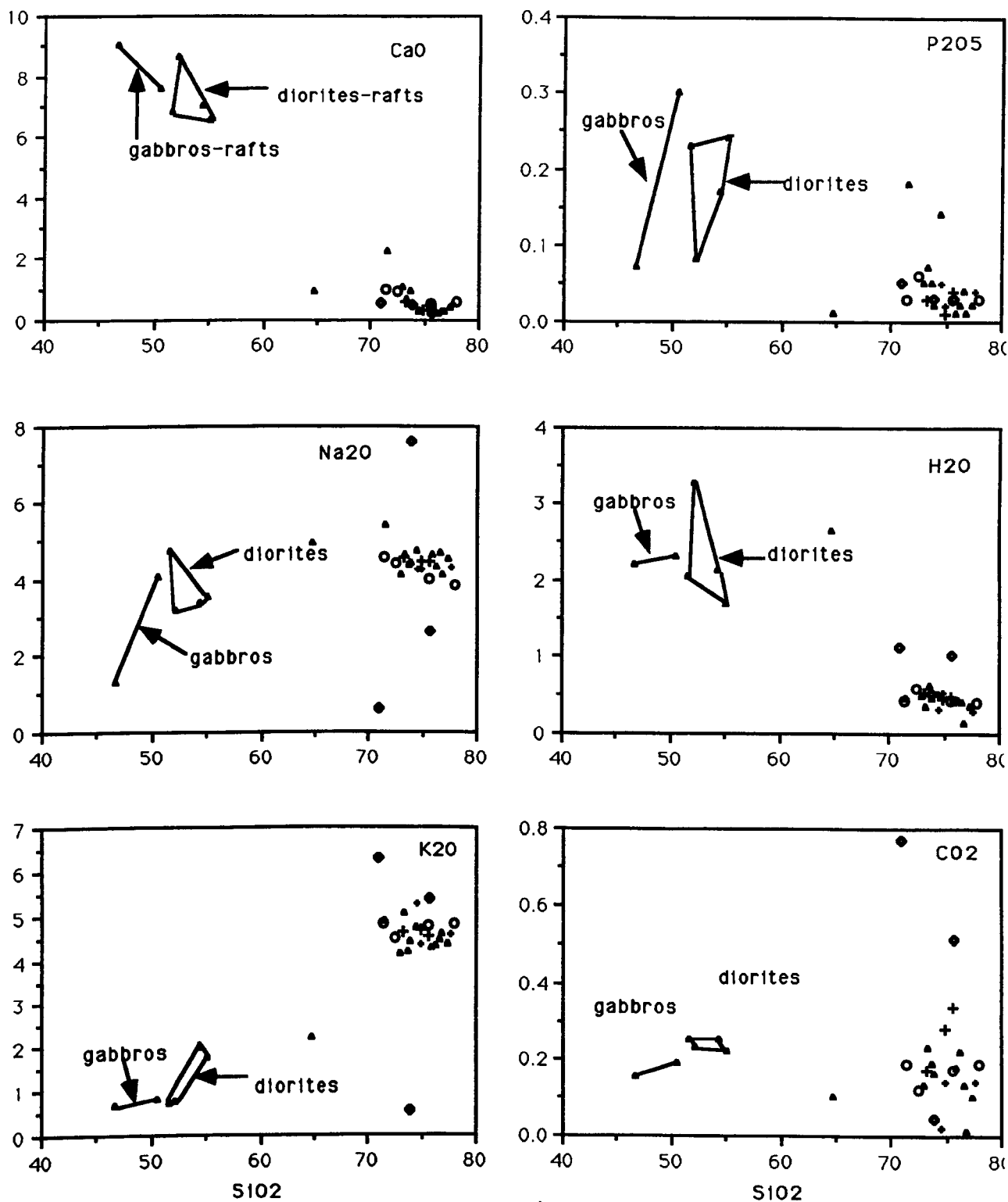
FIGURE 5.4b plots of 6 major element oxides (CaO, Na2O, K2O, P2O5, H2O, CO2) vs. SiO2 for Granites to the North of Bixter Voe and west of of WBF. See Fig. 4.4a for key. Gabbros and diorites are rafts in the Ronas Hill granite.
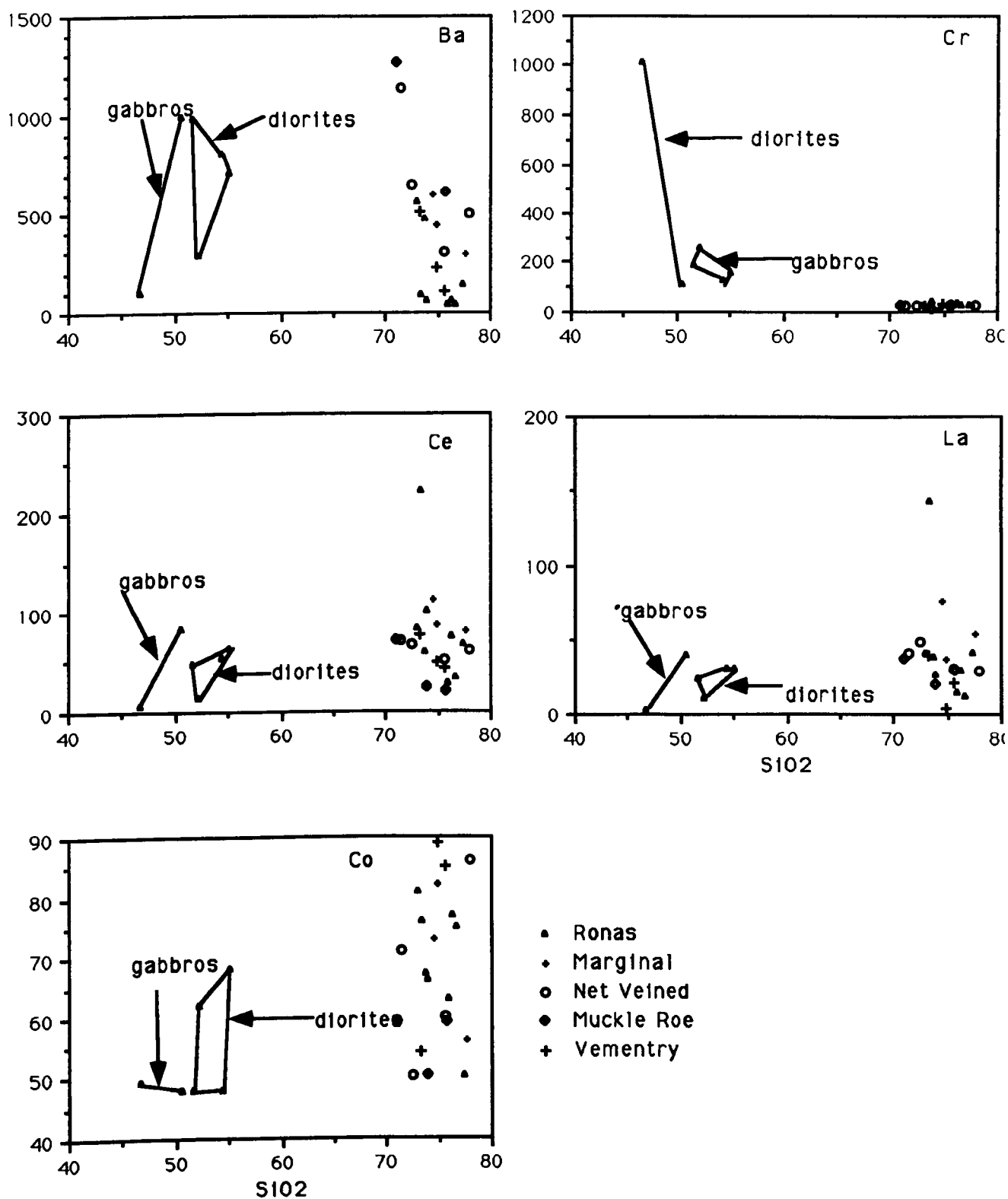
FIGURE 5.4c plots of 5 trace elements (Ba, Ce, Co, Cr, La) in ppm vs.
SiO2 for Granites to the North of Bixter Voe and west of WBF. Gabbros and diorites
are rafts in the Ronas Hill granite.
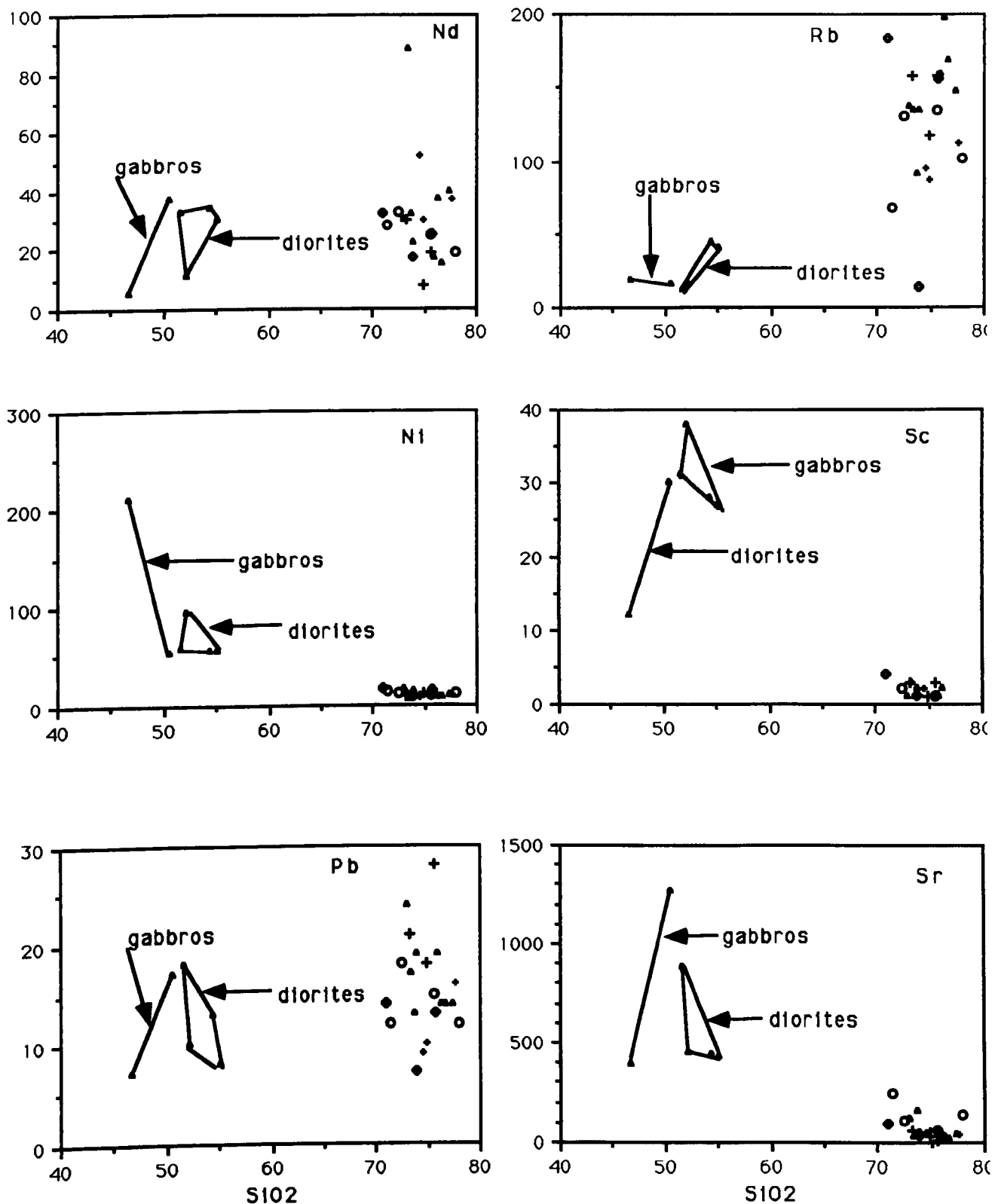
FIGURE 5.4d plots of 6 trace elements (Nd, Ni, Pb, Rb, Sc, Sr) in ppm vs.
SiO2 for Granites to the North of Bixter Voe and west of WBF. See Fig.
4.4c for key. Gabbros and diorites are rafts in the Ronas Hill granite.
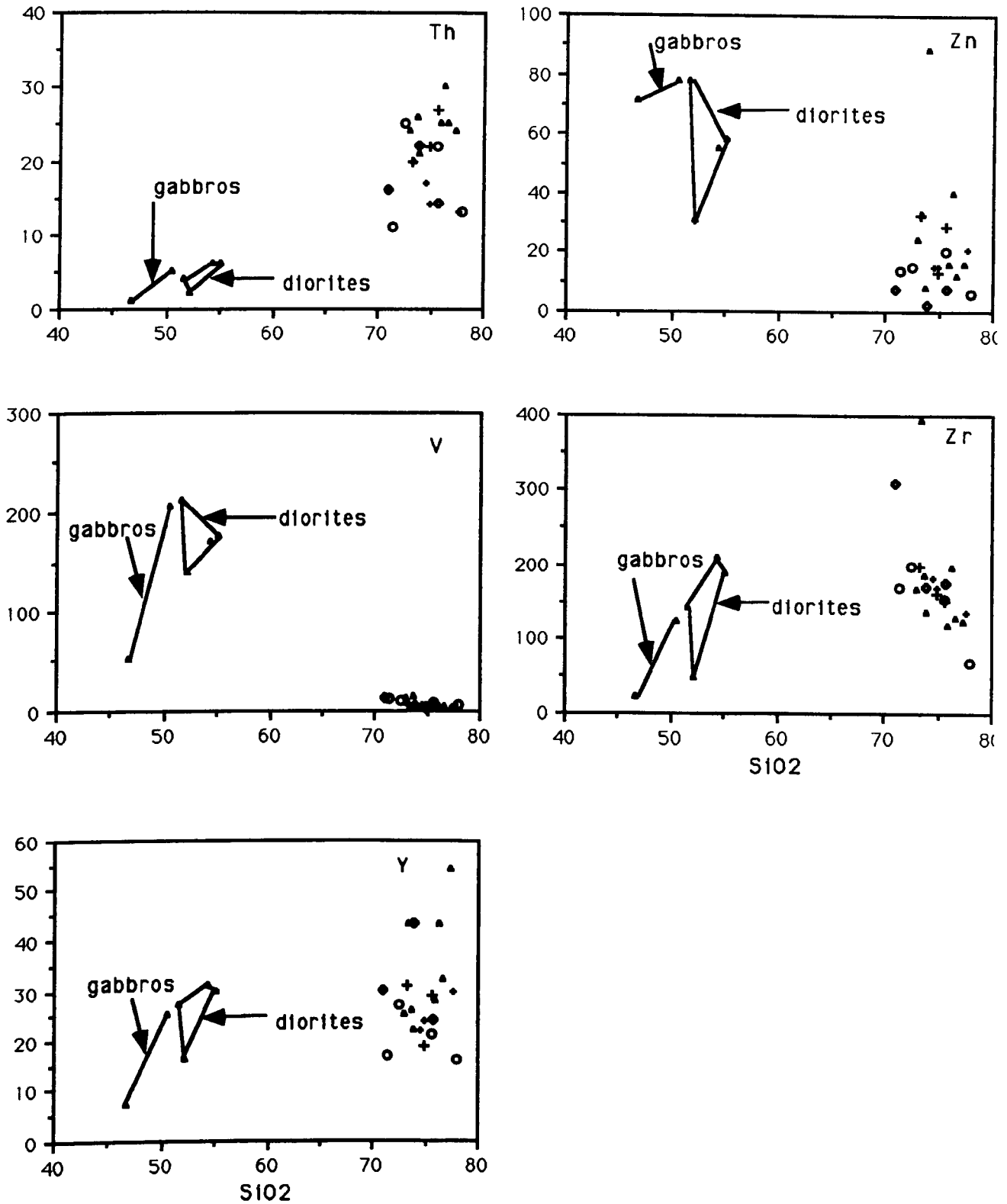
FIGURE 5.4e plots of 5 trace elements (Th, V,Y, Zn, Zr) in ppm vs.
SiO2 for Granites to the North of Bixter Voe and west of WBF. See
Fig. 4.4c for key. Gabbros and diorites are rafts in the Ronas Hill granite.

5.7 Trace Element Chemistry of Ronas Hill Granite and its Granitic Satellites

The samples of Ronas Hill Granite and its granitic satellites were analysed for trace elements (data in appendix 2). The trace element values are plotted against silica contents in Figures 4.4c, 4.4d & 4.4e. It is clear that there is no correlation for the elements Ba, Co, Ce, La, Nd, Pb, Rb, Th and Y with increasing silica contents. Cr, Ni, Sc, Sr and V are do not vary with increasing silica contents. Zr decreases with increasing silica contents, presumably due to zircon precipitation. Scandium is below its limit of detection in some samples of the Ronas Hill Granites. Crude separation of the data i.e low Ba in the Ronas Hill granite, suggest rather different sources and/or melting for these separate intrusions.

5.7.1 **Rubidium-Strontium Ratio**

In the Ronas Hill Granites the Rb/Sr (Figure 4.8b) data indicate that the Marginal granite (Rb/Sr = 1.58-2.89), Net Veined granite (Rb/Sr = 0.73-2.25) and Muckle Roe granophyre (Rb/Sr = 0.41-4) have limited ranges compared with Ronas Hill (Rb/Sr = 0.02-10.56) and Vementry (Rb/Sr = 2.87-11.29) Granites. The Rb/Sr ratio shows a crude correlation with increasing DI with Rb/Sr values up to 11.29. These high values are a characteristic feature of the Ronas Hill Granite and its satellites. Note Ronas Hill and Vementry form a steep positive correlation suggesting extreme fractionation and a family likeness.

5.8 The Relation of Esha Ness volcanic rocks with Ronas Hill Granites and its Satellites.

Volcanic rocks of Old Red Sandstone age in Shetland lie immediately to the west of the Ronas Hill granite near Esha Ness. The O.R.S. sequence of Esha Ness is dominantly volcanic and has been described by Finlay (1930) and summarized by Flinn in Mykura (1976). The older beds are sandstones, which are faulted by the
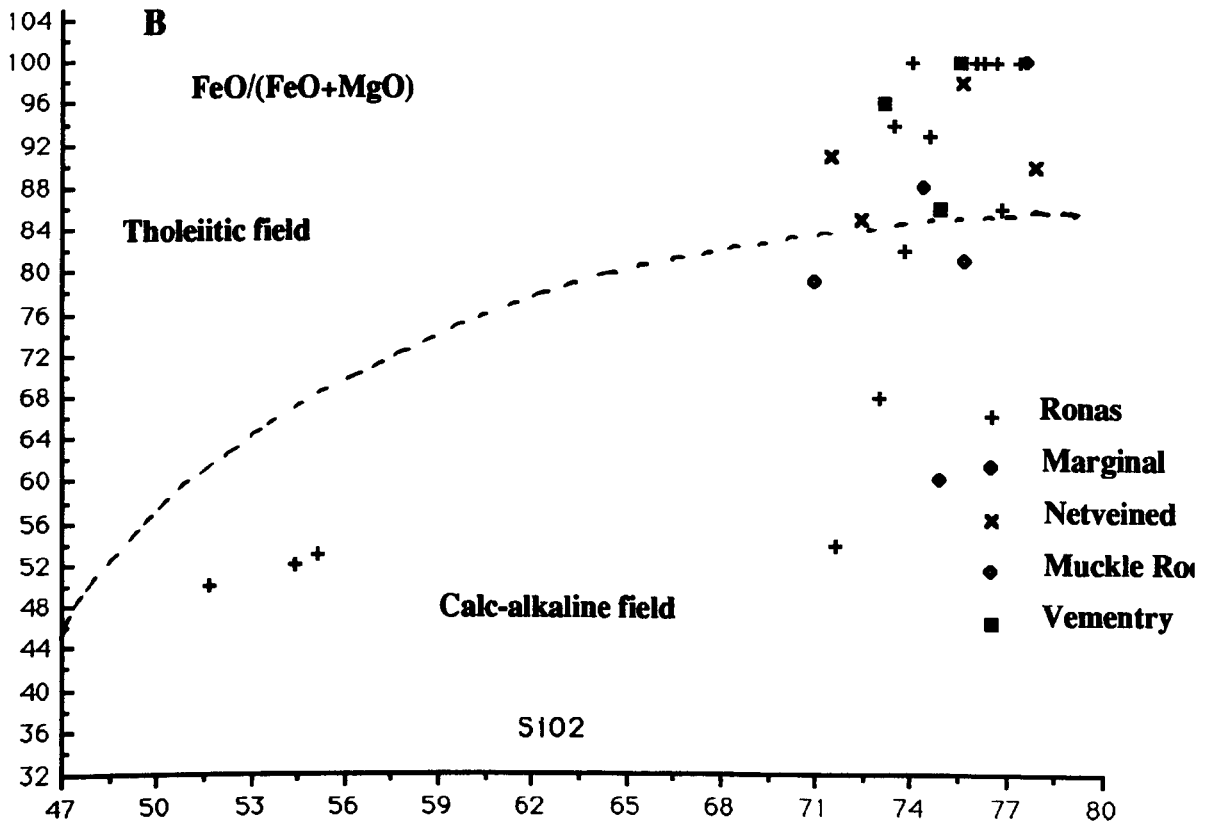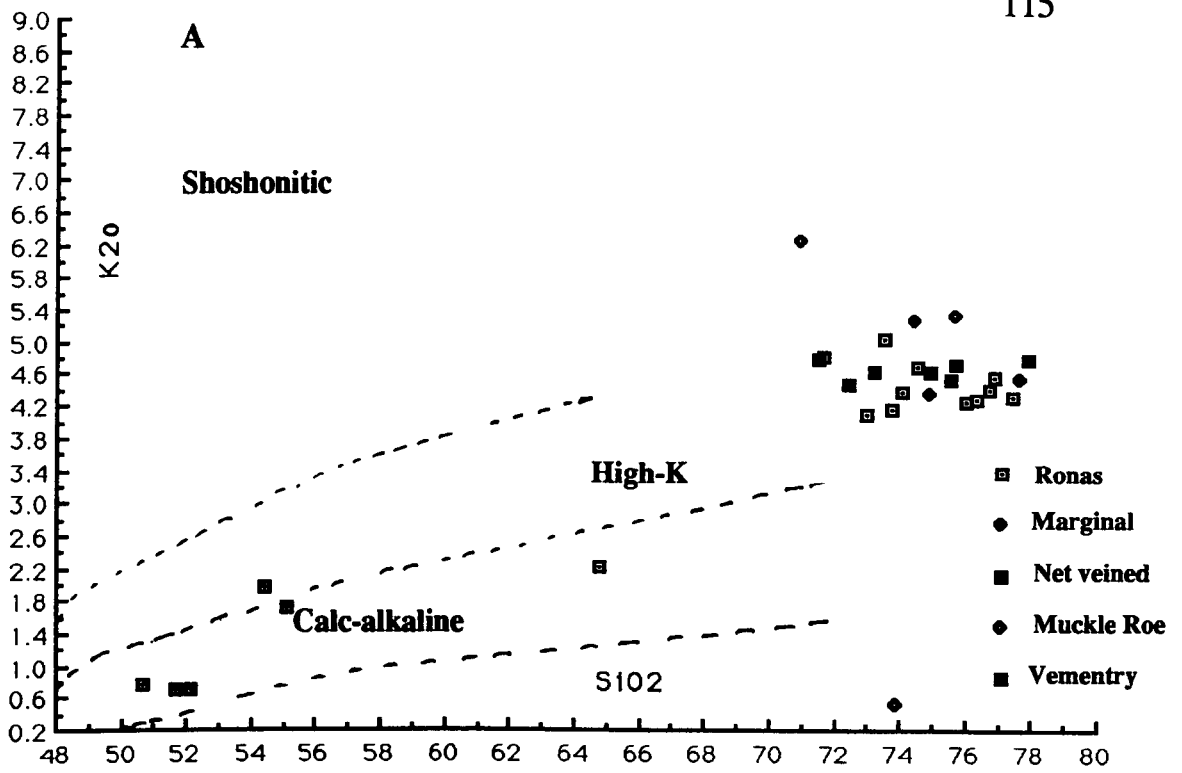
Figure 4.5a. A) plot of K2O versus SiO2 for Ronas Hill granite and its satellites, boundaries from Peccerilo and Taylor (1976). B) plot of FeO/(FeO+MgO) versus SiO2 for same rocks (Miyashiro, (1974).

Fig. 5. 5b of Shetland (after Thirlwall, 1979) (field for Esha Ness ignimbrites)

a : boundaries from Peccerilo and Taylor (1976)
b : boundary from Miyashiro (1974)
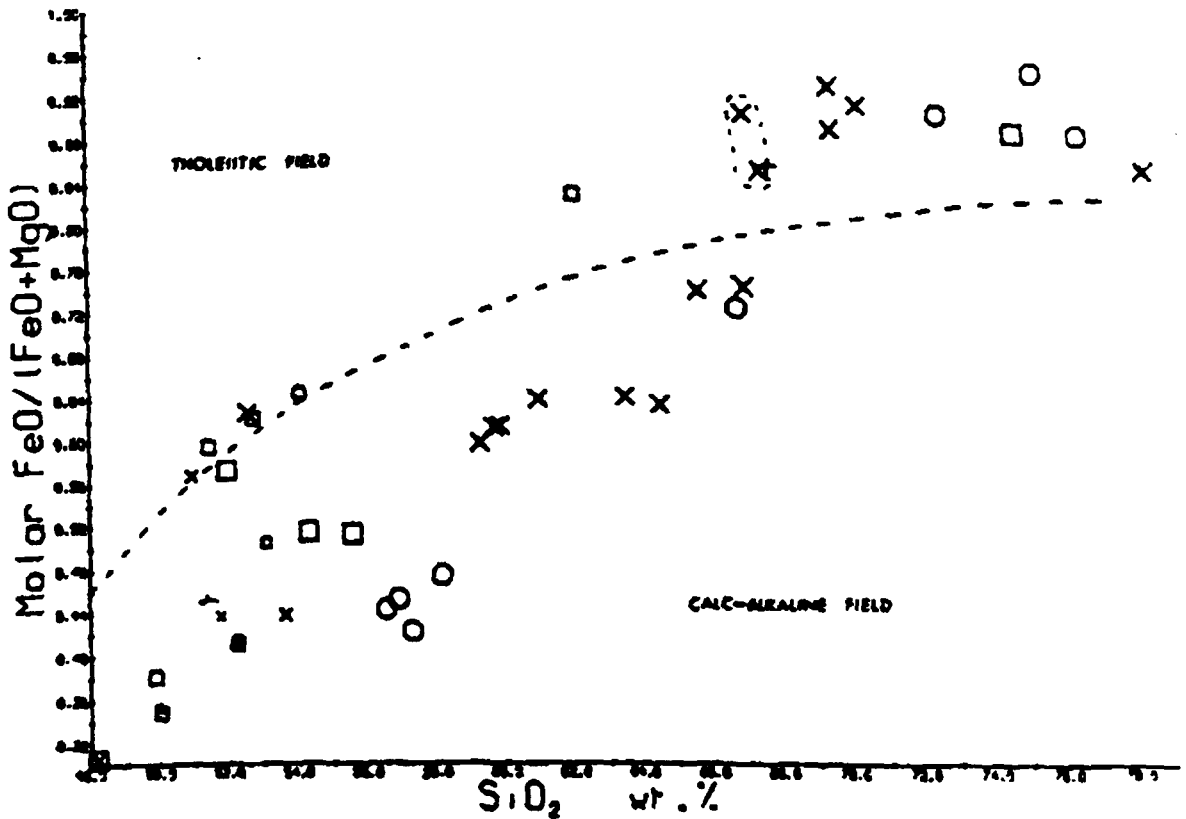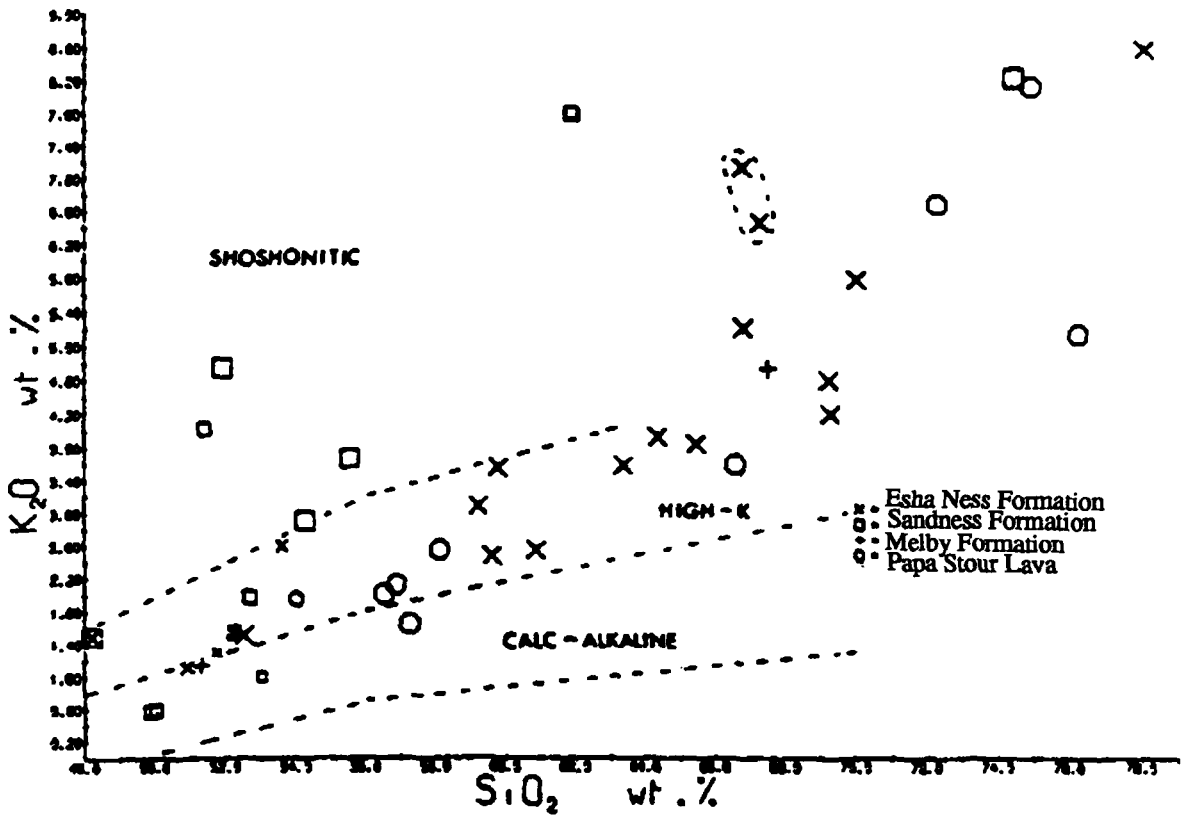
Magnus Bay fault against the Northmaven plutonic complex, but the rest of the sequence is volcanic, and includes olivine-basalts, andesites, pyroxene-andesites, rhyolites and tuffs, with a mugearite and an ignimbrite. The Ronas Hill granite and its satellites have given K-Ar ages near to 350 Ma (Miller and Flinn, 1966), while the Esha Ness volcanic are Eifelian in age (381 Ma) (J. Marshall, 1981). Thirlwall (1981) pointed out that the lower Old Red Sandstone Volcanics of the Midland Valley of Scotland are calc-alkaline and show a spatial chemical variation which may be explained by their being generated at differing distances from an active subduction zone. As to Shetland, Thirwall (1981) points out that the Shetland lavas i) have relatively iron-rich pyroxene; ii) show a different fractionation history with basic parental magmas fractionating under low pressure; and iii) the more basic rocks are distinctly more alkali-rich than the rest of the province. However, the Shetland lavas are not at all alkaline, some are transitional between calc-alkaline and tholeiitic. The Shetland lavas are in fact more chemically similar to modern arc volcanics than the mainland ORS lavas. Thirwall (1982) stated that Shetland lavas show most of the characterstic features of the modern arc volcanics including the marked enrichment in hydrophile elements (K, Rb, Ba, Sr) relative to REE and HFS elements. Their relationship to their adjacent Ronas Hill granitic rocks is not clear because of the difference in age and chemistry. The Ronas Hill granite and its satellites (Figure 4.5a) have compositions which in the K2O-SiO2 classification of Peccerilo and Taylor (1976) span the range from shoshonitic to calc-alkaline. The volcanic rocks of Esha Ness exhibit the same range with a more regular distribution, half of the Esha Ness analyses plot in the shoshonitic field (Figure 4.5b).

On the Fe/Mg plot versus SiO2 most of the Ronas Hill granite and its satellites plot within the tholeiitic field of Miyashiro (1974) , although many Shetland lavas (Figure 4.5b) plot close to the dividing line. Most of the Esha Ness volcanic rocks are very similar to Ronas Hill granite and its satellites rocks and mostly plot in the tholeiitic field. Thirlwall (1979) has described the volcanic rocks of Shetland as

having low to moderate alumina (<16.5%) and this feature also is present in the

Ronas Hill granite and its satellites. These criteria and the relatively iron-rich

pyroxenes suggest that the volcanic rocks are best classified as transitional between

calc-alkaline and tholeiitic, despite the high levels of K2O (Figure 4.5b). The high-

K character of the volcanic and plutonic rocks suggest the source may be similar,

although the trace elements are not compatible as the volcanic rocks have high Sr

and low Rb which is the opposite to that seen in the Ronas Hill granite.

5.9 Major Element Chemistry of the Sandsting and Bixter Granites.

The Sandsting and Bixter Granites are situated to the west of the Walls Boundary

Fault and south of Bixter Voe. The samples of Sandsting and Bixter Granites were

analysed for major elements (data in appendix 2). The Harker variation diagrams

(Figure 4.6a & 4.6b) show good decreasing trends for the major oxides TiO2,

Al2O3, total iron, MnO, MgO, CaO and to a lesser extent P2O5 with increasing

silica contents. Na2O contents are nearly constant at between 3.5 and 4.5%. K2O

contents increase with increasing silica contents. H2O shows a crude decrease

with silica increase and the CO2 contents varies randomly. The major element

variation of Sandsting Granite shows that it is consistent with a differentiation

model and suggests the Bixter granite as an end product of magmatic differentiation

of Sandsting; the phases involved in the fractionation include rutile, ilmenite,

magnetite, hornblende, biotite, plgioclase, apatite and K-feldspar.

5.10 Trace Element Chemistry of the Sandsting and Bixter Granites

The samples of Sandsting and Bixter Granites discussed above were analysed for

trace elements (data set in appendix 2). The values for the trace elements

determined are plotted against SiO2 contents (Figures 4.6c, 4.6d and 4.6e). A

broad negative correlation can be seen for the elements Ba, Ce, Cr, , Ni, Sc, Sr, Zn

and Nd with increasing silica contents. V and Ti show a sharp negative

correlations while Co, Rb and Th give positive correlations with increasing silica
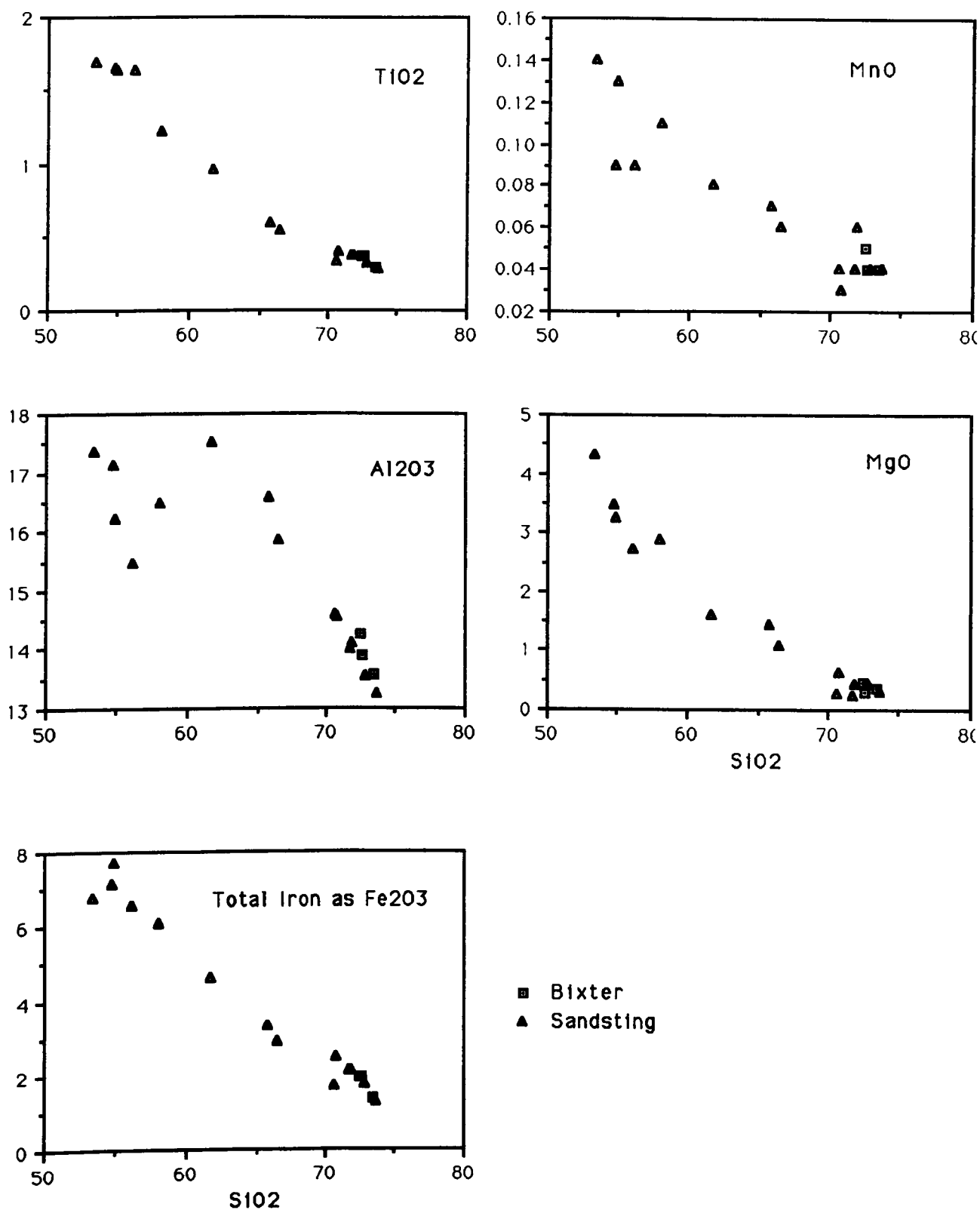
FIGURE 5.6a plots of 5 major element oxides (TiO2, Al2O3, Fe2O3, MnO, MgO) vs. SiO2 for Granites to the west of WBF and South of Bixter Voe, all values are in wt%.
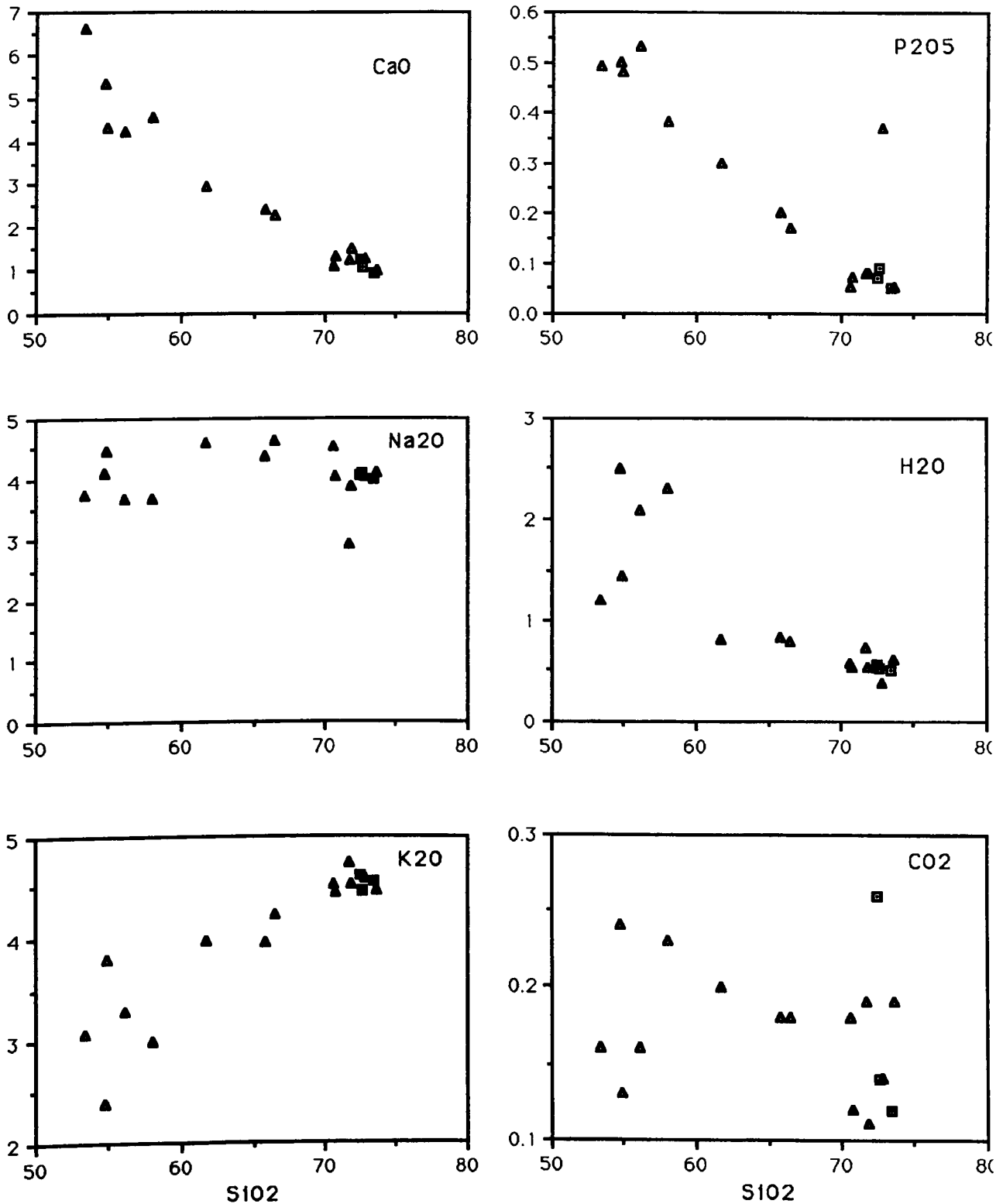
FIGURE 5.6b plots of 6 major elements oxides (CaO, Na2O, K2O, P2O5, H2O, CO2) vs. SiO2 for Granites to the west of WBF and South of Bixter Voe, all values are in wt%. See Fig. 4.6a for key.
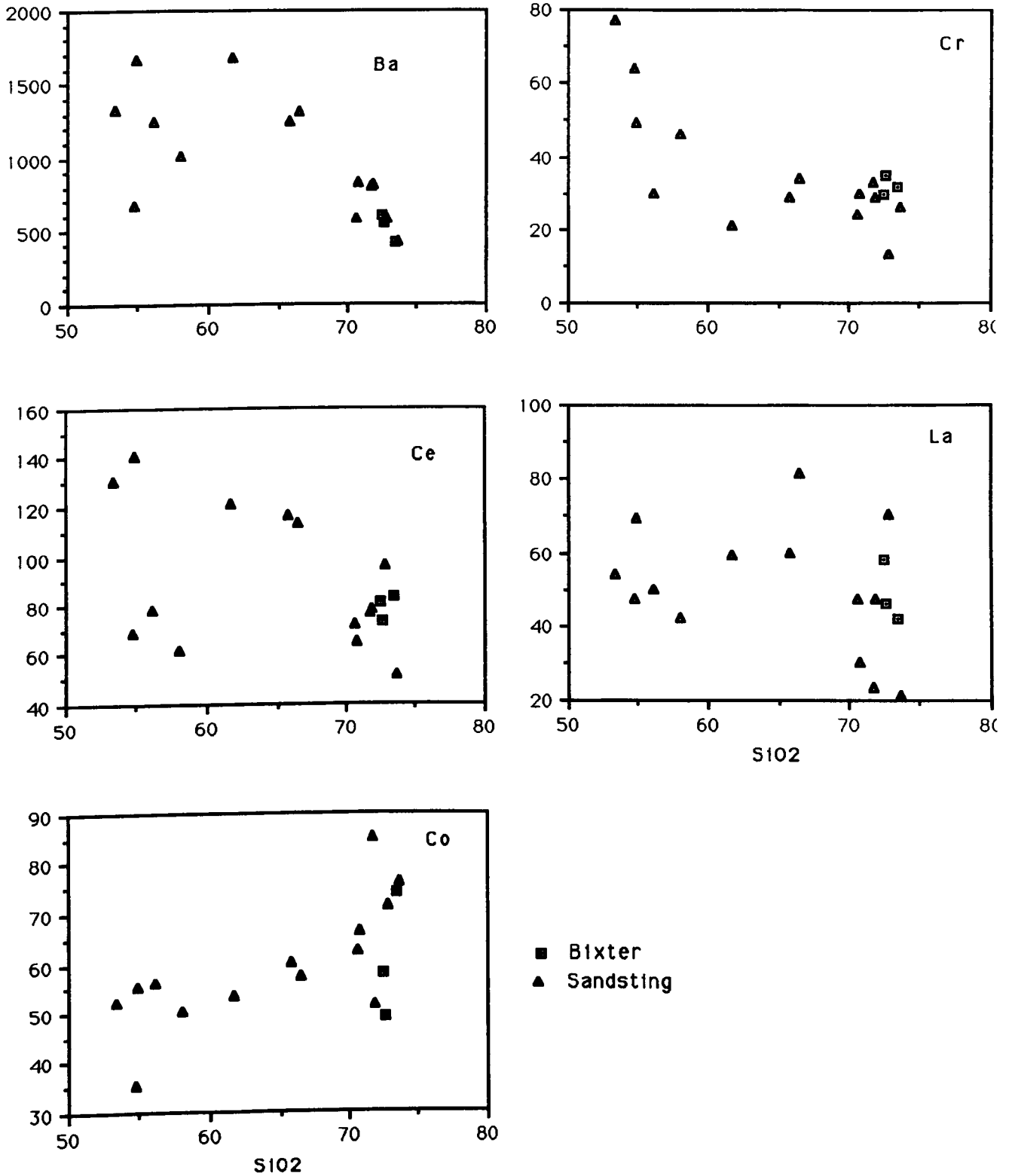
FIGURE 5.6c plots of 5 trace elements (Ba, Ce, Co, Cr, La) in ppm
vs. SiO2 for Granites to the west of WBF and South of Bixter Voe.
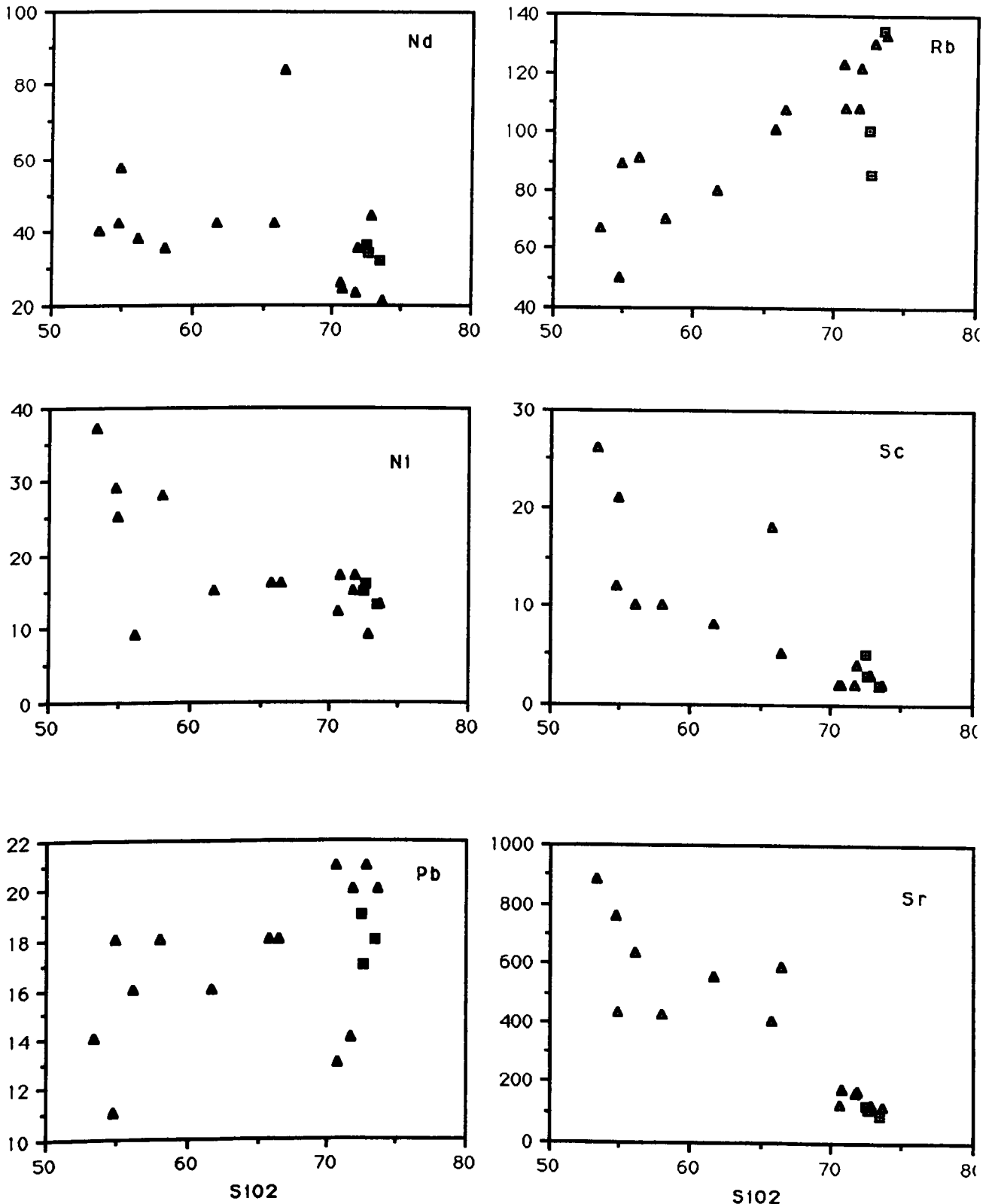
FIGURE 5.6d plots of 6 trace elements (Nd, Ni, Pb, Rb, Sc, Sr) in ppm
vs. SiO2 for Granites to the South of Bixter Voe and west of WBF
See Fig. 4.6c for key.
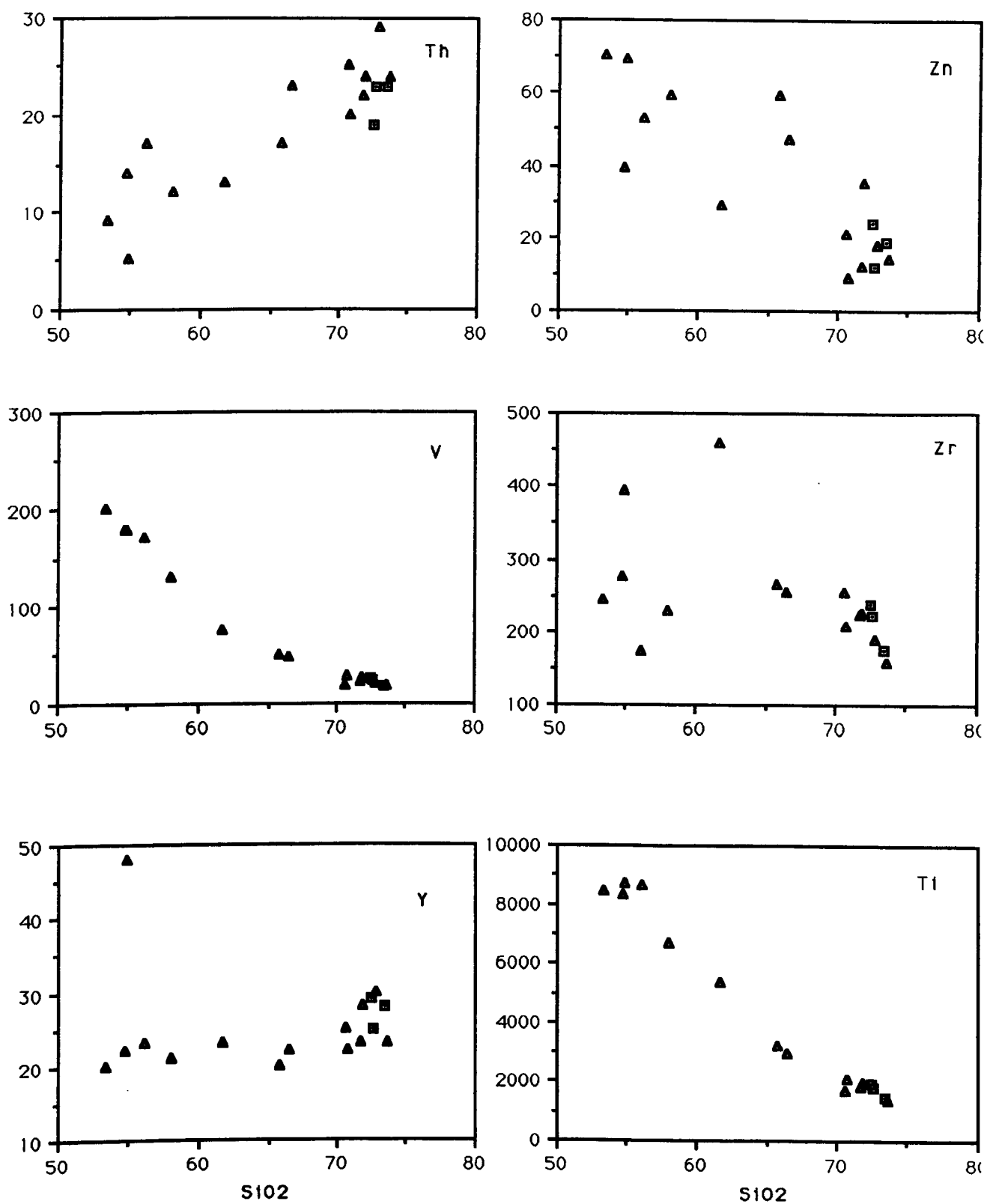
FIGURE 5.6e plots of 6 trace elements (Th, V, Y, Zn, Zr, Ti) in ppm
vs. SiO2 for Granites to the South of Bixter Voe and west of WBF
See Fig. 4.6c for key.

contents. The La, Pb and Zr show a random distribution, Y is constant with increasing silica. The Bixter granite data on the trace element diagrams plot at the end of the Sandsting trends. This may be good evidence for derivation of the Bixter granite from Sandsting granitoid by differentiation.

5.10.1 Rubidium-Strontium Ratio

For the Sandsting (Rb/Sr = 0.08-1.15) and Bixter (Rb/Sr = 0.21-1.52) Granites the Rb/Sr ratio (Figure 4.8a) shows a good smooth trend with increasing DI. Few rocks do not lie on the trend and most of these are from the Bixter Granite. The graph of Rb/Sr ratio shows that the Rb concentration of the more highly differentiated rocks increases as their Sr contents decrease and is consistent with the fact that rubidium is concentrated in the residual liquid during fractional crystallisation of a magma.

5.11 Major Element Chemistry of the Funzie and Rova Head Granitic Pebbles.

The granite pebbles from two separate localities; Funzie (deformed meta conglomerate of pre-Middle Old Red Sandstone) and Rova Head conglomerate (Old Red Sandstone), were collected and analysed for major elements (data set in appendix 2). The Harker variation diagrams (Figures 4.7a & 4.7b) shows that Rova Head rocks show a regular trends for the major element oxides TiO_2, Al_2O_3, Total Iron, MnO, MgO, CaO and to lesser extent P_2O_5 with increasing silica contents. Both Na_2O and K_2O vary randomly in Rova Head and Funzie granite pebbles and lie in separate fields. The H_2O and CO_2 contents show a crude decrease with the increasing silica contents. The major element oxides of Funzie tend to form fields rather than trends as Rova Head does. Generally Funzie is characterized by high Na_2O and low K_2O and vice versa for Rova Head.
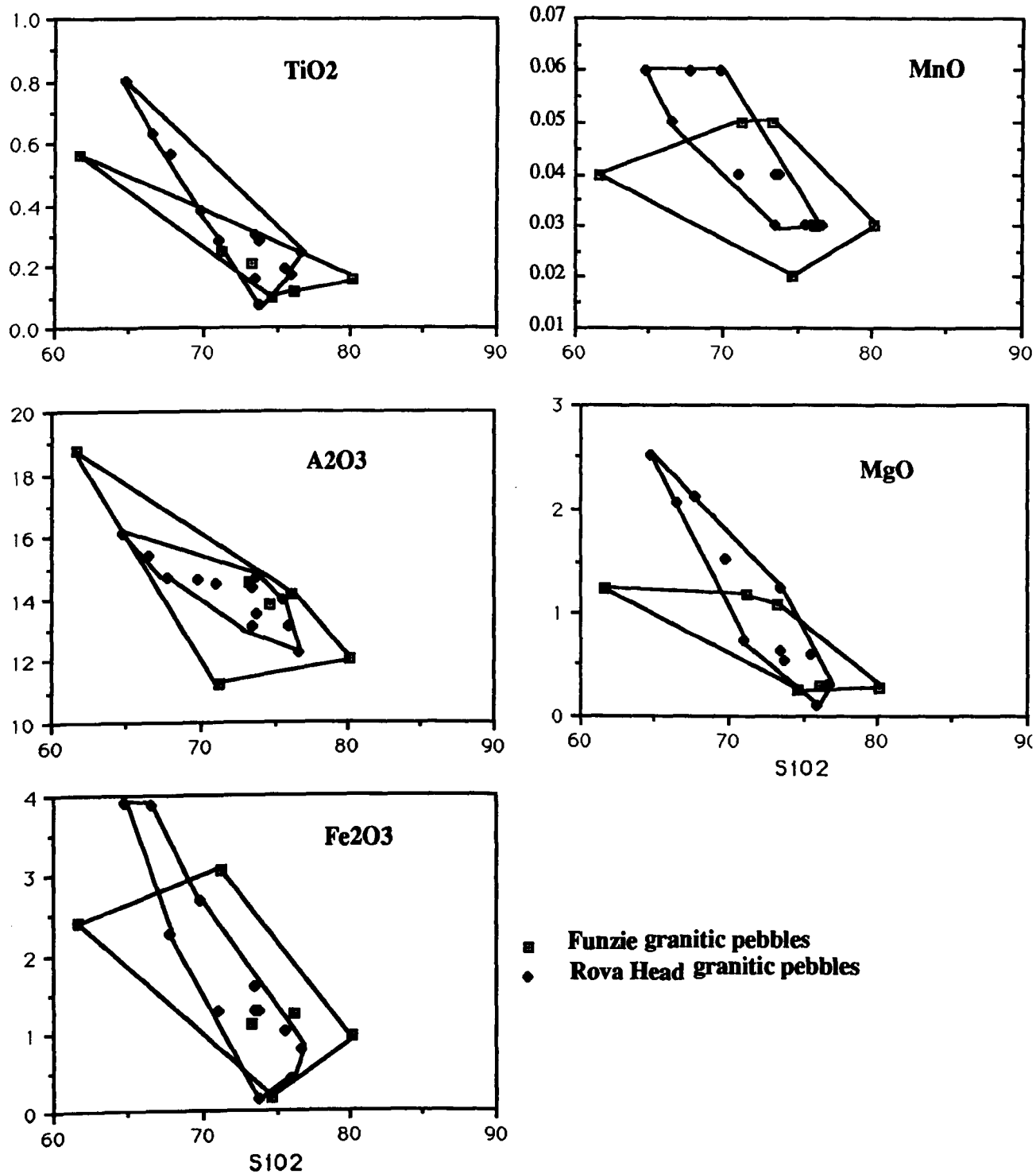
Figutre 5.7a plots of 5 majors elements (TiO2, Al2O3, Fe2O3, MnO, MgO) versus SiO2 for pebbles of granites from Funzie and Rova Head Conglomerates. All values are in wt%.
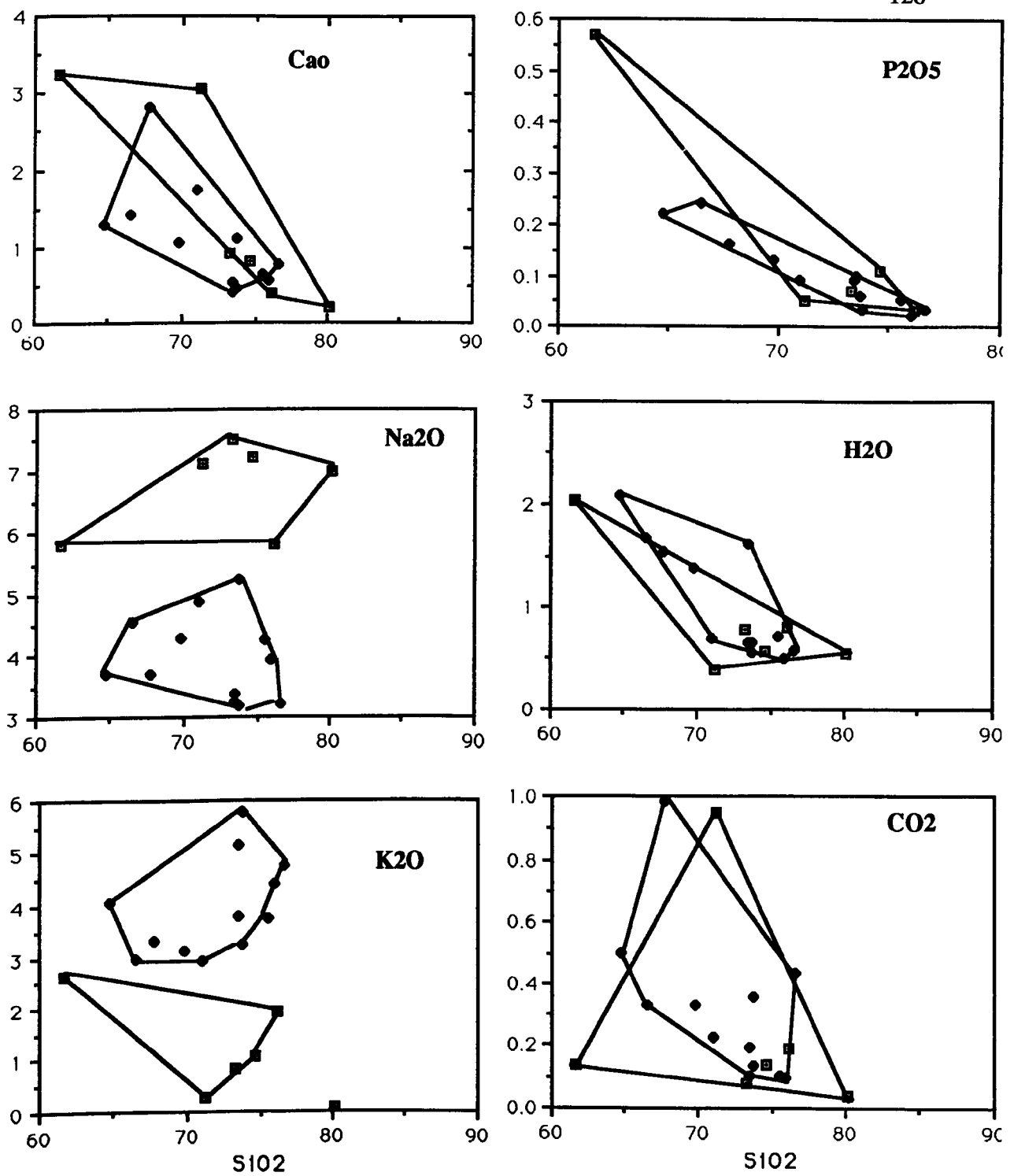
Figure 5.7b plots of 6 major elements (CaO, Na2O, K2O, P2O5, H2O, CO2) versus
SiO2 for pebbles of granites from Funzie and Rova Head conglomerates. All values are in wt%.
See Fig. 4.7a for key.
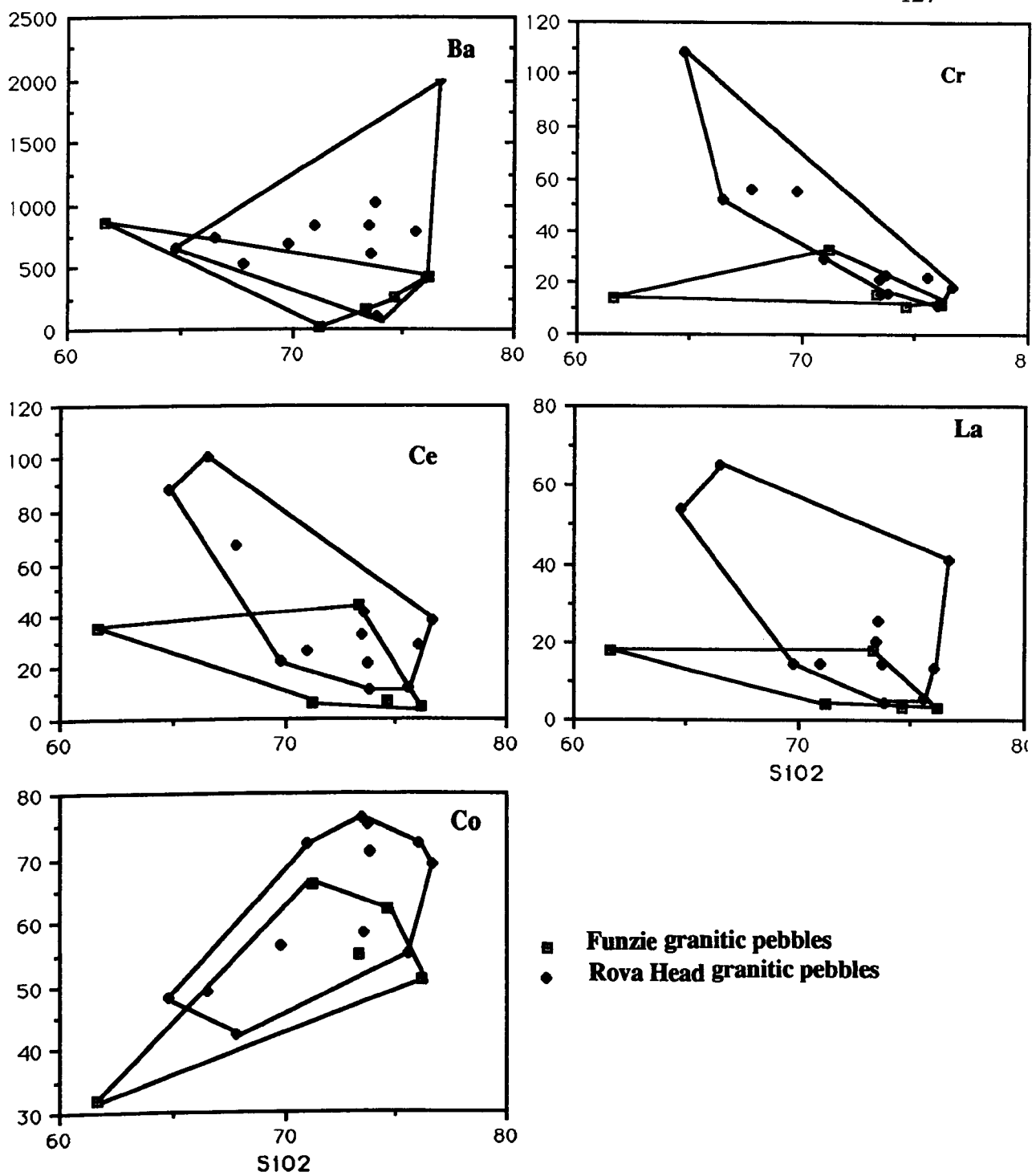
Figure 5.7c plots of 5 trace elements (Ba, Ce, Co, Cr, La) in ppm versus
SiO2 for pebbles of granites from Funzie and Rova Head conglomerates.
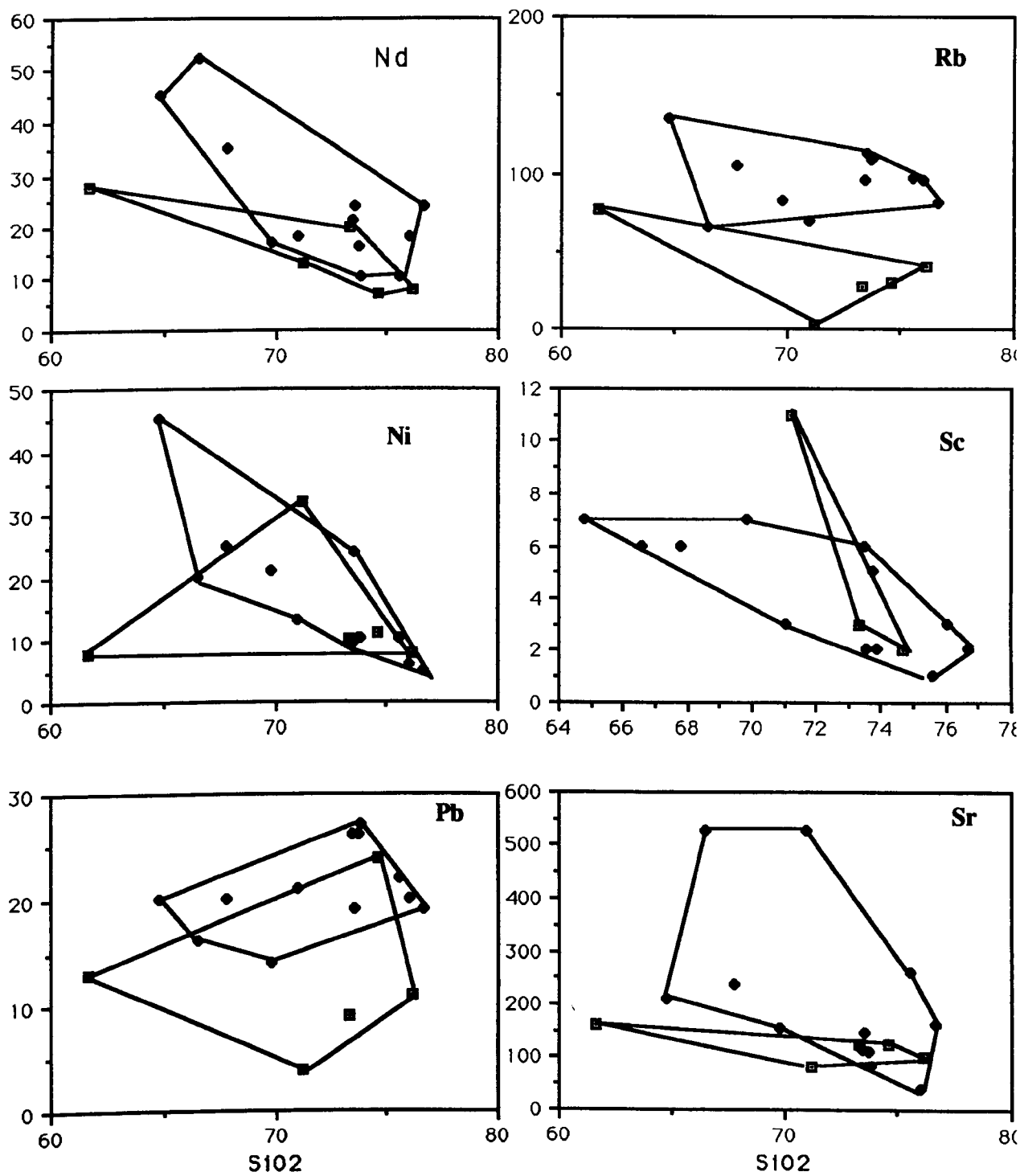
Figure 5.7d Plots of 6 trace elements (Nd, Ni, Pb, Rb, Sc, Sr) in ppm versus wt% SiO2 for pebbles of granites from Funzie and Rova Head conglomerates to the east of WBF. See Fig. 4.7c for key.
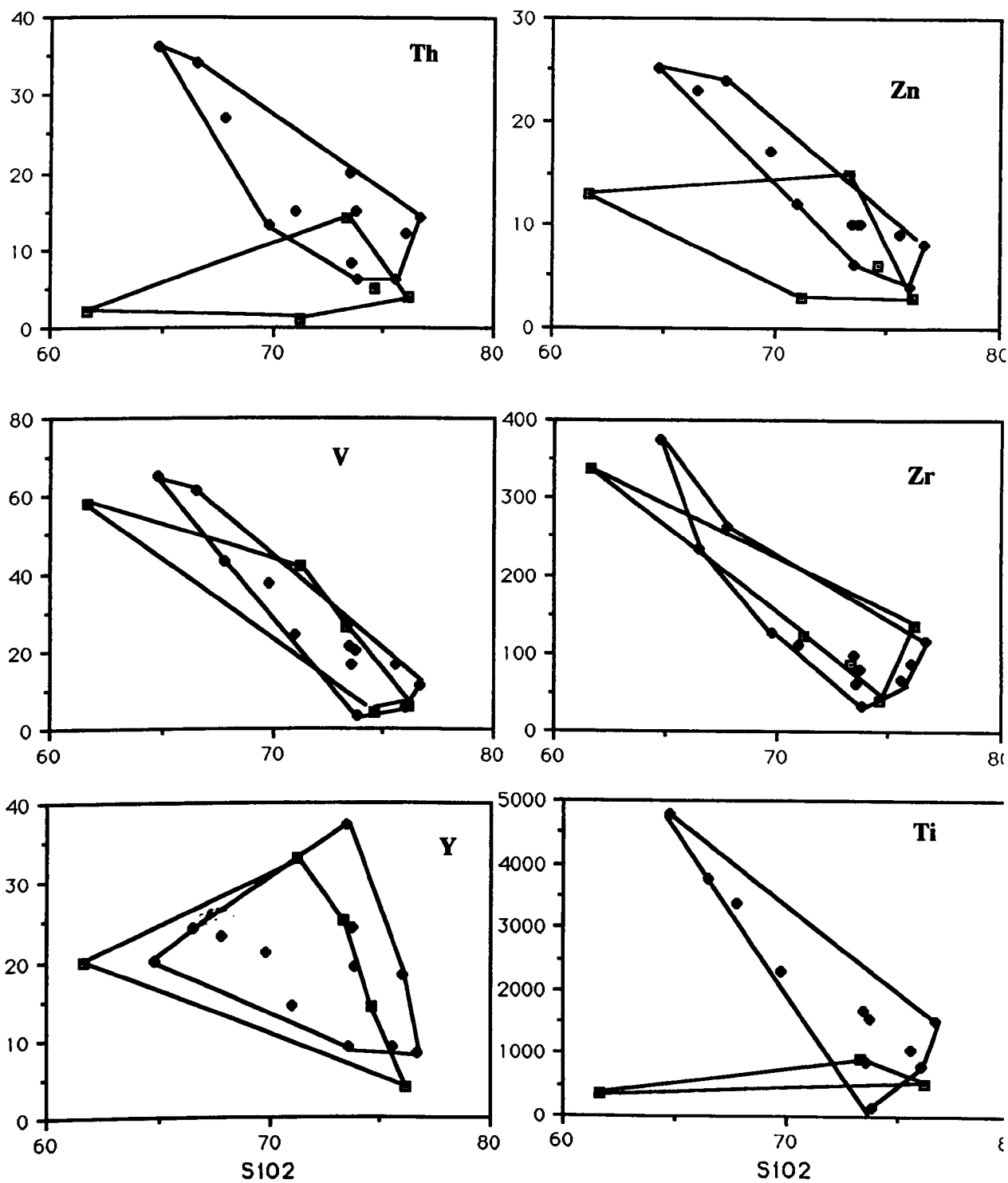
Figure 5.7e Plots of 6 trace elements (Th, V, Y, Zn, Zr, Ti) in ppm versus SiO2 for pebbles of granites from Funzie and Rova Head Conglomerates to the east of WBF. See Fig. 4.7c for key.

5.12 Trace Element Chemistry of the Funzie and Rova Head granitic Pebbles.

The samples of Funzie and Rova Head granitic pebbles were also analysed for trace elements (data set in appendix 2). The ranges of values found for trace elements are plotted versus silica contents (Figures 4.7c, 4.7d & 4.7e). The Rova Head rocks show negative trends for the elements Ce, Cr, Nd, Ni, Sc, Th, V, Zn, Zr, Ti and to lesser extent Sr and Y. Positive correlation can be seen for elements Co, and Pb with SiO_2 contents. Rb shows constant values with silica contents. In contrast the Funzie trondhjemitic pebbles plot in different fields than the Rova Head rocks and are characteristically lower in Rb.

5.12.1 Rubidium-Strontium Ratio

In the Funzie and Rova Head granitic pebbles Rb/Sr (Figure 4.8b) show differences between Funzie (Rb/Sr = 0.04-0.48) and Rova Head (Rb/Sr = 0.13-1.34); whereas the Rova Head shows a smooth increasing trend with increasing DI plus some scatter, the Funzie granitic pebble Rb/Sr ratios are correspondingly low and plot away from the Rova Head trend. In most respects, Funzie granitic pebbles have trace element chemistry different from those of Rova Head, relating to the differences in petrology.

5.13 Major Element Chemistry Of Shetland Granitoids.

Plots of CaO versus SiO_2 and Na_2O+K_2O versus SiO_2, Na_2O versus K_2O and K_2O versus SiO_2 for the different plutons of Shetland granitoids will be discussed in this section.

The Na_2O+K_2O plot and CaO plot against SiO_2 (Figure 4.9a) show that the Shetland Granitoids are generally alkali-calcic (Peacock,1931). However, due to the poor correlation between SiO_2 and Na_2O+K_2O; it is very difficult to position a
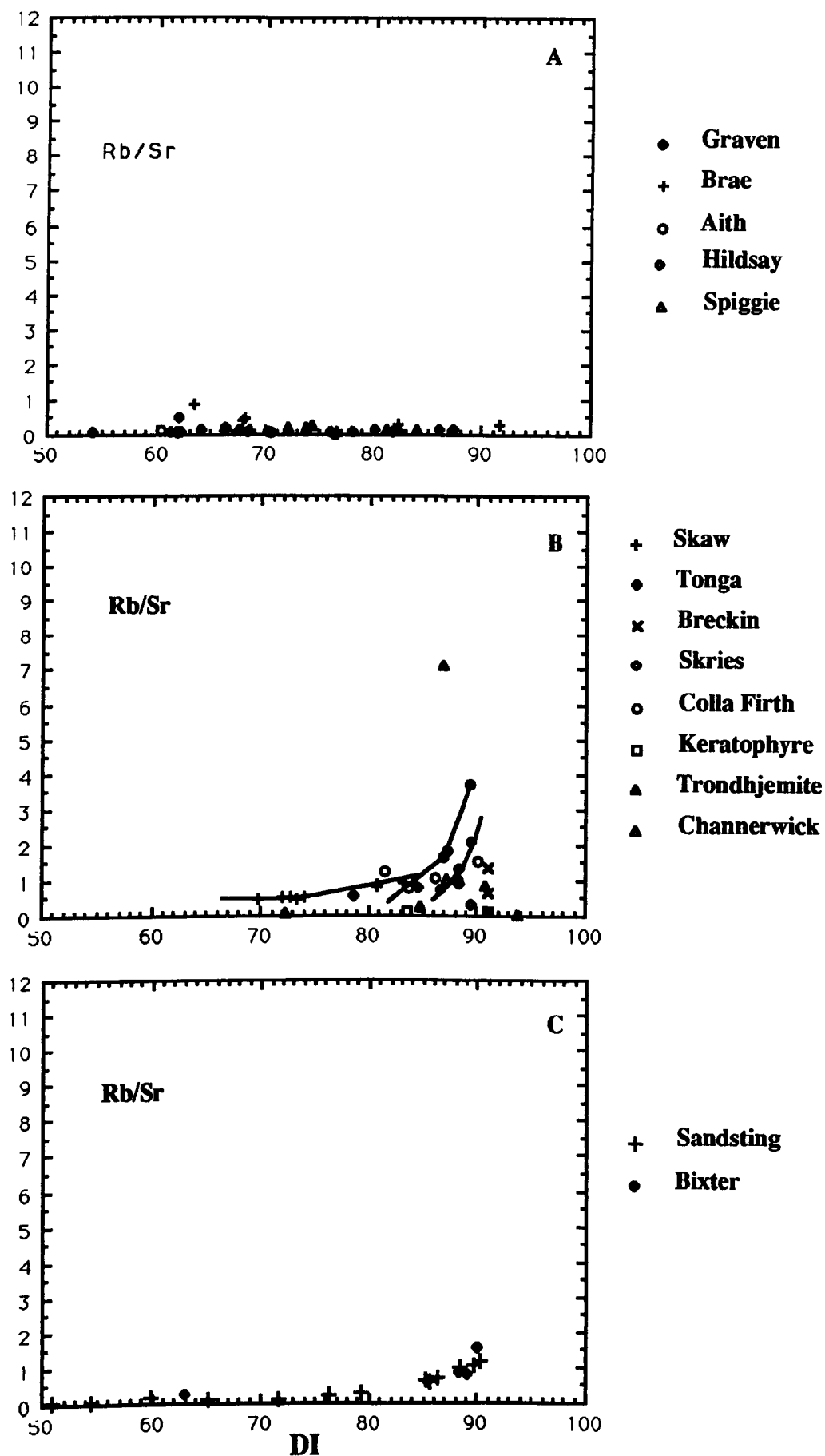
Figure 5.8a plot of Rb/Sr versus DI for A) hornblende-bearing granites, B) hornblende-free granites and C) for Sandsting and Bixter granites.
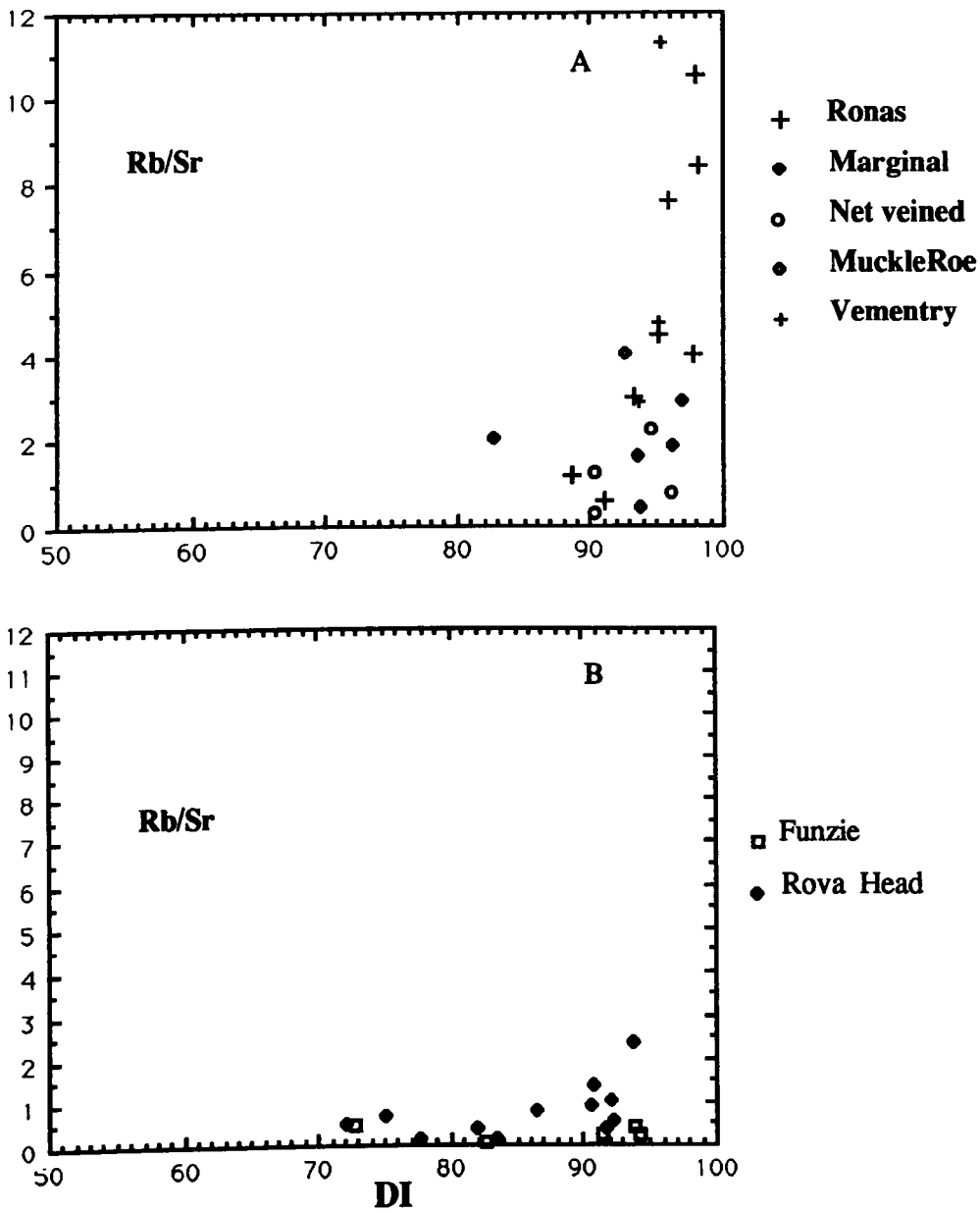
Figure 5.8b plot of Rb/Sr versus DI for A) Ronas Hill granite and its satellites, B) Granitic pebbles of Funzie and Rova Head Conglomerates.

best fit line through the data and thus estimate the SiO2 value at which Na2O+K2O = CaO

The K2O *versus* SiO2 in Figure 4.9a shows that Shetland Granitoids with relatively low SiO2 fall into the fields defined as high-K calc-alkaline and a very few in the shoshonite field (Peccerillo and Taylor,1976). The K2O vs SiO2 (Kuno plot, 1966, Figure 8.7) shows clearly that Shetland Granitoids fall into the high alumina field and alkali field . Very few plot in the pigeonitic rock field or tholeiitic series.

The K2O versus Differentiation Index (DI) plot for Shetland granitoids in (Figure 4.9b) shows a positive trend for the hornblende-bearing granites, Sandsting granite and Skaw granite (hornblende-free granite) with a little scatter. The rest of Shetland granitic data show no particular correlation with increasing DI. The Ronas Hill and its satellites plot together and form a separate group due to their high silica content and thus possession of the highest values of DI. Trondhjemite dykes and keratophyre do not follow this trend because they are very poor in potassium and very rich in sodium.

The SiO2 plot versus DI (Figure 4.9b) show a relatively smooth positive correlation i. e. an increase of SiO2 with increasing differentiation. Monzonitic rocks are associated with the Spiggie granite and its two offshoots (Hildasay and Aith) and the low silica hornblende-free granites (Skaw). The Ronas Hill Granite and its satellites, show a little positive correlation with the DI.

The variation in Na2O+K2O versus DI (Figure 4.9c) is nearly constant, and show slightly positive correlation and has very smilar features to the plot of K2O versus DI.

The MgO versus DI plot (Figure 4.9c) shows a little variation for hornblende-bearing and Sandsting granites (at between 0.3 and 0.9). This very poor correlation of the MgO with increasing DI and the variation within this narrow field,
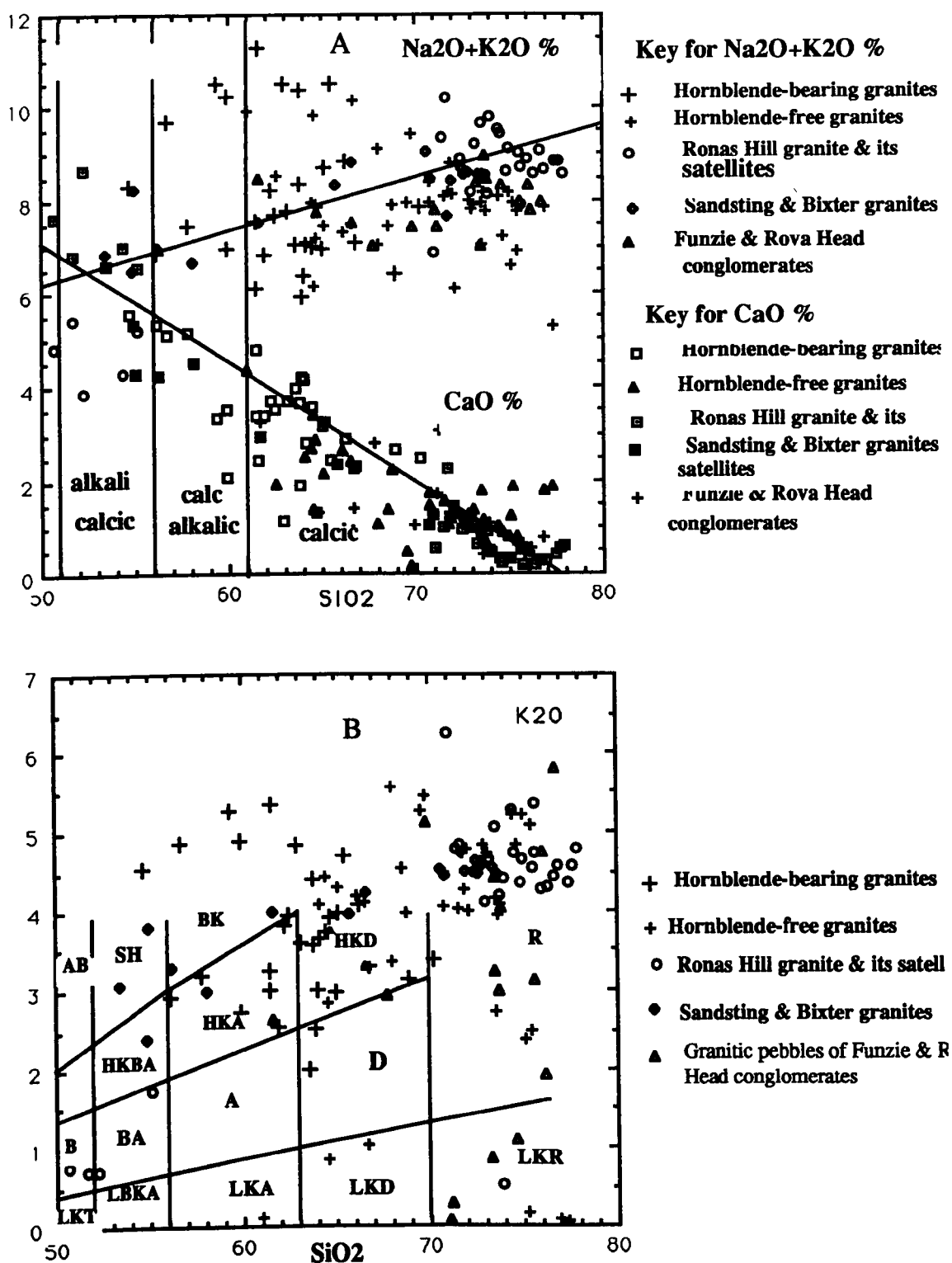
Figure 5.9a A) Na2O+K2O and CaO versus SiO2 plot, and B) K2O versus SiO2 with fields of Peccrillo and Taylor (1976). For Shetland granitoids
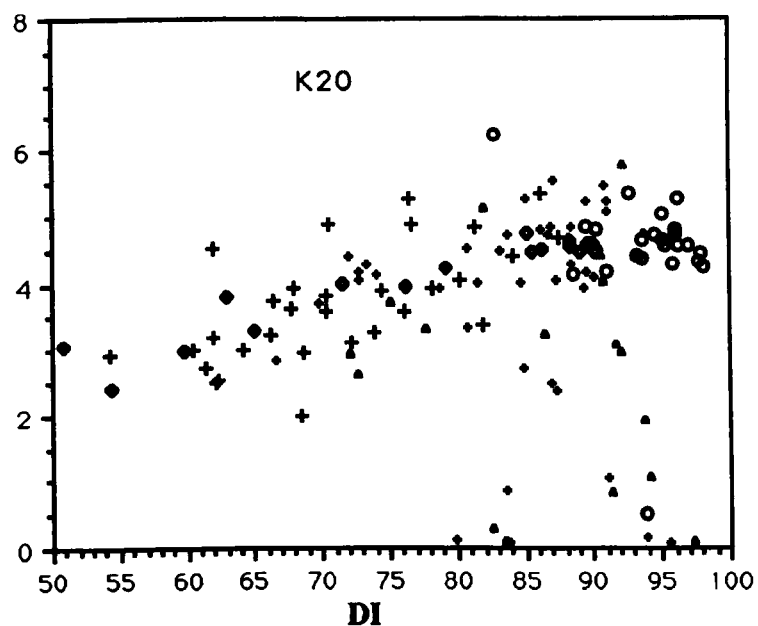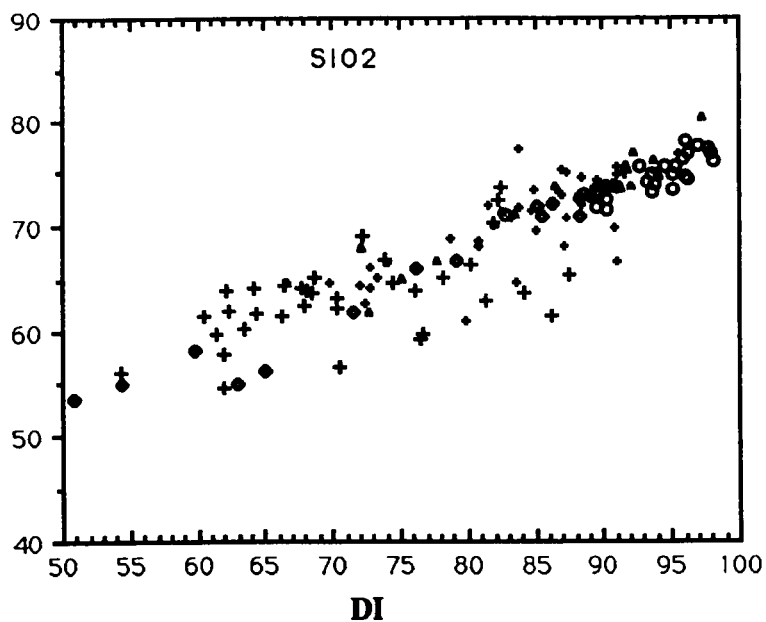
Figure 5.9b plots of SiO2 and K2O versus DI for Shetland granitoids. See Fig. 4.9a B for key. Both show positive correlation with increasing silica content but a bit highly for K2O..
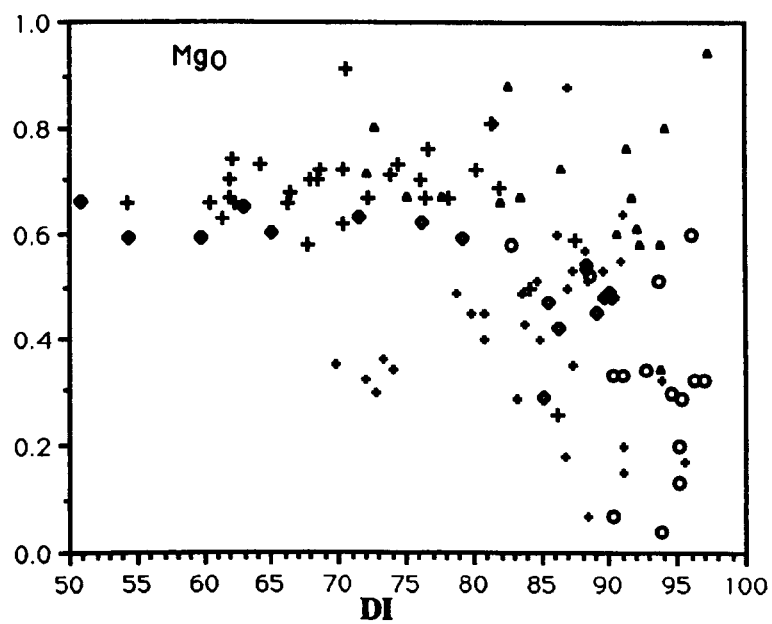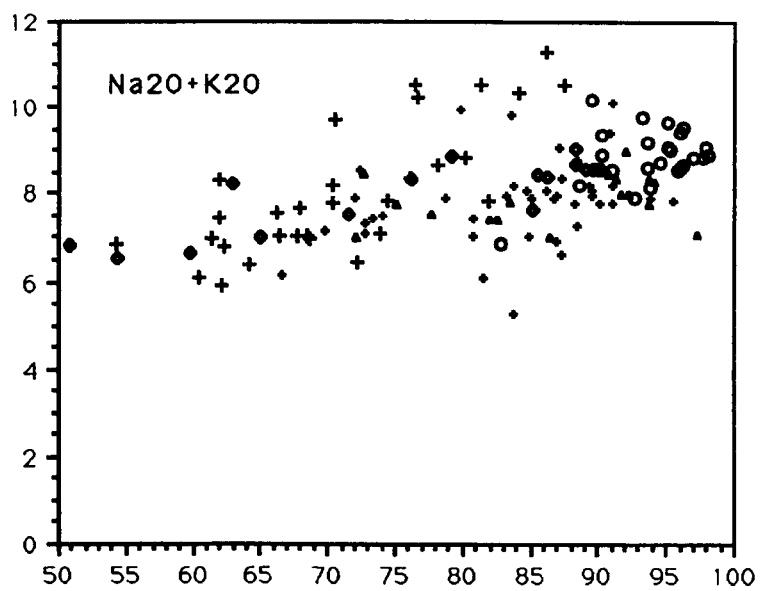
Figure 5.9c plots of Na2O+K2O and MgO values against DI, for Shetland granitoids. See Fig. 5.9a B for key.
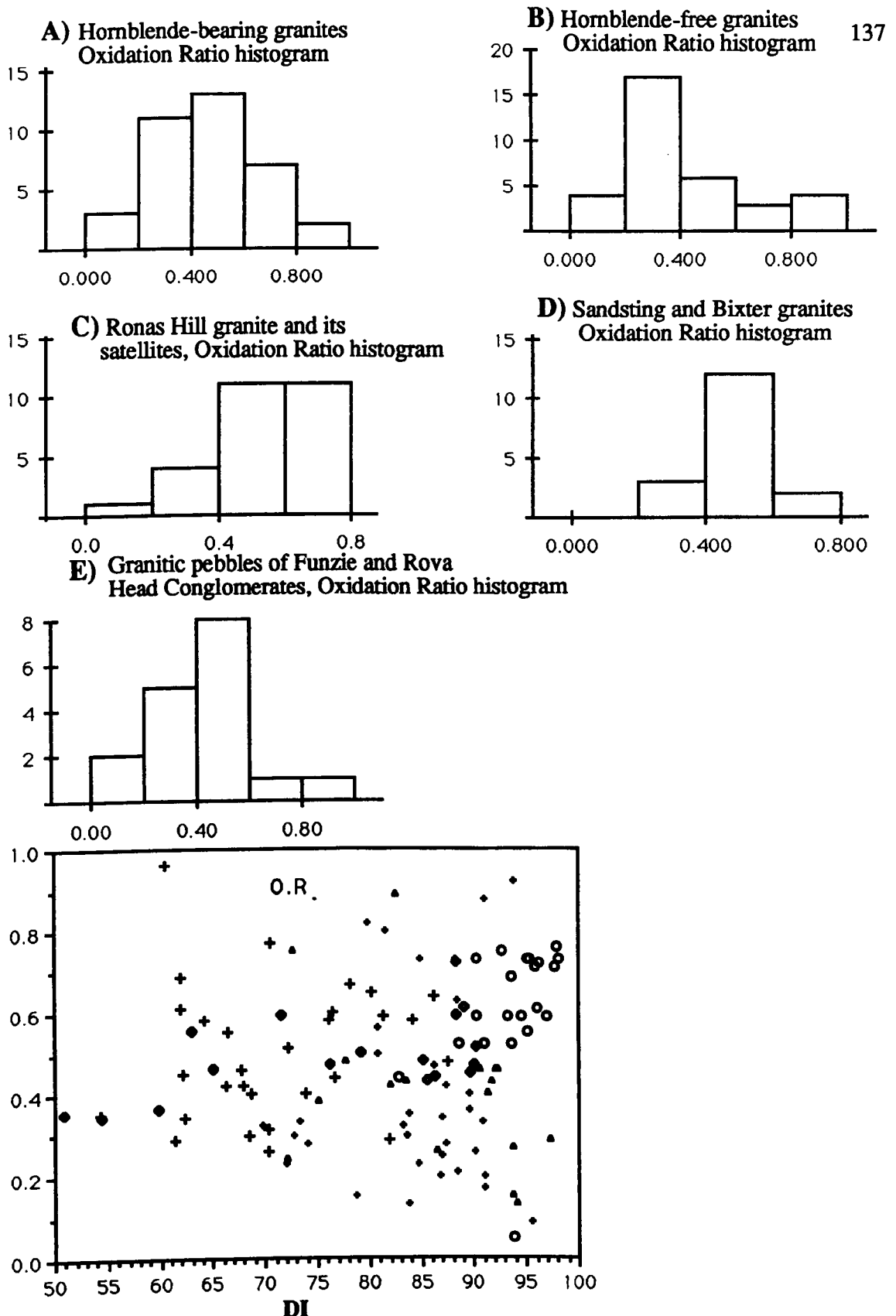
Figure 5.9d Showing the different histograms of oxidation ratios of Shetland Caledonian granites and plot of oxidation ratios versus DI (F, see Fig. 5.9a for key) . Note that the oxidation ratios of Shetland granitoids can tell the differences between the five groups of Shetland granitoids.

A) Hornblende-bearing granites
Corundum histogram

B) Hornblende-free granites
Corundum histogram   138

C) Ronas Hill granite and its satellites
Corundum histogram

D) Sandsting and Bixter granites
Corundum histogram

E) Granitic pebbles of Funzie & Rova
Head Conglomerates, corundum histogram
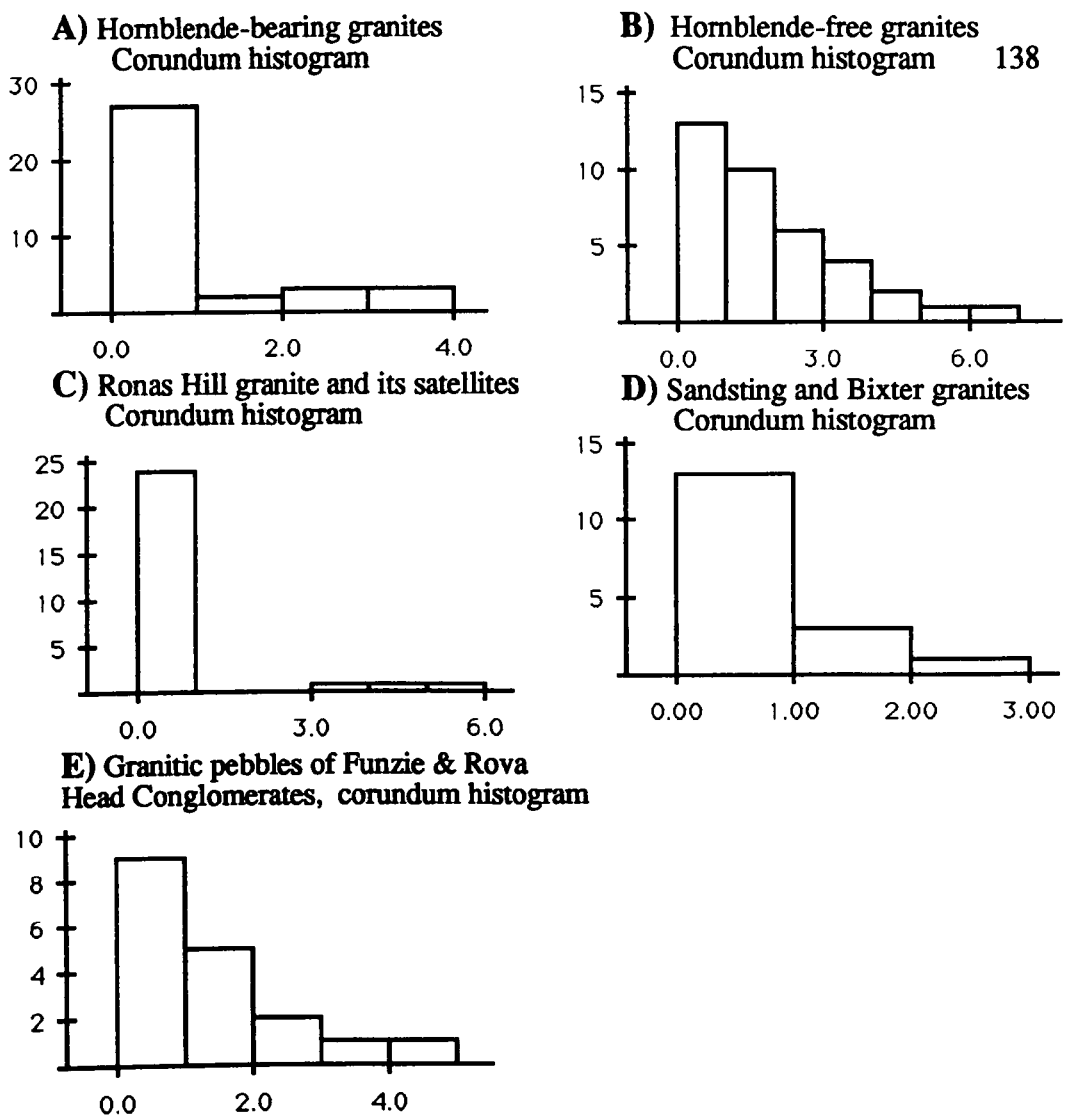
Figure 5.9e Corundum histograms of Shetland Caledonian granitoids, note that each one differ from the others as same as in the Oxidation Ratio histograms.

Normative Corundum. Most samples are slightly corundum normative with a maximum of 6% in the hornblende-free granites. Most of Shetland granite samples are clinopyroxene normative, the amount of CPX in the norm decreases and that of corundum increases with increasing SiO2. Cawthorn et al. (1976) have shown that A trend of diminishing diopside and increasing corundum with SiO2 of whole rocks has been shown to hold for many calc-alkaline plutons, batholiths and extrusives from a wide range of tectonic settings. Hornblende-free granites appear to be slightly more corundum normative than the hornblende -bearing granites (Figure 4.9e)

indicate that MgO is independent of differentiation. The various suites of Shetland granitoids could be discriminated on the MgO-DI plot, where they form fields rather than trends in which MgO values drop at high DI. Sometimes even within a single group of rocks such as the hornblende-free granites, individual granites form their own field e.g. Skaw. Some of the hornblende-free granites, trondhjemite dykes and Funzie trondhjemitic pebbles plot in the field of high Mg-values and this is owing to their possession very low-Fe contents compare with their Mg-values.

The oxidation ratios $2 Fe^{3+}/(2 Fe^{3+}+Fe^{2+})$ are plotted versus DI in Figure 4.9d which shows that the different members of Shetland granitoids plot in separate fields as for the Mg-ratios. The Ronas Hill granite and its satellites plot in the field of high OR, due to their very low-Fe^{2+} and Fe^{3+} contents compared with hornblende-bearing and hornblende-free granites. The hornblende-free granites show lower OR than the hornblende-bearing granites. Thus the hornblende-bearing granites, Ronas Hill granite and its satellites, Sandsting and Bixter granites and the trondhjemitic dykes are considered to belong to the "magnetite series" on the basis of their higher OR and mineral probe analyses while the hornblende free granites (except trondhjemite dykes and keratophyre) represent "ilmenite series" according to lower OR and mineral probe analyses (Ishihara, 1977).

ORs are also summarized in histograms in Figure 4.9d , the main features are very clear in that the Ronas Hill and its satellites are more oxidised rocks, than the hornblende-bearing and free granites respectively. The different patterns shown by the OR histograms indicate the wide range of oxidation ratios of Shetland granitoids .

5.14 Trace Element Chemistry Of Shetland Granitoids.

The trace elements that show striking enrichment in the Shetland granitoids are Sr and Ba. Halliday et al (1984b) pointed out that there is a pronounced enrichment in Ba (up to 6000 ppm) and Sr (up to 10000 ppm) in the SW Scottish Highland

granitoids which is named a provincial characteristic. Some fine grained chilled diorites and andesites in the late Caledonian suite have high Ba and Sr, and Nickel > 100 ppm and these have to be mantle-derived liquids (Halliday et al; in preparation; Stephens, unpublished data; Thirlwall, 1982). The high Sr and Ba contents (> 1000 pmm) appear to be more commonly associated with continental rather than oceanic calc-alkaline magma suites (e.g. Noble et al 1974) although alkaline magmas are quite commonly Sr and Ba rich (Halliday etal,1985). Halliday and Stephens (1984) concluded that the Sr enrichment was a mantle-derived characteristic but noted that it is a similar but much less pronounced characteristic of the c. 2.9 Ga Lewisian complex, suggesting it is a regional feature and points to the existence of an ancient lithospheric chemical province.

The Sr-Harker plot (Figure 4.10a) shows a pronounced enrichment for the Hornblende-bearing granites of Shetland granitoids at SiO_2 values between 55-65%, but is not so apparent at the higher SiO_2 values. This is powerful evidence that they are primary features and not due to different schemes of fractional crystallisation of the same parental magmas for such a process would lead to divergence at high SiO_2 rather than at low SiO_2. It is clear that the overall Sr enrichment is between 52 and 67% silica and very poor in the very acidic end. Each member of the Shetland granitoids on this plot forms its own special field.

The higher Sr values of Shetland hornblende-bearing granites is better seen on the Sr-CaO plot (Figure 4.10a), Ca being the most suitable major oxide against which to normalize Sr for bulk compositional effects cf. Stephens and Halliday (1984) for the Scottish granitoids.

5.14.1 Strontium versus DI plot.

The distribution of Sr in rocks is controlled by the extent to which Sr^{2+} can substitute for Ca^{2+} in calcium-bearing minerals and the degree to which potassium-feldspar can capture Sr^{2+} in place of K^+ ions (Faure and Powell, 1972). In

Shetland granitoids, Sr vs.DI plot (Figure 4.10b) shows a crude increase for hornblende-bearing granites with increasing DI and a poor negative correlation for the remaining members of the Shetland granitoids.

5.14.2 The Barium versus SiO2 plot

Barium is taken up selectively by biotite and fractionation of this phase could be significant. Figure 4.10c shows a pronounced Barium enrichment (up to 3098 ppm) in the hornblende-bearing granite compared with the other members of Shetland granitoids and may reflect a provincial characteristic as defined by Halliday and Stephens (1984). In Shetland granitoids, Ba shows very weak negative correlation for hornblende-bearing granites with increasing SiO2 and no correlation with the rest of Shetland granitoids.

5.14.3 The Barium versus K2O plot

In Figure 4.10c shows that, generally Ba exhibits a positive correlation with increasing K2O for hornblende-bearing granites, Sandsting and Skaw granites, although there is some scatter. There is no correlation with the rest of Shetland granitoids.

5.14.4 On the Barium versus DI plot

Figure 4.10b shows a positive correlation can be detected with increasing DI for Hornblende-bearing granites. At high DI there is a negative trend for hornblende-free granites and Ronas Hill granite and its satellites. All other members of the Shetland granitoids form their own separate trends except Sandsting and Skaw Granites which plot within hornblende-bearing granites due to their coincidence in silica range.

5.14.5 The Zr versus SiO2 plot

Figure 4.10d shows a negative correlation with increasing SiO2 content for hornblende-free granites and Ronas Hill and its satellites. The keratophyre shows
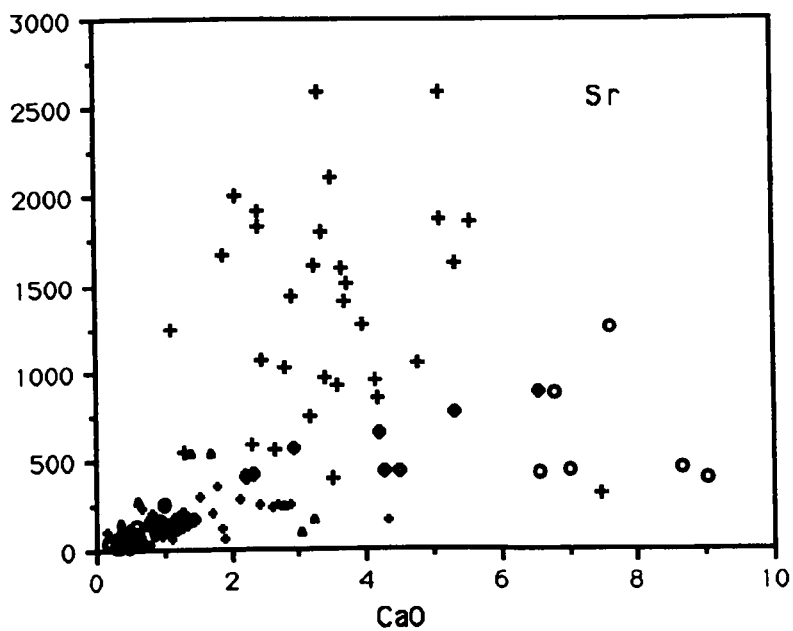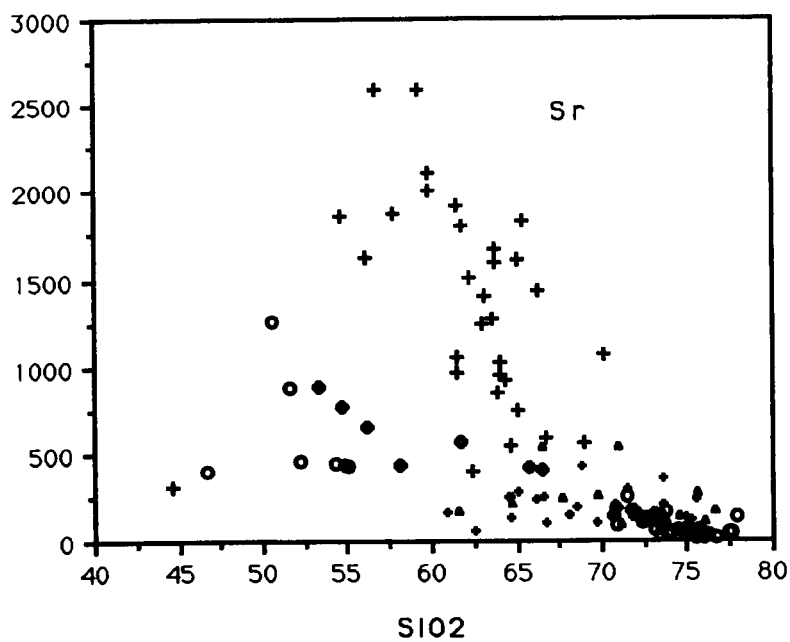
Figure 5.10a plots of Sr versus SiO2 and Sr versus CaO, for Shetland granitoids. See Fig. 5.9a B for key.
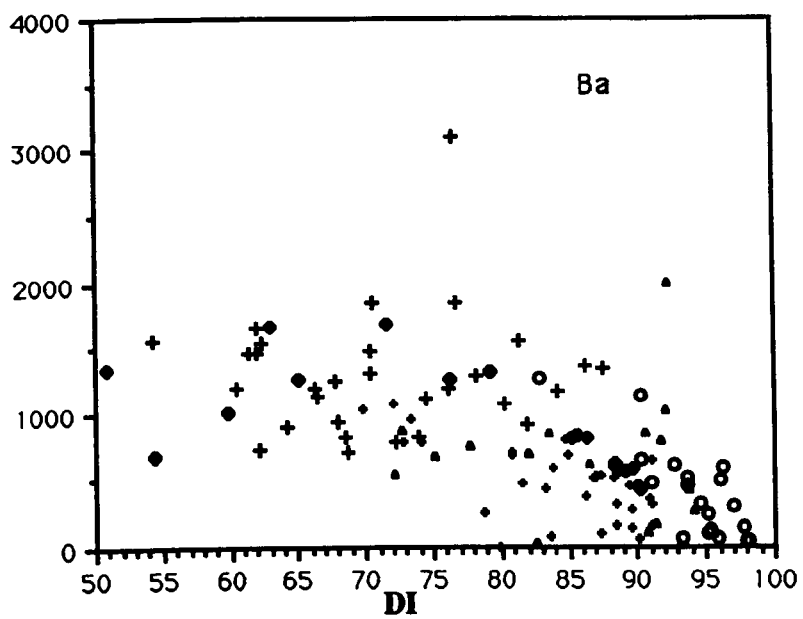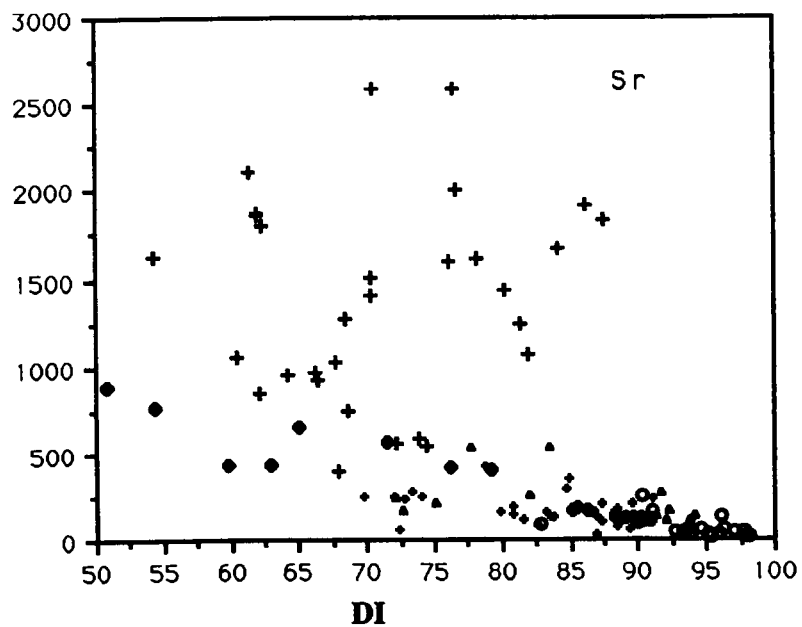
Figure 5.10b plots of Sr and Ba versus DI, for Shetland granitoids. See Fig. 5.9a B for key.
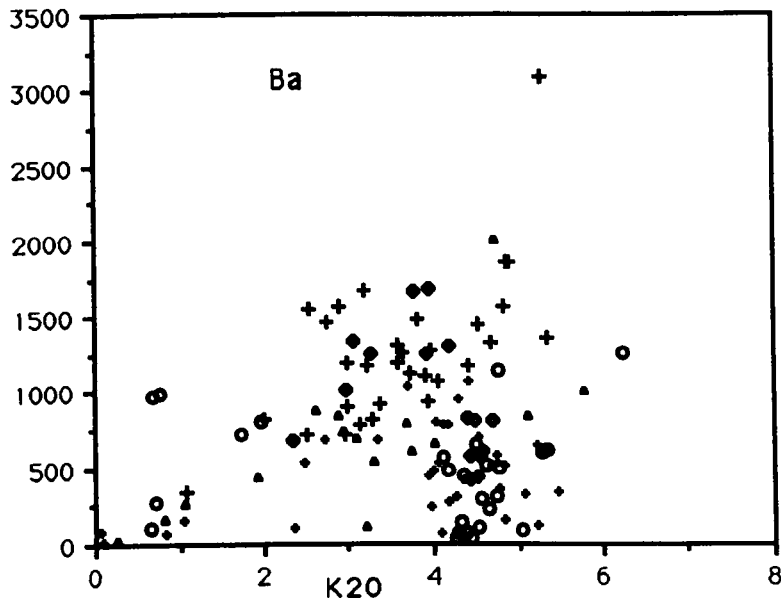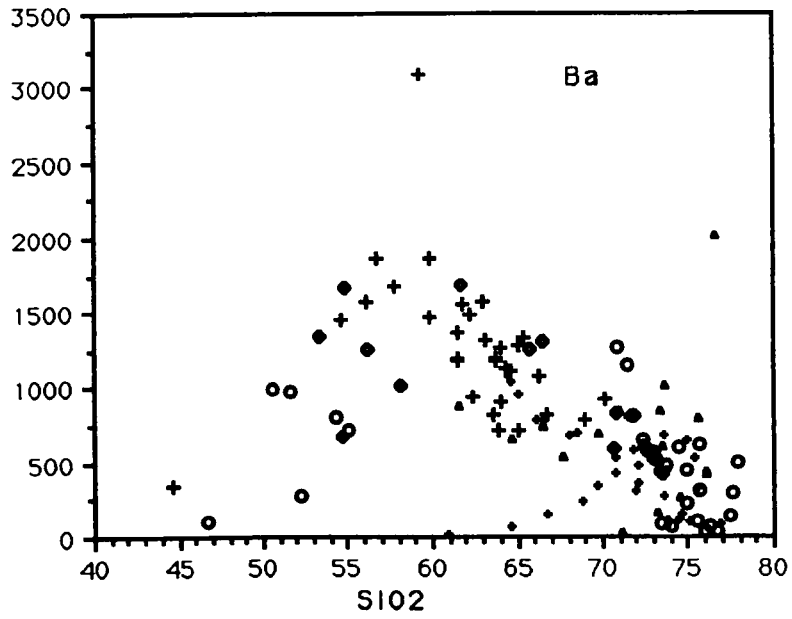
Figure 5.10c plots of Ba versus SiO2 and Ba versus K2O, for Shetland granitoids. See Fig. 5.9a B for key.
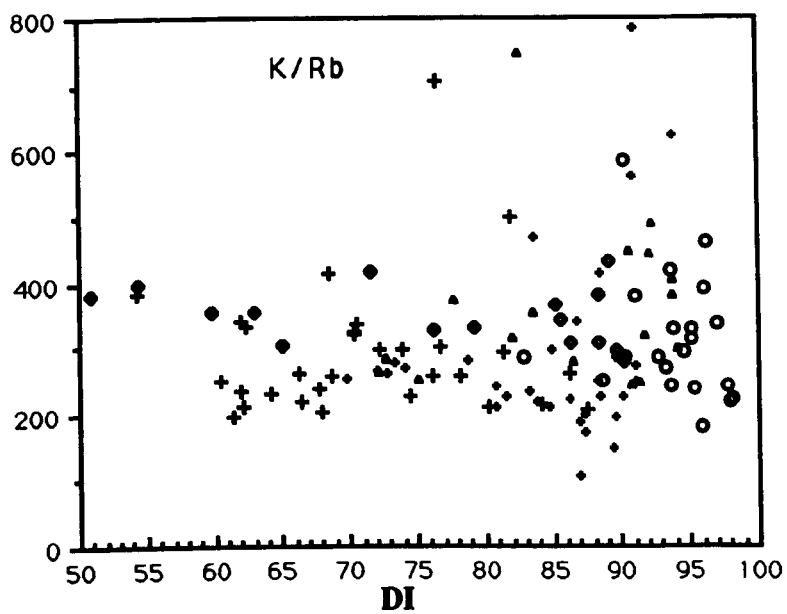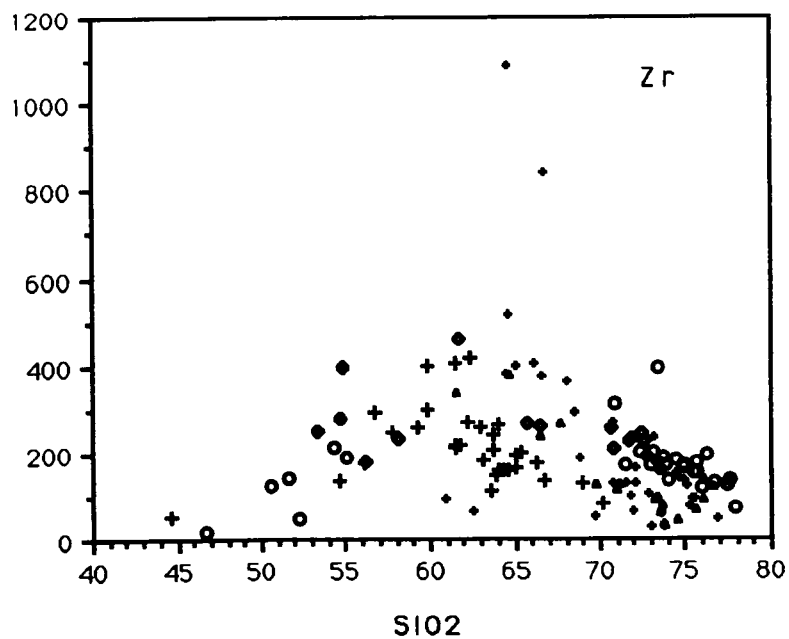
Figure 5.10d plots of Zr versus SiO2 and K/Rb versus DI, for Shetland granitoids. See Fig. 5.9a B for key.

high zirconium values and which may be due to an irregular distribution of zircon in the keratophyre (Flinn, pernsonal communication). This is due to the precipitation of zircon in the more fractionated magmas.

5.14.6 Potassium-Rubidium Ratio

The close geochemical coherence between potassium and rubidium has led to the suggestion that the K/Rb ratio of igneous rocks is constant (Ahrens, Pinson and Kearns, 1952), and typically has an average value of 230. Heier (1972) has shown that in the range from mafic to felsic rocks, the Rb concentration increases two orders of magnitude while the K increase is only about one order of magnitude. A constant K/Rb ratio is therefore not probable and it should decrease with differentiation. Shaw (1968), has suggested that the available data indicate that most common silicate minerals other than mica and amphibole have generally similar K/Rb ratios. Accordingly, with the exception of the above , silicate crystallisation would have little if any effect on the K/Rb of the magma. However, Philpotts and Schnetzler (1970), in a paper dealing with partition coefficients between common silicate minerals and liquid magma, for K, Rb, Ba and Sr, show that sizeable differences do occur in K_D/Rb for various minerals other than mica and amphibole. More importantly the size of the actual partition coefficients involved indicates that during magmatic differentiation the general trend would be one of a slight lowering of the K/Rb ratio in the liquid. Thus they are essentially in agreement with the "main trend "of Shaw (1968), but differ in concluding "that it appears likely that feldspar is a more potent control than the mica or amphibole favoured by Shaw", on the K/Rb ratio in a differentiating silicate magma.

In Shetland granitoids the K/Rb ratio (Figure 4.10d) shows no evidence of any correlation with fractionation as measured by the differentiation index and it is constant through them, except for a few scattered samples of low K and Rb which are off the trend and exibit high K/Rb ratios; these are keratophyre, trondhjemite

dykes and a few samples from the rest of Shetland granitoids. In view of the arguments above, these data almost certainly represent the mobile behaviour of K and / or Rb.

5.15 Trace Element Spider Diagrams.

Incompatible trace elements in granites from the four main tectonic settings and their respective sub-setting (ORG, VAG, WPG,syn-COLG) are normalized to a hypothetical ocean ridge granite (ORG) and plotted as geochemical patterns known as spider diagrams (Pearce et al., 1984). Several variants of the spiderdiagram plot have been used in the literature, in which the order of the elements plotted varies slightly, and different normalization constants have been adopted. For example, Wood et al. (1979) normalize to a hypothetical primordial mantle composition, whereas Thompson et al. (1984) and Sun (1980) normalize their data to chondritic abundances with the exception of K and Rb, which may be volatile during planetary formation, and P, which may be partly contained in the core. Here the normalization of Pearce et al., (1984) is used (table 5.1)

5.15.1 Spider Diagrams Of Trace Elements For Hornblende-bearing Granites.

In the subsequent section the Pearce et al (1984) spider diagram plot will be used to discuss the trace element geochemistry of Shetland granitoids. The trace element distributions are summarised in Figure 4.11a. The patterns are typical of volcanic arc granites; they are broadly similar in shape to the Jamaica volcanic-arc type, differing mainly in the absolute abundance of the elements. The rocks are characterized by enrichments in K, Rb, Ba, Th and (in calc-alkaline and shoshonitic series) Ce and Sm relative to Ta, Nb, Hf, Zr, Y and Yb. A further significant feature is the low values of Y and Yb to the normalizing composition. Figure 4.11a shows that Ce and Sm for monzonitic rocks (Aith-12a.25 and Spiggie-12c.44) are enriched relative to the rest. The sample patterns in Figure 4.11a

exhibit clear Th peaks which are relatively enriched compared with patterns of the hornblende-free granites.

5.15.2 Spider diagrams of trace elements for Hornblende-free Granites.

The patterns of hornblende-free granites are broadly very similar to these from two tectonic settings: within plate granites and syn-collision granites. The patterns of Skaw Granite (Figure 4.11b) are similar to within-plate granites patterns, as exemplified by the Skaergaard complex (Pearce et al.,, 1984). They exhibit high ratios of Rb and Th relative to the other elements, and differ from the other within plate patterns in having no large Ta negative anomaly and in their flatter (more MORB-like) trends from Ta to Y. Despite their large intra-group variability, however, the within plate granite patterns are distinctive in their combinations of (1) values of Hf to Y that are close to the normalising value; and (2) high values of K, Rb and Th. Tonga and Breckin granites have very similar patterns to syn-collision granites as shown in Figure 4.11b. It is evident that, superficially at least, most of the patterns resemble those from volcanic arc granites of calc-alkaline type. There are , however, some distinctive characteristics, notably the exceptionally high contents of Rb and the very low contents of Ce, Zr, Hf and Sm in many of the patterns from syn-collision granites (Pearce et al, (1984). In the Tonga and Breckin granites the distinctive characteristics are the high contents of Rb and Th and the very low contents of Ce, Zr, Hf and Sm (except sample 4b.2 from Breckin) which is characteristic of the patterns of syn-collision granites.

The Out Skerries, Colla Firth and Channerwick granitoids (Figure 4.11b) exhibit very similar patterns to syn-collision granites. Of the four samples of this group, two samples from Colla Firth (9.22) and Channerwick (10.1) show a strong Ba negative anomaly and high contents of Rb and Th and, Ba apart, these samples show a very low contents of Ce, Zr, Hf and Sm which are similar to the syn-collision granites patterns from Barousse and Tibet intrusions.

5.15.3 Spider diagrams of Trace Elements for Ronas Hill and its satellites.

The patterns of the Ronas Hill granite and its satellite are very similar to within plate and post-collision granites (Figure 4.11c), the Ronas Hill granite patterns are marked by high and approximately equal normalized abundances of Rb and Th and large negative Ba anomaly and, Ba apart, a general increase in normalized abundances from Yb to Rb, this type of pattern belong to within plate granites. The second type of within plate granites differ from the other patterns in having no large Ba negative anomaly and have flatter trends from Ta to Yb. This type of pattern applies to two sample patterns from the Net Veined and Muckle Roe Granites (Figure 4.11c). Four samples from Ronas Hill (two feldspar granite), Marginal, Net Veined and Vementry granites have post-collision granites patterns (Figure 4.11c). They are characterised by high contents of Rb and Th and the very low contents of Ce, Zr, Hf and Sm as in the Novate and Querigut post-collision intrusion patterns (Pearce et al., 1984).

5.15.4 Spider diagrams of Trace Elements for Sandsting and Bixter Granites.

The patterns of Sandsting and Bixter Granites (Figure 4.11d) are broadly similar to post-collision granites and in particular to the Novate and Querigut intrusion patterns discribed above. The sample (19.4) from the Sandsting Granite is slightly different in having no Ba anomaly (Figure 4.11d) but its agreement with the rest of the pattern may reflect its petrography as it was collected from the porphyritic microadamellite within the Sandsting granitoid.

5.15.5 Spider diagrams of Trace Elements for Trondhjemite dykes.

The patterns of trondhjemite dykes (Figure 4.11e) are similar to ocean ridge granite patterns. They exhibit negative anomalies in K2O, Rb and Ba, which may be
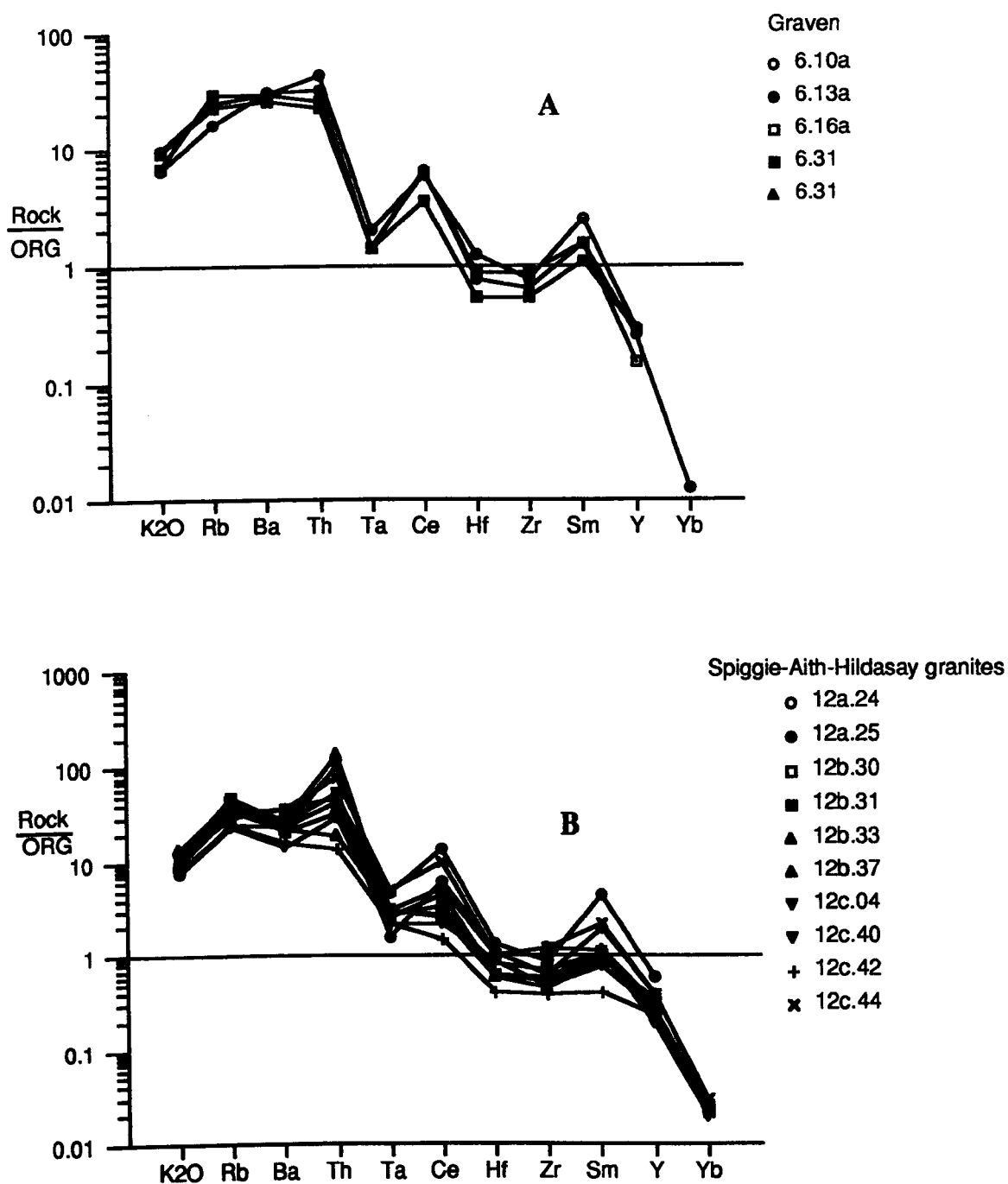
FIGURE 5.11a Oceanic Ridge Granite (ORG) normalized geochemical patterns of hornblende-bearing granites A) Graven granitoid, B) Spiggie granite and its two offshoots Aith and Hildsay granites.
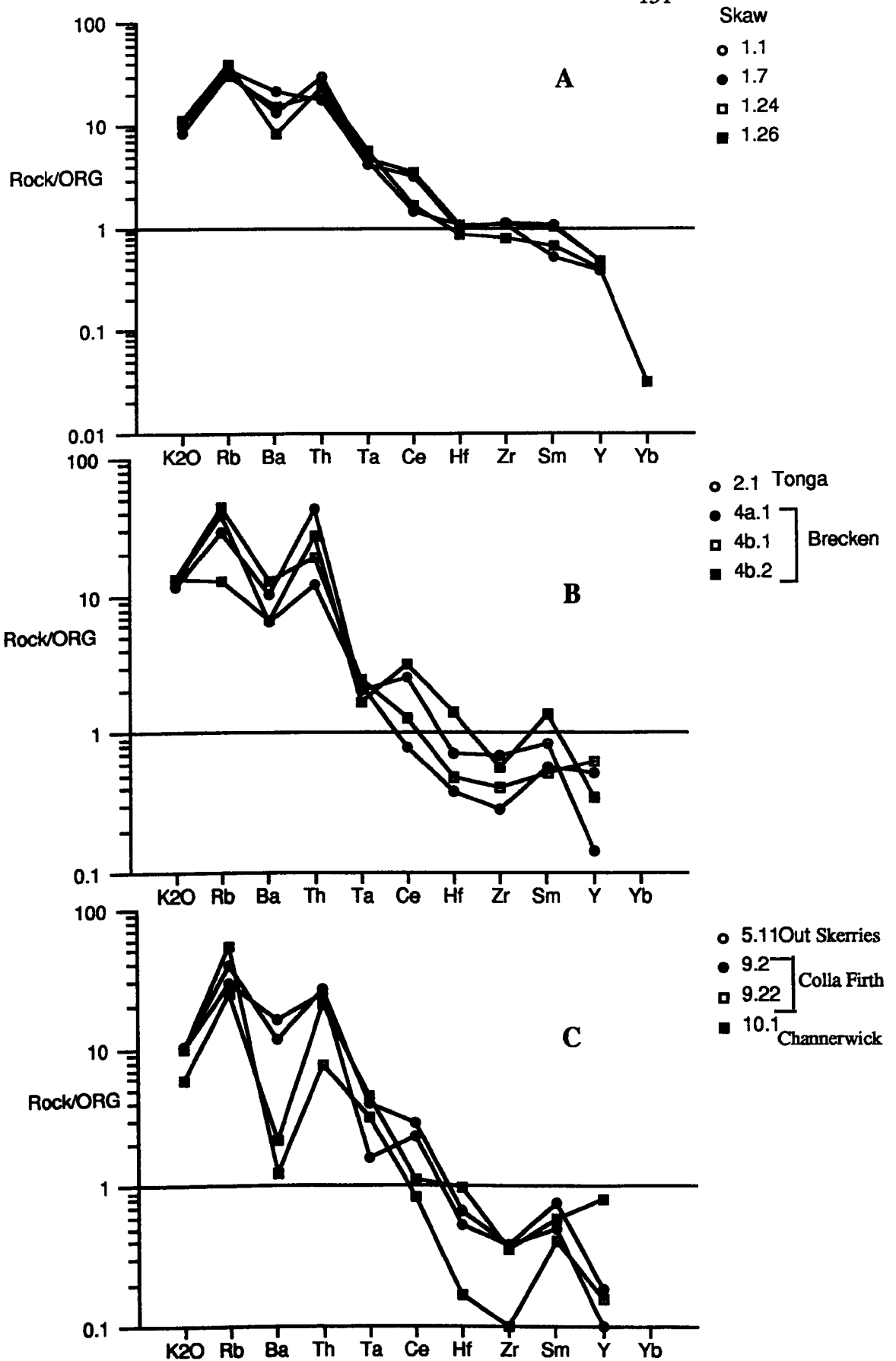
Figure 5.11b Oceanic ridge granite (ORG) normalized geochemical patterns of hornblende-freegranites (normalizing values from Pearce et al., 1981), A) Skaw granite, B) Tonga and Brecken, and C) Colla Firth and Out Skiries.
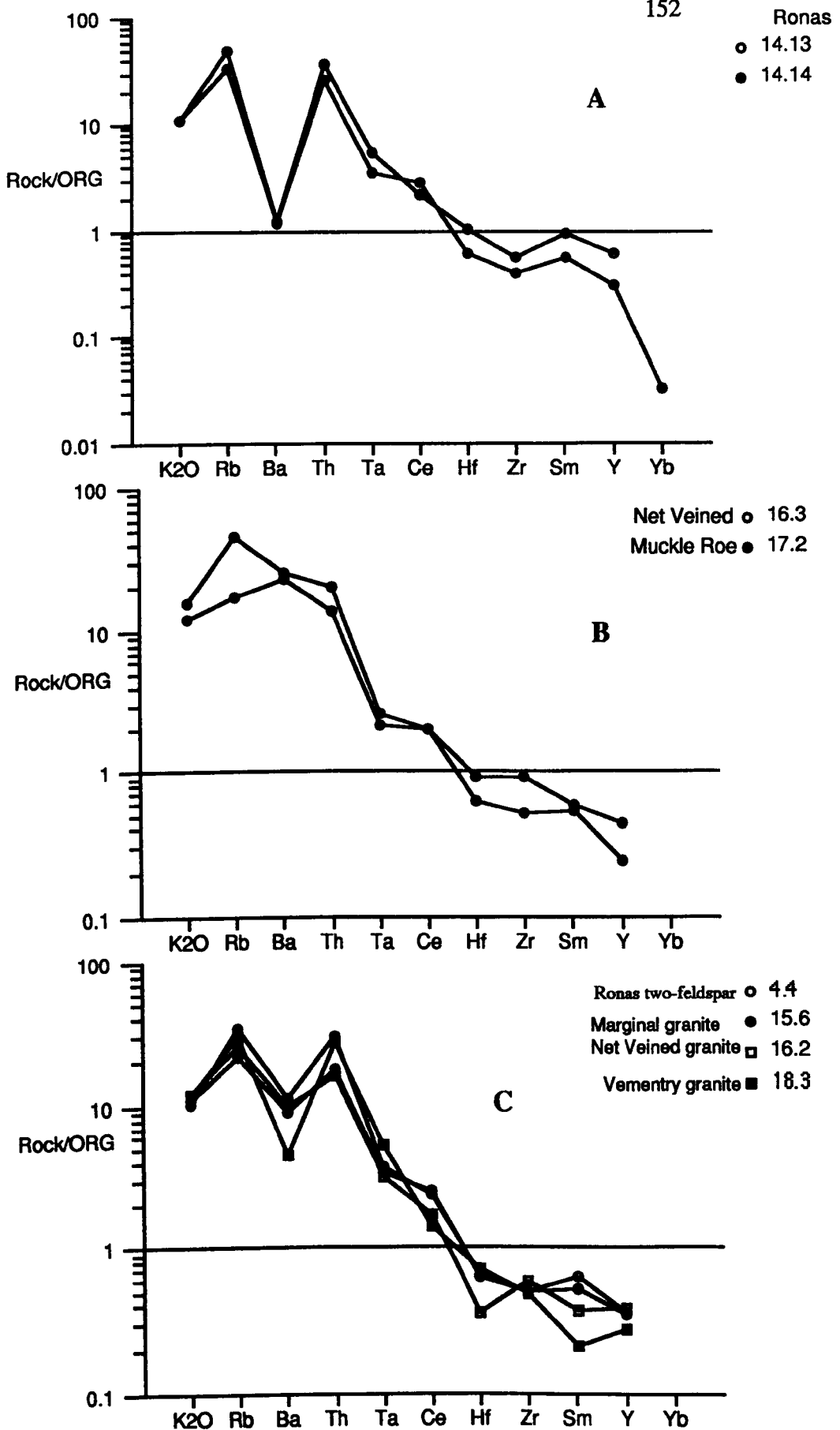
Figure 5.11c Oceanic ridge granite (ORG) normalized geochemical patterns of A) Ronas Hill granite, B) Muckel Roe and Net Veined and C) group Similar samples from Ronas (two feldspar granite), Marginal, Net Veined and Vementry granites.
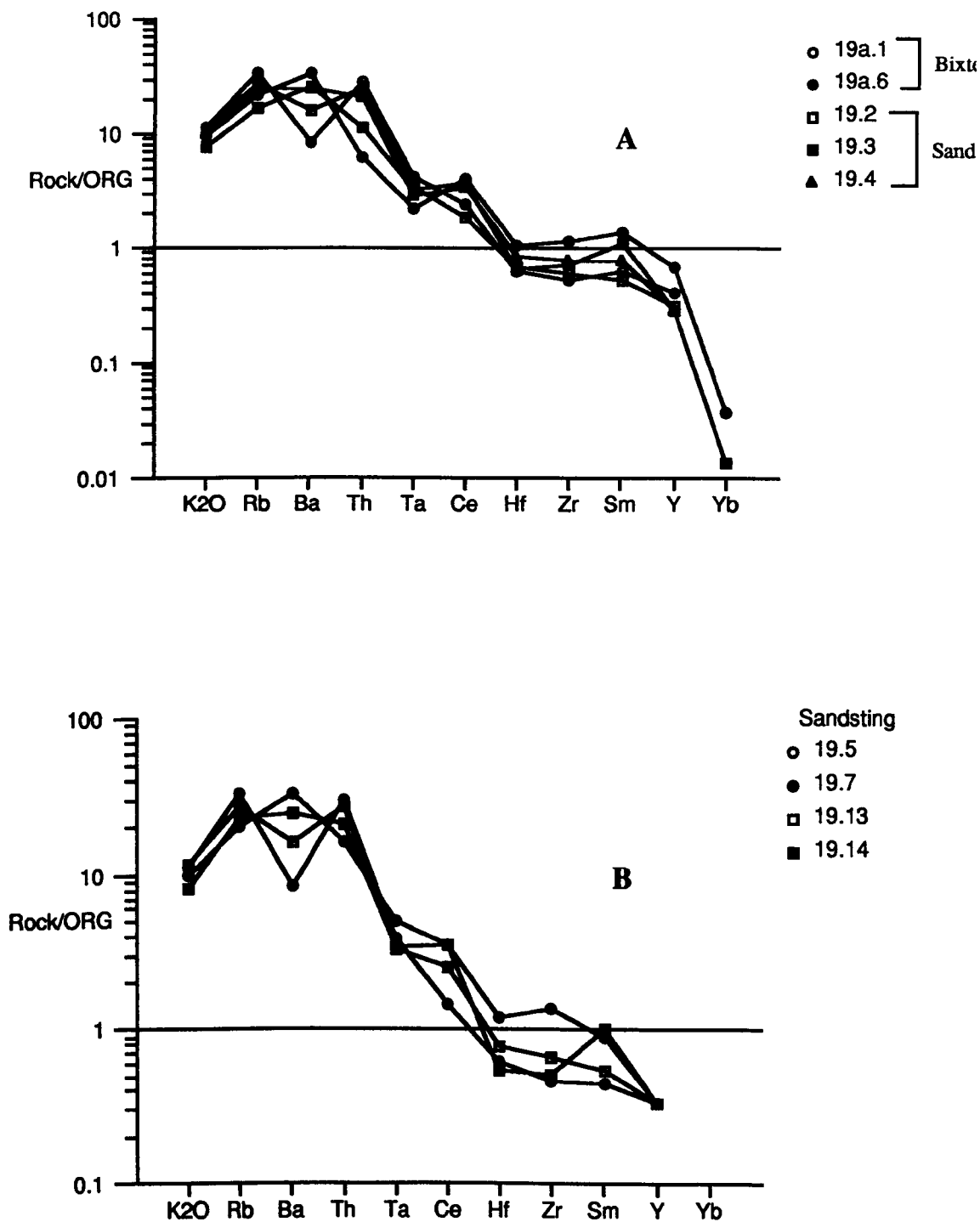
Figure 4.11d Oceanic ridge granite (ORG) normalized geochemical patterns of
A) Bixter (19a.1 and 19a.6) and Sandsting granites, B) rest of Sandsting samples.
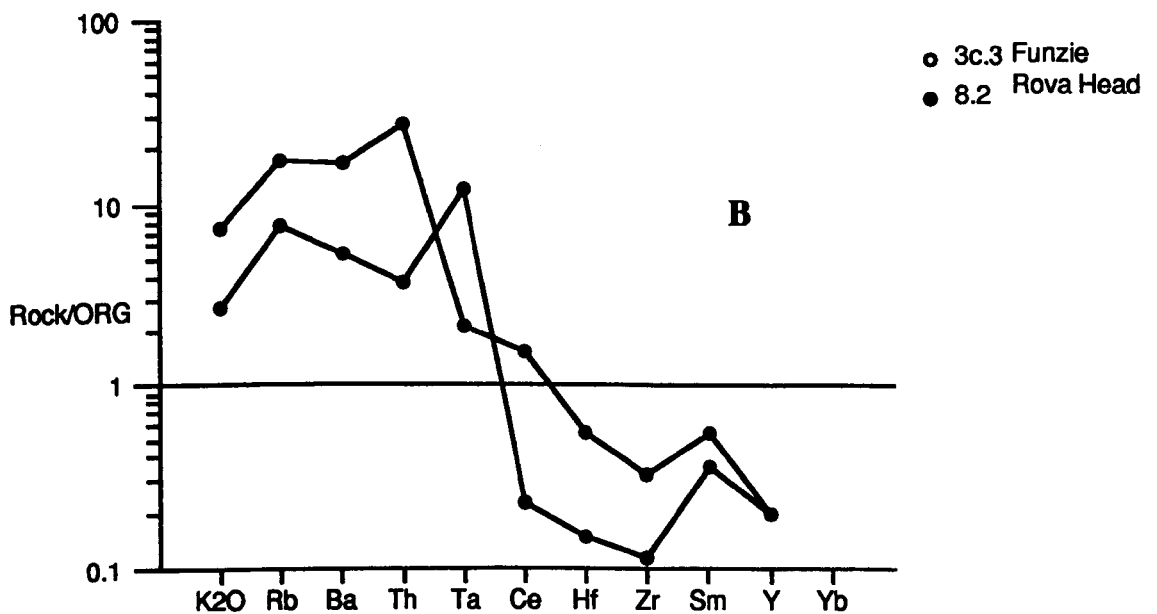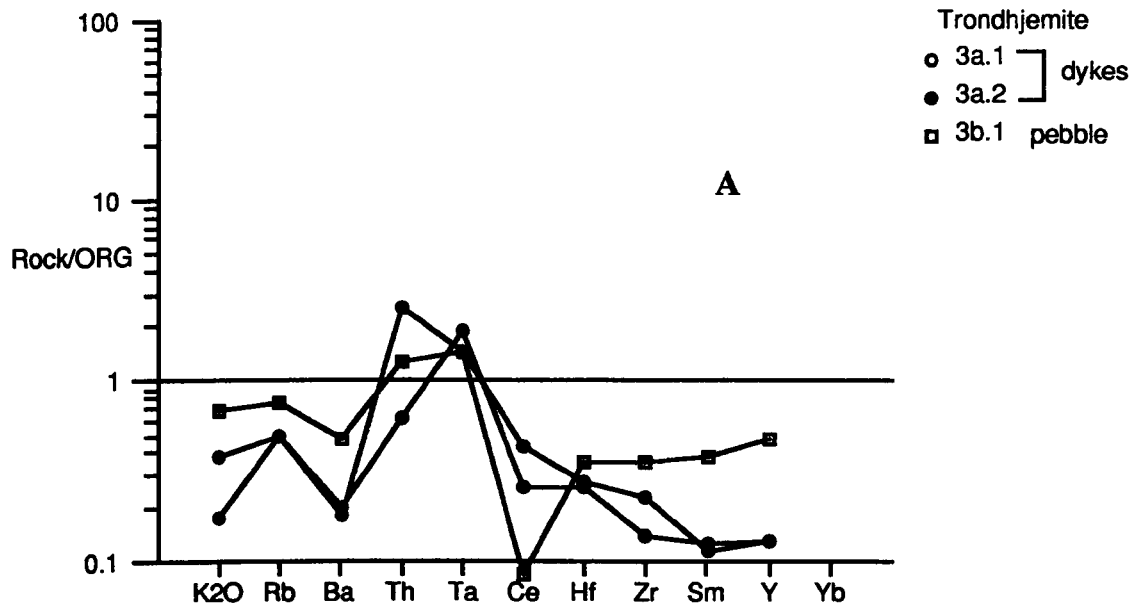
Figure 5.11e Oceanic ridge granite (ORG) normalized geochemical patterns of
A) trondhjemite dykes (3a.1 and 3a.2) and trondhjemitc pebble (Funzie, 3.b1), and
B) granitic pebbles from Funzie and Rova Head conglomerates.

attributed to the loss of these elements in a volatile phase or to alteration (Pearce etal, 1984). The patterns of trondhjemite dykes deviate from the ocean ridge granite patterns in having low abundances Ce to Y.

5.15.6 Spider diagrams of Trace Elements for Funzie and Rova Head Graintic pebbles.

The patterns of trondhjemite dykes and pebble (Figure 4.11e) from the Funzie Conglomerate are similar to the oceanic ridge pattern and deviate only in having strong Ce negative anomaly and unique positive Ta anomaly which can be a special feature of Shtland trondhjemite.

The patterns of the other granitic pebbles (Figure 4.11e) from the Funzie (3c.3) and Rova Head (8.2) conglomerates are similar to syn-collision granites and in particular the pattern of 3c.3 sample is similar to the Barousse syn-collision intrusion and only deviates in its high Ta content. The pattern of sample 8.2 (Rova Head conglomerate) shows relatively high abundances of elements (except Ta) compared with sample of 3c.3 (Funzie conglomerate).

5.16 Rare Earth Element geochemistry of Shetland Granitoids.

5.16. 1 Introduction

Although the term rare earth elements (REE) is considered to be a misnomer to many, a comparison of their crustal abundance with other better known rare elements shows that at least some are indeed relatively rare. The elusiveness of the REE is a consequence of their dispersion as substitutional impurities in many common rock-forming minerals. The mineralogy of the REE is extensive (Clark, 1984), but only a few minerals contain major quantities of REE and are sufficiently concentrated to constitute economic deposits. Despite chemical similarities, the REE may show significant distribution variations in different minerals or in the same mineral crystallized under different environmental conditions. Some of the factors that control the distribution of REE in minerals include: (1) ionic radius
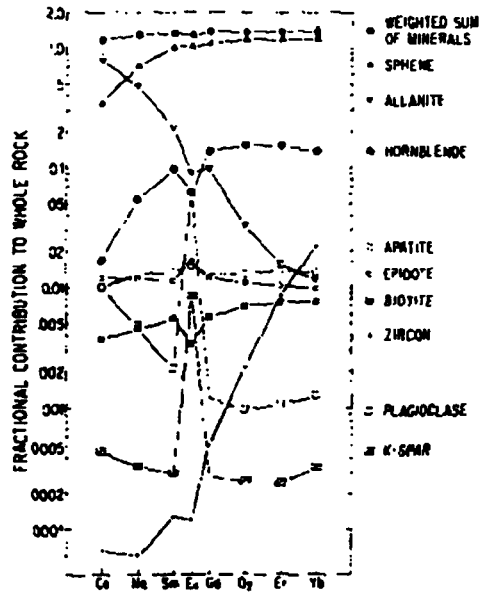
Fractional contribution of each mineral to the whole rock REE abundances in the granodiorite. A composite reconstructed rock calculated from the sum of the mineral contributions is also plotted. Error bar on Ce and Yb for this sum indicate the uncertainty arising solely from the statistical uncertainties in the modal abundances of allanite and sphene. Allanite contributes most of the uncertainty in Ce, whereas sphene does so for Yb. Note that most of the REE in this rock are present in sphene and allanite. The shapes of the patterns on this diagram are equivalent to whole-rock normalized values.

Figure 4.12a Figure 3 of Gromet and Silver (1983)

differences; (2) crystal structure; (3) basicity differences; (4) oxidation states; (5) stability of complexes; (6) melt structure in magmas; (7) REE content and distribution in source fluids; (8) the role of tempreture and pressure; and (9) relative solubility of REE and their migratory capacity in hydrothermal solutions and in the weathering environment (Mariano, 1990).

The REE (also called lanthanides) are lithophile elements (with atomic numbers 57 through 71), and yttrium (atomic number 39) is commonly included because of its similar chemical behaviour. REE of even atomic number (including Ce, Nd, Sm, Gd, Dy, Er, and Yb as well as Y) are geochemically more abundant than those of odd atomic number (La,Pr, Pm, Eu, Tb, Ho, Tm, and Lu), which produce a "zig-zag" effect in plots of rare earth data. This effect is eliminated by plotting REE analyses normalized to average REE abundances in chondritic meteorites. All REE have an identical +3 valence and an ionic radius that gradually decreases with increasing atomic number (the "lanthanide contraction"). Exceptions in nature are mainly Ce which can have a valence of +4 under oxidizing conditions and Eu which can have a valence of +2 under reducing conditions. The +4 valence of cerium is important in weathering ; the +2 valence of europium under reducing conditions can give rise to a "europium anomaly" (normally produced by fractional crystallisation of plagioclase in igneous rocks).

The light rare earths (called cerium-group or LREE) have relatively large ionic radii similar to that of Ca^{2+} and Th^{4+}, whereas the heavy rare earths (plus Y and therefore called the yttrium-group or HREE) have smaller ionic radii approaching that of Mn2+. All of the REE commonly substitute for each other in minerals. The Ce-group or LREE tend to be concentrated in highly fractionated basic rocks such as carbonatites, whereas HREE and especially Y tend to be concentrated in fractionated acid rocks such as alkaline granites and pegmatites.

The distributions of rare earth elements during fractional crystallisation or partial melting are dispersed as minor or trace constituents into major phases, in which

they are not essential components (Figure 4.12a).

In granitic rocks the REE are mainly concentrated in accessory minerals such as sphene, apatite, allanite, zircon and monazite which are widespread. Fleischer, (1978b) showed that sphene in the sequence alkaline pegmatite, alkaline rock, gabbro and pyroxenite, granodiorite, granite pegmatite, the average contents of the LREE decrease and the contents of the intermediate and heaviest REE and Y increase.

Lee et al, (1973) determined the REE compositions of a number of apatites from hybrid granitoid rocks of the southern Snake Range, Nevada, and found that apatites from the more mafic rocks contained rare earth assemblages richer in the lighter REE. Brooks et al (1981), have shown that REE partition between phenocrystic allanite and glass of the Sandy Bares perlitic obsidian of Northern Ireland strongly favours the LREE in allanite. Exley (1980), also found variations in the degree of REE fractionation in allanites from rocks in Skye. Zircon is isostructural with xenotime YPO_4 and Y-group are the dominant REE in zircon and minor amounts of the REE are thought to enter zircon through isomorphous substitution. Khomyakov and Manukhova (1971) have found that the proportion of heavier REE is greater in zircons from nepheline syenite than from granites. Monazite is strongly selective of the Ce-group; Jensen (1967) concludes that the monazite structure will accept REE ions with ionic radii between those of La and Eu, based on the existence of a solid-solution series between $(La,Ce)PO_4$ and $CaTh(PO_4)_2$, implying that the structure will accommodate ions with radii between those of Ce and Ca.

These accessory minerals tend to concentrate the LREE and consequently, whole-rock samples of these minerals are frequently enriched in the light REE. Thus these minerals (Figure 4.12a), notably apatite, sphene, zircon and allanite have been shown to have crucial influence in determining the REE patterns in acid rocks (see Fourcade and Allegre, 1981; Gromet and Silver, 1983). Of the major rock-forming

minerals, hornblende, plagioclase, K-feldspar, and biotite, in that order of abundance, act as hosts for the remaining REE (Condie and Lo, 1971).

5.17 Rare Earth Elements To the East of Walls Boundary Fault (WBF).

5.17.1 Rare Earth Elements of the Hornblende-bearing Granites.

a) Chondrite-normalized REE plots for hornblende-bearing granites are shown in Figure 4.12b, in which the REE patterns of the basic granodiorite and lucogranodiorite of the Graven complex (Figure 4.12b-A) are notable for some lack of coherence which could be due to the innumerable tiny xenoliths of hornblendite associated with the Graven granitoid rocks . The Figure also shows that LREE patterns are strongly fractionated, whereas HREE show a flatter patterns which is confirmed by the Ce_N/Yb_N ratios (59, 27, 21, 13), the four patterns are also LREE-enriched. Of the four patterms two have small europium anomalies e.g. sample 6.24a which has a small positive europium anomaly (Eu/Eu*=1.5) and sample 6.13a has a negative europium anomaly (Eu/Eu*=0.65) . The most evolved rock of the Graven pluton (6.29a) shows depletion in both LREE and HREE relative to the other three samples and greater depletion in Dy as well.

b) The second of hornblende-bearing granite suite is Aith-Hildasay-Spiggie . The rare earth patterns of the 5 analysed rocks from Aith-Hildasay (Figure 4.12b-B) show strong fractionation of the light REE indicated by the Ce_N/Yb_N ratios (24, 21, 18, 11, 7), whereas HREE show a flatter pattern. They have to some extent similar LREE-enriched shapes except sample 12b.32 which has a small positive Ce anomaly. All have small negative europium anomalies except sample 12b.32, three with Eu/Eu* ratios (0.75, 0.66, 0.66) and the fourth one with Eu/Eu* = 0.34. The sample 12a.28 is a rock from the Aith Granite and the others are all from the Hildasay granite. Sample 12b.35 is the most evolved (highest SiO_2 content) and depleted sample among the Hildsay samples in both LREE and
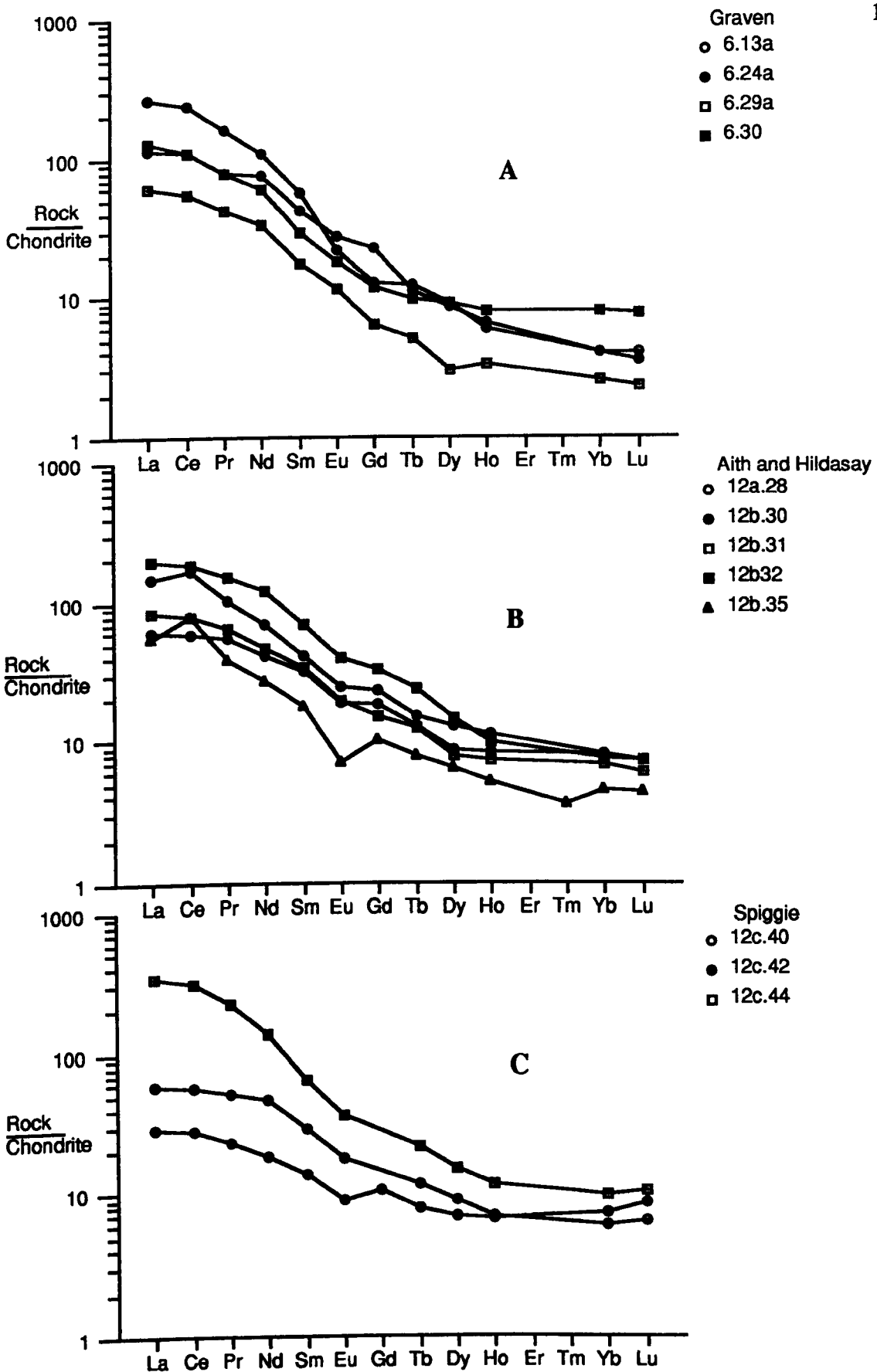
Figure 5.12b Chondrite-normalized rare earth element plots of hornblende-bearing granites, from A) Graven granitoid, B) Aith and Hildsay granites (two offshoots of Spiggie), and C) Spiggie granite.
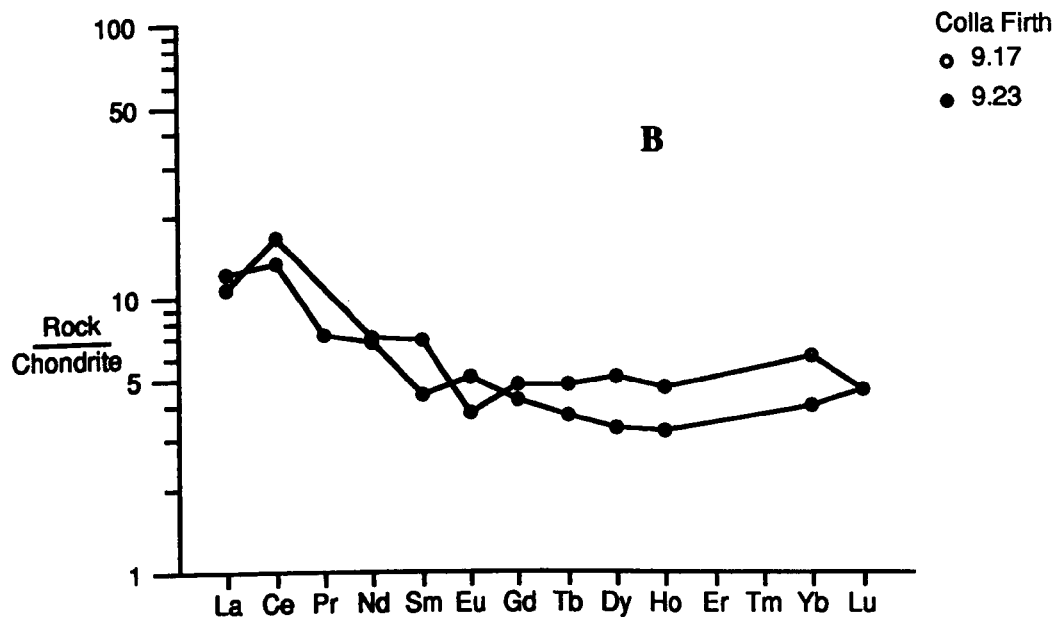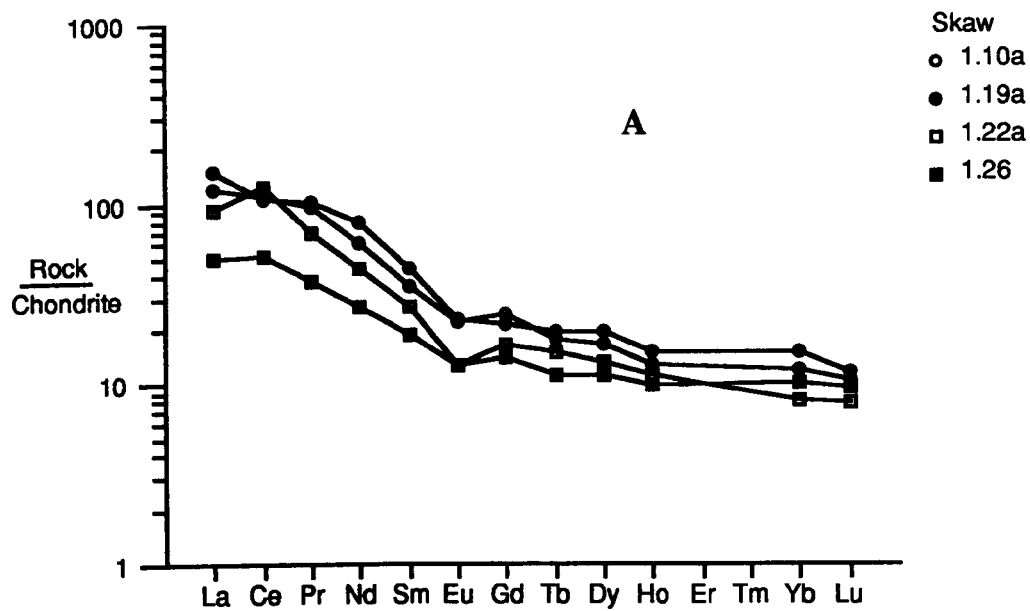
Figure 5.12c Chondrite normalized REE plots for hornblende-free granites, from A) Skaw granite, and B) Colla Firth.

HREE. The development of a larger negative europium anomaly in the most depleted sample could be explained by the fractionation of plagioclase, as the divalent Eu is geochemically very similar to Ca and can be preferentially incorporated into divalent Ca sites in plagioclase (Hanson,1980) during fractional crystallisation. HREE and LREE depletion is probably due to accessory phase precipitation (see Zr data discussed earlier)

c) The third type of hornblende-bearing granite REE paterrns is that for the Spiggie granite. Rare earth patterns of three analysed rocks (Figure 4.12b-C) from the Spiggie complex show strong fractionation of light REE especially in the basic monzonite rock (12c.44) with increasing acidity from 59 to 69 % in the granitic rock which is confirmed by the CeN/YbN ratios (32, 9, 4). There is a marked depletion in LREE and to some extent HREE. These clues indicate the consistent behaviour of the rocks due to fractional crystallisation from the same parental magma. The smooth variation leaves no doubt that all three rocks are genetically related. They have similar LREE-enriched shapes and the most acid rock (12c.42) has a small negative europium anomaly (Eu/Eu* = 0.6) and less depletion in HREE. This may be due in part to fractional crystallisation of plagioclase which will result in the enrichment of HREE, as suggested by Nagasawa and Schnetzler (1971). The great decrease of LREE from the basic monzonite toward the granite may be due to the removal of sphene and allanite, which are the main sources of LREE, as indicated by Condie (1978).

5.17.2 **Rare Earth Elements of the Hornblende-free Granites**

a) Figure 4.12c-A shows the chondrite normalised REE patterns for the rocks of the Skaw granite, 4 samples have been analysed. They have similar LREE-enriched patterns and indicate a LREE enrichment with CeN/YbN ratios 7, 9, 15, 5, whereas the HREE shows a flat pattern . All have small negative europium anomalies which increase toward the most acidic rock (av. Eu/Eu* = 0.68). This indicates that the plagioclase fractionation was important. The most evolved sample (1.26) shows depletion in LREE, but conversely shows less depletion in HREE, the slight enrichment of HREE could be due to the removal of plagioclase (Nagasawa and Schnetzler, 1971).

b) The rather irregular REE patterns (Figure 4.12c-B) for the Colla Firth granite in the Colla Firth permeation belt show less fractionated LREE with low CeN/YbN ratios(3, 5), sample (9.17) shows a small negative europium anomaly (Eu/Eu* = 0.61), whereas sample (9.23) in contrast shows a small positive europium anomaly (Eu/Eu* = 1.31) and HREE depletion and that may be due to the effect of zircon and apatite which have larger K_D values for the HREE, which are the main sources of HREE (Hanson, 1980).

5.18 **Rare Earth Elements To the West of Walls Boundary Fault.**

5.18.1 **Rare Earth Elements of the Ronas Hill Granite**

Figure 4.12d-A shows the chondrite normalised rare earth patterns for the rocks of the Ronas Hill Granite. The REE patterns of three analysed samples, have moderate LREE , show less fractionated LREE with CeN/YbN ratios (8, 8, 5), in which sample (14.7) is from a diorite intruded by the Ronas Hill granite and shows no europium anomaly, subdued LREE 's and an enrichment of HREE. The two feldspar granite (14.3) is distributed within the Ronas Hill complex main magma (14.14) as an early phase, and evolved independent of the main magma which produced the main granite massif of Ronas Hill. The REE pattern of the two
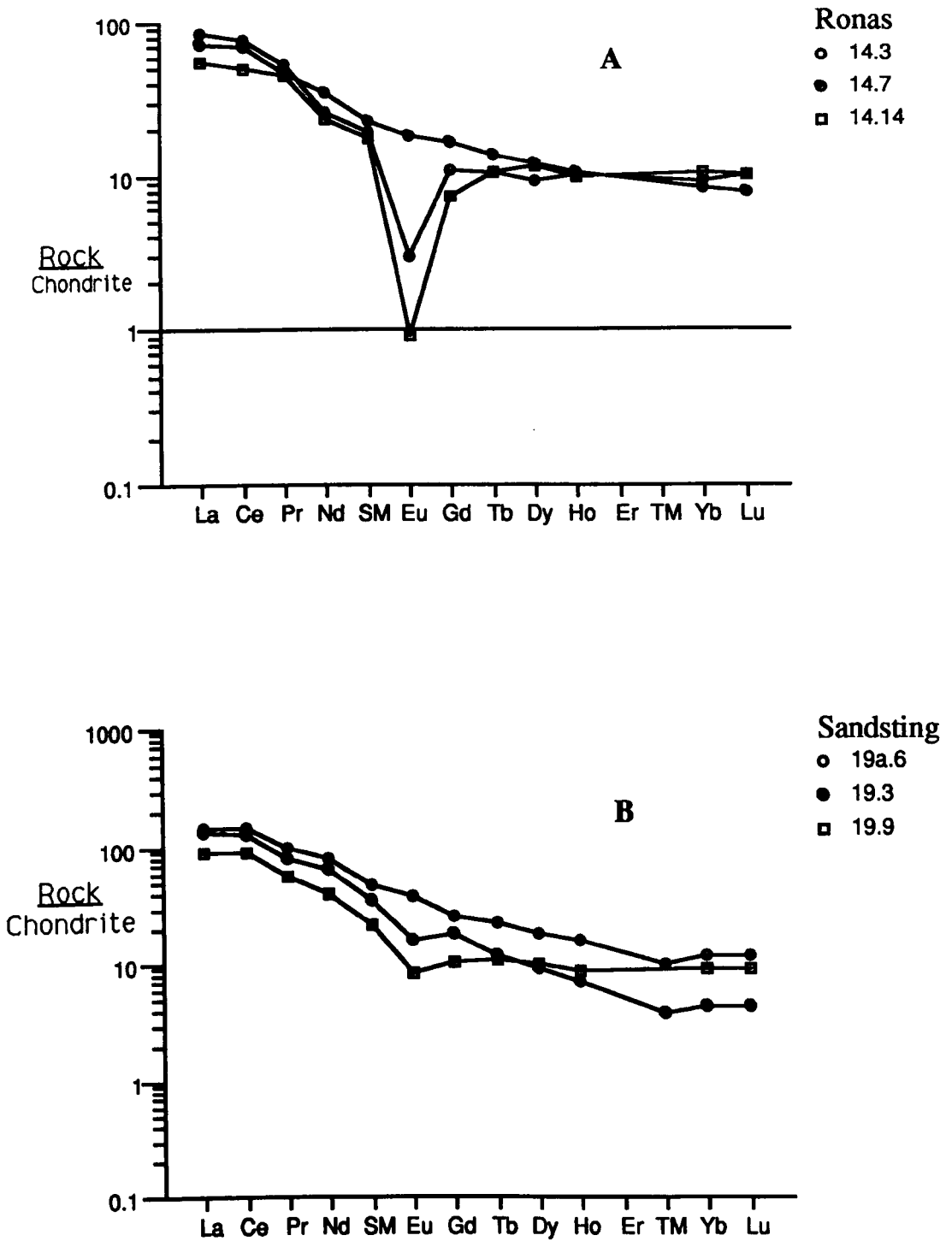
Figure 5.12d Chondrite- normalized rare earth element from A) Ronas Hill grante and B) Sandsting and Bixter granites (19a.6) to the west of WBF and north and south of Bixter Voe respevtively.

Table 5.1   Normalising values used in trace element diagrams.

4.1A. Chondritic normalising values. La, Ce, Nd, Sm, Eu, Gd,

Dy, Er, Yb, Lu, Pr, Tb, Ho and Tm. Courtesy of MP Atherton.

La	0.387 ppm
Ce	0.967 ppm
Pr	0.138 ppm
Nd	0.716 ppm
Sm	0.230 ppm
Eu	0.086 ppm
Gd	0.311 ppm
Tb	0.057 ppm
Dy	0.390 ppm
Ho	0.087 ppm
Er	0.255 ppm
Tm	0.050 ppm
Yb	0.249 ppm
Lu	0.038 ppm

4.1B. ORG (oceanic ridge granite) normalising values
(from Pearce et al., 1984).

K2O	0.4
Rb	4
Ba	50
Th	0.8
Ta	0.7
Nb	10
Ce	35
Hf	9
Zr	340
Sm	9
Y	70
Yb	80

feldspar granite (14.3) shows less LREE depletion than (14.14), has negative europium anomaly (Eu/Eu* = 0.12) and an enriched, flat HREE pattern. Sample (14.14) shows a depletion in LREE, negative europium anomaly (Eu/Eu* = 0.09) and enriched, flat HREE. The similarity between the two feldspar and the perthite granite of the main body of Ronas Hill granite in terms of their smooth variations and large negative europium anomalies indicate that they are genetically related.

5.18.2 Rare Earth Elements of the Sandsting Granitoid and Bixter Granite.

Figure 4.12d-B shows the chondrite normalised rare earth patterns for three analysed samples: one is a diorite from the Bixter granite (19a.6) and the other two are a diorite (19.3) and a granite (19.9) from the Sandsting Complex. The Sandsting diorite (19.3), which together with the gabbro, is the most basic component in the evolution of the Sandsting complex while the granite is the most evolved (19.9). The REE pattern for the diorite from Bixter (19a.6), shows an enrichment in both LREE and HREE and no europium anomaly, whereas the diorite in the Sandsting complex (19.3) shows less enrichment of LREE and a depletion in the HREE, and a small negative europium anomaly (Eu/Eu* = 0.6). The REE pattern (Figure 4.12d) for the granite (19.9) from the Sandsting pluton shows a negative europium anomaly (Eu/Eu* = 0.44). The similar shape of the curves and the development of a Eu anomaly from the diorite towards the granitic rock in the Sandisting intrusion could be explained in terms of the removal of plagioclase which concentrates Eu (Hanson,1980) during fractional crystallisation . The "fractionation" of plagioclase is also indicated by the variation of Rb, Sr, and Ba (see Figure 4.5c-d). However, an accessory mineral such as apatite must also be involved as the LREE are depleted.

5.19 The system An-Ab-Or-Oz (-H2O)

The normative mineral compositions of the Shetland granitoid rocks clearly illustrate differences in major element compositions. These normative data also show that there are differences between the suites discussed and these can be considered simply in terms of the granite system as Ab+An+Or+Qz always exceeds 75. The An-Ab-Or-Qz (-H2O) system is the basis for discussion of the different granitic plutons of Shetland area.

5.19.1 Hornblende-bearing granites.

The ranges of normative composition for the Graven granite and Spiggie-Aith-Hildsay granite are given in the appendix2. The Graven granite contains normative An-Ab-Or-Qz between 71.66 and 92.27. In terms of phase petrology, the Graven bulk composition can be represented on the quaternary phase system $NaAlSi_3O_8$-$CaAl_2Si_2O_8$-$KAlSi_3O_8$-SiO_2 (Figure 4.13a-A) which is useful in describing the crystallisation sequence and lineage character of most granitic rocks. Plagioclase-rich composition rocks lie in the plagioclase volume at or near the An-Ab-Or face. Acid plagioclase-poor compositions, trend away from the plagioclase volume towards the K-feldspar or quartz liquidus surfaces (near the Ab-Or-Qz face) indicative of plagioclase fractionation. The low An-contents of the Graven rocks means that crystallisation in the plagioclase volume would rapidly move the liquid to the plagioclase-K-feldspar surface, and then to the cotectic. According to Presnal and Bateman (1973) such trends lying at a high angle to the quartz liquidus surface are incompatible with derivation of the magma series by fractional melting of lower crustal material. Rather, they are compatible with equilibrium fusion of the lower crust followed by fractional crystallisation of plagioclase from the magma at a high level. This is confirmed texturally, both in the quartz-monzodiorite and the granodiorite which shows the liquidus nature of plagioclase. Plagioclase crystallized first, then K-feldspar and later quartz during cotectic crystallization (Figure 4.13a-A).

In the Spiggie-Aith-Hildsay granite, normative An-Ab-Or-Qz varies from

78.28% to 95.47%. Since Spiggie rocks all have > 75% normative An-Ab-Or-Qz, their bulk compositions are well represented on a tetrahedral An-Ab-Or-Qz plot (Figure 4.13a-B). The Spiggie basic plagioclase-rich compositions lie higher in the plagioclase volume than the Graven granite. Liquids of this composition crystallize plagioclase initially and liquid compositions trend away from the plagioclase volume towards the K-feldspar or quartz liquidus surfaces. The Spiggie rocks with low An-contents indicate crystallisation in the plagioclase volume would move the liquid to the plagioclase-K-feldspar surface, and then to the cotectic. As in the Graven rocks such trends lying at high angle to the quartz liquidus surface are incompatible with derivation of the magma series by fractional melting of lower crustal material. Rather, they are compatible with equilibrium fusion of the lower crust followed by fractional crystallisation of plagioclase from the magma at a high level (Presnall and Bateman (1973). This is confirmed texturally in all Spiggie rocks which show the liquidus nature of plagioclase. Firstly plagioclase, and then K-feldspar and later quartz crystalize during cotectic crystallisation (Figure 4.13a-B).

5.19.2 **Hornblende-free granite.** The ranges of normative composition for the Skaw granite and Colla Firth granite are given in the Appendix 2. The Skaw granite has between 82.01 and 89.37 wt% normative An+Ab+Or+Qz. Most samples are slightly corundum normative, with a maximum of 4.03 wt%. In the quaternary phase system $NaAlSi_3O_8$-$CaAl_2Si_2O_8$-$KAlSi_3O_8$-SiO_2, the Skaw rocks have low An compositions, indicating minor or no crystallization of plagioclase until the K-feldspar or quartz liquidus surface is reached (Figure 4.13b-A). These low An rocks appear to lie on the join or in the quartz field of the system Ab-Or-Qz. Thus they must be a product of fusion of acid material and cannot be the product of melting or fractionation of a basic source unless major amounts of silicic material have been added (Atherton, 1988).

In the quaternary phase system An-Ab-Or-Qz Figure 4.13b-B two distinctive

groups can be shown. One represents Tonga, Brecken and Out Skerries granites and the other Colla Firth garnet-bearing granite plots which has between 86.90 and 94.70 wt% normative An-Ab-Or-Qz. The samples are corundum normative, with a maximum of 5.33 wt%. These are poorer in An than Skaw granite and lie close to the quaternary cotectic. The two groups are similar to the Skaw granite in that some rocks lie in the quartz volume of the system An-Ab-Or-Qz, and must be a product of fusion acid material.

The Ronas Hill granite and its satellites (Eastern granite, Net Veined granite, Muckle Roe granite and Vementry granite) to the west of Walls Boundary Fault (WBF) have between 93.39 and 99.14 wt% normative An-Ab-Or-Qz. They are alkali-feldspar granites, most of them show K-feldspar-quartz intergrowth in terms of micrographic and granophyric textures. A full normative analysis of these rocks are found in Appendix 2. The two feldspar granite within Ronas Hill, some of the Net-Veined granite and the mafic inner Vementry granite seem to form separate plots distinct from the other plots of Ronas Hill granite and its satellites (Figure 4.13c-A). On the quaternary phase system An-Ab-Or-Qz, the Ronas Hill granite and its satellite granitic rocks show a marked clustering of data points,which lie mostly on the cotectic close to the "minimum melt" (M. P. Atherton, 1988), indicating a low temperature melt of granitic (s.s) composition. They are texturally distinctive as mentioned above and show Sr and Ba depletion. No field relations or other geochemical evidence indicate that they are "S-type" granites as shown by the quaternary phase system.

The Sandsting and Bixter granites have between 79.86 and 94.81 wt% normative An+Ab+Or+Qz. Normative analyses of the Sandsting and Bixter granitic rocks are shown in Appendix 2. In terms of phase petrology, some of the Sandsting rocks crystallized in the plagioclase volume, then evolved by plagioclase fractionation until the K-feldspar or quartz liquidus surface was reached. The basic granodiorite, porphyritic microadamellite and most evolved acidic samples of Sandsting and Bixter granite form two contrasting groups in the quaternary phase

system An-Ab-Or-Qz (Figure 4.13c-B). Many of the acid rocks have crystallized near or on the cotectic. The Sandsting and Bixter granites are following Presnal and Bateman (1973), compatible with equilibrium fusion of the lower crust followed by fractional crystallisation of plagioclase from the magma at a high level. Rock textures confirmed this nature by showing that plagioclase formed first. K-feldspar and quartz formed later during cotectic crystal growth.

In the quaternary phase system, the Shetland granitoid rocks show separate crystallisation paths. The hornblende-bearing granites (Graven and Spiggie, Figure 4.13a A-B) and the Sandsting granitoid (Figure 4.13c) clearly show their own curves, extending from the plagioclase field across the tetrahedron above and at a high angle to the quartz-plagioclase and two feldspar surfaces. Further, the individual curves of the plutons, originate at different points within the plagioclase field and do not "fan out" from a common origin. This may be interpreted to mean that each pluton has a separate image or crystallisation path from a primary magma. Two main methods of magma extraction from source region are considered by Presnal and Bateman in their work on the Sierra Nevada Batholith.

a) **Fractional Fusion**; which is defined as the continuous extraction of small increments of completely liquid magma from the source region.

b) **Eqilibrium fusion**; in which the melt remains both in contact and equilibrium with the residual crystals at the site of melting.

A fundamental distinction between these two processes with respect to the above system, is that an important feature of fractional fusion is that the only liquids that can be obtained within the tetrahedron lie on the quartz saturation surface. This conclusion holds regardless of the specific composition, of the source region chosen as long as it can be closely approximated by some point within the system An-Ab-Or-Qz. It is clear that the hornblende-free granite and Ronas Hill granite and its satellites plot near to the quartz saturation surface with some of the more fractionated hornblende-bearing granites and the Sandsting granitoid. Clearly the hornblende-free granites and the Ronas Hill granite can be produced by the process
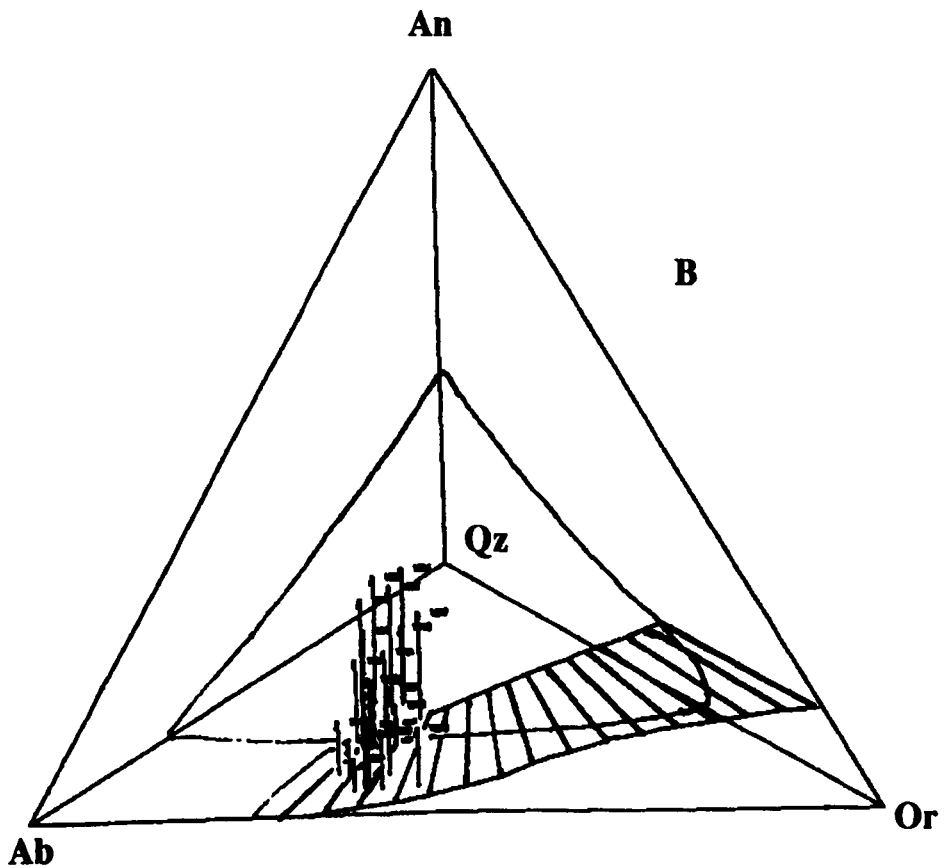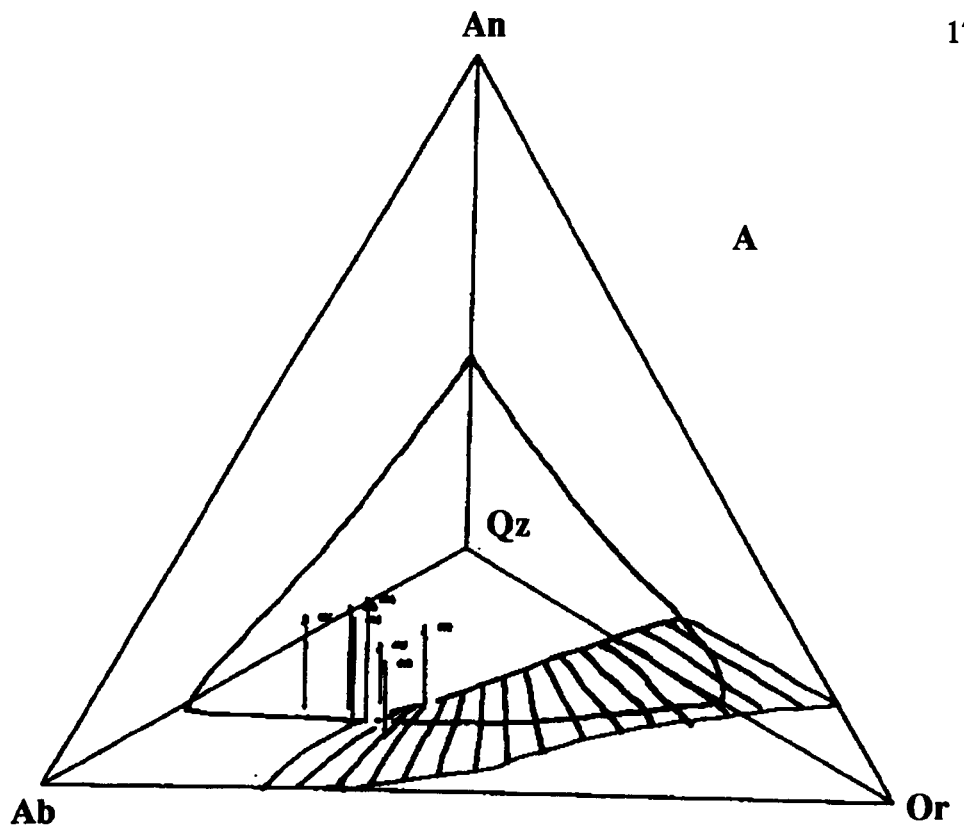
Figure 5.13a An-Ab-Or-Qz tetrahedral plots from hornblende-bearing granites for A) the Graven rocks and B) the Spiggie-Aith-Hildasay granites. Note the spread of data points in B from plagioclase field to quartz field.
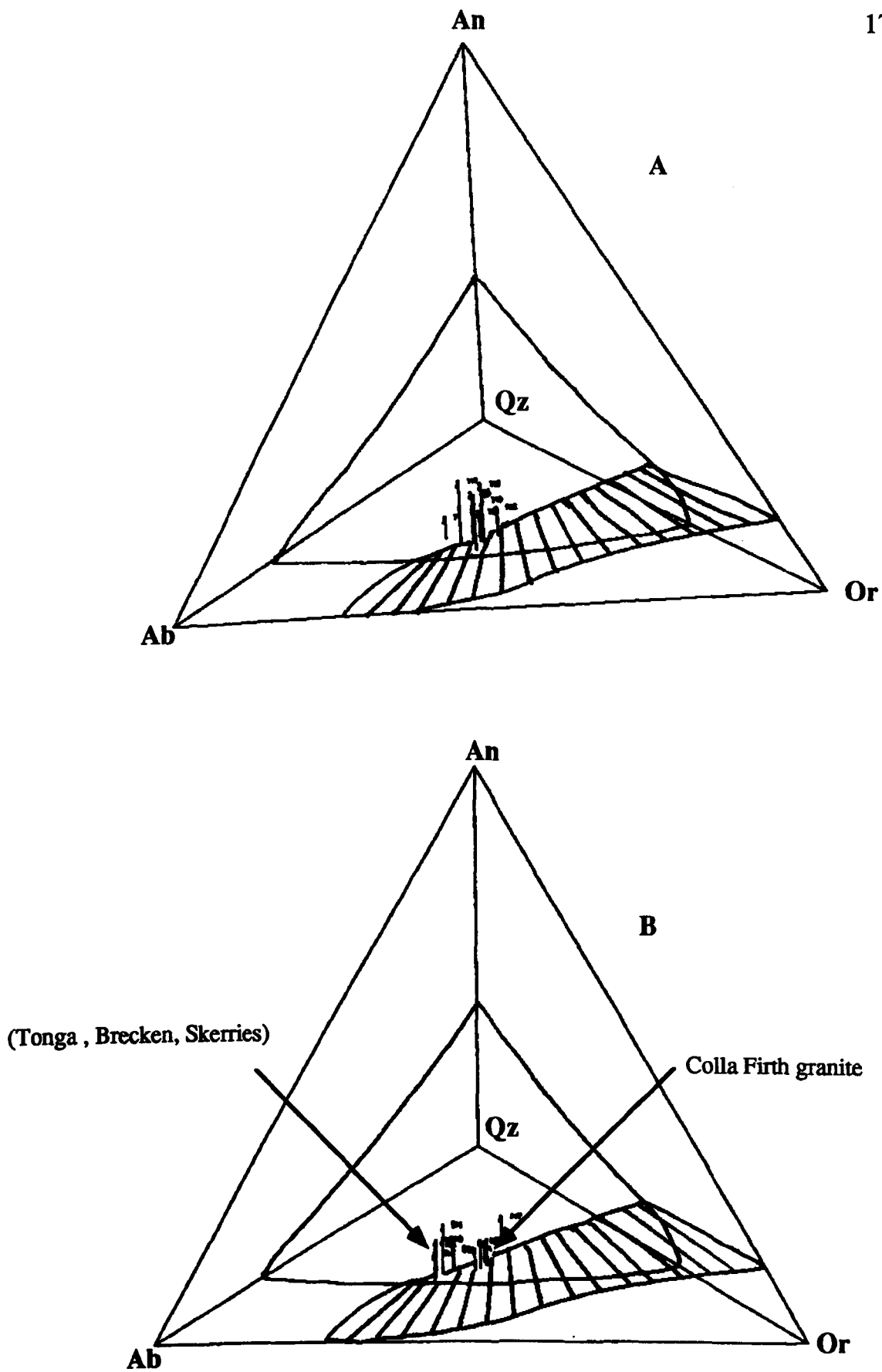
Figure 4.13b An-Ab-Or-Qz tetrahedral plots from Homblende-free granites for A) Skaw granitic rocks and B) include Tonga, Brecken, Out Skerries (note that their data generally grouped to the left) and Colla Firth granitic rocks (clotted to the right).
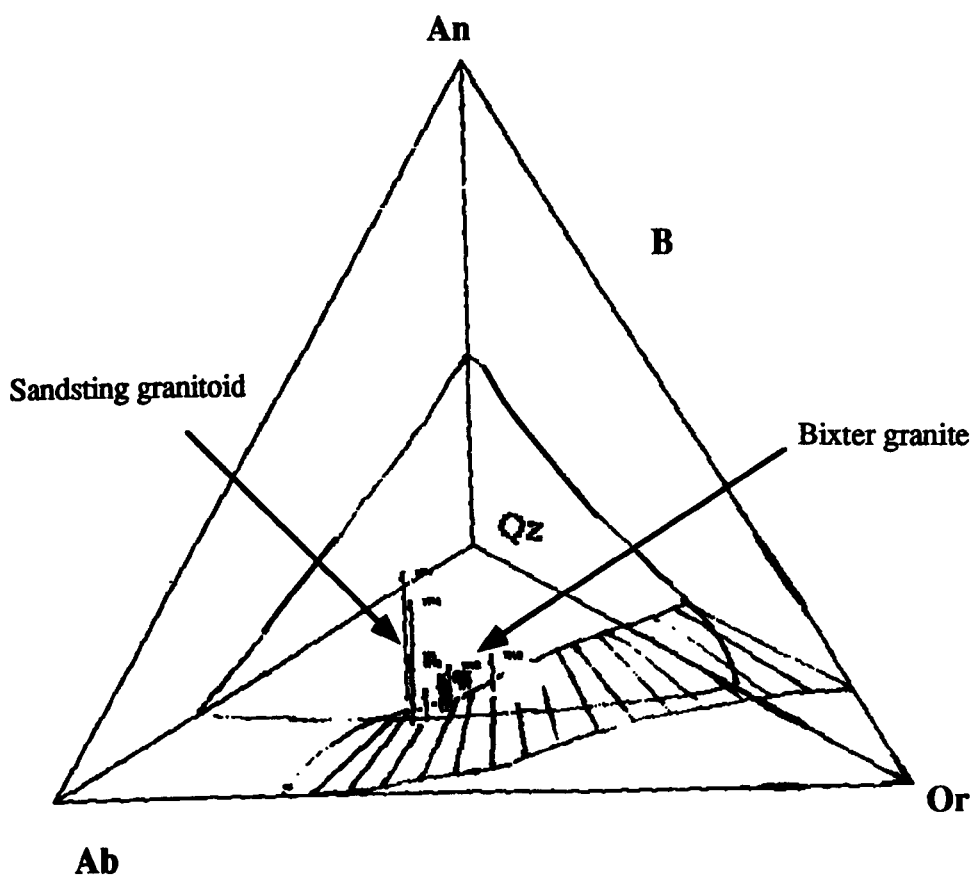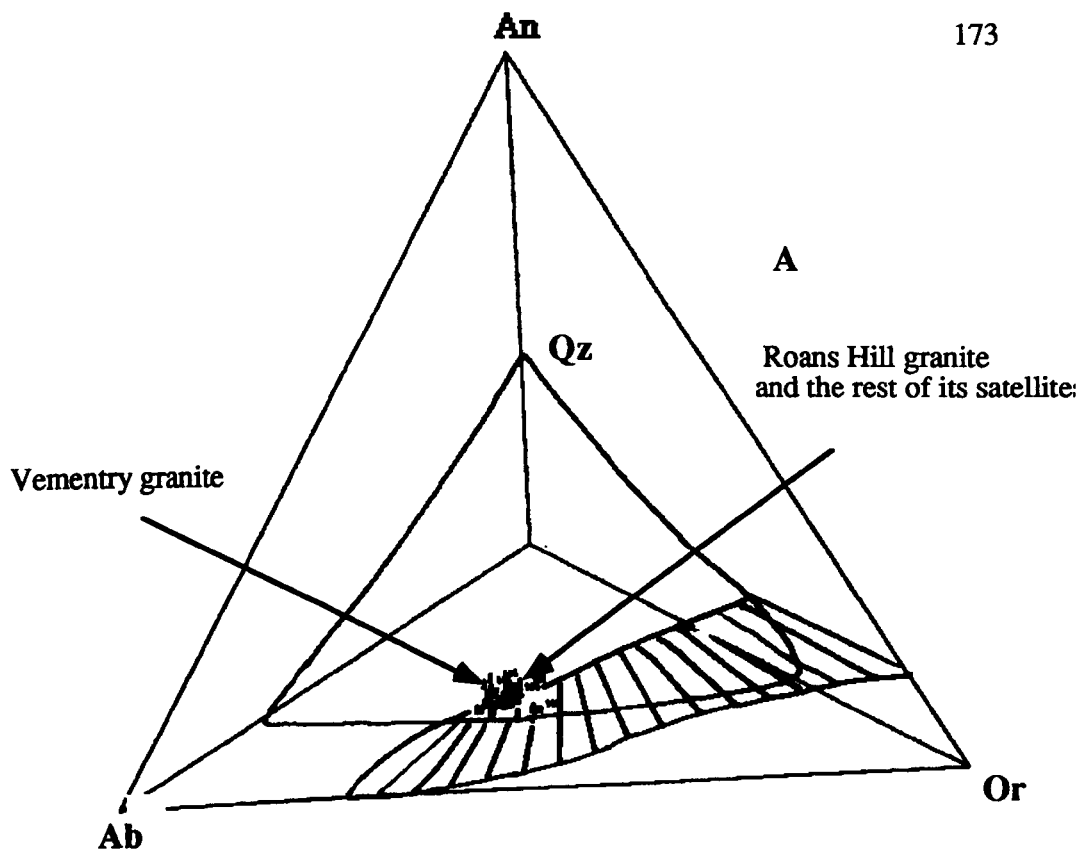
Figure 5.13cAn-Ab-Or-Qz tetrahedral plots of A) Ronas Hill granites and its satellites and B) Sandsting and Bixter granites. Note the data grouping and Net Veined granite show slightly high Ca than the others.

of fractional fusion, but the hornblende-bearing granite and the Sandsting granitoid cannot. Presnal and Bateman (1973) concluded that regardless of the degree of melting or proportion of crystals carried along with the rising liquid fraction, equilibrium fusion is capable of producing the observed trends in the Sierra Nevada Batholith. These trends are (1) mafic to felsic sequence of intrusions, (2) compositions which lie above and at a high angle to the quartz-saturation surface. Thus it may be concluded that a process of equilibrium fusion is responsible for the origin of the parent magmas in the case of hornblende-bearing granites and the Sandsting complex. Further, Presnal and Bateman (1973) point out that a field association involving a well established mafic to felsic sequence of intrusion is not satisfactorily explained by a series of equilibrium fusion events from a single source region. Such an association is best explained by a single equilibrium fusion event, with subsequent fractional crystallisation of the derived magma higher in the crust. This conclusion is in agreement with the present work which proposes equilibrium fusion and then higher level fractional crystallisation, confirmed by the common occurrence of normal zoning in the plagioclase crystals (from a calcic core to a sodic outer shell) as well as the presence of mafic minerals characteristic of low pressures.

<u>CHAPTER SIX.</u>

6.1 <u>Modelling of Major Elements, REE and LILE .</u>

6.1.1 <u>Introduction.</u>

Modelling is an attempt to explain variation in chemical composition, i.e. by removing (fractional crystallisation) or adding (partial melting) of minerals of relevant composition from a given initial composition, and then observing whether the compositions of the evolved "residues" agree favourably with the target compositions. The aim of this part is to find hypotheses to explain the compositional variation in the hornblende-bearing granites and the Sandsting granite. All the available evidence (major and trace element variation, petrological and textural) emphasises the importance of differentiation in the evolution of Shetland granitoids. Following the models of Presnal and Bateman (1973) the normative crystallisation paths (Figures 4.13a) for hornblende-bearing granites (Graven and Spiggie) and the Sandsting granite are in accord with a generative mechanism of equilibrium fusion of the lower crust source region followed by fractionation during and post intrusion dominantly in situ.

If one accepts that in *situ* fractionation was dominant in producing the observed trends, attention must then be focussed on the behaviour of those minerals found in the granites.

The decreasing Sr content of the granites with increasing silica content probably relates to plagioclase fractionation. The metals Ce, Cr, La , Nd, Sc, V, Y and Zn are strongly partitioned into clinopyroxene, hornblende, biotite and magnetite co-existing with intermediate/acid melt and fractionation of these phases could explain the observed trends. Barium and Rb are taken up selectively by biotite and fractionation of this phase could be significant. The decreasing Zr contents of the granites with the increasing SiO_2 contents most likely relates to zircon precipitation. The poor correlation of the elements Ni, Pb, and Th with SiO_2 contents may be due

to an irregular distribution of host accessory and major minerals and to the scale at which I sampled (7g pellet for XRF). It is not simply due to analytical error since it can be seen that the rest of trace elements contents are well correlated with SiO_2.

Co shows a slightly positive correlation with SiO_2 (Figure 4.2c). Co 2^+ ion (radius $= 0.72A^o$) in the iron-magnesium bearing minerals rather than Mg (Mg+2 radius $= 0.65$ A^o). The decrease in modal content of hornblende from the early - crystallising phases of the hornblende-bearing granites toward the acidic end product may be reflected in the increase in Co.

Rb contents of hornblende-bearing granites do not show a regular trend in the range 40-190 ppm while those of the Sandsting granitoid show positive correlation. Potassium is the only major element for which Rb can substitute and the higher ionic radius of Rb causes it to be concentrated in the residual magma during fractional crystallisation. The Rb contents would therefore be expected to increase and the K/Rb ratios decrease during crystallisation differentiation. All these are evidences that there is a substantial fractional crystallisation which will be used in the major and REE modelling.

I attempted to model hornblende-bearing granites (Graven and Spiggie granites) and the Sandsting granite using the modal mineral proportions of the rocks to produce a satisfactory evolution, but it did not work. However, the target can be reached by using hypothetical extract proportions.

6.2 Major Element Modelling using Fractional Crystallisation.

Major element variations of hornblende-bearing granites (Graven and Spiggie) and the Sandsting and Bixter Granites were modelled using a computer programme (M.P. Atherton and Sanderson, 1985) which works upon the following input data :

1) Initial concentration of starting melt (% element oxide).

2) Minerals used for fractionation: including the chemical analysis of each mineral and mineral proportions (estimated from the modal contents of the rocks or from

assumption if the mode does not produce a satisfactory result, fit with the appropriate results) total to 1. The mass balance calculation based on a) sums all the elements (as oxides) associated with the fractionated mineral phases using the equation :

$$S_k = \{ \sum [\sum_i^m (X_{i,k} * P_i)]\} * W$$

where P_i = proportion of mineral i   i : 1-m (m = number of minerals)

S_k = sum of kth element oxide (concentration of the element left in the melt)

k : 1-n (n = No. oxide

$X_{i,k}$ = weight % of element oxide in mineral i

W = fraction of the melt that has been crystallized (fractionated)

The modelling is carried out in fractionation steps of 0.05 : i.e. 0.05, 0.10, 0.15, 0.20, 0.25 etc. After each fractionation a test is carried out to find out whether all the elements are available for a further fractionation :

Element available for further fractionation = (Initial concentration of element in starting melt) - Sk (concentration of element left in the melt).

The concentration of each element left in the melt is calculated and normalized to give a total oxide concentration of 100%. If at this stage of the fractionation, the above calculation for any element is found to be negative; i.e. Sk > intial concentration of element in the starting melt, then the fractionation is terminated.

Variation in the major element abundances in the above plutons can be seen in the Harker diagram plots in (See Figures 4.2a-e in chapter4). The trends from these plutons show a decrease of most major and trace elements (except Na2O and K2O) with increasing SiO2 contents, i.e with fractional crystallisation. In order to model the major element evolution of a melt during fractional crystallisation, it is necessary to make several assumptions regarding 1) the initial composition of the melt and 2), the minerals involved and their proportions removed during fractionation. The first method by graphical modelling calculating the way in which a liquid changes composition during fractionation is described by Cox et al. (1974). Using this method, 8 rocks, including the entire compositional range from the Graven granitoid
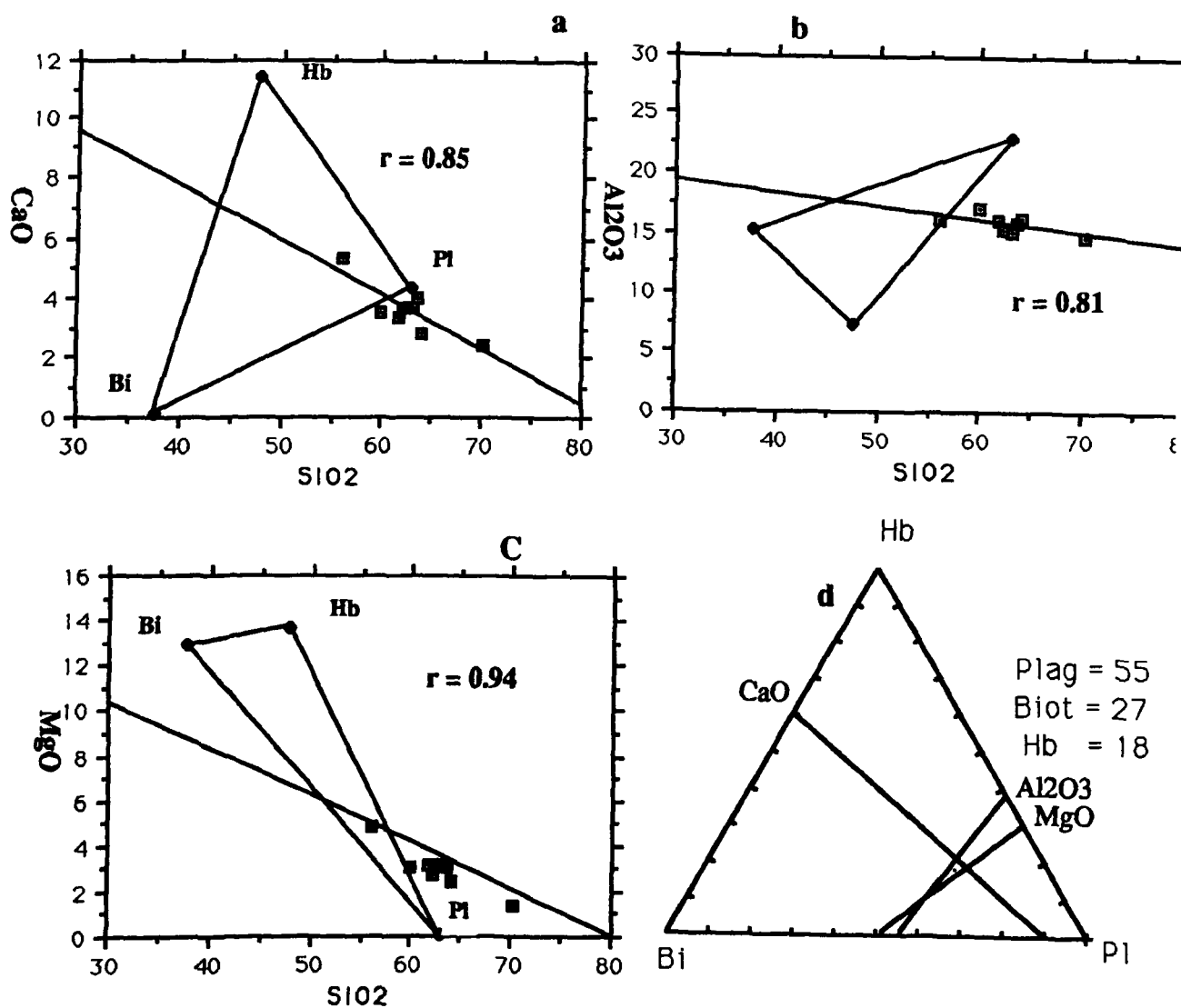
Figure 6.1a-d Extract polygons calculated from the mineral chemistry data in table 6.2 for CaO, Al2O3 and MgO and SiO2 plotted with 8 rocks that span the compositional range in the Graven granitoid (one of the hornblende-bearing granites). During fractional crystallisation, progressively evolved liquids are constrained to lie along a liquid line of descent (defined by regression lines for the rocks) that plots away from a respective extract polygon. The most basic rock (SiO2 56.08) plots inside each polygon and may represent a cumulate extract. Hb = hornblende, Bi = biotite, Pl = plagioclase. Regression lines from a-c replotted on an equilateral triangle. The intersection of all 3 lines gives the relative proportions of a 3 phase extract that represents an initial liquid composition to the more evolved Graven rocks. .

rocks have been plotted on Harker diagrams for MgO, Al2O3 and CaO (Figure 6.1a). Onto these diagrams the extract polygons are plotted from the average compositions of plagioclase, hornblende and biotite (all major phases in the granitoids). During fractionation, the bulk composition of the extract will lie inside a polygon. The residual liquid is driven by fractionation to evolve away from the extract polygon along a liquid line of descent. Figure 6.1a shows that the calculated regression lines for the data plot through all the extract polygons, indicating that the compositional variation may be achieved by fractionatating Pl + Hb + Bi from the melt. Interestingly, sample 6.24a (SiO2 56.08) lies inside all three extract polygons, and may be taken to be represent a cumulate extract. The extract polygons can be further used to determine whether the liquid lines of descent actually represent a coherent suite of rocks, by transposing each triangle and its intersecting bulk compositional trend onto an equilateral triangle (Figure 6.1a-D). The three superimposed compositional trends come close to intersecting, implying a degree of consanguinity. The origin of intersection gives the relative proportions of a three phase extract of plagioclase 55%, hornblende 18% and biotite 27% that represents the relative mineral proportions of the initial liquid composition. These results suggest that it is possible using graphical methods to evolve the monzogranite from the more basic counterparts by three phase fractionation. This method is adequate for modelling the variation of four major elements. To model further the computer programme described above was used for the variation of nine major elements modelled by removing proportions of minerals thought to be involved in the fractionation from a starting melt composition.

	Start Comp (W%) (6.13a)	Liquid Composition at 50% fractionation (Wt%)	Target Composition (6.29a)
SiO2	61.84	68.07	70.19
TiO2	0.79	0.77	0.36
Al2O3	16.04	12.99	14.80
Fe2O3	1.43	1.83	0.50
FeO	2.81	0.21	1.07
MgO	3.13	1.92	1.34
CaO	3.37	3.02	2.47
Na2O	4.24	1.87	4.47
K2O	2.55	2.47	3.38
Total	96.20	93.15	98.58

Mineral extract proportions
Plag. 58
Horn. 16
Biot. 26

Table 6.1 Smmary results obtained from the major element fractionation experiments Of th **Graven granite**. The start is basic granodiorite composition. The target composition is a leucogranodiorite. Liquid composition similar to the target in some elements was obtained after 35% fractionation of plagioclase, biotite and hornblende.

	Plagioclase	Hornblende	Biotite
SiO2	63.18	47.92	37.82
TiO2	0	0.95	2.68
Al2O3	22.92	7.18	15.04
Fe2O3	0	0	0
FeO	0.18	14.00	17.33
MnO	0	0.37	0.17
MgO	0.02	13.62	12.86
CaO	4.28	11.39	0.09
Na2O	9.65	1.68	0.11
K2O	0.22	0.59	9.41
Total	100.45	97.50	95.51

Table 6.2 Microprobe analyses of mineral compositions used to plot the extract polygons in figure 6.1, and in the crystal fractionation modelling experiments of the Graven granitoid.

	Start Comp (W%) (12a.24)	Liquid Composition at 35% fractionation (Wt%)	Target Composition (Wt%) (12c.42)
SiO2	61.49	68.86	68.94
TiO2	0.59	0.50	0.40
Al2O3	16.04	12.75	16.11
Fe2O3	2.12	2.12	1.40
FeO	2.93	2.10	1.90
MgO	3.19	2.72	2.12
CaO	4.79	2.52	2.65
Na2O	3.10	3.18	3.28
K2O	2.99	3.22	3.14
Total	97.24	96.97	99.94

Mineral extract proportions
Plag. 65
Horn. 9
Biot. 25
Mag 1

Table 6.3 sumary results obtained from the major element fractionation experiments of Spiggie granite. The start is a quartz monzonite, the target composition is a coarse grained monzogranite. A liquid composition similar to the target was obtained after 40% fractionation of plagioclase, hornblende, biotite and magnetite in the listed proportions.

	Plagioclase	Hornblende	Biotite	Magnetite
SiO2	52.96	42.8	38.02	0
TiO2	0	0.53	1.72	0
Al2O3	29.72	10.31	15.20	0
Fe2O3	0.84	0	0	69.00
FeO	0	19.56	17.58	31.00
MnO	0	0.45	0.24	0
MgO	0	9.00	12.64	0
CaO	12.28	10.71	0.06	0
Na2O	4.21	2.21	0.13	0
K2O	0.13	1.45	9.42	0
Total	100.14	97.02	94.63	100.00

Table 6.4 Microprobe analyses of mineral compositions used (average composition of hornblende and biotite) in the crystal fractionation modelling experiments of Spiggie granite.

	Start Comp (W%) (19.11)	Liquid Composition at 40% fractionation (Wt%)	Target Composition (Wt%) (19.4)
SiO2	58.15	65.84	65.83
TiO2	1.22	1.28	0.59
Al2O3	16.45	12.23	16.57
Fe2O3	2.15	2.39	1.55
FeO	3.51	0.53	1.55
MgO	2.87	1.06	1.43
CaO	4.53	2.54	2.36
Na2O	3.65	4.41	4.35
K2O	2.98	2.47	3.95
Total	95.51	92.75	98.18

Mineral extract proportions
Plag. 55
Horn. 7
Biot. 38

Tbale 6.5 Summary results obtained from the first stage major element fractionation experiments of **Sandsting granitoid.** The start is a diorite composition. The target composition is quartz-monzodiorite. A liquid composition similar to the target was obtained after 45% fractionation of plagioclase, hornblende and biotite in the listed proportions. Mineral compositions used are in table 6.4

	Start Comp. (19.4)	Liquid Comp at 15% fract.	Target Comp. (19.9)
SiO2	65.83	70.42	70.68
TiO3	0.59	0.51	0.33
Al2O3	16.57	14.87	14.58
Fe2O3	1.55	1.66	1.91
FeO	1.55	0.22	0.41
MgO	1.43	0.58	0.27
CaO	2.36	0.85	1.05
Na2O	4.35	4.74	4.60
K2O	3.95	4.18	4.61
Total	98.18	98.03	98.44

Mineral extract proportions
Plag 60
Biot 30
Horn 10

Table 6.6 Summary results obtained from the second stage major element fractionation experiments of **Sandsting granitoid.** The start is a quartz monzonite composition. The target composition is a coarse grained monzogranite. A liquid composition similar to the target was obtained after 15% fractionation of plagioclase, biotite and hornblende in the listed proportions. Mineral compositions uesd are in table 6.4

6.2.1 For this experiment, in the Graven granite the start melt rock 6.13a (table 6.1) used is a basic granodiorite and fractionation was respectively. The target was rock 6.29a, a leucogranodiorite from the same pluton. The results are shown in the table along with the relative proportions of minerals removed. Mineral compositions used are listed in table 6.2

6.2.2 In the Spiggie-Hildsay-Aith granites, the start melt rock 12a.24 (table 6.3) used is a quartz monzonite and modelling was by fractionating plagioclase, hornblende, biotite and magnetite using the mineral proportions 63 : 9 : 23 : 1 respectively. The target was rock, 12c.42, which is a coarse grained rock from the same pluton (modelling results, relative mineral proportions and mineral compositions used are all listed in table 6.4). The result shows that after 40% fractionation a liquid composition was reached which agreed with the target rock 12c.42

6.2.3 In the Sandsting granite, the modelling was carried out in two stages. The first one from diorite (rock 19.11) to quartz-monzodiorite (rock 19.4), then the second stage from quartz monzodiorite (rock 19.4) to monzogranite (rock 19.9). The first stage modelling started with the melt composition (19.11) (table 6.5), and fractionation of plagioclase, hornblende and biotite using the mineral proportions 55 : 7 : 38 respectively. The second stage modelling started with the start melt composition (19.4), (table 6.6), and fractionation of plagioclase, hornblende and biotite in the mineral proportions 60 : 10 : 30 respectively. The target was the most acid rock in the pluton (modelling results, relative mineral proportions and mineral compositions are listed in table 6.4.

The results show that after 35% fractionation in the Graven, 40% fractionation in the Spiggie and 45% and 15% fractionation in the Sandsting complex, a liquid composition was reached that agreed with the target rocks from

three different plutons. These results suggest that fractional crystallisation involving the above minerals can reasonably account for the observed major elements variation between the basic and more evolved rocks of the three plutons and provides, in simple terms, a general model on which the chemical evolution of the plutonic rocks can be further constrained.

6.3 Rare Earth Element Modelling.

The usefulness of rare earth elements for petrogenetic modelling stems primarily from four factors. First the values of their partition coefficients for any particular mineral vary systematically with atomic number (some by order of magnitude). Thus, each mineral which fractionates or remains as restite during the series of events culminating in the formation of an igneous rock leaves its own signature on the REE pattern of that rock, so their distributions are indicators of source and fractionation.

Second, a useful exception to the systematic variation of REE partition coefficients with atomic number is the well-known europium anomaly. So that anomalous Eu abundances can be a strong diagnostic for the involvement of certain minerals in petrogenetic processes, eg. K-feldspar and plagioclase which shows a degree of mineral crystallisation during the magma differentiation in igneous rocks.

Third, an additional usefulness of the REE, particularly in modelling petrogenetic processes, is that the REE are highly refractory, and hence the relative abundances of these elements in most undifferentiated materials from our solar system are generally assumed to be proportional to their relative abundances in the sun and in chondritic meteorite (G. A. McKay, 1990).

A final characteristic of REE which lends utility to their use in petrogenetic modelling is that they are involved in three important isotopic systems, Sm-Nd, Lu-Hf, and La-Ce. As a result, they can provide information not only about the nature of the mineral separations which occurred during a petrogenetic process, but also the times at which these separations occurred.

6.3.1 REE Modelling by Fractionational Crystallisation.

I have discussed above how some granitic plutons at the present erosion level in Shetland are the end product of crystal fractionation, from REE plot showing a variation between the basic and acidic rocks of the analysed samples of Shetland granitoids (Figurs 412b &c). Fractional crystallisation was chosen as it provided good results for the REE variation. The modelling works upon the assumption that the fractionation is Rayleigh fractionation in the form of :

$$C_{LIQUID}=C_{ORIGINAL} * F^{(D-1)} .$$

Where   CL =   trace element concentration in evolved liquid

   CO =   trace element concentration in initial liquid

   F   =   fraction of intitial liquid remaining

   D   =   bulk partition coefficient   = $\sum K_i P_i$ and P_i is the proportion

   of each mineral in the mix.

6.3.1a *Hornblende-bearing Granites*

a)   Graven Complex.

In this model the production of an evolved liquid from a start melt composition similar to the target leucogranodiorite was modelled via fractional crystallisation. The start composition used was rock 6.13a quartz-monzodiorite (DI 62) which was used as the starting material in the major element modelling. The target (as in major element modelling is 6.29a) was the leucogranodiorite 6.29a (DI 82). The REE profile of the observed start and target compositions used in the modelling together with the calculated melt profile are shown in figure 6.2 and summarised in table 6.7 The results show that an evolved liquid similar in composition to that of rock 6.29a the most evolved leucogranodiorite analysed for REE can be successfully fractionated from a start quartz-monzodiorite composition by the removal of 65% solid of the mineral proportions. In the major element modelling,

variation between a start and target was modelled by fractionating major phases. However, experimentation using the same mineral mix as in the major element modelling failed to produce the observed REE profile in the target rock composition. Only the addition of accessory minerals (notably apatite, sphene, zircon and allanite have been shown to be crucial in controlling the REE patterns in granitoid rocks; Gromet and Silver, 1983) can produce REE profiles which closely match the target granodiorite REE profile (6.29a) Figure (6.2). The partition coefficients or mineral Kds used in the experiment are from Arth (1976), Cullers and Medaris (1977), Simmons and Hedge (1978), Hellman and green (1979), Michael (1983), Nash and Crecraft (1985) and are listed in table 6.10.

c) Spiggie Granite.

The variation in this pluton was modelled via fractionational crystallisation. The start composition used was rock 12c.44 monzonite (DI 72) which is not the same as in major element modelling . The target was the same as in the major element modelling i.e. coarse grained granite 12c.42 (DI 76). The REE profile of the observed start and target compositions used in the modelling, together with the calculated melt profile are shown in figure 6.2 and summarised in table 6.7. The results show that an evolved liquid similar in composition to that of rock 12.42 the most evolved granite rock analysed for REE can be successfully fractionated from a start monzonite composition by the removal of 55% of the monzonite mineral proportions including 3% apatite, 0.5% allanite, 0.3% sphene and 0.3% magnetite.

6.3.1b *Hornblende-free Granites*

Skaw Granite.

The variation between light Skaw granite and dark Skaw granite was modelled via fractional crystallisation. The start composition used was rock 1.19a dark Skaw granite (DI 69). The target was the light Skaw granite 1.26 (DI 83). The REE Profile of the observed start and target compositions used in the modelling

experiment, together with the calculated melt profile are shown in figure 6.2 and summarised in table 6.8 The results show that an evolved liquid similar in composition to that of rock 1.26 the evolved light Skaw granite analysed for REE can be successfully fractionated from a start dark Skaw granite composition by the removal of 70% of the mineral proportions of dark granite including 4% apatite, 0.35% allanite, 0.1% zircon and 1.05% magnetite.

6.3.1c *Granites to the West of Wall Boundary Fault.*

a) Ronas Hill Granite.

In this model the production of an evolved liquid similar in composition to the Ronas Hill perthite granite was modelled via fractional crystallisation. The start compositions used was rock 14.3 two feldspar granite (DI 90). The target was perthite granite 14.14 (DI 93). During the course of the fractionation experiment, a progressive Eu anomaly was not developed in the calculated REE profile of the evolved liquid which is seen in the target (Eu = 0.08). To remain consistent with the target, a Kd of 0.08 was opposed to 2.4 for Eu in the plagioclase, and then used in the modelling experiment. The REE profile of the observed start and target compositions used in the modelling experiment, together with the calculated melt profile are shown in figure 6.3 and summarised in table 6.8. The results show that an evolved liquid similar in composition to that of rock 14.14 the perthite granite can be successfully fractionated from a start two feldspar granite composition by the removal of 65% of the mineral proportion of two feldspar including 0.7% apatite, 0.1% zircon and 0.2% allanite.
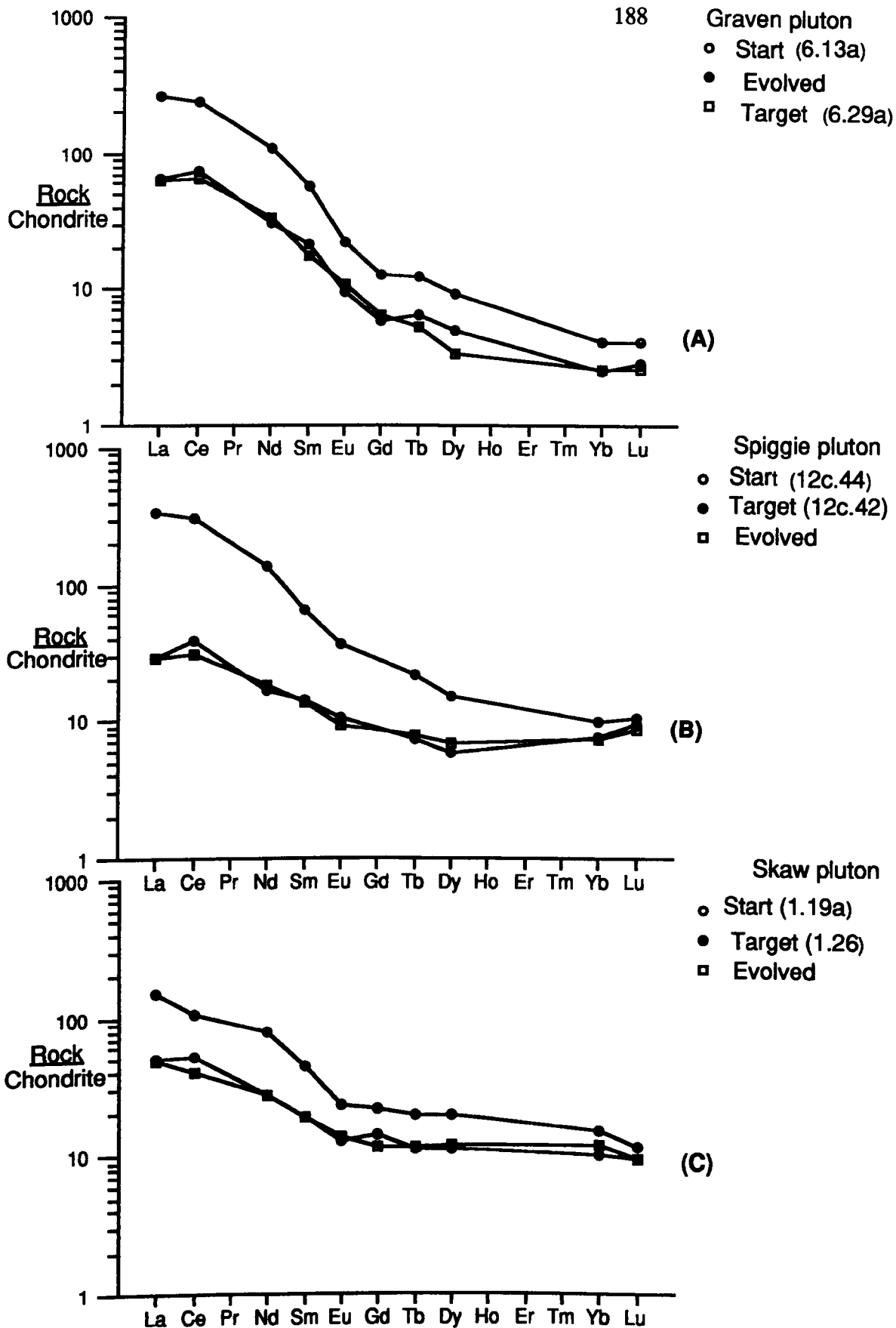
Figure 6.2 REE modelling plots for A) Graven pluton after a 65% fractionation of mineral proportions in step 1 table 6.7, B) Spiggie pluton after 55% fractionation of mineral proportions in step 2 table 6.7, C) Skaw pluton after 70 % fractionation of mineral proportions in step 1 table 6.8 `

Table 6.7 Results obtained from REE fractional crystallisation
experiments after removal of 65% and 55% solid from Graven and
Spiggie granitoids respectively.

1) Graven Granitoid

	START (6.13a)	EXTRACT PROP.%	EVOLVED LIQUID	TARGET (6.29a)	BULK K_d
La	100	Bi 15	24.33	24	4.28
Ce	232	Pl 58	71.16	64	3.743
Nd	79	Hb 5	22.17	24	3.95
Sm	13	Kf 5	4.95	4.10	3.243
Eu	1.9	Qz 13	0.82	0.952.	963
Gd	4	Ap 3	1.82	2	2.833
Tb	0.7	Al 0.4	0.36	0.30	2.518
Dy	3.6	Sp 0.45	1.93	1.20	2.448
Yb	1	Zr 0.15	0.63	0.64	2.058
Lu	0.16		0.11	0.10	1.956

2) Spiggie Granitoid.

	(12c.44)			(12c.42)	
La	130	Bi 5	11.11	11	5.273
Ce	300	Hb 7	36.96	30	4.502
Nd	99	Pl 50	11.8	13	4.558
Sm	15	Kf 34	4.18	3.1	3.597
Eu	3.10	Ap 3	0.91	0.80	3.055
Gd	0	Al 0.5	0	3.2	3.112
Tb	1.2	Sp 0.3	0.42	0.44	2.753
Dy	5.9	Mag 0.3	2.29	2.70	2.582
Yb	2.40		1.88	1.80	1.405
Lu	0.41		0.37	0.33	1.176
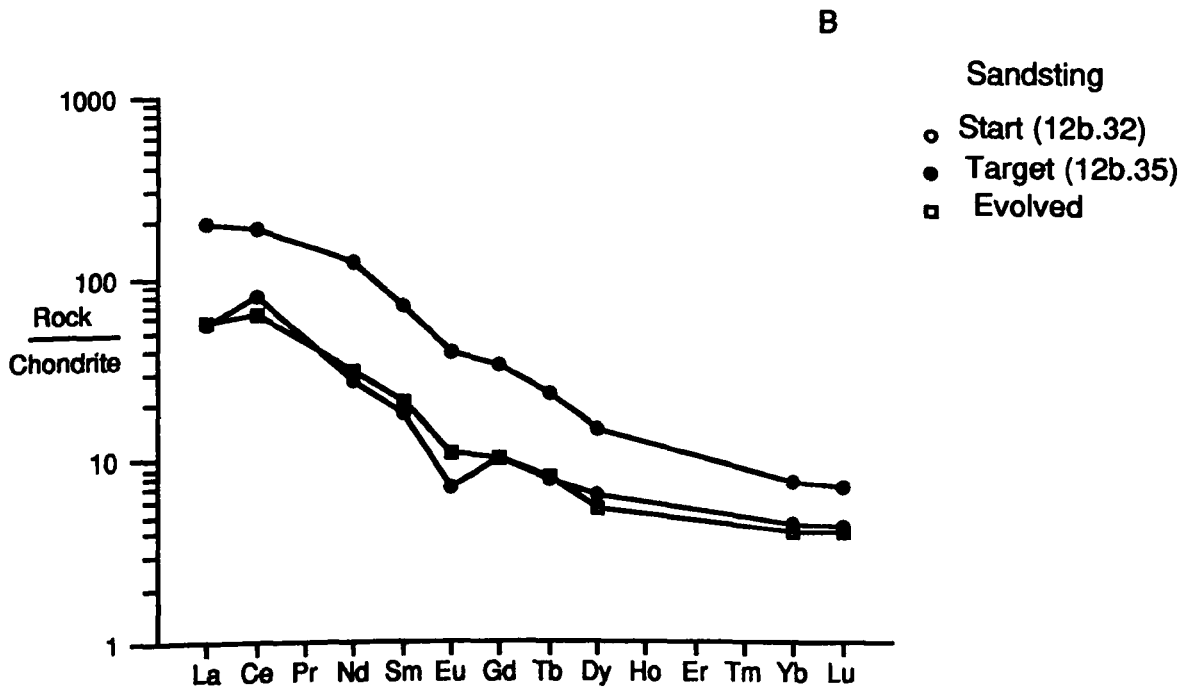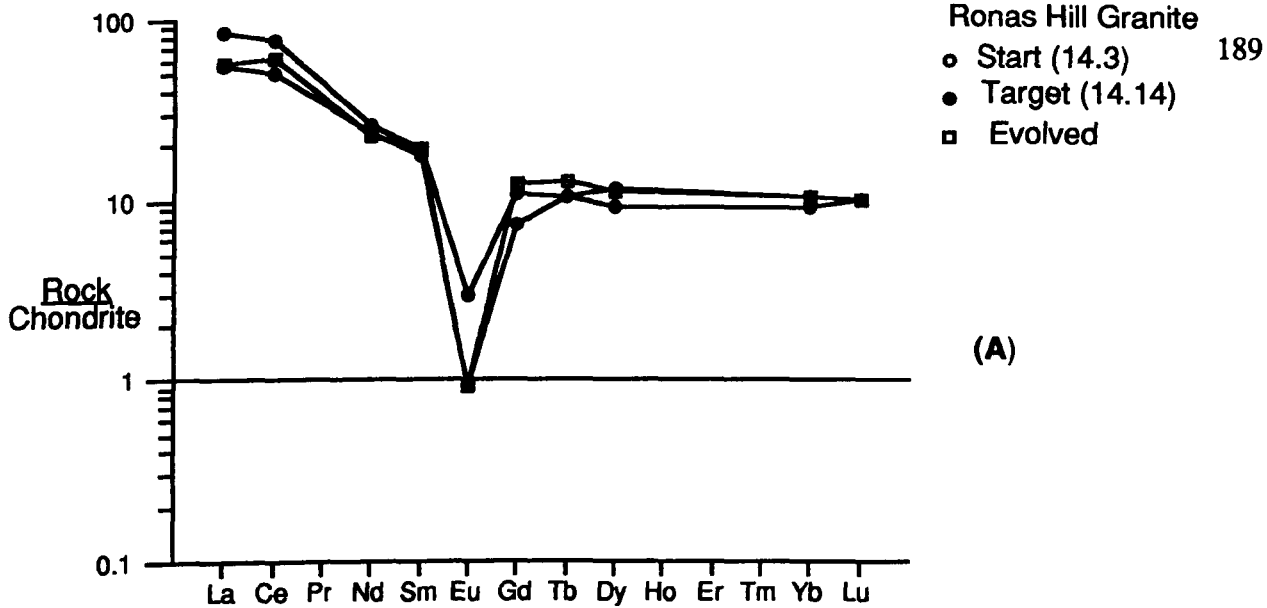
Figure 6.3. REE modelling for A) Ronas Hill granite after a 65% fractionation of mineral proportions in table 6.8 B) Sandsting pluton after a 70% fractionation of the mineral proportions listed in table 6.9.

Table 6.8 Results obtained from REE fractional crystallisation experiments after removal of 70% and 65% solid of mineral proportions from Skaw and Ronas granites respectively.

1) Skaw Granite.

	START (1.19a)	EXTRACT PROP.%	EVOLVED LIQUID	TARGET (1.26)	BULK K_d
La	57	Bi 13.5	18.07	19	4.221
Ce	104	Pl 38	39	50	3.757
Nd	56	Kf 20	19.14	19	4.009
Sm	10	Qz 23	4.34	4.30	3.343
Eu	2	Ap 4	1.19	1.10	2.446
Gd	6.70	Al 0.35	3.6	4.30	2.806
Tb	1.10	Zr 0.10	0.65	0.63	2.493
Dy	7.60	Mag 1.05	4.63	4.40	2.388
Yb	3.70		2.95	2.50	1.632
Lu	0.45		0.37	0.37	
	1.541				

2) Roans Hill granite.

	(14.3)	EXTRACT	EVOLVED	(14.14)	BULK K_d
La	32	Pl 35	21.80	21	1.889
Ce	75	Kf 43	59.12	50	1.552
Nd	19	Qz 21	16.32	17	1.353
Sm	4.50	Ap 0.70	4.45	4.10	0.881
Eu	0.26	Zr 0.10	0.08	0.08	3.770
Gd	3.40	Al 0.20	3.88	3.10	0.695
Tb	0.61		0.74	0.61	0.566
Dy	3.60		4.34	4.5	0.566
Yb	2.30		2.55	2.6	0.760
Lu	0.4		0.32	0.4	
	0.811				

Table 6.9 Results obtained from REE fractional crystallisation experiments after removal of 70% and 75% solid from Sandsting and Hildasay granitoid.

1) Sandsting granitoid.

	START	EXTRACT PROP.%		EVOLVED LIQUID	TARGET	BULK K_d
La	51	Bi	17.5	32	35	2.381
Ce	124	Hb	14	85	90	2.072
Nd	46	Pl	53	29.02	29	2.292
Sm	8	Qz	4	5.56	5.10	2.019
Eu	1.40	Ap	1.5	0.89	0.74	2.283
Gd	5.70	Al	0.20	4.05	3.30	1.957
Tb	0.69	Mag	0.80	0.51	0.63	1.854
Dy	3.50			2.62	3.90	1.812
Yb	1.10			1.04	1.04	1.151
Lu	0.17			0.32	0.35	1.021

Table 6.10 Kd's used in LIL Element Modelling

	Biotite	K-feldspar	plagioclase	Hornblende	Quartz
Ba	3.0 - 9.7	3.0 - 24	0.13 d 0.36 r	0.14 d 0.044 r	0.001
Rb	2.2 - 9.0	0.34 r	0.041 d 0.048 r	0.064 d 0.014 r	0.001 r
Sr	0.12 d	2.0 - 3.9	2.0 - 4.4	0.19 d 0.022 r	0.001 r

Where - is shown Kds used fall in this range; d = dacite value, r = rhyolitic value.

Table 6.11. Shows solid/liquid partition coefficient values used in REE modelling.

Major Phases.

	Biotite	K-feldspar	plagioclase	Hornblend	Quartz
La	0.03 - 0.35	0.050	0.02 -0.30	0.06 -0.08 - 1.0	0.015
Ce	0.04 - 0.32	0.04	0.02 - 0.24 - 0.27	0.9 - 1.5	0.014
Nd	0.04 - 0.29	0.02	0.02 - 0.17 - 0.21	0.16 - 2.8 - 4.3	0.016
Sm	0.06 - 0.26	0.018	0.02 - 0.13	0.24 - 4.0 - 7.8	0.014
Eu	0.15 - 0.24	0.40	2.10 - 0.50	0.26 - 3.4 - 5.1	0.06
Gd	0.08 - 0.28	0.011	0.02 - 0.09 - 0.1	1.10 - 5.5 - 10	0.015
Tb	0.09 - 0.29	0.008	0.02 - 0.09 - 0.08	1.10 - 5.9 - 12	0.017
Dy	0.10 - 0.29	0.006	0.01 - 0.09 -0.064	1.00 - 6.2 - 13	0.014
Er	0.12 - 0.35	0.006	0.01 - 0.08 - 0.055	1.00 - 5.9 - 12	0.015
Yb	0.18 - 0.34	0.0.12	0.006 - 0.08- 0.049	1.00 - 4.9 - 8.4	0.017
Lu	0.19 - 0.33	0.006	0.005 - 0.06 - 0.046	0.82 - 4.5 - 5.5	0.015

Minor and Accessory Phases

	Magnetite	Ilmenite	Apatite	Sphene	Allanite	Zircon
La	1.2	7.1	30	15	820 - 3500	7
Ce	1.6	7.8	35	25	635 - 2600	10
Nd	2.3	7.6	57	78	463 - 1550	5
Sm	2.8	6.9	63	107	205 - 735	11
Eu	1.0	2.5	30	94	81 - 300	20
Gd	3.0	6.7	56	113	130 - 250	29
Tb	3.3	6.5	53	112	71 - 200	38
Dy	2.6	4.9	51	111	46- 100	108
Er	2.0	4.4	37	107	20 - 50	336
Yb	1.5	4.1	24	83	9- 5	564
Lu	1.2	3.6	20	62	8 - 15	648

b) Sandsting Granite.

The variatiation of REE between start and target was modelled via fractional crystallisation. The start composition used was rock 19.3, a coarse grained diorite (DI 51). The target was the same as in major element modelling 19.9, a coarse grained granite (DI 88). The REE profile of the observed start and target compositions used in the modelling, together with the calculated melt profile are shown in figure 6.3 and summarised in table 6.9. The results show that an evolved liquid similar in composition to that of rock 19.9 the evolved granite analysed for REE can be successfully fractionated from a start diorite composition by the removal of 70% solid of the mineral proportions.

6.4 *LIL Elements modelling For Shetland Granitic Rocks*

Trace element compositions of coarse-grained igneous rocks are determined firstly by the composition of their parent magma, and subsequently, by the virtue of the crystallisation process. The LIL elements Sr, Ba and Rb are of considerable use in determining the types and amounts of major phase fractionation in intermediate and acid rocks since they occur predominantly in the major silicate phases and each behaves somewhat differently - Rb is taken up preferentially by biotite, Ba by biotite and K-feldspar and Sr by plagioclase and K-feldspar. The mineral vectors (indicate the paths of evolved liquids for increments of 20% mineral fractionation calculated from the Rayleigh crystal fractionation law) are superimposed on each diagram and indicate the net change in composition of the liquid for 20% Rayleigh fractionation of the named phases :

This was calculated using the equation:-

$$C_{liquid} = C_{initial} * (F^{(D-1)}).$$

where C_{liquid} = the final concentration of the element in the liquid

$C_{initial}$ = the initial concentration of the element in the liquid

F = fraction of melt remaining (0.8 in this case)

D   =   Kd for the particular element in a mineral in a melt of

intermediate-acid composition (see Table 6.10)

6.4.1   *LIL Element Modelling for Hornblende-bearing Granites and the Sandsting Granite*

6.4.1a   a) *Graven Complex:-*

Inter-element variation diagrams for the pairs Sr-Ba, Ba-Rb and Rb-Sr are shown in Figure 6.4. The variation of Rb, Sr and Ba in the rocks from quartz monzodiorite through granodiorite to monzogranite are 40 ppm to 126 ppm, 1028 ppm to 2105 and 820 ppm to 1546 ppm, respectively. The plot of Sr v Ba shows that both increase from quartzmonzodiorite to monzogranite. The mineral vectors indicate that plagioclase and K-feldspar can cause Sr to decrease and Ba to increase in the case of plagioclase in the liquid during fractional crystallisation. The mineral vectors for Ba v Rb predict that plagioclase and hornblende can cause enrichment of Ba and Rb in the liquid during fractional crystallisation. The mineral vectors for Rb v Sr indicate that plagioclase ($\pm$ K-feldspar) can cause enrichment of Rb and depletion of Sr, and hornblende can cause enrichment for both Rb and Sr in the liquid during fractional crystallisation.

6.4.1b   b) *Spiggie-Aith-Hilldsay Granite:-*

On log LIL plots (Figure 6.5) the Spiggie rocks show a good positive trend on the Sr v Ba plot which indicates the compatible behaviour of both elements in acid magma. It is related to the crystallisation of K-feldspar, biotite and plagioclase crystallisation. On a Ba v Rb plot (Fig. 6.5), Rb increases from ~ 62 ppm in the most basic monzonite to 189 in the leucocractic granodiorite over a relatively wide Ba range of 724-1667, except one sample is 3098ppm. The mineral vectors for Sr v Ba shows that Sr decreases with precipitation of plagioclase and K-feldspar, while Ba increases in the case of plagioclase and decreases in case of K-feldspar. The mineral vectors for Ba v Rb shows that biotite and K-feldspar can cause depletion for Ba, while plagioclase and hornblende can cause enrichment of it and
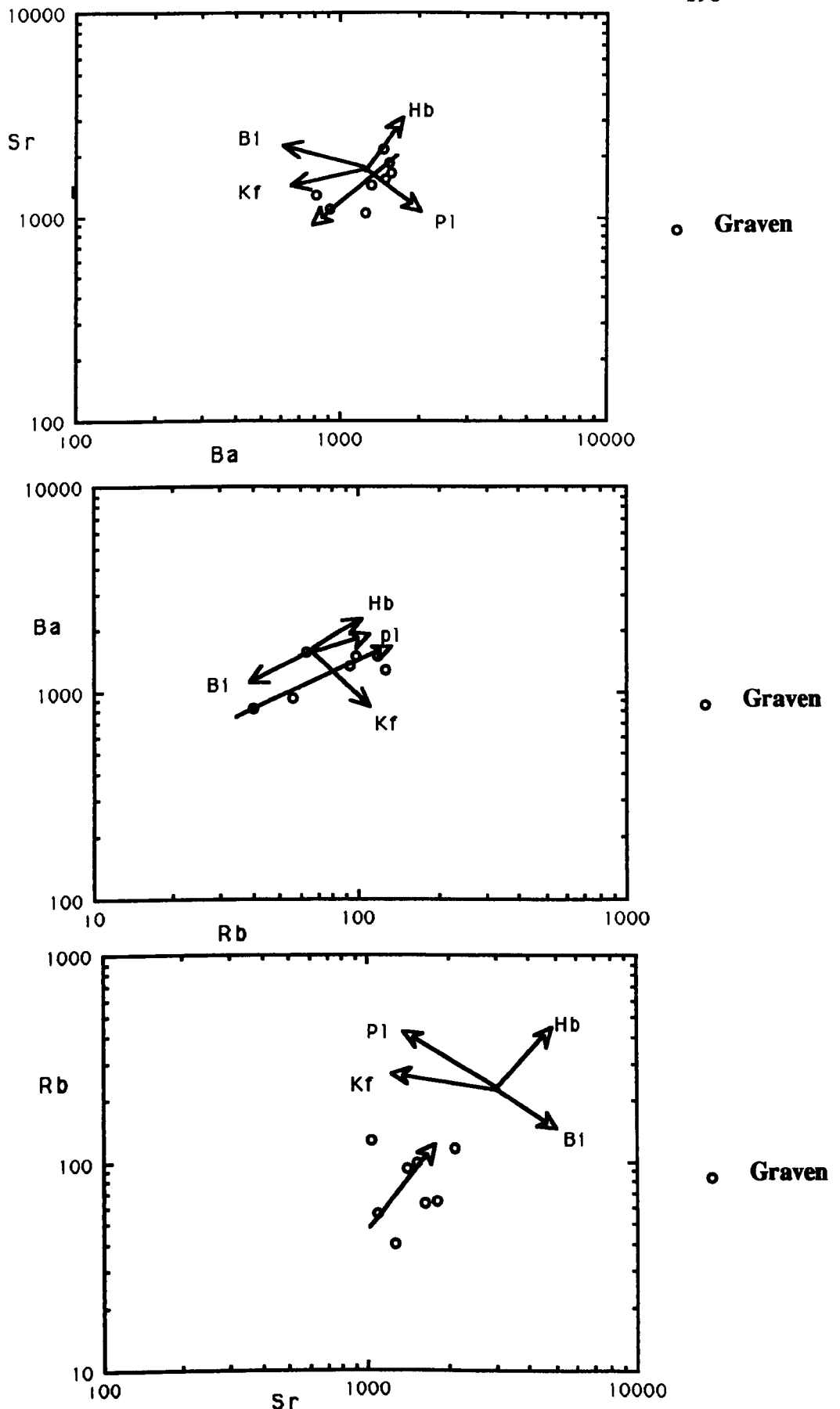
Figure 6.4 Logarithmic LIL inter-element variation plots for the Graven granitoid
rocks. Mineral vectors indicate the paths of evolved liquids for increments of 20% mineral
precipitation calculated from the Rayleigh crystal fractionation law . Pl = plagioclase
Kf = K-feldspar, Bi = biotite, Hb = hornblende. KD's used are listed in table 6.9
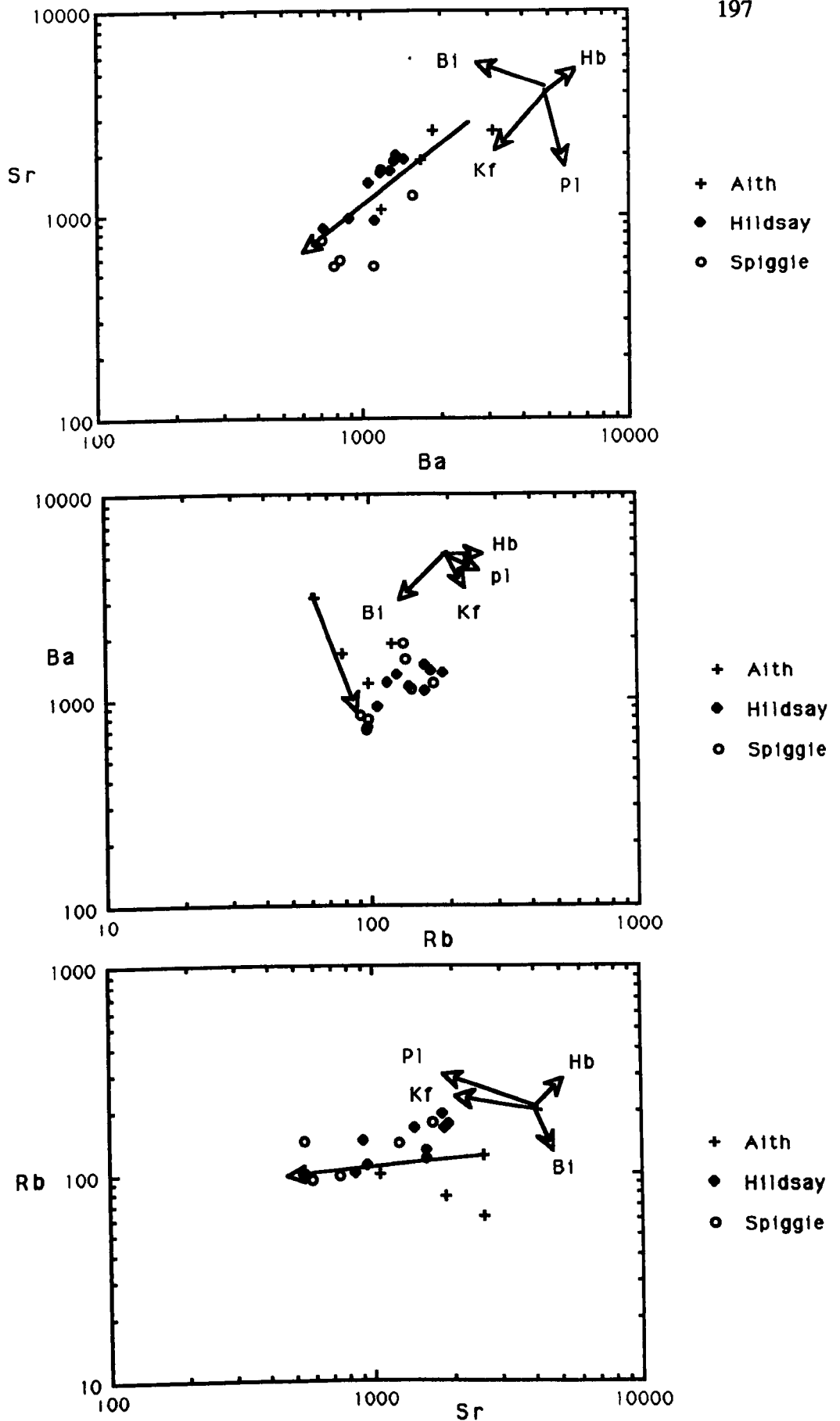
Figure 6.5 Logarithmic LIL element-element plots for the Spiggie granite and its two offshoots (Aith and Hildsay granites). Mineral vectors indicate the paths of evolved liquids for increments of 20% mineral precipitation calculated from the Rayleigh crystal fractionation law. Pl, Kf, Bi and Hb as in Fig.6.4. KDs used are listed in table 6.9.
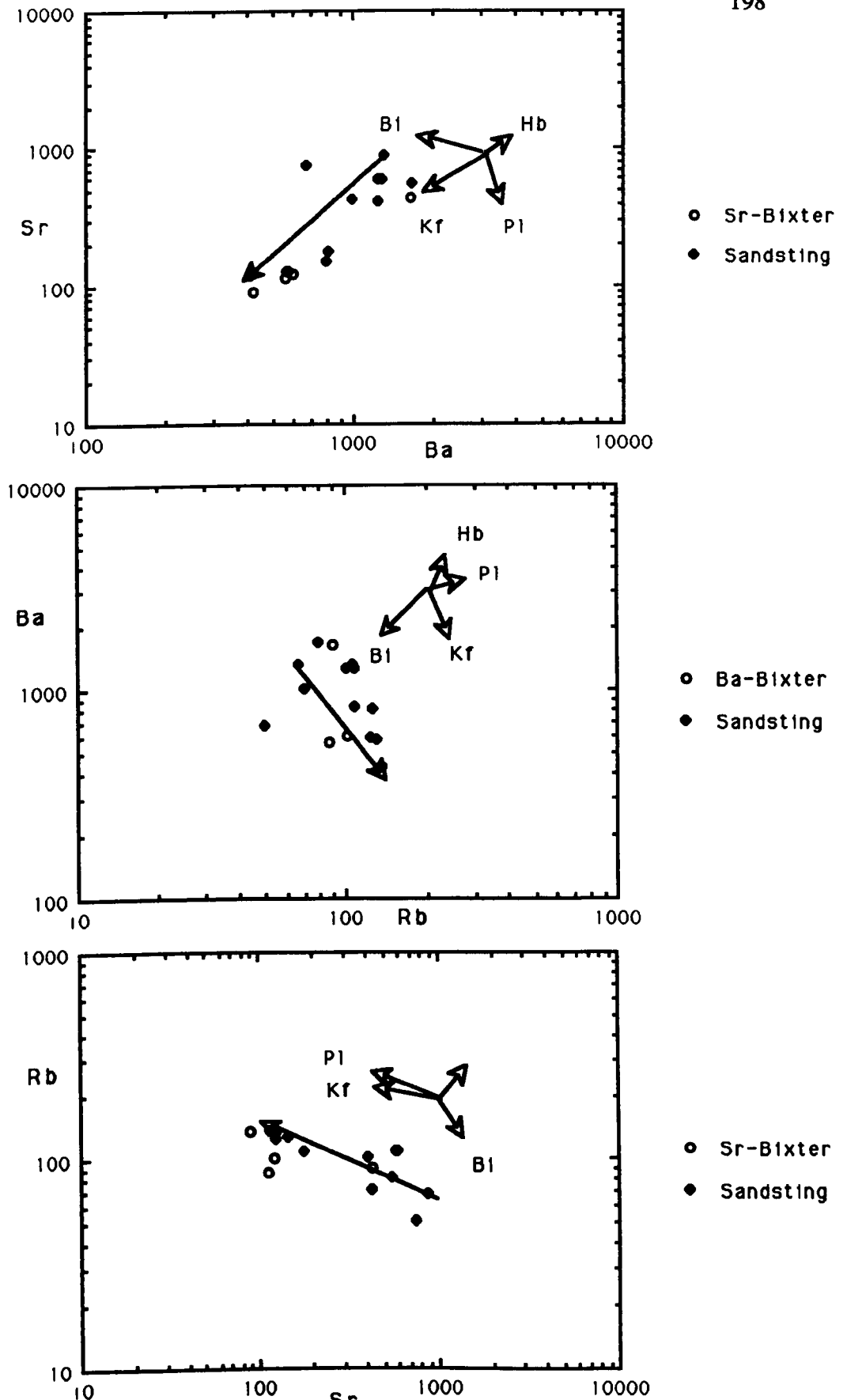
Figure 6.6 Logarithmic LIL element-element plots for Sandsting granitoid and Bixter granite Mineral vectors indicate the paths of evolved liquids for increments of 20% mineral precipitation calculated from Rayleigh crystal fractionation law. Pl, Kf, Bi and Hb as in Figure 6.4. KDs used are listed in table 6.9.

Rb in the evolved liquid. The plot of Rb v Sr shows that the mineral vectors indicate that plagioclase (± K-feldspar) and hornblende can cause enrichment of Rb and depletion of Sr during the evolved liquid, the various plots shown in Figure 6.5.

6.4.1c *c) Sandsting granites:-*

The Sandsting and Bixter LILE plots show that Sr v Ba have a good positive trend, which indicates the compatible behaviour of both elements in the granitic magma. The variation of Sr and Ba in the rocks from diorite through quartzmonzodiorite, granodiorite to monzogranite are 89-880 ppm and 416-1324 ppm, respectively. The mineral vectors for Sr v Ba shows that plagioclase and hornblende can cause Sr to decrease and Ba to increase in the evolved liquid. For Ba v Rb the mineral vectors of plagioclase and hornblende indicate that Ba and Rb were enriched in the liquid during fractional crystallisation. The mineral vectors of Rb v Sr shows that plagioclase and hornblende cause enrichment of Rb and depletion in Sr during the fractional crystallisation, on the various plots shown in Figure 6.6. These different inter-element variation diagrams for the pairs Sr-Ba, Ba-Rb and Rb-Sr are compatible with fractionation of plagioclase, hornblende and biotite. Fractionation of K-feldspar and quartz also have been important in producing the monzonite and coarse grained quartz granite of Spiggie, but is unlikely to have been important in the Graven granodiorite and Sandsting monzodiorite and granodiorite because of the smaller fraction of these phases (K-feldspar and quartz) and their relative presence in the crystallisation sequence.

Chapter Seven.

7.1 Typology Of Shetland Granites.

7.2 The previous classification literature on the plutonic granitoid rocks.

Classification is a cornerstone for each branch of the natural sciences, and has been one of the prime interests of physical and biological sciences. Its aim is to distinguish and categorize common or contrasting features of related objects. In geology this is very important as it provides a shorthand method of referring to groups of objects sharing common properties. Without classification the comparison of objects would be impossible. Clearly, for discussion of magmatic processes we have to classify igneous rocks.

Streckeisen (1976) pointed out that many sciences have arranged their terminology on an international basis. This is to ease communication and discussion. It has not been the case in petrology, where long usage and venerable traditions have hindered an international classification.

Streckeisen and Le-Maitre (1979) introduced a geochemical equivalent of the Streckeisen modal diagram, based on the norm calculation which they called a Q-ANOR normative diagram. The purpose is to classify volcanic rocks by chemical criteria, because modal mineral contents of many volcanic rocks cannot be accurately determined, because of micro or cryptocrystalline or even glassy texture of the groundmass. For such rocks chemical composition has to be used. To deduce the mineral content of a rock from its composition , Streckeisen and Le-Maitre have used the Niggli and Barth molecular norm. These authors used factors plotted on a rectangular diagram (Fig.7.1b), which shows the normative fields (2,
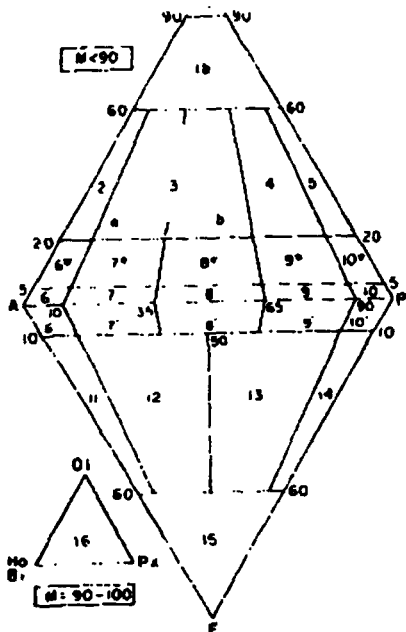
Fig. 7.1a. General classification and nomenclature of plutonic rocks according to mineral content (in vol. %).

Q + A + P = 100, or A + P + F = 100.

1a, quartzolite (silexite); 1b, quartz-rich granitoids; 2, alkali-feldspar granite; 3, granite; 4, granodiorite; 5, tonalite, 6*, quartz alkali-feldspar syenite; 7*, quartz syenite; 8*, quartz monzonite; 9*, quartz monzodiorite/quartz monzogabbro; 10*, quartz diorite/quartz gabbro/quartz anorthosite; 6, alkali-feldspar syenite; 7, syenite; 8, monzonite; 9, monzodiorite/monzogabbro; 10, diorite/gabbro/anorthosite; 6', foid-bearing alkali-feldspar syenite; 7', foid-bearing syenite; 8', foid-bearing monzonite; 9', foid-bearing monzodiorite/monzogabbro; 10', foid-bearing diorite/gabbro; 11, foid syenite; 12, foid monzosyenite (syn. foid plagisyenite); 13, foid monzodiorite/foid monzogabbro (essexite = nepheline monzodiorite/monzogabbro); 14, foid diorite/foid gabbro (theralite = nepheline gabbro, teschenite = analcime gabbro); 15, foidolites; 16, ultramafic plutonic rocks (ultramafitol) (after Streckeisen and Le Maitre, 1979).
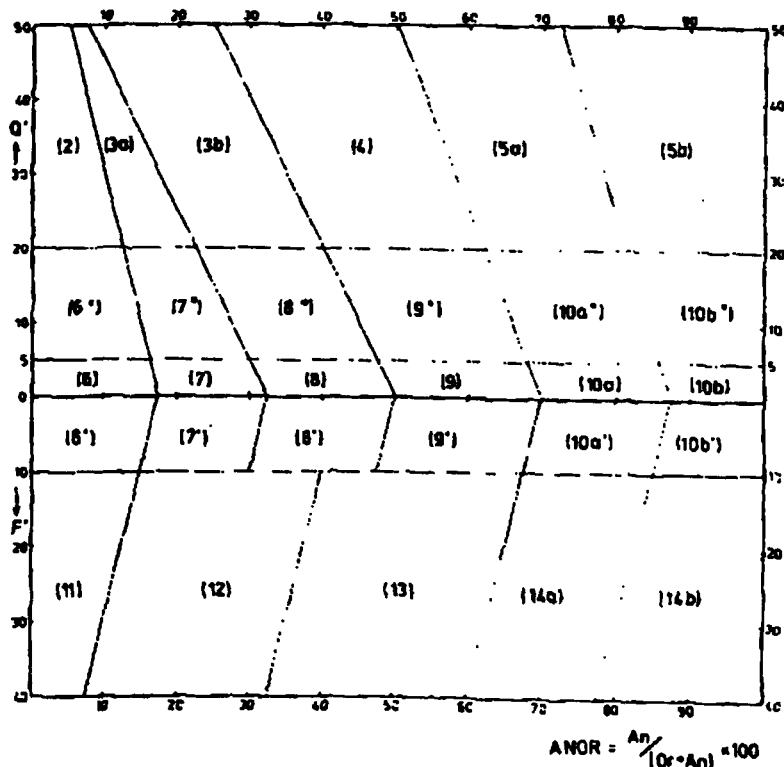
Fig. 7.1b. Diagram Q'(F')-ANOR showing the normative fields (2), (3 a), (3 b), etc., which correspond approximately to the fields 2, 3 a, 3 b, etc. of the modal QAPF diagram. (after Streckeisen and Le Maitre, 1979).

3a, 3b, etc.), which correspond approximately to the modal fields (2, 3a, 3b, etc.) of the QAPF diagram. The validity of the method proposed by Streckeisen and Le-Maitre has been examined by using Clair data system (Le-Maitre & Ferguson 1978), to calculate the norms of 15488 analyses of rocks and group them according to their rock types.

Bowden et al (1984) have used the Q-ANOR normative diagram to show that the various granitic series from different tectonic settings are better separated than in the QAP Streckeisen diagram plot for the same series of granite rocks (fig. 7.1c).

Lameyre and Bowden (1980) have shown that the IUGS Streckeisen diagram is valuable for identifying and distinguishing various granitic series and their relation to associated intermediate and basic rock associations. The diagram displays various granitoid series proposed by Lameyre and Bowden. The granitoid rocks on the Streckiesen diagram can diverge from basaltic composition toward granitic differentiates (fig.7.1d). The calc-alkaline series had been subdivided into (a) calc-alkaline trondhjemite or low K (b) calc-alkaline granodiorite or medium. K (c) calc-alkaline monzonite or high K (fig. 3b). It is possible to relate the major trends of the calc-alkaline series to their position within the orogen and their chronology with an evolution from an early internal low K magmatism toward late external high K ones (Lameyre & Bowden). The alkaline series shows divergent trends in the syenite field, one converging toward nordmarkite granite , the other toward pulaskite-nepheline syenite (fig. 7.1e).

Bowden et al (1984) have shown that five distinctive lineages can be plotted within the Streckeisen diagram (Fig. 7.1f) They have been given the abbreviated symbols CAT (calc-alkaline T-types where T stand for tonalite or trondhjemite), CAG (calc-alkaline granodiorite), SAM (sub-alkaline monzonite), ALK (aluminous potassic), and ANA (alkaline sodic).
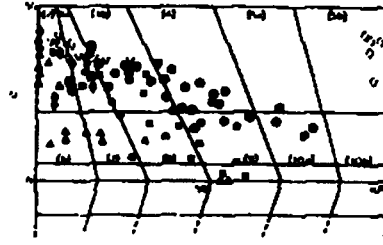
$$ANOR = \frac{An}{Qz+An} *100$$

Fig. 7.1c Q-ANORplot (after Streckeisen and Le Maitre, 1979) of various granite series 1- open diamonds plagiogranites from Cyprus and Oman (Coleman and Peterman, 1975; Coleman and Donato, 1979). 2-closed circles-Cordilleran granitic rocks characterized tectonically as plate margin magmatism (Bateman et al, 1963; Bateman and Nockleberg, 1978). 3-closed squares Caledonian granitic rocks, post -orogenic group (Brown et al, 1981) represented by the data for Ben Nevis (Haslam, 1968). 4-closed diamonds 2-mica cordierite granites Strathbogie batholith, Australia (Phillips et al, 1981). 5-closed triangles A-type granites and related rocks from the Niger Nigerian anorogenic province (Bowden, unpublishe data). 6- open inverted triangles A-type granites from the Lachlan fold belt, SE Australia (Collins et al, 1982).
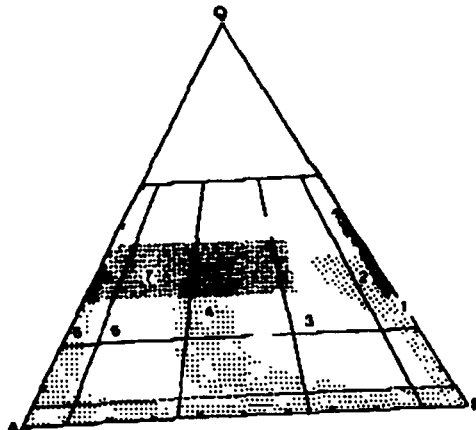
Fig. 7.1d Summary QAP diagram showing important fields of various granitoid series (greater than 20% vol. Q), discussed in the text. 1= tholeiitic; 2= calc-alkaline trondhjemite (low K); 3 = calc-alkaline granodiorite (medium K); 4 = calc-alkaline monzonitic (high K) 5 = aluminous granitoids found in alkaline provinces; 6 = alkaline and peralkaline; 7 = overlapping field of granitoids formed by crustal fusion; black star = median minimum composition. (after Lameyre and Bowden, 1982)
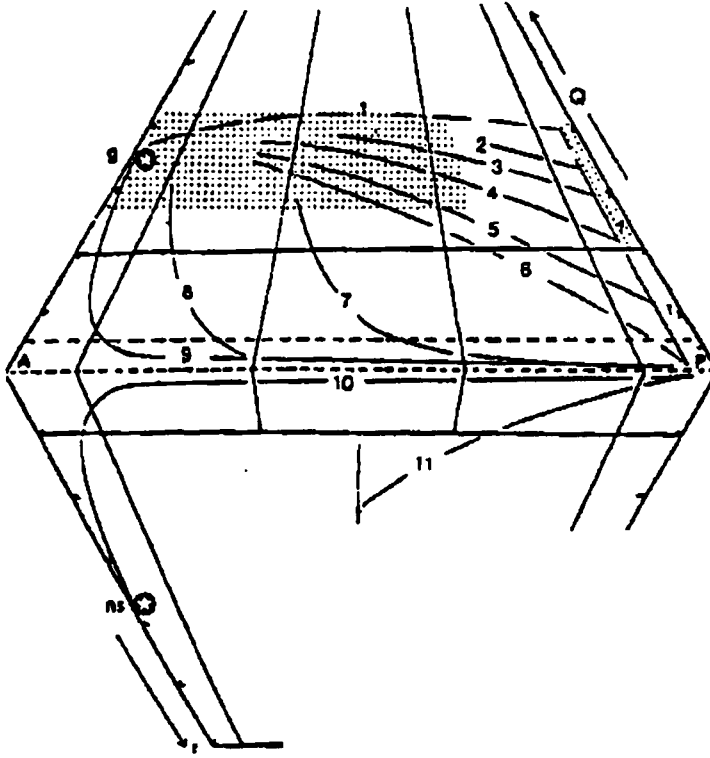
Fig.7.1e. Main Trends of some plutonic type series (modal compositions)

1: tholeiitic series after COLEMAN and PETERMAN (1975), WAGER and BROWN (1967).

2: Calc-alkaline trondhjemitic series after ARTH et al. (1978).

3: Calc-Alkaline-Granodioritic series: ORSINI (1976).

4: ISHIHARA and ULRIKSEN (1980).

5: ATHERTON et al. (1979).

6: BATEMAN et al. (1963).

7: Monzonitic series after ORSINI (1976) and PAGEL (1980).

8,9,10,11: Alkaline series after STRECKEISEN (1967), BOWDEN and TURNER (1974); BONIN (1980); GIRET et LAMEYRE (1980); GIRET (1979).

g: average granite minima ; ns: nepheline syenite. Shaded area: granitic rocks of crustal origin. (after Lameyre et al, 1980).
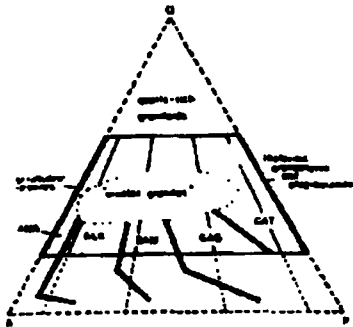
Fig. 7.1f QAP Streckeisen modal diagram with the classification groupings of granite-rock series adapted from Lameyre and Bowden (1982). Various granite rock series delineated by symbols or text. CAT -calc-alkaline tonalitic or trondhjemitic; CAG -calc-alkaline granodiorite; SAM -sub-alkaline monzonit ALK -aluminous potassic; ANA -alkaline sodic. Double lines denote arbitrary fields of the various granitic series, including their related suites of intermediate rocks. (after Bowden et al, 1984)

Lameyre et al (1982) pointed out that the comparative studies of granitic rocks have generated binary classifications, which lead towards an oversimplification of the complex nature of granite . That is the case for the I & S type (Chappell & White, 1974) and the ilmenite & magnetite series (Ishihara, 1977). These being classification approaches have many points in common, but are not in some cases possible (DiDier et al, 1982). It is important to note that most two-fold classifications apply only to orogenic granites which are the most abundant granites, and even today they are commonly the only ones to be considered with regard to reworking of previous continental material.

7.2.1 Classification Based On Source Criteria.

The classification of granitic rocks into S-and I-types by **Chappell and White (1974) and White and Chappell (1977),** have involved source criteria. They studied granites forming major batholiths of the Tasman orogenic zone of Eastern Australia. This classification is based on chemical parameters which require whole rock analysis for its application. S-type granites are from sedimentary source and are formed by partial melting of continental crust, whereas I-type granites are derived from an igneous source in the mantle or lower crust. The distinctive mineralogical and chemical properties are shown in table 7.1, which discriminates characteristics of "I" and "S" type granites.

Ishihara (1977) described a two fold classification of granitoid rocks into ilmenite series and magnetite series (ILM & MAG). This subdivision is very important in mineral exploration where Sn, W, Nb, and Ta deposits are associated with ilmenite series granitoids and Mo, Cu, Pb, Zn, Ag, and Au deposits with magnetite series.

Takahashi et al. (1980) compared the "S" and "I"-types classification based on chemical parameters with the ilmenite-magnetite classification of Ishihara (1977), and they found that most "S"-type granitoids were also ilmenite bearing, and that

TABLE 7.1 Discriminant characteristics of "I" and "S" type granites (from Chappell and White, 1974).

I-types	S-types
Relatively high sodium, Na_2O normally > 3.2% in felsic varieties, decreasing to > 2.2% in more mafic types	Relatively low sodium, Na_2O normally < 3.2% in rocks with approx. 5% K_2O, decreasing to < 2.2% in rocks with approx. 2% K_2O
Mol $Al_2O_3/(Na_2O + K_2O + CaO) < 1.1$	Mol $Al_2O_3/(Na_2O + K_2O + CaO) > 1.1$
C.I.P.W. normative diopside or < 1% normative corundum	> 1% C.I.P.W. normative corundum
Broad spectrum of compositions from felsic to mafic	Relatively restricted in composition to high SiO_2 types
Regular inter-element variations within plutons, linear or near-linear variation diagrams	Variation diagrams more irregular
hornblende, sphene common	muscovite common, biotite abundant, garnet, cordierite, Al_2SiO_5 and monazite can occur
apatite as small inclusions in biotite and hornblende	apatite as large discrete crystals
initial $^{87}Sr/^{86}Sr$ in the range 0.704 - 0.706 isochrons regular	initial $^{87}Sr/^{86}Sr$ > 0.708 isochrons show scatter
often contain mafic hornblende-bearing xenoliths	metasedimentary xenoliths common
generally late in intrusive sequence	generally early in intrusive sequence
massive or have dominant primary foliation	generally have a strong secondary foliation
W and porphyry-type Cu and Mo deposits associated	Sn mineralization in highly silicic types

Table 7.2 Geochemical characteristics of A-type granitoids (after White & Chappell, 1983)

Parameter	Characteristic value	Explanation
SiO2	Usually high, often near 77%	Small degree of partial melting
Na2O	High	Small degree of partial melting
CaO	Low	Small degree of partial melting, Ca not compatible with melt structure
Ca/Al	High	Ca complexed in melt, plagioclase in residue
Y & REE	High except Eu	Complexed in melt, with much Eu remaining in anorthite
Nb & Sn	High	Complexed in melt
Zr	Normally high, particularly in the more mafic varieties	Comlexed in melt
F & Cl	High	Source rock is a residue from earlier melt & is rich in F & Cl an

most "I"-type granitoids were magnetite bearing and may apply for some areas and does not apply for others.

Miller and Bradish (1980) described a belt of muscovite-bearing granites of "S"-type affinity present on the continental side of a belt of "I"-type granites along the western margin of north America.

Haliday et al (1980b) demonstrated that the late Caledonian Criffell, Doon and Fleet plutons emplaced into shales in the south of Scotland are zoned plutons which mafic granodiorites with "I"-type characterstics at the margins and muscovite granite with "S"-type affinity in the cores. They concluded that melts of high level crustal rocks had intruded the differentiated margins of lower crustal melt "I"-type plutons.

Clemens and Wall (1981) showed exprimentally that magmas with broadly "S"-type affinity could be generated by partial fusion of crustal source rocks either pelitic or psammitic and even altered igneous rocks. White and Chappell (1983) have recently grouped the LFB (Lachlan Fold Belt) into 3 suites "I"-, "S"- and "A"-type granitoids; "A"-type has been derived from crust that had previously produced "I"-type magmas, the source rocks being residual from the prior melting event. Table 7.2, shows the geochemical characteristics of "A"-type granitoid.

Pitcher (1983) merged his earlier granite classification based on tectonic environment (Hercynotype, Andinotype, Alpinotype, Fig. 7.2a and 7.2b; Pitcher 1979) with "I"/ "S" classification of Chappell and White (1974) to produce a 5-fold division of granite types (table 3a). Pitcher in his classification (1983) has recognized two sorts of "I"-type granite one termed "I"-Cordilleran and the other "I"-Caledonian, table 7.3.

Todd and Shaw (1985) defined a boundary between predominantly "I"-type and predominantly "S"-type granitoids in the central and eastern parts of the peninsular ranges batholiths of southern California. They proposed that the change from I to S type represents a fundamental change in the Mesozoic crust. They suggested that "S"-type granitoids and associated migmatites developed at

208
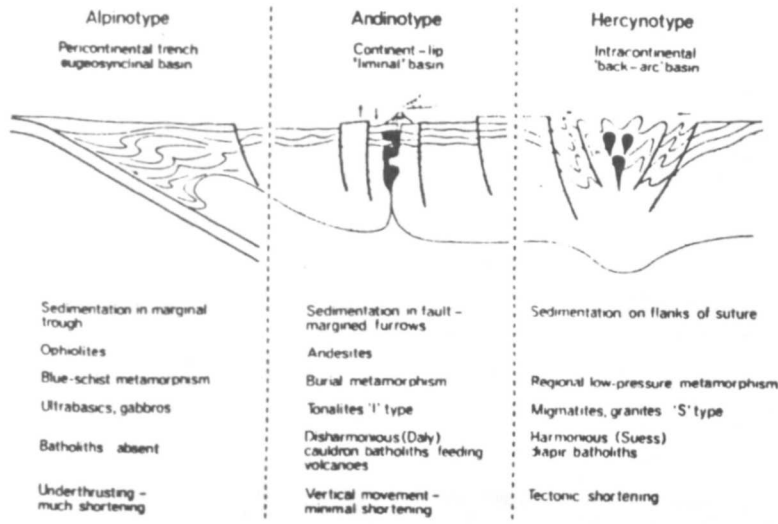
Fig. 7.2a Schematic representation of three orogenic environments to illustrate the differing environments of granitic rocks (after Pitcher in Atherton and Tarney, 1979).
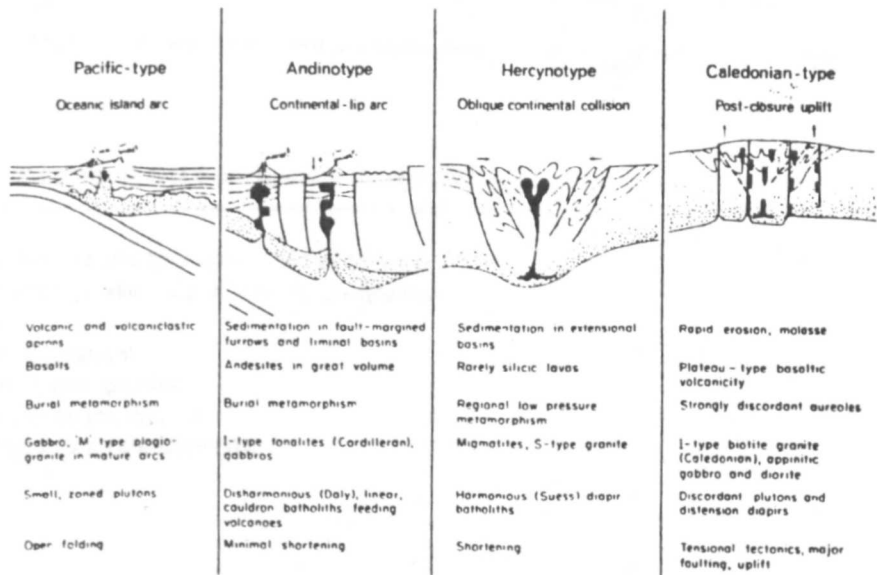
Figure 7.2.b. Caption depicting the various geological environments of Phanerozoic granitic rocks Normal changes in composition of the crust above an assumed Moho are indicated by density of the stipple and under the continental lip the denser stipple represents underplated material in the Andinotype model a wedge of lithospheric mantle is presumed to overlie the subduction zone.

Table 7.3 Granite-types, their character and geological environments (after Pitcher, 1982).

M-type	I- (Cordilleran) type	I- (Caledonian) type	S-type	A-type
Plagiogranite subordinate to gabbro	Tonalite dominant but broad compositional spectrum – diorite to monzogranite — with wide SiO₂-range. Major association with gabbro	Granodiorite-granite in contrasted association with minor bodies of hornblende diorite and gabbro	Granites with high but narrow range of SiO₂. Leucocratic monzogranites predominate but granitoids with high biotite content locally important	Biotite granite in evolving with alkalic granite and in Highly contrasted acid-ba relationship
Hornblende and biotite; pyroxene	Hornblende and biotite; magnetite, sphene	Biotite predominates; ilmenite and magnetite	Muscovite and red biotite; ilmenite, monazite, garnet, cordierite.	Green biotite. Alkali amp and pyroxenes in alkalic t astrophyllite.
K-feldspar interstitial micrographic	K-feldspar interstitial and xenomorphic	K-feldspar generally interstitial and invasive. Often quartz-rich	K-feldspar often as megacrysts with protracted history. Autometasomatic variants	Perthites
Basic igneous xenoliths	Dioritic xenoliths: may represent restitic material	Mixed xenolith populations	Metasedimentary xenoliths predominant	Cognate xenoliths, also b magma blebs
Typical initial ⁸⁷Sr/⁸⁶Sr ratios <0·704	$Al/(Na+K+\frac{Ca}{2})<1\cdot1$ (often <1) <0·706	$Al/(Na+K+\frac{Ca}{2})$ ca. 1 >0·705 <0·709	$Al/(Na+K+\frac{Ca}{2})>1\cdot05$ >0·708	Peralkaline, relatively rich Considerable range, 0·703
Small, quartz diorite-gabbro composite plutons	Great multiple, linear batholiths with arrays of composite cauldrons	Dispersed, isolated complexes of multiple plutons and sheets	Multiple batholiths, plutons and sheets, less voluminous and more commonly diapiric than I-types	Multiple, centred, cauldro complexes of relatively sm volume
Associated island-arc volcanism	Associated with great volumes andesite and dacite	Sometimes associated basalt-andesite lava "plateaux"	Can be associated with cordierite-bearing lavas but characteristically lacking in voluminous volcanic equivalents	Associated with caldera or alkalic lavas
Short, sustained plutonism	Very long-duration episodic plutonism	Short, sustained plutonism; post-kinematic	Sustained plutonism of moderate duration; syn- and post-kinematic	Short-lived plutonism
Oceanic island arc	Andinotype marginal continental arc	Caledonian-type post-closure uplift	Hercynotype continental collision. Also cratonic ductile shear-belts	Post-orogenic or anorogen situations
Open folding: burial-type metamorphism	Vertical movements, little lateral shortening: burial-type metamorphism	Dip-slip and strike-slip faulting: retrograde metamorphism	Much shortening; low-pressure metamorphism in slate belts; part of a Granite Series	Doming and rifting
Porphyry-Cu, Au, mineralization	Porphyry-Cu, Mo, mineralization	Rarely strongly mineralized	Sn and W-greisen and vein-type mineralization	Columbite, cassiterite and

Table 7.4

Geochemical classification of granitoids (Tauson & Kozlov,1973)

(1) Plagiogranite
(2) Ultrametamorphic granites (products of partial melting)
(3) Palingenic granites (product of total melting divided into two subdivisions:
(a) normal palingenic granites
(b) subalkaline palingenic granites
(4) Plumasitic leucogranites, tin type
(5) Agpaitic leucogranites, columbite type

Table 7.5
Concentration ratios in granitic types devised by Tauson and Kozlov (1973)

Concentration ratios	Plagio-granites	Ultra metamorphic granites	Palingenic granites	Plumasitic leuco granites	Agpaitic leuco-granites
K/Na	0.16	2.2	1.1	1.4	1.2
K/Rb	1250	385	240	100	290
(Li*1000)/K	0.4	0.15	1.1	2.4	0.9
F/Li	75	16	16	31	29
Ba/Rb	45	11.5	5.3	0.5	0.3

midcrustal levels as a result of collision and crustal thickening, and rose as diapirs, some dragging an envelope of migmatite and wall rocks with them.

White et al (1986) compared the peraluminous granites of south-western North America (some of them reported to be "S"-types), with those of the Lachlan Fold Belt (LFB) in S. E. Australia. They indicate that the "S"-type granites are not always foliated bodies associated with regional metamorphism and migmatites. Cordierite is the dominant peraluminous mineral in the LFB "S"-type granite, while cordierite is absent from "S"-type granites of S. W. North America. Na, Sr, and Ba elements are higher in the peraluminous granite of S. W. North America (Keith et al. 1980),thus they are unlike any rocks of the LFB. They concluded that "S"-type granites of the LFB of S. E. Australia either do not exist in S. W. North America, or that insufficient data have been presented to identify them.

The survey of the "I" and "S" classification given above shows that the genetic nature of this classification is debatable and not all authors agree about its usefulness and its precise definition. The problem is that many authors have expanded the range of the "S"-type term to include all peraluminous and muscovite-biotite granite (Baker 1981), while others have restricted the definition of "S"-type granitoids to these containing cordierite as essential feature (White et al., 1986); according to this definition the "S"-type granitoids are likely to be associated with high grade metamorphism {migmatites}. Thus, this "S"-type classification is relatively useless outside the LFB of S.E. Australia, as less than 1 % of granites throughout the world are cordierite bearing (Miller et al 1986).

7.2.2 Classification based on Tectonic Environment.

Martin and Piwinskii (1972) defined two distinctive tectonic environments, each characterized by diagnostic magmatism. A compressional environment occurs at the loci of plate convergence (orogenic magmatism) and tensional environment occurs at the loci of plate divergence (non-orogenic magmatism).
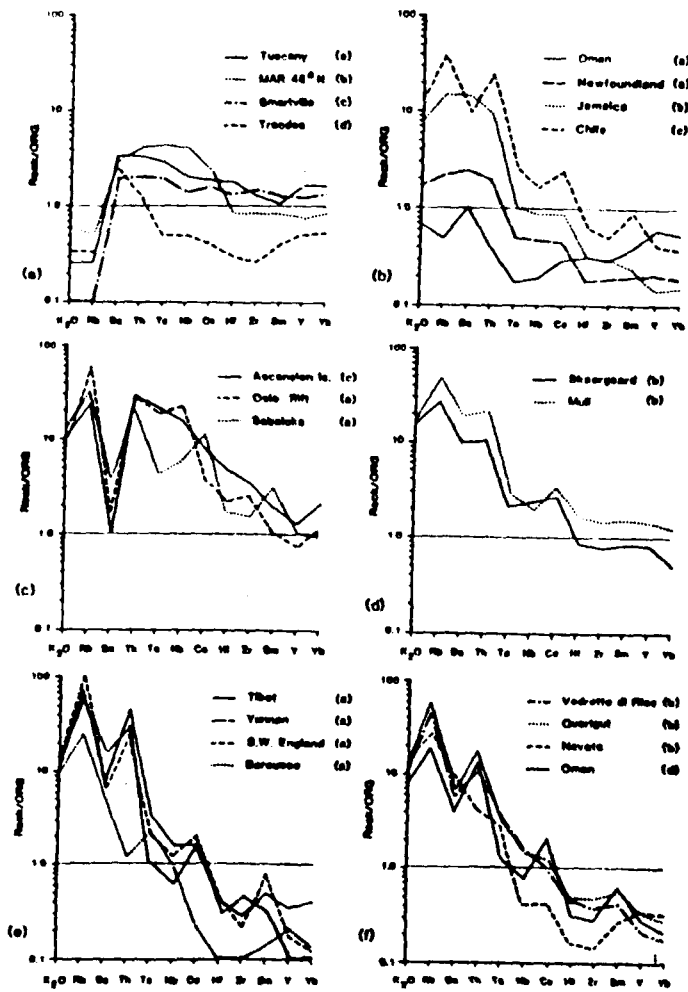
Fig. 7.2a Ocean ridge granite (ORG) normalized geochemical patterns for the representative analyses, of ocean ridhge granites (a), volcanic arc granites (b), within plate granites (c), within plate granites (attenuated continental lithosphere) (d), syn-collision granites (e) and post-collision granites (f). (after Pearce et al, 1984).
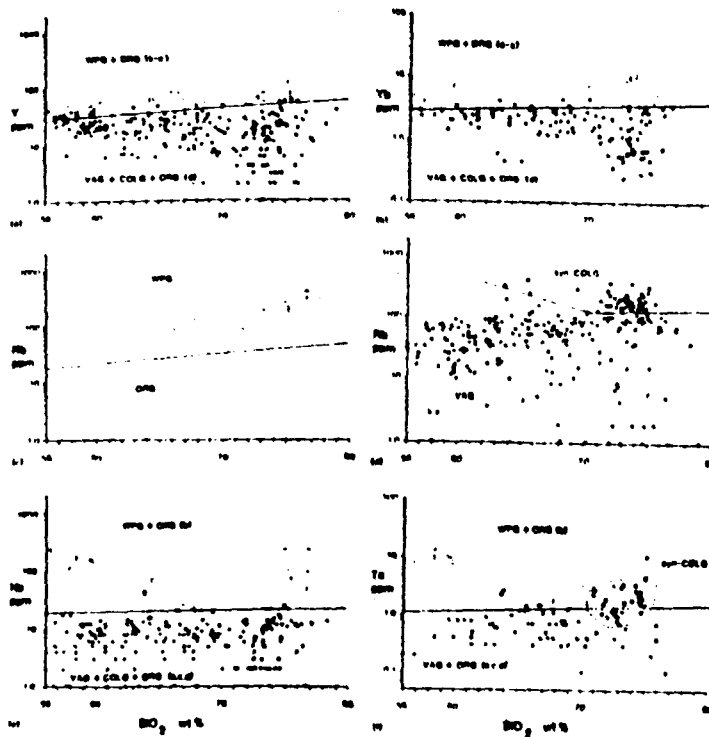
Fig. 7.2b SiO2 variation diagrams for Rb, Y, Yb, Ta and Tb based on analyses in the data bank. Open circles represent ORG, closed circles represent VAG, open squares represent WPG, and closed square represent COLG. For clarity ORG (d) which have the same Y values as VAG, have not been plotted in Figs. 7.2a (a) and 7.2a (b) and post-COLD which are generally transitional between syn-COLG & VAG have not been plotted in Figs. 7.2a (d) & 7.2a (f).
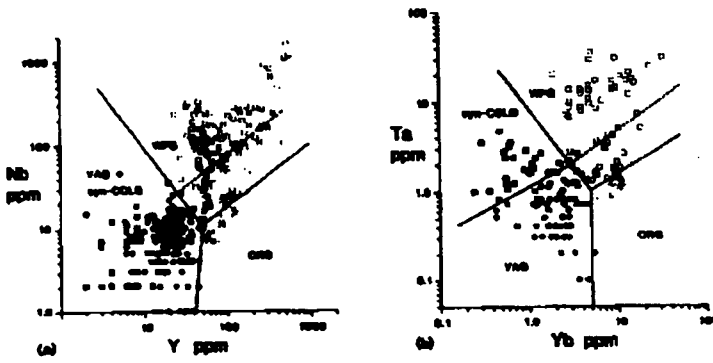
Fig.7.2c Nb-Y (a) and Ta-Yb (b) discriminant diagrams for syn-collision granites (syn-COLG),volcanic arc granite (VAG), within plate granite (WPG), and ocean ridge granite (ORG). The dashed line represents the upper copositional boundary for ORG from anomalous ridge segments. Note that post-collision granites can plot in all but the ORG fields, and that supra-subduction zone ocean ridge granites plot in the VAG field. Symbols as in Fig. 7.2b. Co-ordinations of the discriminantboundaries are: for the Y-Nb diagram:
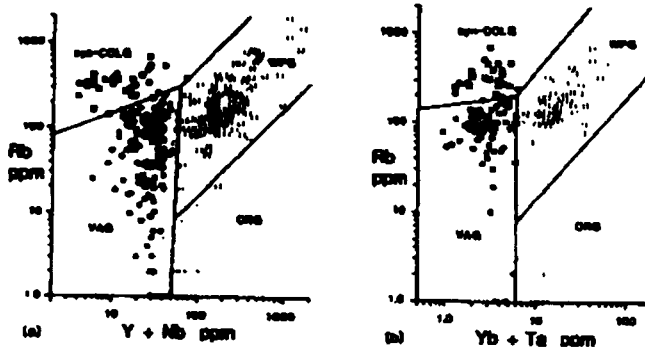
Figure 7.2d Rb-(Y+Nb) (a) and Rb-(Yb+Ta) (b) discriminant diagrams for syn-COLG, VAG, WPG and normal and anomalous ORG. Note that post-collision granites can plot in all but the OR fields and thatsupra-subduction zone ocean ridge granite plot in the VA field. Symbols as in Fig. 7.2b. Co-ordination of the discriminantboundaries are: for the Rb-(Y+Nb) diagram;

(after Pearce et al, 1984)
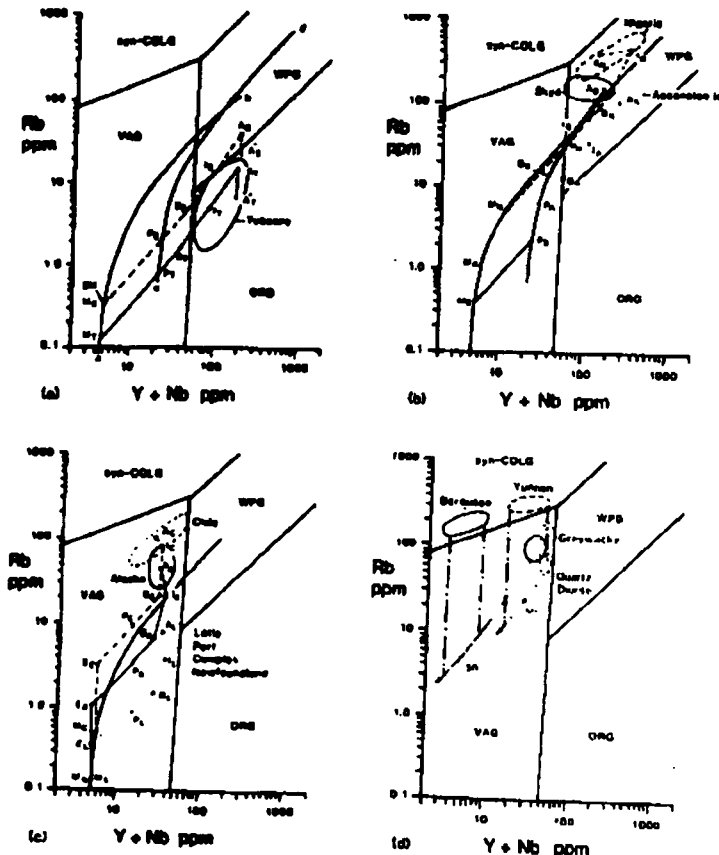
Fig. 7.2e Petrogenetic modelling of the Rb-(Y+Nb) to demonstrate the theoritical basis for the discriminant boundaries. (after Pearce et al, 1984).

Pearce et al (1984) introduced a trace element discrimination diagram for tectonic classification of granitic rocks. They subdivided granitoid rocks according to their intrusive settings into four main groups: Oceanic Ridge Granite (ORG), Volcanic Arc Granite (VAG), Within Plate Granite (WPG), and Collision Granite (COLG). Pearce et al. used high quality trace element analyses of granites from known settings to provide geochemical patterns (normalized to a hypothetical ORG) revealing systematic trace element differences between many of the tectonic groups and subgroups. The most significant are the high Y and HREE concentration in oceanic ridge and within plate granites; high Nb and Ta in mainly within plate granite and high Rb in syn-collisional granites (Fig. 7.2a). Trace element-SiO2 variation diagrams confirm that these features hold over the SiO2 range studied (56-80 %) Fig. 7.2b. Discrimination of ORG, VAG, WPG, and syn-COLG are most effective in Rb-Y-Nb and Rb - Yb - Ta space, particularly on the projection of Y-Nb, Yb-Ta, Rb-(Y + Nb) and Rb-(Yb + Ta), Figs. 7.2c and 7.2d. Discrimination boundaries, although, drawn empirically, can be shown by geochemical modelling to have a theoretical basis in the different petrogenetic histories of the various groups (fig. 7.2f). The post- collision granites present the main problem of tectonic classification, since their charactersitics depend on the thickness and composition of the lithosphere involved in the collision event, and on the precise timing and location of magmatism (Fig. 9f), they can plot in the VAG, WPG, or syn-collision fields, depending on the relative proportions of mantle and crust-derived magmas and on the enrichment history of the mantle concerned.

7.2.3 Classification based On Associated Mineralization.

Tauson and Kozolov (1973) have used specifically Russian models for trace element geochemical behavior to distinguish five main types of granitic rocks (table 7.4). Genetic classification is based on associated mineralization. The associated mineralizations have been used by some authors as genetic constraints for granitoid rocks within which distinctive metal deposits are associated. Ore deposits can be
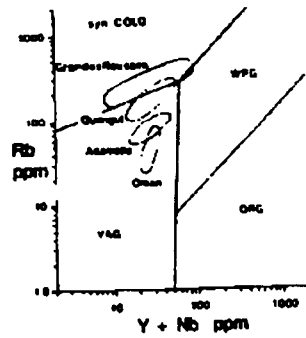
Fig. 7.1f Distribution of some post-collision granites on the Rb-(Y+Nb) discriminant diagram of Fig. 7.2a
(after Pearce et al, 1984).
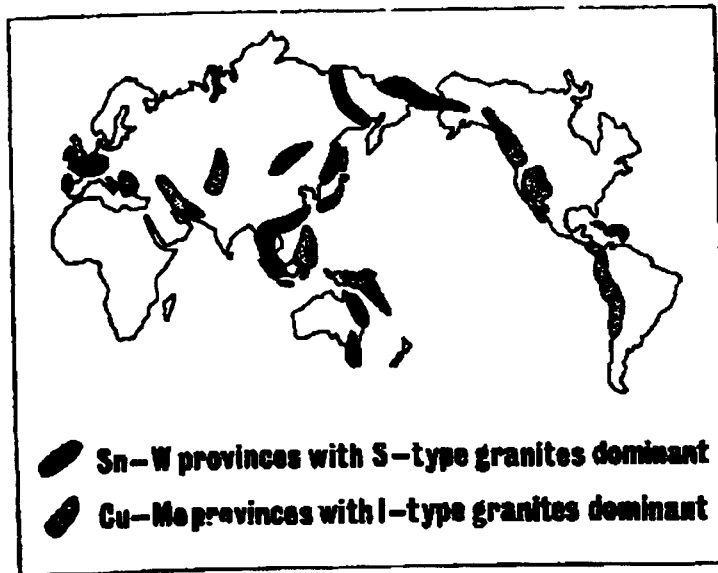
Fig. 7.3 Map showing distribution of I-type and S-type granites on a world scale,
based on the work of Ishihara (1977). (after Beckinsale in Atherton & Tarney, 1979)
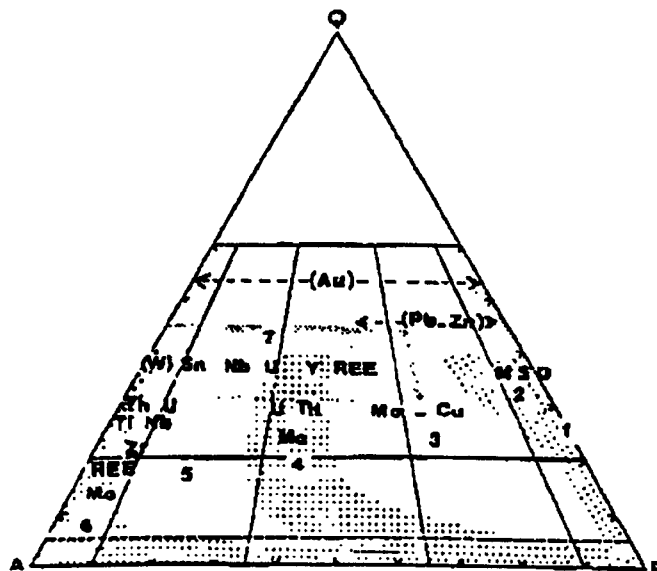
Fig. 7.4 Mineralizations associated with granitoids in the fields defined on Fig. 7.1d.
(after Lameyre et al, 1980)

TABLE 7.6 Characteristic features of "I" and "S" type granites (from Beckinsale in Atherton and Tarney, 1979).

I-type or magnetite-series granites	S-type or ilmenite-series granites
Tend to be the acid end of a broad compositional spectrum from basic to acid	Tend to occur in restricted ranges of only acidic compositions
Relatively high sodium contents	Relatively low sodium contents ($<3.2\%\,Na_2O$ in rocks with $\sim 5\%\,K_2O$)
Low initial $^{87}Sr/^{86}Sr$ ratios (<0.708)	High initial $^{87}Sr/^{86}Sr$ ratios (>0.708)
Normal range of $\delta^{18}O$ values (approx. $6-10\%_o$, SMOW)	Enriched in ^{18}O ($\delta^{18}O$ values $>$ about $10\%_o$, SMOW)
Magmas with relatively high oxygen fugacity; relatively high ferric/ferrous ratios; characterized by magnetite	Magmas with relatively low oxygen fugacity; relatively low ferric/ferrous ratios; characterized by ilmenite
Hornblende and sphene commonly present	Muscovite, monazite, cordierite and garnet commonly present

Table 7.7 Contrasting characters of orogens (on a structural, not time-stratigraphic basis, partly after Zwart, 1967)

Alpinotype Orogenies:	Island-arc derived volcaniclastic sediments and lavas deposited in oceanic trenches; crustal shortening involving thrusting with nappes predominant; high pressure regional metamorphism with wide progressive zonation; ultrabasic rocks abundant. Granitoid batholiths characteristically absent
Andinotype Orogenies:	Island-arc volcaniclastic sediments and lavas deposited in troughs of eugeosynclinal type located within the continental lip and paired with belts of shelf-facies clastics; little crustal shortening but vertical movements dominant, with open, drape-folding lacking cleavage; regional burial metamorphism. Compositionally expanded, disharmonious, granitoid batholiths with important basic plutonic and andesitic volcanic associations. I-type granites with crustal involvement only in the later stages of evolution: $^{87}Sr/^{86}Sr \leqslant 0.706$; include restite material from subcrustal source
Hercynotype Orogenies:	Non-volcanic, continentally-derived sediments in intra-cratonic basins of miogeosynclinal type; crustal shortening with upright folding and cleavage; low-pressure metamorphism with prograde zonation; ultrabasic rocks rare. Compositionally contracted, harmonious, granitoid batholiths with only minor basic association and generally lacking contemporaneous volcanics. S-type or mixed S- and I-type granites; $^{87}Sr/^{86}Sr > 0.706$; inherited xenocrysts derived from recycled crustal rocks

broadly divided into those generated by endogenetic processes and those generated by exogenetic processes; the former associated with thermal processes, that can be related to magmatic and tectonic events promoted by plate activity. The exogenic processes or deposits formed by surficial processes such as weathering or shallow marine sedimentation will have a relationship to their tectonic environment.

Tauson and Kozlov (1973) showed that the majority of trace elements are not dispersed in mineral lattices during crystallisation, but migrate with volatiles to form residual concentrations toward the top of a magma chamber. This tendency has been called "emanation concentration", though the actual concentration mechanism remains obscure. Five granitoid rock types have been recognized by Tauson and Koslov, each one has a distinctive assemblage of trace elements which is known as element concentration ratio (table 7.5). These assemblages are not only characteristic of the granites themselves, but also the geochemical anomalies formed in the surrounding country rocks. Each of the granites has a different geochemical potential, two of them are economically very important; tin type-plumasitic leucogranites and columbite type-agpaitic leucogranite.

Beckinsale (in Atherton and Tarney 1979) and others have shown the relationship between granite types and their associated mineralization (Fig. 7.3). "I"-type granites are characterized by Cu-Mo porphyry and "S"-types granites by Sn-W greisen and vein-type mineralization. Beckinsale added $\partial 18O$, $Fe2+ / Fe3+$ ratios to the list of discrimination characteristics (table 7.6).

Lameyre et al (1980) showed that the plutonic series associated with mineralization are well distinguished on a QAP Streckeisen diagram (fig. 7.4). Thus Massive Sulfide Deposits (MSD) are associated with tholeiitic and calc-alkaline-trondhjemitic series, Cu-Mo porphyry with calc-alkaline (mainly granodiorite), Pb-Zn in many cases concentrate around granitic bodies belonging to calc-alkaline series as veins. The late orogenic granite monzonite series, frequently have small concentrations of Mo and to some extent high U and Th .

REE-Zr-Nb in addition to U and Th are concentrated in the alkaline and silica

undersaturated series. The presence of F is very important in micas, amphibole

and in fluorite. Mobilizates granitoids are enriched with REE and W (Fig.7.4)

V.I.Kovalenko and N.I.Kovalenko (1984) discussed the probable

origin of rare-metal Li-F granite which ranges from leucogranites to albite-

lepidolitic granites enriched in flourine, rare alkaline elements Sn, Nb, Ta, and

depleted in Sr, Ba, REE, and Y, compared to their mean content in acid igneous

rocks. They suggested that they have been formed either as the latest stage

differentiates of a common granitic magma or partial melting of rare-metal

metasomatic rocks.

Sawkins (1984) has described in length in his book (metal deposits in relation

to plate tectonics) the relationship of metal deposits to the various types of tectonic

settings; whether in orogenic or anorogenic magmatism. He recognized 3 main

environments of metal deposits; 1) Convergent plate boundary environment, which

may be subdivided into A = principle arcs and their associated metal deposits (Cu,

Skarn deposits). B = metal deposits on the inner sides of principle arc (Ag-Pb-Zn-

Cu). C = metal deposits of arc related rifts (Mo-porphyry, massive sulfide

deposits). 2) Divergent plate boundary environments, including the following

subdivisions A= metalliferous deposits of oceanic-type crust (massive sulfide

deposits of the Troodos ophiolite, chromium deposits in ophiolite complexes). B =

intracontinental hot sposts, anorogenic magmatism; the associated metal deposits

are (Sn, Fe-Ti, Cu-Ni, Pt). C = metal deposits associated with the early stages of

continental rifting (hydro. Cu, Mo, Cu-Ni, carbonate-hosted Pb-Zn). D = metal

deposits related to the advanced stages of rifting (Red sea deposits, massive sulfide

deposits). 3) Collision environments, include; A = metal deposits related to

collision events (ophiolite-hosted metal deposits, Sn, W, U). The utilization of

plate tectonic concepts in mineral exploration obviously provides a meaningful

framework within which the geological and geochemical processes that lead to

economic metal concentrations can be more fully understood.

7.2.4 Genetic Classification Based On Enclaves within the granitoid rocks.

Mafic xenoliths are of world-wide occurrence in granitoidrocks, implying a general mechanism for their production rather than a local mechanism. The specific character of the xenoliths in each suite indicates two possible sources. First,the xenoliths could represent material produced by earlier crystallization at depth, which has been incorporated in the magma. Second, they could represent material residual from partial melting at the source of magma generation. Gilbert (1906) proposed that xenoliths are clots of early-formed minerals. Harker (1909) regarded the mafic inclusions as products of an early crystallization in an intercrustal reservoir.

Didier (1973) reviewed all the mafic enclaves that are particularly abundant in the granitoid rocks especially basic enclaves associated with granodiorites and monzogranites.

Chappell and White (1974) on the distinction between "I" and "S"-type granitoids, indicate that "I"-types contain mafic hornblende-bearing xenoliths of igneous appearance which are rare in "S"-type granites in which metasedimentary xenoliths may be common.

Didier et al. (1982) proposed that granitoid rocks could originate in the mantle or crust, and this would be shown by their enclaves. The distinction is made between C-type granite (crustal) and M-type granite (mantle or mixed, i.e crustal + mantle). The C-type granites can be subdivided into CS-type (anatexis of sedimentary rocks), and CI-type granites (anatexis of igneous rocks), rather than a distinction between S-type granites of sedimentary origin and I-type granites of igneous origin. This classification has been applied to the Variscan granites in the Massive Central granites of France.

Wall et al (1987) suggested that most plutons contain a number of different enclaves of various provenances (see Vernon 1984). These enclaves grouped into: 1) Accidental inclusions derived from wall rocks near the

emplacement level, and those derived at deeper levels and related to neither the present wall rocks nor the primary source region. 2) Magma mixing products; **Larsen et al (1938) and Eichelberger (1978-1980)** have shown that partial mixing of mafic and silicic magmas is wide spread in calc-alkaline volcanic associations. Clear examples of the mingling of mafic and silicic magmas also occur in plutonic suites (Reid et al. 1980, 1983; Contagerl et al., 1984). For some metaluminous granites magma mixing seems to have been particularly important. 3) Cognate cumulates are common and may dominate the enclave populations. Such cognate inclusions are well documented among suites of mafic igneous rocks.

Phillips et al. (1981) and Vernon and Flood (1982) believe that many microgranite enclaves with igneous textures represent accumulations of near-liquid phases formed on the cool walls of magma chambers and in volcanic conduits. Didier (1973) cites numerous examples of such mafic-enriched chilled margins and enclaves derived from them, the fine grained cognates attributed to high degree of undercooling and rapid crystal growth. Such cognates are enriched in early crystallized ferromagnesian phases and calcic plagioclase.

7.2.5 Genetic Classification Based On Zircon Morphology.

The petrogenetic classification of granitoid rocks have been proposed according to the careful study of zircon morphologies in granites. The fundamental basis of population in zircons had been given earlier by Pupin and Turcu (1972 a). **Pupin (1980)** introduced the following petrogenetical classification on the basis of typological studies of zircon populations from granitic rocks, field observations, petrographical, geochemical data of the granites examined and their typological evolutionary trend (T.E.T.). A - Granites of crustal or mainly crustal origin (orogenic granites) of two types; 1) Autochthonous and intrusive aluminous leucogranite, 2) Subautochthonous monzogranites and granodiorites. B -Granites of crustal+mantle origin; hybrid granites {orogenic granite} ; this can be

subdivided into: 1) calc-alkaline series granite 2) sub-alkaline series granites. C - Granite of mantle or mainly mantle origin {anorogenic granites}; and subdivided into; 1 - alkaline series granites and 2) tholeiitic series granites. It appears that the study of granite-zircon populations can provide extremely valuable data about the genetic classification of granitoid rocks.

7.2.6 Petrographical classification Based On Major Element-Cations.

Debon and Le Fort (1982) have used De La Roche (1966) ideas on classification which are based on major element analytical data plotted in three diagrams. The first diagram is termed a nomenclature diagram (Fig. 7.5), which is formed on the basis of two parameters; Q = Si/3-(K + Na + 2Ca/3) and P = K - (Na + Ca). Debon and La Fort have superimposed on it a new classification grid in which each division (1-12) corresponds to a petrographical group. The evolutionary trends of the magmatic associations have also been drawn on this diagram. The second diagram or characteristic minerals diagram (see Debon & Le Fort, 1982) uses two parameters A = Al - (K + Na + 2Ca) which were used by Shand (1927) to define the peraluminous or metaluminous characters, and B = (Fe + Mg + Ti), used by De La Roche (1964). This diagram shows the nature and proportions of minerals other than quartz and feldspars, and is used to discriminate three types of magmatic associations: 1) The Cafemic types mainly located in the metaluminous domain with a negative slope. 2) The aluminous type entirely located in the peraluminous domain of the diagram with a vertical or positive to slightly negative slope. 3) Alumino-Cafemic type intermediate between these two types, mainly located in the peraluminous domain of the diagram, with a more or less pronounced negative slope. The third diagram or Q-B-F diagram associates the three chemical parameters used by La Roche (1964); Q is the same for the first diagram, B of the second diagram and F = 555-(Q + B), these parameters recalculated as percentages and plotted on the Q-B-F diagram as proposed by Moine (1974, See Debon & Le Fort for calculations). Each plutonic rock is compared in

Figure 1. Nomenclature diagram for common igneous rocks modified after Le Roche (1964, 1966). Its parameters are expressed as gram-atoms × 10³ of each element in 100 g of material (rock or single mineral); method of calculation is set out in Table 2. Each pigeon-hole of the classification grid corresponds to a petrographical group: 1 (gr) granite, 2 (ad) adamellite, 3 (gd) granodiorite, 4 (to) tonalite (trondhjemite), 5 (sq) quartz syenite, 6 (mzq) quartz monzonite, 7 (mzdq) quartz monzodiorite, 8 (dq) quartz diorite (quartz gabbro - quartz anorthosite), 9 (s) syenite, 10 (mz) monzonite, 11 (mzg) monzogabbro (monzodiorite), 12 (go) gabbro (diorite - anorthosite). The twelve model compositions adopted for a reference system (Table 1) are marked by asterisks. Ab and An stand for albite and anorthite respectively.

Examples of different plutonic associations are shown (symbols and notations explained in Figures 2 to 4).

For volcanic rocks the corresponding nomenclature is 1 rhyolite, 2 dellenite, 3 rhyodacite, 4 dacite, 5 quartz trachyte, 6 quartz latite, 7 quartz latiandesite, 8 quartz andesite (quartz basalt), 9 trachyte, 10 latite, 11 latibasalt (latiandesite) 12 basalt (andesite).

Figure 2. "Characteristic minerals" diagram. Both parameters are expressed as gram-atoms × 10³ of each element in 100 g of material (see Table 2 for calculation). The diagram is divided into six sectors numbered from I to VI. Plots of minerals using actual and theoretical compositions are given in the inset: And andalusite, Ap apatite, Bi biotite (hatched field), Cd cordierite, Chl chlorite, Ct calcite, Di diopside, Ep epidote, Fk potassium feldspar, Gr pyralspite, Hb hornblende, Hy hypersthene, Ilm ilmenite, Mt magnetite, Ol olivine, Pl plagioclase, Q quartz, Sill sillimanite, Sph sphene, Tr tourmaline.

Figure 7.5 Figures 1 and 2 0f Debon and Le Fort (1982)

this diagram to a system of references made up of a set of modal compositions of the main petrographical groups of common plutonic rocks. The Q-B-F diagram is used concurrently with the nomenclature diagram to discriminate between the main different subtypes and variants of the three main types of magmatic associations as the following: Cafemic associations: subdivided into the following subtypes and variants: A) Tholeiitic (or gabbroic-trondhjemitic). B) Calc-alkaline (or granodioritic). C) Subalkaline (or monzonitic), D) Alkaline & peralkaline (saturated, oversaturated). Alumino-cafemic association: using the same diagram, similar sudivisions to those adopted for the cafemic associations are proposed and a granitic-trondhjemite subtype is added. Aluminous associations: three main types are recognized through the Q-B-F diagram (quartz-rich subtype, quartz-normal subtype, quartz-poor subtype. Debon and La Fort said from a descriptive point of view, that cafemic and aluminous associations are respectively equivalent to the "I" and "S" types of **Chappell and White (1974).**

7.3 The previous Classification of Shetland Granites

All the previous classifications of Shetland igneous rocks were based on petrographical descriptions. No real geochemical parameters have been used before this work for the purpose of classification of Shetland plutonic granitoids, which include small and large areas of granite. The plutonic complexes exposed on Shetland fall into two groups lying, respectively, east and west of the Walls Boundary Fault. The eastern complexes are in places weakly foliated, indicating that they were emplaced before Caledonian tectonism ceased, and give K-Ar ages about 400 Ma and are all cut by the Walls Boundary Fault (WBF) and the Nesting Fault. The Old Red Sandstones of the eastern group are cut neither by these complexes nor by associated dyke rocks, and the Spiggie granite is unconformably overlain by the Sandstones. The western complexes crop out just to the west of the WBF and form a north-south trending series with K-Ar ages nearer to 350 Ma, while some of the dykes associated with them and Sandsting granite itself cut the

Old Red Sandstones. These complexes are not foliated and are thus essentially post-tectonic intrusions. Besides these late and post-Caledonian complexes there are several premetamorphic, now gneissose, granites in the Yell Sound division. A partially tectonized, very coarsely porphyritic Skaw Granite (Read, 1934) forms a forceful intrusive near the Ophiolite Complex; and a series of schistose aplogranites of Colla Firth, varying in size from a fraction of a metre to a kilometre across and giving a Rb-Sr age 530 Ma is associated with the Colla Firth permeation gneiss belt or Colla Firth granite (Flinn and Pringle 1976; Mykura 1976).

7.4 Classificaiton Of Shetland Granites According to Streckeisen Classification Diagram.

The best classifications are generally those which have no reference to the origin of geological materials. Indeed once genetic factors are used in classifications, difficulties arise. Thus most of the igneous classifications in use today are essentially free of genetic parameters and should be in terms of mineralogy and mode using the Streckeisen (1976) diagram. There are many igneous rock classification schemes that have been set up by individuals or by small groups, but none has become universally used. The first attempt to develop a systematic classification for igneous rocks and in particular for granitoid plutonic rocks was Streckeisen and the subcommision created by the (IUGS). The subcommision started with plutonic rocks and reviewed all the previous schemes of plutonic rock classification. They put forward a system of classification and nomenclature for plutonic rocks that has since been called the Streckeisen classification (Figure 7.1a). Thus plutonic rocks are named according to their actual (modal) mineral contents, expressed in volume percent. Prior to being plotted on the QAPF diagram, the values of the light-coloured constituents are recalculated to total 100 (that is, Q + A + P = 100, or A + P + F = 100).

7.4.1 The Streckeisen Classification for Hornblende-Bearing Granites.

The modal data from all three plutons (Graven, Brae and Spiggie granites) of the Hornblende-bearing granites are plotted on a Streckeisen diagram, Figure 7.6a-A, (the complete data set are given in appendix 2). The modal analyses from the Graven complex fall in the fields quartzmonzodiorite, tonalite grading to granodiorite, granodiorite and monzogranite. It seems from the distribution of the samples within the QAP diagram that granodiorite is the main lithological type of the Graven complex and has a wide range of petrological variation. In case of the Brae Complex the modal plots mostly lie in the tonalite field, two on the boundary between quartzmonzodiorite and granodiorite and two in the fields of quartzmonzonite and monzogranite. According to the modal measurements the Aith-Hildsay-Spiggie granite falls mostly in the fields of granodiorite and quartzmonzonite and monzonite, then a few rocks in quartzmonzodiorite, quartzsyenite and monzogranite, one sample from Hildasay lies in the tonalite field. The Streckeisen diagram of hornblende-bearing granite shows overlap in the field of granodiorite and to some extent in the quartzmonzodiorite field. It is clear that the Spiggie granite is calc-alkaline-monzonite high K and the Graven pluton is calc-alkaline-granodiorite medium K and the Brae Complex is calc-alkaline-monzonitic low K.

7.4.2 Streckeisen Classification Of Hornblende-Free Granites.

The modal analysis data of Hornblende-free granites (Skaw, Tonga & Brecken, Skerries and Colla Firth, Channerwick & Cunningsburgh and trondhjemite dykes) plotted on the QAP Streckeisen diagram, Figure 7.6a-B, shows that they fall in monzogranite and syenogranite zones, both of them form the granite field, and few samples from Skaw and Skerries granites plotted in the granodiorite field very close to the monzogranite. The modal values of Skaw

A) Hornblende-bearing granites

- ○ **Graven granitoid**
- ● **Brae granitoid**
- ■ **Spiggie and its two offshoots Hildsay and Aith granites**

B) Hornblende-free granites

- o **Skaw granite**
- • **Tonga and Brecken granites**
- • **Out Skerries granite**
- ■ **Colla Firth granite**
- + **Trondhjemite dykes**

- ○ **Ronas Hill granite**
- * **Marginal granite**
- • **Net veined granite**
- + **vementry granite**

C) Ronas Hill granite and its satellites

Figure 7.6a Streckeisen QAP diagrams showing the modal data plots for the three main groups of granites in A, B and C.
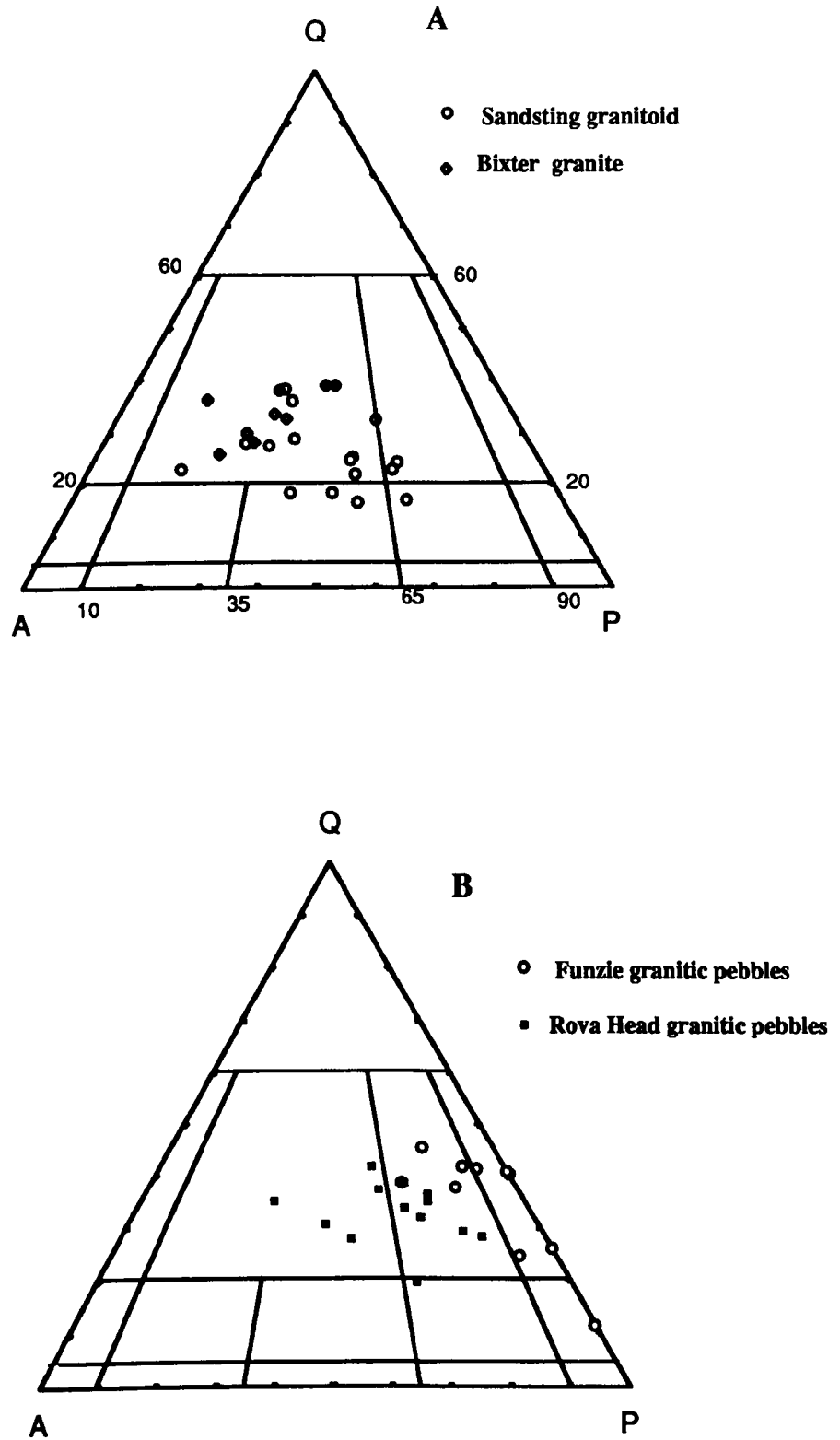
Figure 7.6b Streckeisen QAP diagrams showing modal data plots for two main groups of Shetland granitoids in A and B.

granite have been calculated on the basis of 80% matrix measured by point counter under the microscope, and 20% of K-feldspar phenocrysts, determined by point counting phenocrysts on photographs of the Skaw granite (plate 2.1). An average K-feldspar phenocrysts content of 20% was obtained. The plagiogranite or trondhjemite dykes (Na-granite intrusives) associated with the ophiolite sequence adjacent to Skaw Granite, plot on the Q-P side, which characterizes the plagiogranite group, the end product of magma differentiated from the ophiolitic rocks.

7.4.3 Streckeisen Classification for Ronas Hill and Its Satellite Granites .

This group of rocks lies to the west of the Walls Boundary Fault and North of Bixter Voe; they include the Ronas Hill granite, Marginal granite, Net-Veined granite, Muckle Roe granite and Vementry granite. The modal analyses of Ronas Hill granite and its satellite plotted on the QAP Streckeisen diagram, Figure 7.6a-C, (data modes in appendix 2) are located in the field of granite, either syenogranite or monzogranite, with some samples from Ronas and marginal granites plot in the alkali-feldspar granite field (as they are microperthite granites). The overlap of the data indicating the homogeneity of this granitic group supports the suggestion that the granites form north-south trending series of possibly interconnected plutons which extend from North Roe to the southern side of the Walls Peninsula.

7.4.4 Streckeisen Classification for Sandsting and Bixter Granites

The Sandsting and Bixter lie to the west of Walls Boundary Fault and South of Bixter Voe. The modal analysis of the components of the Sandsting granite and Bixter granite are shown on the QAP Streckeisen diagram Figure 7.6b-A (modes data in appendix 2). The Sandsting range from quartzmonzodiorite, through quartzmonzonite to granite and only one sample in the field of monzodiorite, two samples plot on the boundary between granodiorite and granite and some samples

show high quartz content, representing quartz-rich biotite granite. The Bixter granite plots only in the field of monzogranite and one diorite sample in the field of quartmonzodiorite and petrographically is similar to the Ronas Hill group and lies with in the same plot envelope.

7.4.5 Streckeisen Classification for Pebbles of granites in Rova Head & Funzie Conglomerates to the east of the Walls Boundary Fault.

The modal analyses of granitic pebbles from Funzie and Rova Head Conglomerates Figure 7.6b-B (modes data in appendix 2) plotted on the QAP Streckeisen diagram range from plagiogranite, through tonalite to granodiorite, and this is calc-alkaline trondhjemite low K (Lameyre and Bowden (1982). There are two types of granitic pebbles in Rova Head conglomerate, one is intermediat with range of silica between 64-71 and the other one is acidic and silica range between 71-76.74%. The modal data of the more basic one lies in the field of granodiorite and two of them grade in to the granitic field, and one sample lie on the boundary between granodiorite and quartzmonozodiorite, the modal data of the acidic one lies in the field of granite.

Introduction To the Geochemical Classification of Shetland Granites.

A potential problem with the geochemical classification of granitic rocks is the degree to which the analysed composition reflects the primary composition or secondary alteration effects. This can be particularly so when a geochemical classification involves the use of elements which are mobile during water-rock interaction. For example, the De La Roche et al. (1980) scheme relies on the concentrations of Na and K for one of its parameters (R1), K would normally be expected to increase with differentiation (see Figures 5.2b &5.3b). However, in the present study, K and Rb contents often show no systematic variation with SiO_2 content (see Figures 5.2d & 5.3d). There is some petrographic evidence for alteration of feldspars (see plates 3.2 & 3.6). Thus in the following geochemical

classification schemes envoling elements of Na, K, Rb, Sr Should be viewed with caution.

7.5 Classification of Shetland Granites Using the De La Roche R1 R2-Diagram

De La Roche (1980) and De La Roche et al. (1980) have put forward a classification based on the cationic proportions of the major oxides, that permit ready recognition of the mineralogical significance of the chemical variations used to define granitic rocks of calc-alkaline affinities.

7.5.1 Hornblende-bearing Granite Classification Using R1 R2-Diagram

The De La Roche R1 R2 parameters have been calculated for the various rocks of hornblende-bearing granites and are displayed in Figure 7.8a-A. which indicates the calc-alkaline character trend of Shetland granitoids. An intermediate trend between the calc-alkali and alkaline series is seen too. The Spiggie monzonite is characterize by high total alkalis, owing to that it is plot in the alkaline field, on the curved classification grid they fall into the gabbro-diorite field through diorite then tonalite to granodiorite. Some of the Spiggie granite plotted on the border between diorite and monzodiorite and some in quartzmonzonite field but none plotted in the fields of granite, monzonite and quartzsyenite as they do on a Streckeisen diagram.

7.5.2 Hornblende-free Granites Classification Using the R1 R2-Diagram.

The major cation proportions for the hornblende-free granites samples have been calculated and R1 R2 parameters are displayed in Figure 7.8ab-B, they are more acidic than the hornblende-bearing granites and similar to the plutonic complexes of Ploumanac'h, Brittany (Barriere, 1977) and Corsica (Orsini,1976). They are restricted into two fields, granodiorite and granite with one sample of the

A

3000
2000
1000
0

Alkaline

Shoshonitic

Calc-alkali

Ploumanac'h

O Graven
◆ Brae
+ Spiggie

B

R2=6Ca+2Mg+Al

3000
2000
1000
0

Alkaline

Shoshonitic

Calc-alkali

Ploumanac'h

O Skaw
● Tonga & Brecken
■ Skerries
◉ Colla Firth
+ Channerwick
□ Keratophyre
▲ Trondhjemite dykes

C

3000
2000
1000
0

Alkaline

Shoshonitic

Calc-alkali

Ploumanac'h

+ Ronas
◆ Marginal
O Net-Veined
● Muckle Roe
✕ Vementry

R1= 4Si - 11(Na+K) - 2(Fe+Ti)

Figure 7.8a Variation diagrams for the rocks of A) hornblende-bearing granites, B) hornblende-free granites, and C) Ronas Hill granite and its satellites after Dela Roche et al., (1980). Various trends shown the distinctive character of the hornblende-bearing granites compared to hornblende free granites and the Ronas group.
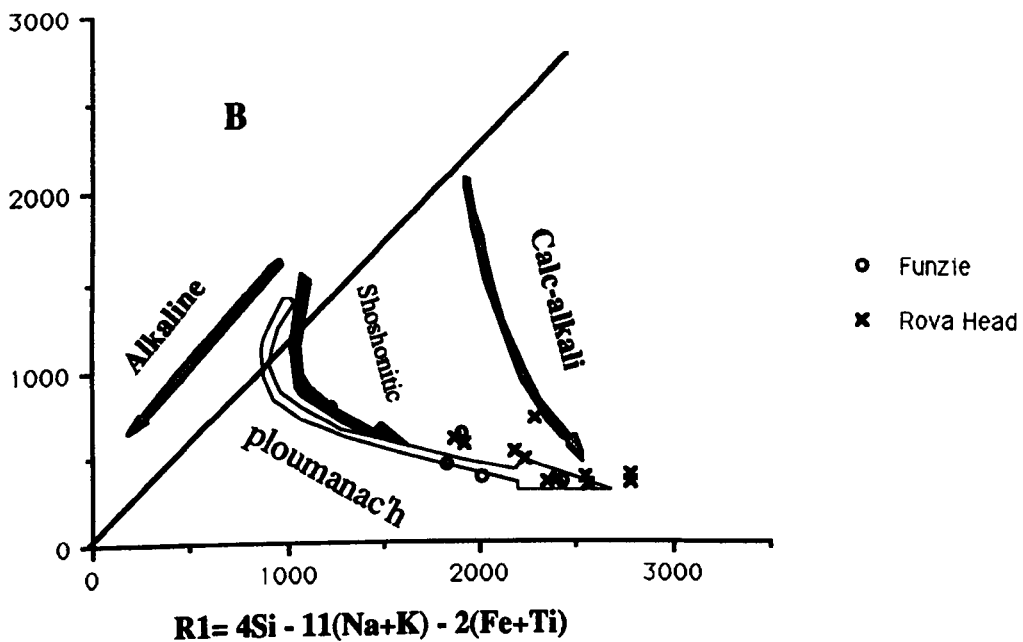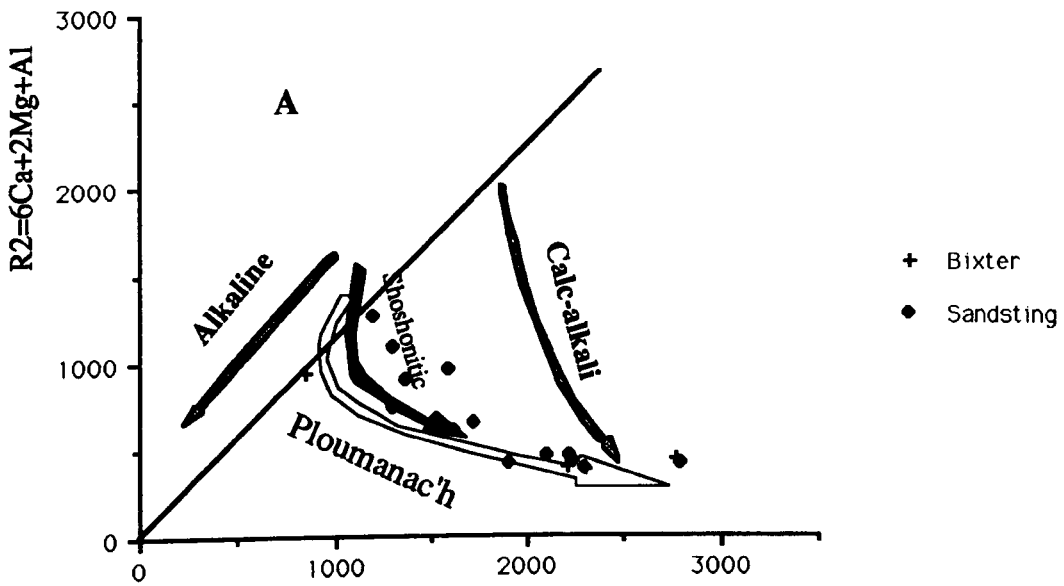
Figure 7.8b Variation diagrams for A) Sandsting granitoid and Bixter granites, and B) Granitic pebbles from Funzie and Rova Head Conglomerates. Note the Shoshonitic trend of the Sandsting and Bixter granites.

trondhjemite dykes lying in the dioritic field, and the keratophyre and trondhjemite dykes close to the calc-alkaline trend. The difference between the data in R1 R2-classification diagram and in the Streckeisen-classification diagram is that the bulk composition of rocks on Streckeisen lie in the field of granite, while on the R1 R2 diagram they lie in the field of granodiorite.

7.5.3 <u>Ronas Hill Granite and its satellites Classification Using the R1 R2-Diagram</u>

R1 R2-values have been calculated for the Ronas Hill Granite and its satellites and displayed in Figure 7.8a-C. The gabbro and diorites show a calc-alkali trend and the granitic portions are indistinguishable from the Ploumanac'h trend. They plot as in the Streckeisen diagram in the alkali granite and granite fields. Two of Ronas samples qouted from work of Phemister plot in the granodiorite field. The Ronas basic rocks are drawn in the gabbro-diorite and pyroxenite fields. While the basic sample plots in the diorite field.

7.5.4 <u>Sandsting and Bixter Granites Classification Using R1 R2-Diagram.</u>

The De La Roche R1 R2 parameters have been calculated for the Sandsting and Bixter Granites and are displayed in Figure 7.7b-A. The more basic samples plot in the shoshonitic field with more acidic ones grading to the Ploumanac'h trend. The more basic rocks R1 R2-parameters plot in the gabbro-norite, gabbro-diorite and diorite fields, the acidic ones plot in the tonalite and granodiorite fields. No samples plot in the quartzmonzonite and granite fields of the R1 R2 diagram as they do in Streckeisen diagram. In contrast no samples plotted in tonalite and gabbro fields as they do in R1R2-Diagram.

7.5.5 Classification of Granitic Pebbles from Funzie and Rova Head Conglomerates Using the R1R2-Diagram.

The De La Roche R1R2 parameter have been calculated for the granitic pebbles and are displayed in Figure 7.7b-B. The Rova Head plot has a calc-alkaline character while Funzie takes the Ploumanac'h trend. They fall in the granodiorite and granite fields, with one sample from Funzie plotting in the tonalite field.

7.6 Geotectonic Setting of Shetland Granites According to Pitcher Granite Type and Tectonic Environments.

According to Read (1948) there are granites and granites, this means that there is no single origin for granites and furthermore no single path of evolution. **Pitcher (1979)** formalized or proposed a variety of tectonic settings for granitoid rocks (table 7.2) and related batholith emplacement. The different granitoids associated with the contrasted types of orogenic environments are shown on Figure. 7.a and table 7.3.

Pitcher (1983), expanded the earlier classification to include Pacific-type or oceanic island arc, Caledonian-type or post-closure uplift type and omitted tha Alpinotype environment (Figure 7.b).

Pitcher (1987) further has modified his earlier diagrams to show the various sources of granitic rocks in relation to orogenic and anorogenic environments (Figure 7.9) while **Brew (1990)** has modified Pitcher's geotectonic settings classification to avoid some provincial terms (Hercynian etc.), mixed geochemical and tectonic terms (M, I,S and A) and to put a tectonic orientation on the classification rather than a geochemical one (table 7.8)

Pitcher (1982) has suggested at least five types of granites exist, namely 1) M-type which includes the plagio-granite of the oceanic island arcs; 2) an I-
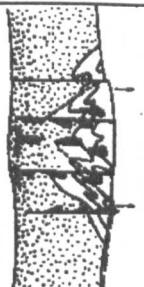
OROGENIC				ANOROGENIC
IOK	**IMT**	**Ss**	**Si Ikk**	**IMA**
W. Pacific-type — Oceanic island Arc	Andinotype — Continental-lip arc, liminal basin	Hercynotype — Oblique continental collision	Caledonian-type — Post-closure uplift	Nigeria-type — Major rifting
Volcanic and volcaniclastic aprons	Sedimentation in fault margined furrows and marginal basins	Sedimentation in fore-thrust and 'A'anatexite,'B' batch-melt	Erosion/flanking molasse basins	Rift infills
Burial metamorphism	Burial metamorphism	Regional, low-pressure metamorphism	Strongly discordant aureoles	Alkali lavas, tuffs, as caldera infill
Basalts	Andesites in great volume	Rarely silicic lavas	Plateau-type basaltic volcanicity	Rifting
Open folding	Spreading-Minimal shortening	Shortening and thickening	Tensional faulting, uplift	Encratonic or post-orogenic rifting
Ocean-ocean subduction	Ocean-continental subduction	Continent-continent "subduction"	Rapid, post-closure uplift	Relatively short-lived
Short-lived	Long-lived	Episodic recycling	Relatively short-lived	Resurgent subsidence cauldrons
Small zoned plutons	Disharmonious (Daly), linear, cauldron batholiths feeding volcanoes	Harmonious (Suess) deep batholiths in early phase	Discordant plutons and distension diapirs	Biotite granite, alkali granite and syenite
Gabbro, M-type granitoids in mature arcs	I-type tonalite, granodiorite, with gabbro	Migmatites, reworked as S-type granites	Biotite granite, aplinitic diorite and gabbro	Partial melting of old mantle, or exhausted lower crust, under anhydrous but F,B-rich conditions
Partial melting of mantle-derived, metamorphosed underplate	Partial melting of mantle-derived underplate; crustal contribution within continental lip	Partial melting of recycled crustal material by metamorphic anatexis; reworking as batch-melts	Partial melting of old, tonalitic lower crust plus mantle contribution	Relatively cool, fluidal magma, rising to near surface with sub-solidus crystallization
Hot, 7°dry; quartz-diorite magma	Hot, "dry" Tonalitic magma rising high into the crust	Hot, "wet" granitic mush freezing at depth, with high-level crystal-bearing anatexis recrystallization	Moderately hot and "dry", evolved, crystal-bearing magma rising to various levels	Decompression on release from deep crustal trap
Subduction energy - transfer of heat by basic magmas		Blanketing by tectonic thickening of redogenic crust	Adiabatic decompression, heat transfer by basic magma	

Figure 7.b **(after Pitcher, 1987)**

Table 7.8 (after David. A. Brew, 1990)

MODIFIED PITCHER (1982) CLASSIFICATION OF GRANITIC BATHOLITHS AND INTRUSIONS, THEIR CHARACTER AND GEOLOGICAL ENVIRONMENTS

	Oceanic Island (OI)	Continental-Margin-I.Up (CL)	Continental-Margin-Uplift (CU)	Continental-Collision (CC)	Anorogenic/Post-orogenic Environments (AP)
Type Name Used in This Report (Abbreviation)					
Distribution	Small, quartz diorite-gabbro composite plutons; sometimes zoned	Great multiple, linear batholiths; arrays of composite calderons at higher levels; migmatitic roots at lower levels	Dispersed, isolated complexes of multiple plutons and sheets; more multiple linear batholiths	Multiple plutons and sheets, less voluminous and more commonly alkalic than CL and CU types	Multiple, centered, cauldron-complexes of relatively small volume
Lithologies	Plagiogranite subordinate to gabbro	Tonalite dominant, but broad compositional spectrum—diorite to monzogranite—with wide SiO2-range major association with gabbro	Granodiorite-granite in narrow range of SiO2; leucocratic monzogranites predominate but granitoids with high biotite content locally important	Granite with high but evolving series with alkalic granite and syenite; highly contrasted felsic-mafic relationship	Biotite granite in evolving series with alkalic granite and syenite, highly contrasted felsic-mafic relationship
Varietal and Accessory Minerals	Hornblende and biotite; pyroxene	Hornblende and biotite; sphene	Biotite predominant; limonite and magnetite	Muscovite and red biotite; limonite, muscovite, garnet; cordierite	Green biotite; alkali amphiboles and pyroxenes in alkalic granites
Inclusions and Screens	Mafic igneous	Dioritic; may be restitic, cognate, or from separate magma	Mixed dioritic and metasedimentary	Metasedimentary rocks dominant	Cognatic; also mafic from separate magma
Chemical Classification (Irvine and Barger, 1971)	Tholeiitic, calc-alkalic	Calc-alkalic	Calc-alkalic	Calc-alkalic'	Calc-alkalic to alkalic to peralkalic
Chemical Classification (Shand, 1969)	Subaluminous to metaluminous	Metaluminous	Metaluminous and peraluminous	Peraluminous to strongly peraluminous	Peraluminous to strongly peraluminous
Typical Initial 87Sr/86Sr Ratios	<0.704	<0.706	>0.705 <.709	>0.708	0.703-0.712
Duration and Kinematic Setting	Short, sustained; pre-kinematic	Very long-duration episodic; syn-kinematic and late kinematic	Short, sustained; post-kinematic	Sustained of moderate duration; syn- and post-kinematic	Short-lived stable environments'
Associated Volcanism	Island arc basalt and andesite	Great volume of andesite and dacite	Sometimes with basalt-andesite rhyolite	Lacking in voluminous volcanic equivalents; may have silicic lavas	Caldera-centered alkalic lavas
Associated Deformation; Metamorphism	Open folding; burial	Vertical movement, open to isoclinal folding; burial to intermediate P and T	Vertical and transcurrent faulting; low P in dissected areas, intermediate T; also retrograde	Lacking in volcanic equivalents; regional folding; intermediate T, low P and T	Doming; rifting; low P and T'
Associated Metallic Mineralization	Au, porphyry Cu	Porphyry Cu, porphyry Mo	Caledonian-type peridotite splits; tensional tectonics; major faulting	Sn and W stern, vein; and replacement	Sn, F, Nb, U, Th
Tectonic Setting Given By Pitcher (1982, Table 1, fig. 7)	Oceanic island arc	Andinotype marginal continental arc	Hercynotype continental collision. Also aseismic ductile shear belts	Hercynotype continental collision. Also aseismic ductile shear belts	Post-orogenic or anorogenic situations
Associated Sedimentation	Volcaniclastic apron	Volcanic fillings of fault-bounded basins and shallow troughs	Rapid erosion results in molasse	Filling of extensional basins	Uplift may produce molasse(?)
Selected Examples	Bougainville, New Ireland (Papua, New Guinea), Cordillera Occidental (Colombia)	Coastal batholith (Peru); great tonalite cliff (SE Alaska, U.S.A. and Canada)	Sierra Nevada (California, U.S.A.); Idaho batholith (Idaho-Montana, U.S.A.)	White Mountains (California, U.S.A.); Ladra and Manaslu batholiths (Nepal)	Bega and New England batholiths (Australia)

(Cordilleran) - type representing the voluminous gabbro-quartz diorite-tonalite assemblages of active continental plate edge; 3) an I-(Caledonian) - type which represents the granodiorite and granite of the immediate post-orogenic uplift regimes; 4) S-type which is the peraluminous granite assemblage of encratonic and continental-collision fold belts; 5) an A-type which includes the alkaline granites of both the stabilised fold belts and the swells and rifts of the cratons. The detailed characteristics of these five types of granite are summarised in table 7.3, and these criteria will now be discussed in relation to the granites of Shetland.

All the five categories of Shetland granites have wide and narrow ranges of SiO_2 content. In the hornblende-bearing granites, granodiorite is predominate in the Graven Complex, in the Spiggie Complex quartzmonzonite and granodiorite is predominant and in the Brae Complex granodiorite and tonalite predominate. The basic minor intrusions are hornblendite, hornblende-diorite (appinite). Common mafic minerals are hornblende, biotite plus epidote and pyroxene in the Spiggie Complex. In hornblende-free granites, characterised by a narrow range of SiO_2 content, monzogranite is the predominant rock and the mafic minerals are biotite and muscovite plus some garnet in theTonga, Breckin and Colla Firth granites. In the Ronas Hill granite and its satellites, there is a narrow range of SiO_2; syenogranite and alkali-granite predominate and stilpnomelane is the mafic mineral. In the Sandsting granite, quartzmonzodiorite and granite predominat. Hornblende-bearing granites, Ronas Hill and its satellites and the Sandsting, all contain magnetite rather than ilmenite as the ore phases, while it is ilmenite in hornblende-free granites. K-feldspar occurs as interstitial and xenomorphic grains in hornblende-bearing granites, but occurs sometimes as megacryst as it is in Spiggie granodiorite and as megacrysts i.e. in most of the hornblende-free granites. Sphene and allanite occur in all hornblende-bearing plutons and only in Skaw among the hornblende-free granites. The hornblende-bearing plutons, Ronas Hill Granite and its satellites normally show small amounts of normative corundum, usually less than 1% while the hornblende-free granites normally show

values usually greater than 1% (appendix). The initial values of the 87Sr/86Sr ratios

are not determined yet for the Shetland granites, so that we cannot judge if they

conflict or are compatible with other results.

The chemical and mineralogical characterstics listed above lead to the conclusion

that the granitic rocks of Shetland should be considered as I-Caledonian type and

some of the hornblende-free granites (except Skaw) including Tonga, Breckin,

Colla Firth and Skerries are S-type granites.

7.7 Shetland granitoids Classification Using "I" and "S" types binary Classification.

The "I" and "S" types granite classification of **Chappell and White (1974)**,

has become perhaps the most widely used in the last 15 years because of its simple

criteria, apparently broad applicability and genetic implications. Chappell and

White suggested this mineralogical and chemical classification (Table 7.1) could be

used to infer an origin for continental orogenic granites; I-types having been

derived by melting of igneous source rocks and S-types by melting of sedimentary

or metasedimentary source rocks.

The criteria of "I" and 'S' types will now be discussed in relation to the Shetland

granitoids. The hornblende-bearing granites to the east of the WBF, the Ronas Hill

granite and its satellites and the Sandsting and Bixter granites have Na2O values

normally > 3.2%; A/CNK<1.1; less than 1% normative corundum; they are

characterised by a broad spectrum of composition from mafic to felsic; all of them

show regular inter-element variation within plutons. The mafic minerals are

hornblende, sphene, biotite, plus pyroxene and epidote in the Spiggie granite. The

accessory mineral apatite exists as small inclusions in biotite. The field relations

indicate that they are massive and generally late in the intrusive sequence. No

evidence for mineral deposits associated with these plutons is available.

The chemical and mineralogical characteristics lead to the conclusion that the

hornblende-bearing granites to east of the WBF, Ronas Hill granite and its satellites

and Sandsting and Bixter are I-type by the criteria of Chappell and White (1974).
Some of the hornblende-free granites, (Tonga, Breckin, Colla Firth and Skerrie),
however, have the characteristic features of S-type granites listed in the discriminant
characteristics of "I" and "S" types (see Table 7.1).

7.8 Rubidium-Hafnium-Tantalum Triangular plot.

An extensive study of the geochemical characteristics of intermediate-acid
intrusive rocks from a range of tectonic settings indicates that in many cases, trace
elements may be used as discriminants for the tectonic setting in which the magma
was intruded (**Pearce et al, 1984**). The close relationship between the
geochemistry and tectonic setting of collision magmatism has been examined and
demonstrated by **Harris et al (1986)** who presented a 4-fold classification of
collision magmatism based on the petrology, field relations and geochronology of
intrusions found in the Himalayan, Alpine and Hercynian collision zones as
follows;

Group-1 intrusions pre-date collision and typically form a high-level calc-alkaline
suite ranging from gabbro to biotite granite, in which diorites, tonalites and
granodiorites are the dominant rock types. Group-1 intrusions are similar in field
relations, mineralogy, and geochemistry to intrusions found in active continental
margins and are thus assumed to be of volcanic-arc origin, equivalent to "I" type
granites.

Goup-11 intrusions are syn-orogenic granites which are commonly known as
leucogranites. They produce conformable or semiconformable intrusions which
often contain pelitic enclaves and are broadly similar to the S-type granite group of

A

Rb/10

+ Graven granodiorite
□ Brae tonalite & granodiorite
○ Aith granite
× Hildsay granite
△ Spiggie granite

VA   WP

OF

Hf   Ta*3

B

Rb/10

+ Skaw granite
□ Tonga granite
○ Brecken granite
× Out Skiries & Coll Firth granites
△ Channerwick granite

VA

WP

OF

Hf   Ta*3

C

Rb/10

+ Ronas Hill granite
□ Marginal granite
○ Net Veined granite
× Muckle Roe granophyre
△ Yementry granite

VA   WP

OF

Hf   Ta*3
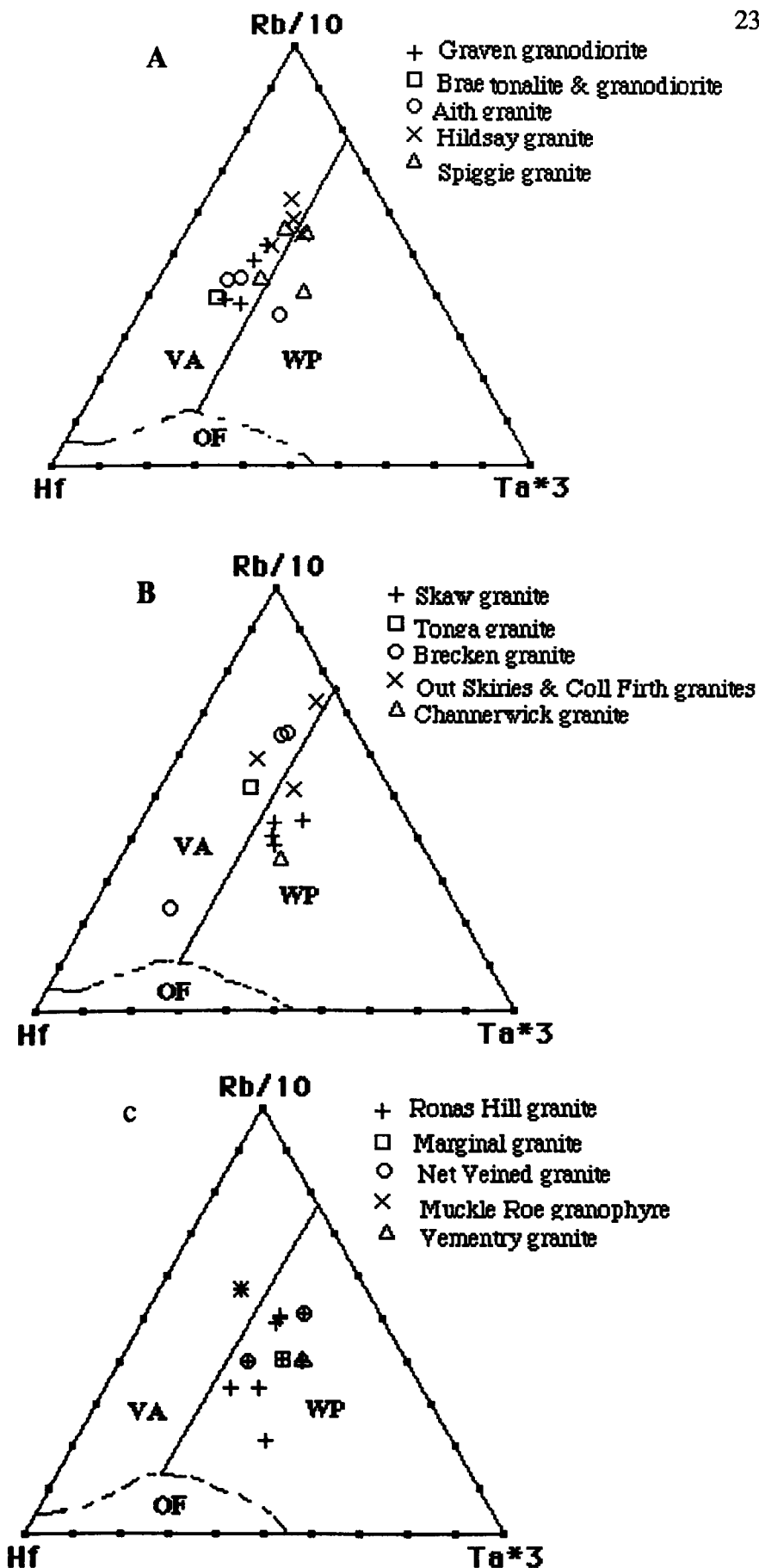
Figure 7.10a Rb-Hf-Ta triangular plots for Shetland granitoids; A) hornblende-bearing granites, B) hornblende-free granites, and C) Ronas Hill and its satellites.

Rb/10

A

+ Bixter granite
□ Sandsting granitoid
O Trondhjemite dykes
X Funzie granitic pebbles

VA

WP

OF

Hf   Ta*3

Rb/30

B

+ Hornblende-bearing granites
□ Hornblende-free granites
O Ronas Hill & its satellites
X Sandsting & Bixter granites
△ Granitic pebbles of Funzie
  and Rova Head conglomerates

Group 2

Group 3

VA

WP

Hf   Ta*3
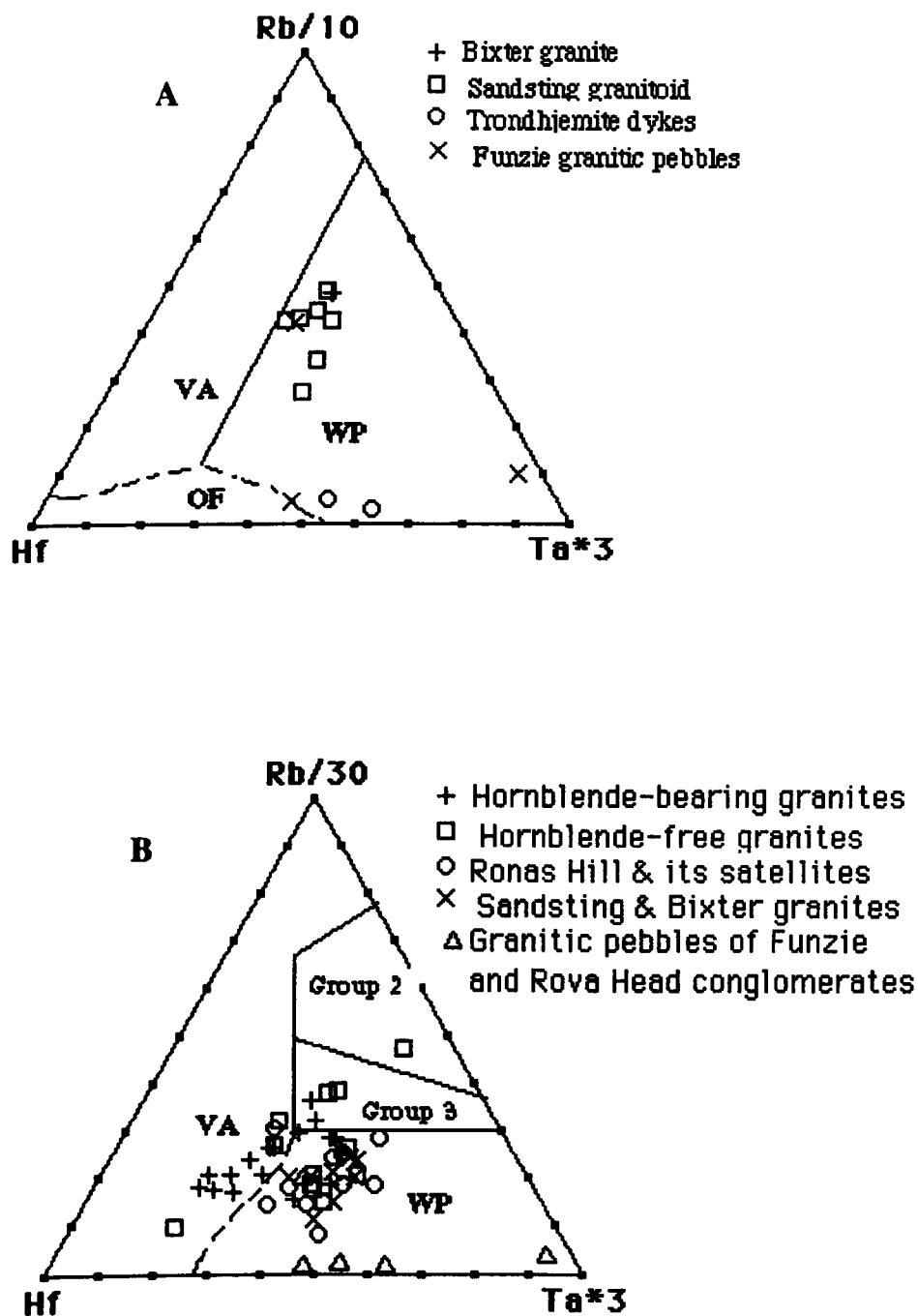
Figure 7.10b Rb-Hf-Ta triangular plots for A) two main granitic groups of Shetland (Sandsting and Bixter, granitic pebbles of Funzie and Rova Head conglomerates), B) plot based on Rb/30 for Shetland granitoids to show their relation to groups 2 and 3.
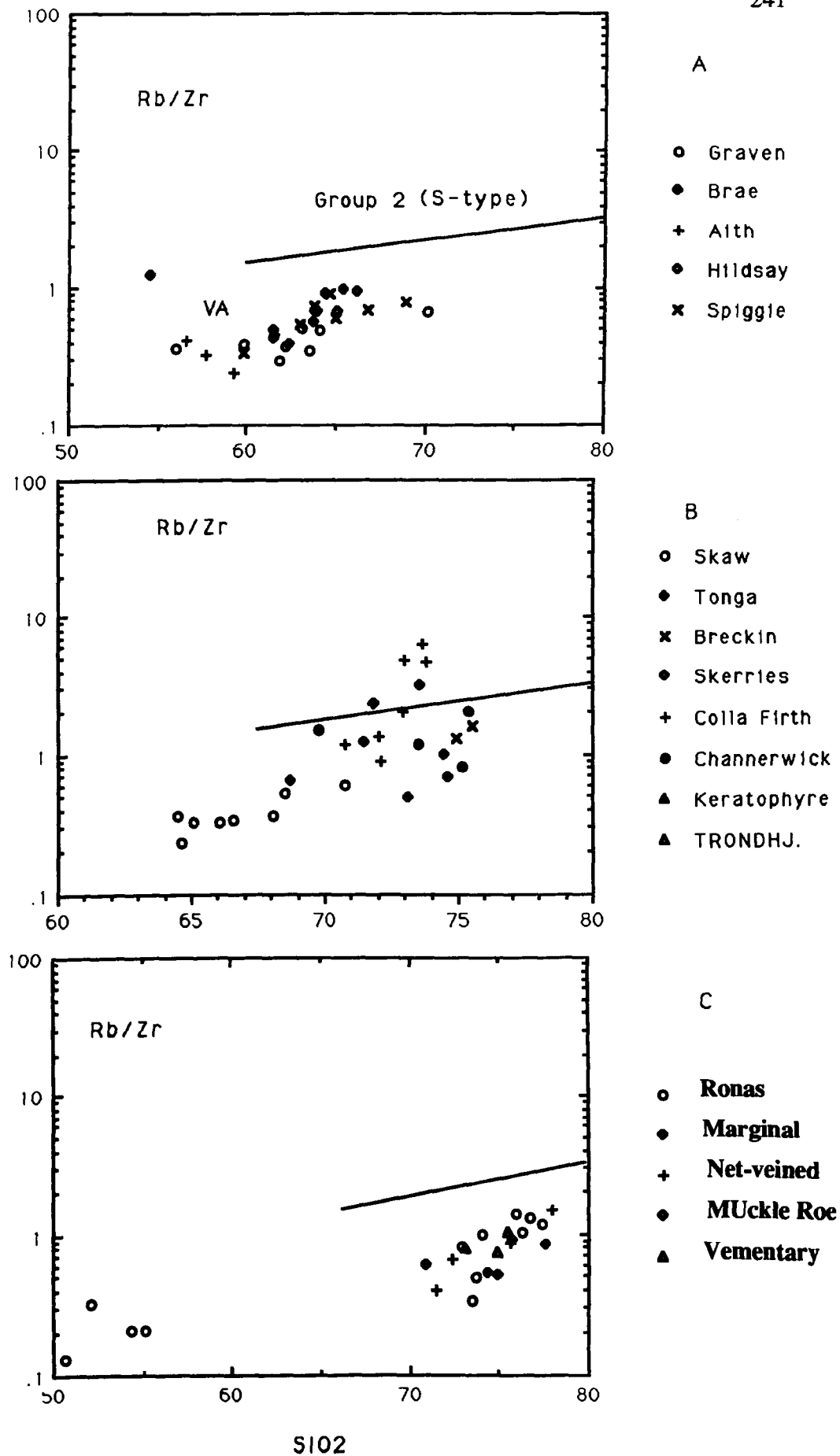
Figure 7.11a Plots of Rb/Zr against SiO2 for A) hornblende-bearing granites, B) hornblende-free granites, and C) Ronas Hill and its satellites.
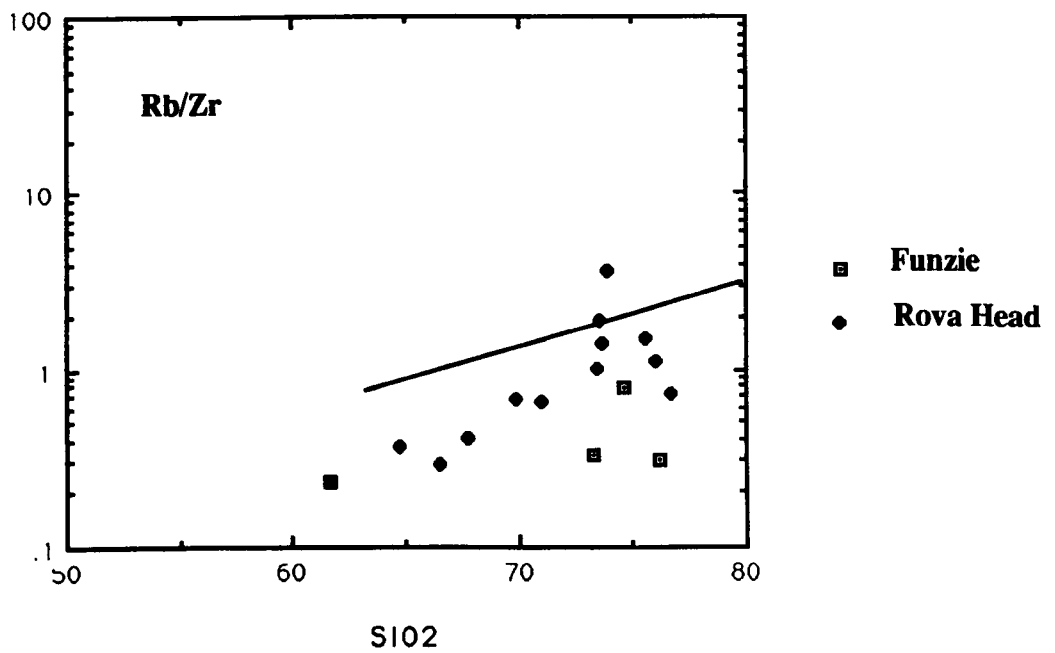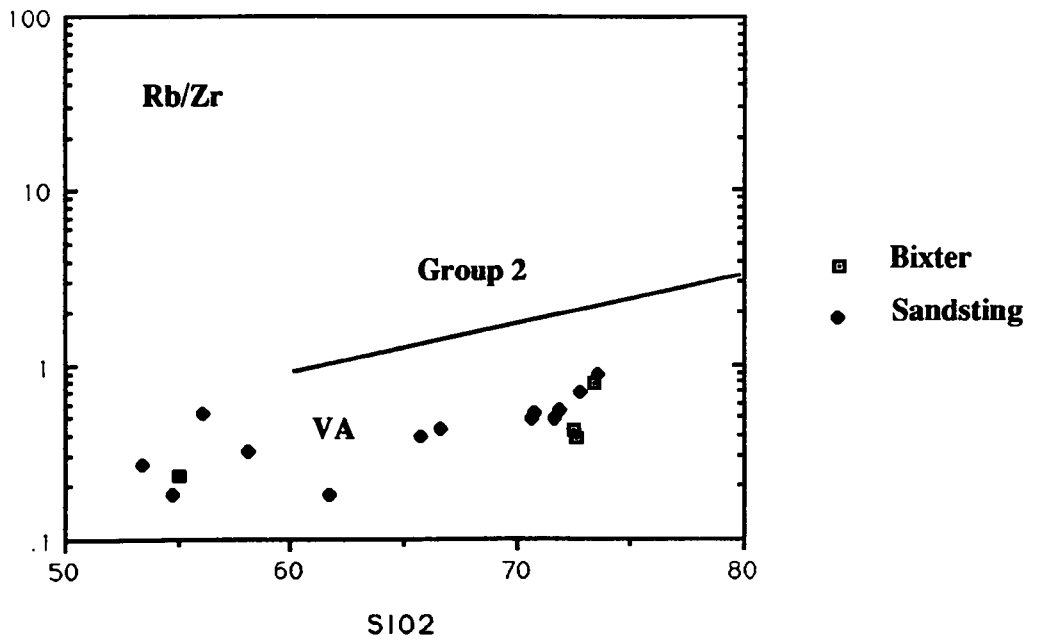
Figure 7.11b Rb/Zr against SiO2 plots for Sandsting and Bixter and granitic pebbles of Funzie and Rova Head conglomerates.

the Australian classification (**Chappell and White, 1974**). Mineralogically they are characterized by the presence of muscovite, with or without biotite and tourmaline is also common. Silica contents of Group-11 intrusions usually exceed 70%. They are emplaced within metamorphic terranes which often include migmatites.

Group-111 intrusions form calc-alkaline suites ranging from gabbro through to granite but are dominantly biotite-hornblende tonalite and granodiorites. They are emplaced as high level-intrusions with sharp cross-cutting contacts and they frequently contain enclaves of intermediate, basic and even ultrabasic plutonic rocks. Despite their petrographic similarities, they differ from Group-1 in having been emplaced after the collision event.

Group-1V intrusions form minor hypabyssal or high-level plutonic suites. In the Alps they are of alkali basaltic and shoshonitic composition and are emplaced in a post-collision environment (**Deutsch, 1980**). In the Hercynides, post-tectonic alkaline granites and syenites of this type were emplaced in the Pyrenees (**Fourcade and Allegre, 1981; Brotzu et al., 1978**) and a Cretaceous alkaline province, including lamprophyric and nepheline syenitic minor intrusions, was developed in western Iberia and the Pyrenees (**Rock, 1982**)

7.8.1 **On the Rb-Hf-Ta triangular plot** (Figure 7.10b-B) of Harris et al 1986 which purports to distinguish the tectonic settings of collision granitoids, the various members of Shetland Granitoids have been plotted. Hornblende-bearing and hornblende-free granites (Figure 7.10A and B) clearly fall in the Volcanic-arc and within plate type fields, while Ronas Hill Granite and its satellites, Sandsting and Bixter and Rova Head granitic pebbles fall in the within plate type field. Trondhjemite dykes and Funzie trondhjemite pebbles plot in within plate field but very close to ocean floor field. The plotting of Shetland granitoids on the Rb/30-Hf-Ta triangle (Figure 7.10b-B) which aims to classify granitoids into the group of intrusions which is discussed above, it shows that a very few samples plot in the

Group ll and Group lll fields and that most of Shetland granitoids plot in within plate and volcanic arc fields respectively.

One of the most effective discriminate, **the Rb/Zr ratios** which separate the syn-collision granites from pre-collision and post-collision types (Harris et al, 1986) in which some samples of the hornblende-free granites (Skirier and Colla Firth) (Figure 7.11a) fall in the syn-collision (field) peraluminous group (*Group 11*) of Harris et al, (1986) which are characterized by high Rb/Zr and low K/Rb ratios. The hornblende-bearing granites, Ronas Hill and its satellites, Sandsting and Bixter and granitic pebbles (Funzie and Rova Head) are plotted in *Group 1 and Group 111* (Figures 7.11a and 7.11b), which are pre-collision and post-collision granites and if these plots are good discriminators, they show that the pre-collision (Tonga, Brecken and Colla Firth) and post-collision (the remainings) setting is indicated as the most plutonic type for Shetland granitoids.

7.9 Shetland Granitoids and their relation to the Trace Elements Classification of Pearce et al. (1984).

On a (Y + Nb)-Rb plot (Pearce et al. 1984) which purports to distinguish different granites from each other, all the Shetland granitoid samples clearly fall in the within plate (WPG) and volcanic arc fields (VAG) (Figures 7.12a and 7.12b) and none in the syn-collision field (Syn-COLG) and that may be because of using fixed value for Nb which is calculated as Ta * 14.4 = Nb; 14.4 representing the natural abundances of Nb element in the nature, because of lack of Nb analytical values and because Ta behaves geochemically like Nb and camouflages it.

7.10 **Na2O** *versus* **K2O** plot (Figure 8.4) shows that only two samples of the Shetland Granitoids falls within the field of S-type granites from the Lachlan fold belt (White and Chappell, 1983); all fall within the ranges of the Lachlan I-types and A-types. Keratophyre, trondhjemite dykes and Funzie trondhjemitic
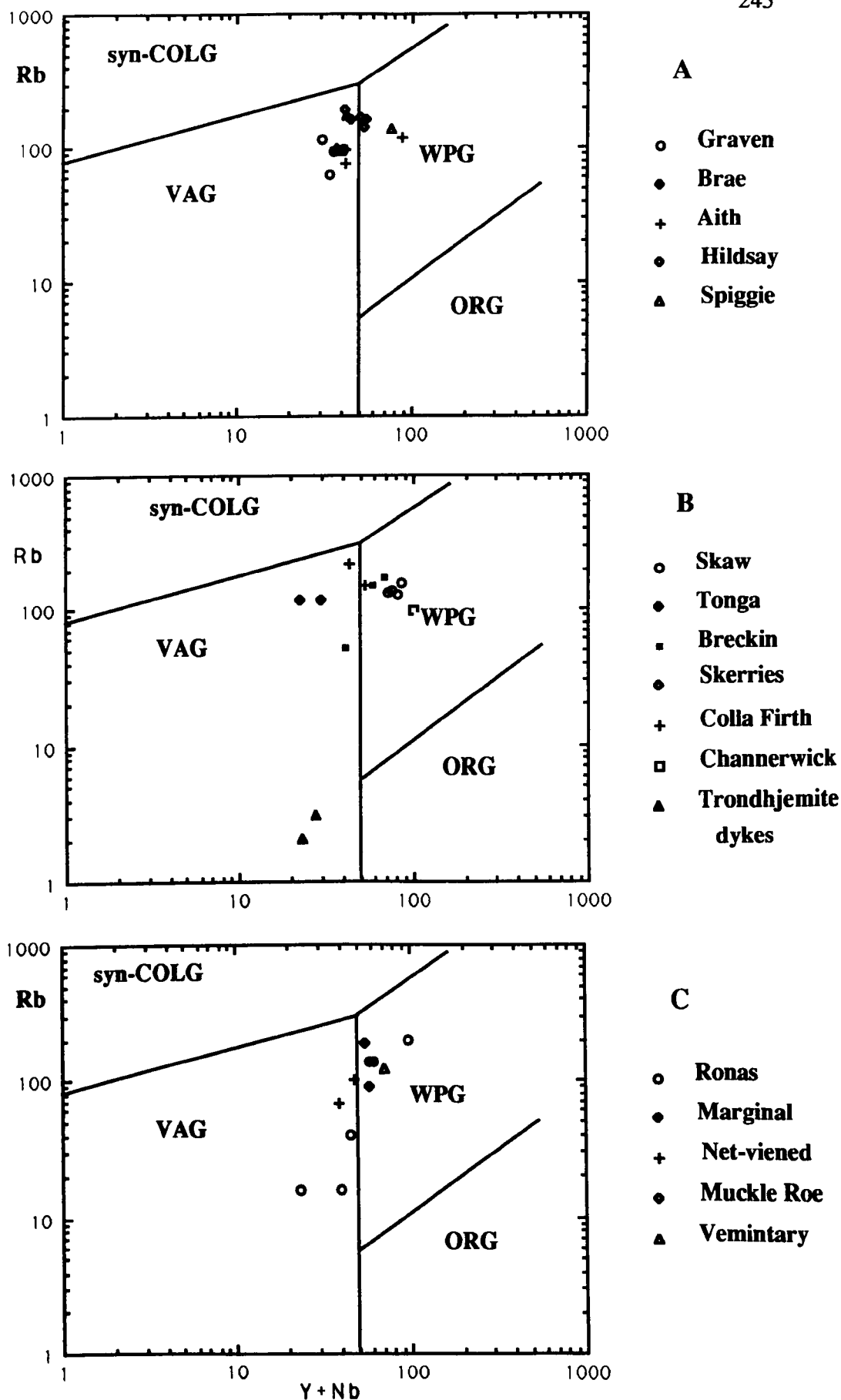
Figure 7.12a Rb versus Y+Nb discriminant diagrams of Shetland granitoids for A) hornblende-bearing granites, B) hornblende-free granites, and C) Ronas Hill granite and its satellites.
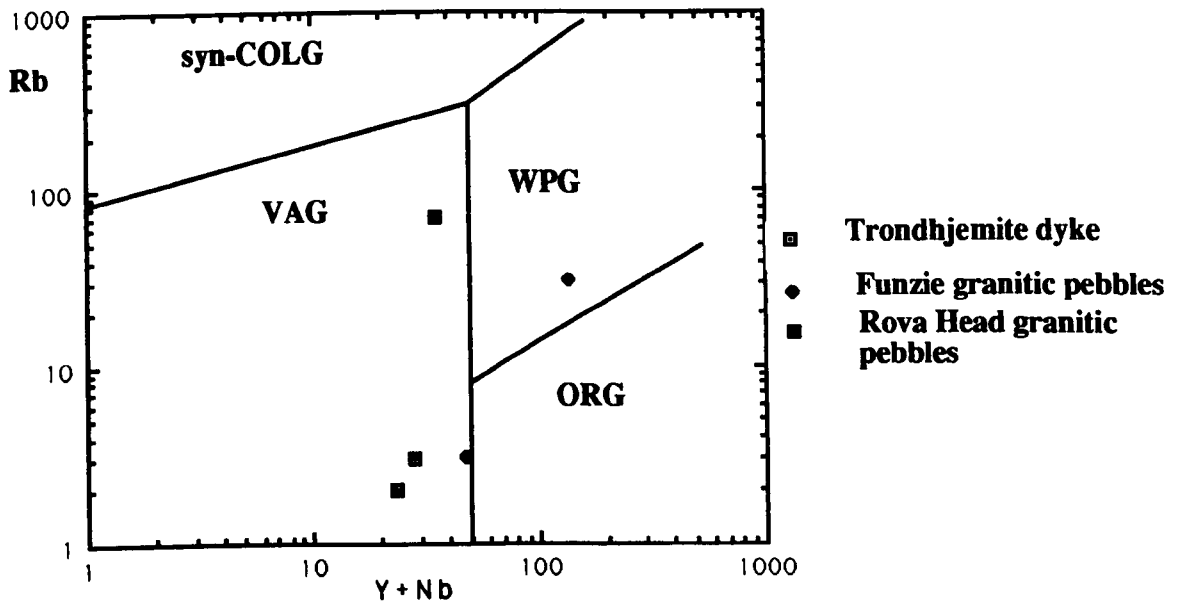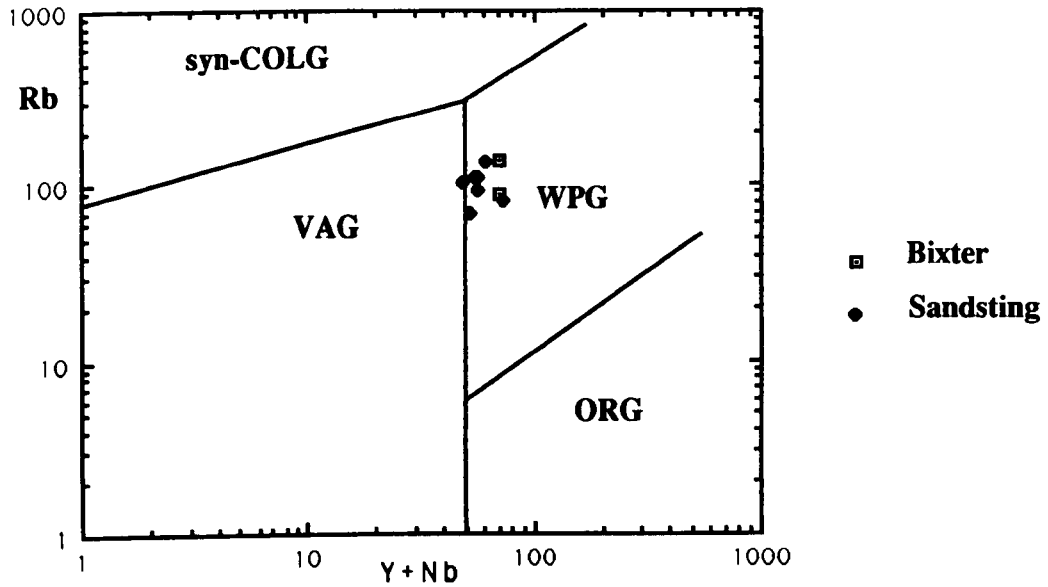
Figure 7.12b Rb versus Y+Nb discriminant diagrams of the Sandsting granitoid and the Bixter granite and granitic pebbles of the Funzie and Rova Head conglomerates..
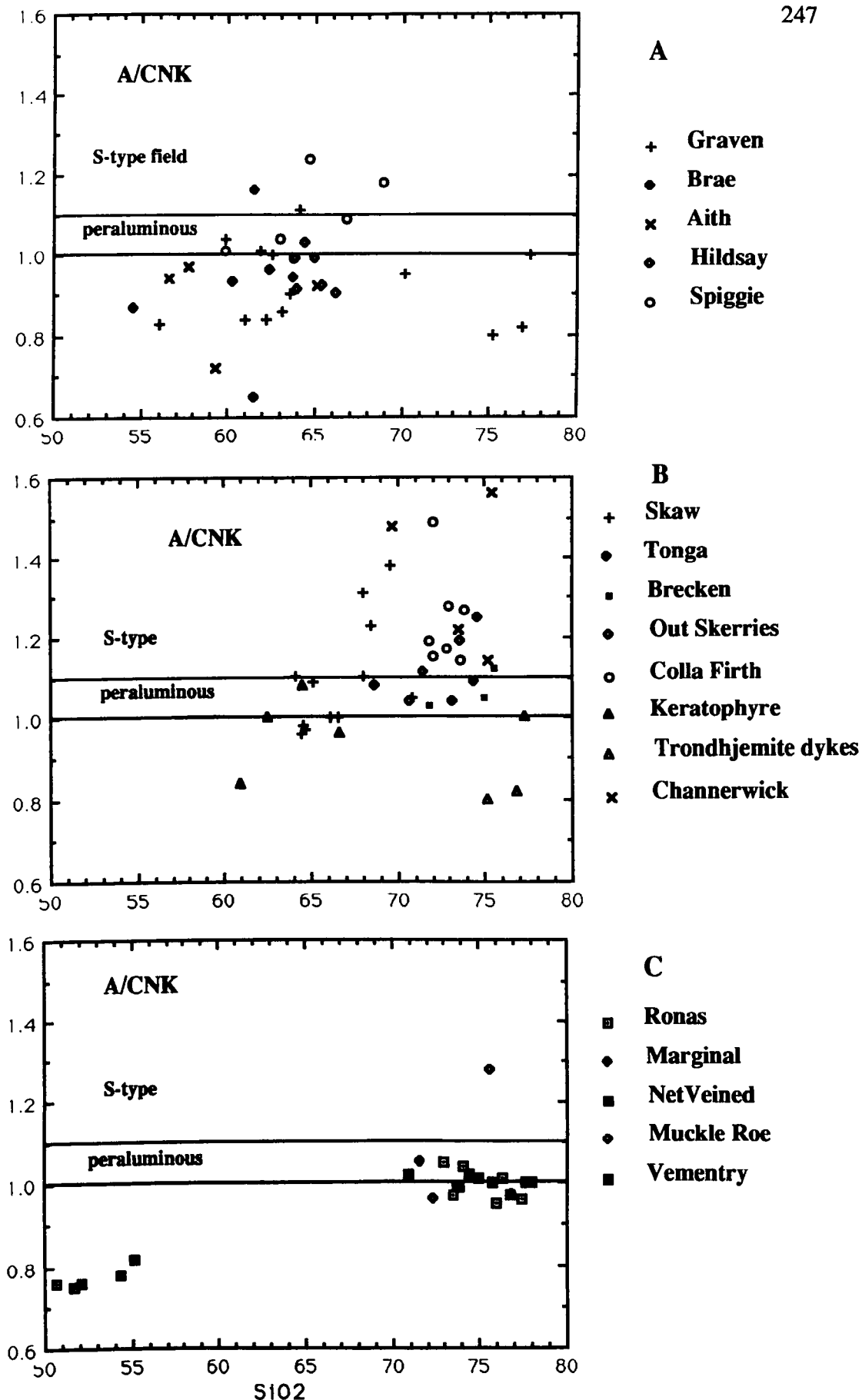
Figure 7.13a Plots of mole Al2O3/(CaO+Na2O+K2O) versus SiO2 for A) hornblende-bearing granites, B) hornblende-free granites, and C) Ronas Hill & its satellites. Data points above 1.0 define peraluminous compositions and above 1.1 S-type granites.
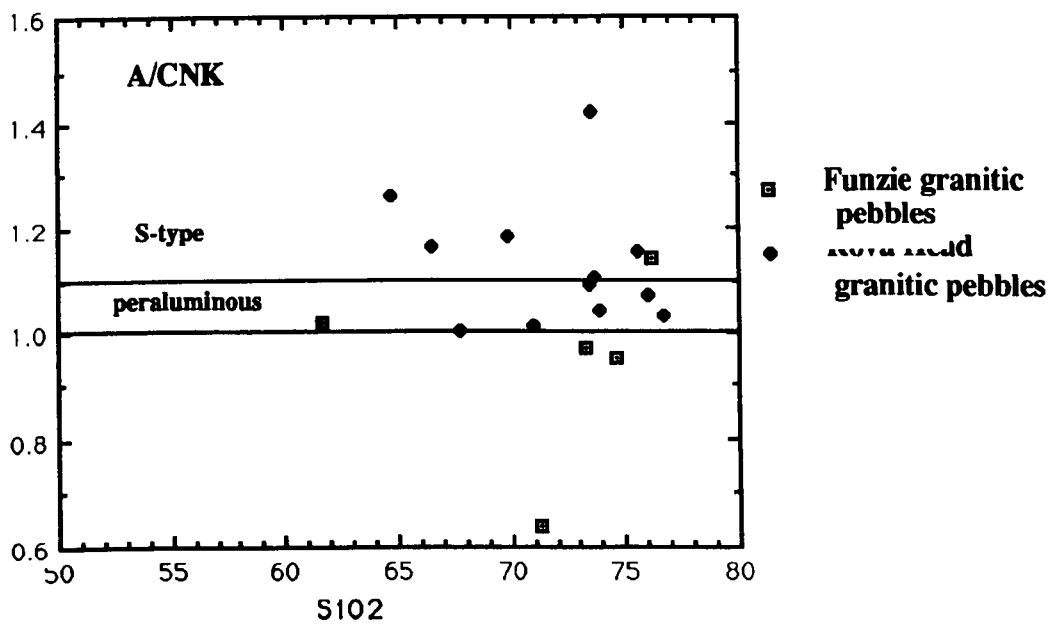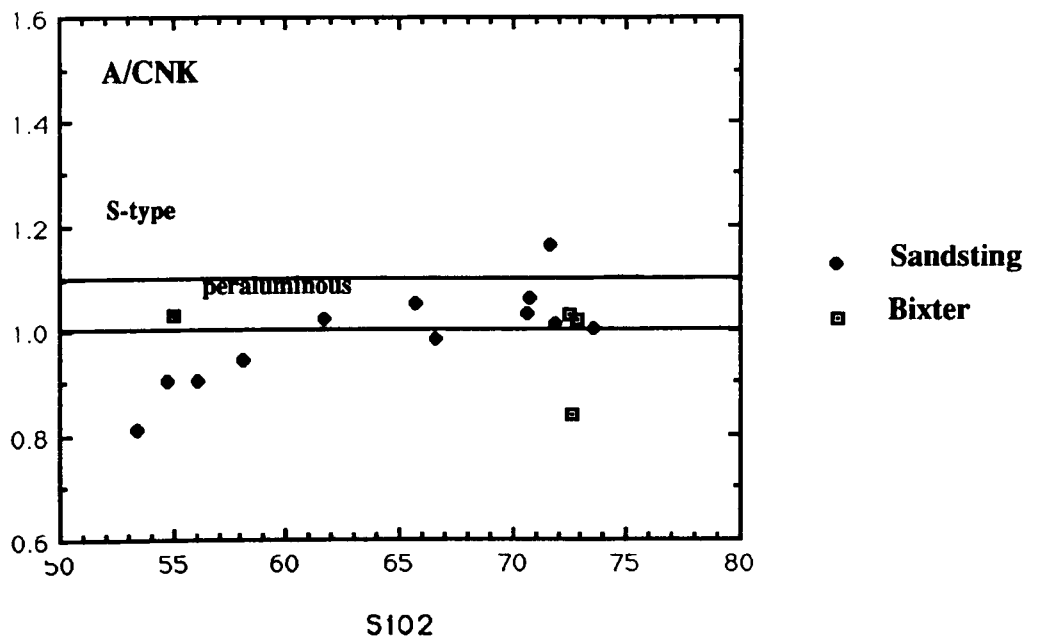
Figure 7.13b Plots of mole Al2O3/(CaO+Na2O+K2O) versus SiO2 for the Sandsting and Bixter granites and granitic pebbles from Funzie and Rova Head conglomerates..

pebbles, all characterised by low K values and plot outside the Lachlan "I" and "S"
types.

7.11 The alkali-alumina balance.

In Figure 7.13a and 7.13b, the ratios of **mol $Al_2O_3/(CaO+Na_2O+K_2O)$**
(hereafter referred to as **A/CNK**), is plotted against SiO_2. Compositions above
the line **A/CNK= 1** are peraluminous. Samples with **A/CNK> 1.1** are S-type
according to the definition of Chappell and White (1974). Note that some samples
of hornblende-bearing granites , Ronas Hill granite and its satellites and Sandsting
and Bixter granites fall in the S-type and peraluminous fields. Most samples of
hornblende-free granites plot in S-type and peraluminous group, Funzie and Rova
Head Conglomerates mostly plot in peraluminous and S-type fields. Several
possible processes can produce peraluminous granites, these include fractional
crystallisation of amphibole **(Cawthorn et al., 1976)**, vapour phase transport of
alkalis **(Luth et al., 1964)** and melting of a peraluminous metasedimentary
protolith **(White and Chappell, 1977)**.

Chapter Eight .

8.1 The Relation of Shetland Granites to the Scottish Granites.

The aim of this chapter is to correlate Shetland granites with Scottish granites as there initial indications of significant similarities in the major and trace elements geochemistry. Trace elements, major elements and REE will be used to elucidate the relationship of Shetland granites to the Scottish granites, and in particular to those which have available data similar to Shetland granites. The geochemical characteristics of Shetland granites have been outlined and interpreted in the preceding sections. Magmatic differentiation has been used as a means of producing suites of igneous rocks which geologically, temporally and spatially are strongly related. Such a comparative study may enhance the geological and geochemical knowledge of the Shetland Caledonian granites and could have implications for a greater understanding of the overall Caledonian geology of Britain.

8.2 Historical Background Of the Caledonian Granites in Britain.

Most acceptable models for the evolution of the British and Irish Caledonian orogeny postulate a cycle lasting for more than 200 Ma. related to the closing of the proto-Atlantic ocean, Iapetus. This ocean existed for much of the Cambrian and Ordovician until suturing occurred at the end of the Silurian to form the Devonian ORS continent (Phillips et al. 1976). The last events in the cycle involved sinistral strike-slip movements (Watson, 1984, McKerrow, 1984) which juxtaposed the American continental plate, of which north-west Ireland and Northern Scotland formed a part, and a younger European plate which now comprises much of south and south-east Ireland, England and Wales.

The late Caledonian sinistral displacements of Britain and North Atlantic
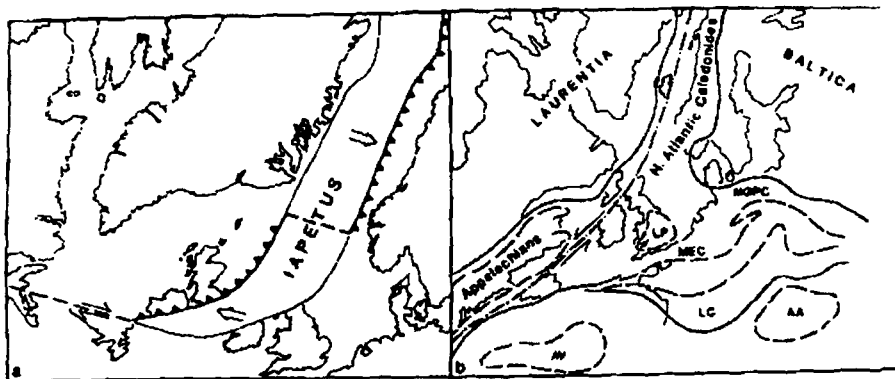
Fig. 1 (a). Two-plate model for the final closure of Iapetus, with dextral transpression in the British sector, after McKerrow [1982, Figure 4]. (b) Late Caledonian reconstruction of the N. Atlantic region, with a hypothetical major sinistral displacement of post-Devonian age restored, after Ziegler [1982]. AA, Austro-Alps; AV, Avalonia; LC, Ligerian Cordillera; LP, London Platform; MEC, Mid-European Caledonides; NGP, North German-Polish Caledonides.
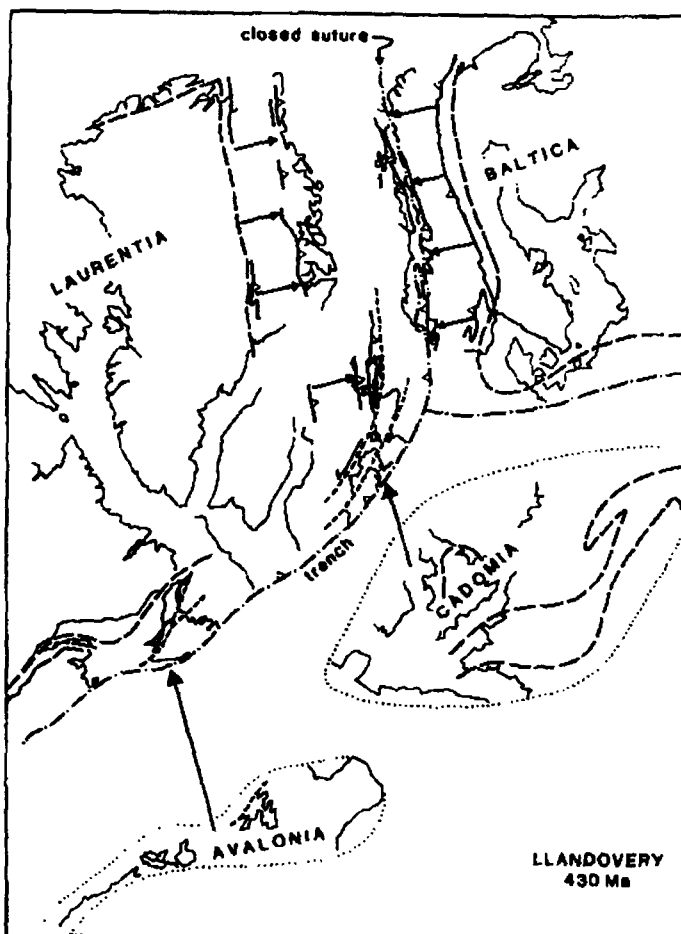
Fig. 4. Reconstruction of the N Atlantic Caledonides in Llandovery time (430 Ma). Collision has already taken place between Baltica and Laurentia in the Greenland-N Scotland/Scandinavian sector, but within-plate deformation is continuing by crustal imbrication (short arrows). Cadomia has yet to collide with N Britain-S Baltica and Avalonia with the Appalachians. These terranes are positioned assuming a 2 cm/year convergence rate (long arrows).

Figure 8.1 Figures 1 and 4 of Soper and Hutton (1984)

Caledonides have adopted a two plate configuration, with a roughly E-W closure direction between Laurentia and Baltica producing the N-S striking Scandinavian and East Greenland Caledonides and inducing dextral srike-slip along the NE-SW oriented British sector of the Iapetus suture (Figure 8.1A &B). The North German-Polish Caledonides are the third arm to the Appalachain-N. Atlantic Caledonide orogen. Recently, Ziegler has proposed that the mid-palaeozoic deformation belts of S. Britain - N. Germany-Poland and also of central Europe were produced by the northward impact of microcontinental fragments onto the southern margin of the already sutured continental mass of the Laurentia-Baltica (Figure 8.1 C). Some ascribe the whole Applachain orogen to a sequence of terrane accretion events in mid-Ordovician through mtd-Devonian time. A N-S collision direction would induce sinistral shear across the British sector of the Iapetus suture.

There have been several attempts to classify the Caledonian intrusive complexes on the basis of age and petrology, and while most workers agree that several major episodes of magmatism took place, there has been some debate about how many subgroups should be identified (Plant et al. 1981). The attempt to unravel the history of magmatism by Read (1961), based on the relationship of the intrusions to the deformation of their host rocks, has dominated later attempts to fit radiometric ages into an evolutionary sequence summarised by Leake (1978), Pankhurst and Southerland (1981) and Plant et al (1980).

Granitic intrusions in Scotland were divided by Read into two groups: *"older and younger granites"*; the older granites comprising pretectonic intrusions and vein complexes, predate the climax of Caledonian metamorphism at 485-500 Ma in the cover rocks of the northern province. These intrusions are relatively small in outcrop area and are generally concentrated (although not exclusively so) in northern Scotland (Figure 8.1); they are dominated by biotite-hornblende gneisses, often with augen texture and adamellite to diorite compositions, and occasional alkaline complexes. There are many associated migmatite complexes (for example, the most northerly Strath Halladale complex of mainland Soctland) in which it is
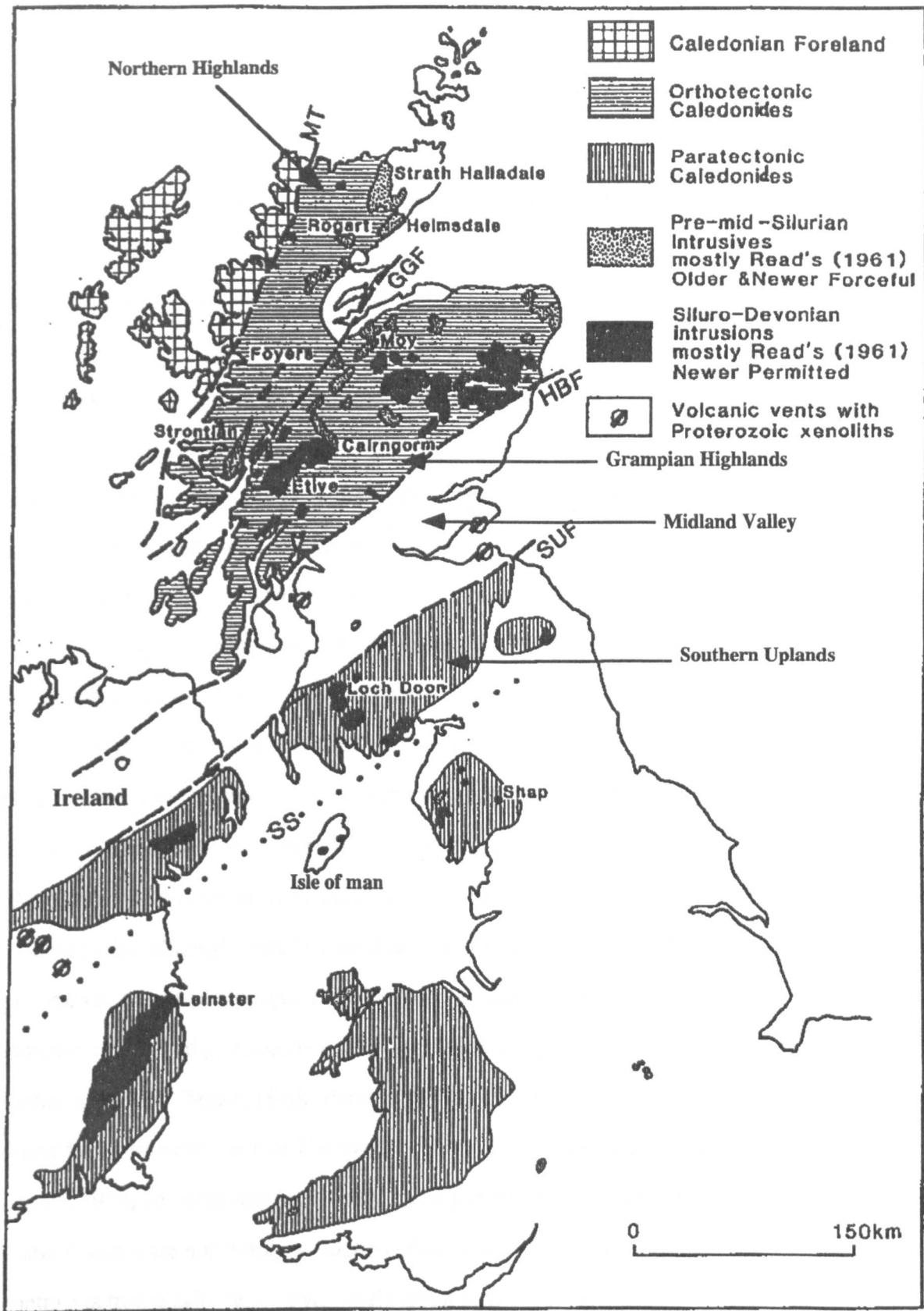
Figure 8.2. The major structural and tectonic sudivisions of the British Caledonides including the main intrusive complexes referred to in the text. MT, Moine Thrust; GGF, Great Glen Fault; HBF, Highland boundary Fault; SUF, Southern Upland Fault; and SS, Solway-Shannon line or Iapetus Suture.

(after Brown et al., 1981).

often difficult to distinguish intrusive contacts between deformed plutons and high grade country rocks.

By far the largest volumes of granite magmas are postmetamorphic *"newer granites"* which were subdivided by Read (1961) into an earlier *"forceful"* suite (the later orogenic granites) around which country rock deformation due to the intrusive processes and occasional contact aureoles may be traced (e.g. Rogart, figure 8.2). Compositions varies from alkaline complexes (such as Loch Borrolan), to tonalite-granodiorite-adamellite complexes emplaced mainly to the north of Great Glen Fault, Reads' other suite is a later *"permitted"* (the post-orogenic granites) group of discordant granites with low pressure aureoles (e.g. the Cairngorm and Etive complexes in figure 8.2) which were emplaced in the period 430-390 Ma, as judged by the available radiometric age data. It is now known that emplacement style does not strictly relate to absolute age as suggested by Read (1961), primarly because their Rb/Sr ratios are too low to obtain reasonable isochron ages or because they have marked inherited zircon components (Pidgeon and Aftalion, 1978; Halliday et al. 1979). They are found mainly in the southwestern and eastern Grampian Highlands. Most of the newer granites vary internally from dioritic to adamellitic or granitic facies, although there is a trend with time from mainly dioritic to more granitic intrusions on average. For example, the forceful Rogart and Foyers intrusions are zoned granodiorites with significant marginal tonalites and cores of biotite adamellite (Soper, 1963; Marston, 1970), whereas some of the permitted discordant intrusions, such as Cairngorm (Harry, 1965) and Shap (Locke and Brown, 1978) are relatively felsic, varying only in the range adamellite to granite. These features are not simply a function of erosion level because intrusions which contrast petrologically (e.g. Foyers and Cairngorm) are known from field evidence to be exposed at similar levels. Thus there appears to be a definite petrological change with time and an intermediate stage is represented by the Loch Doon pluton (Brown et al. 1979a), which is mainly quartzmonzonite at outcrop but has cumulate hypersthene diorite margins and a residual granite core. The implication that crystal

fractionation has occurred is fundamental in studies of magmatic evolution in all such zoned Caledonian plutons.

The newer granites have relatively unmetamorphosed fabrics, and all have radiometric ages younger than about 460 Ma and so were emplaced during or after the closure of Iapetus (Phillips et al. 1976). But whereas most of the forceful intrusions are indeed older, radiometrically, than most of the permitted intrusions, there are exceptions and it is possible (cf. Pankhurst and Southerland, 1981) that changes in the style of emplacement took place at different times in different places in responce to local factors. However, with the exception of some early Ordovician (c. 460 Ma old) intrusions that are concentrated in northeast Scotland, Plant et al. in 1981 have pointed out the two main age groups which are represented among the newer granites of both the northern and southern Caledonide provinces as the following:

1. Pre-410 Ma intrusions of mid-Ordovician and early Silurian age such as the Strontian {435 Ma (Pidgeon and Aftalion, 1978)}, Helmsdale and Foyers {420 and 415 Ma (Brown et al. 1968)} intrusions of figure 8.2.

2. Post-410 Ma Silurian-Devonian intrusions at a time of major calc-alkaline magmatism in Scotland north of the Southern Uplands Fault {392-408 Ma (Halliday et al. 1980)}, Etive {400 Ma (Fleet Brown, 1972)} and Shap {394 Ma (Wadge et al. 1978)} in figure 8.2.

Geophysical and geochemical data show that the boundary between groups 1 and 2 as defined above, is associated with an important change in magma volume, type, evolution, and possibly provenance. Therefore, group 1 intrusions, the older granites of Read (1961) and a pre-410 Ma suite (pre-mid-Silurian) are distinguished in figure 8.2, from the later, post-410 Ma (Silurian-Devonian) group of intrusions.

8.3 The Caledonian Granites: The Shetland and Scottish Geochemical Relationships.

The Caledonian Shetland granites are now, with this study, suffiently well known for a meaningful correlation to be made with the Scottish granites. Plutons from Shetland are well represented in the geochemical sampling which is shown in Appendix 2, Over one hundred and thirty samples representative of most of the lithologies of the plutons, have been used for the geochemical studies. Most of the samples are taken from localities for which detailed petrographic descriptions have previously been published by different authors (e.g. Flinn in Mykura, 1976), and this is the first time a comprehensive study of the trace and major element geochemistry of Shetland granitoids has been made.

8.3.1 Major Elements Geochemistry.

Figure 8.2 shows variation in the plots of total alkali oxides and CaO versus SiO_2 relationships for all Caledonian granitic suites from Scotland and Shetland regions. The plots are very similar and they have a very good correlation, and are alkalic-calcic in the terminology of Peacock (1931) for Shetland and calc-alkalic for Scotland. This is supported by FAM plots for both Scotland & Shetland regions (Figure 8.3) showing the calc-alkaline trend normally associated with orogenic granitoids. The Na_2O-K_2O plots (Figure 8.4), show the similar behaviour of alkalis and CaO with a few samples of Shetland granitoids falling within the field of S-type granites of the Lachlan fold belt (White & Chappell, 1983), while none of the Scotland Caledonian granitoids fall within that field; all fall within the ranges of the Lachlan I- and A-types. However, plutons with S-type characteristics do occur in Shetland, in hornblende-free granites (Brecken, Tonga, Colla Firth and Out Skerries), and in Scotland, in the NE Highlands (but all are older than about 430 Ma, Stephens and Halliday, 1984). In bulk terms, therefore, the late Caledonian granitoids of Scotland and Shetland are largely metalumenous of high-K and calc-
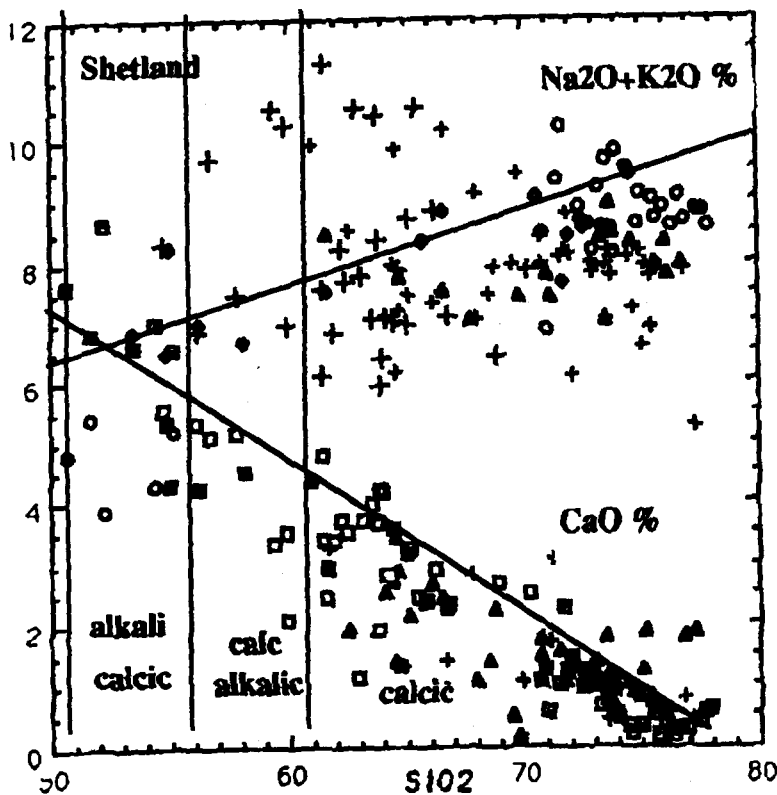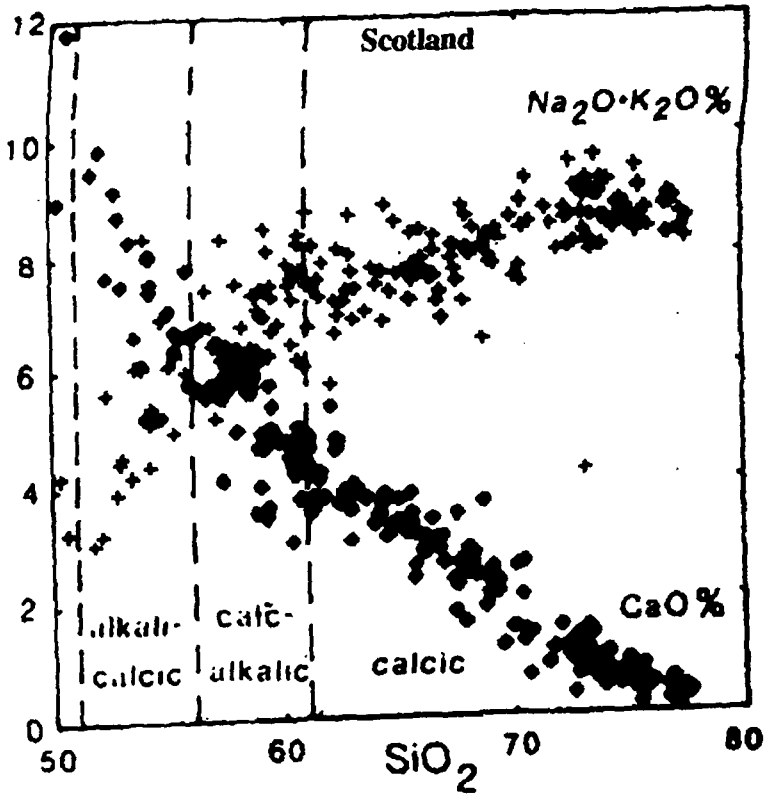
Figure 8.2 Na2O+K2O and CaO versus SiO2 for Shetland and Scotland granit·
For Scotland plots of Na2O (crosses) and CaO (diamonds). All samples
with > 5o% Si O2.

Fe^{tot}(as Fe$_2$O$_3$)

KEY for b,c,d

+ N E Highlands
■ S W Highlands
◆ S Highlands
✳ Midland Valley
✕ Southern Uplands

Scotland

Na$_2$O·K$_2$O

MgO

Fe total (as Fe2O3)

Shetland AFM diagram

□ Hornblende- bearing granite
■ Hornblende - free granites
  Ronas Hill & its satellites
■ Sandsting & Bixter granite
+ Granitic pebbles of Funzie
  Rova Head Conglomerates

Shetland

(Na2O+K2O)

MgO
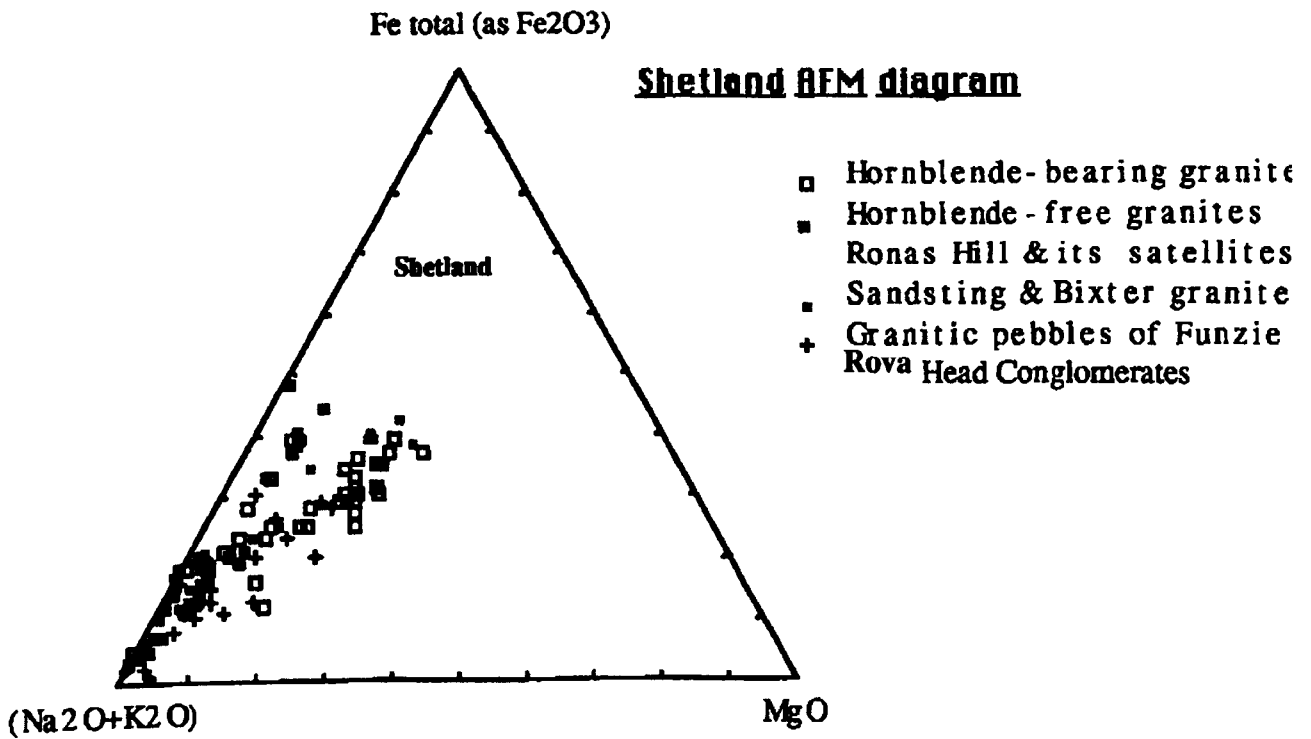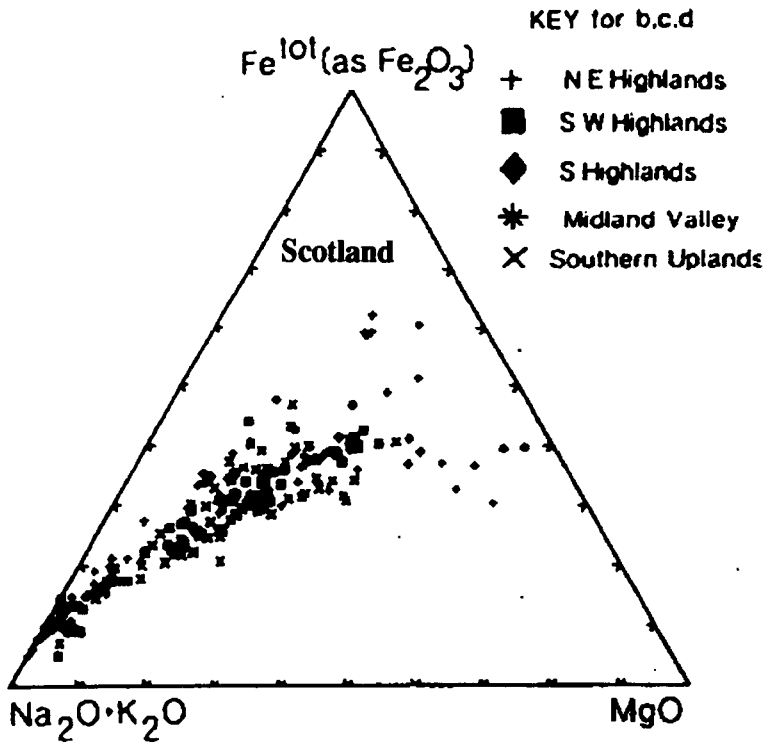
Figure 8.3 AFM plot for Scotland and Shetland showing calc-alkaline
nature of the Caledonian granitoid suites.
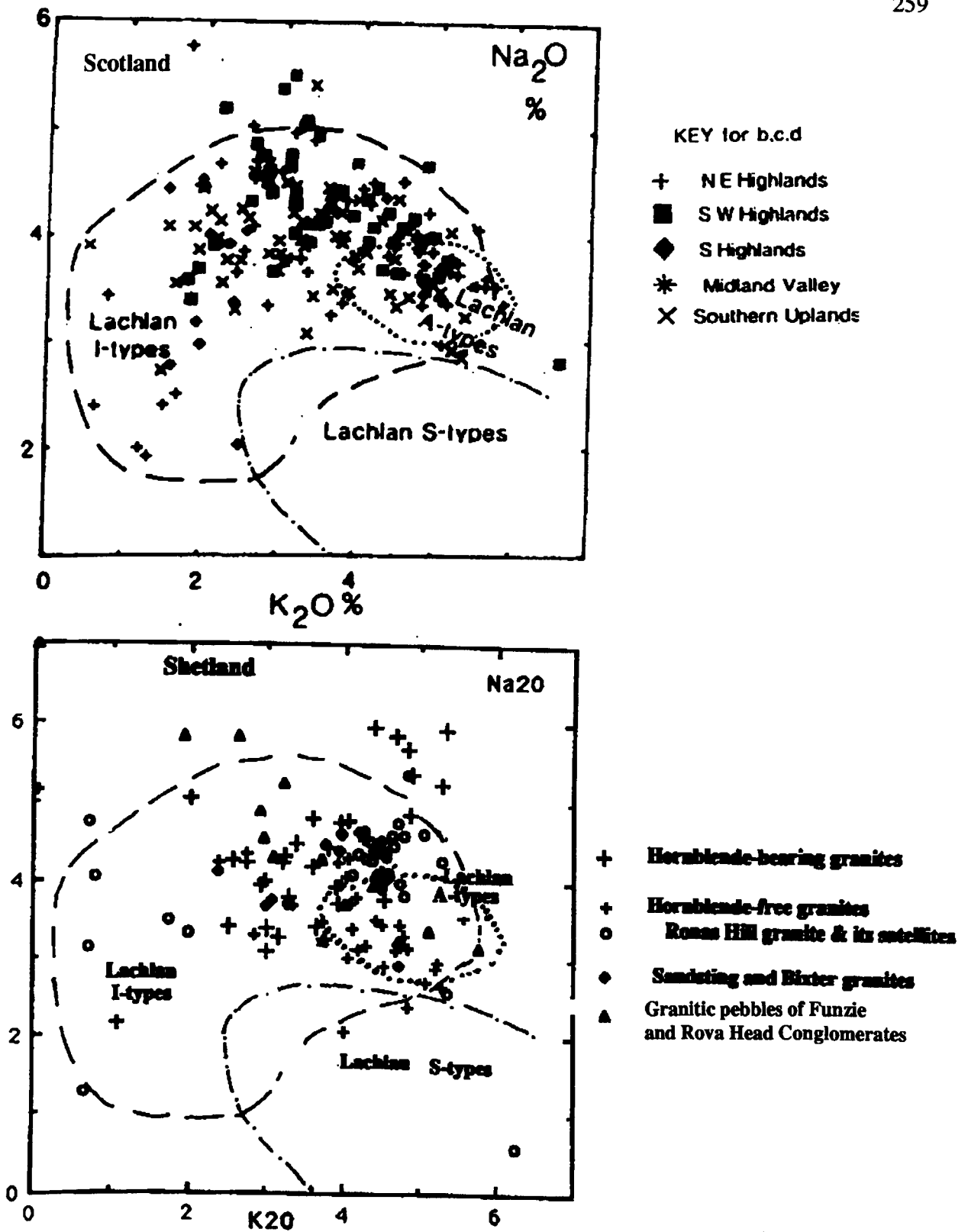
Figure 8.4. Plots Na2O versus K2O for Shetland and Scotland graintoids with fields for I-, S- and A-type granites of the Lachlan fold belt, Australian (White & Chappell, 1983) shown for comparison.
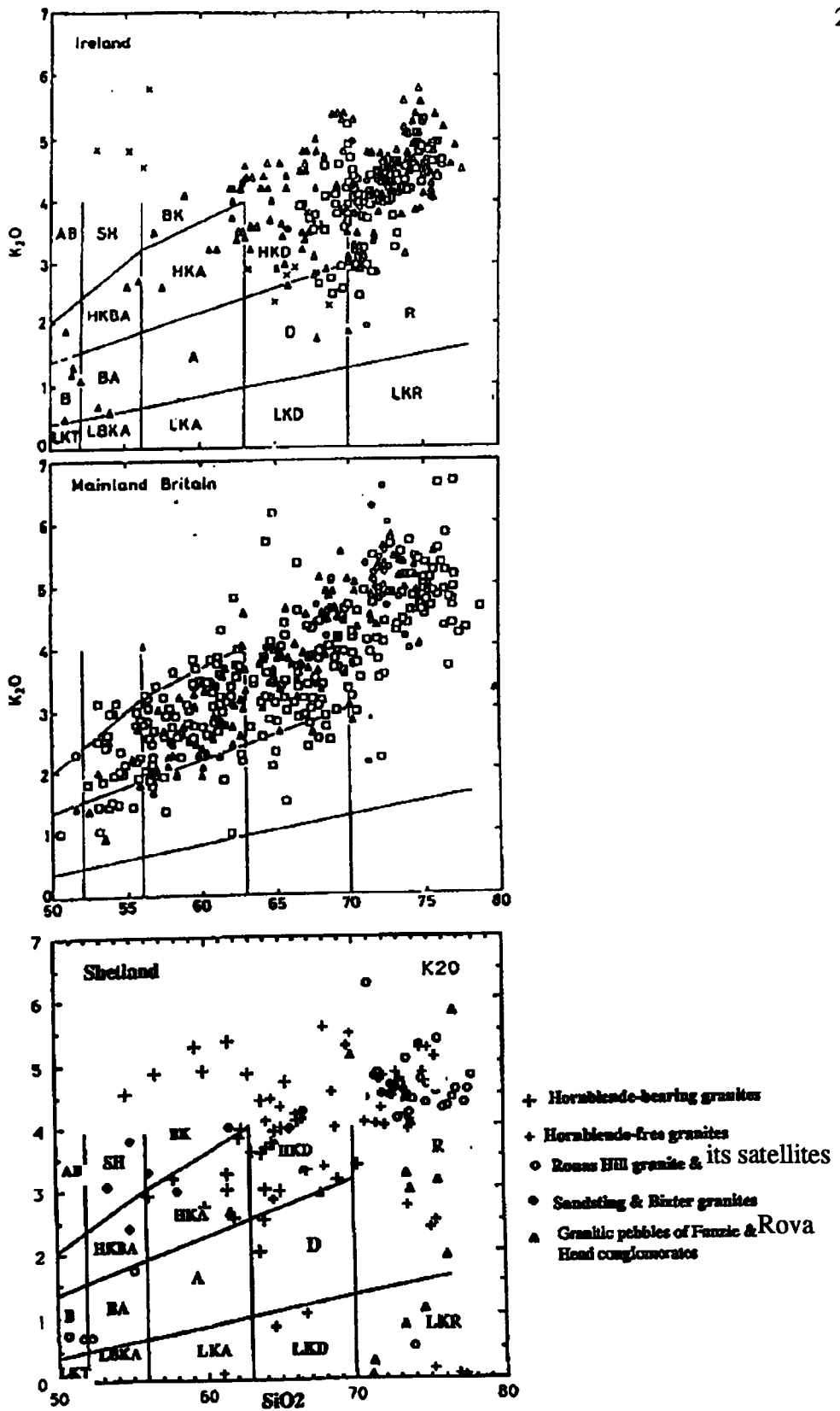
Figure 8.5. K2O versus SiO2 plots with fields of Peccrillo and Taylor (1976). For Ireland, symbols are; Crosses-Newry, triangles-Donegal, squares-Conemara, circles-Leinster. For Soctland, symbols as in Figure 8.7.

alkalic affinities, and have the major oxide compositions of I- and A-type granites. The K2O versus SiO2 plot (Figure 8.5) shows relationships for late granitic suites from Shetland, Scotland and Ireland. The data for the three regions clearly mainly fall in the fields of high-K calc-alkaline magmas as defined by Peccerillo and Taylor (1976) which reflect their common source region. Recent circum-Pacific volcanics display the same K-enrichment where the magmas have passed through thick continental crust (e.g. western U.S.A. and western South America) (Ewart and Le Maitre, 1980).

In Figure 8.6, the ratio of mol Al2O3/(CaO+Na2O+K2O) (hereafter referred to as A/CNK) is plotted against SiO2 for Shetland and correlated with the Scotland and Ireland, an index of peraluminous character. Compositions above the line A/CNK = 1 are peraluminous. Samples with A/CNK > 1.1 are S-type granites according to the definition of Chappell and White (1974). Note the moderately to strongly peraluminous nature of the Older granitoids of Shetland hornblende-free granites samples which include Tonga, Brecken, Colla Firth, Out Skeries and Channerwick granites (except Skaw granite and Keratophyre) tend to plot in the field of S- types, and also some of Rova Head granitic pebbles. The samples from English granites and Leinster (Ireland), all south of the Iapetus suture, tend to plot with high SiO2 and relatively high A/CNK.

The generation of peraluminous granites can be explained by a variety of mechanisms (see Halliday et al., 1980). These include vapour phase transport of alkalis (Luth et al., 1964), fractional crystallisation of amphibole (Cawthorn et al., 1976) and melting of a peraluminous metasedimentary protolith (White and Chappell, 1977). In the British Isles, Leinster (Ireland), Fleet (Southern Uplands), Eskdale (Lake District), Foxdale (Isle of Man) and Weardale (English Pennines) are all highly peraluminous (Stephens and Halliday, 1984). Those which have been analysed have high $\partial^{18}O$ (> 10 % , Harmon and Halliday, 1980). All occur within thick geosynclinal prisms of Palaeozoic sediment at low metamorphic grade which had not suffered a previous orogeny. In also being compositionally
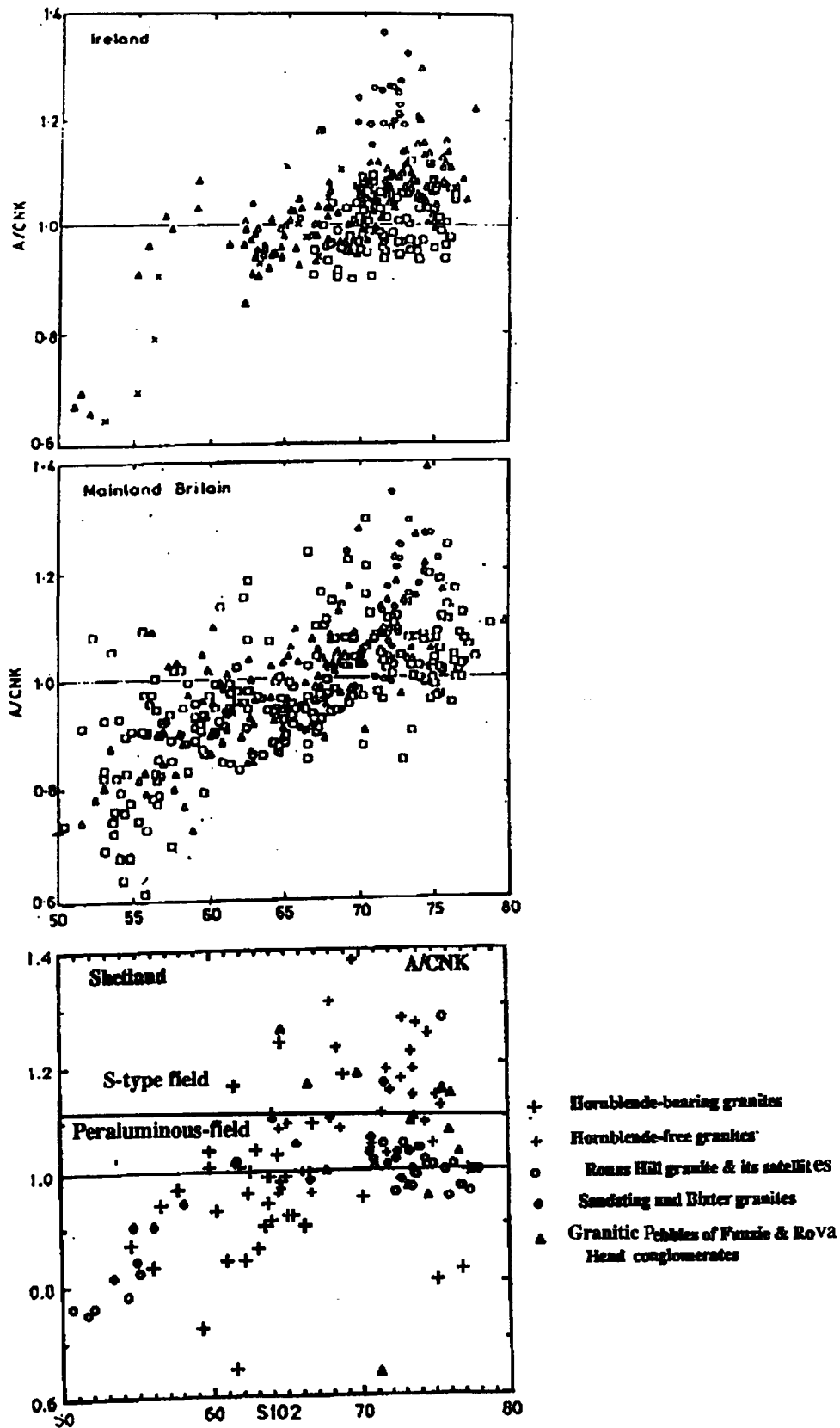
Figure 8.6. Plots of mol Al2O3/(CaO+Na2O+K2O) versus SiO2. Data points above horizontal line define peraluminous compositions. Symbols as in Figure 8.7. (Scotland and Ireland after Halliday & Stephens, 1984).

restricted, these granites fulfil the S-type definition of Chappell and White (1974) with the exception of their K/Na low ratio.

Stephens and Halliday (1984), when they discussed the total alkalis versus SiO2, pointed out that the Caledonian granites all have high Na at a given K concentration compared with the Variscan granites (Hall, 1971) and compared with the Caledonian granites of the Lachlan fold belt Australia (Chappell and White, 1974). White and Chappell (1977) explain the low Na in S-type granites as owing to removal of alkalis by seawater during diagenesis of sedimentary protoliths.

In Figure 8.7 are shown the total alkalis versus SiO2 plot for the granitic suites from Ireland, Scotland and Shetland. From this, it is apparent that most of Caledonian granitoids of Britain including Shetland and Ireland largely plot in the alkali field of Kuno which indicates the specific feature of high alkali content of Shetland, Scotland and Ireland granitoids. All three diagrams of the alkali plots show a positive trend with increasing SiO2. In short, even Caledonian granites that in other respects appear to be S-types, for example hornblende-free granites in Shetland, and those in Scotland which are mainly found to the south of the Iapetus suture (Stephens and Halliday,1984), are not depleted in alkalis relative to SiO2 and are not depleted in Na2O relative to K2O.

With respect to the high Na feature of the Caledonian granites, Hall (1967) attributed the high Na (normative albite) content of the Caledonian granites to melting at higher H2O pressures. He cited as supporting evidence the apparent relationship between high normative albite and association with appinites (hydrous mafic intrusions).

Stephens and Halliday (1984) introduced an alternative explanation, which should be considered, that the British Isles is a high alkali, low K/Na province. Supporting evidence for this comes from the following:

1. Appinites (probably volatile emplaced cumulates related to the granite genesis) are also alkali rich (Wright and Bowes, 1979), the alkali enrichment is therefore not due to fractional crystallisation.
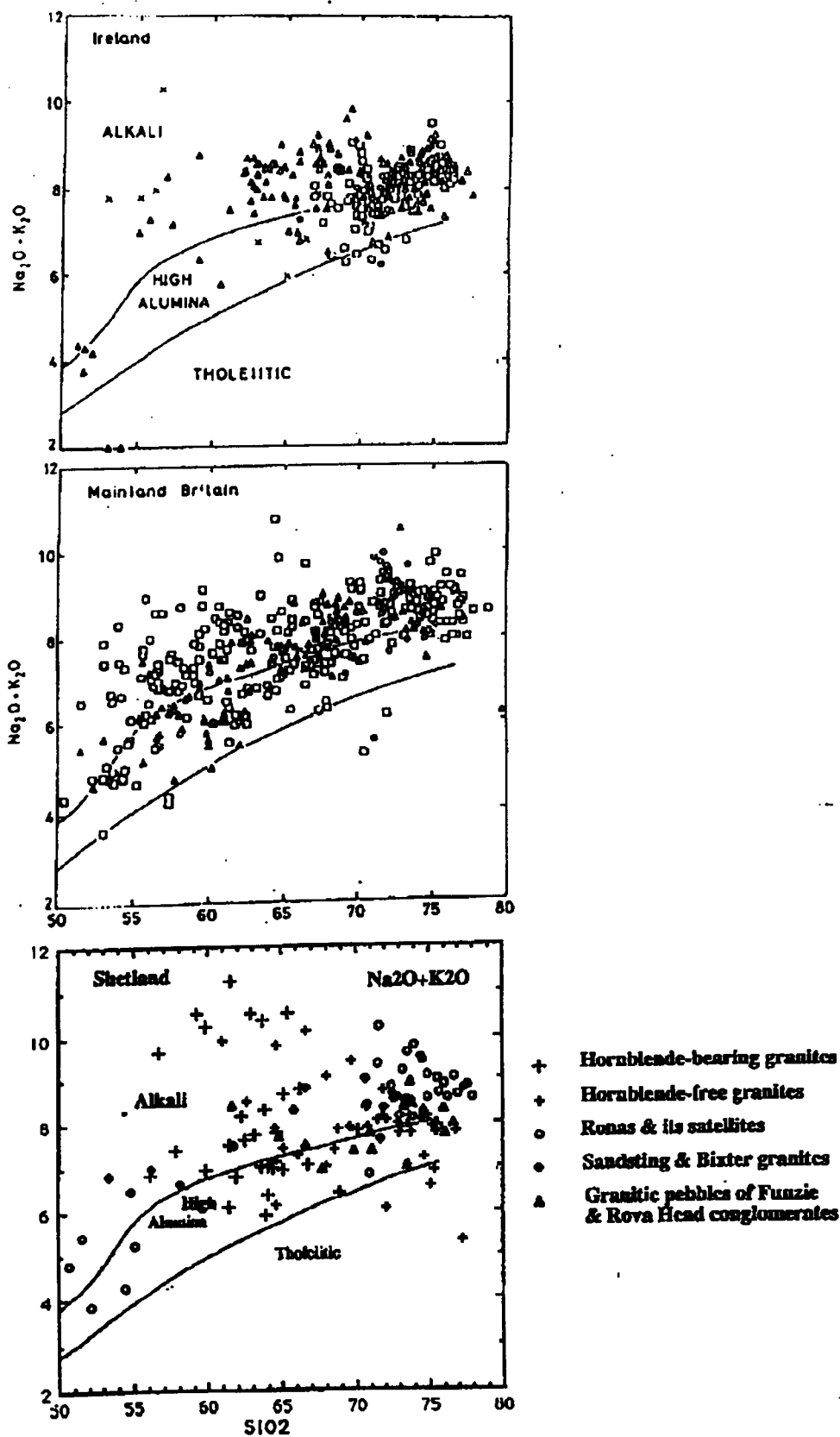
Figure 8.7. Plots of total alkalis versus SiO2 with fields of Kuno (1966). For Scotland and Shetland granitoids, symbols are circles-England, triangles-Southern Uplands and Midland Valley, squares Highlands. (Scotland and Ireland after Halliday & Stephens).

2. Dalradian pelites have relatively low K2O/Na2O of 2.0 (Senior and Leake, 1978), compared with the average shale values of 3.5 (Krauskopf, 1967, p.639).

3. The oldest rocks in the British Isles, the Lewisian Complex, exhibit extreme depletion in K and this would be expected to be carried on in sedimentary detritus to yield a Caledonian crust that also had low K/Na unless the K that had been lost during granulite facies metamorphism of the Lewisian was also recycled in the British Isles crust.

A third explanation for the high alkali (both K and Na) content is involvement of metasomatising fluids in the generation of the granites. The most striking argument for this is the chemistry of the Shap granite in the Lake District of northern England which is a high K granite with I-type mineralogy, but high $\partial^{18}O$ indicating the involvement of metasomatism (Halliday and Stephens, 1984).

8.3.2 Trace Element Geochemistry.

The Scottish Caledonian granites define a chemical province characterized by high Na, Ba and Sr abundances, particularly towards the north and west where they also have higher Zn, REEs and La/Y and lower Rb and Th (Stephens and Halliday, 1984). Halliday and Stephens (1984) show the most remarkable variations, particularly in relation to major oxide parameters and to trace elements of Sr and Ba Harker plots. A Sr versus SiO2 plot (Figure 8.8) shows a distinct divergence or separation at about 65% SiO2 between the Shetland hornblende-bearing granites and those of hornblende-free granites, Ronas Hill and its satellites, Sandsting and Bixter and granitic pebbles of Funzie and Rova Head conglomerates. Stephens and Halliday (1984) have pointed to the divergence at low SiO2 (Figure 8.8) between granitoids of the SW Highlands and those of the Midland Valley, Southern Uplands and Southern Highlands . The granitoids of Shetland and the SW Highlands (as stated by Stephens and Halliday) are markedly enriched in Sr, more than three times that of the Lachlan fold belt at the same SiO2 level. The whole province, in fact, is Sr-rich compared with the Lachlan fold belt and granitoids in
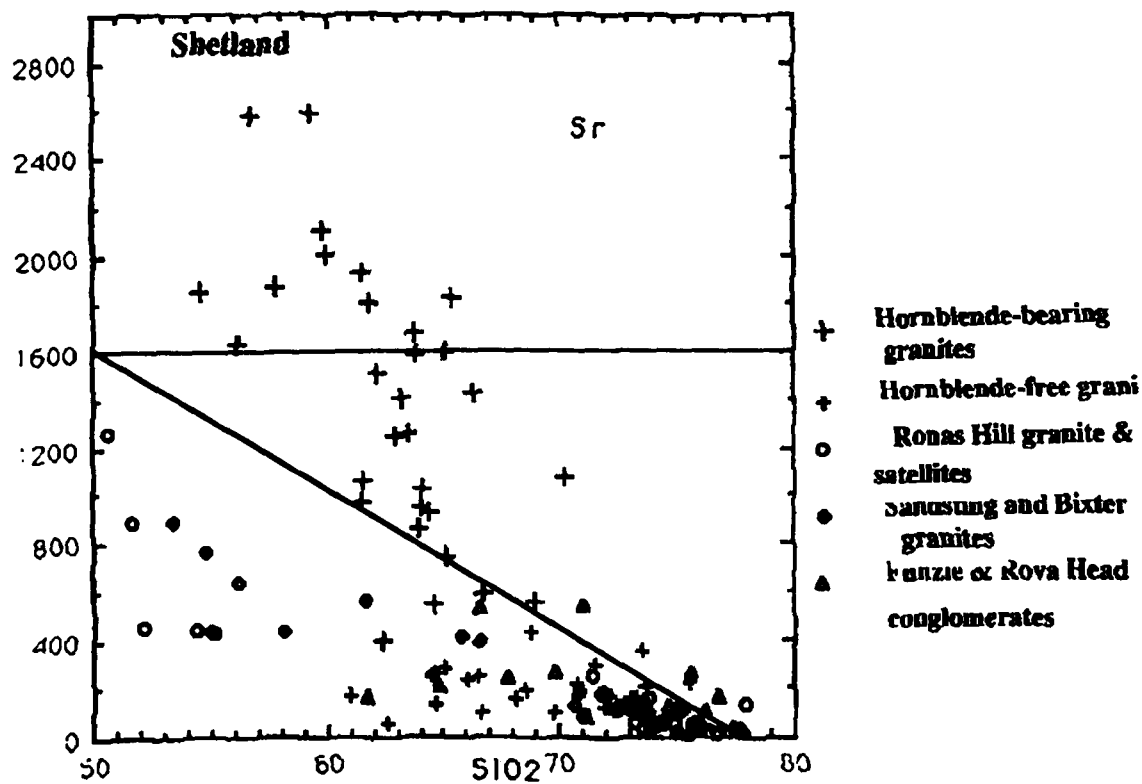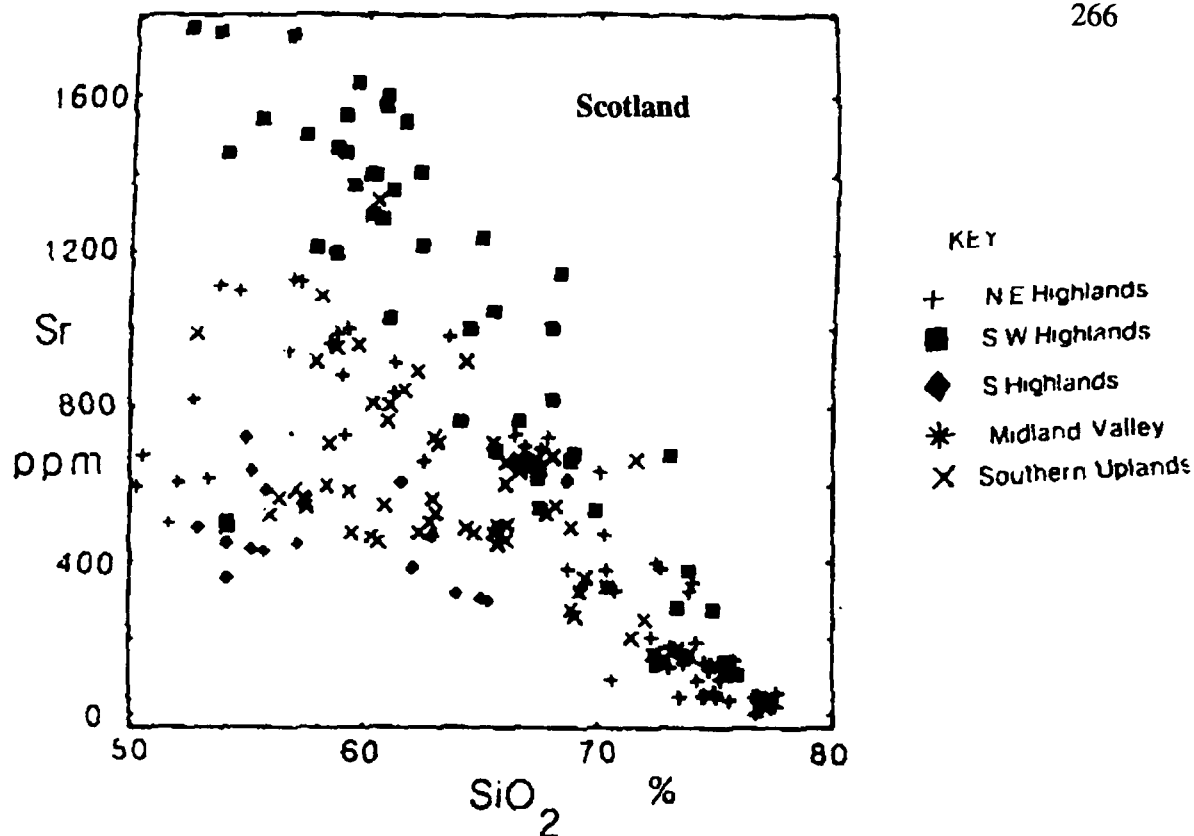
Figure 8.8 plots of Sr versus SiO2 for Scotland and Shetland granitoids.
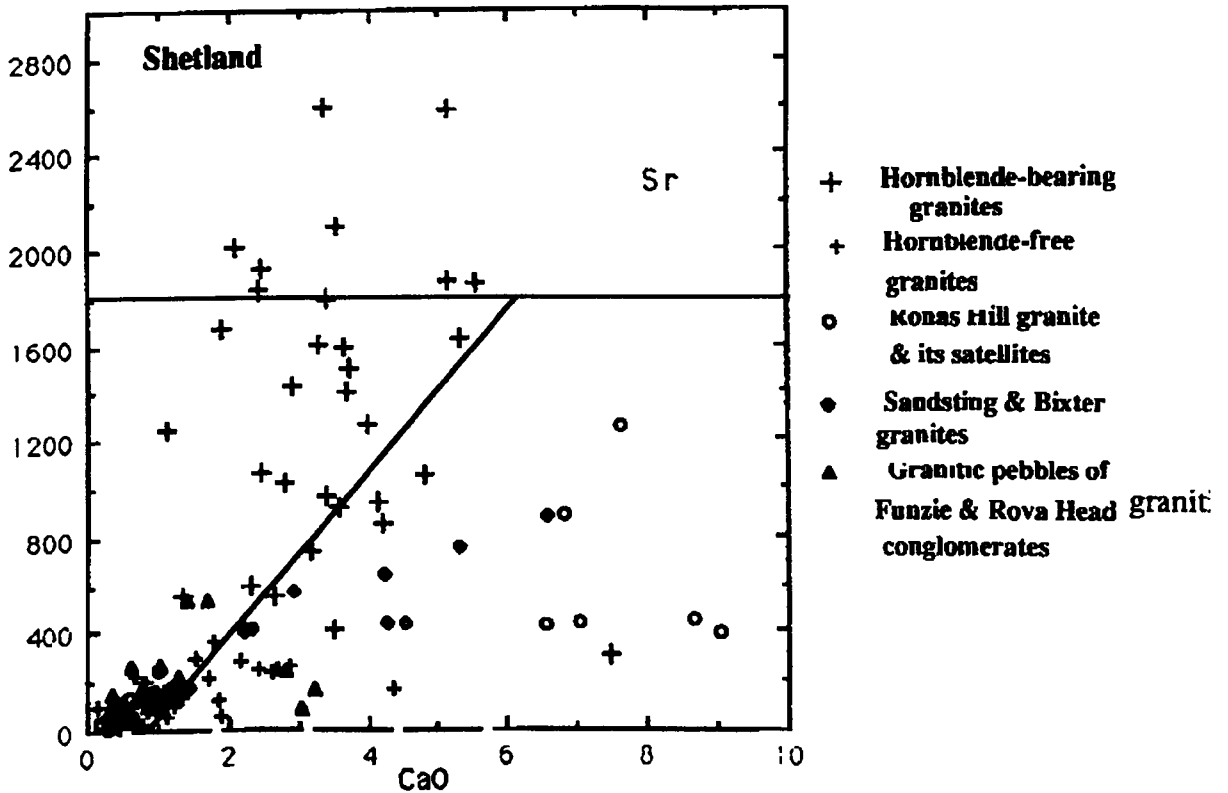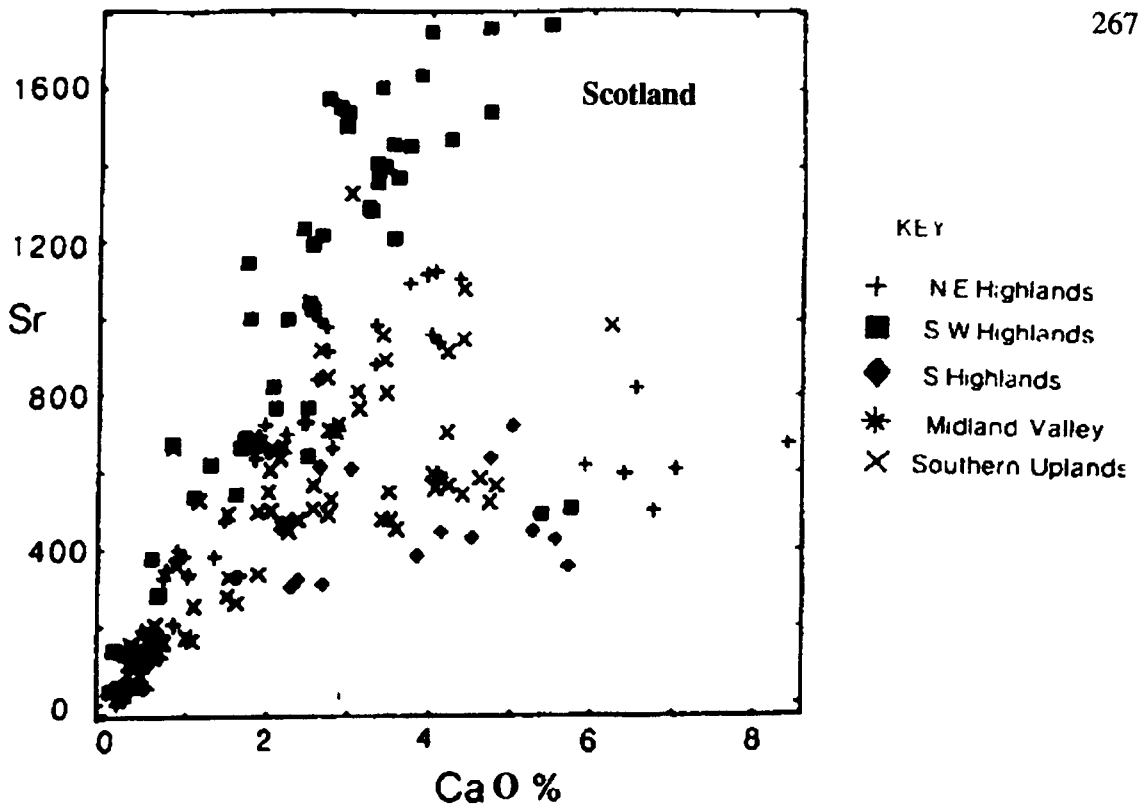
Figure 8.10 plots of Sr versus SiO2 for Scotland and Shetland granitoids.
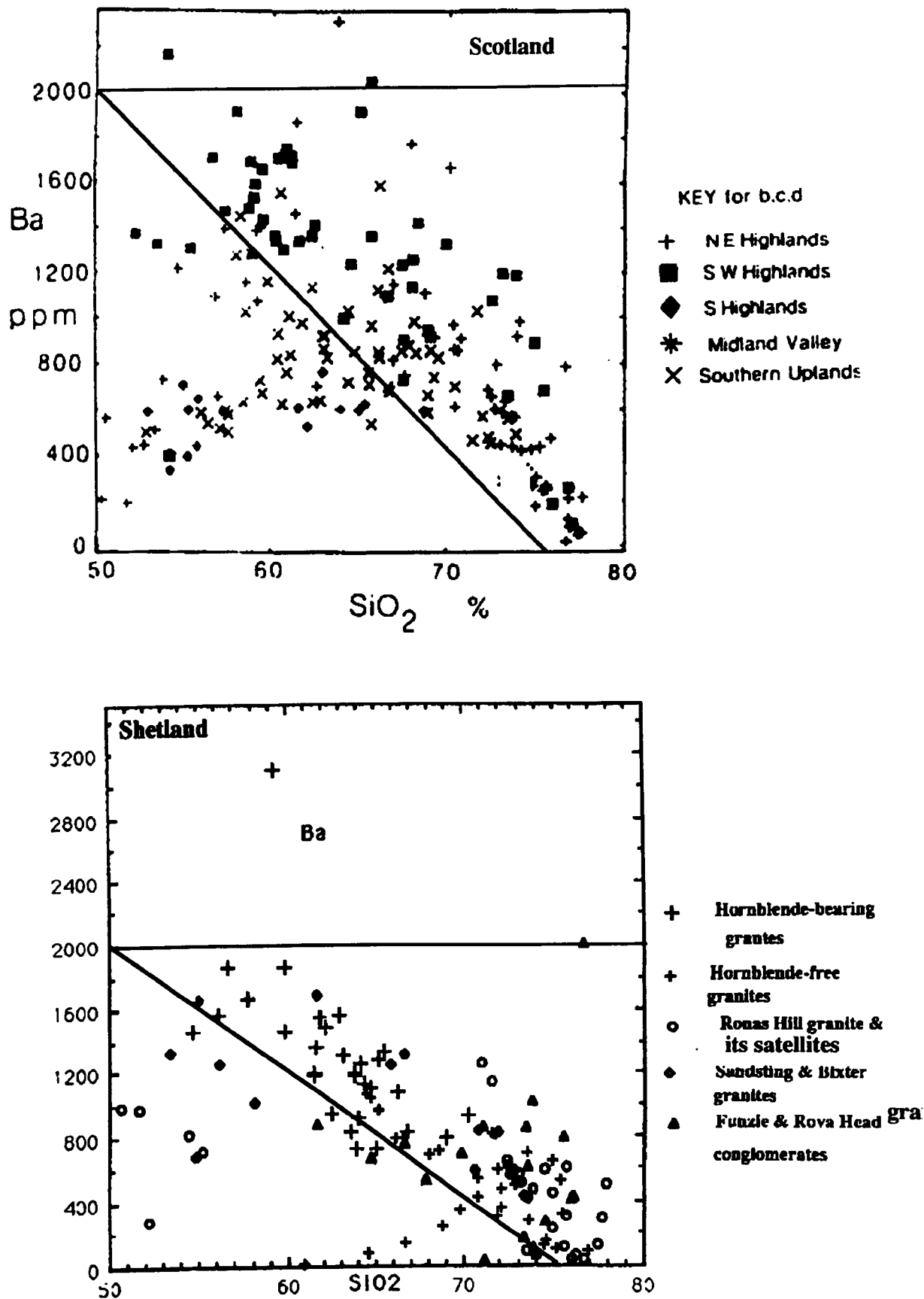
Figure 8. 9 plots Ba versus SiO2 for Scotland and Shetland granitoids. All samples with > 50% SiO2.
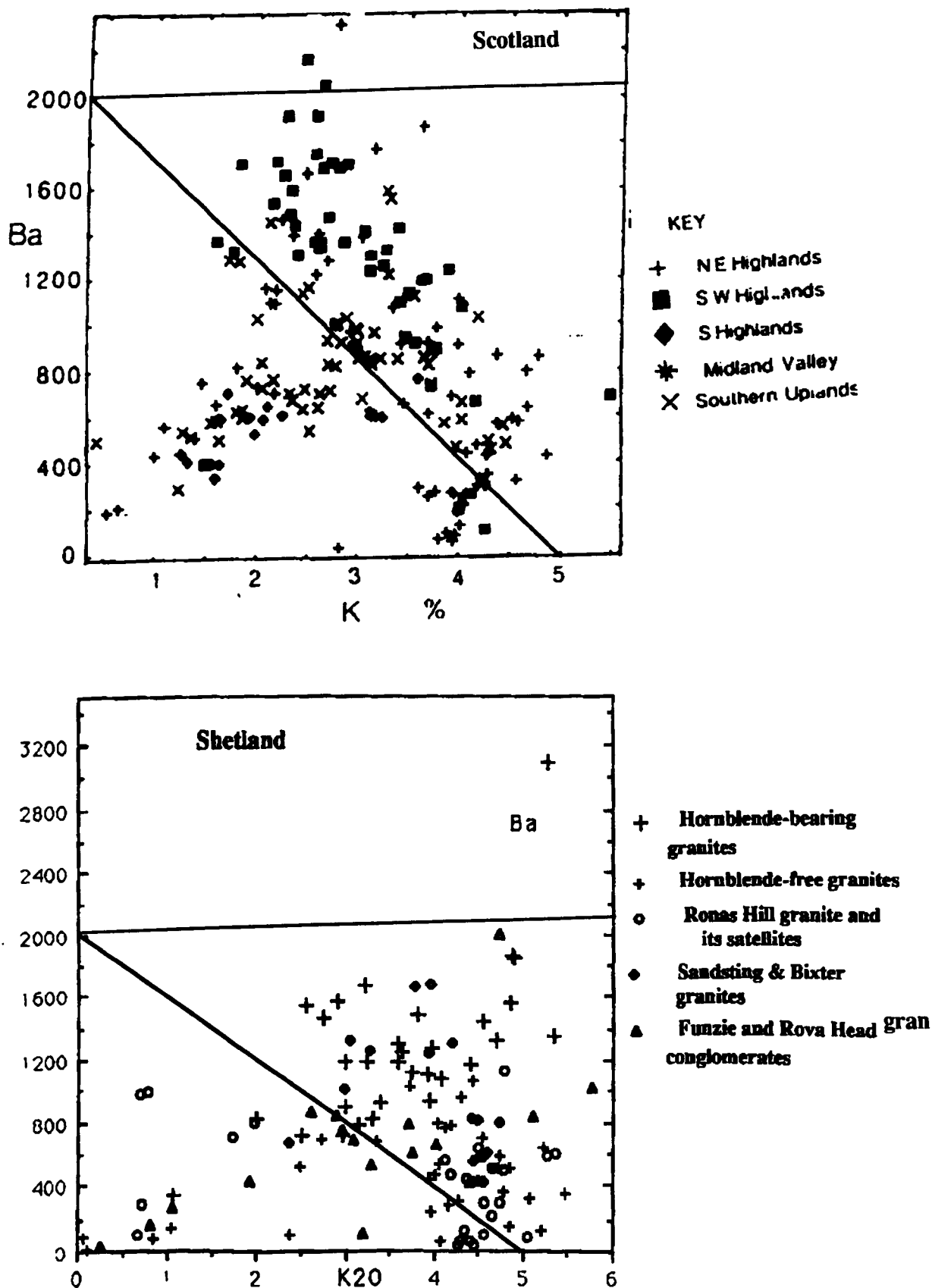
Figure 8.11 plots Ba versus K2O for Scotland and Shetland granitoids.

other parts of the Caledonian orogen in N America and Europe and appears to represent a significant enrichment in this respect.

The Sr versus CaO plot (Figure 8.9) is used as Ca is the most suitable major oxide against which to normalise Sr for bulk compositional effects. The Sr enrichment of Shetland and also SW Highlands granitoids are persistent even down to low CaO levels. A similar effect is seen for Ba versus SiO2 (Figure 8.10) and Ba plotted against K (Figure 8.11), these plots illustrate well the separation of Shetland hornblende-bearing granites from the rest of Shetland granitoids and divergence of the late granitoids of the Southern Highlands from those of the SW and NE Highlands, and the geochemical association of the Southern Highlands with Maidland Valley and Southern Uplands.

Stephens and Halliday (1984) have shown that the Sr and Ba enrichment feature for the Caledonian granitoids is pronounced at lower SiO2 values but is not so apparent at the higher range. They added that the fact that the trends are best shown at the more primitive SiO2 end of the range and disappear with increasing SiO2 is powerful evidence that they are primary features and not due to different schemes of fractional crystallisation of the same parental magmas. Such a process would lead to divergence at high SiO2 rather than at low SiO2. The Shetland hornblende-bearing granites (Graven pluton, Brae pluton, Spiggie and its two offshoots Aith & Hildasay plutons) clearly represent a high Sr and Ba province and show distinct trends with the plots of Sr-SiO2, Sr-Ca, Ba-SiO2 and Ba-K at low SiO2 as they do in the Scotland granites, and very similar to those of the SW Highlands. Where both lie on the same alignment as the hornblende-bearing granites lying immediately to the east of Walls Boundary Fault (WBF) which crosses Shetland Mainland from south to north and divides it into two parts. Many geologists had extrapolated that the Walls Boundary Fault as an extension of the Great Glen Fault (e.g. Flinn) (Figure 8.12).

8.3.3 **Rare Earth Elements**

Very little is known about the REE abundances in the Scottish Caledonian granites, while the isotopic compositions of the Scottish Caledonian granites are reasonably well known. Pankhurst in 1979, shows the REE patterns for Strontian and Foyers complexes from the Scottish Highlands. He confirm the strong light-to heavy REE fractionation suggested by the Ce/Yb ratios, which are 2-3 times higher than in typical calc-alkaline granites from destructive plate margins (e.g. Thorpe and Francis, 1976).

A composite plot for the Strontian, Foyers and Cairngorm granites (Figure 8.13) shows a strong fractionation from light to heavy rare earth elements with a large negative Eu* in the Cairngorm intrusion (about 0.30) A similar but slightly smaller negative Eu anomaly is present in the Foyers adamellite (Eu* 0.70) and a slightly positive Eu anomaly in the Foyers tonalite and granodiorite (Eu/Eu* ~ 1.1). The Strontian intrusion lacks any Eu anomaly. A common feature of Strontian and Foyers intrusions the smooth REE variations within each intrusion which leave no doubt that all the rock types in each intrusion are genetically related (i.e. the Foyers adamellite is not a much later magma unrelated to the earlier units, Pankhurst, 1979). However, The individuallity of the three intrusions (Foyers, Strontian & Cairngorm) is clearly established because of their differences in the Eu contents and light to heavy REE fractionation.

The composite plot of 24 samples analysed for REE from Shetland Caledonide granites including hornblende-bearing granites (Graven and Spiggie plutons), hornblende-free granites (Skaw), Ronas Hill granite and Sandsting pluton (Figure 8.13) confirms the strong light to heavy REE fractionation and their total abundances decrease with increasing SiO_2 suggesting rather compatible behaviour during fractional crystallisation, which is clearer for the Graven complex and Spiggie granite (see chapter 4 Figure 4.12b). The Eu* anomalies are slightly negative in the Spiggie (0.6), Sandsting (0.63) and Skaw (0.68) and slightly
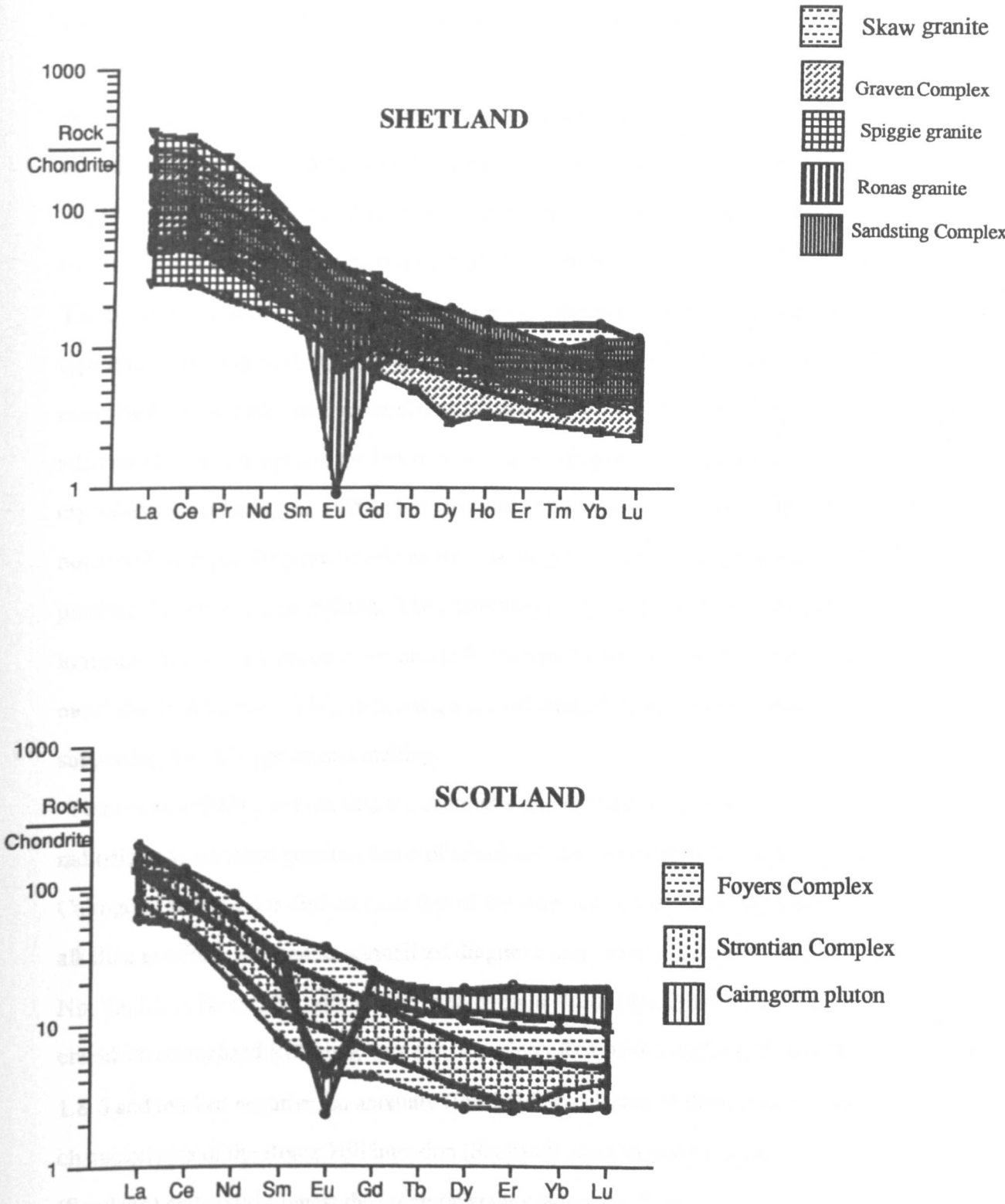
Figure 8.12 Chondrite normalised rare-earth element abundances for Shetland and Scotland. (data for Scotland come from Pankhurst, 1979, and Plant et al., 1980).

positive Eu* anomaly is present in the Graven granite (1.5). The contrasting

incompatible behavior of REEs in the Ronas Hill granite coupled with a strong

negative Eu* anomaly (0.08) (chapter 4 Figure 4.12d) which is very similar to the

contrasting incompatible behaviour of REEs in the Cairngorm intrusion (Brown et

al., 1981) with its strong negative anomaly about (0.3) suggests refractory feldspar

residue in the melt zone or cumulate feldspar at depth or both.

The petrogenetic models and isotopic data for the Cairngorm granite preclude "S'-

type crustal melting models for its genesis; instead the preferred model involves

combined assimilation and fractional crystallisation (AFC) as the result of the

addition of diorite magma to the lower crust following up to 50% fractional

crystallisation (Plant et al., 1990). For the Ronas Hill granite the isotopic data is

not established yet, the petrogenetic models for its genesis like Cairngorm also

preclude "S"-type crustal melting. The quaternary phase system of the Ronas Hill

intrusion lies on the cotectic in the quartz-K-feldspar fields, close to the "minimum

melt" (M. P. Atherton, 1988), indicating a crustal melt of granitic composition,

supporting the "S"-type crustal melting.

Plant et al. (1990) point out that the chemistry and tectonic setting of

radioelement-enriched granites, some of which are also enriched in Sn (e.g.

Cairngorm intrusion) is distinct from that of the more commonly occurring calc-

alkaline granites. On mantle-normalized diagrams they are enriched in U, Th, Rb,

Nb, Ta, Li, F, Be and Sn with marked depletion in Ba and Sr, Ti and P; and on

chondrite normalized REE diagrams they have high REE with La_N/Lu_N values of

1.8-6 and marked negative Eu anomaly (Eu/Eu* 0.3). Some of these features are

characteristics of the Ronas Hill intrusion (Shetland) and Cairngorm intrusion

(Scotland) and could suggest the common source origin for them.

Pitcher (1982), in classifying British granites as I-(Caledonian)-type, gives

mean values of 4.7 ppm U and 14. 6 ppm Th, in comparison with the average

values for the hornblende-free granites of 3.32 ppm U and 22 ppm Th, for the

hornblende-bearing granites of the Graven granitoid of 5 ppm Uand 26 ppm Th

and for the Spiggie granite of 6.10 ppm U and 50 ppm Th, for the Ronas Hill

granite and its satellites of 4 ppm U and 19 ppm Th and for the Sandsting and

Bixter granites of 3.1ppm U and 21 ppm Th. O'Connor (1981) gives mean values

for the British and Irish Caledonian granitic plutons of 4.0 ppm U and 14.1 ppm

Th, these averages including the result of Hennessy (1981). It seems that the

Shetland granitoids have slightly higher Th values than their Scottish counterparts

and more or less and sometimes the same U values.

8.4 Conclusion.

When all the analyses of Shetland granites are plotted on variation

diagrams, the resulting pattern of variation is very similar to that found in the

Caledonian granites of the British Isles. The Caledonian granites of the British

Isles (Scotland mainland, Ireland, Shetland) are high K-calc-alkaline (using criteria

of Peccerillo and Taylor, 1976) and Na-rich compared with Hercynian granites and

Australian Caledonian granites (Figure 8.4). Most of the granodiorites and diorites

are very rich in Ba and Sr, more so than almost any other area of the world.

K, Sr and Ba enrichment is common in calc-alkaline magmas erupted through

continental crust. The extreme enrichment in Sr and the low K/Na is thought to

reflect, at least in part a feature of the crust of the British Isles including Shetland

which extends back to Lewisian times. The high Na is not due to extensive

metasomatism with seawater-derived fluids. Neither is it likely to be due to a

greater pressure of H2O in the source. Many of the Caledonian granites were

probably initially quite dry magmas. Nockolds and Mitchell (1946) considered

pyroxene-mica diorite, a common rock type in the Caledonian granites, to be

parental to other magmas.

The high Sr and Ba province of the British Isles Caledonian granites to the

east of the Great Glen Fault extends northeast to include Shetland equivalents which

occur to the east of the WBF (Walls Boundary Fault). The granitoids of 400 Ma

age in eastern Canada, eastern U.S.A., Norway and eastern Greenland, which are

not notably Sr rich, provide an evidence that the British Isles crust has not been affected by >2000 Km transcurrent movements as suggested on the basis of palaeomagnetic data by Piper (1979) and Van der Voo and Scotese (1981).

The high Sr granitoids, lacking as they do major Eu anomalies (e.g. Pankhurst, 1979) were almost certainly derived from a feldspar free source, which had not been associated with a previous upper crustal history. This, coupled with the isotopic evidence and the occurrence of high Ni liquid indicates a fundamentally mantle-initiated magmatism (Halliday and Stephens, 1984).

The REEs of the British Isles Caledonian granites,including Shetland granitoids typically show light REE enrichments, and are behaving as compatible elements with bulk solid-liquid partition coefficients (D) greater than unity, and the REE patterns constitute independent evidence for the prime cause of petrological variation in these complexes. These evidences support the hypothesis of crystal fractionation of plagioclase, hornblende and minor phases in a parental magma, fractionation occurring below the level of emplacement and accomplished by successive intrusion, but with no major Eu anomalies and compatible behaviour due to plagioclase fractionation.

Chapter Nine.

9.1 Conclusions

9.1.1 This is the first comprehensive petrological and geochemical study to have been completed on Shetland granitoids on which very little data has been published. For the purpose of this thesis the Shetland granites have been subdivided into five main groups according to their location to the east or west of the Walls Boundary Fault (WBF), the continuation of the Great Glen Fault, according to their mineralogy and according to their occurrence as granitic pebbles. The granites to the east of the WBF have been subdivided on the basis of their mineralogy into two groups : hornblende-bearing granites and hornblende-free granites and the third group according to their occurrence as granitic pebbles in the Funzie and the Rova Head Conglomerates. The two groups to the west of WBF are the Ronas Hill granite and its satellite and the Sandsting and Bixter granites, which contain minor hornblende. Each of the Shetland granitoids described here is considered to be a single intrusion, which exhibits distinctive trends in chemistry.

Granites to the East of Walls Boundary Fault (WBF).

(1) The hornblende-free granites have a restricted range of SiO_2 between 71-75 % except for the Skaw granite which has a range : 64-70 SiO_2 %. They include granites of widely different ages and compositions such as the Brecken orthogneiss, the garnet -bearing Tonga and Colla Firth granites, trondhjemite dykes (associated with the ophiolite complex) and albite-keratophyres occurring as small masses and tiny veins in metavolcanic rocks associated with komatiitic serpentinites in the Cunningsburgh area southeast Shetland.

(2) The hornblende-bearing granites lie immediately to the east of the WBF. They have a wide range of silica content (60-71SiO_2%) compared with the hornblende-

free granites. They have approximately the same ages (about middle Devonian) and they include the Graven, Brae and Spiggie granites of different lithological and mineralogical compositions eg. the Spiggie granitoid (s. l.) is epidote-bearing.

(3) Granitic pebbles include a) these in the Funzie conglomerate which are mostly trondhjemites in the deformed metaconglomerate of pre-middle Old Red Sandstone. The trondhjemites pebbles are indistinguishable from quartz-albite porphyry minor intrusions in the greenstone slice at Staves Geo (Fetlar) and at North Tonga in the Muness phyllites. Their provenance by the means of natural erosion has been inferred by Flinn (1956) to be from these minor intrusions.

b) The granitic pebbles within the Rova Head Conglomerate have a range in SiO2 from 64 to 76 %) suggesting varied granitic sources. There are four types of pebble:- basic granodiorite, leucocratic porphyritic granodiorite, basic micrographic granite and leucocratic granite. None of these pebbles can be matched with the present Shetland granitoids, thus their original provenance lies somewhere to the NW under the sea, or alternatively large post-Devonian displacements along the Walls Boundary Fault and associated faults have obscured the provenance of these granitic clasts.

Granites to the West of WBF

(4) The Ronas Hill granite and its satellites are perthitic granites and granophyres characterized by drusy cavities containing crystals of stilpnomelane, quartz and epidote. They show a very limited silica variation : 72 to 76 SiO2%.

(5) The Sandsting complex and Bixter granite are both considered as one group because of their proximity and because on the Harker diagrams the Bixter granite lies at the acidic end of the Sandsting granitoid trend which varies from porphyritic microadamellite through granodiorite containing minor amounts of hornblende to granite, the whole showing a wide silica range (64-71SiO2%). Both the Ronas Hill granite and its satellites, the Sandsting complex and Bixter granite have ages of 360 Ma (upper Devonian time).

9.1.2 Classification of the Caledonian granitoid complexes of Shetland on the basis of age and petrology has not previously been attempted. Caledonian plutonic magmatism was classified by Read (1961) into two groups on the basis of structure and relationship of the intrusions to the deformation of their host rocks: the Older Pre- and Syn-tectonic intrusions and the younger post-tectonic Newer and Last intrusions. According to the Read classification the Caledonian hornblende-free granites of Shetland (except Skaw which lies within the Unst nappe structure) are pretectonic and syntectonic intrusions (about 530 Ma) equivalent to Read's older granites as they are single, garnet-bearing intrusions (Tonga, Brecken and Colla Firth). They lie to the east of WBF on the Shetland mainland and in a group of small Isles. They occur in areas of medium to high metamorphic grade country rocks and are all small vein complexes. Turner in 1968 mentioned that such rocks are thought to have been derived locally from relatively low-volume peraluminous melts at depths of up to 30 Km. By contrast the hornblende-bearing granites (Brae complex, Graven complex, Aith-Hildsay-Spiggie granite) to the east of WBF have K-Ar ages of about 400-430 Ma (Miller and Flinn, 1966). The Aith - Hildasay - Spiggie granite seems to be a forceful Younger- Newer granite, while the Brae and Graven Complexes appear to belong to the earlier Appinite Suite. In Shetland, the Spiggie granite (s.l) appears to have been emplaced at the same time as the Graven Complex (Miller and Flinn, 1966), whereas according to Read the forceful Newer Granites were emplaced just after the appinite suite.

The upper Devonian to early Carbonferous granites of Ronas Hill and its satellites and Sandsting and Bixter granites seem to be permitted last granites (K-Ar ages about 350 Ma) but do not appear to be of the cauldron or ring-complex type typical of those in Scotland. The classification applied to Shetland granitoids is not convincing when considered in detail, and suggests that Shetland granites may not fit the simple scheme put forward by Read.

9.1.3   A/CNK ranges from 0.8 to 1.1 (see Figures 8.6) making all Shetland granitic rocks (except the trondhjemite dykes and keratophyre) transitional between metaluminous and peraluminous compositions. The hornblende-free granites (Figure 7.13a) appear to be slightly more peraluminous in general than the hornblende-bearing granites. Peraluminous calc-alkali plutons granitoids (A/CNK above 1) in which peraluminosity increases with SiO_2 content have been ascribed by Cawthorn and Brown (1976) to be due to the precipitation of metaluminous hornblende from the magma. In Shetland, however, only the hornblende-free granites are clearly peraluminous and there is no petrographic evidence to suggest that rocks of this composition were formed by extraction of hornblende from a melt and the source, therefore, may be essentially sedimentary (Chappell and White, 1974)

9.1.4   Consideration of typology (Pitcher, 1982) indicates that the hornblende-bearing granites to the east of the WBF, the Ronas Hill granite and its satellites, the Sandsting complex and Bixter granite to the west of WBF are I-Caledonian type, while the hornblende-free granites are closer to S-type. The De La Roche system of classification shows that all 5 groups of Shetland granites are high-K calc-alkaline granites (except the trondhjemite dykes and pebbles) mostly plotting on the shoshonitic trend, while the Spiggie monzonite rocks, owing to their high total alkalis and to some extent iron and titanium plot on the alkaline trend.

9.1.5 The 5 groups of Shetland granitoids have been plotted on the Streckeisen classification diagram. This shows that granodiotite and monzonite are the main lithologies of hornblende-bearing granites, while the hornblende-free granites plot in the monzogranite field. The Ronas Hill granite and its satellites plot in the monzogranite and alkali-feldspar granite field, Sandsting and Bixter granite in the monzogranite and granodiorite fields and Funzie and Rova Head plot in the field of

granodiorite. The plagiogranite samples from Funzie lie on the Q-P tie line and in the tonalite field.

9.1.6   The observed patterns of major elemental variation are typical of calc-alkali granitoids in general (cf. Nockolds and Allan, 1953; McBirney, 1980; Atherton in Harmon and Barreiro, 1984). In the terminology of Peacock (1931), the Shetland granitoids have an alkali-calcic chemistry but using the criteria of Peccerillo and Taylor (1976), they belong to high-K calc-alkaline series (except the trondhjemite dykes and keratophyre). This is confirmed by the variation on the AFM plot (Figure 8.3).

9.1.7   In the quaternary An-Ab-Or-Qz phase diagram the five main groups of Shetland granitoid rocks show their own crystallisation paths. Within each group there are similar trends reflecting the differences between the individual intrusions. The bulk of the hornblende-bearing granites plot as a group low in the plagioclase volume, while the bulk of the hornblende-free granites plot near to the quartz saturation surface and Ronas Hill and its satellites plot on the cotectic between the quartz and K-feldspar field. The bulk composition plot for the Sandsting and Bixter granites show them to be a group low in plagioclase volume. The hornblende-free granites and the Ronas Hill granite can be inferred on the basis of their plots to be produced by the process of fractional fusion, while the hornblende-bearing granites and Sandsting complex on the basis of their plots are produced by equilibrium fusion. The fundamental distinction between these two processes is that in the fractional fusion the only liquid obtainable within the tetrahedron lies on the quartz saturation surface whereas the equilibrium fusion liquid can originate in the plagioclase volume and then move towards the K-feldspar or quartz liquidous surfaces and is capable of producing the parent magmas of the hornblende-bearing granites and the Sandsting complex.

9.1.8   On the Rb/Sr versus DI plots, each of the 5 groups of Shetland granitoids form separated trends. Also within each group there are sometimes different trends which indicate the difference between individual intrusions. Rb/Sr ratios of the Ronas Hill granite and its satellites are exteremly high due to the very low content of Sr (sometimes it is below the detection limit) and high Rb content. As such, it is very tempting to say that the Rb/Sr ratio for the Ronas Hill granite and its satellites indicates a special continental crust for the North Maven Caledonian granites, very depleted in Sr . Such low Sr magmas are found in Scotland eg. Lochnagar, Hill of Fare, Meall Odhar and Cairngorm and have been attributed by some workers to the melting of a distinct source region (e.g., Brown and Locke, 1979). The other chemical features of these granites which distinguish them from the high Sr magmas are depletion in Sr, Zr and Ba, enrichment in Rb and U, and a marked negative Eu anomaly. These features are most easily explained by low pressure fractionation of zircon, K-feldspar, and minor biotite. If this is so there is no feature of the geochemistry that requires a different source region of these granites.

9.1.9   The high Sr hornblende-bearing granites to the east of the WBF, the Sandsting granitoid to the west of the WBF and the Skaw granite (hornblende-free granite), lack major Eu anomalies. They must have been derived from a feldspar-poor source and or suffered a little feldspar fractionation.

9.1.10   REEs of Shetland granitoids show very high enrichment in the light rare earth elements and strong light to heavy rare earth elements fractionation. The CeN/YbN ratios range between 59 to 4 in the hornblende-bearing granites and from 15 to 5 in the hornblende-free granites. The least evolved patterns are in the more basic granitoid rocks and REE concentrations decreases progressively with the increasing SiO2 contents. Generally most patterns lack a Eu anomaly, but some show a small negative Eu anomaly. Only the Ronas Hill granite shows a big negative Eu anomaly (0.08) which is due to feldspar fractionation. It has been

postulated that the REE in Shetland granitoids are largely contained in the accessory minerals such as sphene, allanite, apatite and zircon and these are responsible for the progressive depletion of REE with increasing SiO2. The reasons for this are:-

a) Studies by e.g. Gromet and Silver (1983), Watson and Harrison (1984) have shown that in most intermediate-acid plutons, the bulk of the rare earth complement of the rock is held in the accessory minerals. This is confirmed by the REE modelling.

b) The K_D's of the common rock-forming minerals are inadequate to explain the depletion of rare earth elements in the more evolved rocks of the Shetland granitoids.

9.1.11   Major elements and REE modelling gave results which are in agreement with the targets. It was inferred from major and trace element variation diagrams and REE patterns that crystal fractionation was the dominant process in producing the observed chemical variations: fractionation of plagioclase, biotite and hornblende is suggested from major elements modelling whereas allanite, sphene, apatite and zircon are suggested by REE modelling.

9.1.12 On the basis of his work on geochemistry of the Old Red Sandstone volcanic rocks associated with the Ronas Hill granite and those in Scotland Thirlwall (1981) points out that the Shetland ORS volcanics have a high SiO2 assemblage (olivine-pyroxene-plagioclase) leading to higher K (and other incompatible elements) at constant SiO2 in evolved rocks than fractionation of a low-SiO2 assemblage e.g. magnetite, hornblende- or garnet-bearing. This also leads to higher Fe/Mg, i.e. a tholeiitic differentiation trend. Thirlwall (1982) stated that Shetland lavas show most of the characteristic features of the mordern arc volcanics including the marked enrichment in hydrophile elements (K, Rb, Ba, Sr) relative to REE and HFS elements. A direct relationship to the adjacent Ronas Hill

granite and its satellites is unlikely because of the difference in age and chemistry. The age of the Shetland volcanics associated with the Ronas Hill granite is Eifelian (381 Ma) while the Ronas Hill granite and its satellites are Upper Devonian to early Carboniferous about 358 Ma and in contrast to 381 Ma for the volcanics, there is a difference between silica contents as Shetland volcanics ranges from 52 to 60 SiO2 % and few samples have silica over 70% while Ronas Hill and its satellites have a silica range between 71-77%. There are differences in Rb and Sr values too as the Ronas Hill granitoid shows high Rb and low Sr values while the ORS volcanics of Shetland on the contrary show high Sr and low Rb values and that is reflected in their difference in the Rb/Sr ratios where Ronas and its satellites show wide range of Rb/Sr (0.09-11.29) while Rb/Sr ratios of Shetland voalcanics are between 0.01-0.38 and only one sample gives 6.5 Rb/Sr value. Therefore there appears to be no link between the Ronas Hill granite and its satellites and the adjacent Shetland volcanics.

9.2.1 The British Caledonian granites, including Shetland granitoids have high Na concentrations compared with the Variscan granites (Hall, 1971) and compared with the Caledonian granites of the Lachlan fold belt Australia. Chappell and White (1974), consider the low Na in S-type granites is due to removal of alkalis by seawater during diagenesis of sedimentary protoliths. Hall attributed the high Na (normative albite) content of the Caledonian granites to melting at high H2O pressures; the supporting evidence comes from the apparent relationship between high normative albite and association with appinites (hydrous mafic intrusions).

9.2.2 The comparison between Caledonian Shetland and Scottish granitoids reveals the nature of their similarity in chemistry. Thus they have high K-calc alkaline (Peccerillo and Taylor, 1976), high alumina and alkali (Kuno, 1966) characteristics and are generally calc-alkalic or alkali-calcic (Peacock, 1931).

9.2.3   The hornblende-bearing granites of Shetland (to the east of the WBF)

clearly represent a high Sr and Ba province very similar to that of the Scottish

granitoids in the SW Highland (immediately to the east of Great Glen Fault),

perhaps the most important conclusion in this thesis. The Sr and Ba province of

the British Isles Caledonian granitoids (defined by Stephens and Halliday, 1984)

can be extended 200 miles toward the NE into Shetland immediately to the east of

WBF. Thus Sr and Br enrichment is a mantle derived characteristic (Halliday and

Stephens, 1984) relating to a major ancient lithospheric chemical province.

9.3 Suggestions for further work

Further conclusions concerning the source of Shetland granitoids should

be reached through a detailed Rb-Sr, Sm-Nd and U-Th-Pb radiogenic isotopes

study. Similarly, a detailed study is necessary of the oxygen stable isotope

compositions of the different groups of Shetland granites and in particular the

oxygen isotope composition of mineral separates from the syntectonic peraluminous

facies is needed if the processes involved in high-level fluid/rock interaction in

modifying primary magmatic composition are to be understood more precisely.

Such studies , linked with fluid inclusion studies and argon-argon geochronology

from the deformed rocks could provide useful information on how mineral ages are

reset by deformation and recrystallisation during fault movements in the upper

crust. It would also be fruitful to make a more detailed study of the petrology of

Shetland granites from the textural point of view to determine the proper order of

crystallisation of the phases of each Shetland granite. No study has been made or

exploration at regional or local scale of the mineralization associated with Shetland

granites and such a study is needed.

APPENDIX A1 ANALYTICAL METHODS.

A1.1a) Modal analysis of Granites

Modal analyses were made for all medium and coarse grained rocks of the granitic plutons of Shetland on both side of Wall Boundary Fault (WBF) by the traditional point counting method using 1000 orthogonally spaced points over an area of approximately 960 sqmm on a standard size thin section using a Swift Model E automatic point counter. The author was aware of the errors attendant on the use of such small counting areas in rocks of this grain-size (Chayes, 1956) and in view of these could see little advantage in repeating the count to increase the precision associated with such a small area of thin-section. Modes of the following minerals were determined: plagioclase, K-feldspar, quartz, clinopyroxene, hornblende, biotite, epidote and accessory minerals (sphene, epidote, apatite, opaques, zircon and tourmaline). The modal proportions of each mineral had to be determined from the thin section count.

Errors on accessory mineral modal proportions are likely to be considerably larger than those determined on major minerals, especially because of the relatively low total counts I have used (1000 points). Authors interested in accurate determination of accessory mineral proportions (e.g. Gromet and Silver, 1983) have counted of the order of 20,000 points over a number of thin sections. The results obtained in the modal analysis of the Shetland granitoids are shown in appendix 2

A1.1b) <u>Preparation of samples for whole rock chemical analysis</u>

Granite samples collected for chemical analysis weighed not less than 2Kg. The freshest available material was chosen and this usually involved starting with quite a large sample (up to 4 kg) and removing the outer weathered layers. Occasionally, fracture and joint planes could not be removed and consequently small amounts of altered material may be present in some samples.

The granite samples were then spilt or sawn into two portions :- a) a ~2" cube was removed for thin sectioning; b) the rest of the material was cut into pieces for jaw crushing and crushed to a coarse grit in a jaw crusher and 100g of the homogenised material was then further reduced in a tungsten carbide "tema". 3 samples of rock powder were taken:- a) After 15 seconds grinding, 5g of homogenised rock powder was removed for FeO determination. The grinding time was kept short since oxidation of fine powders is known to occur if they get too hot (Fitton and Gill, 1970). This material was passed through a 150μm diameter brass seive and any material retained was hand-ground in an agate mortar and pestle until it also passed through.

The remaining powder was returned to the tema and ground for a further 30 seconds.

b) A 15g sample of the homogenised powder was removed and passed through a 150μm brass sieve. In most cases, no material was retained, so no hand-grinding was necessary. This sample of the whole rock was the one used in most of the analytical techniques. c) 7g of the homogenised rock powder were removed and passed through a 53μm brass sieve. Further grinding of the retained portion in an automatic agate mortar and pestle was necessary in all cases to get all the rock powder through. This rock powder was used for making a pressed powder pellet for XRF trace elements analysis. Rock powders were dried at 110c overnight to drive off moisture before conducting any analysis.

A1.1c) Whole rock major oxide and trace element analysis.

Major and trace element abundances of Shetland granitoids were determined by XRF at the Geology Department, Liverpool University :- SiO2, TiO2, Al2O3, total iron as Fe2O3, MnO, MgO, CaO, Na2O, K2O, P2O5, Ba, Ce, Co, Cr, La, Nd, Ni, Pb, Rb, Sc, Sr, Th, V, Y, Zn, Zr. The equipment used was a Siemens Krystalloflex-4 generator and controlled by an Apple 11+ computer via a Hiltonbrooks controller and drive unit. Major elements were determined using Cr primary beam radiation generated at 50kv and 40mA, and trace elements using W primary beam radiation generated at 45kv and 60mA. Accuracy in major element analysis was checked by routine analysis of the USGS standard G2.

Major element pression is given in the following table (courtesy of J. Sharman).

Element	x	n	sigma n-1	C%
SiO2	72.60	6	0.24	0.33
TiO2	0.30	6	0.0041	1.36
Al2O3	14.27	6	0.094	0.66
Fe2O3	1.76	6	0.015	0.86
MnO	0.16	4	0.0040	2.46
MgO	1.46	4	0.046	3.14
CaO	1.86	6	0.0063	0.34
Na2O	5.81	4	0.101	1.74
K2O	4.10	6	0.011	0.27
P2O5	0.08	6	0.012	15.1

Table of XRF major element precision (courtesy J. Sharman).

Accuracy and precision data for trace elements analysed by XRF were obtained by analysing 4 separate pellets of rock V4 which has been independently analysed (by XRF) at Nottingham University. Analysis courtesy of J. Sharman.

Element	Notts. val.	x	n	sigma n-1	c%
Ba	1140	1053	5	13.53	1.28
Ce	62	59	4	1.71	2.89
Cr	<det	<det	4	-	-
La	26	32	4	2.45	7.66
Nd	-	39	4	1.26	3.23
Ni	<det	<det	4	-	-
Pb	1.6	17	4	1.50	8.82
Rb	59	61	4	0.00	0.00
Sc	-	15	5	1.15	7.70
Sr	232	234	4	1.50	0.64
Th	12	12	4	2.22	18.5
V	18	19	4	0.58	3.05
Y	53	47	4	1.41	3.00
Zn	114	101	4	0.96	0.95
Zr	297	288	4	0.82	0.28

Table of XRF trace element Precision (courtesy J. Sharman).

The sample preparation techniques employed in this study were:-

1) Glass discs for major elements.

Glass fusion discs were used for the analysis of all major elements except MgO, MnO and Na2O. These were prepared using the method of Norrrish and Hutton (1969) which was the powder mix with "spectraflux", fused and moulded into a disc using an aluminium disc and plunger.

2) pressed powder pellets for MgO, MnO, Na2O, and trace element.

7g of the <53micron powder was made into pellets by mixing the rock powder with 15 drops of moviol solution (4g moviol + 10ml ethanol + 50ml distilled water). The mixture was then pressed into a 4cm diameter disc under 5 tons pressure.

A1.1d) <u>Ferrous and Ferric iron</u>

5g of the dried, <150μm, 30-second crushed rock powder was dissolved in a mixture of sulphuric and hydrofluoric acids and then titrated with potassium dichromate using sodium diphenylamine sulphonate indicator.

The titration is undertaken in the presence of boric acid to complex flouride, and phosphoric acid to suppress ferric iron. All analysis were carried out in duplicate and if the discrepancy between the 2 determinations was more than 0.1%, a further analysis was carried out. The concentration in the rock sample was calculated from the XRF total iron value and the wet chemical FeO analysis using the following relationship:

$$Fe_{XRF} - 1.111 FeO = Fe_2O_3$$

"wet"

A1.1e) <u>Analysis of H2O+ and CO2</u>

H2O+ and C2O were determined simultaneously in the granite samples. This was done by heating 1g of the 110c-dried <150 μm rock powder in an alumina boat inside a tube furnace to 1000c for half an hour whilst passing a stream of dry nitrogen over it continuously. The nitrogen + evolved vapour and CO2 were then passed through a U-tube filled with anhydrous magnesium perchlorate to absorb water and then a U-tube filled with carbasorb (a mixture of NaOH and asbestos) to absorb CO2. This U-tubes were weighed before and after the experiment and the wt% H2O and CO2 calculated from the differences. Blanks were performed on empty alumina boats to account for any absorption of moisture from the

atmosphere.

Analysis was carried out in duplicate and if the discrepancy between the determinations was greater than 0.1 wt%, a further analysis was carried out. Problems can arise when using this method if the rock contains sulphide since any evolved SO_2 will also be absorbed by the carbasorb. It is likely that the CO_2 determination in the case of the granites represents evolved CO_2 from carbonate minerals + SO_2 evolved during combustion of the sulphides in the rock powder (the N_2 carrier gas was unfortunately not 100% pure).

A1.1 f) Electron probe analysis

Sample preparation

Rocks suitable for electron microprobe analysis were chosen after examination of the ordinary thin sections. Offcuts remaining from the manufacture of the ordinary thin sections were impergnated with epoxy resin and glued to a standard size glass slide (28 *47mm). These were then sawn and ground down to a thickness of ~40μm by standard thin section making techniques. The final polish was achieved by polishing with progressively finer diamond pastes (6μ, 3μ, 1μ, 1/4μ) for a day at a time. The specimen surface was made conducting by coating it with a 20nm carbon film.

All mineral compositions were determined by electron microprobe analysis (EMPA). The EMPA technique allows non-destructive analysis of selected points or areas on a thin section by means of characteristic X-rays generated by the irradiation of the specimen with a finely focused electron beam.

Experimental procedure.

The microprobe used were of two types, both of which are housed in the Geology Department, Manchester University.

1) Modefied Cambridge Instrument Company Geoscan, running under the following operating conditions: Energy Dispersive Spectrometer (EDS) analysis, focused beam diameter c.3microns, 15Kv beam accelerating potential, 3nA specimen current on cobalt metal and Take Off Angle of 75 degree with a count time of 100 liveseconds. Beam current drift was checked by analysing a specific plagioclase feldspare at ~1/2 hourly intervals and adjusting the controls to gives 100% totals. Link systems ZAF-4/FLS software package (Statham, 1977) was used to convert X-ray spectra into chemical analyses.

2) A CAMECA Camebax probe

Operating under similar conditions to the Geoscan: EDS analysis, beam diameter 1-2 microns, 15Kv beam accelerating voltage, 3nA beam current and 100 liveseconds counting time. The spectra processing and ZAF correction used was the the same as for the Geoscan machine, the only major difference being that the Take Off Angle is 40 degree instead of 70 degree.

EPMA determined iron as FeO. Formula calculation and estimation were performed in the following ways.

Feldspar: based on 8 oxygens. Analysis described in terms of three end-members - albite (Ab), anorthite (An) and orthoclase (Or). Pyroxenes: Amphiboles: calculation on the basis of SI+AL+TI+FE3+FE2+MG+MN= 13 and oxygen equivalent of 23 as recommended by LEAKE (1978).

Ilmnite: Fe partitioned on the basis of 4 cations and 6 oxygens . Analysis described in terms of end-members ilmenite and haematite. Magnetite: Fe partitioned on the basis of 24 cations and 32 oxygens . Biotite: Based on 22 oxygens.

A1.1g) Neutron Activation Analysis

54 granite samples from Shetland granitoids were analysed by neutron activation

analysis for U, Hf, Ta, Th and certain other trace elements. To prevent contamination of powder by Ta during grinding in a tungsten carbide tema (Wood et al, 1979) powder to be used in INNA were crushed to <150 microns in an agate tema. INNA was carried out at the Universities' Research Reactor (URR) at Risley near Warrington. The experimental techniques used was based upon that of BRUNFELT AND STEINNES (1969).

Samples comprising c.o.25g of rock powder are enclosed in aluminium vials and packed into an aluminium can lined with cadmium (1mm). The samples are irradiated for 7-7.5 hours in a flux of c.3 X 10^{12} n cm-2 sec-1. The samples are left to decay for seven days and counted for 1000 seconds. Following a further decay period of 3-4 weeks a second count of 10000seconds is made. Samples are counted on a PGT (Princetown Gamma Technology) Ge (Li) detector (80cm^3) and 4096 analyser. Peak areas were determined using Geligam software running on an IBM PC. Decay corrections were carried out at dept. of Geological sciences using software wrtten by M.S.Brotherton running on an Apple 11 microcomputer. The raw data obtained using this method are given in appendix 2.

A1.1h) Whole rock rare earth element analysis

24 samples of granites were analysed for REE concentrations and determined by Radiochemical neutron activation analysis (RNAA) using the <150 micron rock powder.

REE analysis was undertaken at the Universities Research Reactor (URR) at Risley, near Warrington. The experimental procedure used is that of DUFFIELD AND GILMORE (1979).

Rock powders, weighed at c.200mg, are enclosed within aluminium capsules. Standard solutions (400mg) are sealed in silica tubes and leak tested. One standard contains the REEs La, Nd, Eu, Dy, Tm, Tb, and Lu and the other Ce, Pr, Sm, Gd,

Ho, and Er. Concentrations chosen for the standards represent a typical rock but with amounts of the more difficult REEs enhanced.

Samples and standards are placed in an "A" can and irradiated for 7-8 hours under a thermal neutron flux of c. 10^{12} n cm-2 sec -1.

After irradiation the samples are removed from their capsules and each placed in a platinum capsule containing 1ml of La^{+3} (10 mg g^{-1}) solution. 10ml of 40% HF is added and the crucibles are evaporated to dryness. Evaporation is repeated, first with a further 10ml of 40% HF and finally with a mixture of 5ml 40% HF and 5ml concentrated $HClO4$ solution.

The resulting residue is washed into a beaker using concentrated HCl acid and 10ml of saturated borax is added. Hydroxides are precipitated by netralising with concentrated $NH4OH$ and the supernatant liquid discareded. The precipitate is dissolved by adding concentrated HCL acid and the resultant solution is diluted to 30ml. Concentrated $NH4OH$ is added until the hydroxides again precipitate. A few drops of concentrated HCL acid are added to clear the solution which is then boild . On cooling oxalic acid is added to precipitate REE oxalates which are separated, washed twice with water and once with acitone before being transferred to a polythene tube for analysis.

The standard solutions are washed into tubes containing 1ml of $La+3$ carrier solutions. Oxalates are then precipitated using the method described above.

Gamma ray spectra are measured by detector system, only two counts were taken, one immediately after separation and the other one week later. Dy is measured using the isotope 165mDy, which has a half life of 1.3 minutes, by re-irradiation of the REE oxalate precipitate for 30 seconds using the rapid sample retrieval system. The system allows for rapid sample input/output from the reactor. The precipitates were counted for 30 seconds. La140 is also measured in order to determine the

chemical yield of the separation. The consistency of the neutron flux is determined by irradiation of a Cu flux monitor with each sample.

SANDERSON (1981) has shown the technique described above to be accurate, comparing REE concentrations presented in the literature with determinations made on the same rock at the URR.

The results of REE analyses are given in appendix 2, the analyses are given with an error quoted at the 2 sigma limit of detection.

APPENDIX A2 CHEMICAL, MINERALOGICAL DATA AND SAMPLE NUMBERS USED IN THIS THESIS.

A2.1 List of abbreviations used in listings

Chemistry:

LOI	loss on ignition
O and -	below limit of detection of experimental

Modes:

n.d	not determined
Plag	plagioclase
Ksp	K-feldspar
Qz	quartz
Bi	biotite
Hb	hornblende
Chl	chlorite
Musc	muscovite
Grn	garnet
opq	opaques
epi	epidote
Aeg	aegerine
sph	sphene
Zr	zircon
Al	allanite
Alkli	alkali-feldspar
access.	accessory

Norms:

Qz	quartz
Or	orthoclase
ab	albite
an	anorthite
c	corundum
diwo	diopside-wollastonite
dien	endiopside
difs	diopside-ferrosalite
hyen	hypersthene-enstatite
hyfs	hypersthene-ferrosilite
mt	magnetite
iL	ilmenite
ap	apatite
olfo	olivine-forsterite
olfa	olivine-fayalite
he	hematite

A2.1) Hornblende-bearing granites: XRF analysis (whole rocck major oxide and trace elements), modal mineralogy, normative mineralogy.

Sample	6.10	6.13a	6.16a	6.24a	6.26a	6.29a	6.30	6.31	7.5	7.10a	7.14
SiO2	62.17	61.84	59.84	56.08	63.54	70.19	64.09	63.15	62.43	61.48	44.56
TiO2	0.73	0.79	0.98	1.09	0.61	0.36	0.72	0.70	0.86	0.40	1.31
Al2O3	15.23	16.04	16.98	16.00	15.90	14.80	16.22	15.06	16.16	19.52	17.10
Fe2O3	1.26	1.43	1.87	2.02	1.34	0.50	1.38	2.06	0.95	1.28	4.3
FeO	2.98	2.81	3.24	4.47	2.25	1.07	3.05	2.19	2.38	1.60	7.38
MnO	0.07	0.08	0.10	0.10	0.07	0.05	0.08	0.08	0.06	0.07	0.17
MgO	2.75	3.13	3.08	4.81	3.00	1.34	2.39	3.11	3.07	1.77	7.88
CaO	3.72	3.37	3.52	5.33	3.97	2.47	2.79	3.69	3.51	3.39	7.47
Na2O	4.40	4.24	4.22	3.94	5.05	4.47	3.40	4.17	3.71	4.31	2.16
K2O	3.81	2.55	2.74	2.91	2.00	3.38	3.64	3.59	3.94	3.23	1.07
H2O	1.33	1.40	1.05	1.63	1.01	0.54	0.88	0.95	0.91	1.93	3.45
P2O5	0.33	0.31	0.47	0.42	0.19	0.16	0.28	0.29	0.22	0.17	0.16
CO2	0.22	0.17	0.17	0.21	0.11	0.09	0.12	0.08	0.12	0.33	0.57
Total	99.00	98.16	98.26	99.06	99.04	99.42	99.00	99.04	98.32	99.48	97.61
Ba	1486	1546	1467	1564	820	923	1258	1312	941	1184	346
Ce	96	188	172	70	52	33	80	77	94	176	23
Co	58	46	50	45	52	57	49	47	57	30	46
Cr	103	68	60	141	65	35	65	113	120	28	215
La	46	126	87	43	28	28	44	52	51	112	10
Nd	60	90	93	49	32	22	45	45	46	65	28
Ni	48	36	32	79	36	21	27	53	52	8	44
Pb	21	22	21	22	21	32	29	36	24	21	11
Rb	98	64	117	63	40	56	126	93	160	102	24
Sc	9	3	7	16	9	4	11	8	7	4	43
Sr	1511	1803	2105	1630	1268	1072	1028	1406	400	971	304
Th	16	27	21	8	6	11	23	19	20	33	89
V	83	83	95	11	20	84	96	82	86	42	284
Y	21	18	11	18	10	8	24	20	28	6	40
Zn	74	85	104	104	72	34	59	68	53	46	102
Zr	267	217	301	175	114	83	263	182	414	209	54
Ti		4284	5768	879	1564	4311	5849	3862		2328	7267

	modl mineralogy (percent)										
Plag	36.60	60.00	53.60	52.80	55.00	41.70	47.00	56.20	42.50	69.20	n.d.
Ksp	26.80	5.00	4.60	9.20	4.80	19.60	7.00	12.40	21.90	0.00	n.d.
Qz	17.00	13.50	16.22	5.00	16.00	29.10	25.60	9.80	18.90	17.20	n.d.
Bi	6.80	15.50	21.80	7.6	9.8	5.10	20.20	6.80	15.50	11.00	n.d.
Hb	10.60	6.00	3.40	24.40	11.20	3.50	0.00	13.40	6.00	0.00	n.d.
Opq	2.20	0.00	0.00	1.00	0.00	0.00	0.00	0.00	0.00	0.00	n.d.
Chl	0.00	0.00	0.00	0.00	2.20	0.00	0.00	0.00	0.00	0.00	n.d.
Access.	0.00	0.00	0.40	0.00	1.00	1.00	0.20	1.40	0.60	2.60	n.d.

	normative mineralogy (percent)										
Qz	10.56	11.35	9.53	3.74	13.87	24.12	17.98	13.83	13.31	10.61	0.00
Or	22.52	15.07	16.19	17.20	11.82	19.98	21.51	21.22	23.28	19.09	6.32
ab	37.23	35.88	35.71	33.34	42.73	37.83	28.77	35.29	31.39	36.47	18.28
an	10.55	15.61	14.40	17.38	14.81	10.34	12.01	11.77	15.81	15.71	33.80
C	0.00	0.85	1.80	0.00	0.00	0.00	2.33	0.00	0.00	3.18	0.00
diwo	2.40	6.52	6.01	2.64	1.52	0.36	5.02	1.94	0.07	6.29	0.92
dien	1.51	4.42	4.01	1.74	1.08	0.25	3.02	1.48	0.05	4.41	0.62
difs	0.74	1.60	1.55	0.71	0.31	0.08	1.73	0.25	0.02	1.35	0.25
hyen	5.34	3.38	3.66	10.24	6.39	3.08	2.94	6.26	7.57	0.00	12.34
hyfs	2.62	1.22	1.42	4.21	1.84	0.97	1.69	1.06	2.26	0.00	5.11
mt	1.83	2.07	2.71	2.93	1.94	0.72	2.00	2.99	1.38	1.86	6.28
iL	1.39	1.50	1.86	2.07	1.16	0.68	1.37	1.33	1.63	0.76	2.94
ap	0.78	0.40	1.11	0.99	0.45	0.38	0.66	0.69	0.52	0.40	0.38
olfo	0.00	0.00	0.00	0.00	0.00	0.00	0.00	0.00	0.00	0.00	4.68
olfa	0.00	0.00	0.00	0.00	0.00	0.00	0.00	0.00	0.00	0.00	2.14

Hornblende-bearing Granites: XRF analysis (whole rock major oxides and trace elements), modal mineralogy, normative mineralogy.

Sample	12a.24	12a.25	12a.27	12a.28	12b.12	12b.30	12b.31	12b.32	12b.33	12b.34	12b.35	12b.36	12b.37
SiO2	61.49	56.65	59.28	57.76	65.06	66.23	65.43	54.62	61.54	63.79	64.04	63.90	64.39
TiO2	0.59	0.80	0.43	0.65	0.41	0.39	0.31	0.94	0.36	0.47	0.50	0.53	0.52
Al2O3	16.04	16.19	19.80	18.22	16.14	16.11	16.57	13.68	18.84	16.68	16.25	16.35	15.87
Fe2O3	2.12	6.51	2.37	3.49	2.04	2.05	1.56	4.01	1.70	2.44	2.48	2.69	1.95
FeO	2.93	0.27	0.62	2.06	1.16	0.91	0.75	3.96	0.70	1.22	1.63	1.75	2.16
MnO	0.13	0.13	0.07	0.12	0.08	0.10	0.10	0.14	0.08	0.10	0.10	0.10	0.14
MgO	3.19	1.61	0.70	2.74	1.34	1.34	0.61	4.45	0.14	1.59	2.45	2.84	2.62
CaO	4.79	5.12	3.33	5.13	3.26	2.90	2.43	5.55	2.44	3.66	4.14	4.19	3.57
Na2O	3.10	4.83	5.23	4.23	4.73	4.75	5.83	3.76	5.93	4.77	3.39	3.40	3.26
K2O	2.99	4.86	5.28	3.20	3.96	4.07	4.69	4.54	5.34	3.58	2.99	2.51	3.74
H2O	1.43	0.66	1.53	1.39	0.83	0.91	0.51	1.50	0.63	0.48	1.35	1.58	1.33
P2O5	0.22	0.50	0.10	0.36	0.16	0.24	0.14	0.77	0.15	0.23	0.19	0.19	0.19
CO2	0.11	0.17	0.14	0.15	0.00	0.23	0.22	0.18	0.20	0.18	0.11	0.12	0.18
Total	99.13	98.24	98.88	99.50	99.17	100.23	99.15	98.10	98.05	99.19	99.62	100.15	99.92
Ba	1194	1862	3098	1667	1285	1079	1338	1456	1359	1189	906	724	1127
Ce	110	214	127	153	136	77	110	141	134	133	61	46	84
Co	48	42	34	40	60	50	47	42	38	51	58	51	49
Cr	62	24	12	34	24	25	23	62	27	20	57	69	52
La	72	120	57	85	106	27	39	81	55	59	27	14	48
Nd	56	109	50	70	65	33	38	80	42	51	29	18	45
Ni	16	10	10	11	13	6	9	28	11	9	15	15	15
Pb	17	30	26	17	20	24	36	33	52	24	18	18	23
Rb	99	120	62	78	128	161	189	161	170	116	107	98	141
Sc	13	9	3	-1	4	5	2	19	1	5	10	9	8
Sr	1059	2583	2591	1869	1604	1428	1832	1854	1924	1595	944	854	924
Th	23	18	18	32	26	28	44	23	111	29	17	17	20
V	114	150	72	124	66	59	49	200	50	77	84	90	92
Y	26	42	17	28	24	18	16	27	21	22	13	13	24
Zn	77	89	34	65	36	46	42	101	43	46	61	72	78
Zr	214	291	255	245	194	177	200	134	404	206	159	147	156
Ti			3058	4023		2107	1646	5151	1917	2524	2940	3147	3027

modal mineralogy (percent)

	12a.24	12a.25	12a.27	12a.28	12b.12	12b.30	12b.31	12b.32	12b.33	12b.34	12b.35	12b.36	12b.37
Plag	35.40	22.00	33.00	28.80	39.30	45.80	24.60	36.40	19.80	32.4	40.60	41.40	40.80
ksp	18.90	37.00	50.40	32.80	17.10	24.00	50.00	17.20	60.40	25.20	14.00	10.10	16.40
Qz	20.70	28.00	2.80	11.40	29.00	21.60	12.60	5.00	11.80	24.00	20.80	28.20	19.60
Bio	11.60	5.00	1.20	12.80	4.80	2.60	3.00	7.20	0.00	7.60	13.80	10.10	13.60
Hb	10.10	5.50	1.00	0.00	0.00	1.40	4.80	8.80	2.60	0.00	0.00	4.10	0.00
cp	0.00	12.20	2.00	0.00	0.00	0.00	0.00	20.80	0.00	0.00	0.00	1.00	0.00
ep	3.40	1.00	7.60	11.60	9.80	4.40	3.60	3.20	3.80	9.00	10.80	4.80	8.60
opq	0.00	0.00	0.00	0.00	0.00	4.40	0.00	0.00	0.00	0.00	0.00	0.00	0.00
access.	0.90	2.30	2.00	2.60	0.00	0.20	1.40	1.40	1.60	1.80	0.00	0.30	1.00

normative mineralogy (percent)

	12a.24	12a.25	12a.27	12a.28	12b.12	12b.30	12b.31	12b.32	12b.33	12b.34	12b.35	12b.36	12b.37
Qz	16.58	1.01	0.95	7.21	14.72	15.96	9.28	1.18	2.11	13.65	16.89	17.86	15.99
or	17.67	28.27	31.20	18.91	23.40	24.05	28.16	27.83	32.46	21.47	18.00	15.08	22.46
ab	26.23	40.87	44.26	35.79	40.03	40.19	50.13	33.00	51.62	40.97	29.22	29.25	28.03
an	21.02	8.14	14.96	21.28	11.11	10.62	5.28	7.30	9.28	13.73	19.66	19.87	16.74
C	0.00	0.00	0.00	0.00	0.00	0.00	0.00	0.00	0.00	0.00	0.37	0.89	0.43
diwo	0.55	4.64	0.38	0.76	1.68	0.92	1.79	6.70	0.42	1.33	7.47	8.30	6.99
dien	0.37	4.01	0.33	0.65	1.45	0.80	1.54	4.89	0.36	1.15	6.22	7.08	5.01
difs	0.13	0.00	0.00	0.00	0.00	0.00	0.00	1.18	0.00	0.00	0.31	0.12	1.35
hyen	7.58	0.00	1.41	6.17	1.89	2.54	0.00	6.60	0.00	2.87	0.00	0.11	1.62
hyfs	2.76	0.00	0.00	0.04	0.00	0.00	0.00	1.59	0.00	0.00	0.00	0.00	0.44
mt	3.07	-1.02	0.98	5.06	2.81	2.13	1.87	6.03	1.52	2.94	3.66	3.97	2.87
he	0.00	7.22	1.69	0.00	0.10	0.58	0.29	0.00	0.70	0.45	0.00	0.00	0.00
iL	1.12	1.52	0.82	1.26	0.78	0.74	0.60	1.85	0.70	0.91	0.97	1.02	1.00
ap	0.52	1.18	0.24	0.87	0.38	0.57	0.34	1.89	0.37	0.55	0.46	0.46	0.46

Hornblende-bearing graanites: XRF analysis (whole rock major oxide and trace elements), modal mineralogy, normative mineralogy.

Sample	12c.4	12c.39	12c.40	12c.41	12c.42	12c.43	12c.44
SiO2	65.03	62.93	63.75	66.76	68.94	64.66	59.87
TiO2	0.44	0.33	0.30	0.36	0.40	0.45	0.67
Al2O3	15.31	17.22	17.80	15.27	16.11	16.19	18.04
Fe2O3	2.24	0.71	1.41	1.93	1.40	2.35	4.81
FeO	1.63	0.94	0.88	1.27	1.90	2.07	0.57
MnO	0.07	0.05	0.07	0.06	0.08	0.07	0.13
MgO	2.35	2.21	0.49	1.78	2.12	3.14	1.01
CaO	3.16	1.11	1.90	2.32	2.65	1.32	2.09
Na2O	4.00	5.68	5.95	3.79	3.28	3.92	5.37
K2O	2.96	4.85	4.41	3.29	3.14	3.91	4.89
H2O	1.81	1.74	1.59	1.51	0.53	1.60	1.20
P2O5	0.18	0.13	0.08	0.13	0.14	0.18	0.15
CO2	0.09	0.14	0.20	0.20	0.13	0.41	0.17
Total	99.27	98.04	98.83	98.67	100.68	100.27	98.97
Ba	712	1565	1180	821	787	1104	1857
Ce	53	155	59	55	55	86	256
Co	46	36	47	56	45	36	37
Cr	51	23	21	43	48	34	15
La	29	113	27	22	12	60	161
Nd	29	69	31	29	21	50	108
Ni	13	32	9	12	14	10	10
Pb	17	26	42	18	23	19	29
Rb	96	137	172	92	98	143	135
Sc	8	3	3	6	6	10	5
Sr	741	1248	1675	592	551	546	2006
Th	15	70	75	16	13	15	62
V	78	50	48	57	59	89	134
Y	18	23	13	13	16	26	27
Zn	20	15	42	18	34	28	51
Zr	164	256	238	134	127	159	400
Ti		1731	1551	2125	2204	2658	4453

modal mineralogy (percent)

	12c.4	12c.39	12c.40	12c.41	12c.42	12c.43	12c.44
Plag	46.20	51.60	44.40	50.60	44.30	54.20	49.00
Ksp	13.50	35.60	38.40	16.40	15.00	16.20	36.00
Qz	24.50	7.20	13.20	24.40	24.10	17.00	4.00
Bio	2.70	4.40	0.00	0.00	10.40	0.00	0.60
Hb	0.00	0.00	1.20	0.00	0.70	0.00	0.00
Chl	3.90	0.00	0.00	7.20	3.30	11.80	0.00
epi	9.20	0.00	2.00	1.40	2.20	0.00	9.00
opq	0.00	1.20	0.80	0.00	0.00	0.00	1.40
access.	0.00	0.00	0.00	0.00	0.00	0.80	0.00

normative mineralogy (percent)

	12c.4	12c.39	12c.40	12c.41	12c.42	12c.43	12c.44
Qz	17.28	4.70	7.66	22.44	25.93	18.16	2.33
or	17.49	28.66	26.06	19.44	18.56	23.11	28.90
ab	33.85	48.06	50.35	32.07	27.76	33.17	45.44
an	14.50	4.66	8.84	10.66	12.23	5.37	9.39
C	0.21	0.92	0.00	1.57	2.83	3.54	0.47
diwo	6.06	1.94	0.03	4.45	5.11	2.24	2.91
dien	4.89	1.54	0.02	3.69	3.50	1.73	2.52
difs	0.46	0.19	0.00	0.21	1.21	0.28	0.00
hyen	0.97	3.97	1.20	0.75	1.78	6.09	0.00
hyfs	0.09	0.50	0.08	0.04	0.61	0.97	0.00
mt	3.25	1.03	2.04	2.80	2.03	3.41	0.32
he	0.00	0.00	0.00	0.00	0.00	0.00	4.59
iL	0.84	0.63	0.57	0.68	0.76	0.85	1.27
ap	0.43	0.31	0.19	0.31	0.33	0.43	0.36

A2.2) Hornblende-bearing Granites: :Trace Elements Determined by I.N.A.A.
(all values in ppm: error given in brackets)

Sample	6.10	6.13a	6.16a	6.31	7.5	12a.24	12a.25	12a.28
La	81(1.93)	125 (3)	87 (2)	55 (1)	83(2.03)	110(2.59)	227(5.15)	83 (2)
Ce	206 (9.83)	230 (10)	220 (10)	122 (6)	189 (9.43)	208 (10)	484 (22)	195 (9)
Sm	22 (0.15)	14 (0.10)	14 (0.10)	10 (0.10)	16 (0.12)	17 (0.11)	39 (0.26)	12 (0.10)
Eu	2.39 (0.21)	14 (0.10)	14 (0.10)	10 (0.10)	1.74 (0.18)	1.73 (0.18)	4.30 (0.35)	3 (0.20)
Tb	1.61 (0.8)	0.80 (0.04)	0.72 (0.04)	0.76 (0.04)	1.83 (0.09)	1.62 (0.08)	3.23 (0.14)	1 (0.10)
U	5 (0.72)	3 (0.40)	4 (0.50)	4 (0.50)	9 (1.24)	3 (045)	7 (0.94)	2 (0.20)
Th	34.44 (1.35)	26 (1)	21 (1)	18 (1)	31 (1.22)	34 (1.32)	38 (1.51)	31 (0)
Ba	1637 (86)	1495 (80)	1755 (90)	1310 (70)	1023 (55)	1230 (65)	1944 (102)	1830 (95)
Rb	106 (6)	73 (40)	125 (7)	97 (5)	173 (9.09)	108 (6)	130 (7)	92 (5)
Sr	1538 (84)	1890 (100)	2200 (120)	1390 (80)	400 (23)	1107 (61)	2797 (152)	1910 (100)
Hf	11.19 (0.41)	7 (0.30)	8 (0.30)	5 (0.20)	18.41 (0.60)	9.45 (0.34)	12 (0.42)	7 (0.20)
Zr	602 (63)	290 (30)	480 (40)	250 (25)	812 (81)	549 (62)	695 (75)	330 (25)
Cs	4.62 (0.26)	2 (0.10)	4 (0.20)	6 (0.30)	10.61 (0.59)	3.41 (0.20)	1.48 (0.11)	1 (0.10)
Sc	10.49 (0.53)	7 (0.30)	8 (0.40)	9 (0.50)	9.69 (0.49)	14.61 (0.74)	10.90 (0.56)	13
(1)								
Ta	1.40 (0.6)	1 (0.10)	1 (0.10)	1 (0.10)	1.91 (08)	1.08 (0.05)	3.31 (0.24)	1 (0.10)
Co	36.67 (1.86)	66 (4)	32 (2)	60 93)	33.16 (1.69)	28.36 (1.45)	25.59 (1.31)	50 (30)

	12b.30	12b.31	12b.33	12b.37	12c.4	12c.40	12c.42	12c.44
La	31 (1)	42 (10)	56 (1)	47 (1)	40.05 (1.06)	32 (1)	14 (0.40)	170 (30)
Ce	114 (6)	150 (7)	180 (9)	91 (5)	73.68 (4.11)	92 (5)	51 (30)	350 (15)
Sm	8.50 (0.10)	9.30 (0.10)	10.30 (0.10)	8.30 (0.10)	7.07 (0.05)	9.70 (0.10)	3.70 (0.03)	19 (0.10)
Eu	2.10 (0.20)	2.10 (0.20)	2.10 (0.20)	1.70 (0.20)	0.96 (0.12)	1.90 (0.20)	1.10 (0.20)	3.60 (0.30)
Tb	0.71 (0.04)	0.73 (0.04)	0.80 (0.04)	0.87 (0.04)	0.96 (0.06)	0.66 (0.04)	0.44 (0.03)	1.30 (0.10)
U	4.40 (0.60)	6.90 (1)	11 (2)	4.00 (0.60)	5.23 (0.74)	1.20 (0.20)	2.10 (0.30)	11 (2)
Th	26 (1)	43 (2)	108 (4)	15 (1)	23.18 (091)	81 (3)	11.20 (0.40)	62 (2)
Ba	1175 (65)	1485 (80)	1495 (80)	1195 (65)	741 (39)	1425 (75)	895 (50)	1970 (100)
Rb	180 (10)	205 (11)	175 (9)	145 (8)	102 (5)	195 (11)	110 (6)	150 (8)
Sr	1520 (80)	1935 (100)	1950 (110)	900 (50)	747 (43)	1890 (100)	560 (30)	1965 (100)
Hf	5.60 (0.20)	5.60 (0.20)	9.30 (0.30)	5.30 (0.20)	7.55 (0.28)	7.30 (0.30)	3.60 (0.20)	9.00 (0.30)
Zr	215 (30)	285 (30)	530 (40)	<60	379 (51)	340 (35)	150 (25)	460 (35)
Cs	6.00 (0.30)	3.00 (0.20)	4.70 (0.30)	5.70 (0.30)	3.47 (0.20)	3.70 (0.20)	3.20 (0.20)	1.30 (0.10)
Sc	6.00 (0.30)	3.00 (0.20)	1.70 (0.10)	10 (1)	9.87 (0.50)	2.40 (0.10)	7.40 (0.40)	5.20 (0.30)
Ta	1.90 (0.10)	1.80 (0.10)	2.10 (0.10)	2.10 (0.10)	1.54 (0.06)	2.10 (0.10)	1.50 (0.10)	3.50 (0.10)
Co	69 (4)	61 (3)	47 (3)	66 (4)	26.46 (1.35)	66 (4)	61 (3)	51 (3)

Hornblende-bearing Granite: RNAA- rare earth elements

	6.13a	6.24	6.29a	6.30	12a.28	12b.30	12b.31	12b.32	12b.35	12c40	12c.42	12c.44
La	100	42	23	48	55	23	32	74	21	22	11	130
Ce	232	106	54	107	165	58	76	180	77	55	27	300
Pr	22	11	5.90	11	14	7.50	9	21	5.30	7	3.10	31
Nd	79	55	24	44	50	29	34	85	19	33	13	99
Sm	13	9.60	4.10	6.80	9.50	7.30	7.80	16	4.10	6.50	3.10	15
Eu	1.90	2.40	1.00	1,60	2.10	1.60	1.70	3.40	0.61	1.50	0.77	3.10
Gd	4.00	7.00	2.00	3.70	7.00	5.60	4.60	10	3.10	-	3.20	0.00
Tb	0.70	0.63	0.29	0.56	0.84	0.72	0.68	1.30	0.44	0.65	0.44	1.20
Dy	3.60	3.30	1.20	3.60	5.00	3.40	3.00	5.70	2.50	3.50	2.70	5.90
Ho	0.53	0.58	0.29	0.69	0.96	0.72	0.64	0.84	0.44	0.60	0.57	1.00
Er	-	-	-	-	-	-	-	-	-	-	-	-
Tm	-	-	-	-	-	-	-	-	0.18	-	-	-
Yb	1.00	1.00	0.64	2.00	2.00	2.00	1.70	1.90	1.10	1.50	1.80	2.40
Lu	0.16	0.14	0.09	0.30	0.28	0.28	0.23	0.28	0.17	0.25	0.33	0.41

A2.3) Hornblende-free Granites: XRF analysis (whole rock major oxides and trace elements), modal mineralogy,
normative mineralogy.

Sample	1.1	1.7	1.10a	1.19a	1.22a	1.24	1.25	1.26	2.1	2.2	2.5
SiO2	68.03	64.47	65.07	64.65	68.52	66.08	66.08	70.78	73.15	74.45	74.65
TiO2	0.69	0.77	0.86	1.01	0.60	0.75	0.78	0.49	0.33	0.21	0.17
Al2O3	15.17	14.83	15.03	14.40	14.98	14.46	14.42	13.82	13.36	13.23	13.39
Fe2O3	2.58	1.24	2.03	2.08	1.90	1.57	1.83	1.12	0.26	0.71	0.95
FeO	1.80	3.76	3.69	4.05	1.74	3.57	3.49	2.35	0.95	0.97	0.51
MnO	0.06	0.10	0.10	0.11	0.07	0.11	0.11	0.08	0.02	0.05	0.05
MgO	0.83	0.97	1.10	1.23	0.64	1.01	0.82	0.54	0.12	-0.05	0.02
CaO	1.06	2.67	2.14	2.86	1.35	2.41	2.61	1.43	1.34	0.98	0.85
Na2O	3.68	3.50	3.16	3.45	2.90	3.39	3.12	3.44	3.19	2.88	2.39
K2O	3.34	4.42	4.29	3.71	4.53	4.12	4.18	4.50	4.72	5.21	4.85
H2O	1.58	1.08	1.40	1.30	2.02	1.42	1.23	1.05	0.55	0.51	0.70
P2O5	0.19	0.31	0.30	0.28	0.17	0.25	0.26	0.14	0.08	0.06	0.04
CO2	0.16	0.31	0.13	0.16	0.29	0.23	0.24	0.21	0.17	0.07	0.22
Total	99.17	98.43	99.30	99.29	99.71	99.85	99.17	99.95	98.24	98.56	98.79
Ba	679	1070	960	1033	705	777	778	429	510	128	153
Ce	55	95	94	99	110	101	119	51	86	43	53
Co	51	41	49	49	51	46	46	54	74	58	78
Cr	22	12	8	10	10	11	7	18	12	11	11
La	30	56	50	75	47	56	68	24	54	17	54
Nd	28	50	52	69	45	54	58	27	54	28	34
Ni	9	6	4	0.42	11	4	11	4	9	7	6
Pb	22	19	23	22	25	20	20	24	34	35	33
Rb	131	138	129	121	155	126	133	158	115	151	97
Sc	7	7	6	9	10	8	5	5	0	0.44	0.67
Sr	153	251	280	255	192	245	240	168	159	74	75
Th	25	14	14	15	20	16	19	18	33	28	28
V	38	44	49	65	34	40	39	22	14	6	6
Y	27	33	37	44	31	33	34	28	10	20	15
Zn	83	81	90	90	66	84	86	65	39	40	24
Zr	365	382	400	516	295	373	402	268	232	151	142
Ti	n.d.	n.d.	5005	5815	3568	4401	4477	2698	n.d.	1075	789
Plag	n.d.	38.22	34.24	39.00	36.80	38.06	29.44	29.64	23.20	17.80	23.80
ksp	n.d.	20.00	24.48	22.00	22.40	24.02	25.76	30.44	51.20	28.40	27.80
Qz	n.d.	26.25	23.20	25.00	20.88	23.44	28.48	29.02	20.30	45.20	39.80
Bio	n.d.	15.26	18.08	11.50	17.92	14.48	16.32	8.32	3.60	6.80	0.60
Musc	n.d.	0.00	0.00	0.00	0.00	0.00	0.00	0.00	0.50	1.6	7.20
Grn	n.d.	0.00	0.00	0.00	0.00	0.00	0.00	0.00	0.00	0.20	0.00
opq	n.d.	0.00	0.00	1.50	0.00	0.00	0.00	2.08	0.00	0.00	0.80
access.	n.d.	0.27	0.00	1.00	2.00	0.00	0.00	0.50	1.20	0.00	0.00
Qz	29.93	16.29	21.26	18.60	29.39	20.95	21.68	27.49	31.91	34.42	39.59
or	19.74	26.12	25.35	21.93	26.77	24.35	24.70	26.59	27.89	30.79	28.66
ab	31.14	29.62	26.74	29.19	24.54	28.69	26.40	29.11	29.54	24.37	20.22
an	4.02	11.22	8.66	12.36	5.59	10.32	11.25	6.18	6.13	4.47	3.96
c	4.03	0.18	2.02	0.18	3.36	0.64	0.64	1.03	0.76	1.21	2.76
diwo	1.68	4.69	3.62	5.16	2.33	4.31	4.70	2.58	1.25	0.86	0.06
dien	1.38	1.61	1.51	2.22	1.48	1.64	1.68	0.88	0.30	0.02	0.05
difs	0.10	3.20	2.13	3.01	0.71	2.75	3.13	1.78	1.02	0.94	0.00
hyen	0.69	0.80	1.23	0.89	0.12	0.88	0.37	0.47	0.00	0.00	0.00
hyfs	0.05	1.59	1.74	1.24	0.06	1.48	0.68	0.95	0.00	0.00	0.00
mt	3.74	1.80	2.94	3.02	2.75	2.28	2.65	1.62	0.38	1.03	1.31
he	0.00	0.00	0.00	0.00	0.00	0.00	0.00	0.00	0.00	0.00	0.04
iL	1.31	1.46	1.63	1.92	1.14	1.42	1.48	0.93	0.63	0.40	0.32
ap	0.45	0.73	0.71	0.66	0.40	0.59	0.62	0.33	0.19	0.14	0.09

Hornblende-free Granites: XRF analysis (whole rock major oxdies and trace elements), modal mineralogy, normative mineralogy.

Sample	4a.1	4b.1	5.1	5.9	5.11	5.12	9.1a	9.2	9.5a	9.17
SIO2	75.49	74.95	71.87	73.60	68.74	71.50	70.75	71.81	72.03	72.07
TIO2	0.22	0.26	0.19	0.18	0.46	0.31	0.31	0.26	0.27	0.36
Al2O3	12.51	12.44	14.65	14.59	16.01	15.34	15.08	15.11	14.63	14.88
Fe2O3	0.17	0.28	0.14	0.23	0.32	0.31	0.23	0.52	0.57	1.42
FeO	0.77	1.01	0.46	0.37	1.58	0.94	1.34	0.64	0.59	0.31
MnO	0.03	0.03	0.04	0.06	0.06	0.06	0.05	0.05	0.05	0.04
MgO	0.11	0.10	0.27	0.23	0.84	0.56	0.57	0.41	0.50	0.75
CaO	0.68	0.75	1.19	0.82	2.21	1.52	1.71	1.06	1.29	1.25
Na2O	2.70	2.96	4.52	3.78	3.94	4.05	4.28	3.44	3.31	2.06
K2O	5.07	5.22	4.28	4.17	3.96	4.03	4.06	4.74	4.79	4.01
H2O	0.52	0.67	0.53	0.78	1.00	0.81	0.69	1.00	0.98	1.64
P2O5	0.16	0.11	0.05	0.09	0.12	0.09	0.10	0.16	0.11	0.19
CO2	0.10	0.14	0.23	0.11	0.28	0.21	0.11	0.13	0.20	0.30
Total	98.53	98.25	98.42	99.01	99.52	99.77	99.05	99.33	99.31	99.73
Ba	321	643	281	244	803	533	587	362	476	512
Ce	20	41	29	23	59	27	48	23	23	11
Co	76	79	58	65	51	55	63	51	59	48
Cr	19	25	19	14	12	11	24	12	16	27
La	6	22	16	16	17	10	27	13	11	3
Nd	16	25	16	13	30	13	24	16	14	11
NI	11	8	11	6	5	6	10	6	6	9
Pb	17	22	39	37	35	36	31	25	38	20
Rb	153	175	156	178	117	158	154	230	178	147
Sc	3	3	2	0.5	4	2	3	1	4	4
Sr	228	131	175	199	427	291	209	125	165	120
Th	7	15	19	13	18	18	13	13	18	4
V	12	13	11	11	33	21	24	22	15	33
Y	36	44	14	8	7	8	13	10	14	14
Zn	10	12	34	26	48	35	33	51	46	48
Zr	96	137	67	57	185	131	131	101	131	166
TI				842	2607	1626		1415	1455	2160
Plag	35.70	33.40	42.00	42.00	41.40	40.80	11.20	27.90	22.20	n.d.
ksp	22.30	18.30	19.80	20.20	16.40	19.20	39.40	33.20	30.60	n.d.
Qz	31.40	40.50	26.30	31.20	32.20	31.80	29.60	30.10	28.40	n.d.
Bio	2.50	3.30	5.90	1.40	3.80	5.00	0.00	1.80	0.00	n.d.
Musc	8.10	4.50	4.00	5.20	6.20	3.20	16.20	7.00	13.40	n.d.
Chl	0.00	0.00	1.10	0.00	0.00	0.00	0.60	0.00	3.00	n.d.
Gar	0.00	0.00	0.00	0.00	0.00	0.00	3.00	0.00	0.00	n.d.
epl	0.00	0.00	0.00	0.00	0.00	0.00	0.00	0.00	2.40	n.d.
Qz	38.27	35.09	24.96	32.91	21.91	26.69	30.13	23.55	29.90	40.41
or	29.96	30.85	25.29	24.64	23.40	23.82	28.01	23.99	28.31	23.70
ab	22.85	25.05	38.25	31.99	33.34	34.27	29.11	36.22	28.01	17.83
an	2.33	3.00	5.58	3.48	10.18	6.95	4.21	7.83	5.68	4.96
C	1.75	0.82	0.54	2.58	1.56	1.77	2.78	0.77	1.92	5.33
diwo	0.97	1.25	1.21	0.93	4.17	2.56	1.54	3.32	1.67	2.07
dien	0.23	0.22	0.67	0.57	2.09	1.39	1.02	1.42	1.25	1.79
difs	0.80	1.13	0.49	0.30	1.99	1.07	0.41	1.85	0.26	0.00
hyen	0.05	0.02	0.00	0.00	0.00	0.00	0.00	0.00	0.00	0.08
hyfs	0.16	0.12	0.00	0.00	0.00	0.00	0.00	0.00	0.00	0.00
mt	0.25	0.41	0.20	0.33	0.46	0.45	0.75	0.00	0.83	0.09
he	0.00	0.00	0.00	0.00	0.00	0.00	0.00	0.00	0.00	1.36
iL	0.42	0.49	0.36	0.34	0.87	0.59	0.49	0.59	0.51	0.68
ap	0.38	0.26	0.12	0.28	0.29	0.21	0.38	0.24	0.26	0.45

Hornblende-free granites: XRF analysis (whole rock major oxide and trace elements), modal mineralogy, normative mineralogy.

Sample	9.19	9.20	9.22	9.23	10.1	10.2	10.3	11.1	13.1	1D-14	(Trondhjemite dyks) 3a.1	3a.2	3a.4	15
SiO2	72.95	72.88	73.6	73.80	75.14	73.53	69	75.39	66.65	64.57	76.87	75.24	60.95	77.30
TiO2	0.13	0.26	0.12	0.14	0.09	0.11	0.13	0.17	0.17	0.16	0.12	0.15	0.15	0.19
Al2O3	15.26	4.85	15.08	14.81	13.39	16.26	18.79	15.19	17.05	19.57	13.15	13.05	20.39	11.95
Fe2O3	0.36	0.26	0.00	0.11	0.09	0.09	0.92	0.08	2.28	0.78	0.01	0.45	1.57	1.02
FeO	0.12	0.72	0.31	0.28	0.10	0.21	0.31	0.14	0.27	1.65	0.09	0.39	0.31	1.73
MnO	0.04	0.05	0.05	0.04	0.14	0.08	0.03	0.04	0.02	0.02	0.02	0.03	0.04	0.04
MgO	0.09	0.40	-0.02	0.15	0.03	0.08	0.21	0.55	0.27	0.89	0.01	0.10	0.14	0.39
CaO	0.95	1.27	1.13	0.65	1.21	1.78	0.15	0.77	0.88	1.35	1.77	1.87	4.34	1.86
Na2O	3.11	3.14	4.23	3.70	4.22	4.33	3.96	3.42	9.09	8.99	7.76	7.77	9.83	5.16
K2O	4.68	4.85	3.94	4.08	2.37	2.72	5.47	2.49	1.04	0.85	0.07	0.15	0.10	0.06
H2O	0.98	0.83	0.47	0.99	1.00	0.81	0.65	0.68	0.56	0.60	0.28	0.48	0.43	0.64
P2O5	0.10	0.16	0.05	0.09	0.03	0.04	0.03	0.16	0.06	0.04	0.04	0.04	0.04	0.04
CO2	0.15	0.19	0.10	0.13	0.81	0.72	0.66	0.26	0.85	n.d.	0.07	0.11	0.34	n.d.
Total	98.92	99.83	99.16	99.02	99.02	100.76	101.06	99.34	99.20	99.47	100.26	99.85	98.63	100.38
Ba	505	444	61	174	107	691	349	524	75	85	-12	9	-69	n.d
Ce	14	31	20	6	11	7	13	5	73	274	-24	13	7	n.d.
Co	54	52	59	65	53	50	64	38	57	40	87	66	49	n.d.
Cr	18	22	17	27	13	22	24	19	15	11	-5	20	18	n.d.
La	4	18	10	4	9	4	7	4	46	221	4	9	4	n.d
Nd	13	21	14	8	13	6	10	8	23		-12	10	10	n.d
Ni	8	8	8	11	5	11	11	8	5	1	7	10	7	n.d
Pb	45	31	36	34	11	15	22	7	8	13	7	6	6	n.d
Rb	155	217	218	149	98	76	81	199	11	15	-2	2	-0.22	n.d
Sc	3	2	1	2	3	2	5	3	-1	0	1	2	3	n.d
Sr	158	133	59	97	101	355	99	28	104	132	-3	118	167	n.d
Th	4	10	7	2	12	5	3	8	20	22	4	2	2	n.d
V	3	15	6	8	8	3	12	18	7	30	5	9	107	n.d
Y	14	13	11	9	56	10	15	42	23	49	9	9	23	n.d
Zn	21	51	24	20	15	17	6	36	8	30	1	9	2	n.d
Zr	32	108	34	32	121	65	54	94	844	1086	47	77	91	n.d
Ti	672	1404	466	589		521	812	572					547	n.d
Plag	9.20	12.20	26.60	15.80	38.50	29.80	n.d.	n.d.	n.d.	n.d.	70.80	69.10	67.40	n.d
ksp	29.20	38.20	37.40	32.40	8.20	26.20	n.d.	n.d.	n.d.	n.d.	0.00	0.00	2.20	n.d
Qz	40.40	33.20	22.20	39.60	34.20	31.80	n.d.	n.d.	n.d.	n.q.	27.40	29.60	23.80	n.d
Bio	0.00	2.20	1.00	0.00	3.80	0.00	n.d.	n.d.	n.d.	n.d.	1.80	0.00	3.80	n.d
Hb	0.00	0.00	0.00	0.00	0.00	0.00	n.d.	n.d.	n.d.	n.d.	0.00	1.30	1.40	n.d
Musc	21.20	14.20	12.20	12.20	15.30	12.20	n.d.	n.d.	n.d.	n.d.	0.00	0.00	0.00	n.d
Gar	0.00	0.00	0.60	0.00	0.00	0.00	n.d.	n.d.	n.d.	n.d.	0.00	0.00	0.00	n.d
opq	0.00	0.00	0.00	0.00	0.00	0.00	n.d.	n.d.	n.d.	n.d	0.00	0.00	1.40	n.d
Qz	34.18	31.70	30.35	34.61	37.61	32.13	25.11	43.35	7.96	2.54	29.24	27.24	0.00	n.d.
or	27.66	28.66	23.28	24.11	14.01	16.07	32.33	14.72	6.15	5.02	0.14	0.89	0.59	n.d
ab	26.32	26.57	35.79	31.31	35.71	36.64	33.51	28.94	76.96	76.07	65.67	65.75	74.80	n.d.
an	4.06	5.26	5.28	2.64	5.81	8.57	0.55	2.78	2.65	6.44	0.84	0.29	11.22	n.d
C	3.59	2.51	1.92	3.34	1.75	3.05	6.15	5.85	0.00	1.50	0.00	0.00	0.00	n.d
diwo	0.27	1.83	0.40	0.67	0.28	0.48	0.23	1.16	0.55	2.69	0.03	0.42	0.40	n.d
dien	0.22	1.00	0.00	0.37	0.07	0.20	0.20	1.00	0.48	1.33	0.02	0.25	0.35	n.d
difs	0.00	0.77	0.46	0.27	0.22	0.28	0.00	0.00	0.00	1.30	0.00	0.15	0.00	n.d
wo	1.44	0.36	1.80	0.43	2.14	3.10	0.00	0.00	0.00	0.00	3.18	3.22	3.79	n.d
hyen	0.00	0.00	0.00	0.00	0.00	0.00	0.33	0.37	0.20	0.88	0.00	0.00	0.00	n.d
hyfs	0.00	0.00	0.00	0.00	0.00	0.00	0.00	0.00	0.00	0.86	0.00	0.00	0.00	n.d
mt	0.14	0.38	0.01	0.16	0.13	0.13	0.72	0.09	0.44	1.13	0.00	0.65	0.69	n.d
he	0.26	0.00	0.00	0.00	0.00	0.00	0.42	0.02	1.97	0.00	0.00	0.00	1.09	n.d
iL	0.25	0.49	0.23	0.27	0.17	0.21	0.25	0.32	0.32	0.30	0.23	0.28	0.28	n.d.
ap	0.24	0.38	0.12	0.21	0.07	0.09	0.07	0.38	0.14	0.09	0.09	0.09	0.09	n.d

A2.4) Hornblende-free Granites: Trace Elements Determined by I.N.A.A.

(all values in ppm; error given in brackets)

Sample	1.1	1.7	1.24	1.26	2.1	4a.1	4b.1	4b.2
La	28.78 (0.84)	61.04 (1.46)	58 (1)	24 (1)	51.04 (1.240	4.20 (0.28)	20.34 (0.61)	52.79 (1.34)
Ce	50.95 (2.73)	115 (5.20)	125 (6)	60 (3)	88.36 (4.13)	26.98 (1.68)	45.37 (2.46)	111 (5.59)
Sm	4.69 (0.34)	9.76 (0.07)	9.50 (0.10)	6.00 (0.10)	7.47 (0.05)	5.00 (0.10)	4.58 (0.36)	12.28 (0.08)
Eu	1.06 (0.15)	2.19 (0.21)	1.90 (0.20)	1.30 (0.10)	0.94 (0.13)	0.20 -	0.61 (0.13)	0.67 (0.11)
Tb	0.77 (0.07)	1.20 (0.05)	1.10 (0.10)	0.92 (0.04)	0.52 (0.03)	0.82 (0.04)	1.16 (0.05)	1.61 (0.08)
U	4.50 (0.64)	2.35 (0.33)	2.60 (0.40)	1.90 (0.30)	2.21 (0.32)	2.11 (0.30)	5.76 (0.81)	2.85 (0.41)
Th	23.59 (0.94)	13.98 (0.55)	16 (1)	19 (1)	33.91 (1.33)	9.68 (0.38)	14.68 (0.58)	22.25 (0.88)
Ba	708 (37)	1192 (61)	815 (45)	510 (25)	576 (30)	401 (22)	752 (39)	332 (18)
Rb	141 (7.21)	158 (8.13)	135 (7)	185 (10)	123 (6.39)	171 (9)	201 (10)	56 (3.10)
Sr	158 (13)	257 (17)	240 (16)	140 (10)	157 (11)	236 (15)	155 (12)	266 (160
Hf	9.69 (0.31)	8.95 (0.29)	10.00 (0.30)	7.90 (0.30)	6.28 (0.21)	3.43 (0.13)	4.33 (0.16)	12.66 (0.42)
Zr	429 (37)	488 (40)	485 (40)	375 (30)	246 (24)	131 (21)	193 (26)	535 (56)
Cs	2.74 (0.15)	3.42 (0.19)	4.00 (0.20)	5.30 (0.30)	1.32 (0.08)	0.70 (0.05)	2.35 (0.13)	2.62 (0.15)
Sc	8.81 (0.45)	9.31 (0.47)	1.63 (0.10)	5.00 (0.30)	1.63 (0.10)	3.10 (0.17)	3.73 (0.20)	3.43 (0.19)
Ta	3.17 (0.12)	2.95 (0.11)	3.30 (0.10)	4.00 (0.20)	1.39 (0.05)	1.55 (0.06)	1.71 (0.07)	1.15 (0.05)
Co	68 (4)	62 (3)	65 (3)	76 (4)	62 (3)	65 (3)	73 (4)	43 (2.17)

	5.11	9.2	9.22	10.1	3a.1	3a.2	3b.1	3c.3	8.2
La	43 (1)	51.15 (1.32)	13.70 (0.40)	18.09 (0.57)	3.06 (0.27)	115.07 (2.63)	4.08 (0.27)	12.91 (0.73)	24.25
Ce	79 (4)	101 (5.23)	29 (2)	38.79 (2.77)	8.55 (0.88)	14.73 (1.03)	3.48 (0.99)	7.84 (1.45)	53.99
Sm	4.40 (0.10)	6.74 (0.05)	3.60 (0.05)	5.23 (0.04)	1.14 (0.01)	1.03 0.01	3.39 (0.03)	3.20 (0.03)	4.92
Eu	1.30 (0.10)	0.88 (0.12)	0.60 (0.10)	0.53 (0.10)	0.95	0.37 (0.10)	0.64 (0.13)	1.01	1.11
Tb	0.31 (0.02)	0.85 (0.05)	0.42 (0.03)	1.93 (0.09)	0.23 (0.02)	0.16 (0.02)	0.76 (0.04)	0.28 (0.03)	0.64
U	1.80 (0.20)	5.76 (0.810	5.10 (0.70)	5.23 (0.04)	0.28 (0.06)	0.40 (0.8)	0.56 (0.90)	8.29 (1.17)	1.86
Th	20 (1)	20.69 (0.81)	5.90 (0.20)	16.66 (0.66)	0.43 (0.02)	2.39 (0.10)	0.63 (0.28)	2.5 (1.01)	21.58
Ba	880 (45)	656 (34)	160 (15)	164 (11)	17 (4.96)	52 (5.51)	67 (7.19)	297 (17.51)	918
Rb	130 (7)	167 (9)	230 (12)	106 (6)	2.45	2.96 (0.73)	3.33 (0.82)	34.24 (2.12)	76
Sr	390 (20)	211 (14)	60 (8)	88 (9)	34 (6.33)	119 (8.79)	65 (8.45)	117 (11.57)	527
Hf	4.80 (0.20)	6.02 (0.26)	1.50 (0.10)	8.80 (0.32)	2.3 (0.09)	2.45 (0.10)	3.24 (0.13)	1.35 (0.10)	4.91
Zr	210 (20)	278 (47)	<65 -	244 (44)	45 (16.25)	81 (15.42)	44.45 (16.25)	89.13 (20.42)	299
Cs	3.60 (0.20)	5.72 (0.32)	5.00 (0.30)	3.72 (0.22)	0.07	0.08 (0.009)	0.14 (0.03)	2.21 (0.13)	2.05
Sc	4.20 (0.20)	3.29 (0.18)	1.20 (0.10)	2.98 (0.16)	1.08 (0.07)	1.93 (0.11)	9.84 (0.50)	2.77 (0.16)	3.38
Ta	1.10 (0.10)	2.80 (0.11)	2.20 (0.10)	3.19 (0.12)	1.33 (0.05)	0.95 (0.04)	0.97 (0.04)	8.51 (0.31)	1.49
Co	66 (4)	36.90 (1.88)	76 (4)	30.69 (1.56)	0.69	0.67	68.98	0.73	42.09

Hornblende-Free Granites: RNAA - rare earth elements.

	1.10a	1.19a	1.26	9.23
La	46	57	19	4.60
Ce	106	104	50	13
Pr	13	14	5.10	1.00
Nd	44	56	19	4.80
Sm	8.10	10	4.30	1.00
Eu	1.90	2.00	1.10	0.44
Gd	7.60	6.70	4.30	1.30
Tb	1.00	1.10	0.63	0.21
Dy	6.40	7.60	4.40	1.30
Ho	1.10	1.30	0.86	0.18
Er	-	-	-	-
Tm	-	-	-	-
Yb	3.00	3.70	2.50	0.58
Lu	0.41	0.45	0.37	0.18

A2.5) Granitic rocks to the west of WBF and North of Bixter Voe: XRF analysis (whole rock major oxides and trace elements), modal mineralogy, normative mineralogy.

Sample	14.1	14.2	14.3	14.4	14.5	14.6	14.7	14.8	14.9	14.10	14.11	14.13	14.14	14.15
SiO_2	73.50	55.13	73.77	73.00	52.17	46.74	54.38	77.41	50.63	76.02	51.63	76.30	74.04	76.71
TiO_2	0.18	1.19	0.24	0.24	0.61	0.27	1.06	0.11	1.18	0.12	1.24	0.12	0.14	0.12
Al_2O_3	13.68	15.91	13.32	13.66	16.58	23.64	15.95	12.33	16.22	12.32	15.65	12.19	13.31	12.55
Fe_2O_3	1.34	2.56	0.61	0.64	1.79	1.57	2.22	0.73	4.95	0.57	4.87	0.84	0.62	0.59
FeO	0.43	5.76	0.50	0.52	3.88	3.25	5.66	0.27	3.85	0.19	4.47	0.31	0.39	0.17
MnO	0.05	0.02	0.03	0.05	0.10	0.09	0.12	0.03	0.14	0.03	0.15	0.04	0.05	0.03
MgO	0.06	4.50	0.14	0.32	8.12	11.82	4.41	-0.06	6.26	-0.03	5.56	-0.11	-0.04	-0.11
CaO	0.63	6.55	0.92	1.03	8.65	9.04	7.01	0.39	7.61	0.34	6.80	0.20	0.47	0.29
Na_2O	4.59	3.48	4.34	4.06	3.15	1.26	3.33	4.49	4.05	4.62	4.72	4.27	4.38	4.63
K_2O	5.05	1.72	4.18	4.12	0.71	0.66	1.97	4.34	0.77	4.27	0.69	4.30	4.40	4.44
H_2O	0.34	1.68	0.61	0.48	3.26	2.19	2.12	0.35	2.31	0.40	2.04	0.41	0.44	0.40
P_2O_5	0.07	0.24	0.05	0.05	0.08	0.07	0.17	0.02	0.30	0.01	0.23	0.02	0.02	0.04
CO_2	0.23	0.22	0.19	0.13	0.23	0.15	0.25	0.10	0.19	0.18	0.25	0.22	0.16	0.13
Total	100.15	98.97	98.90	98.30	99.33	100.75	98.65	100.57	98.46	99.07	98.30	99.26	98.42	100.12
Ba	93	709	472	563	281	100	802	134	992	39	976	63	60	35
Ce	221	50	59	63	11	5	53	66	55	27	48	55	64	33
Co	76	46	67	62	44	49	48	50	34	63	48	57	43	75
Cr	11	155	20	24	257	1015	128	25	107	21	187	29	37	22
La	142	30	38	40	7	3	30	41	32	14	23	27	21	12
Nd	88	30	32	30	11	5	34	40	37	17	33	37	22	15
Ni	6	54	10	15	95	210	54	10	53	9	56	8	14	7
Pb	17	8	13	24	10	7	13	14	17	19	18	14	19	14
Rb	134	40	92	137	16	18	45	148	16	160	12	198	135	169
Sc	3	27	1	1	38	12	28	-0.3	30		1	310.27	0.12	0.24
Sr	30	427	158	116	449	395	443	37	1261	19	883	26	45	16
Th	20	5	26	28	5	0.5	6	24	7	25	4	29	22	25
V	3	177	14	12	140	51	170	2	206	5	211	2	4	3
Y	43	30	26	25	16	7	31	54	25	28	27	43	22	32
Zn	33	58	8	24	31	71	55	16	78	16	78	40	88	12
Zr	391	188	186	167	48	20	210	124	122	117	140	195	136	129
Ti		6796	1222	1284	3180	1318	5779	385	6870	445	6845	393	508	412

modal mineralogy (percent)

	14.1	14.2	14.3	14.4	14.5	14.6	14.7	14.8	14.9	14.10	14.11	14.13	14.14	14.15
Plag	0.00	n.d.	27.00	29.20	n.d.	n.d.	44.40	4.80	n.d.	10.60	n.d.	3.20	19.00	4.60
ksp	60.20	n.d.	50.60	43.40	n.d.	n.d.	4.60	54.40	n.d.	60.40	n.d.	58.40	52.20	56.20
Qz	32.20	n.d.	20.40	24.60	n.d	n.d.	8.60	38.20	n.d.	27.80	n.d.	37.10	27.40	36.70
Aeg	6.20	n.d.	2.00	0.00	n.d.	n.d.	0.00	1.80	n.d.	0.70	n.d.	1.30	1.40	2.50
Bio	0.00	n.d.	0.00	1.60	n.d.	n.d.	3.80	0.00	n.d.	0.00	n.d.	0.00	0.00	0.00
Hb	0.00	n.d.	0.00	1.20	n.d.	n.d.	37.40	0.00	n.d.	0.00	n.d.	0.00	0.00	0.00
opq	0.00	n.d.	0.00	0.00	n.d.	n.d.	1.20	0.80	n.d.	0.50	n.d.	0.00	0.00	0.00
access.	1.50	n.d.	0.00	0.00	n.d.	n.d.	0.00	0.00	n.d.	0.00	n.d.	0.00	0.00	0.00

normative mineralogy (prcent)

	14.1	14.2	14.3	14.4	14.5	14.6	14.7	14.8	14.9	14.10	14.11	14.13	14.14	14.15
Qz	26.41	6.95	29.54	29.98	1.41	0.00	5.51	34.13	1.33	32.38	0.97	34.43	30.25	32.44
or	29.84	10.16	24.70	24.35	4.20	-3.50	11.64	25.65	4.55	25.23	4.08	25.41	26.00	26.24
ab	38.84	29.45	36.37	34.36	26.66	0.00	28.18	37.99	34.27	39.09	39.94	36.13	37.06	39.10
an	1.81	22.71	4.24	4.78	29.01	44.39	22.76	0.67	23.81	0.27	19.84	0.86	2.20	0.35
C	1.52	0.00	0.10	0.77	0.00	4.58	0.00	0.00	0.00	0.00	0.00	0.20	0.54	0.00
diwo	0.17	3.43	0.47	1.03	5.59	18.54	4.56	0.03	5.01	0.03	5.33	0.03	0.09	0.03
dien	0.15	2.04	0.35	0.80	4.09	14.39	2.65	0.02	4.07	0.02	4.06	0.02	0.02	0.02
difs	0.00	1.22	0.07	0.12	0.98	2.15	1.70	0.00	0.34	0.00	0.71	0.00	0.07	0.00
wo	0.19	0.00	1.30	0.97	0.00	0.00	0.00	0.44	0.00	0.54	0.00	0.33	0.83	0.32
hyen	0.00	9.17	0.00	0.00	16.14	0.00	8.34	0.00	11.52	0.00	9.78	0.00	0.00	0.00
hyfs	0.00	5.50	0.00	0.00	3.85	0.00	5.34	0.00	0.95	0.00	1.71	0.00	0.00	0.00
olfo	0.00	0.00	0.00	0.00	0.00	10.55	0.00	0.00	0.00	0.00	0.00	0.00	0.00	0.00
olfa	0.00	0.00	0.00	0.00	0.00	1.76	0.00	0.00	0.00	0.00	0.00	0.00	0.00	0.00
mt	1.03	3.71	0.88	0.90	2.60	2.28	3.34	0.65	7.18	0.36	7.06	0.78	0.90	0.30
he	0.63	0.00	0.00	0.00	0.00	0.00	0.00	0.28	0.00	0.32	0.00	0.30	0.00	0.38
iL	0.34	2.26	0.46	0.46	1.16	0.51	2.01	0.21	2.24	0.23	2.36	0.23	0.27	0.23
ap	0.17	0.57	0.12	0.12	0.19	0.17	0.40	0.05	0.71	0.02	0.54	0.05	0.05	0.09

Granites from the west of WBF and North of Bixter Voe: XRF analysis (whole rock major oxides and trace elements),
modal mineralogy, normative mineralogy.

Sample	1	A	B	2	15.1	15.5	15.6	16.1	16.2	16.3	16.4	17.1	17.2	17.3	18.1	18.3	18.4
SiO2	76.90	74.57	71.66	64.75	74.45	77.63	74.91	77.93	72.43	71.46	75.68	73.89	70.97	75.71	73.19	74.95	75.54
TiO2	0.07	0.02	nill	0.31	0.20	0.18	0.18	0.14	0.26	0.19	0.17	0.16	0.30	0.20	0.21	0.15	0.15
Al2O3	12.20	13.39	13.28	18.25	12.89	13.06	12.93	12.74	13.72	14.70	12.57	13.35	14.11	13.26	13.57	13.25	13.19
Fe2O3	0.96	1.46	1.24	0.29	0.86	0.57	0.55	0.30	1.07	1.00	0.62	0.02	1.19	1.54	0.93	0.53	0.77
F2O	0.27	0.32	0.10	0.80	0.30	0.36	0.46	0.17	0.66	0.33	0.38	0.31	1.36	0.45	0.37	0.39	0.26
MnO	0.01	n.d.	nill	0.02	0.02	0.04	0.03	0.03	0.05	0.03	0.03	0.02	0.06	0.04	0.05	0.03	0.04
MgO	0.12	0.08	0.64	4.68	0.08	-0.05	0.39	0.03	0.18	0.08	0.01	0.24	0.39	0.26	0.03	0.09	-0.07
CaO	0.29	0.24	2.24	0.91	0.30	0.53	0.33	0.59	0.94	0.99	0.51	0.48	0.55	0.19	0.62	0.32	0.48
Na2O	4.10	4.72	5.37	4.92	4.25	4.30	4.24	3.80	4.37	4.57	3.97	7.60	0.59	2.55	4.57	4.44	4.46
K2O	4.57	4.72	4.84	2.21	5.27	4.56	4.36	4.79	4.50	4.79	4.74	0.51	6.25	5.35	4.64	4.66	4.55
H2O	0.12	0.49	0.45	2.65	0.31	0.28	0.53	0.38	0.58	0.42	0.42	0.50	1.09	0.99	0.51	0.44	0.48
P2O5	0.01	0.14	0.18	0.01	0.05	0.04	0.02	0.03	0.06	0.03	0.03	0.03	0.05	0.03	0.03	0.01	0.04
CO2	0.01	-0.00	nill	0.10	0.02	0.14	0.14	0.19	0.12	0.19	0.17	0.04	0.77	0.51	0.17	0.28	0.34
Total	100.19	100.01	100.00	99.95	99.33	101.69	99.07	101.12	98.84	98.78	99.30	97.15	99.68	101.08	98.89	99.53	100
Ba					594	296	443	496	645	1139	304	-11	1262	607	509	225	109
Ce		All of them			111	80	80	38	67	54	51	23	50	20	77	39	44
Co					73	56	64	57	50	52	60	50	61	59	54	66	85
Cr		not			11	26	24	24	26	25	23	11	25	26	26	29	25
La					76	53	37	29	49	41	30	20	30	29	39	7	21
Nd					52	37	30	19	33	28	25	17	32	25	30	8	19
Ni					7	10	10	12	11	13	10	8	15	14	10	11	11
Pb		dteremined			9	16	10	12	18	12	15	7	14	13	21	18	28
Rb					95	113	87	102	131	68	135	13	183	156	158	118	158
Sc					2	-0.20	1	-1	2	0.13	0.60	1	4	1	3	1	3
Sr					52	39	55	139	108	246	60	32	92	39	55	25	14
Th					17	13	16	14	25	14	22	22	15	14	20	27	27
V					6	6	5	5	10	11	7	4	12	5	6	2	5
Y					22	30	24	16	27	17	21	43	30	24	31	19	29
Zn					15	21	15	6	15	14	20	2	7	7	33	13	29
Zr					182	135	170	68	198	171	155	169	308	174	200	162	152
Ti						744	790	597	1345	1001	761		627	612	1108	622	591

modal mineralogy.

	1	A	B	2	15.1	15.5	15.6	16.1	16.2	16.3	16.4	17.1	17.2	17.3	18.1	18.3	18.4
Plag	n.d.	n.d.	n.d.	n.d.	6.70	11.20	25.60	12.40	26.60	22.40	9.00	n.d.	n.d.	n.d.	33.00	27.30	28.60
ksp	n.d.	n.d.	n.d.	n.d.	59.40	53.60	38.80	49.00	40.00	48.20	53.60	n.d	n.d	n.d.	37.80	40.40	43.40
Qz	n.d.	n.d.	n.d.	n.d.	31.70	32.80	30.60	36.40	27.80	27.60	32.20	n.d.	n.d.	n.d.	26.40	29.80	26.00
Bio	n.d.	n.d.	n.d.	n.d.	2.20	2.40	5.00	0.00	3.10	1.20	4.40	n.d.	n.d.	n.d.	2.00	0.00	1.00
Aeg	n.d.	n.d.	n.d.	n.d.	0.00	0.00	0.00	0.00	2.50	0.00	0.00	n.d.	n.d.	n.d.	0.00	2.50	0.00
opq	n.d.	n.d.	n.d.	n.d.	0.00	0.00	0.00	0.60	0.00	0.60	0.80	n.d.	n.d.	n.d.	0.80	0.00	1.00
access.	n.d.	n.d.	n.d.	n.d.	0.00	0.00	0.00	1.60	0.00	0.00	0.00	n.d.	n.d.	n.d.	0.00	0.00	0.00

normative mineralogy (percent)

	1	A	B	2	15.1	15.5	15.6	16.1	16.2	16.3	16.4	17.1	17.2	17.3	18.1	18.3	18.4
Qz	34.49	28.75	19.65	17.47	29.07	33.61	31.93	35.68	26.75	23.37	32.92	26.58	40.96	39.53	27.57	30.13	30.79
or	27.01	27.89	28.60	13.06	31.14	26.95	25.77	28.31	26.59	28.31	28.01	3.01	36.94	31.62	27.42	27.54	26.89
ab	34.69	39.94	41.36	41.63	35.96	36.39	35.88	32.16	36.98	38.67	33.59	64.31	4.99	21.58	38.67	37.57	37.74
an	1.37	0.28	0.00	4.45	0.54	2.37	1.51	2.73	4.27	4.72	2.33	0.81	2.40	0.75	2.81	1.52	2.12
C	0.00	0.42	0.00	6.13	0.00	0.18	0.68	0.30	0.09	0.27	0.05	0.00	5.49	3.00	0.00	0.34	0.15
diwo	0.35	0.12	2.01	1.86	0.28	0.03	0.63	0.09	0.52	0.23	0.03	0.58	1.00	0.31	0.03	0.34	0.03
dien	0.30	0.10	1.59	1.53	0.20	0.02	0.49	0.07	0.45	0.20	0.02	0.35	0.46	0.27	0.03	0.22	0.02
difs	0.00	0.00	0.19	0.10	0.00	0.00	0.07	0.00	0.00	0.00	0.00	0.19	0.54	0.00	0.00	0.09	0.00
wo	0.23	0.00	2.14	0.00	0.03	0.96	0.00	1.05	1.26	1.74	0.95	0.00	0.00	0.00	0.00	0.30	0.86
hyen	0.00	0.10	0.00	10.13	0.00	0.00	0.48	0.00	0.00	0.00	0.00	0.25	0.51	0.39	0.05	0.00	0.00
hyfs	0.00	0.00	0.00	0.66	0.00	0.00	0.07	0.00	0.00	0.00	0.00	0.13	0.60	0.00	0.00	0.00	0.00
mt	0.70	1.01	-0.00	0.42	0.45	0.77	0.80	0.24	1.54	0.61	0.83	0.03	1.73	1.01	0.75	0.77	0.53
he	0.48	0.77	0.00	0.00	0.55	0.04	0.00	0.13	0.01	0.58	0.05	0.30	0.00	0.85	0.41	0.00	0.40
iL	0.13	0.04	0.02	0.59	0.38	0.34	0.34	0.27	0.49	0.36	0.32	0.30	0.57	0.38	0.40	0.28	0.28
ap	0.02	0.33	0.43	0.02	0.12	0.09	0.05	0.07	0.14	0.07	0.07	0.07	0.12	0.07	0.07	0.02	0.09

A2.7) Granites from the west of WBF and North of Bixter Voe: Trace Elements Determined by I.N.A.A.

(all values in ppm; error given in brackets)

Sample	14.2	14.4	14.5	14.9	14.13	14.14	15.6	16.2
La	30 (1)	41 (1)	10.1(0.30)	39 (1)	29 (1)	26 (1)	36 (1)	29 (1)
Ce	63 (3)	83 (4)	14 (1)	83 (4)	75 (4)	100 (5)	87 (4)	60 (3)
Sm	6.00(0.10)	5.60(0.10)	2.40(0.02)	7.2(0.10)	8.0(0.10)	5.20(0.10)	4.6(0.05)	3.3 (0.05)
Eu	2.20(0.20)	0.26(0.08)	0.40(0.10)	2.0(0.20)	<0.20	0.21(0.05)	0.4(0.10)	0.40 (0.10)
Tb	0.86(0.04)	0.68(0.03)	0.40(0.03)	0.85(0.04)	1.3(0.10)	0.67(0.03)	0.62(0.04)	0.43 (0.03)
U	1.60(0.20)	3.80(0.50)	0.52(0.08)	1.0(0.10)	5.5(0.80)	3.3(0.50)	2.60(0.40)	2.40(0.30)
Th	6.10(0.20)	24 (1)	2.40(0.10)	4.6(0.20)	30 (1)	21 (1)	14 (1)	13 (1)
Ba	740 (40)	680 (35)	310 (20)	1055 (55)	130 (12)	123 (10)	520 (30)	615 (35)
Rb	45 (2)	155 (8)	22 (2)	19 (1)	230 (12)	150 (8)	90 (5)	115 (6)
Sr	405 (20)	113 (10)	440 (25)	1270 (65)	25 (7)	48 (6)	56 (7)	140 (10)
Cr	130 (10)	<5	-	-	100 (8)	32 (5)	22 (3)	-
Hf	4.70(0.20)	5.80(0.20)	1.60(0.10)	2.90(0.10)	9.30(0.30)	5.60(0.5)	0.50(0.20)	3.20 (0.10)
Zr	230 (25)	185 (20)	<55	-	190 (20)	170 (20)	145 (15)	190 (25) <60 -
Cs	1.40(0.10)	2.50(0.10)	0.73(0.06)	0.20(0.03)	1.0(0.10)	0.96(0.06)	0.65(0.05)	0.53 (0.04)
Sc	26 (1)	2.50(0.10)	34 (2)	28 (1)	1.50(0.10)	2.10(0.10)	1.20(0.10)	1.20(0.10)
Ta	1.04(0.04)	2.60(0.10)	0.49(0.03)	0.74(0.03)	3.80(0.10)	2.50 (0.	2.40(0.10)	2.20 (0.10)
Co	68 (4)	81 (4)	62 (3)	48 (3)	77 (4)	66 (3)	82 (4)	86 (5)

	16.3	17.2	18.3
La	39 (1)	36 (1)	3.5(0.20)
Ce	71 (4)	71 (3)	49? (3)
Sm	4.80(0.03)	5.30(0.10)	1.90(0.01)
Eu	0.60(0.08)	1.00(0.10)	0.40(0.06)
Tb	0.55(0.03)	0.74(0.04)	0.40(0.03)
U	1.60(0.20)	2.80(0.40)	2.00(0.30)
Th	10.90(0.40)	16 (10	22 (1)
Ba	1360 (70)	1390 (70)	295 (20)
Rb	78 (4)	205 (10)	125 (7)
Sr	245 (15)	81 (7)	20? -
Hf	5.60(0.20)	8.30(0.30)	6.30(0.20)
Zr	270 (30)	320 (35)	225 (30)
Cs	0.35(0.04)	0.45(0.05)	0.56(0.05)
Sc	1.60(0.10)	4.40(0.20)	2.40(0.10)
Ta	1.50(0.10)	1.80(0.10)	3.70(0.10)
Co	71 (7)	59 (3)	89 (5)

	14.3	14.7	14.14
La	32	27	21
Ce	75	69	50
Pr	7.50	6.50	6.40
Nd	19	25	17
Sm	4.50	5.30	4.10
Eu	0.26	1.60	0.08
Gd	3.40	5.20	2.30
Tb	0.61	0.77	0.61
Dy	3.60	4.70	4.50
Ho	0.88	0.92	0.87
Er	-	-	-
Tm	-	-	-
Yb	2.30	2.10	2.60
Lu	0.40	0.30	0.40

A2.8) Granites from the west of WBF and South of Blxter Voe: XRF analysis (whole rock major oxides and trace elements), modal mineralogy, normative mineralogy.

Sample	19a.1	19a.6	19a.7	19a.9	19.1	192	19.3	19.4
SIO2	73.42	54.99	72.63	72.53	72.87	70.84	53.43	65.83
TIO2	0.29	1.64	0.36	0.36	0.32	0.39	1.69	0.59
Al2O3	13.57	16.19	13.88	14.25	13.52	14.54	17.34	16.57
Fe2O3	0.64	4.23	1.19	1.15	0.78	1.06	2.37	1.55
FeO	0.66	3.11	0.68	0.72	0.85	1.27	3.94	1.55
MnO	0.04	0.13	0.04	0.05	0.04	0.03	0.14	0.07
MgO	0.35	3.25	0.31	0.46	0.43	0.62	4.32	1.43
CaO	0.91	4.29	1.05	1.24	1.22	1.27	6.57	2.36
Na2O	3.94	4.43	4.08	4.05	4.01	4.01	3.73	4.35
K2O	4.55	3.78	4.46	4.61	4.56	4.43	3.06	3.95
H2O	0.51	1.43	0.52	0.57	0.37	0.53	1.20	0.82
P2O5	0.05	0.48	0.09	0.07	0.37	0.07	0.49	0.20
CO2	0.12	0.13	0.14	0.26	0.14	0.12	0.16	0.18
Total	99.09	98.03	99.39	100.32	99.18	99.18	98.44	99.45
Ba	420	1657	555	600	571	820	1324	1247
Ce	65	89	73	81	96	46	72	87
Co	58	38	49	58	71	52	37	43
Cr	32	49	35	30	13	30	77	29
La	46	62	46	58	70	30	54	60
Nd	32	57	34	36	44	24	40	42
NI	13	25	16	15	9	17	37	16
Pb	18	18	17	19	21	13	14	18
Rb	135	89	86	101	130	108	67	101
Sc	2	21	3	5	3	2	26	18
Sr	89	431	113	121	124	178	880	407
Th	25	6	23	19	29	22	8	16
V	18	178	24	25	20	28	200	49
Y	28	48	25	29	30	22	20	20
Zn	19	69	12	24	18	9	70	59
Zr	175	392	222	238	189	206	244	264
Tl	1476	8700	1804	1952		2115	8444	3210

modal mineralogy (percent)

Plag	17.00	54.00	25.40	27.60	23.90	41.20	54.00	47.00
ksp	43.60	15.70	44.60	37.20	33.70	21.80	9.60	21.70
Qz	32.80	6.90	26.6	30.60	36.50	30.00	3.20	22.10
Bio	6.20	6.50	3.40	4.60	5.90	7.00	14.00	6.20
Hb	0.00	13.80	0.00	0.00	0.00	0.00	19.20	2.20
opq	0.40	0.00	0.00	0.00	0.00	0.00	0.00	0.00
access.	0.00	3.10	0.00	0.00	0.00	0.00	0.00	0.80

normative mineralogy (percent)

Qz	29.49	3.15	28.37	26.95	28.88	25.45	1.33	16.21
or	26.89	22.34	26.36	27.24	26.95	26.18	18.08	23.34
ab	33.68	37.49	34.53	34.27	33.93	33.93	31.56	36.81
an	4.19	13.13	4.62	5.69	3.64	5.84	21.53	10.40
C	0.56	0.00	0.65	0.51	0.65	1.01	0.00	1.33
diwo	1.25	2.10	0.89	1.33	1.52	2.44	3.28	4.34
dien	0.87	1.81	0.77	1.15	0.99	1.48	2.38	3.25
difs	0.28	0.00	0.00	0.00	0.43	0.83	0.61	0.66
wo	0.49	0.00	1.04	1.05	0.00	0.00	0.00	0.00
hyen	0.00	5.28	0.00	0.00	0.08	0.07	8.38	0.31
hyfs	0.00	0.00	0.00	0.00	0.04	0.04	2.14	0.06
mt	0.93	5.69	1.28	1.44	1.13	1.54	3.44	2.25
he	0.00	0.30	0.31	0.16	0.00	0.00	0.00	0.00
iL	0.55	3.11	0.68	0.68	0.61	0.74	3.21	1.14
ap	0.12	1.14	0.21	0.17	0.88	0.17	1.16	0.47

Granites from the west of WBF and South of Bixter Voe: XRF analysis (whole rock major oxides and trace elements), modal mineralogy, normative mineralogy.

Sample	19.5	19.6	19.7	19.9	19.10	19.11	19.12	19.13	19.14
SiO_2	73.65	54.84	61.72	70.68	66.64	58.15	71.95	71.77	56.21
TiO_2	0.28	1.65	0.96	0.33	0.54	1.22	0.37	0.36	1.64
Al_2O_3	13.23	17.13	17.52	14.58	15.83	16.45	14.08	13.98	15.46
Fe_2O_3	0.64	2.41	2.70	1.91	1.44	2.16	0.91	1.02	2.94
FeO	0.55	4.22	1.70	0.41	1.31	3.51	1.04	0.98	3.19
MnO	0.04	0.09	0.08	0.04	0.06	0.11	0.06	0.04	0.09
MgO	0.29	3.47	1.59	0.27	1.08	2.87	0.43	0.22	2.70
CaO	0.97	5.32	2.93	1.05	2.24	4.53	1.45	1.20	4.22
Na_2O	4.07	4.10	4.57	4.50	4.60	3.65	3.87	2.90	3.67
K_2O	4.46	2.37	3.97	4.51	4.21	2.98	4.50	4.73	3.28
H_2O	0.60	2.49	0.80	0.56	0.78	2.30	0.53	0.73	2.07
P_2O_5	0.05	0.50	0.30	0.05	0.17	0.38	0.08	0.08	0.53
CO_2	0.19	0.24	0.20	0.18	0.18	0.23	0.11	0.19	0.16
Total	99.02	99.19	99.04	98.35	99.08	98.59	99.38	98.20	96.21
Ba	416	669	1676	576	1303	1002	807	749	1248
Ce	36	68	86	71	113	61	78	76	78
Co	56	35	41	62	57	50	51	61	40
Cr	26	64	21	24	34	46	29	33	30
La	21	47	55	47	81	42	47	23	50
Nd	21	42	42	26	84	35	35	23	38
Ni	13	29	15	12	16	28	17	15	9
Pb	20	11	16	21	18	18	20	14	16
Rb	133	50	80	123	107	70	122	108	91
Sc	2	12	8	2	5	10	4	2	10
Sr	116	756	558	125	388	427	167	164	637
Th	26	14	17	25	23	12	24	26	18
V	17	179	75	17	48	129	25	22	171
Y	23	22	23	25	22	21	28	23	23
Zn	14	39	29	21	47	59	35	12	53
Zr	157	274	457	253	255	227	226	223	173
Ti	1388	8301	5384	1698	2928	6663	1966	1815	8616

modal mineralogy (percents)

	19.5	19.6	19.7	19.9	19.10	19.11	19.12	19.13	19.14
Plag	26.70	63.40	50.30	14.60	34.00	59.20	22.70	30.20	52.80
ksp	35.50	5.20	22.60	59.20	42.40	6.40	44.80	37.20	13.20
Qz	34.60	3.80	14.80	22.40	16.60	8.20	25.90	27.20	10.40
Bio	1.30	14.60	6.70	3.8	7.00	13.00	6.60	5.40	12.00
Hb	0.00	9.00	4.50	0.00	0.00	11.40	0.00	0.00	11.60
opq	0.00	0.00	1.10	0.00	0.00	1.80	0.00	0.00	0.00
access.	1.90	0.00	0.00	0.00	0.00	0.00	0.00	0.00	0.00

normative mineralogy (percents)

	19.5	19.6	19.7	19.9	19.10	19.11	19.12	19.13	19.14
Qz	29.52	5.68	9.42	23.68	15.48	11.36	26.95	32.75	11.33
or	26.36	14.01	23.46	26.65	24.88	17.61	26.59	27.95	20.64
ab	34.44	34.69	38.67	38.08	38.93	30.89	32.75	24.54	33.06
an	4.49	21.34	12.58	4.88	10.00	19.70	6.67	5.43	17.06
C	0.06	0.00	1.10	0.51	0.04	0.00	0.40	2.10	0.00
diwo	0.92	0.75	4.58	0.78	3.50	0.12	1.82	1.02	0.65
dien	0.72	0.50	3.96	0.67	2.69	0.08	1.07	0.55	0.51
difs	0.09	0.19	0.00	0.00	0.44	0.03	0.66	0.44	0.07
wo	0.96	0.00	0.67	1.26	0.68	0.00	0.97	1.25	0.00
hyen	0.00	8.14	0.00	0.00	0.00	7.07	0.00	0.00	6.65
hyfs	0.00	3.01	0.00	0.00	0.00	2.82	0.00	0.00	0.88
mt	0.93	3.49	2.96	0.50	2.09	3.13	1.32	1.48	4.54
he	0.00	0.00	0.66	0.85	0.00	0.00	0.00	0.00	0.00
IL	0.53	3.13	1.82	0.63	1.03	2.32	0.70	0.68	3.32
ap	0.12	1.18	0.71	0.12	0.40	0.90	0.19	0.19	1.34

A2.9) Granites from the west of WBF and South of Bixter Voe: Trace Elements Determined by I.N.A.A.

(all values in ppm; error given in brackets)

Sample	19a.1	19a.6	19.2	19.3	19.4	19.5	19.7
La	42 (1)	69 (2)	31 (1)	65 (1)	60 (1)	20 (1)	59 (1)
Ce	83 (3)	140 (6)	64 (3)	130 (6)	116 (5)	51 (3)	121 (5)
Sm	5.60(0.10)	12.00(0.10)	4.70(0.10)	10.00(0.10)	6.90(0.10)	4.00(0.10)	8.00(0.10)
Eu	0.68(0.05)	2.80(0.20)	1.10(0.10)	2.30(0.20)	1.20(0.10)	0.59(0.10)	2.10(0.20)
Tb	0.71(0.03)	1.60(0.10)	0.56(0.03)	0.83(0.04)	0.72(0.03)	0.59(0.03)	0.78(0.04)
U	3.60(0.50)	1.60(0.20)	3.20(0.40)	2.80(0.40)	2.20(0.30)	2.90(0.40)	2.30(0.30)
Th	23 (1)	4.90(0.20)	20 (1)	9.40(0.40)	17 (1)	24 (1)	13 (1)
Ba	515 (30)	1725 (90)	945 (50)	1400 (70)	1435 (75)	530 (30)	1810 (90)
Rb	146 (8)	105 (5)	117 (6)	85 (5)	115 (6)	157 (8)	85 (4)
Sr	83 (8)	415 (20)	175 (10)	880 (45)	405 (20)	117 (20)	530 (30)
Cr	<5 -	66 (7)	<5 -	69 (6)	14 (3)	<5 -	<5 -
Hf	5.60(0.20)	9.60(0.30)	6.00(0.20)	5.80(0.20)	7.50(0.20)	5.60(0.20)	10.60(0.30)
Zr	210 (20)	445 (35)	260 (20)	230 (25)	360 (25)	223 (15)	490 (35)
Cs	1.40(0.10)	3.30(0.20)	3.60(0.20)	1.40(0.10)	1.90(0.10)	2.10(0.10)	2.30(0.10)
Sc	2.80(0.20)	18 (1)	4.00(0.20)	22 (1)	6.40(0.30)	2.90(0.20)	6.50(0.30)
Ta	2.90(0.10)	1.50(0.10)	2.40(0.10)	2.30(0.10)	2.00(0.10)	2.70(0.10)	3.50(0.10)
Co	74 (4)	55 (3)	66 (4)	52 (3)	60 (3)	76 (4)	53 (3)

	19.13	19.14
La	25 (1)	64 (1)
Ce	89 (4)	122 (6)
Sm	4.90(0.10)	9.10(0.10)
Eu	1.20(0.10)	2.20(0.20)
Tb	0.68(0.03)	0.84(0.04)
U	2.60(0.40)	3.80(0.50)
Th	22 (1)	17 (1)
Ba	975 (50)	1355 (70)
Rb	125 (7)	108 (6)
Sr	146 (10)	595 (30)
Cr	<5 -	49 (7)
Hf	7.10(0.20)	4.90(0.20)
Zr	320 (25)	225 (20)
Cs	1.30(0.10)	1.90(0.10)
Sc	4.10(0.20)	15 (1)
Ta	2.30(0.10)	2.40(0.10)
Co	85 (4)	56 (3)

Granites from the west of WBF and South of Bixter Voe: RNAA - rare earth elements.

	19a.6	19.3	19.9
La	56(0.20)	51(0.20)	35(0.20)
Ce	145 (1)	124 (1)	90 (1)
Pr	14(0.30)	11(0.20)	7.80(0.20)
Nd	57 (1)	46 (1)	29 (1)
Sm	11(0.10)	8(0.10)	5.10(0.10)
Eu	3.30(0.10)	1.40(0.10)	0.74(0.05)
Gd	8(0.40)	5.70(0.50)	3.30(0.30)
Tb	1.30(0.02)	0.69(0.02)	0.63(0.02)
Dy	7.30(0.10)	3.50(0.10)	3.90(0.10)
Ho	1.40(0.02)	0.61(0.02)	0.75(0.02)
Er	-	-	-
Tm	0.51(0.02)	0.19(0.02)	-
Yb	2.90(0.10)	1.10(0.10)	2.30(0.20)
Lu	0.47(0.02)	0.17(0.01)	0.35(0.02)

A2.10) Pebbles of Granites from Rova Head Conglomerate: XRF analysis (whole rock major oxides and trace elements),modal mineralogy, normative mineralogy.

Sample	8.1	8.3	8.4	8.6	8.7	8.8	8.9	8.11	8.12	8.13	8.14	8.15
SiO2	71.09	67.83	66.62	73.78	76.74	76.08	73.50	69.89	75.64	64.80	73.90	73.59
TiO2	0.28	0.56	0.63	0.28	0.24	0.17	0.30	0.38	0.19	0.80	0.07	0.16
Al2O3	14.45	14.67	15.33	13.45	12.21	13.09	13.08	14.60	13.93	16.11	14.66	14.30
Fe2O3	0.54	0.55	1.84	0.58	0.35	0.06	0.72	1.11	0.42	1.47	-	0.33
FeO	0.64	1.54	1.82	0.61	0.37	0.31	0.76	1.40	0.51	2.19	0.14	0.84
MaO	0.04	0.06	0.05	0.04	0.03	0.03	0.04	0.06	0.03	0.06	0.04	0.03
MgO	0.72	2.12	2.05	0.53	0.29	0.09	0.63	1.51	0.58	2.51	-	1.24
CaO	1.72	2.81	1.42	0.45	0.77	0.56	0.53	1.05	0.62	1.29	1.09	0.39
Na2O	4.87	3.68	4.53	3.15	3.21	3.92	3.35	4.29	4.25	3.67	5.22	3.23
K2O	2.91	3.30	2.96	5.78	4.74	4.40	5.12	3.10	3.71	4.03	3.22	3.76
H2O	0.69	1.53	1.67	0.64	0.57	0.49	0.65	1.38	0.70	2.08	0.54	1.60
P2O2	0.09	0.16	0.24	0.06	0.03	0.02	0.09	0.13	0.05	0.22	0.03	0.10
CO2	0.22	1.45	0.33	0.13	0.43	0.09	0.19	0.33	0.10	0.50	0.35	0.10
Total	98.31	100.26	99.30	99.48	99.98	99.31	99.00	99.23	100.73	99.73	99.29	99.62
Ba	840	528	739	1015	1994	414	841	682	780	654	105	605
Ce	26	67	100	21	38	28	32	22	12	88	11	41
Co	72	42	49	75	69	72	76	56	55	48	71	58
Cr	29	56	52	23	18	11	21	55	22	108	16	16
La	14	0.40	65	14	41	13	20	14	5	54	4	25
Nd	18	35	52	16	24	18	21	17	10	45	10	24
Ni	13	25	20	10	5	6	9	21	11	35	7	14
Pb	21	20	16	26	19	20	26	14	22	20	27	19
Rb	69	105	66	109	81	96	96	82	97	134	110	112
Sc	3	6	6	5	2	3	6	7	1	7	2	2
Sr	525	235	524	109	161	41	112	154	259	208	82	144
Th	15	27	34	15	14	12	20	13	6	36	6	8
V	24	43	61	20	11	5	21	37	16	65	3	16
Y	14	23	24	24	8	18	37	21	9	20	19	9
Za	12	24	23	10	8	4	10	17	9	25	10	6
Zr	109	261	233	79	115	86	96	125	66	375	31	59
Ti		3375	3759	1505	779	1661	2274	1044	4757	128	853	

modal mineralogy

	8.1	8.3	8.4	8.6	8.7	8.8	8.9	8.11	8.12	8.13	8.14	8.15
Plag	35.00	47.60	a.d.	30.80	38.40	42.00	21.00	51.00	43.00	31.40	46.20	44.80
Ksp	21.90	23.40	a.d.	33.00	23.20	18.00	39.60	12.20	19.80	26.20	18.20	15.40
Qz	40.70	17.00	a.d.	28.20	36.00	38.00	31.60	25.80	32.20	22.00	29.80	32.40
Musc	0.00	0.00	a.d.	0.00	0.00	1.00	0.00	0.00	o.80	0.00	5.80	3.40
Chl	2.40	9.20	a.d.	7.20	1.80	1.00	6.80	9.00	4.00	20.40	0.00	0.00
Cal	0.00	2.40	a.d.	0.00	0.00	0.00	0.00	2.00	0.00	0.00	0.00	0.00
epq	0.00	0.40	a.d.	0.80	0.60	0.00	1.00	0.00	0.20	0.00	0.00	0.00

normative mineralogy.

	8.1	8.3	8.4	8.6	8.7	8.8	8.9	8.11	8.12	8.13	8.14	8.15
Qz	25.25	21.57	21.94	31.30	37.12	34.45	31.98	27.48	33.92	20.34	27.74	37.04
Or	17.20	19.50	17.49	34.16	28.01	26.00	30.26	18.32	21.93	23.82	19.03	22.22
ab	41.21	31.14	38.33	26.66	27.16	33.17	28.35	36.30	35.96	31.06	44.17	27.33
an	7.95	12.90	5.48	1.74	3.62	2.65	2.04	4.36	2.75	4.96	5.21	1.61
C	0.38	0.32	2.67	1.37	0.47	0.91	1.28	2.59	1.92	3.89	0.68	4.33
diwe	2.38	5.38	2.29	0.73	0.88	0.52	0.58	1.82	1.15	2.07	0.18	0.67
dien	1.79	3.80	1.75	0.55	0.72	0.22	0.62	1.28	0.84	1.50	0.00	0.46
difs	0.34	1.12	0.30	0.11	0.05	0.29	0.15	0.39	0.19	0.38	0.21	0.16
we	0.94	0.00	0.00	0.00	0.63	0.59	0.00	0.00	0.00	0.00	0.00	1.99
hyen	0.00	1.48	3.36	0.77	0.00	0.00	0.95	2.48	0.60	4.75	0.00	2.63
hyfs	0.00	0.44	0.58	0.15	0.00	0.00	0.23	0.75	.14	1.21	0.00	0.90
mt	0.78	0.80	2.67	0.84	0.51	0.09	1.04	1.61	0.61	2.13	0.01	0.49
iL	0.53	1.06	1.20	0.54	0.46	0.32	0.57	0.72	0.36	1.52	0.13	0.31
ap	0.21	0.38	0.57	0.14	0.07	0.05	0.21	0.31	0.12	0.52	0.07	0.12

Pebbles of granites from Funzie Conglomerate to the east of WBF: XRF analysis (whole rock major oxides and trace elements), modal mineralogy, normative mineralogy.

sample	3a.1	3a.2	3a.4	3b.1	3c.3	3c.5	3c.10	3c.11	K	15
SiO2	76.87	75.24	60.95	71.22	74.65	76.17	61.68	73.33	62.58	77.30
TiO2	0.12	0.15	0.15	0.25	0.10	0.12	0.56	0.21	0.25	0.19
Al2O3	13.15	13.05	20.39	11.26	13.77	14.09	18.74	14.51	18.07	11.95
Fe2O3	0.01	0.45	1.57	2.73	0.02	0.15	1.79	0.44	a.d	1.02
FeO	0.09	0.39	0.31	0.30	0.12	0.37	0.55	0.59	6.13	1.73
MnO	0.02	0.03	0.04	0.05	0.02	0.03	0.04	0.05	0.06	0.04
MgO	0.01	0.10	0.14	1.18	0.26	0.29	1.24	1.07	1.62	0.39
CaO	1.77	1.87	4.34	3.06	0.81	0.38	3.24	0.91	1.90	1.86
Na2O	7.76	7.77	9.83	7.11	7.21	5.82	5.82	7.51	8.54	5.16
K2O	0.07	0.15	0.10	0.27	1.07	1.93	2.62	0.83		0.06
H2O	0.28	0.48	0.43	0.40	0.57	0.80	2.04	0.78	1.34	0.64
P2O5	0.04	0.04	0.04	0.05	0.11	0.03	0.57	0.07	0.03	a.d
CO2	0.07	0.11	0.34	1.95	0.14	0.19	0.14	0.08	0.01	0.04
Total	100.26	99.85	98.63	99.83	98.85	100.22	99.02	100.38	100.51	100.38
Ba	-12	9	-69	24	263	424	865	161		
Ce	-24	13	7	6	7	5	35	44		
Co	87	66	49	66	62	51	32	55		not
Cr	-5	20	18	33	11	12	14	16		
La	4	9	4	4	3	3	18	18		
Nd	-12	10	10	13	7	8	28	20		
Ni	7	10	7	32	11	8	8	10		
Pb	7	6	6	4	24	11	13	9		
Rb	-2	2	-0.22	3	30	40	77	28		
Sc	1	2	3	11	2	-1	-0.50	3		determined
Sr	-3	118	167	83	127	100	160	127		
Th	4	2	2	1	5	4	2	14		
V	5	9	107	42	4	6	58	26		
Y	9	9	23	33	14	4	20	25		
Zn	1	9	2	3	6	3	13	15		
Zr	47	77	91	122	39	135	336	87		
Ti		547					521	348	910	

modal mineralogy (percents)

	3a.1	3a.2	3a.4	3b.1	3c.3	3c.5	3c.10	3c.11	K	15	
Plag	70.80	69.10	67.40	83.70	58.50	51.40	a.d	65.40	n.d	n.d	n.d
ksp	0.00	0.00	2.20	0.00	0.00	6.60	a.d	5.60	n.d	n.d	n.d
Qz	27.40	29.60	23.80	10.80	39.70	42.00	a.d	23.60	n.d	n.d	n.d
Bit	0.00	0.00	0.00	4.00	0.00	0.00	a.d	0.00	n.d	n.d	n.d
Hb	0.00	1.30	1.40	0.00	0.00	0.00	a.d	0.00	n.d	n.d	n.d
epi	1.80	0.00	3.80	0.00	0.00	0.00	a.d	0.00	n.d	n.d	n.d
Musc	0.00	0.00	0.00	0.00	1.80	0.00	a.d	0.00	n.d	n.d	n.d
cal	0.00	0.00	0.00	1.50	0.00	0.00	a.d	0.00	n.d	n.d	n.d
opq	0.00	0.00	1.40	0.00	0.00	0.00	a.d	0.00	n.d	n.d	n.d

normative mineralogy (percents)

	3a.1	3a.2	3a.4	3b.1	3c.3	3c.5	3c.10	3c.11	K	15
Qz	29.42	27.24	0.00	24.72	26.96	33.22	7.94	23.04	0.00	39.54	38.01
Or	0.41	0.89	0.59	1.60	6.32	11.41	15.48	4.91	0.06	0.35	0.35
ab	65.67	65.75	74.80	56.42	61.01	49.16	49.25	63.55	72.27	43.66	59.07
an	0.84	0.29	11.22	0.00	2.05	1.69	12.35	3.43	9.23	9.23	0.99
C	0.00	0.00	0.00	0.00	0.00	1.82	1.80	0.00	0.63	0.01	0.12
ac	0.00	0.00	0.00	3.30	0.00	0.00	0.00	0.00	0.00	0.00	0.00
diwo	0.03	0.42	0.40	3.40	0.52	0.71	3.57	0.26	3.85	2.97	0.41
dien	0.02	0.25	0.35	2.94	0.35	0.39	3.09	0.20	1.09	0.97	0.21
difs	0.00	0.15	0.00	0.00	0.13	0.29	0.00	0.03	2.95	2.09	0.20
wo	3.18	3.22	3.79	2.80	0.00	0.00	1.58	0.00	0.00	0.88	0.00
hyen	0.00	0.00	0.00	0.00	0.30	0.33	0.00	2.47	2.38	0.00	0.49
hyfs	0.00	0.00	0.00	0.00	0.11	0.24	0.00	0.34	6.47	0.00	0.46
mt	0.00	0.65	0.69	0.41	0.03	0.01	0.28	0.64	0.01	1.48	0.39
he	0.00	0.00	1.09	1.31	0.00	0.00	1.60	0.00	0.00	0.00	0.00
il	0.23	0.28	0.28	0.47	0.00	0.23	1.06	0.40	0.47	0.36	0.30
ap	0.09	0.09	0.09	0.12	0.26	0.07	1.35	0.17	0.07	0.00	0.00

A2.11) Hornblende-bearing Granites: mineral analysis
Plagiocase

| Sample | 6.26a | 6.26a | 6.26a | 6.26a | 6.29a | 6.29a | 6.29a | 12c.42 | 12c.42 | 12c.42 |
Code	rim	cdre	rim	rim	core	rim	core	core	core	core
SiO2	65.08	61.65	63.08	65.46	62.07	63.38	61.46	59.32	61.16	59.51
Al2O3	22.48	23.06	22.57	22.52	23.35	22.77	23.60	25.60	25.46	25.30
FeO	0.27	0.25	0.29	0.20	0.05	0.04	0.10	0.04	0.09	0.05
MgO	0.00	0.00	0.03	0.03	0.00	0.02	0.00	0.00	0.02	0.00
CaO	3.51	4.69	3.85	3.43	4.84	3.98	5.43	7.42	6.71	6.91
Na2O	10.30	9.42	10.09	10.58	9.19	9.49	8.72	7.81	8.35	7.59
K2O	0.17	0.12	0.34	0.11	0.12	0.42	0.25	0.08	0.13	0.12
Total	101.81	99.19	100.02	102.22	99.62	100.10	99.56	100.27	101.92	99.84
SI	2.830	2.763	2.795	2.832	2.763	2.803	2.744	2.642	2.675	2.663
AL	1.152	1.218	1.179	1.148	1.225	1.187	1.242	1.344	1.313	1.334
TI	0.000	0.000	0.002	0.000	0.002	0.002	0.000	0.002	0.000	0.004
FE2	0.010	0.009	0.011	0.007	0.002	0.002	0.004	0.001	0.003	0.002
MG	0.000	0.000	0.000	0.000	0.000	0.000	0.000	0.000	0.004	0.000
CA	0.164	0.225	0.183	0.159	0.231	0.189	0.260	0.354	0.314	0.331
NA	0.868	0.819	0.867	0.888	0.794	0.814	0.755	0.675	0.708	0.658
K	0.009	0.007	0.019	0.006	0.007	0.024	0.014	0.004	0.007	0.007
AN	15.75	21.41	17.12	15.10	22.38	18.40	25.27	34.27	30.52	33.23
AB	83.38	77.93	81.10	84.33	76.94	79.26	73.37	65.34	68.80	66.06
OR	0.87	0.66	1.78	0.57	0.68	2.34	1.36	0.39	0.68	0.71

Hornblende-free Granites: mineral analysis
Plagioclase

| Sample | 1.19a | 1.19a | 1.19a | 1.24 | 1.25 | 1.25 |
Code	core	core	coreq	rim	core	rim
SiO2	60.65	62.46	59.60	69.67	60.97	66.73
Al2O3	25.27	25.19	25.80	25.58	25.98	21.71
FeO	0.04	0.14	0.00	0.05	0.18	0.15
MgO	0.06	0.00	0.08	0.13	0.00	0.00
CaO	6.68	6.02	7.34	0.22	6.99	1.50
Na2O	8.93	9.00	7.81	11.51	7.44	10.63
K2O	0.11	0.17	0.07	0.00	0.19	0.21
Total	101.20	102.98	100.70	102.16	101.75	100.93
SI	2.673	2.702	2.643	2.975	2.667	2.902
AL	1.313	1.284	1.349	1.036	1.340	1.113
FE2	0.001	0.005	0.000	0.002	0.007	0.005
MG	0.000	0.000	0.000	0.002	0.000	0.001
CA	0.316	0.279	0.349	0.010	0.328	0.070
NA	0.717	0.755	0.672	0.953	0.631	0.896
K	0.006	0.009	0.004	0.000	0.011	0.007
AN	30.41	26.75	34.05	1.04	33.81	7.19
AB	67.01	72.39	65.56	98.96	65.05	92.09
OR	0.85	0.86	0.39	0.00	1.13	0.72

Grantes to the west of WBF : mineral analysis
Plagioclase

Sample	14.6	14.6	15.6	19a.6	19a.6	19a.6	19.4	19.4	19.4	19.4	19.4
Code	core	core	core	core		core	rim	core	rim	core	rim
SiO2	47.28	49.33	61.91	58.57	60.79	64.36	61.96	62.63	62.05	62.36	63.41
Al2O	33.75	32.61	24.11	25.24	23.97	21.30	23.56	22.31	22.40	23.14	22.67
FeO	0.51	0.50	0.02	0.45	0.23	0.15	0.24	0.12	0.54	0.21	0.25
MgO	0.00	0.00	0.00	0.00	0.00	0.00	0.00	0.00	0.00	0.00	0.00
CaO	16.93	15.28	5.31	6.04	5.65	2.57	4.89	4.23	3.73	4.77	4.05
Na2O	1.84	2.67	9.29	7.15	8.59	10.42	8.93	9.65	9.57	9.28	9.81
K2O	0.08	0.19	0.02	1.19	0.10	0.09	0.26	0.10	0.33	0.08	0.08
Total	100.39	100.58	100.66	98.64	99.33	98.89	99.84	99.04	98.62	99.84	100.29
SI	2.165	2.243	2.733	2.656	2.723	2.868	2.756	2.802	2.095	2.770	2.802
AL	1.822	1.748	1.254	1.349	1.266	1.119	1.235	1.176	0.892	1.212	1.181
FE2	0.019	0.019	0.003	0.017	0.009	0.006	0.009	0.004	0.015	0.008	0.009
MG	0.000	0.000	0.000	0.000	0.000	0.000	0.000	0.000	0.000	0.000	0.000
CA	0.830	0.745	0.251	0.294	0.271	0.123	0.233	0.203	0.135	0.227	0.192
NA	0.163	0.235	0.795	0.629	0.746	0.901	0.770	0.837	0.627	0.799	0.840
K	0.005	0.011	0.001	0.069	0.006	0.005	0.015	0.005	0.014	0.005	0.004

AN
AB
OR

MINERAL ANALYSIS
AMPHIBOLE

	{	Hornblende-bearing Granites				}	Ronas	(Bixter &Sandsting)			
Sample	6.26a	6.29a	6.29a	12a.25	12a.25	12b.32	12b.32	14.6	19a.6	19.4	19.4
SiO2	46.05	45.98	51.14	41.77	41.01	44.41	44.01	50.51	48.43	48.43	49.98
TiO2	1.13	1.19	0.54	0.83	0.47	0.45	0.37	0.38	0.55	1.17	0.97
Al2O3	9.03	8.39	4.13	10.87	11.61	9.39	9.39	5.55	5.08	5.90	4.69
FeO	14.39	15.34	12.27	20.49	21.14	18.51	19.10	8.99	13.39	13.97	13.73
MnO	0.41	0.44	0.25	0.50	0.50	0.37	0.43	0.77	0.33	0.65	0.35
MgO	13.18	12.46	15.22	8.05	7.64	10.15	10.14	18.78	14.82	14.00	14.73
CaO	11.02	11.09	12.05	10.67	10.37	10.49	10.88	9.63	10.45	10.83	11.23
Na2O	2.02	2.11	0.91	1.94	2.13	2.33	2.44	1.15	0.63	1.68	1.38
K2O	0.74	0.69	0.34	1.73	1.83	1.22	1.39	0.05	0.40	0.54	0.42
Cl2O	0.01	0.07	0.03	0.13	0.23	0.13	0.10	0.19	0.06	0.15	0.12
Total	97.98	97.78	96.88	96.98	96.93	97.90	98.25	96.01	94.41	97.32	97.60
SI	6.788	6.831	7.475	6.493	6.670	6.717	6.680	7.304	7.318	7.154	7.318
AL1V	1.212	1.169	0.060	1.507	1.330	1.283	1.320	0.606	0.682	0.846	0.682
ALV1	0.357	0.300	0.210	0.483	0.810	0.391	0.359	0.339	0.217	0.180	0.127
TI	0.128	0.132	0.531	0.097	0.053	0.051	0.042	0.041	0.062	0.130	0.112
FE3	0.264	0.284	0.224	0.396	0.411	0.349	0.361	0.163	0.251	0.257	0.25
FE2	1.498	1.611	1.267	2.244	2.329	1.979	2.045	0.921	1.425	1.459	1.421
MN	0.051	0.056	0.031	0.065	0.067	0.048	0.055	0.094	0.044	0.081	0.04
MG	2.896	2.760	3.311	1.866	1.781	2.289	2.294	4.049	3.464	3.081	3.214
CA	1.741	1.765	1.884	1.776	1.738	1.773	1.770	1.492	1.756	1.714	1.762
NA	0.578	0.609	0.259	0.584	0.646	0.684	0.717	0.322	0.191	0.481	0.392
K	0.138	0.131	0.064	0.343	0.365	0.235	0.269	0.008	0.081	0.103	0.080

GRANITES TO THE EAST OF WBF: MINERAL ANALYSIS
BIOTITE

	Hornblende-bearing granites					Hornblende-free granite				
Sample Code	6.26a core rim	6.29a core cor	6.29a rim	12b.32 core	12b.32 rim	1.19a core	1.19a core	1.19a rim	1.24 rim	1.24	1.25
SiO2	38.19	38.11	37.15	38.24	37.80	37.09	36.75	36.33	36.67	35.45	36.24
TiO2	2.86	2.17	3.00	1.56	1.88	2.07	2.10	1.84	1.81	2.03	2.53
Al2O3	15.02	15.72	14.39	14.15	16.24	17.83	18.02	17.27	17.47	16.98	16.63
FeO	17.03	16.73	18.23	17.79	17.36	24.30	24.09	24.73	27.33	26.00	20.15
MnO	0.12	0.22	0.18	0.34	0.14	0.60	0.41	0.39	0.34	0.57	0.15
MgO	13.04	13.57	11.97	13.42	12.03	6.17	6.52	5.77	5.80	5.31	11.01
CaO	0.01	0.02	0.00	0.090	0.02	0.04	0.02	0.024	0.00	0.11	0.06
Na2O	0.09	0.17	0.07	0.21	0.05	0.22	0.34	0.24	0.27	0.29	0.48
K2O	9.39	9.42	9.41	9.46	9.40	9.27	9.48	8.91	9.61	9.27	9.01
Total	95.75	96.13	94.40	95.26	94.92	97.58	97.73	95.72	99.30	96.01	96.26

Structural formulae on the basis of 22 oxygens

SI	5.710	5.670	5.692	5.788	5.704	5.626	5.572	5.638	5.570	5.554	5.485
AliV	2.290	2.330	2.308	2.212	2.296	2.374	2.428	2.362	2.430	2.446	2.515
AlVi	0.358	0.427	0.292	0.312	0.593	0.815	0.793	0.797	0.698	0.690	0.452
TI	0.322	0.242	0.345	0.177	0.214	0.236	0.239	0.215	0.207	0.239	0.288
FE3	0.159	0.155	0.174	0.168	0.163	0.229	0.227	0.238	0.257	0.253	0.190
FE2	0.900	0.878	0.985	0.950	0.924	1.297	1.285	1.349	1.455	1.431	1.075
MN	0.015	0.027	0.023	0.043	0.017	0.077	0.053	0.051	0.043	0.075	0.020
MG	2.906	3.008	2.735	3.029	2.707	1.396	1.606	1.335	1.313	1.240	2.484
CA	0.002	0.003	0.000	0.014	0.003	0.007	0.003	0.040	0.000	0.020	0.011
NA	0.027	0.050	0.021	0.061	0.016	0.063	0.099	0.073	0.087	0.088	0.141
K	1.791	1.788	1.840	1.827	1.809	1.794	1.833	1.765	1.771	1.853	1.740

GRANITES TO THE EAST AND WEST OF WBF: MINERAL ANALYSIS
BIOTITE.   PYROXENE.

Sample Code	19a.6	19.4	19.4	19.4	12a.25	12a.25	12b32	12b.32	14.6	14.6
	Granites to the South of Bixter Voe				(Aith-Hildsay-Spiggie Granite)				(Ronas Hill gabbro)	
SiO2	36.68	36.71	36.34	36.15	52.59	51.51	52.57	52.16	55.38	51.39
TiO2	2.24	3.99	5.30	4.41	0.25	0.44	0.34	0.39	0.53	0.12
Al2O3	14.46	14.90	14.41	14.68	2.62	3.21	2.07	2.17	2.80	18.04
FeO	18.03	17.86	18.16	17.33	10.28	10.86	8.44	7.32	7.71	3.99
MnO	0.24	0.33	0.31	0.45	0.68	0.49	0.36	0.34	0.14	0.02
MgO	13.29	11.48	10.61	11.96	11.36	10.80	13.01	13.54	19.53	9.71
CaO	0.08	0.01	0.00	0.07	22.35	21.68	21.37	21.94	12.50	13.25
Na2O	0.27	0.33	0.26	0.20	1.97	2.01	1.47	1.21	0.86	1.96
K2O	7.88	9.10	8.79	8.71	0.00	0.00	0.06	0.01	0.05	0.00
Total	93.17	94.71	94.18	93.96	102.29	101.05	99.72	99.09	99.50	98.55

Structural formulae on the basis of 22 oxygens   Structural formulae on the basis of 6 oxygens

SI	5.652	5.599	5.580	5.555	1.943	1.930	1.966	1.956	1.996	1.826
AliV	2.348	2.401	2.420	2.445	0.114	0.142	0.091	0.096	0.119	0.756
AlVi	0.279	0.279	0.188	0.215	0	0 0	0	0	0	
TI	0.260	0.457	0.612	0.509	0.007	0.012	0.009	0.011	0.014	0.003
FE3	0.173	0.170	0.174	0.165	0.179	0.176	0.099	0.088	0.000	0.000
FE2	0.980	0.961	0.983	0.938	0.134	0.159	0.162	0.140	0.232	0.119
MN	0.031	0.043	0.041	0.019	0.021	0.016	0.012	0.011	0.004	0.001
MG	3.053	2.610	2.430	2.741	0.626	0.603	0.726	0.757	1.049	0.514
CA	0.014	0.001	0.000	0.011	0.885	0.870	0.856	0.881	0.483	0.505
NA	0.081	0.098	0.077	0.059	0.141	0.146	0.107	0.088	0.060	0.135
K	1.549	1.771	1.722	1.708	0.000	0.000	0.003	0.001	0.002	0.000

Granites to the East of WBF: mineral analysis
Epidote

Sample Code Spot	6.26a	12a.25	12a.25	12b.32	12b.32	1.24	1.25
SIO2	30.55	29.56	36.08	38.50	37.90	38.51	37.38
TIO2	37.74	34.66	8.05	0.14	0.09	0.02	0.17
AL2O3	1.27	1.65	18.11	21.47	21.40	29.77	23.96
FE2O3	1.60	1.70	10.74	14.19	13.91	5.15	11.57
MNO	0.06	0.00	0.36	0.00	0.20	0.06	0.06
MGO	0.00	0.00	0.23	0.04	0.01	0.14	0.18
CAO	27.03	26.86	23.86	20.91	21.71	23.93	23.34
NA2O	0.03	0.01	0.30	0.12	0.07	0.15	0.37
K2O	0.05	0.00	0.00	0.00	0.00	0.00	0.00
Total	98.33	94.44	97.73	95.37	96.29	97.73	97.03

structural fomulae on the basis of 13 oxygens

	6.26a	12a.25	12a.25	12b.32	12b.32	1.24	1.25
SI	2.639	2.662	3.090	3.345	3.308	3.128	3.181
TI	2.451	2.347	0.519	0.009	0.006	0.001	0.011
AI	0.129	0.175	1.829	2.200	2.202	2.851	2.404
FE3	0.115	0.128	0.769	1.031	1.016	0.350	0.824
MN	0.004	0.000	0.026	0.000	0.015	0.004	0.004
CA	2.502	2.592	2.189	1.946	2.031	2.083	2.128
NA	0.005	0.001	0.049	0.020	0.012	0.023	0.060
K	0.005	0.000	0.000	0.000	0.000	0.000	0.000
Total	7.850	7.905	8.941	8.556	8.591	8.457	8.635

Granites to the east of WBF: mineral analysis
Allanite

Sample Code Spot	6.26a	6.26a	1.19a
SIO2	26.40	27.12	3.45
TIO2	1.25	1.25	5.45
AL2O3	10.58	10.65	6.46
FE2O3	17.17	16.76	45.57
MNO	0.00	0.00	0.00
MGO	0.97	1.00	0.62
CAO	7.87	8.41	0.63
NA2O	1.27	1.44	1.33
K2O	0.60	0.55	0.06
Tota	66.11	67.18	63.54
SI	3.445	3.408	0.595
TI	0.123	0.118	0.706
AL	1.628	1.623	1.313
FE3	1.873	1.762	6.567
MN	0.000	0.000	0.000
MG	0.189	0.186	0.158
CA	1.101	1.132	0.117
NA	0.320	0.350	0.445
K	0.100	0.088	0.013

Granites to the East of WBF: mineral analysis
K-feldspar

	Hornblende-bearing Granites				Hornblende-free Granites			
Sample	6.29a	12a.25	12b.32	12b.32	1.19a	1.24	1.24	1.25
Code	core	rim	core	rim	core	core	rim	rim
SiO2	64.88	65.13	65.40	63.92	66.13	67.33	63.42	69.47
TiO2	0.24	0.23	0.11	0.28	0.23	0.18	0.00	0.07
Al2O3	18.51	19.46	18.87	18.46	18.75	19.12	17.87	20.44
FeO	0.05	0.09	0.15	0.04	0.00	0.00	0.13	0.11
MnO	0.00	0.10	0.04	0.00	0.05	0.16	0.11	0.00
MgO	0.00	0.05	0.00	0.00	0.00	0.00	0.00	0.00
CaO	0.00	0.06	0.00	0.02	0.00	0.09	0.21	0.11
Na2O	0.77	1.09	0.66	0.63	0.79	7.36	0.48	11.67
K2O	15.15	14.86	15.07	14.83	15.61	6.65	15.38	0.13
Tota	99.60	101.07	100.30	98.18	101.56	101.11	97.60	101.98
SI	2.995	2.963	2.994	2.990	2.996	2.989	3.00	2.976
AL	1.007	1.044	1.018	1.018	1.001	0.997	0.996	1.032
FE2	0.002	0.003	0.006	0.001	0.000	0.000	0.005	0.004
MG	0.000	0.003	0.006	0.000	0.000	0.000	0.000	0.000
CA	0.000	0.003	0.000	0.001	0.000	0.004	0.011	0.005
NA	0.069	0.096	0.059	0.057	0.069	0.630	0.044	0.969
K	0.892	0.863	0.880	0.885	0.902	0.376	0.928	0.007
AN	0.0	0.30	0.0		0.0	0.40	1.12	
AB	7.2	10	6	6	7.11	62.38	4.48	
OR								

Granites to the west of WBF
K-feldspar

	marginal Gr.		Granites to the South of Bixter Voe					
Sample	15.6	19a.6	19a.6	19a.6	19a.6	19a.6	19.4	19.4
Code	core	core	rim	rim	core	core	core	rim
SiO2	65.6	65.96	65.55	63.56	63.06	57.13	65.13	66.69
TiO2	0.09	0.10	0.31	0.23	0.28	0.32	0.13	0.05
Al2O3	18.33	18.70	18.99	17.73	17.95	26.15	18.73	19.51
FeO	0.19	0.23	0.22	0.09	1.04	0.37	0.17	0.09
MnO	0.08	0.06	0.00	0.00	0.08	0.03	0.00	0.03
MgO	0.00	0.03	0.00	0.00	0.00	0.00	0.00	0.00
CaO	0.02	0.24	0.00	0.00	0.00	5.91	0.06	0.68
Na2O	3.89	8.45	0.98	1.21	2.73	4.87	3.98	10.48
K2O	11.58	5.17	14.96	14.17	12.13	3.77	10.83	1.95
Total	100.15	98.94	101.00	97.00	97.17	98.62	99.03	100.38
SI	2.996	2.978	2.983	3.005	2.972	2.614	2.985	2.961
AL	0.984	0.995	1.018	0.988	0.997	1.410	1.012	1.021
FE2	0.007	0.009	0.009	0.003	0.041	0.014	0.006	0.003
MG	0.000	0.002	0.000	0.000	0.000	0.001	0.000	0.000
CA	0.017	0.012	0.000	0.000	0.000	0.290	0.003	0.032
NA	0.344	0.739	0.086	0.110	0.250	0.432	0.354	0.903
K	0.673	0.298	0.869	0.855	0.729	0.220	0.633	0.110
AN	1.64	1.14	0.0	0.0	0.0	30.79	0.30	3.06
AB	33.27	70.45	9.01	11.40	25.54	45.86	35.76	86.41
OR	65.09	28.41	90.99	88.60	74.46	33.35	63.94	10.53

Granite to the West and East of the Walls Boundary Fault

Fe-Ti oxides (magnetite and ilmenite)

Sample Code	12a.25	12b.32	12b.32	1.25	15.6	19a.6	19.4
	Hornblende-bearing granites						
SiO2	0.34	0.46	0.41	2.28	0.587	0.597	0.742
TiO20	0.05	0.03	0.00	0.00	6.706	4.498	0.105
Al2O3	0.12	0.00	0.16	0.242	0.137	0.105	0.184
FeO	90.69	90.33	89.91	57.29	80.41	81.69	85.47
MnO	0.00	0.13	0.18	0.00	0.00	0.195	0.009
MgO	0.22	0.19	0.23	0.00	0.154	0.232	0.212
CaO	0.14	0.06	0.01	0.00	0.029	0.000	0.131
Na2O	0.01	0.47	0.41	0.012	0.507	0.083	0.616
K2O	0.00	0.00	0.04	0.00	0.00	0.00	0.31
Total	91.56	91.67	91.35	60.00	89.00	87.00	88.00
	Structural formulae based on 32 oxygen for magnetite & 6 oxygen for ilmenite)						
Si	0.140	0.190	0.168	1.383	0.276	0.246	0.319
Ti	0.015	0.008	0.000	0.000	2.024	1.394	0.034
Al	0.059	0.000	0.078	0.172	0.065	0.051	0.093
Fe2							
Fe3							
Mn	0.000	0.044	0.062	0.000	0.068	0.003	0.21
Mg	0.135	0.118	0.145	0.000	0.000	0.143	0.136
Ca	0.063	0.027	0.004	0.009	0.000	0.044	0.060

Granites to the East and to the West of the Walls Boundary Fault

Sphene

Sample	6.29a	6.29a	12a.25	12a.25	19a.6
SiO2	30.01	29.95	29.37	28.84	29.19
TiO2	36.99	38.11	34.99	34.19	36.76
Al2O3	1.34	1.10	1.83	1.48	1.00
FeO	1.38	1.16	1.83	2.02	1.99
MnO	0.161	0.00	0.00	0.00	0.00
MgO	0.026	0.00	0.00	0.00	0.039
CaO	27.13	26.79	26.43	26.11	25.61
Na2O	0.171	0.094	0.092	0.220	0.178
K2O	0.057	0.002	0.00	0.041	0.033
Total	97.30	97.11	94.00	93.00	95.0
	structural formulae based on 20 oxygen				
Si	1.009	1.005	1.016	1.017	1.005
Ti	0.935	0.962	0.910	0.907	0.952
Al	0.053	0.044	0.075	0.060	0.040
Fe3	0.039	0.032	0.053	0.060	0.057
Mn	0.005	0.000	0.000	0.000	0.000
Mg	0.001	0.000	0.000	0.000	0.002
Ca	0.977	0.964	0.980	0.987	0.945
Na	0.011	0.006	0.006	0.015	0.012
K	0.002	0.000	0.000	0.002	0.004

A2.12) IGNEOUS ROCKS (mostly granites)
Hornblende-bearing-granites (Sample used only for mode analysis)

modal mineralogy percent

SampleNO.	Plag	Ksp	Qz	Bio	Hb	Chl	Ep	Op	Ap	Sph	Zr
Graven Complex											
6.3	49.10	9.10	21.80	0.00	0.00	20.00	0.00	0.00	0.00	0.00	0.0
6.4	56.80	6.90	14.50	0.00	0.00	21.80	0.00	0.00	0.00	0.00	0.0
6.7	35.50	17.0	10.9	13.7	22.9	0.00	0.00	0.00	0.00	0.00	0.0
6.8	50.60	15.4	25.3	7.50	0.00	1.20	0.00	0.00	0.00	0.00	0.0
6.17	52.20	20.10	16.5	9.20	1.00	0.60	0.00	0.00	0.00	0.40	0.0
6.20	46.90	12.70	27.00	11.90	0.00	1.50	0.00	0.00	0.00	0.00	0.0
6.23	50.60	3.00	17.30	10.90	17.50	0.00	0.70	0.00	0.00	0.00	0.0
6.26	54.40	5.00	20.30	7.00	12.40	0.00	0.00	0.00	0.00	0.90	0.0
6.27	42.60	18.60	28.40	2.90	0.00	7.50	0.00	0.00	0.00	0.00	0.0
Brae Complex											
7.1	55.00	2.40	32.00	3.90	0.00	6.70	0.00	0.00	0.00	0.00	0.0
7.3	40.50	24.40	11.60	15.0	5.00	0.30	0.60	0.70	0.30	0.00	0.0
7.5	42.50	21.90	18.90	15.5	0.60	0.00	0.00	0.00	0.00	0.00	0.0
7.7	47.00	19.50	16.10	14.0	2.30	0.00	0.40	0.00	0.00	0.70	0.0
7.8	41.60	16.10	31.50	4.40	0.00	6.4	0.00	0.00	0.00	0.00	0.0
7.9	49.30	2.00	18.00	27.2	1.90	0.20	0.00	0.00	0.30	1.10	0.0
7.13	57.00	3.30	26.10	13.2	0.00	0.00	0.00	0.40	0.00	0.00	0.0
Aith-Hildsay-Spigie Granite											
12c.1	41.0	7.20	32.70	0.00	0.00	4.20	14.80	0.00	0.00	0.00	0.0
12c.3	44.30	22.20	20.80	0.00	0.00	8.30	4.40	0.00	0.00	0.00	0.0
12c.5	38.20	21.10	35.20	2.30	0.00	0.00	5.50	0.00	0.00	0.00	0.0
12c.8	44.20	11.00	30.00	5.70	0.00	1.60	7.50	0.00	0.00	0.00	0.0
12.b10	37.10	50.20	4.10	0.00	3.70	0.00	3.70	0.00	0.00	0.00	0.0
12b.13	45.30	2.80	29.40	13.3	0.70	6.10	1.30	0.00	0.00	0.00	0.0
12.b15	40.30	13.30	26.10	9.20	0.00	0.00	11.10	0.00	0.00	0.00	0.0
12b.16	47.50	9.20	19.60	7.20	0.00	0.80	15.70	0.00	0.00	0.00	0.0
12a.19	42.50	27.80	11.00	8.10	0.00	0.00	10.60	0.00	0.00	0.00	0.0
12a.22	56.70	8.90	16.40	12.30	0.00	0.00	5.70	0.00	0.00	0.00	0.0
12a.23	43.80	6.80	24.10	15.30	0.00	0.00	10.00	0.00	0.00	0.00	0.0

Hornblende-bearing granites (Non analysed samples either for mode neither for geochemical)

Sample No.	Akli	plag	ksp	Qz	Px	Bi	Hb	Chl	Musc	SPh	Ep	Ap	Op	Zr	Al
Graven Complex.															
6.1	o	xxx	xx	xx	o	xx	o	x	o	o	x	x	o	o	o
6.2	o	xxx	xx	xx	o	xx	xx	x	o	xx	x	x	xx	o	o
6.5	o	xxx	xxx	xxx	o	xx	o	o	o	x	o	x	x	o	x
6.6	o	xxx	xx	xx	o	xx	xx	o	o	x	x	x	o	o	o
6.9	o	xxx	xxx	xxx	o	xx	x	x	o	x	x	x	o	o	x
6.10	o	xxx	xxx	xxx	o	xx	xx	o	o	x	x	x	o	o	o
6.11	o	xxx	xxx	xxx	o	xx	xx	x	o	x	x	x	o	o	x
6.12	o	xxx	xxx	xxx	o	o	xx	x	o	x	x	o	o	o	o
6.13	o	xxx	xxx	xxx	o	xx	o	x	x	o	o	x	x	o	o
6.14	o	xxx	xxx	xxx	o	xx	xx	x	o	x	x	x	o	o	x
6.15	o	xxx	xxx	xxx	o	xx	o	o	o	o	o	x	o	o	o
6.16	o	xxx	xxx	xxx	o	xx	o	x	o	o	o	x	o	o	x
6.18	o	xxx	xx	xx	o	xx	xx	o	o	x	o	x	x	o	o
6.19	o	xxx	xxx	xxx	0	xx	o	x	o	o	o	x	x	o	o

(o : absent; x : rare; xx : frequent; xxx : abundant)

Sample No.	Akli	plag	ksp	Qz	Px	Bi	Hb	Chl	Musc	SPh	Ep	Ap	Op	Zr	Al
6.21	o	xxx	xx	xxx	o	xx	o	o	o	x	x	x	x	o	x
6.22	o	xxx	xx	xxx	o	xx	o	o	o	x	o	x	x	o	x
6.24	o	xxx	x	xxx	o	xx	xx	o	o	x	o	x	x	o	o
6.25	o	xxx	x	xxx	o	xx	xx	o	o	x	o	x	x	o	o
6.28	o	xxx	xx	xxx	o	xx	xx	x	o	o	o	x	o	o	o
Brae Complex															
7.2	o	xxx	xx	xxx	o	xx	o	x	o	o	o	o	o	x	o
7.4	o	xxx	xxx	xxx	o	xx	o	x	o	o	x	x	o	x	o
7.6	o	xxx	xxx	xxx	o	xx	xx	o	o	x	x	x	x	x	o

7.10	O	XXX	X	XXX	O	X	O	XX	O	O	O	O	X	O	O
7.11	O	XXX	X	XXX	O	XX	O	X	O	O	X	O	O	O	O
7.12	O	XXX	XX	XXX	O	XX	O	X	O	O	O	X	O	O	O

Aith-Hildsay-Spiggie Granite

12c.2	O	XXX	XX	XXX	O	O	O	O	O	O	XXX	X	X	O	X
12c.6	O	XXX	XXX	XXX	O	XX	O	X	O	O	XX	X	X	O	O
12c.7	O	XXX	XX	XXX	O	O	O	X	O	O	XX	O	X	O	O
12c.9	O	XXX	XXX	X	O	O	O	O	O	O	O	O	O	O	O
12b.11	O	XXX	XXX	XX	O	X	X	X	O	X	XX	X	X	O	X
12b.14	O	XXX	X	XXX	O	O	O	X	O	X	X	X	X	O	X
12b.17	O	XXX	X	XXX	O	XX	O	X	O	X	X	X	X	X	X
12b.18	O	XXX	X	XXX	O	X	O	X	O	X	X	X	X	O	X
12a.20	O	XXX	XX	XXX	X	XX	XX	X	O	X	X	X	X	O	X
12a.21	O	XXX	XX	XXX	O	O	XX	O	O	X	X	X	X	X	O

Hornblende-free granites (Samples used only for Mode analysis)

Sample No.	Plag	Ksp	QZ	Bio	Chl	Musc	Ep	Sph	Gar	Op	Zr	Al
Skaw Granite												
1.7	38.22	20.00	26.25	15.26	0.00	0.00	0.00	0.34	0.00	0.00	0.00	0.00
1.11	41.20	20.00	22.19	15.57	0.00	0.00	0.00	0.34	0.00	0.50	0.00	0.43
1.17	43.76	20.00	20.64	14.96	0.00	0.00	0.00	0.80	0.00	0.00	0.00	0.00
1.22	33.47	20.00	31.98	13.97	0.00	0.00	0.00	0.00	0.00	0.00	0.00	0.00
Tonga Granite												
2.3	22.40	25.60	45.20	6.80	0.00	1.60	0.00	0.00	0.20	0.00	0.00	0.00
Breckin Granite												
4a.2	27.30	23.70	30.50	5.80	0.00	12.70	0.00	0.00	0.00	0.00	0.00	0.00
4a.6	38.90	10.10	24.90	21.00	0.00	3.60	0.00	1.50	0.00	0.00	0.00	0.00
Out Skerries Granite (It is thought to be a continuation of Colla Firth permeation belt)												
5.2	35.00	19.80	32.00	5.90	1.30	7.00	0.00	0.00	0.00	0.00	0.00	0.00
5.3	40.30	23.10	32.70	3.20	0.70	0.00	0.00	0.00	0.00	0.00	0.00	0.00
5.4	30.80	27.90	30.40	7.00	0.00	3.70	0.00	0.00	0.00	0.00	0.00	0.00
5.5	29.20	33.50	27.40	6.70	0.00	3.20	0.00	0.00	0.00	0.00	0.00	0.00
5.7	34.70	23.80	35.60	0.00	0.00	5.90	0.00	0.00	0.00	0.00	0.00	0.00
Colla Firth granites												
9.4	42.10	24.10	22.50	2.50	0.00	7.30	1.50	0.00	0.00	0.00	0.00	0.00
9.7	23.90	32.50	29.50	3.50	0.00	10.60	0.00	0.00	0.00	0.00	0.00	0.00
9.10	24.50	34.30	28.80	4.10	0.00	7.00	1.30	0.00	0.00	0.00	0.00	0.00
9.13	42.80	25.70	28.00	0.00	0.00	2.70	0.00	0.80	0.00	0.00	0.00	0.00
9.14	38.60	30.50	27.70	3.20	0.00	0.00	0.00	0.00	0.00	0.00	0.00	0.00

Hornblende-free granites (Non analysed samples either for modes neither for Geochemical)

Sample No.	Alkli	plag	ksp	Qz	Px	Bi	Hb	Chl	Musc	SPh	Ep	Ap	Op	Zr	Al
Skaw Granite															
1.2	O	XXX	XXX	XXX	O	XXX	O	O	O	O	O	X	X	O	X
1.3	O	XXX	XXX	XXX	O	XXX	O	X	O	X	O	X	X	X	X
1.4	O	XXX	XXX	XXX	O	XXX	O	O	O	X	O	X	O	X	O
1.5	O	XXX	XXX	XXX	O	XXX	O	X	O	X	O	X	X	X	O
1.6	O	XXX	XXX	XXX	O	XXX	O	X	O	X	O	X	X	X	O
1.8	O	XXX	XXX	XXX	O	XXX	O	X	O	X	O	X	X	X	O
1.9	O	XXX	XXX	XXX	O	XXX	O	X	O	O	O	X	X	X	O
1.10	O	XXX	XXX	XXX	O	XXX	O	X	O	O	O	O	X	X	X
1.12	O	XXX	XXX	XXX	O	XXX	O	X	O	X	O	O	X	X	O
1.13	O	XXX	XXX	XXX	O	XXX	O	O	O	X	O	X	O	X	O
1.14	O	XXX	XXX	XXX	O	XXX	O	X	O	O	O	X	X	X	X
1.15	O	XXX	XXX	XXX	O	XXX	O	X	O	X	O	X	X	X	X
1.16	O	XXX	XXX	XXX	O	XXX	O	X	O	X	O	X	X	O	O
1.18	O	XXX	XXX	XXX	O	XXX	O	X	O	O	O	X	O	X	O
1.19	O	XXX	XXX	XXX	O	XXX	O	O	O	X	O	X	X	X	O
1.20	O	XXX	XXX	XXX	O	XXX	O	X	O	X	O	X	X	X	X
1.21	O	XXX	XXX	XXX	O	XXX	O	X	O	X	O	X	X	X	X
1.23	O	XXX	XXX	XXX	O	XXX	O	X	O	O	O	X	X	X	O
Breckin Granite															
4a.3	O	XXX	XXX	XXX	O	XX	O	O	XX	X	O	X	O	X	O

```
4a.4              o   xxx  xxx  xxx o  xx  o  o   xx   x   o  x  o  x  o
4a.5              o   xxx  xxx  xxx o  xx  o  x   xx   o   o  x  x  x  x
4b.4              o   xxx  x    xxx o  xx  o  x   xx   x   o  x  o  x  o
4b.5              o   xxx  x    xxx o  xx  o  x   xx   x   o  x  o  x  o
4b.6              o   xxx  x    xxx o  xx  o  x   xx   o   x  o  o  x  o
4b.7              o   xxx  xxx  xxx o  xx  o  o   xx   o   o  x  o  x  o
Out Skerries Granit
5.6               o   xxx  xxx  xxx o  xx  o  x   xx   o   o  x  o  o  o
5.8               o   xxx  xxx  xxx o  xx  o  x   xx   o   o  o  o  o  o
Colla  Firth permeation belt
9.5               o   xxx  xxx  xxx o  xx  o  x    x   o   x  o  o  o  o
9.6               o   xxx  xxx  xxx o   o  o  xx   xx  o   x  x  o  o  o
9.8               o   xxx  xxx  xxx o  xx  o  o   xxx  o   o  o  o  o  o
9.9               o   xxx  xxx  xxx o  xx  o  x   xx   x   x  o  o  o  o
9.11              o   xxx  xxx  xxx o   o  o  o   xxx  x   x  o  o  o  o
9.12              o   xxx  xxx  xxx o   o  o  o   xxx  o   o  o  o  o  o
9.13              o   xxx  xxx  xxx o   o  o  o   xxx  x   o  o  o  o  o
9.15              o   xxx  xxx  xxx o   o  o  o   xxx  o   o  o  o  o  o
9.18              o   xxx  xxx  xxx o  xx  o  x   xx   o   x  o  o  x  o
```

(o : absent; x : rare; xx : frequent; xxx : abundant)

IGNEOUS ROCKS (mostly granites)
Ronas Hill Granite and its satellites to the west of WBF (samples used only for mode analysis).

Sample No.	Alkli	Plag	Ksp	Qz	Bio	Aeg	Chl	Al	Ep	Op
Ronas Hill Granite										
28529	49.60	16.20	0.00	32.30	0.90	0.00	0.80	0.00	0.00	0.20
28531	58.60	7.00	0.00	34.40	0.00	0.00	0.00	0.00	0.00	0.00
28537	60.80	2.20	0.00	33.50	0.00	1.00	0.70	0.00	1.10	0.70
29330	40.08	33.60	0.00	26.10	0.00	1.60	0.20	0.00	0.00	1.70
35124	40.11	26.08	0.00	34.21	0.60	0.00	0.00	0.00	0.00	0.00
43394	51.40	15.80	0.00	28.70	0.00	0.00	4.10	0.00	0.00	0.00
43388	63.50	6.50	0.00	30.86	0.00	0.00	0.20	0.00	0.00	0.00
43384	35.90	32.90	0.00	29.30	0.00	0.00	1.90	0.00	0.00	0.00
42696	34.80	29.40	0.00	31.60	0.60	0.70	2.20	0.00	0.20	0.50
42866	30.40	37.20	0.00	28.40	4.00	0.00	0.00	0.00	0.00	0.00
43429	34.50	30.70	0.00	32.20	0.00	0.00	2.60	0.00	0.00	0.00
46238	44.40	21.70	0.00	32.90	1.0	0.00	0.00	0.00	0.00	0.00
58021	34.80	30.20	0.00	31.70	0.00	0.00	2.30	0.00	1.00	0.00
58407	48.20	20.20	0.00	27.20	0.90	0.00	3.50	0.00	0.00	0.00
59127	65.00	0.00	0.00	33.80	0.70	0.00	0.50	0.00	0.00	0.00
Eastern Granite or Marginal Granite										
29419	72.70	6.10	0.00	18.90	2.00	0.00	0.30	0.00	0.00	0.00
42697	47.70	20.00	0.00	30.20	1.2	0.00	1.00	0.00	0.00	0.00
42967	54.10	8.80	0.00	34.40	2.00	0.00	0.70	0.00	0.00	0.00
59126	50.50	2.30	0.00	44.90	1.3	0.00	0.00	0.00	0.00	1.00
15.2	63.80	3.20	0.00	32.40	0.00	0.00	0.00	0.00	0.00	0.60
15.3	49.20	15.00	0.00	31.40	0.00	3.00	0.00	0.00	0.00	1.00
15.4	47.00	15.80	0.00	34.80	0.40	0.00	1.60	0.00	0.00	0.40
15.7	58.20	4.00	0.00	37.20	0.60	0.00	0.00	0.00	0.00	0.00
Vementry Granite										
30734	43.70	18.50	0.00	37.00	0.40	0.00	0.40	0.00	0.00	0.00
30717	35.97	39.71	0.00	23.40	2.80	0.00	0.80	0.00	0.00	0.20
30737	45.70	22.80	0.00	29.50	1.50	0.00	0.50	0.00	0.00	0.00
30712	51.70	20.20	0.00	25.90	1.20	0.00	0.80	0.00	0.00	0.20
50139	45.60	23.10	0.00	28.50	1.80	0.00	0.50	0.50	0.00	0.00

Ronas Hill Granite and its satellites (Non-analysed samples either for mode niether for Geochemistry).

Sample No.	Alkali	Plag	Ksp	Qz	Bio	Chl	Ep	Op	Zr	Al
Ronas Hill granite										
28529	xxx	xxx	o	xxx	xx	x	x	o	o	o
28533	xxx	xxx	o	xxx	o	o	o	x	o	o
35124	xxx	xxx	o	xxx	o	xx	o	x	o	o

43387	xxx	xxx	o	xxx	xx	x	o	x	x	o
43424	xxx	xxx	o	xxx	o	xx	o	x	o	x
47485	xxx	xxx	o	xxx	o	o	o	x	o	o
59132	xxx	xxx	o	xxx	o	o	x	o	o	o
57472	xxx	xxx	o	xxx	xx	o	o	x	o	x
59928	xxx	xxx	o	xxx	o	xx	x	x	o	x
Eastern Granite										
28913	xxx	xxx	o	xxx	o	xx	x	x	o	o
35106	xxx	xxx	o	xxx	o	o	o	o	o	o
44113	xxx	xxx	o	xxx	o	o	o	x	o	o
47599	xxx	xxx	o	xxx	o	o	o	x	o	o
Muckle Roe										
28905	xxx	o	o	xxx	o	xx	o	x	o	o
70500	xxx	xxx	o	xxx	x	o	o	x	o	o

IGNEOUS PETROLOGY (mostly granites)
Sandsting and Bixter Granites (Samples used only for modes analysis)

Sample No.	Alkli	Plag	Ksp	Qz	Bio	Hb	Chl	Ep	Sph	Op	Ap	Al
Bixter Granite												
31133	53.10	21.30	0.00	25.00	0.40	0.00	0.20	0.00	0.00	0.00	0.00	0.0
51548	49.50	13.90	0.00	36.00	0.60	0.00	0.00	0.00	0.00	0.00	0.00	0.0
19a.2	38.80	25.80	0.00	31.80	1.00	0.00	2.60	0.00	0.00	0.00	0.00	0.0
19a.3	28.00	32.00	0.00	38.40	0.40	0.00	0.00	1.20	0.00	0.00	0.00	0.0
19a.4	35.40	24.00	0.00	36.40	4.20	0.00	0.00	0.00	0.00	0.00	0.00	0.0
19a.7	44.60	25..40	0.00	26.60	3.40	0.00	0.00	0.00	0.00	0.00	0.00	0.0
19a.8	26.40	32.60	0.00	37.40	2.6	0.00	0.00	000	0.00	0.00	0.00	0.0
Sandsting Complex.												
28875	0.00	41.80	30.00	24.60	2.40	1.00	0.00	0.00	0.00	0.00	0.00	0.2
29871	0.00	35.10	20.3	7.60	19.20	12.00	0.00	3.70	2.10	0.00	0.00	0.0
29522	0.00	42.40	30.10	19.70	4.40	1.80	0.40	0.00	0.00	1.20	0.00	0.0
29526	0.00	22.80	19.8	55.60	1.60	0.60	0.00	0.00	0.00	0.00	0.00	0.0
31141	0.00	48.10	8.40	4.10	17.70	18.20	0.00	0.70	1.80	1.00	0.00	0.0
31159	0.00	39.20	33.90	15.60	7.20	3.40	0.00	0.00	0.00	00.30	0.00	0.4
33678	0.00	55.60	7.80	11.90	15.40	5.90	0.00	0.40	1.70	1.00	0.40	0.0
51505	0.00	44.70	32.10	15.3	4.90	1.90	0.00	0.30	0.50	0.30	0.00	0.0
51506	0.00	54.20	13.80	8.30	13.00	9.30	0.00	0.60	0.00	0.80	0.00	0.0
51509	0.00	41.10	30.40	22.60	4.0	1.40	0.00	0.00	0.00	0.50	0.00	0.0
51529	0.00	44.60	30.60	7.30	8.00	6.40	0.00	0.00	2.00	1.10	0.00	0.0
51519	0.00	26.90	42.90	26.10	1.90	2.00	0.00	0.00	0.00	0.20	0.00	0.0
19.8	0.00	48.40	24.40	20.60	2.40	2.20	0.00	0.00	1.00	1.00	0.00	0.0

IGNEOUS PETROLOGY (Non analysed samples either for modes niether for Geochemistry.

Sample No	Alkli	Plag	Ksp	Qz	Bio	Hb	Ep	Al	Sph	Ap	OP	Zr
Bixter Granite												
29874	o	xxx	xxx	xxx	xx	o	o	x	o	x	o	o
31130	o	xxx	xxx	xxx	xx	xx	o	o	x	x	x	o
45285	xxx	xxx	o	xxx	o	o	o	o	o	o	x	o
51531	o	xxx	xx	xxx	xx	xx	o	o	o	o	x	o
51550	xxx	xxx	o	xxx	o	o	o	o	o	o	x	o
Sandsting Granite												
28878	o	xxx	xx	xxx	xx	xx	o	o	x	x	x	o
29512	o	xxx	xx	xxx	xx	x	o	o	o	x	x	o
29516	o	xxx	xx	xxx	xx	o	o	o	x	x	x	o
31137	o	xxx	xxx	xx	xx	xx	x	o	x	x	x	o
31141	o	xxx	xx	xx	xx	xx	x	o	x	x	x	o
51508	o	xxx	xxx	x	xx	x	o	o	o	o	x	o
51521	o	xxx	xxx	xx	xx	xx	x	x	x	o	x	o
51525	o	xxx	xxx	xxx	xx	xx	o	o	x	x	x	o
51536	o	xxx	xxx	xx	xx	xx	o	o	x	o	x	o
29525	o	xxx	xxx	xx	xx	xx	x	o	x	o	x	o

GRANITIC PEBBLES TO THE EAST OF WALL BOUNDARY FAULT

Sample No. Tour	Alkli	Plag	Ksp	Qz	Bio	Hb	Chl	Musc	Ep	Cal	Op	
Funzie Conglomerate												
3c.1	0.00	73.70	0.00	26.30	0.00	0.00	0.00	0.00	0.00	0.00	0.00	0.00
3c.2	0.00	59.50	0.00	40.50	0.00	0.00	0.00	0.00	0.00	0.00	0.00	0.00
3.4	0.00	53.80	5.00	41.20	0.00	0.00	0.00	0.00	0.00	0.00	0.00	0.00
3c.6	0.00	41.60	11.60	45.80	0.00	0.00	0.00	1.00	0.00	0.00	0.00	0.00
3c.9	0.00	41.00	18.20	36.80	0.00	0.00	0.00	0.00	4.00	0.00	0.00	0.00
3c.12	0.00	45.60	8.60	33.20	7.20	0.00	0.00	5.40	0.00	0.00	0.00	0.00
3c.13	0.00	65.00	5.60	28.00	0.00	0.00	0.00	0.80	0.00	0.00	0.60	0.00
Rova Head Conglomerate												
8.2	0.00	44.70	15.30	34.10	0.00	0.00	0.00	1.00	0.00	4.90	0.00	0.00
8.5	0.00	55.60	9.80	28.40	2.20	0.00	0.00	4.00	0.00	0.00	0.00	0.00

A2.13) Tables of sample numbers used in this thesis giving name of granite, gric reference,
University of Liverpool catalogue number and analytical details.

Univ. Liv. Cat. No.

this the catalogue number given to a rock specimen when a thin section is cut in the Geology Dept., Liverpool University. The number also identifies the corresponding thin-section.

Analytical details

XRF   - rock analysed for major and trace elements by XRF.
INAA - rock analysed for trace elements by INAA.
RE   - rock analysed for rare earth elements by RNAA.
PC   - point counter data.

Sample Loc.No.	Univ. Liv. Cat. No.	Grid. Ref.	Granite name	Anal. Details
1.1	70505	653145	Skaw granite	XRF, INAA, PC
1.7	70506	676154	Skaw granite	XRF, INAA, PC
1.10a	75435	671158	Skaw granite	XRF, PC, RE
1.19a	75436	660170	Skaw diorite xenolith	XRF, PC, RE
1.22a	75438	653174	Skaw granite	XRF, PC
1.24	75439	669153	Skaw granite	XRF, PC
1.25	75440	672154	Skaw granite	XRF, PC
1.26	75441	666170	Skaw granite	XRF, PC
2.1	70507	581147	Tonga granite	XRF, INAA PC
2.2	75442	581149	Tonga granite	XRF, PC
2.5	75445	582138	Tonga granite	XRF, PC
3a.1	72404	64750595	Trondhjemite dyke	XRF, INAA, PC
3a.2	71817	59939886	Trondhjemite dyke	XRF, INAA, PC
3a.4	75456	6240339	Trondhjemite dyke	XRF, PC
3b.1	71730	599989	Trondhjemite dyke	XRF, INAA, PC
3c.5	75447	667896	Funzie granitic pebbles	XRF, PC
3c.10	75452	67409055	Funzi granitic pebble	XRF, PC
3c.11	75453	67409050	Funzie granitic pebble	XRF, PC
4a.1	70508	524043	Brecken granite	XRF, INAA,PC
4a.2	70508	524043	Brecken granite	XRF, PC
4B.1	70511	449953	Brecken granite	XRF, INAA, PC
4b.2	70509	449954	Brecken granite	XRF, INAA, PC
5.9	75457	69557195	Out Skerries granite	XRF, PC
5.11	75459	68107210	Out Skerries granite	XRF, INAA, PC
5.12	75460	68307255	Out Skerries granite	XRF, PC
6.10	70504	450745	Graven Complex	XRF, PC
6.13a	75463	44507580	Graven Complex	XRF, RE, INAA, PC
6.16a	75464	42957880	Graven Complex	XRF, INAA, PC
6.24a	75465	47605955	Graven Complex	XRF, RE, PC
6.26a	75466	50456050	Graven Complex	XRF, PC
6.29a	75467	49406005	Graven Complex	XRF, RE, PC
6.30	75468	42507925	Graven Complex	XRF, RE, PC

Sample Loc.No.	Univ. Liv. Cat. No.	Grid. Ref.	Rock Type	Anal. Details
6.31	75469	37657750	Graven Complex	XRF, INAA, PC
7.5	70499	368669	Brae Complex	XRF, INAA, PC
7.10a	75471	38456215	Brae Complex	XRF, PC
7.14	75471	38506210	Brae Complex	XRF, PC
8.2	70600	469444	Rova granitic pebble	XRF, INAA, PC
8.3	75472	46704415	Rova granitic pebble	XRF, PC
8.4	75473	46704415	Rova granitic pebble	XRF, PC
8.6	75474	46704415	Rova granitic pebble	XRF, PC
8.7	75476	46704415	Rova granitic Pebble	XRF, PC
8.8	75477	46704415	Rova granitic pebble	XRF, PC
8.9	75478	46704415	Rova granitic pebble	XRF, PC
8.11	75480	46704415	Rova granitic pebble	XRF, PC
8.12	75481	46704415	Rova granitic pebble	XRF, PC
8.13	75482	46704415	Rova granitic pebble	XRF, PC
8.14	75483	47254510	Rova granitic pebble	XRF, PC
8.15	75484	47254510	Rova granitic pebble	XRF, PC
9.1a	75486	34852910	Colla Firth granite	XRF,PC
9.2	70602	395388	Colla Firth granite	XRF, INAA, PC
9.5a	75488	40104520	Colla Firth granite	XRF, PC
9.17	75490	41304420	Colla Firth granite	XRF, RE, PC
9.19	75492	40904620	Colla Firth granite	XRF, PC
9.20	75493	44755075	Colla Firth granite	XRF, PC
9.22	75495	42903610	Colla Firth granite	XRF, PC
9.23	75496	361207	Colla Firth granite	XRF, RE, PC
10.1	70595	403234	Channerwick granite	XRF, INAA, PC
10.2	75497	40302345	Channerwick granite	XRF, PC
11.1	75499	43403060	Cunningsburgh granite	XRF, PC
12a.24	70497	346474	Aith granite	XRF, INAA, PC
12a.25	70603	344521	Aith granite	XRF, INAA, PC
12a.27	75501	3440560	Aith granite	XRF, PC
12a.28	75502	34255650	Aith granite	XRF, INAA, RE, PC
12b.12	70601	368359	Hildasay granite	XRF, PC
12b.30	75504	36703530	Hildasay granite	XRF, INAA, RE, PC
12b.31	75505	36603535	Hildasay granite	XRF, INAA, RE, PC
12b.32	75506	36703520	Hildasay granite	XRF, RE, PC
12b.33	75507	36503550	Hildasay granite	XRF, INAA, PC
12b.34	75508	36403595	Hildasay granite	XRF, PC
12b.35	75509	35353750	Hildasay granite	XRF, RE, PC
12b.36	75510	34903845	Hildasay granite	XRF, PC
12b.37	75511	35754010	Hildasay granite	XRF, INAA, PC
12c.4	70597	357168	Spiggie granite	XRF, PC
12c.39	75513	37501810	Spiggie granite	XRF, PC
12c.40	75514	37701770	Spiggie granite	XRF, INAA, RE, PC
12c.41	75515	35701780	Spiggie granite	XRF, PC
12c.42	75516	35701770	Spiggie granite	XRF, INAA, RE, PC
12c.43	75517	37051560	Spiggie granite	XRF,PC
12c.44	75518	37551620	Spiggie granite	XRF, INAA, RE, PC
13.1	70594	427275	Abite-keratophyre	XRF, PC
14.1	70502	353845	Ronas Hill granite	XRF, PC
14.2	75519	32108720	Ronas diorit raft	XRF, INAA, PC

Sample Loc.No.	Univ. Liv. Cat. No.	Grid. Ref.	Rock Type	Anal. Details
14.3	75520	32158735	Ronas two-feldspar granite	XRF, RE, PC
14.4	75521	32058775	Ronas two-feldspar granite	XRF, INAA,PC
14.5	75522	33308690	Ronas gabbro raft	XRF, INAA,PC
14.6	75523	33308690	Ronas gabbro raft	XRF, PC
14.7	75524	34408620	Ronas diorite raft	XRF, RE, PC
18.8	75525	35178550	Ronas granite	XRF, PC
14.9	75526	32258590	Ronas diorite raft	XRF, INAA, P
14.10	75527	32458560	Ronas granite	XRF, PC
14.11	75528	31958570	Ronas diorite raft	XRF, PC
14.13	75530	35558880	Ronas granite	XRF, INAA, P
14.14	75531	29658130	Ronas granite	XRF, INAA, R
14.15	75532	28109205	Ronas granite	XRF, PC
15.1	70503	337706	Eastern granite	XRF, PC
15.5	75536	34357225	Eastern granite	XRF, PC
15.6	75537	34406940	Eastern granite	XRF, INAA, P
16.1	75539	337070	Net-Veined granite	XRF, INAA, P
16.2	75540	29937799	Net-Veined granite	XRF, PC
16.3	75541	31907780	Net-Veined granite	XRF, INAA, P
16.4	75542	31307350	Net-Veined granite	XRF, PC
17.1	70500	323627	Muckle Roe granophyre	XRF, PC
17.2	75543	3136695	Muckle Roe granophyre	XRF, INAA, P
17.3	75545	31756630	Muckle Roe granophyre	XRF, PC
17.4	75544	30856500	Muckle Roe granophyre	XRF, PC
18.1	75546	29556110	Vementry granite	XRF, PC
18.3	75548	30156075	Vementry granite	XRF, INAA, P
18.4	75549	30656075	Vementry granite	XRF, PC
19a.1	75612	320445	Bixter granite	XRF, INAA, P
19a.6	75617	31404325	Bixter granite	XRF, INAA, R
19a.7	75618	31404325	Bixter granite	XRF, PC
19a.9	75620	32104330	Bixter granite	XRF, PC
19.1	70498	281455	Sandsting granite	XRF, PC
19.2	75621	28354260	Sandsting granite	XRF, INAA, P
19.3	75622	28554340	Sandsting diorite	XRF, INAA, R
19.4	75623	27374580	Sandsting granite	XRF, INAA, P
19.5	75624	27554605	Sandsting granite	XRF, INAA, P
19.6	75625	26954505	Sandsting diorite	XRF. PC
19.7	75626	26954520	Sandsting grandiorite	XRF, INAA. P
19.9	75628	26604425	Sandsting granite	XRF, INAA, R
19.10	75629	27904505	Sandsting granite	XRF, PC
19.11	75630	30454370	Sandsting granite	XRF, INAA, P
19.12	75631	30554290	Sandsting granite	XRF, PC
19.13	75632	303460	Sandsting granite	XRF, INAA, P
19.14	75633	29754230	Sandsting diorite	XRF, INAA, P

Adams, J.A.S., Osmond, J. K. and Rogers, J. J. W., 1967. The geochemistry of thorium and uranium. *In:* In : physics and chemistry of the earth (eds) Ahrens L. H., P., F., Rankema, K. and Runcorn, S. K. (Pergman, London, 3, 298-348.

Allen, P.A., 1981. Sediments and processes on a small streamflow dominated, Devonian alluvial fan, Shetland Islands. Geol., **29**, pp 31-66.

Allen, P.A., 1982. Cyclicity of Devonian fluvial sedimentation, Cunningsburgh-Peninsula, south-east Shetland. J. Geol. Soc. London; **139**, pp. 49-58.

Allen, P. A.and Marshal, J. E. A. 1981. Depositional environments and palynology of the Devonian, south-east Shetland basin. Scott. J. Geol. **17**, pp. 257-273.

Ahrens, L. H., Pinson, W. H., and Kearns, M. M. 1952. Association of rubidium and potassium and their abundance in common igneous rocks and meteorites. Geochim. et Cosmochim. Acta. 2, 229-242.

Arth, J. G. 1976. Behaviour of trace elements during magmatic processes-summary of theoritical models and their applications. J. Res. US Geol. Surv. 4, 41-47.

Astin, T. R. and Thirlwall, M. F. 1983. Discussion on Implications for Caledonian plate tectonic models of chemical data from volcanic rocks of the British Old Red Sandstone. J. geol. Soc. Lond. 140, 315-318.

Atherton, M. P. and Plant, J. A. 1985. High heat production granites and the evolution of the Andean and Caledonian continental margins High heat production (HHP) granites, hydrothermal circulation and ore genesis. Institute of Mining and Metallurgy.

Atherton, M. P. 1988. On the lineage character of evolving granites. Fifth International Symposium on Tin/ Tungsten granites in Southeast Asia and the western Pacific. Shimane University, Matsue, Japan, Pp. 1-6.

Bateman, P.C., and F. C. W. Dodge., 1970. Variations of major chemical constituents across the central Sierra Nevada batholith. B.G.S.A. V **81**, P 409-420.

Barriere M (1977) Le Complexe de Ploumanac'h. Massif armoricain. Thesis Doct Etat. Univ Brest (France). 291 pp.

Beckinsale, R. D. 1979. Ggranite magmatism in the tin belt of South-east Asia. In Atherton, M. P., Tarney, J. (eds). Origin of granite Batholiths: Geochemical evidence. Shiva, Orpington, Kent.

Bowden, P.B., Chappell, B. W., Didier, J. and Lameyre, J., 1984. Petrological, geochemical and source criteria for the classification of granitic rocks: a disscussion. Phys. Earth Planet. Int., **35**, 1-11.

Brooks, C. K., Henderson, P. and Rønsbo, J. G. 1981. Rare-earth partition between allanite and glass in the obsidian of Sandy Braes, Northern Ireland. Mineral. Mag. 44, 157-160.

Brown, G. C., Cassidy, J., Tindle, A. G. and Hughes, D. J. 1979a. The Loch Doon granite: An example of granite petrogenesis in the British Caledonian, J. Geol. Soc. London, 136, 745-753.

Brown, G. C., Cassidy, J., Locke, C. A., Plant, J. A. and Simpson, P. R. 1981. Caledonian Plutonism in Britain (a summary). Journal of Geophysical Research, 86, No. B11, 10502-10514.

Bullard, E. C., Everett, J. E. and Smith, A. G. 1965. The fit of the continents around the Atlantic. Phil. Trans. R. Soc. Lond. A258, 41.

Burnfelt, A. O. and Steinnes, E. 1969. Instrumental Activation analysis of silicate rocks with epithermal neutrons. Anal. Chim. Acta. 48, 13-24.

Carey, S. W. 1958. Continental Drift: a Symposyium. Hobart.

Cawthorn, R. G. and O'Hara, M. J. 1976. Amphibole fractionation in calc-alkaline magma genesis. Am. J. SCi. 276, 309-329.

Cawthorn, R.G., Strong, D.F. & Brown, P.A., 1976. Origin of corundom normative intrusive and extrusive magmas. Nature, 259, 102-104.

Chappell, B.W. 1984. Source rocks of I and S-types granites in LFB, south east Australia, Phil. Trans. R. Soc. Lond. A310, 693-707.

Chappell, B.W. and White, A. J. R., 1974. Two contrasting granite-types. Pacific Geol., 8, 173-174.

Chappell, B.W., White., A. J. R. & Wyborn, D. 1987. The importance of residual source material (restite) in granite petrogenesis. Journal of Petrology. 28, part 6, pp. 1111-1138.

Chappell, B. W. and Stephens, W. E. 1988. Origin of infracrustal (I) type granite magmas. Trans. Roy. Soc. Edin. Earth. Sci. 79, 71-86.

Chayes, F. 1956. Petrographic modal analysis. J. Wiley and sons, New York. 113 PP.

Clark, S. P., Peterman, Z. E. and Heier, K. S., 1966. Abundance of Uranium, thorium and potassium. In: Handbook of physical constants (rev. ed.). Geol. Soc. Am. Memoir, 97, 523-539.

Clark, D. B. 1981. The mineralogy of peraluminous granites: a review Con. Min. 19, 3-17.

Clark, A. M. 1984. Mineralogy of the rare earth elements. In : Henderson, P., ed., Rare earth element Geochemistry. Elsevier, Amsterdam, 33-61.

Clemens, J. D. and Wall, V. J. 1981. Origin and crystallisation of some peraluminous (S-type) magmas. Con. Min. 19, 111-131.

Clemens, J. D. and Vielzeuf, D. 1987. Constraints on melting and magma production in the crust. Earth. Planet. Sci. Lett. 86, 287-306.

Condie, K. C. and Lo, H. H. 1971. Trace element geochemistry of the Louis Lake batholith of early precambrian age, wyoming. Geochim. Cosmochim. Acta. 35, 1099-1119.

Condie, K. C. 1978. Geochemistry of Proterozoic granitic plutons from New Mexico. U.S.A. Chem. Geol. 21, 131-149.

Cox, K.G., Bell, J. D. and Pankhurst, R. J. 1979. *The interpretation of igneous rocks..* George Allen and Unwin, London.

Cullres, R. L. and Medaris, G. 1977. REE in carbonatite and cogenetic alkaline rocks. Contrib. Mineral. Petrol. 65, 143-153.

Curtis, C.D., 1964. Applications of the crystal-field theory to the inclusion of trace transition elements in minerals during magmatic differentiation. Geochim. Cosmochim. Acta. **28**, 389-403.

Brew, D. A., 1990. Modified Pitcher (1982) classificationof granitic batholiths and intrusions, their character and geological environments. U.S. Geological survey.

De la Roche, D., Leterrier, J., Grandelaude, P. and Marchal, M. 1980. A classification of volcanic and plutonic rocks using R1R2 diagram and major element analyses- its relationship with current nomenclature. Chemical geology, **29**, 183-210.

Debon, F. and Le Fort, P. 1982. Chemical-Mineralogical classification of plutonic rocks and association -examples from southern Asia belts. Proceedings of the international Syposium, Held at Nanjing University, Nanjing, China, October 26-30, 1982.

Deer, W.A., Howie, R. A. and Zussman, J. 1962. *In:* (eds.), *Rock-froming minerals. vol.* **1-5.,** Longman,

Didier, J. 1973. Granites and their enclaves the bearing of enclaves on the origin of granites. *In:* (eds.), *Dev. Petrology.* 3 Elsevier, 393.

Didier, J., Duthou, J. L. and Lameyre, J. 1982. Mantle and crustal granites: genetic classifications of orogenic granites and the nature of their enclaves. J. Volcan. Geoth. Res. **14**, 125-132.

Didier, J.and.Lameyre, J. 1969. Les granites du Massif Central francais: etude comparee des leucogranites et granodiorites. Contrib. Mineral Petrol. **24**, 219-238.

Ewart, A. and Taylor, S. R. 1969. Trace element geochemistry of the Rhyolitic volcanic rocks, central North Island, Newzealand. Phenocryst data. Contrib. Mineral. Petrol., **22**, 127-146.

Exley, R. A. 1980. Microporbe studies of REE-rich accessory minerals: implications for Skye granite petrogenesis and REE mobility in hydrothermal systems. Earth Planet. Sci. Lett. 48, 97-110.

Faure, G. and Powell, J. L., 1972. *Strontium isotope geology. Minerals and rocks. V* **5, P 188.** Springer-Verlag, New York.

Finlay, T.M. 1930. The Old Red Sandstone of Shetland. Part 11. North-western area. Trans. R. Soc. Edinb., **56**, 671-694.

Fleet, B. J. Rb-Sr studies and related chemistry on the Caledonian calc-alkaline igneous rocks of North-west Argyllshire, Ph. D. thesis, Univ. of Oxford, Oxford, England.

Fleischer, M., 1978b. Relation of the relative concentrations of lanthanides in titanite to types of host rocks. Am. Mineral., 63: 869-873.

Fleischer, M. and Altschuler, Z. S. 1969. The relationship of the rare-earth composition of minerals to geological environment. Geothim. Cosmochim. Acta, 33: 725-732.

Flinn, D. 1953. On the time relations between regional metamorphism and permeation in Delting, Shetland. Q. J. Geol. Soc. Lond., **110**, pp. 177-199,

Flinn, D. 1956. On the deformation of the Funzie conglomerate, Fetlar, Shetland. J. Geol. 64, 480-505.

Flinn, D. 1958. The nappe structure of north-east Shetland. J. Geol. Soc. Lond., **114**, 120-136.

Flinn, D., Miller, J. A., Evans, A. C. and Pringle, I. R. 1968. On the age of the sediments and contemporaneous volcanic rocks of western Shetland. Soctt. J. Geol., **4**, 10-19.

Flinn, D. 1970. Some aspects of the geochemistry of the metamorphic rocks of Unst and Fetlar, Shetland. Proc. Geol. Ass. **81**, 509-527.

Flinn, D. 1985. The Caledonides of Shetland. In the Caledonide orogen-Scandinavia and related areas. *In this volume.*

Flinn, D. and Moffat, D. T. 1985. A peridotite komatiite from the Dalradian of Shetland. Geol. J., **20**, 287-292.

Flinn, D and Pringle, I. R. 1976. Age of the migmatisation in the Dalradian of Shetland. *Nature, London,* **259**, 299-300.

Foster, M. D. 1960. Interpretation of the composition of Trioctahedral micas. Prof. Pap. U. U. Geol. Surv. 354B, 11-49.

Fourcade, S., and Allegre, C. J. 1981. Trace element behaviour in granite genesis. A case study: the calc-alkaline plutonic association from the Querigut complex, C. Pyrenees, France. Contrib. Mineral. Petrol., 76, 177-195.

Francois Debon and Patrick Le Fort. 1982. Chemical-Mineralogical classification of plutonic rocks and association - examples from southern Asia belts. Proceeding of the international symposium, held at Nanjing University, Nanjing, China October 26-30, 1982.

Gass, I.G., Neary, C. R., Prichard, H. M. and Bartholomew, I. D. 1982. The chromite of the Shetland ophiolite. In a report for the commission of European communities.

Gill, K. R. 1965. The Petrology of the Brae Complex, Delting, Shetland, Ph. D. thesis, University of Cambridge (unpublished).

Gribble, C.D. 1969. Distribution of elements in igneous rocks of the normal calc-alkali sequence. Soctt. J. Geol., **5**, 322-327.

Gromet, L. P. and Silver, L. T. 1983. Rare earth element distributions among accessory minerals in a granodiorite and their petrogenetic implications. Geochim. Cosmochim. Acta. 47, 925-939.

Hall, A. 1971. The relationship between geothermal gradient and the composition of granitic magmas in orogenic belts. Contrib. Mineral. Petrol. 32, 186-192.

Halliday, A. N., Stephens, W. E. and Harmon, R. S. 1980b. Rb-Sr and O isoptopic relationships in three zoned Caledonian granite plutons, southern Uplands, Scotland: evidence for varying sources and hybridisation of magmas. J. Geol. Soc. Lond. 137, 329-348.

Halliday, A. N. and Stephens, W. E. 1984. Crustal controls on the genesis of the 400 Ma old Caledonian granite. Phys. Earth. Planet. Inter., 35, 89-104.

Halliday, A. N., Stephens, W. E., Hunter, R. H., Menzies, M. A., Dickin, A. P. and Hamilton, P. J. 1985. Isotopic and Chemical constraints on the building of the deep Scottish lithosphere. Scott. J. Geol., 21, 465491.

Hanson, G. N. 1980. Rare earth elements in Petrogenetic studies of igneous systems. Ann. Rev. Earth Planet. Sci. 8, 371-406.

Harmon, R. S. and Halliday, A. N. 1980. Oxygen and strontium isotope relationship in the British Late Caledonian granites, Nature, 283, 21-25.

Harris, N. B. W., Pearce, J. A and . A .G .Tindle, A .G . 1986. Collision tectonics. *Geological Society special publication*, No. 19, 67-81.

Harry, W. T. 1965.The form of Cairngorm granite pluton, Soctt. J. Geol., 1,1-8.

Heddle, M.F. 1879. The geognosy and mineralogy of Scotland-part 111. Shetland-Mainland. Mineral. Mag., 2, 155-190.

Heier, K.S and Rogers, J. J. W. 1963. Radiometric detrmination of thorium, uranium and potassium in basalts and in two magmatic differentiation series. Geochi. Cosmochim. Acta. 27, 137-154.

Hellman, P. L. and Green, T. H. 1979. The role of sphene as an accessory phase in the high pressure partial melting of hydrous mafic compositions. Earth. Planet. Sci. Lett. 42, 191-201.

Hennessy, J. 1981. A classification of British Caledonian granites based on uranium and thorium contents. Mineral. Mag. 44, 449-454.

Plant, J. A. Models for granites and thier mineralizing systems in the British and Irish Caledonian.

plant Jane A., Brown, G. C., Simpson, P. R. and Smith, R. T. 1980. Signatures of metalliferous granites in the Scottish Caledonides. Trans. Inst. Min. Metall. 893, 198-210.

Jensen, B. B. 1967. Distribution Patterns of rare earth elements in cerium-rich minerals. Nor. Geol. Tidsskr., 47, 9-19.

Ishihara, S. 1977. The magnetite series and ilmenite series rocks. Minin. Geol., 27, 293-305.

Khomyakov, A. P. and Manukhova, A. A. 1971. Rare earths in zircon from Miaskite. Dokl. Acad. Sci. U.S.S.R., Earth Sci. Sect., 196, 221-223.

Kovalenko, V. I. and Kovalenko, N. I. 1984. Problems of the origin ore-bearing and evolution of rare-metal granitoids. Physics of Earth and Planetary Interiors, 35, 51-62.

Krauskopf, K. 1967. Introduction to geochemistry. McGraw-Hill, New York.

Kuno, H. 1966. Differentiation of basalt magmas. In basalts V.2. Ed. H. H. Hess , Wiley N. Y. London.

Lameyre, J. and Bowden, P. 1982. Plutonic rock type series: discrimination of various granitoid series and related rocks. J. Volcan. Geotherm. Res., 14, 169-86.

Lameyre, J., Black, R., Bonin, B., Bowden, P. and Giret, A. 1982. The granitic terms of Converging plutonic type series and associated minerallisations. au Syposium sur la Geologie des Granites et leurs relations metallogeniques. October1982, Nanlin.

Larsen, E. S. and Irving, J. 1938. Petrologic results of a study the minerals from the Tertiary volcanic rocks of the San Juan region, Colorado. 7. The plagioclase feldspars, Amer. Min. 23, 227-57.

Leake, B. E. 1978. Nomenclature of Amphibole. Min. Mag. 42, 533-563.

Leake, B. E. 1978. Granite emplacement: The granites of Ireland and Their origin, in crustal evolution in northwestern Britain and adjacent regions, edited by D. R. Bowes, and B. E. Leake, Geol. J. Spec. Issue, 10, 221-248.

Lee, D. E., Van Loenen, R. E. and Mays, R. E. 1973. Accessory apatite from hybrid granitoid rocks of southern Snake Range, Nevada. J. Res., U.S. Geol. Surv., 1, 89-98.

Locke, C. A. and G. C. Brown, 1978. Geophysical constraints on strucure and emplacement of Shap granite, Nature, 272, 526-528.

Luth, W.C., Jahns, R.H. & Tuttle, O.F. 1964. The granite system at pressure of 4 to 10 kilobars. J. Geophys. Res., 69, 759-773.

Mahawat, C., Atherton, M. P. and Brotherton, M. S. 1990. Tha Tak Batholith, Thailand; the evolution of contrasting granite types and implications for tectonic setting. J. Southeast Asian Earth. Sci. 4, 11-27.

Marshall, J. E. A. 1988. Devonian miospores from Papa Stour, Shetland. Trans. Roy. Soc. Edinburgh: Earth Science, 79, 13-18.

Mariano, A. N. 1990. Economic geology of rare earth elements. Geochemistry and mineralogy of REE. Reviews in Mineralogy vol. 21.

Marston, R. J. 1970. The Foyers granitic complex, Inverness-shire, Scotland, Q. J. Geol. Soc. London, 126, 331-368.

McKenzie, D. 1988. The generation and extraction of magma from the crust and mantle. Extended Abs.

McKenzie, D. 1989. Some remarks on the movement of small melt fractions in the mantle. Earth. Planet. Sci. Lett. 95, 53-72.

McCarthy, T.S and Hasty, R. A. 1976. Trace element distribution patterns and their relationship to the crystallize of granitic melts. Geochim. Cosmochim. Acta. 40, 1351-1358.

McKerrow, W. S. Arenig-wenlock synthesis. Abstract of meeting; evolution of the Caledonide-Appalachain orogen held at Glasgow University, 3-8 Sept. 1984.

International Geological Correlation Programme Project 27, Caledonide orogen. 1984.

Michael, P. J. 1983. Chemical differentiation of the Bishop tuff and other high-silica magmas through crystallisation processes. Geology 11, 31-34.

Miller, C. F. and Bradfish, L. J. 1980. An inner belt of muscovite-bearing plutons. Geology, 8, 412-16.

Miller, C. F., Stoddard, E. F., Bradfish, L. J. and Dollase, W. A. 1981. Composition of plutonic muscovite: genetic implications. Can. Min. 19, 25-34.

Miller, C. F. 1985. Are strongly peraluminous magmas derived from sedimentary sources?. J. Geol. 93, 673-690.

Miller, J. and Flinn, D. 1966. A survey of the age relations of Shetland rocks. Geol. J., 5, 95-116.

Mykura, W. and Young, B. R. 1969. Sodic scapolite (dipyre) in the Shetland Islands. Rep. Ins. Geol. Sci., No. 69/4.

Mykura, W. 1976. *British regional geology: Orkeny and Shetland.* Edinburgh, OHMS.

Mykura, W and Phemister, J. 1976. The geology of western Shetland. Mem. Geol. Surv. G. B.

Nagasawa, H., and Schnetzler, C. C. 1971. Partitioning of rare earth alkali, and alkali-earth elements between phenocrysts and acidic igneous magma. Geochim. Cosmochim. Acta. 35, 953-968.

Nash, W. P. and Crecraft, H. R. 1985. Partition coefficients for trace elements in silcic magmas. Geochim. Cosmochim. Acta. 49, 2309-2322.

Noble, C. D. Mckee, E. H., Farrar, E. and Petersen, V. 1974. Episodic Cenozoic volcanism and tectonism in the Andes of Peru. Earth. Plan. Sci. Letts. 21, 213-220.

O'Connor, P. J. 1981. Radioelement geochemistry of Irish granites. Mineral. Mag. 44, 485-4895.

Pankhurst, R. J., and Southerland, D. S. 1981. Caledonian granites and diorites of Scotland and Ireland, in igneous rocks of the British Isles, edited by D. S. Southerland, John Wiley, New York, in press.

Peach, B.N.and Horne, J. 1879. The glaciation of the Shetland Islands. Q. J. Geol. Soc. Lond. 35, 778-811.

Peach, B.N. and Horne, J. 1884. The Old Red Volcanic rocks of Shetland. Trans. R. Soc. Edinburgh. 32, 359-388.

Peacock, M.A. 1931. Classification of igneous rocks. J. Geol. 39, 54-67.

Pearce, J.A., Harris, N. B. W. and Tindle, A. G. 1984. Trace element discrimination diagrams for the tectonic interpretation of granitic rocks. J. Petrol., 25, 956-983.

Peccerillo, A.and Taylor, S. R. 1976. Geochemistry of Eocene calc-alkaline volcanic rocks from the Kastamona area, northern Turkey. Contrib. Mineral. Petrol. **58**, 63-81.

Phemister, J., Harvey, C.O. and Sabine, P. A. 1950. The riebeckite-bearing dikes of Shetland. Mineral. Mag. **29**, 359-373.

Phemister, J. 1979. The Old Red Sandstone intrusive complex of Northern-Northmaven, Shetland. *I. G. S.*, **Ref. 78/2, OHMS** .

Philpots, J. A. and Schnetzler, C. C. 1970. Phenocryst-matrix partition coefficients for K, Rb, Sr, and Ba, with applications to anorthosite and basalt genesis. Geochim. et Cosmochim. Acta. 34, 307-323 (also P. 331).

Phillips, F.C. 1926. Note on a riebeckite-bearing rock from the Shetlands. Geol. Mag., **63**, 79-86.

Phillips, W. E. A., Stillman, C. J. and Murphy, T. 1976. A Caledonian plate tectonic model. J. Geol. Soc. Lond. 132, 579-609.

Phillips, W. J., Fuge, R. and Phillips, N. 1981. Convection and crystallisation in the Criffell-Dalbeattie pluton. J. geol. Soc. Lond. 138, 351-66.

Pidgeon, R. T., and M. Aftalion. 1978. Cogenetic and inherited zircon U-Pb system in palaeozoic granites from Soctland and adjacent regions, in crustal evolution in Northwestern Britaib and adjacent regions, edited by D. R. Bowes and B. E. Leake, Geol. J. Spec. Issue, 10, 183-220.

Pitcher, W.S. 1978. The anatomy of a batholith. J. Geol. Soc. London., **135**, 157-182.

Pitcher, W. S. 1979. The nature, ascent and emplacement of granitic magmas. J. Geol. Soc. Lond. 136, 627-662.

Pitcher, W.S. 1982. Granite type and tectonic environment. In : Mountain building Processes. K. Hsu, editor. Academic press, 19-40.

Pitcher, W. S. 1983. In: Granite typology, geological environment and melting relationships-. In : Migmatites, melting and metamorphism. M. P. Atherton and C. D. Gribble, editors. Shiva Publishing Ltd, Cheshire, 277-285.

Pitcher, W. S. 1987. Granites and yet more granites forty years on. Geol. Rundsch. 76, 51-79

Poldervaart, A. and Hess, H. H. 1951. Nomenclature of clinopyroxenes in the system CaMgSi2O6-CaFeSi2O6-Mg2Si2O6-Fe2Si2O6. Journ. Geol. 59, 472.

Poldervaart, A. 1956. Zircon in rocks. 2. Igneous rocks. Am. J. Sci. **254**, 521-554.

Poldervaart, A. 1950. Statisical studies of zircon as a criteria in granitization. *Nature*, **165**, 574-575.

Presnall, D. C. and Bateman, P. C. 1973. Fused relations in the system Ab-An-Or- Qz-H2O and the generation of granitic magmas in the Sierra Nevada Batholith. B.G.S.A. V.84, 3181-3202.

Pringle, I. R. 1970. The structural geology of the North Roe area of Shetland. Geol. J., 7, 147-170.

Pupin, J. P. and Turco, G. 1972a. Une typologie originale du zircon accessoire, Bull Soc. for Mineral Cristallogr, 95, 348-359.

Pupin, J. P. 1980. Zircon and granite petrology. Contrib. Mineral. Petrol., 73, 207-220.

Read, H.H. 1934. The metamorphic geology of Unst in the Shetland Ilands. Q. J. Geol. Soc. Lond., 90, 637-688.

Read, H.H. 1947. The granite problem in origin of granite. Geol. Surevy. Amer. Mem., 28,

Read, H. H. 1961. Aspects of Caledonian magmatism in Britain, Liverpool Manchester Geol. J., 2, 653-683.

Sawkins, F. J. 1984. Metal deposits in relation to Plate tectonics. Springer-Verlag, Berlin Heidelberg, New York, Tokyo, 1984.

Schnetzler, C. C. and John, A. P. 1970. Partition Coefficients of REE between igneous matrix material and rock-forming mineral phenocrysts -11. Geochimica et Cosmochimica. Acta., 34, 331-340.

Simmons, E. C. and Hedge, C.E. 1978. Minor element and Sr isotope geochemistry of tertiary stocks, Colorado. Contrib. Min. Petrol. 67, 379-396.

Soper, N. J. 1963. The structure of the Rogart igneous complex, Sutherland, Scotland, Q. J. Geol. Soc. London, 119, 445-478.

Soper, N. J. and Hutton, D. H. W. 1984. Late Caledonian sinistral displacements in Britain: Implications for a three-plate collision model.

Stephens, W. E. and Halliday, A. N. 1984. Geochemical contrasts between late Caledonian granitoid plutons of northern, central and southern Scotland. Transactions of the Royal Society of Edinburgh: Earth Sciences. 75, 259-273.

Stephens, W. E., John, E. Whitely., Thirlwall, M. F. and Alex N. Halliday. 1985. The Criffell zoned pluton: Correlated behaviour of rare earth element abundances with isotopic systems. Contrib. Mineral. Petrol. 89, 226-238.

Streckeisen, A. L. 1967. Classification and nomenclature of igneous rocks. Neues Jahrb Mineral. Abh. 107 (2/3), 144-240.

Streckeisen, A.L. 1974. Classification and Nomencluture of igneous rocks. Recommendations of the IUGS subcommision on the systematics of igneous rocks. Geol. Rundsch. 63, 773-786.

Streckeisen, A. L. 1976. To each plutonic rock its proper name. Earth Sci. Rev. 12, 1-33.

Streckeisen, A.L. and Le Maitre, R. W. 1979. A chemical approximation to the modal QAPF classification of the igneous rocks. Neues Jahrb Mineral. Abh. 136, 169-206.

Sun, S. S. 1980. Lead isotopic study of young volcanic rocks from mid-oceanic ridges, ocean islands and island arcs. Phil Trans R. Soc. Lond. A297, 409-45.

Takahashi, M., Armaki, S. and Ishihara, S. 1980. Magnetite-series / Ilmenite-series vs. I-type / S-type granitoids. In: Ishihara, S. and Takenouchi, S. (eds). Granitic magmatism and related minerallisation. Mining Geol. Japan Spec. Issue, 8, 13-28.

Tauson, L. V. and Kozlov, V. D. 1973. Distribution functions of and ratios of trace element concentrations as estimators of the ore-bearing potential of granites. Cited in Levinson, A.A. (1974), Introduction to exploration geochemistry, P. 318, Applied publishing, Calgary.

Taylor, G.K. 1984. Geophysical investigations of a Caledonian ophiolite complex, N. E. Shetland. ph. D. thesis, Liverpool.

Thirlwall, M. F. 1979. The Petrochemistry of British Old Red Sandstone volcanic province. Thesis, Ph. D, Uni. Edinburgh (unpubl.).

Thirlwall, M. F. 1981. Implications for Caledonian Plate tectonic models of chemical data from volcanic rocks of the British Old Red Sandstone. J. Geol. Soc. Lond. 138, 123-138.

Thirwall, M . F. 1982. Systematic variation in chemistry and Nd-Sm isotopes across a Caledonian calc-alkaline volcanic and implications for source materials. Earth. Planet. SCI. LEET., 58, 27-50.

Thompson, R. N., M. A. Morrison, G. L. Hendry and S. J. Parry. 1984. An assessment of the relative roles of a crust and mantle in magma genesis: an elemental approach. Phil Trans R. Soc. Lond. A310, 549-90.

Thorpe, R. S., Potts, P. J. and Francis, P. W. 1976. Rare earth data and petrogenesis of andesites from the north Chilean Andes. Contrib. Mineral. Petrol. 54, 65-78.

Todd, V..R. and Shaw, S. E. 1985. S-type granitoids and an I-S line in the Peninsular ranges batholith, southern California. Geology, 13, 231-233.

Vance, J. A. 1969. On synneusis. Contrib. Mineral. Petrol., 24,, 7-29.

Vernon, R. H. 1984. Microgranitoid enclaves in granites -globules of hybrid magma quenched in plutonic envirnment. Nature, 309, 438-9.

Watson, J. V. and Plant, J. 1979. The regional geochemistry of uranium as a guide to deposit formation. Philos. Trans. R. Soc. London., 291A, 321-338.

Watson, J.V. 1984. The ending of the Caledonian orogeny in Scotland. J. Geol. Soc. London., 141, 193-214.

White, A. J. R., & Chappell, B. W. 1983. Granitoid types and their distribution in the LFB, south east Australia. Tectonophysics., 159, 21-34.

White, A. J. R., Clemens, J. D., Holloway, J. R., Silver, L. T., Chappell, B. W. & Wall, V. J. 1986. S-type granite and their probable absence in southwestern North America. *Geology*, 14, 115-118.

White, A. J. R. & Chappell, B. W. 1977. Ultrametamorphism and granitoid genesis. *Tectonophyscs*, 43,, 7-22.

White, A. J. R. and Chappell, B. W. 1983. Granitoid types and their distribution in the Lachlan fold belt, southeastern Australia. Geological Society of America Memoir 159, 1983.

Wilson, G.V. 1932. In: HMSO. (eds.), In summ. progr. Geol. Surv. G. B. for 1932. London, 77-80.

Wood, D. A., Joron, J. L. and Treuil, M. 1979. A re-appraisal of the use of trace elements to classify and discriminate between magma series erupted in different tectonic settings. Earth Planet. Sci. Lett. 45, 326-336.

Wright, A. E., and Bowes, D. R. 1979. Geochemistry of the appinite suite. In Harris, A. L., Holland, C. H. and Leake, B. E. (eds). The Caledonides of the British Isles - Reviewed. 699-703. Spec. Publ. Geol. Soc. Lond. 8.

Ziegler, P.A. 1981. *Evolution ofsedimentary basin in north-west Europe*. Heyden, London, 3-39.